

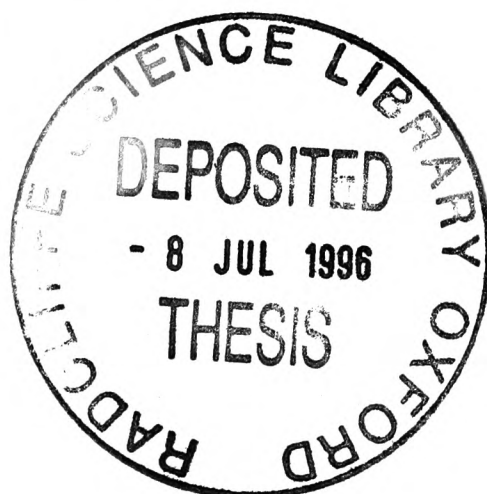
High-Resolution Outcrop Gamma-Ray Spectrometry of the Lower Lias, Southern Britain.

VOLUME 2

FIGURES & APPENDICES

Julian L. Bessa

Saint Edmund Hall and Department of Earth Sciences.



Thesis presented to the University of Oxford for the Degree of Doctor of Philosophy.

Michaelmas Term 1995

High-Resolution Outcrop Gamma-Ray Spectrometry **of the Lower Lias, Southern Britain.**

Contents to Volume 2 - Illustrations and Appendices

CHAPTER 1

Introduction to the Depositional Basins of Southern Britain and the Techniques and Theory of Gamma-Ray Spectrometry.

- Figure 1.01 Simplified regional tectonic map of major Mesozoic depocentres in the Wessex Basin.
Figure 1.02 Summary geological map of the Wessex Basin in south Dorset.
Figure 1.03 Structure of the East Midland shelf in the Chipping Norton District.
Figure 1.04 Outcrop pattern for the Lower Jurassic of the British Isles.
Figure 1.05 Stratigraphic scheme for the Rhaetian to Lower Pliensbachian.
Figure 1.06 Division of the Lower Lias interval in the Winterborne Kingston borehole into lithological gamma-ray units proposed by Whittaker *et al.* (1985)
Figure 1.07 Thorium decay series of naturally occurring radiogenic isotopes.
Figure 1.08 Uranium decay series of naturally occurring radiogenic isotopes.
Figure 1.09 Gamma-ray spectrum for the Th decay series.
Figure 1.10 Gamma-ray spectrum for the U decay series.
Figure 1.11 Gamma-ray spectrum for the 40-K isotope.
Figure 1.12 Depositional sequence stratigraphic interpretation of a total gamma-ray log for a coarse-grained siliciclastic system.
Figure 1.13 The theoretical distribution of clay minerals in terms of potassium and thorium content.
Figure 1.14 Thorium - potassium cross-plot proposed by Hurst 1990.
Figure 1.15 (A) Distribution of thorium-hydroxy and phosphate complexes.
(B) Thorium-ligand complexes.
(C) Thorium complexes vs. pH in a solution containing organic and inorganic species.
Figure 1.16 Plot of the forward sorption rate for Th vs. particle concentration in oceanic environments.
Figure 1.17 Distribution of uranyl-hydroxy and silicate complexes vs. pH.
Figure 1.18 Distribution of uranyl-hydroxy and carbonate complexes vs. pH.

CHAPTER 2

The Methodology and Experimentation Required For Outcrop Gamma-Ray Spectrometry

- Figure 2.01 The GRS-500 portable gamma-ray spectrometer. (Single photograph).
Figure 2.02 The GR-410 and GR-256 gamma-ray spectrometer. (Two photographs).
Figure 2.03 Simplified block diagram of detector unit for spectrometer models GR-410 and GR-256.
Figure 2.04 Interference effects from the reference isotope.
Figure 2.05 Calibration results with temperature drift.
Figure 2.06 Temperature drift.
Figure 2.07 (A) Linear regression between K-U (GR-410) collected from Iron Ledge
(B) Linear regression between K-U (GR-410) collected from the Belemnite Bed.
(C) Linear regression between K-U (GR-410) including Lower Cement Bed.
(D) Relationship between calculated K and U concentration from total counts (GR-410)
Figure 2.08 Linear regression between K (GR-256) and K (GR-410) for Iron Ledge and Belemnite Bed.
Figure 2.09 (A) Linear regression between U (GR-256) and U (GR-410) for the Belemnite Bed

	(B) Linear regression between U (GR-256) and U (GR-410) for the Iron Ledge.
	(C) Positive linear relationship between U (GR-256) and U (GR-410) for the Belemnite Bed and the Iron Ledge.
	(D) Polynomial relationship between U (GR-256) and U (GR-410).
Figure 2.10	Positive linear relationship between K (GR-256) and K (GR-410).
Figure 2.11	(A) Positive linear relationship between Th (GR-410 and GR-256) for the Belemnite Bed. (B) Positive linear relationship between Th (GR-410 and GR-256) for the Iron Ledge.
Figure 2.12	Positive linear relationship between Th (GR-410) and Th (GR-256).
Figure 2.13	Spectral drift within the GR-410 data-set.
Figure 2.14	Individual energy windows used in determination of K, U and Th concentrations.
Figure 2.15	Response of a portable gamma-ray spectrometer to cylindrical pads of varying diameter.
Figure 2.16	Standard deviation curves for GR-256 on the Belemnite Bed.
Figure 2.17	Standard deviation curves for GR-256 on Iron Ledge.
Figure 2.18	Comparison of gamma-ray measurements collected from identical points in St. Mary's Well Bay exactly five hours apart.
Figure 2.19	Relationship between counting geometry and stratigraphic bedding surfaces.
Figure 2.20	Loss of high frequency information with increase in sampling interval.

CHAPTER 3

The Gamma-Ray Characteristics of the Lower Lias in Southern Britain

Figure 3.01	A comparison of lithostratigraphic terms used to delineate the Rhaetian to Lower Sinemurian succession in southern Britain.
Figure 3.02	Stratigraphic Log for the Blue Lias and lower part of the Shales-with-'Beef', Dorset.
Figure 3.03	Stratigraphic log for the Blue Lias at St. Audrie's Bay, Somerset.
Figure 3.04	Stratigraphic log for the Blue Lias at Kilve Pylle, Somerset.
Figure 3.05	Stratigraphic log for the Blue Lias at Kilve Pylle and Hinkley Point, Somerset.
Figure 3.06	Stratigraphic log for the Blue Lias at St. Mary's Well Bay, Glamorgan.
Figure 3.07	Stratigraphic log for the Blue Lias at Nash Point, Glamorgan.
Figure 3.08 A	Stratigraphic log for the upper Shales-with-'Beef'.
Figure 3.08 B	Stratigraphic log for the Black Ven Marls.
Figure 3.09	Stratigraphic log for the Belemnite Marls.
Figure 3.10	Sinemurian - Pliensbachian Stage boundary, Dorset. (Two photographs).
Figure 3.11	Gamma-ray logs for the Lower Lias of the Somerset coast based on 501 sets of measurements.
Figure 3.12	Stratal packaging within the Lower Lias of the Somerset coast based on total gamma-ray signature and divided into nine gamma-ray units.
Figure 3.13 A	Gamma-ray logs for the Lower Lias of the Glamorgan coast based on 196 set of readings.
Figure 3.13 B	Stratal packaging within the Lower Lias of the Glamorgan coast based on total gamma-ray signature and divided into five gamma-ray units.
Figure 3.14	The Blue Lias, St. Audrie's Bay, Somerset. (Two photographs).
Figure 3.15	The Blue Lias, East of Kilve Pylle, Somerset. (Two photographs).
Figure 3.16	The Blue Lias, West of Kilve Pylle and Hinkley Point, Somerset. (Two photographs).
Figure 3.17	The Blue Lias at Doniford Bay, Somerset. (Single photograph).
Figure 3.18	Blue Lias at St Mary's Well Bay and Lavernock Point, Glamorgan. (Two photographs).
Figure 3.19	Blue Lias at St Mary's Well Bay, Glamorgan. (Two photographs).
Figure 3.20	Blue Lias at St Mary's Well Bay and Nash Point, Glamorgan. (Two photographs).
Figure 3.21	Outcrop gamma-ray logs for the Blue Lias exposed at St. Audrie's Bay, Somerset.
Figure 3.22 A	Linear regression correlation between Th concentration and K concentration.
Figure 3.22 B	Linear regression between Th concentration and U concentration.
Figure 3.23	Outcrop gamma-ray logs for the Blue Lias exposed east of Kilve Pylle, Somerset.
Figure 3.24 A	Linear regression correlation between Th concentration and K concentration.
Figure 3.24 B	Linear regression between Th concentration and U concentration.
Figure 3.25	Outcrop gamma-ray logs for the Blue Lias exposed west of Kilve Pylle, Somerset.
Figure 3.26 A	Linear regression correlation between Th concentration and K concentration.
Figure 3.26 B	Linear regression between Th concentration and U concentration.

- Figure 3.27 Outcrop gamma-ray logs for the Blue Lias exposed at Doniford Bay, Somerset.
- Figure 3.28 A Linear regression correlation between Th concentration and K concentration.
- Figure 3.28 B Linear regression between Th concentration and U concentration.
- Figure 3.31 Outcrop gamma-ray logs for the Blue Lias exposed at St. Mary's Well Bay, Glamorgan.
- Figure 3.30 A Linear regression correlation between Th concentration and K concentration.
- Figure 3.30 B Linear regression between Th concentration and U concentration.
- Figure 3.31 Outcrop gamma-ray logs for the Blue Lias exposed at Nash Point, Glamorgan.
- Figure 3.32 A Linear regression correlation between Th concentration and K concentration.
- Figure 3.32 B Linear regression between Th concentration and U concentration.
- Figure 3.33 Outcrop gamma-ray logs for the Lower Lias succession of the Dorset coast.
- Figure 3.34 Stratal packaging within the Lower Lias of the Dorset coast based on total gamma-ray flux and divided into ten gamma-ray units.
- Figure 3.35 The Blue Lias Formation, Dorset. (Two photographs).
- Figure 3.36 Shales-with-'Beef' at Seven Rock Point, Lyme Regis, Dorset. (Single photograph).
- Figure 3.37 The Black Ven Marls, Charmouth, Dorset. (Two photographs.)
- Figure 3.38 Belemnite Marls exposed east of Charmouth, Dorset. (Two photographs).
- Figure 3.39 Outcrop gamma-ray logs for the Blue Lias, Dorset.
- Figure 3.40 A Linear regression correlation between Th concentration and K concentration.
- Figure 3.40 B Linear regression between Th concentration and U concentration.
- Figure 3.41 Outcrop gamma-ray logs for the Shales-with-'Beef'.
- Figure 3.42 A Linear regression correlation between Th concentration and K concentration.
- Figure 3.42 B Linear regression between Th concentration and U concentration.
- Figure 3.43 Outcrop gamma-ray logs for the Black Ven Marls.
- Figure 3.44 Outcrop gamma-ray logs for the Shales-with-'Beef' and Black Ven Marls.
- Figure 3.45 A Linear regression correlation between Th concentration and K concentration.
- Figure 3.45 B Linear regression between Th concentration and U concentration.
- Figure 3.46 Outcrop gamma-ray logs for the Belemnite Marls.
- Figure 3.47 Outcrop gamma-ray logs for the upper Shales-with-'Beef', Black Ven Marls and Belemnite Marls.
- Figure 3.48 Stratal packaging within the Belemnite Marls based on total gamma-ray signature.
- Figure 3.49 Positive linear regression between total gamma-ray flux and radio-elemental concentration within gamma-ray unit BM 1.
- Figure 3.50 Discrete carbonate cycles evident in the gamma-ray signature for the Belemnite Marls.
- Figure 3.51 Positive linear regression between total gamma-ray flux and radio-elemental concentration
- Figure 3.52 A Linear regression correlation between Th concentration and K concentration.
- Figure 3.52 B Linear regression between Th concentration and U concentration.
- Figure 3.53 The *luridum* Subzone at Blockley Pit, Gloucestershire. (Two photographs).
- Figure 3.54 Outcrop gamma-ray log for the Blockley Pit section.
- Figure 3.55 A Linear regression correlation between Th concentration and K concentration.
- Figure 3.55 B Linear regression between Th concentration and U concentration.
- Figure 3.56 Production of a synthetic gamma-ray log using bed-thickness data.
- Figure 3.57 Comparison of the outcrop gamma-ray log with the coded-lithological log for the Dorset coast
- Figure 3.58 A Biostratigraphic divisions of the Burton Row borehole at the zonal level of resolution.
- Figure 3.58 B Correlation of the Hettangian to Lower Sinemurian succession across southern Britain.
- Figure 3.59 Gamma-ray divisions of the Burton Row borehole using the Dorset outcrop gamma-ray log.
- Figure 3.60 Gamma-ray divisions of the Winterborne Kingston borehole using the Dorset outcrop gamma-ray log.

CHAPTER 4

Interpretation of the Gamma-Ray Characteristics shown by the Lower Lias in Southern Britain

- Figure 4.01 Typical signatures that would be expected to be shown by the Th gamma-ray log for a fine-grained depositional system of 100 % clay, a fine-grained depositional system characterised by clay and pelagic carbonate and a coarse-grained depositional system.

- Figure 4.02 Th/K fields shown by gamma-ray units BL 3 to BL 7 for the Pre-*planorbis* Beds to *bucklandi* Zone in Somerset.
- Figure 4.03 Th/K fields shown by gamma-ray units BL 8 to BL 11 for the *bucklandi* Zone and lower *semicostatum* Zone in Somerset.
- Figure 4.04 A Gamma-ray logs for the Lower Lias succession of the Somerset coast divided into gamma-ray facies.
- Figure 4.04 B The total gamma-ray log of the Burton Row borehole divided into gamma-ray facies based on the spectral gamma-ray data collected from the Dorset and Somerset coasts.
- Figure 4.05 Th/K fields shown by gamma-ray units BL 3 to BL 7 for the Pre-*planorbis* Beds to *bucklandi* Zone in Glamorgan.
- Figure 4.06 Gamma-ray logs for the Lower Lias succession of the Glamorgan coast divided into gamma-ray facies.
- Figure 4.07 Th/K fields shown by gamma-ray units BL 1 to SWB 3 for the Pre-*planorbis* Beds to *turneri* Zone in Dorset.
- Figure 4.08 Th/K fields shown by gamma-ray units BVM 1 to BM 2 for the *turneri* Zone to *ibex* Zone in Dorset.
- Figure 4.09 Gamma-ray logs for the Lower Lias succession of the Dorset coast divided into gamma-ray facies.
- Figure 4.10 A Linear regression correlation between Th concentration and K concentration for the Shales-with-'Beef' and Black Ven Marls.
- Figure 4.10 B Linear regression correlation between Th concentration and K concentration for the Blue Lias and Belemnite Marls.
- Figure 4.11 *Obtusum* Shales at Stonebarrow, Charmouth, Dorset. (Two photographs).
- Figure 4.12 Comparison between total gamma ray flux, U concentration, TOC and calcium carbonate for the *Obtusum* Shales.
- Figure 4.13 Comparison between total gamma ray flux, U concentration, smoothed TOC and calcium smoothed carbonate for the *Obtusum* Shales.
- Figure 4.14 Correlation line for the *Obtusum* Shales across southern Britain.
- Figure 4.15 Correlation of total gamma-ray flux for the *Obtusum* Shales across southern Britain.
- Figure 4.16 Correlation of gamma-ray units BM 1 and BM 2 (distal facies) between the fully cored Burton Row borehole, Somerset and the Dorset coastal sections.
- Figure 4.17 Comparison of the gamma-ray signatures for a distal gamma-ray facies and a proximal gamma-ray facies in the *ibex* Zone.
- Figure 4.18 The wire-line log trace for two laterally persistent geophysical marker horizons recognised within the Lower Lias of Oxfordshire.
- Figure 4.19 The '70' and '85' Marker Member, East Midland Shelf. (Two photographs).
- Figure 4.20 Correlation of total gamma-ray flux between the distal Belemnite Marls and the proximal-facies sub-surface equivalents developed on the East Midland Shelf and Worcester Graben.
- Figure 4.21 Line of correlation for the proximal and distal facies between the Bristol Channel Basin, Wessex Basin & East Midland Shelf.
- Figure 4.22 Correlation panel for the Lower Pliensbachian in southern Britain.

CHAPTER 5

A Sequence Stratigraphic Synthesis for the Lower Lias in Southern Britain and Final Conclusions

- Figure 5.01 The complex system of interactions and feedbacks which influence the stratigraphic record.
- Figure 5.02 Sequence stratigraphic interpretation of a total gamma-ray log for a coarse-grained siliciclastic system.
- Figure 5.03 Gamma-ray logs for the Lower Lias succession of the Somerset coast divided into genetic stratigraphic sequences (*sensu* Galloway 1989).
- Figure 5.04 Gamma-ray logs for the Lower Lias succession of the Glamorgan coast divided into genetic stratigraphic sequences (*sensu* Galloway 1989).
- Figure 5.05 Gamma-ray logs for the Lower Lias succession of the Dorset coast divided into genetic

	stratigraphic sequences (<i>sensu</i> Galloway 1989).
Figure 5.06	Possible sequence stratigraphic interpretation of the <i>obtusum</i> Shales (gamma-ray unit BVM 2)
Figure 5.07	The Coinstone at Stonebarrow, Charmouth, Dorset. (Two photographs)
Figure 5.08	Correlation of the Coinstone disconformity across southern Britain.
Figure 5.09	Possible interpretation of the Coinstone in terms of relative sea-level change.
Figure 5.10	Migration of mudrock facies at the Sinemurian - Pliensbachian boundary.
Figure 5.11	Line of correlation for the proximal and distal facies between the Bristol Channel Basin, Wessex Basin & East Midland Shelf.
Figure 5.12	Correlation of total gamma-ray flux between the distal Belemnite Marls and the proximal-facies sub-surface equivalents developed on the East Midland Shelf and Worcester Graben.
Figure 5.13	Correlation panel for the Lower Pliensbachian in southern Britain.
Figure 5.14	A model for the deposition of the Lower Lias and influence of sediment supply on the Th gamma-ray log.
Figure 5.15	The three types of shale that can be distinguished in the Lower Lias of southern Britain based on spectral gamma-ray data.

APPENDIX 1
(TABLES 1.10 to 1.36)

Table 1.10	Data-set representing 20 samples taken at different locations on the Limestone known as Iron Ledge from the Blue Lias. Data collected with the B.P. GR-256 spectrometer.
Table 1.11	Data-set representing 20 samples taken at different locations on the Limestone known as Iron Ledge from the Blue Lias. Data collected with the GR-410 spectrometer.
Table 1.12	Data-set representing 20 samples taken at different locations on the dark laminated shale known as the Belemnite Bed from the Belemnite Marls. Data collected with the B.P. GR-256 spectrometer.
Table 1.13	Data-set representing 20 samples taken at different locations on the dark laminated shale known as the Belemnite Bed from the Belemnite Marls. Data collected with the GR-410 spectrometer.
Table 1.14	Comparison between data collected under conditions of high battery voltage and low battery voltage.
Table 1.15	Temperature drift within the GR-410 gamma-ray spectrometer identified during calibration.
Table 1.16	Data collected with the GR-410 from the Lower Cement Bed of the Black Ven Marls.
Table 1.17	Specifications of Transportable Calibration Pads.
Table 1.18	Program PADWIN.
Table 1.19	Calibration data for the GR-256 gamma-ray spectrometer owned by Leeds University.
Table 1.20	Calibration of the Edinburgh University GR-256 using transportable pads. Data processed and obtained using the PADWIN program for the IBM computer.
Table 1.21	Calibration of total gamma-ray flux to μr using each of the total gamma-ray sensitivity constants determined from the BGS transportable pads. Required for the GR-410.
Table 1.22	The Mann-Whitney statistical test. Procedure for calculation.
Table 1.23	Data collected on the Belemnite Bed, with the B.P. GR-256, with 5 second increments in measurement time upto a maximum of 240 seconds.
Table 1.24	Data collected on Iron Ledge, with the B.P. GR-256, with 10 second increments in measurement time upto a maximum of 360 seconds.
Table 1.25	20 repeated samples taken from a single point on the Belemnite Bed with the B.P. GR-256.
Table 1.26	20 repeated samples taken from a single point on with the B.P. GR-256.
Table 1.27	The percentage error calculated for total gamma-ray flux and radio-elemental concentration for measurements collected at the same location and different locations on the Belemnite Bed.
Table 1.28	The percentage error calculated for total gamma-ray flux and radio-elemental concentration for measurements collected at the same location and different locations on the Iron Ledge.
Table 1.29	Collection of data from identical positions within the Rhaetian succession exposed in St. Mary's Well Bay, Glamorgan. The first and second set of gamma-ray measurements were collected exactly five hours apart.
Table 1.30	Randomised total gamma-ray and radio-elemental data generated for the Belemnite Bed.
Table 1.31	Randomised total gamma-ray and radio-elemental data generated for the Iron Ledge.

- Table 1.32 Comparison between data collected using the Leeds University GR-256 with the detector placed parallel to bedding in the vertical plane and perpendicular to bedding in the horizontal plane.
- Table 1.33 The percentage error calculated for total gamma-ray flux and radio-elemental concentration due to the orientation of the detector during gamma-ray data collection.
- Table 1.34 Data collected at differing sampling intervals from St. Mary's Well Bay, Glamorgan with the Leeds University and Edinburgh University GR-256 spectrometers.
- Table 1.35 Data-set representing 20 samples taken at different locations on the dark laminated shale known as the Belemnite Bed from the Belemnite Marls. Data collected with the Leeds University GR-256 spectrometer.
- Table 1.36 Data-set representing 20 samples taken at different locations on the dark laminated shale known as the Belemnite Bed from the Belemnite Marls. Data collected with the Edinburgh University GR-256 spectrometer.

APPENDIX 2
Tables 2.01 to 2.11

- Table 2.01 Gamma-ray data-set for the Pre-*planorbis* Beds to the lowermost 90 cm of the *angulata* Zone exposed in St. Audrie's Bay, Somerset (ST 102433). The 145 sets of measurements were collected from cliff section. All readings were taken with the Leeds University GR-256 during the period 22nd August - 25th August 1995.
- Table 2.02 Gamma-ray data-set for the *angulata* Zone and *bucklandi* Zone (*conybeari* and *rotiforme* Subzones) exposed east of Kilve Pylle, Somerset (ST 144455 to ST 153452). The 154 sets of measurements were collected from cliff section apart from the stratigraphic interval represented between 51.90 m and 63.30 m, which was measured on the foreshore. All readings were taken with the Leeds University GR-256 during the period 26th August - 30th August 1995.
- Table 2.03 Gamma-ray data-set for the *bucklandi* Zone (*bucklandi* Subzone) exposed west of Kilve Pylle, Somerset (ST 139457 - ST 144455). The 80 sets of measurements were collected from cliff section. All readings were taken with the Leeds University GR-256 during the period 1st September - 3rd September 1995.
- Table 2.04 Gamma-ray data-set for the *semicostatum* Zone (*lyra* Subzone) exposed at the west end of Doniford Bay, Somerset (ST 1079433 - ST 082430). The 122 sets of measurements were collected from cliff section. All readings were taken with the Edinburgh University GR-256 during the period 19th September - 21st September 1995.
- Table 2.05 Gamma-ray data-set for the Pre-*planorbis* Beds to the *liasicus* Zone exposed in St. Mary's Well Bay, Glamorgan (ST 176677 - ST 187681). The 96 sets of measurements were collected from cliff section. All readings were taken with the Edinburgh University GR-256 during the period 23rd September - 27th September 1995.
- Table 2.06 Gamma-ray data-set for the *angulata* Zone and *bucklandi* Zone (*conybeari* Subzone) exposed at Nash Point, South Glamorgan (SS 914684). The 100 sets of measurements were collected from cliff section. All readings were taken with the Leeds University GR-256 during the period 7th September - 10th September 1995.
- Table 2.07 Gamma-ray data-set for the White Lias and Blue Lias Formations that outcrop between Pinhay Bay, Devon and Seven Rock Point, Lyme Regis, Dorset (SY 318908 - SY 328910). A total number of 109 sets of measurements were collected. All readings were taken with the B.P. GR-256. The White Lias (Langport Member) was measured during the period 10th February - 12th February 1992. The remaining sets of measurements were collected during the period February 15th - March 4th 1993.

- Table 2.08 Gamma-ray data-set for the Shales-with-'Beef' that outcrop between Seven Rock Point, Lyme Regis and Stonebarrow, Charmouth (SY 328910 - SY 364390). A total number of 109 sets of measurements were collected. All readings were taken with the B.P. GR-256. The *sciponianum* Subzone was measured during the period 20th March - March 23rd 1993. The remaining sets of measurements were collected during the period April 24th - April 27th 1993 (41.70 m to 61.20 m) and 19th May - 24th May 1993 (61.50 m to 70.80 m).
- Table 2.09 Gamma-ray data-set for the Black Ven Marls that outcrop beneath Stonebarrow, Charmouth (SY 368930 - SY 380927). The 114 sets of measurements were collected from cliff section. All readings were taken with the B.P. GR-256 spectrometer. The stratigraphy represented between 71.20 m and 82.30 m was logged during the period 15th October - 20th October 1993. The remainder of the formation was gamma-ray logged during the period 6th February - 16th February 1993.
- Table 2.10 Gamma-ray data-set for the Belemnite Marls that outcrop between Stonebarrow and Seatown, Dorset (SY 380927 - SY 415918). Beds 103-110 were measured from the cliff exposure east of Westhay Water (SY 386925 - SY 391924). Measurements for beds 116-121 were obtained from the exposure between Golden Cap and Seatown (SY 410918 - SY 416917). A total number of 89 sets of measurements were collected in all. All readings were taken with the B.P. GR-256 during the period 20th October - 27th October 1993.
- Table 2.11 Gamma-ray data-set for the *luridum* Subzone of the *ibex* Zone that is exposed in Blockley Pit, Gloucestershire (SP 182369). The gamma-ray logs were measured from a series of fresh sections in the pit. The measurements taken between 0 m and 4.2 m were obtained from a section exposed at the north end of the pit, measurements taken between 4.2 m and 9.3 m were obtained from a section exposed at the south east end of the pit and the remainder of measurements were obtained from a section at the south-south west end of the pit. The 36 sets of measurements were collected with the Edinburgh University GR-256 on the 10th October 1995.
- Note Artificial radioactive contamination as a possible, additional source of error (with Figure 6.01).

Chapter 1
(Figures 1.01 to 1.18)

**Introduction to the Depositional Basins of Southern
Britain and the Techniques and Theory of
Gamma-Ray Spectrometry.**

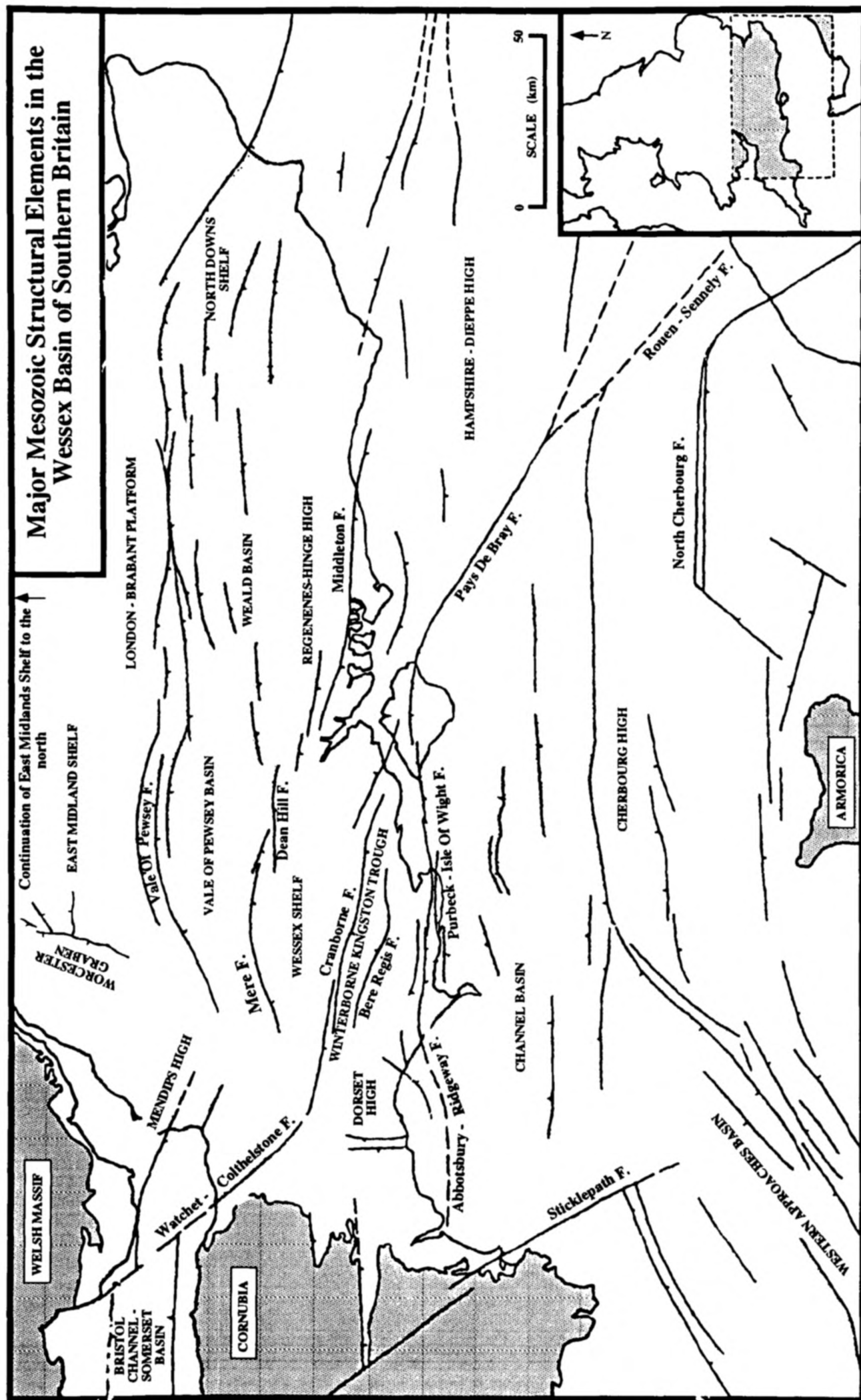


FIGURE 1.01 Simplified regional tectonic map of the major Mesozoic structures in the Wessex Basin. The stippled area represents outcropping basement of pre-Permian age. The diagram is based upon Stoneley (1982), Whittaker (1985) and Karner *et al.* (1987). British Geological Survey sheet maps have also been used in this compilation.

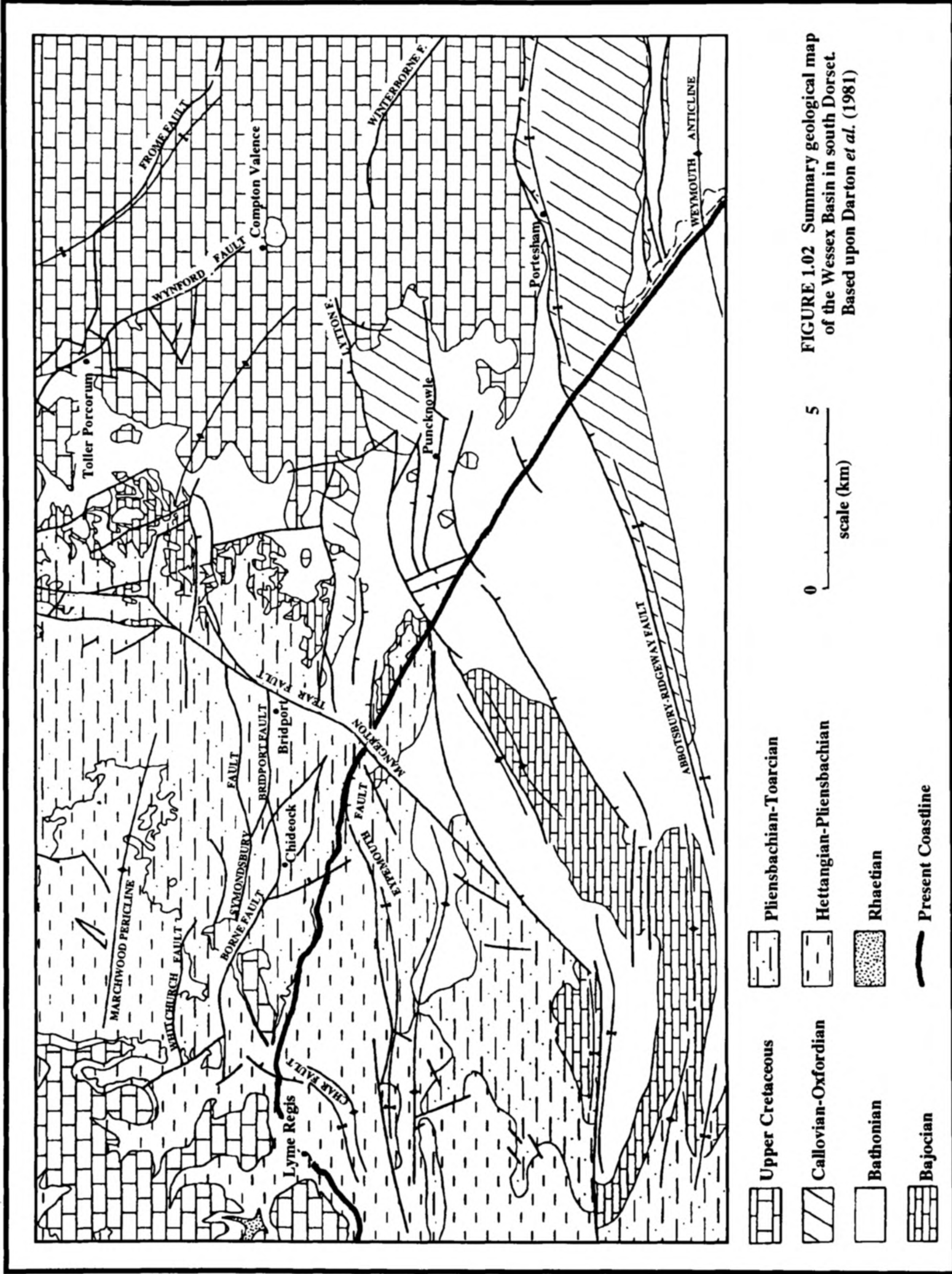


FIGURE 1.02 Summary geological map of the Wessex Basin in south Dorset. Based upon Darton *et al.* (1981)

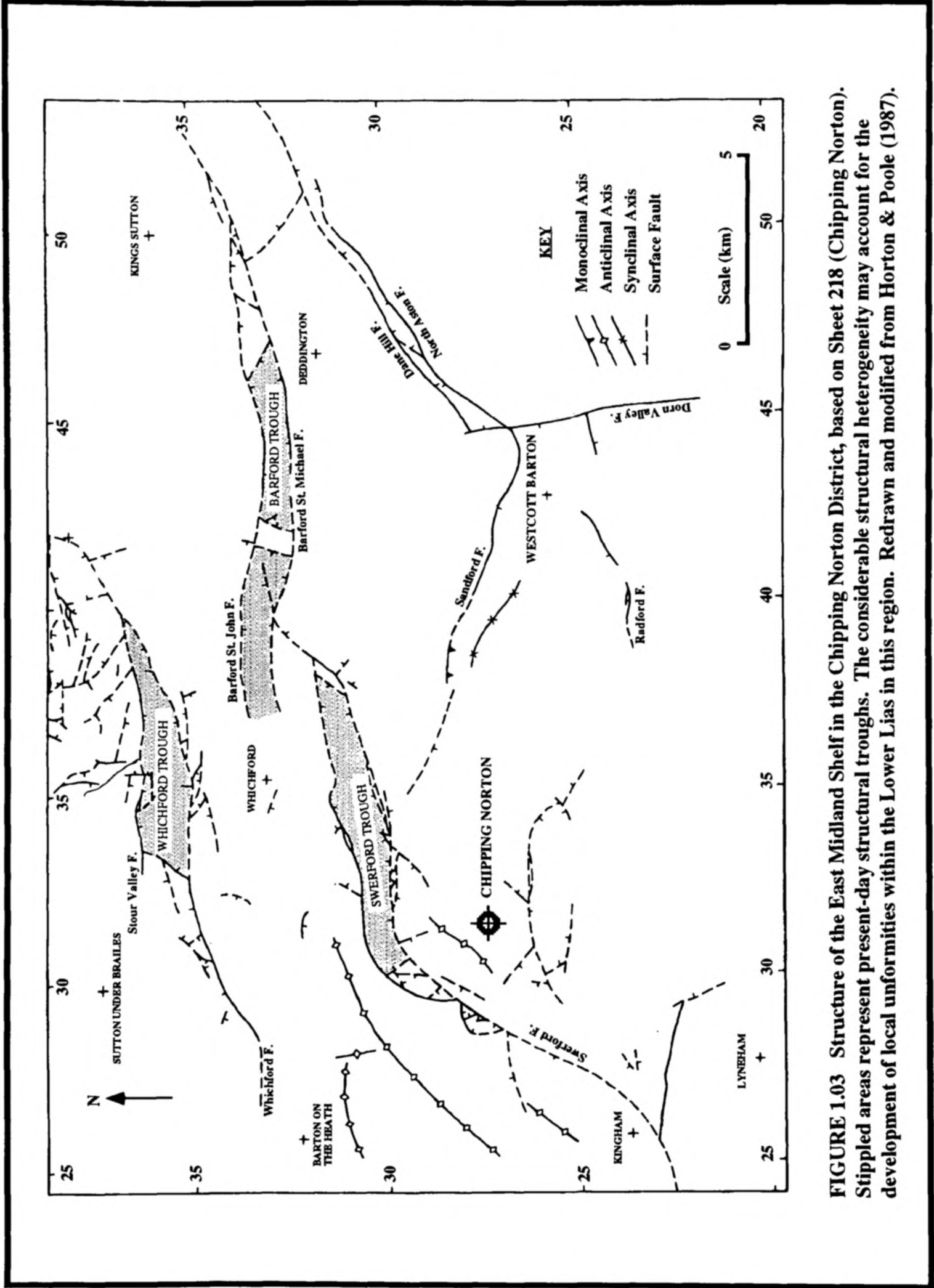


FIGURE 1.03 Structure of the East Midland Shelf in the Chipping Norton District, based on Sheet 218 (Chipping Norton). Stippled areas represent present-day structural troughs. The considerable structural heterogeneity may account for the development of local uniformities within the Lower Lias in this region. Redrawn and modified from Horton & Poole (1987).

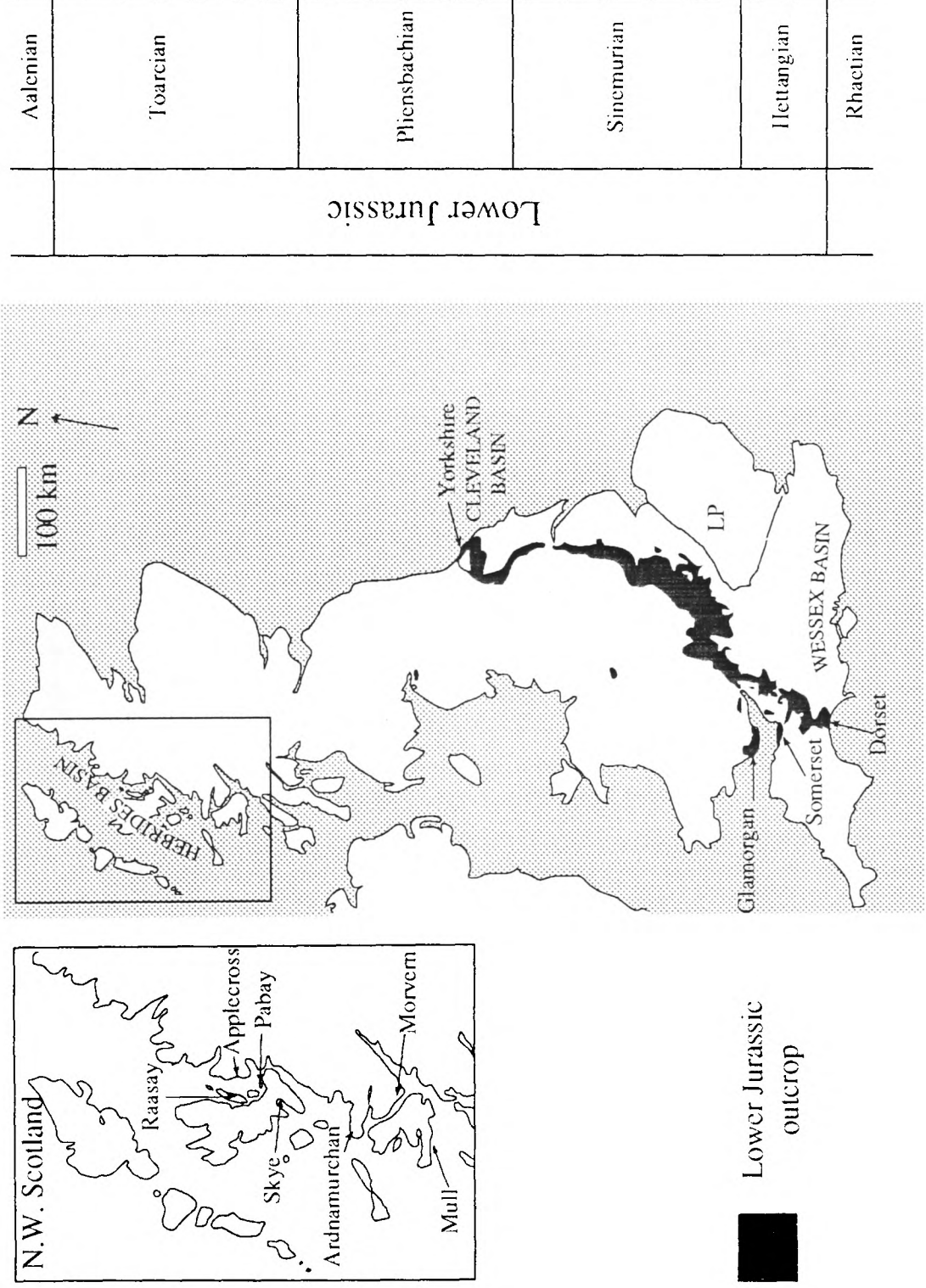


FIGURE 1.04 Outcrop pattern for the Lower Jurassic of the British Isles. This study is concerned with outcrop of Rhaetian to Pliensbachian age found in southern Britain, namely Glamorgan, Somerset and Dorset (LP = London Platform). Taken from Hesselbo & Jenkyns (1995).

Biostratigraphy		Lithostratigraphy	Chronostratigraphy		
Zone	Subzone				
<i>Tragophllyo- ceras ibex</i>	<i>Beaniceras luridum</i>	Belemnite Stone	Lower Pliensbachian		
	<i>Acanthopleuroceras valdani</i>				
	<i>Tropidoceras masseanum</i>				
<i>Uptonia jamesoni</i>	<i>Uptonia jamesoni</i>	Belemnite Marls			
	<i>Platyleuroceras brevispina</i>				
	<i>Polymorphites polymorphus</i>				
	<i>Phricodoceras taylori</i>				
<i>Echioceras raricostatum</i>	<i>Paltechioceras aplanatum</i>	Hummocky			
	<i>Leptechioceras macdonnelli</i>				
	<i>Echioceras raricostatoides</i>	Black Ven Marls			
	<i>Cruciloboceras densinodulum</i>				
<i>Oxynoticeras oxynotum</i>	<i>Oxynoticeras oxynotum</i>	Coinstone			Upper Sinemurian
	<i>Oxynoticeras simpsoni</i>				
<i>Asteroceras obtusum</i>	<i>Eparietites denotatus</i>	Black Ven Marls			
	<i>Asteroceras stellare</i>				
	<i>Asteroceras obtusum</i>				
<i>Caenisites turneri</i>	<i>Microderoceras birchi</i>	Shales-with-'Beef'	Lower Jurassic or Lias		
	<i>Caenisites brooki</i>				
<i>Arnioceras semicostatum</i>	<i>Euagassicerias resupinatum</i>	Shales-with-'Beef'			
	<i>Agassicerias scipionianum</i>				
	<i>Coroniceras lyra</i>				
<i>Arietites bucklandi</i>	<i>Arietites bucklandi</i>	Blue Lias		Lower Sinemurian	
	<i>Coroniceras rotiforme</i>				
	<i>Vermiceras bucklandi</i>				
<i>Schlotheimia angulata</i>	not differentiated	Blue Lias		Hettangian	
<i>Alsatites liasicus</i>	<i>Alsatites laqueus</i>				
	<i>Waehneroceras portlocki</i>				
<i>Psiloceras planorbis</i>	<i>Caloceras johnstoni</i>	Blue Lias			
	<i>Psiloceras planorbis</i>				
Pre-planorbis Beds			Rhaetian	Triassic	

Figure 1.05 Stratigraphic scheme for the Rhaetian - Pliensbachian interval as represented by the sediments of the Dorset coast, based upon Cope *et al.* (1980). The boundary between the Blue Lias and Shales-with-'Beef' is taken from Hallam (1960). The extent of the disconformity/hiatus associated with the Coinstone and Hummocky are indicated.

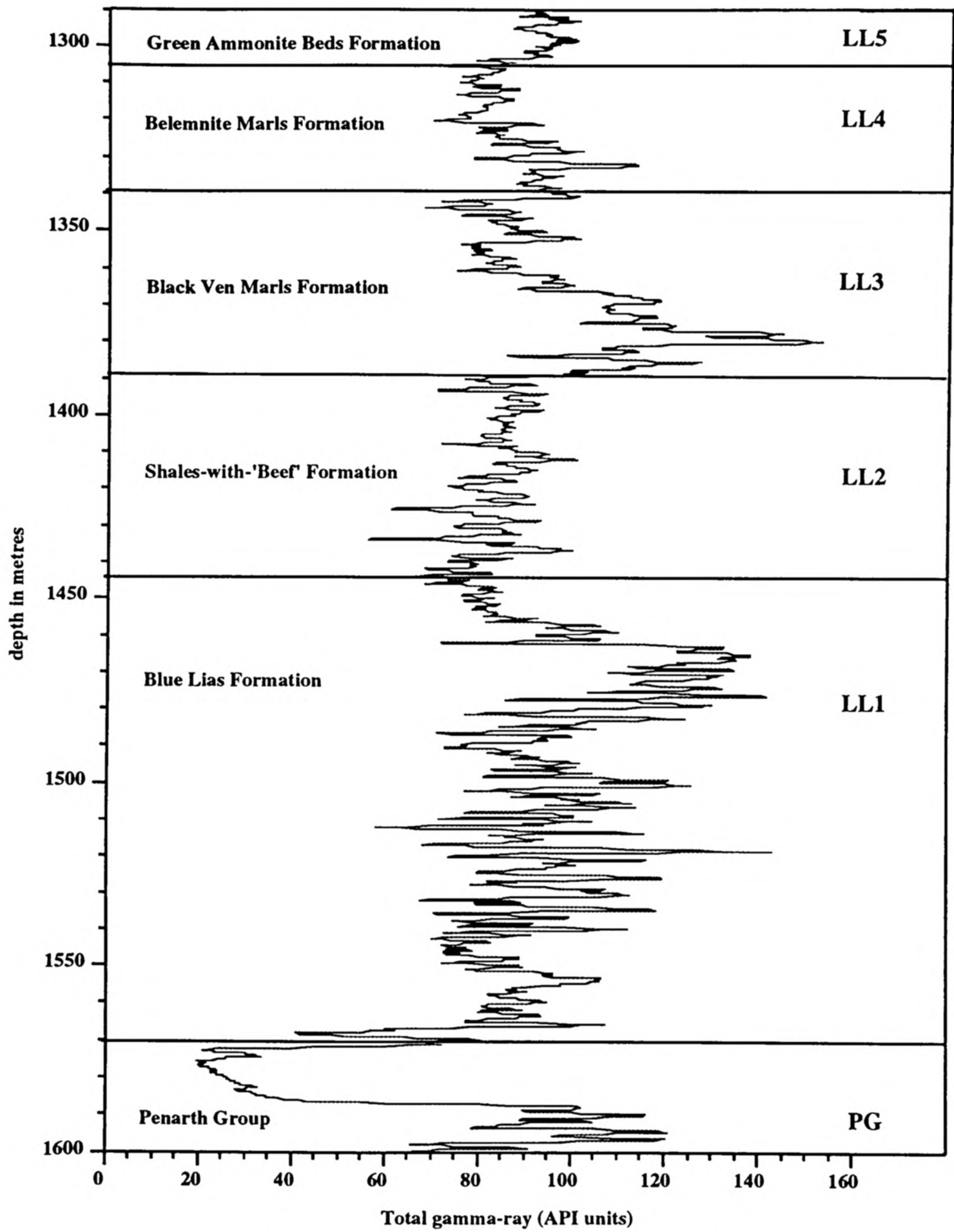


FIGURE 1.06 Division of the Lower Lias interval in the Winterborne Kingston borehole into lithological gamma-ray units as proposed by Whittaker *et al.* (1985). Redrawn from Whittaker *et al.* (1985)

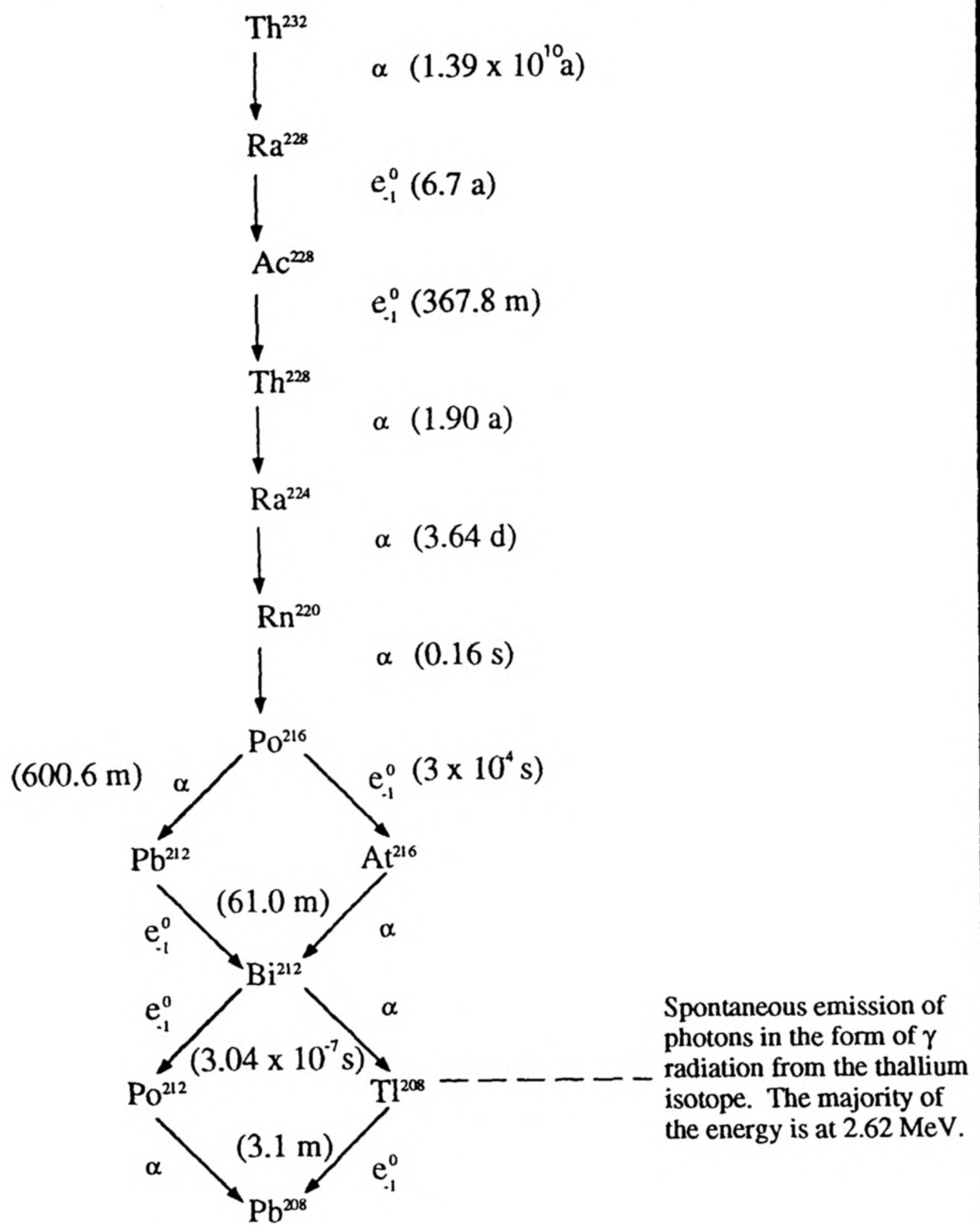
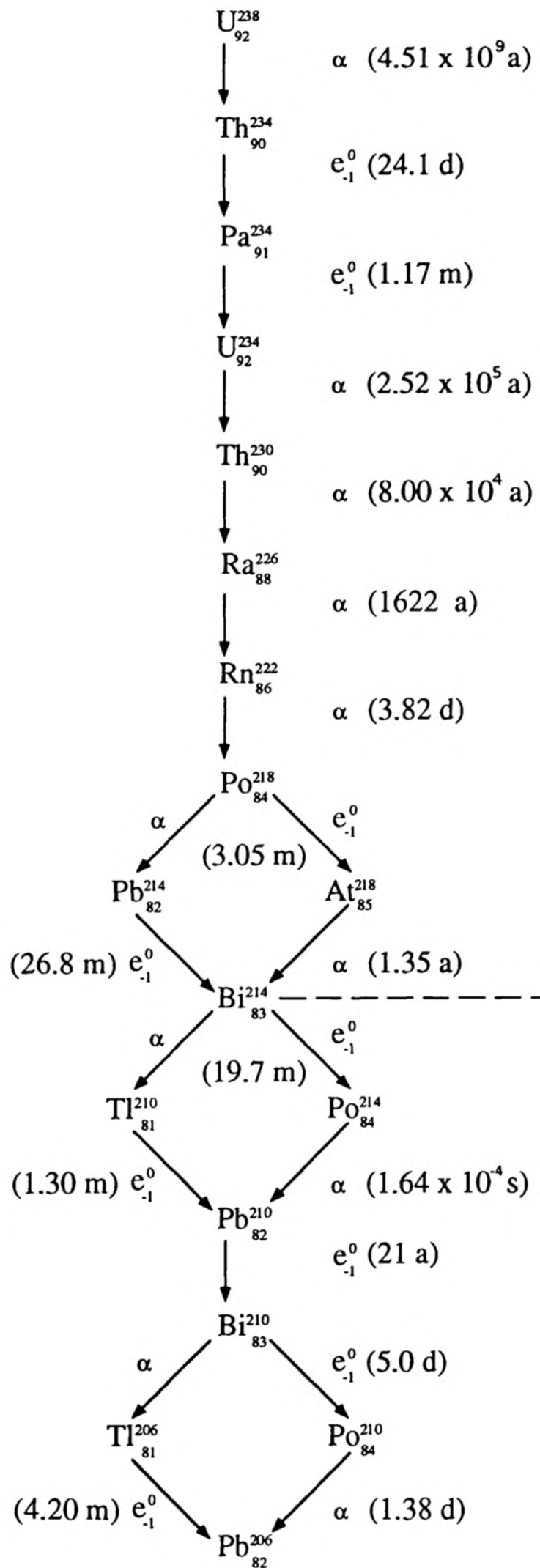


FIGURE 1.07 Thorium decay series of naturally occurring radiogenic isotopes. The thorium series corresponds to the simple formulae $4n$ and terminates with a stable isotope of lead. (Based upon Rankama 1954)



The α and β radiation is followed by spontaneous emission of photons in the form of γ radiation from the bismuth isotope. The majority of the energy is at 1.46 MeV.

FIGURE 1.08 Uranium decay series of naturally occurring radiogenic isotopes. The uranium series corresponds to the simple formulae $4n + 2$ and terminates with a stable isotope of lead. (From Murray 1987)

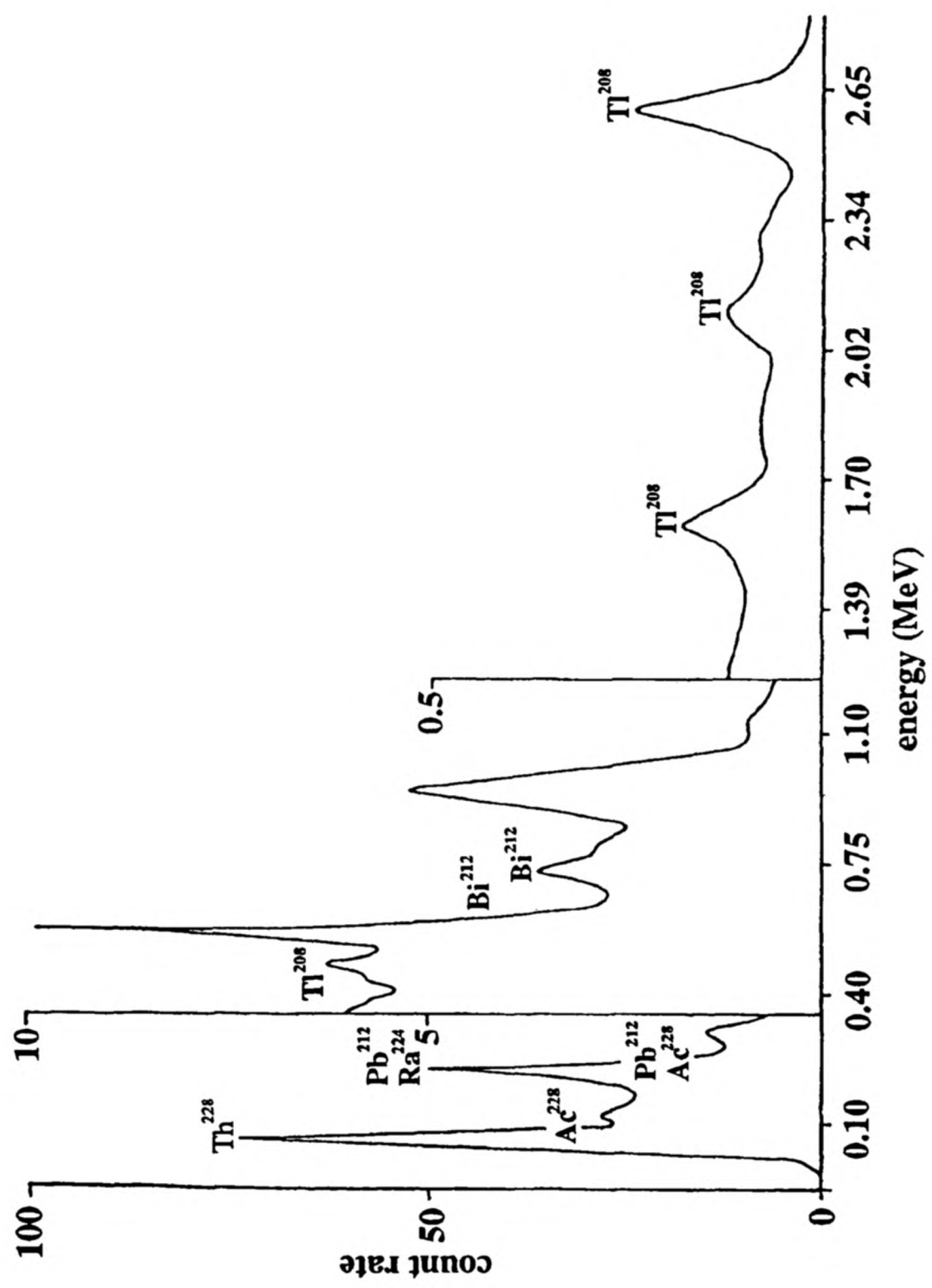


FIGURE 1.09 Gamma-ray spectrum of the Th^{232} decay series (Redrawn from Durrance 1986)

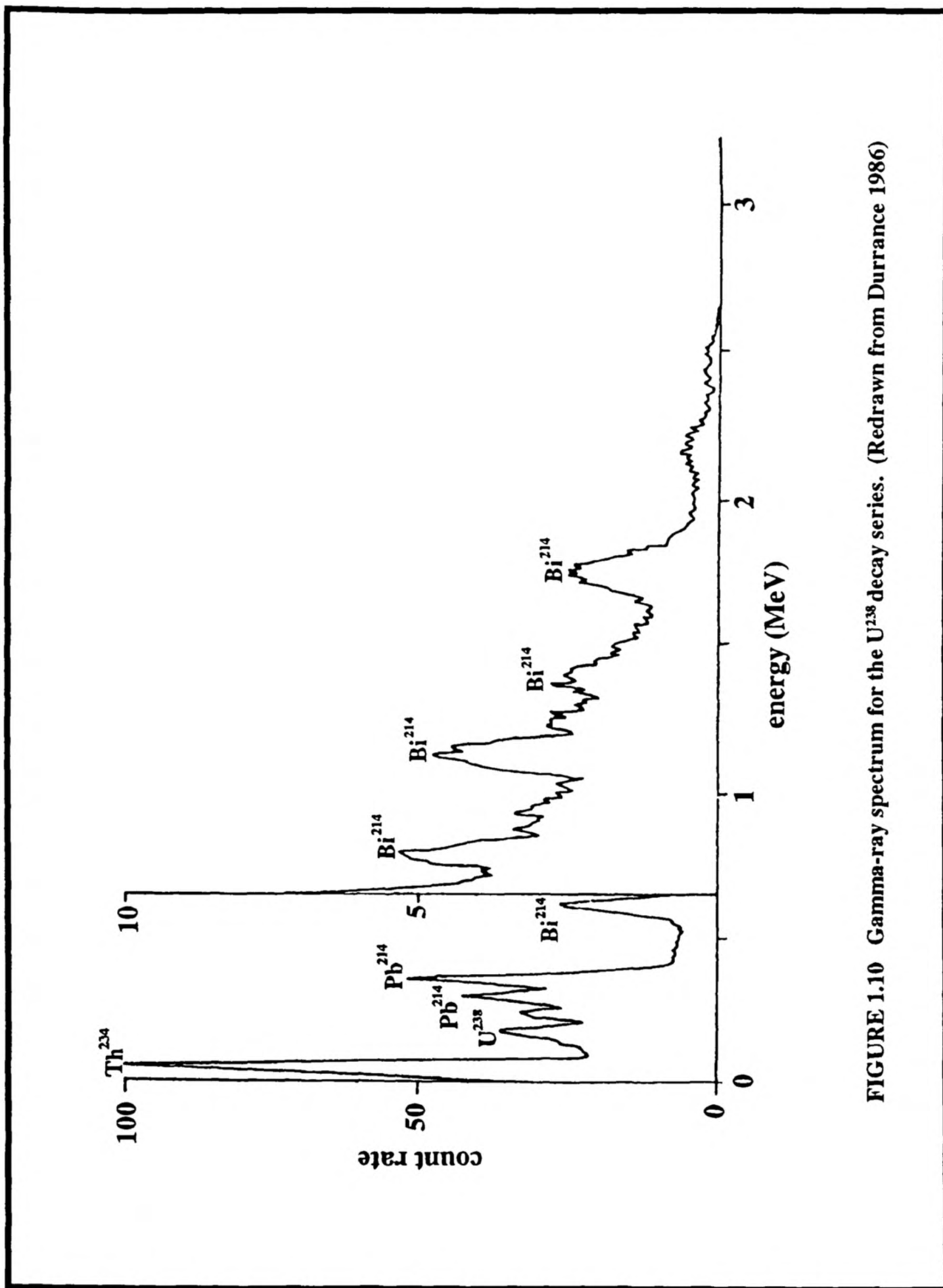


FIGURE 1.10 Gamma-ray spectrum for the U^{238} decay series. (Redrawn from Durrance 1986)

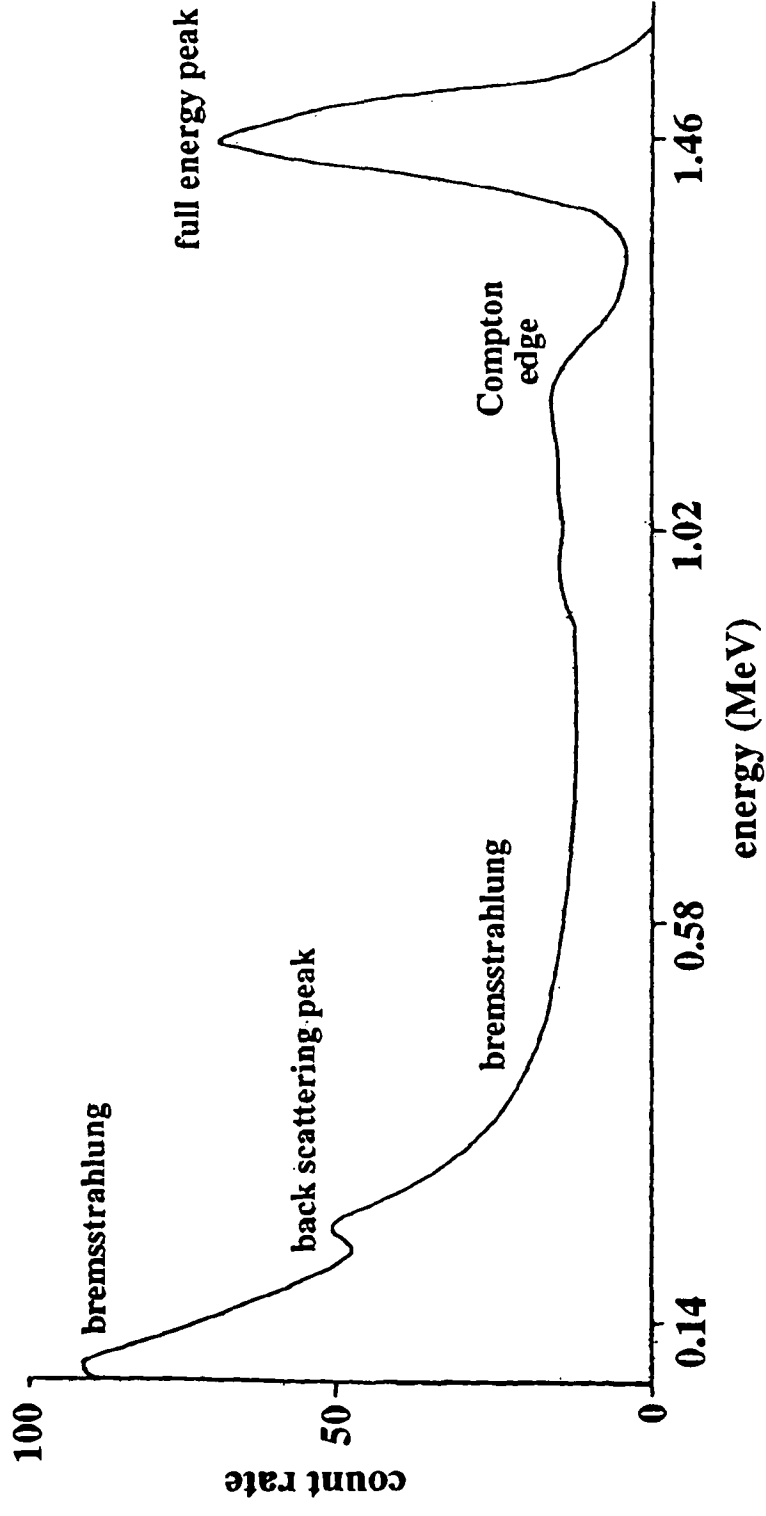


Figure 1.11 Gamma-ray spectrum for the isotope ^{40}K (Redrawn from Durrance 1986).

Bremsstrahlung is known as 'braking radiation' and is a consequence of the interaction between orbital electrons with gamma-rays as photons are emitted from the nucleus. This electrostatic attraction produces an acceleration upon the photon and causes deflection of the gamma-rays from the original pathway resulting in an overall loss of energy.

The Compton Edge marks the boundary at which the gamma radiation received by the detector is lower than would theoretically be expected (full energy peak). The loss of energy is due to Compton scattering (as explained in Chapter One, Section 1.31.)

Back-scattering refers to photons that have been deflected back along their incident pathways through Compton processes.

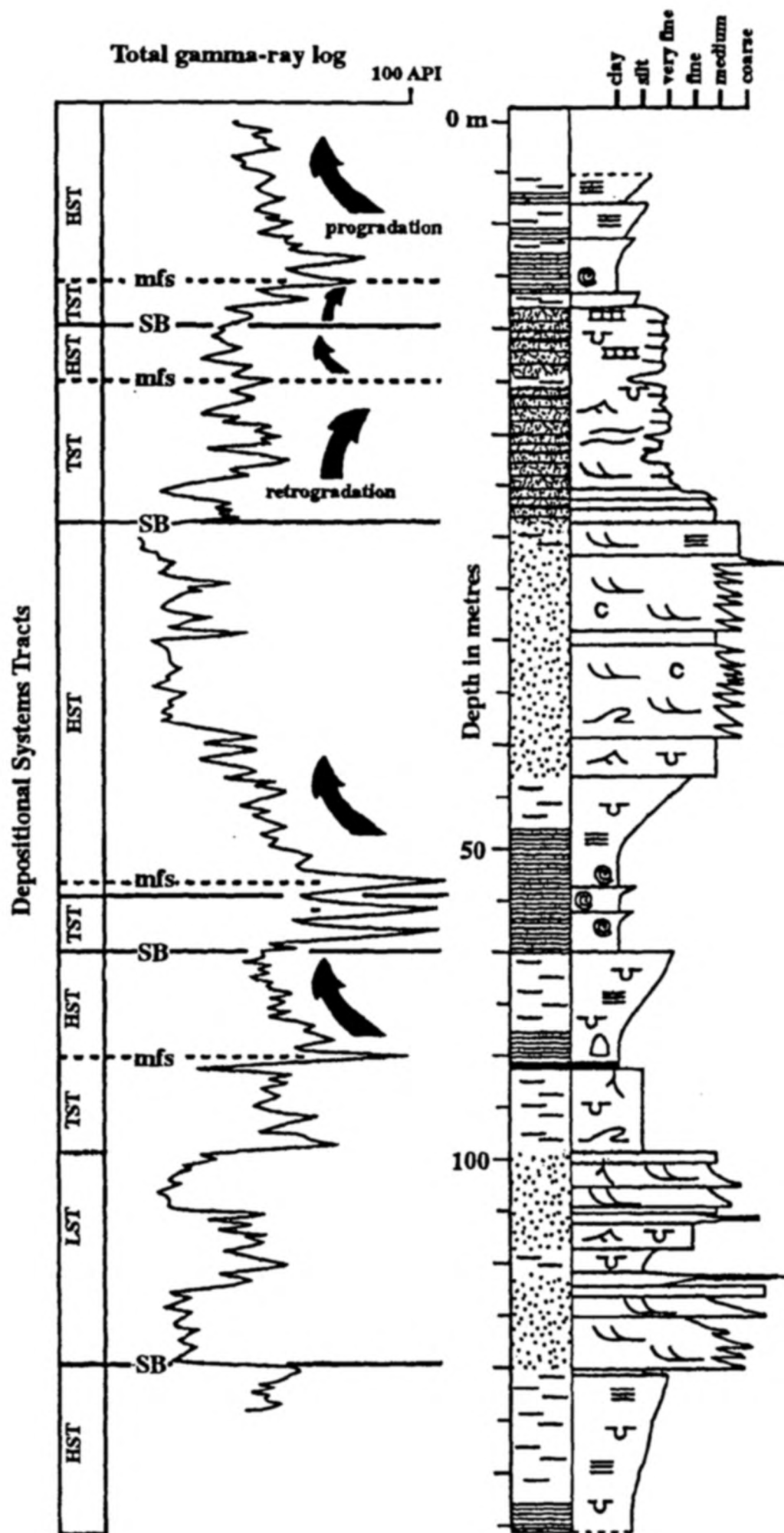


FIGURE 1.12 Depositional sequence stratigraphic interpretation of a total gamma-ray log for a coarse-grained siliciclastic system. The associated lithological log is also given. The interpreted maximum-flooding surface is denoted mfs and the interpreted sequence boundary SB. Interpreted Vail *et al.* (1977) depositional systems tracts are also given. (Based upon Gawthorpe *et al.* 1994)

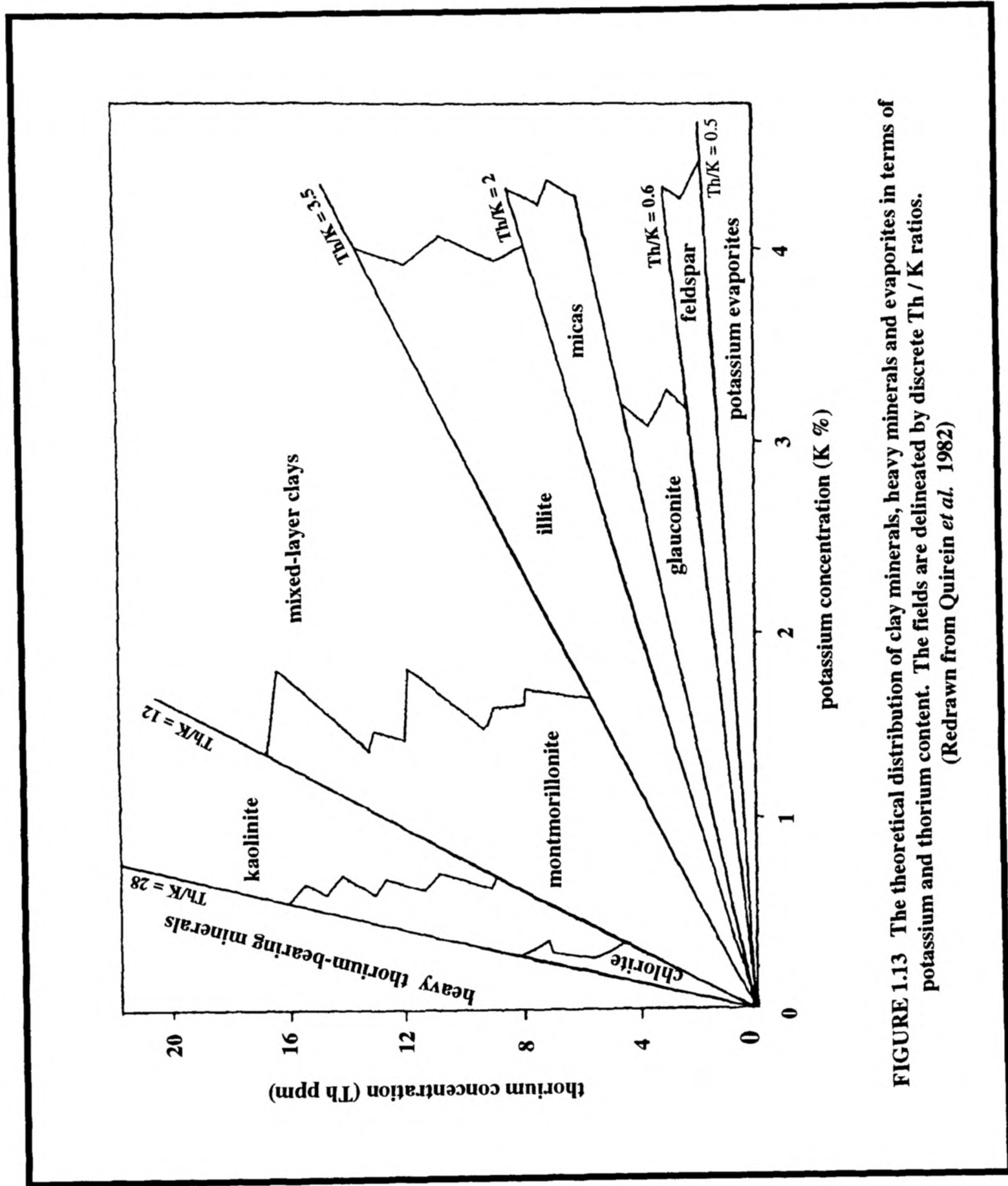


FIGURE 1.13 The theoretical distribution of clay minerals, heavy minerals and evaporites in terms of potassium and thorium content. The fields are delineated by discrete Th / K ratios.
(Redrawn from Quirein *et al.* 1982)

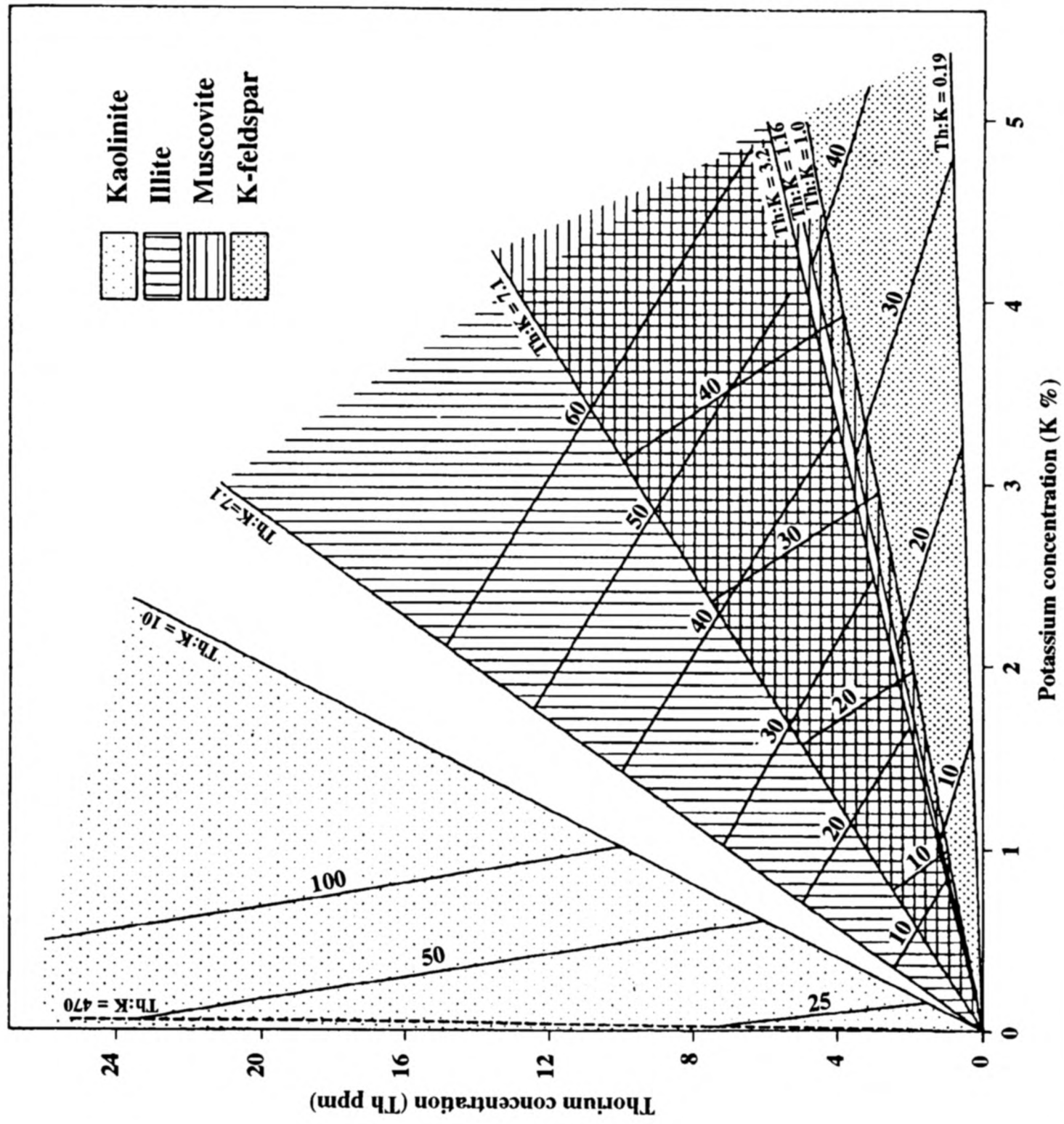


FIGURE 1.14

Thorium - potassium cross-plot given in Hurst (1990). There are considerable areas of overlap between the K-rich minerals and the broader kaolinite field. Kaolinite normally has a negligible K-content. (Redrawn from Hurst (1990))

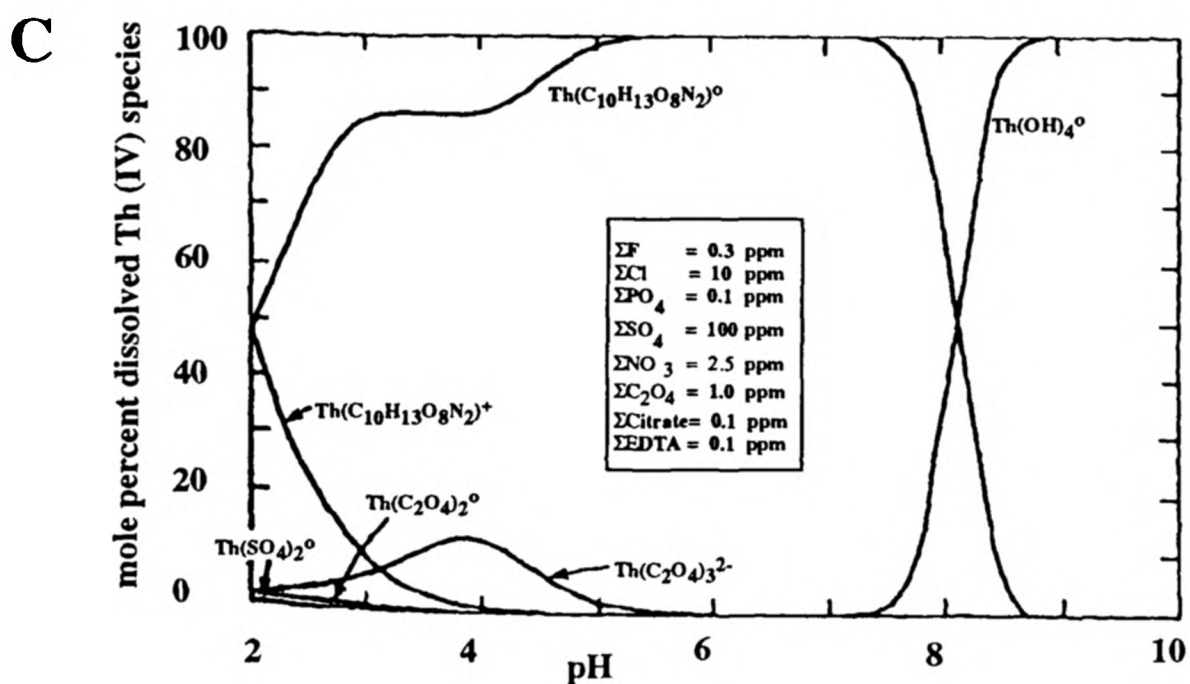
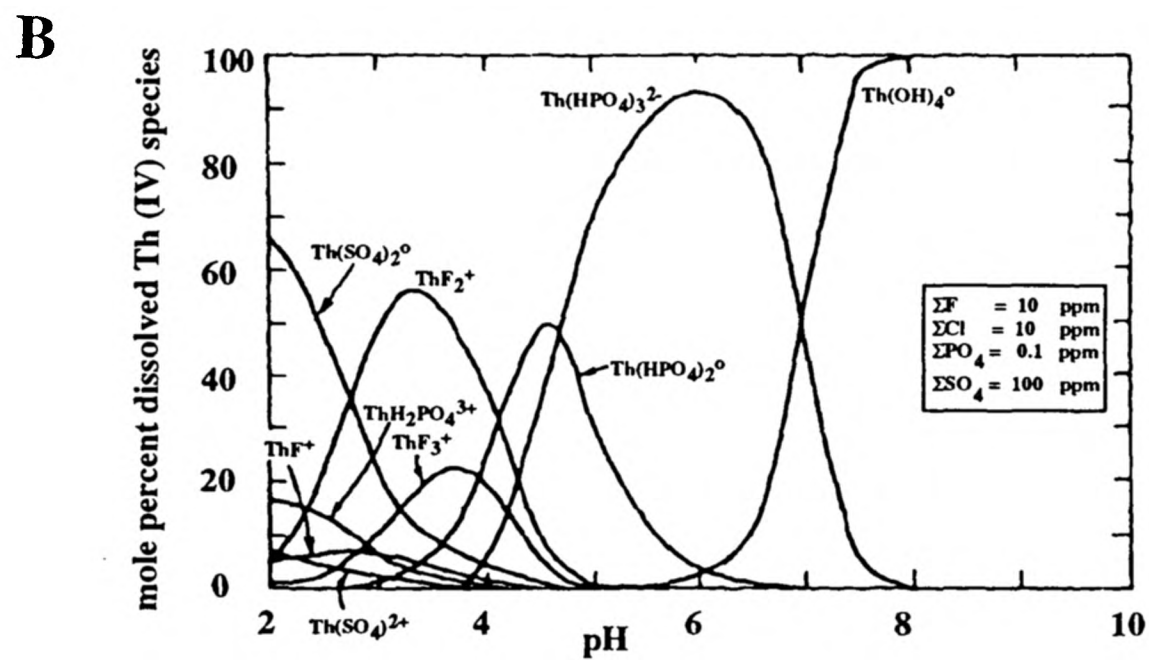
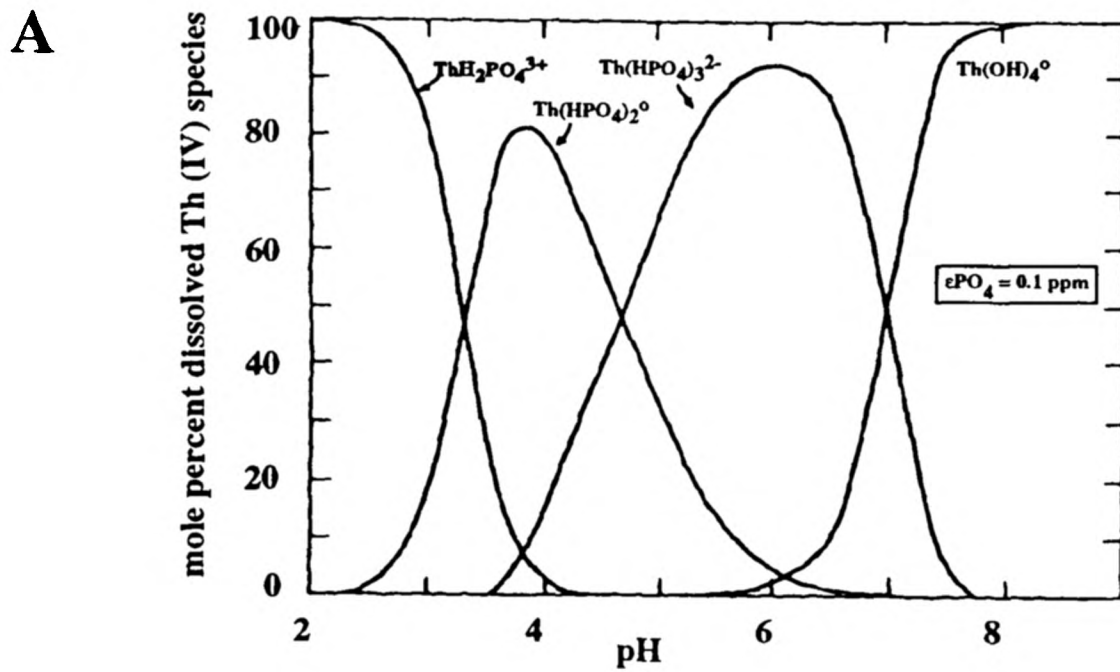


FIGURE 1.15 Distribution of (A) thorium-hydroxy and phosphate complexes (B) thorium-ligand complexes and (C) thorium complexes vs. pH in a solution containing inorganic and organic species at the concentrations indicated and 25°C with $\Sigma\text{Th} = 0.001\text{ppb}$.

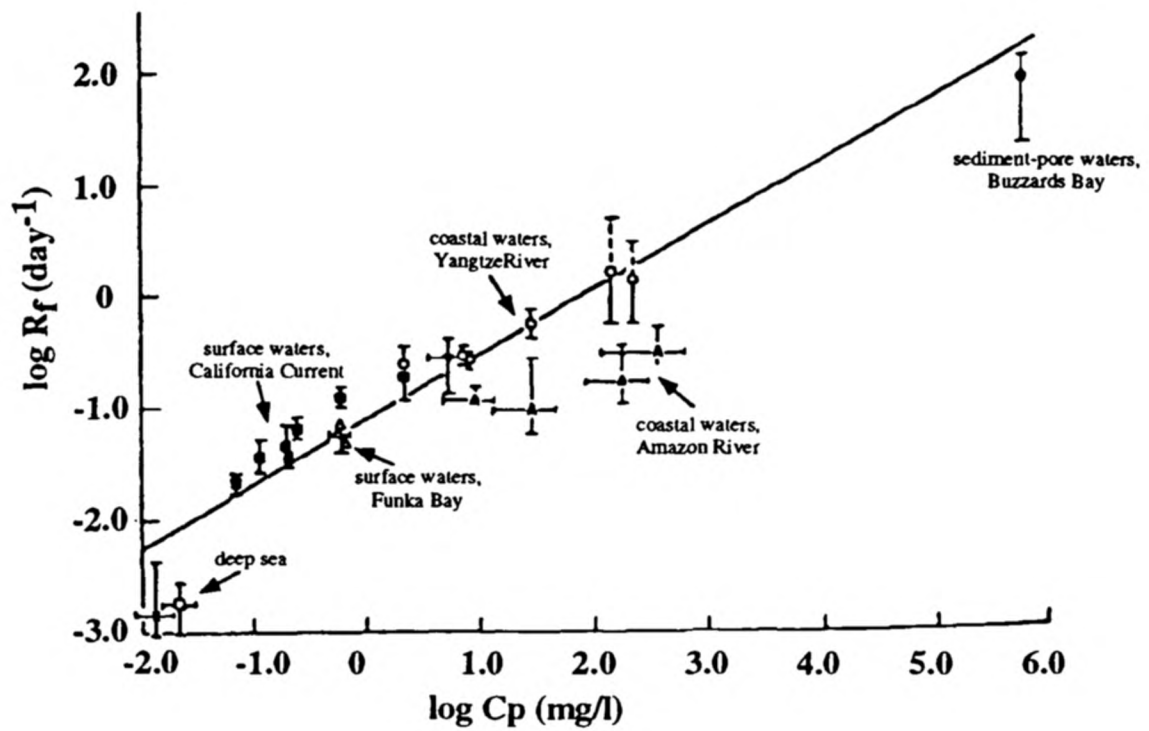


FIGURE 1.16 A plot of the forward sorption (adsorption) rate constant (R_f) for Th versus particle concentration using data from various oceanic regions. The oceanic regions cover a wide variety of particle concentrations, particle type and primary productivity intensities. The full line represents the linear regression (excluding the Amazon data). Redrawn from Honeyman *et al.* 1988

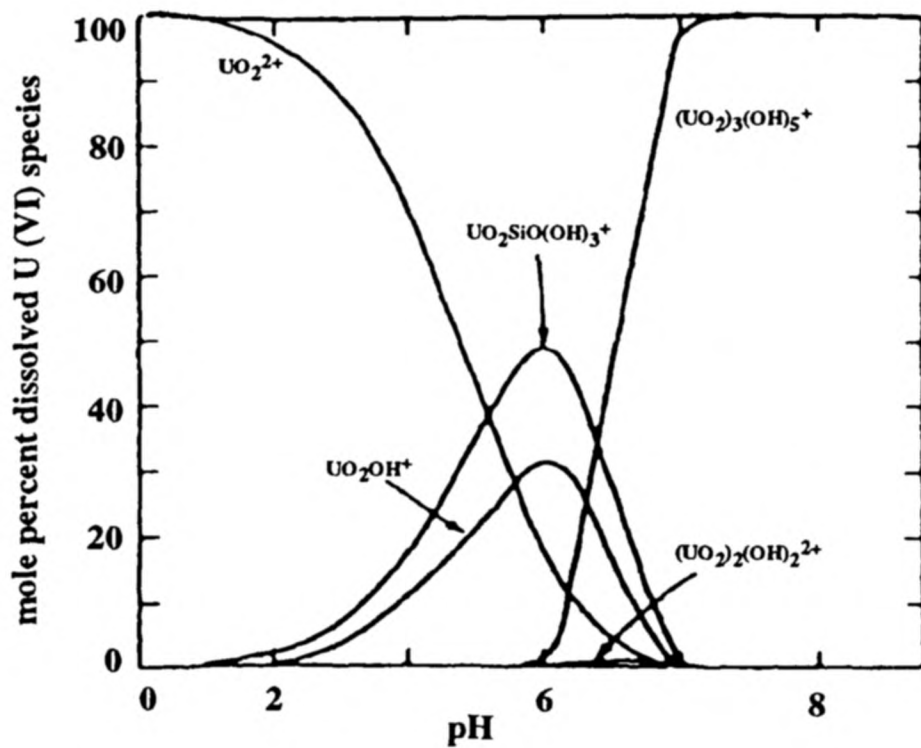


FIGURE 1.17 Distribution of uranyl-hydroxy and silicate complexes vs. pH at 25 °C with $\Sigma U = 10^{-8}$ M and $\Sigma SiO_2 = 1 \cdot 10^{-3}$ M (60 ppm). Redrawn from Langmuir (1978).

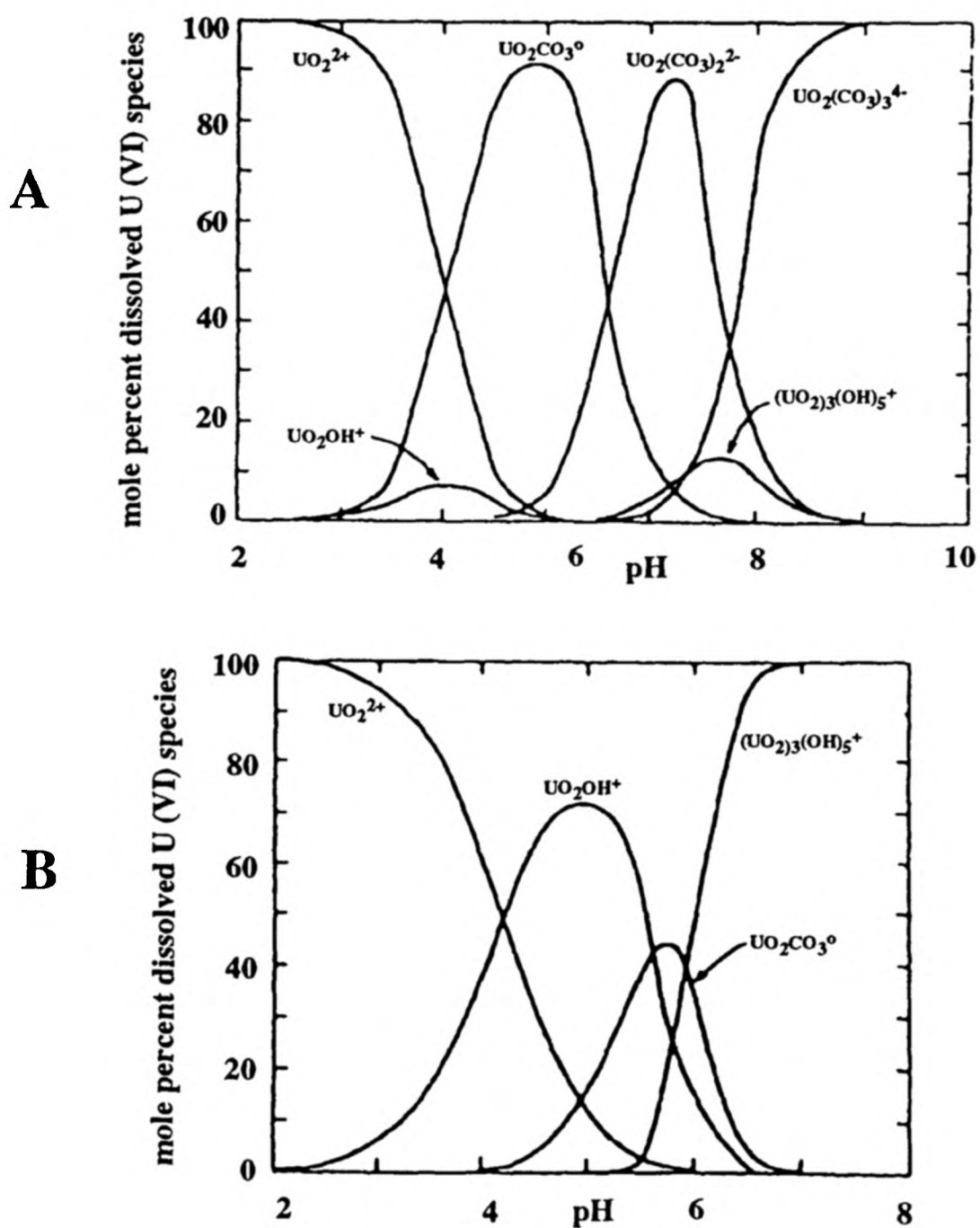


FIGURE 1.18 Distribution of uranyl-hydroxy and carbonate complexes vs. pH at with $\Sigma U = 10^{-8}$ M and $P_{CO_2} = 10^{-2}$ atm at 25 °C (A) and 100 °C (B). Redrawn from Langmuir (1978).

Chapter 2
(Figures 2.01 to 2.20)

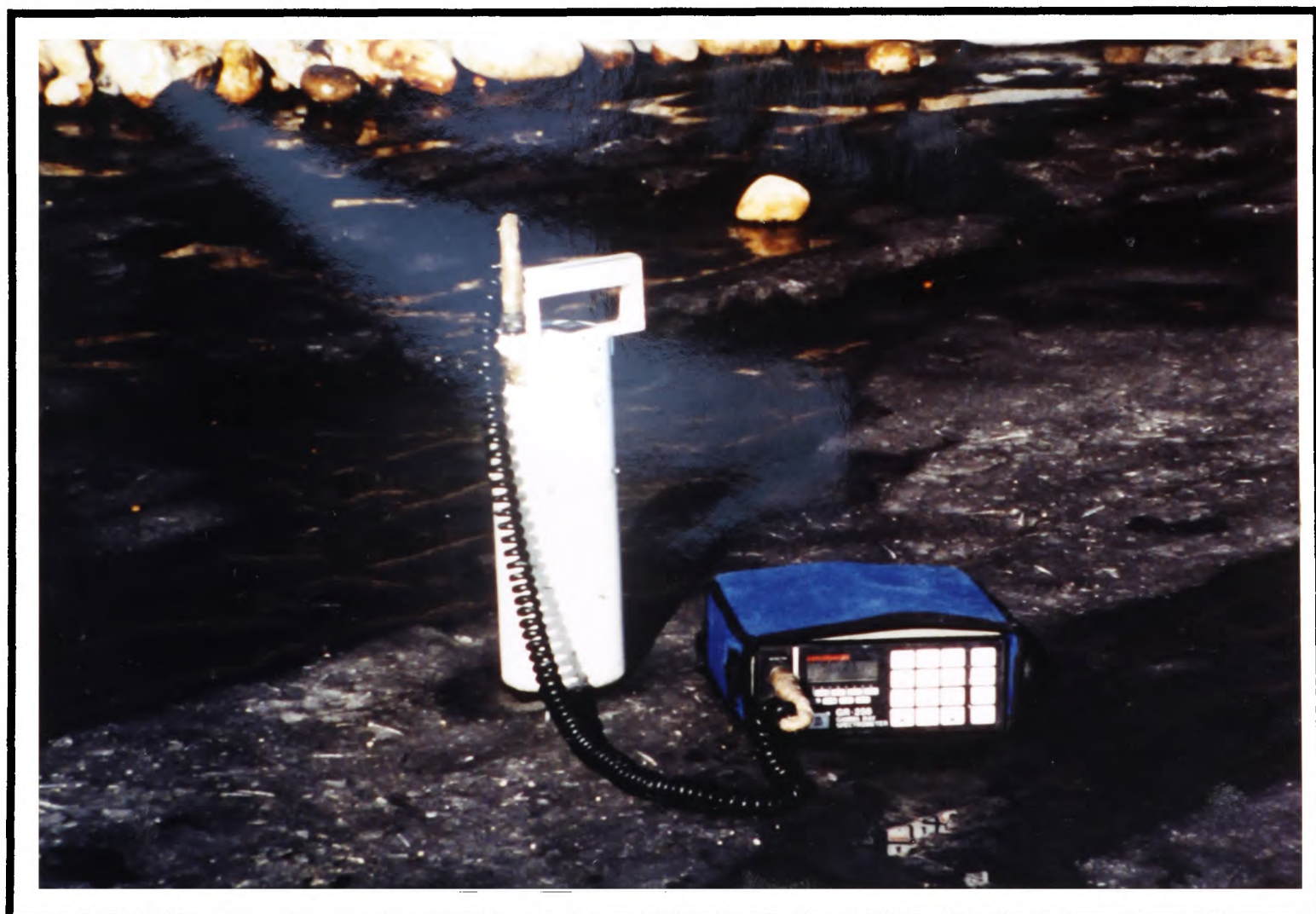
**Methodology and Experimentation Required For
Outcrop Gamma-Ray Spectrometry**



FIGURE 2.01 The GRS-500 portable gamma-ray spectrometer. The machine is ideal for general reconnaissance work involving the detection of local concentrations of radionuclides at outcrop or the rapid location of finite sources (*e.g.* uraninite). However, the maximum sample time is 10 seconds and the machine therefore has limited applicability to studies involving the detection of low radionuclide concentrations.



FIGURE 2.02 The GR-410 gamma-ray spectrometer (above) and the GR-256 gamma-ray spectrometer (below). Both models can be accurately calibrated. The GR-410 records total counts attributed to K, U and Th whilst the GR-256 automatically converts the data to radionuclide ground concentration (*e.g.* K %, U ppm and Th ppm).



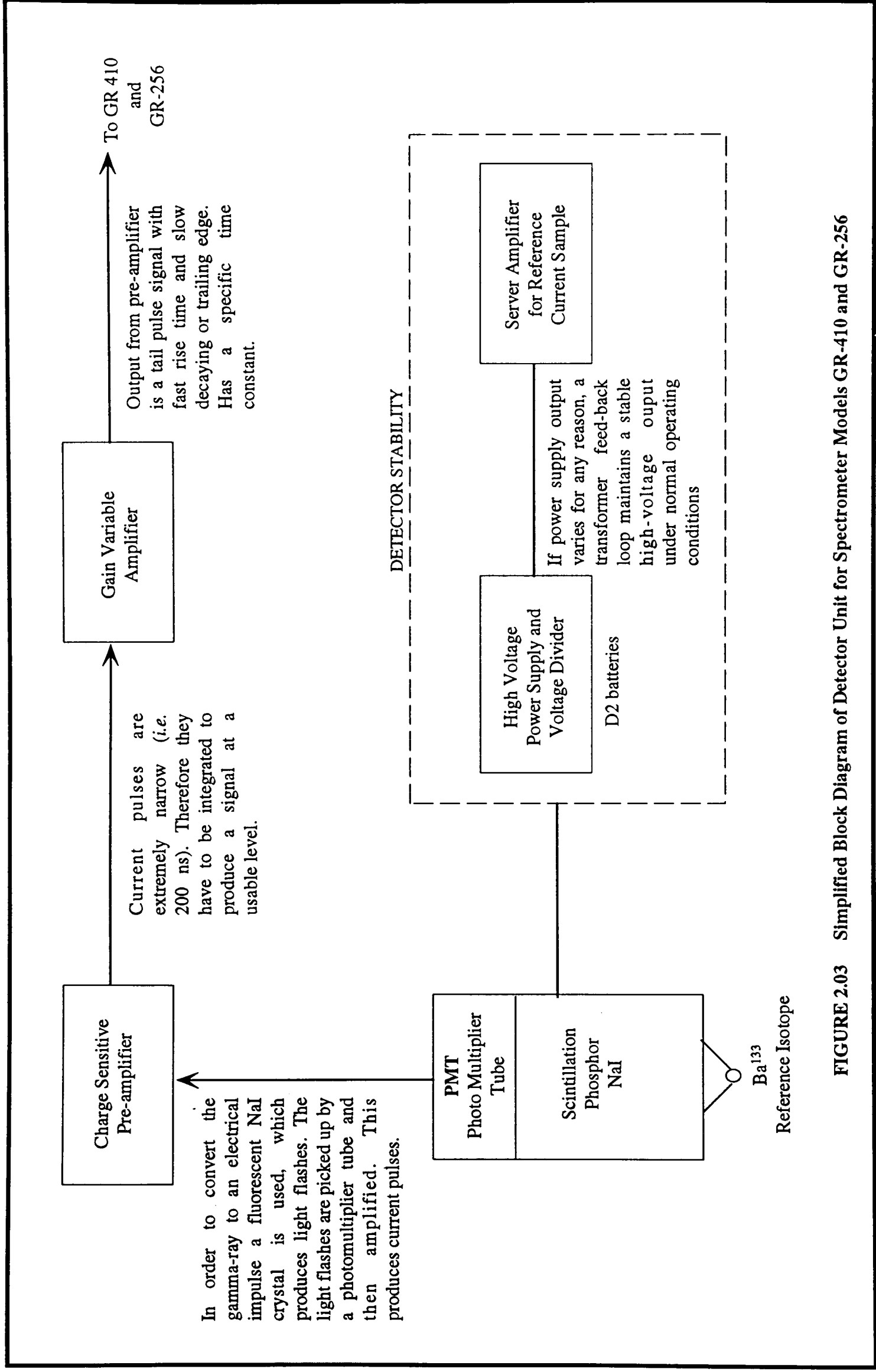
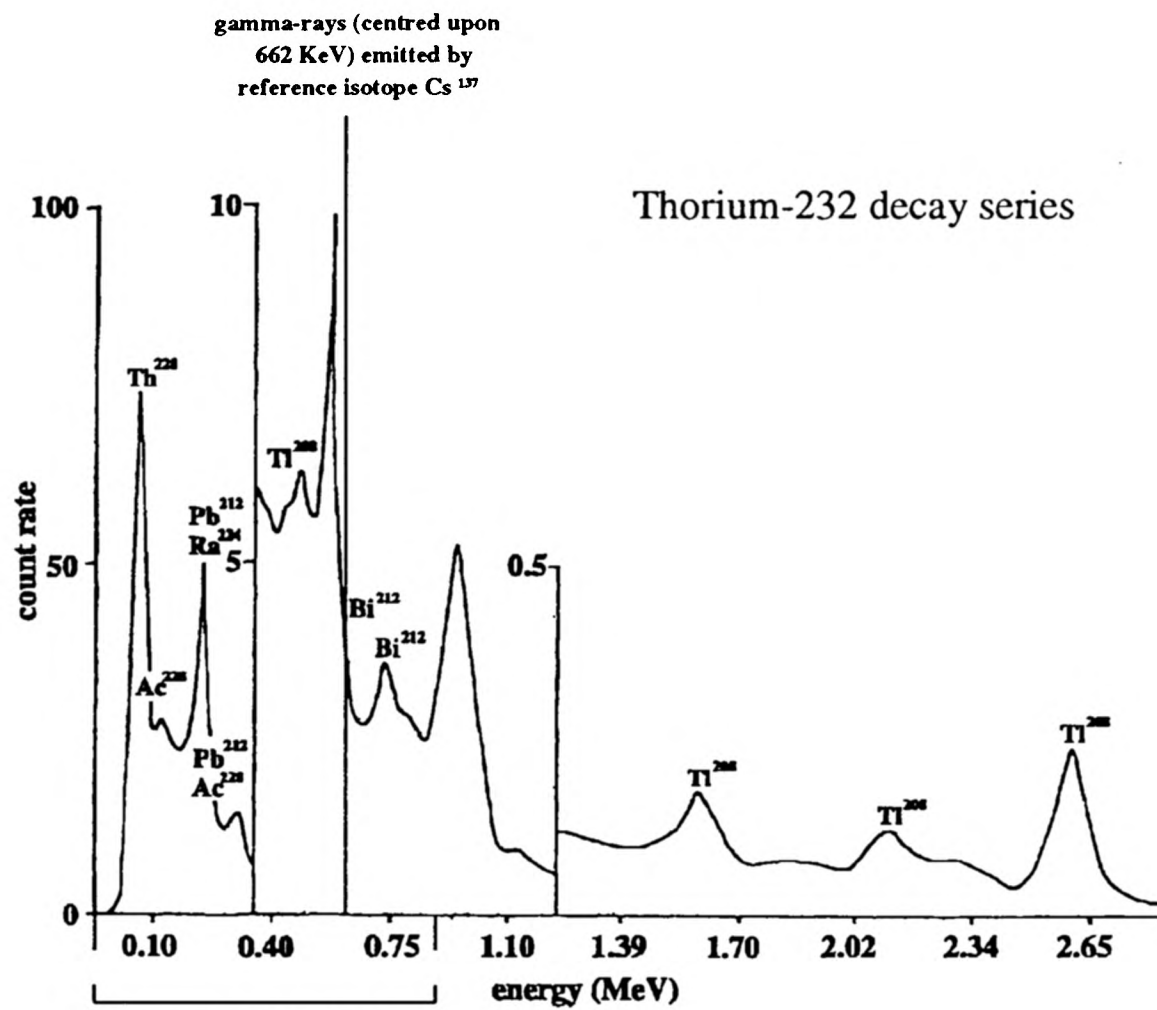
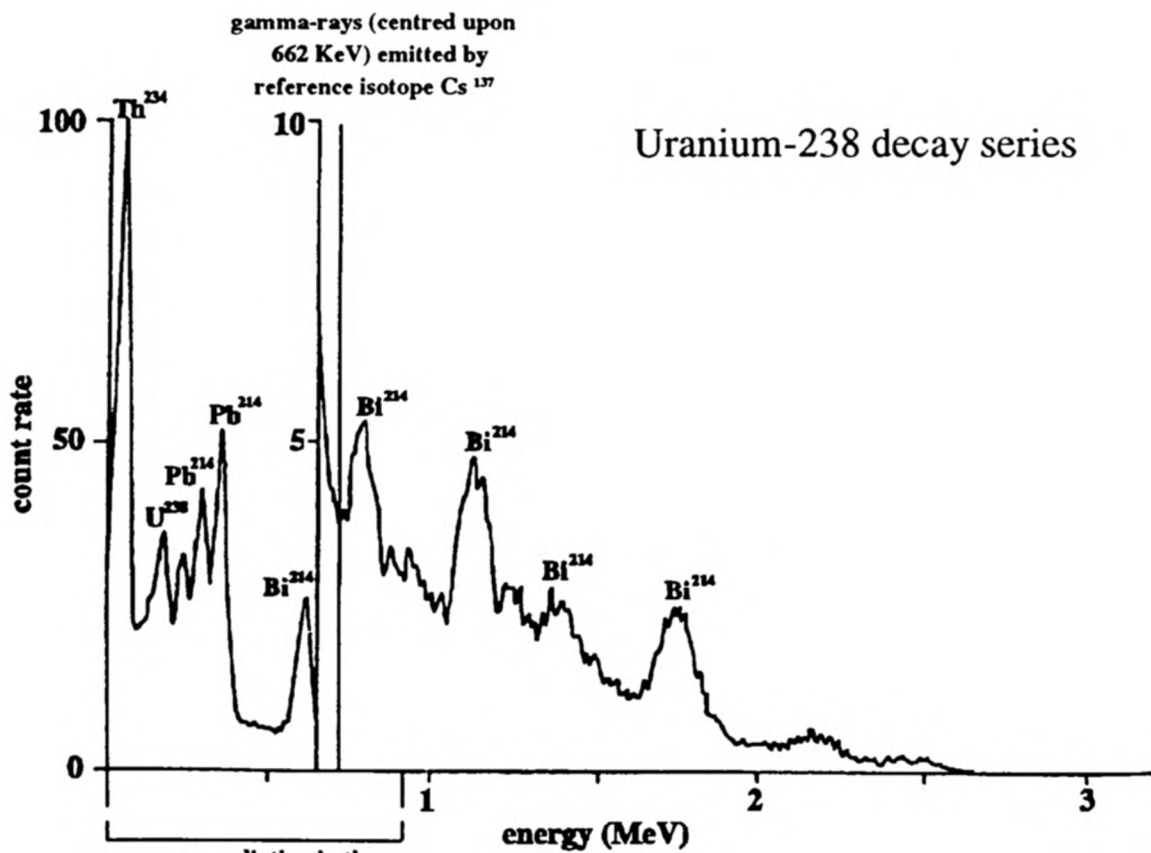


FIGURE 2.03 Simplified Block Diagram of Detector Unit for Spectrometer Models GR-410 and GR-256



gamma-radiation in the
approximate range 800 KeV
and below cannot be measured
due to interference by low-
energy gamma radiation
emitted by the reference isotope



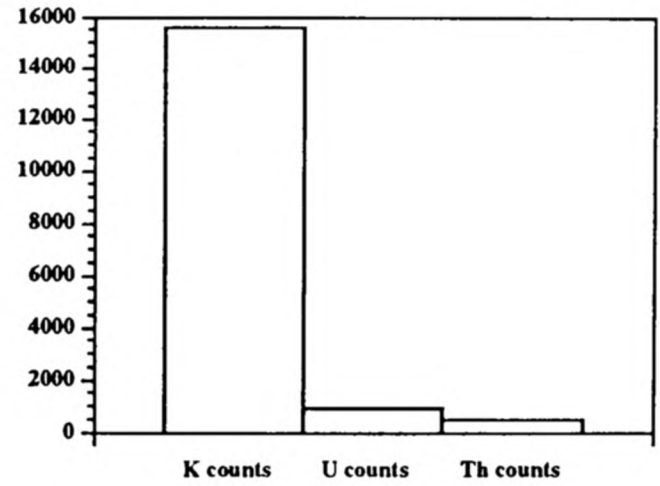
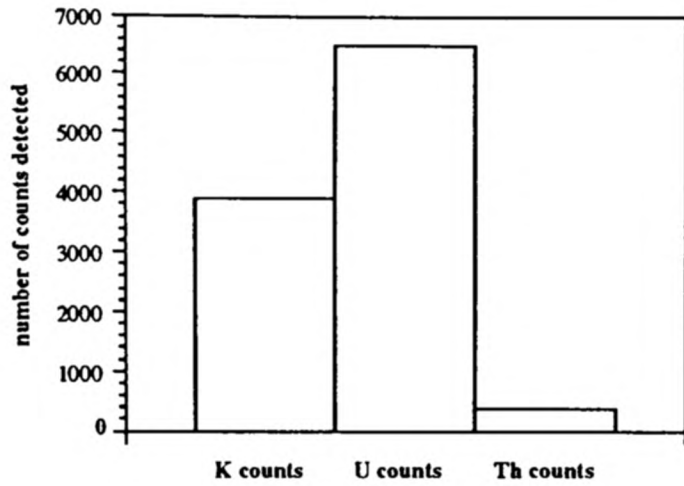
gamma-radiation in the
approximate range 800 KeV
and below cannot be
measured due to
interference by low-energy
gamma radiation emitted by
the reference isotope

FIGURE 2.04 Interference effects with the lower-energy part of the gamma-radiation spectrum from the Caesium reference isotope incorporated into the GR-256 detector system. Gamma radiation in the energy 800 KeV and below cannot be reliably resolved.

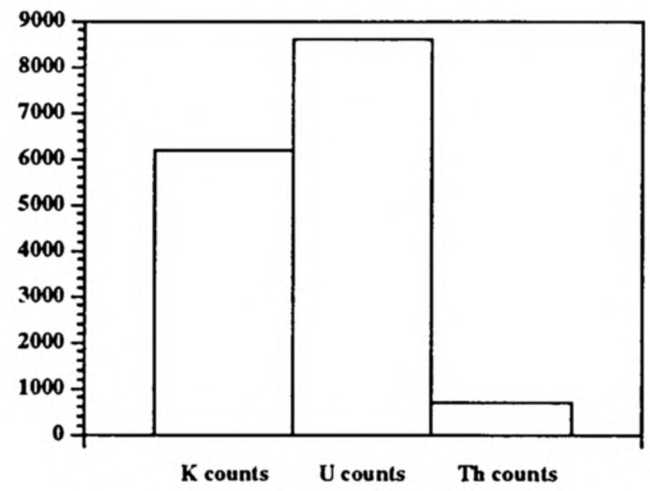
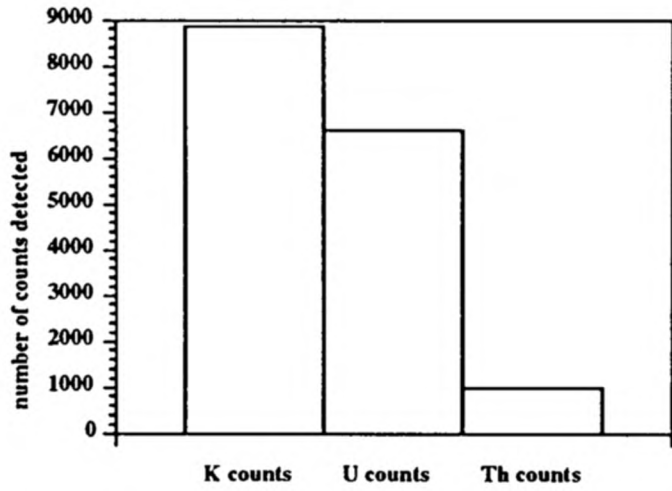
Temperature Drift

Correct Results

(A) K3-88 Pad (High K concentration, low U and Th concentration)



(B) K8-89 Pad (High U concentration, low K and Th concentration)



(C) T3-88 Pad (High Th concentration, low K and U concentration)

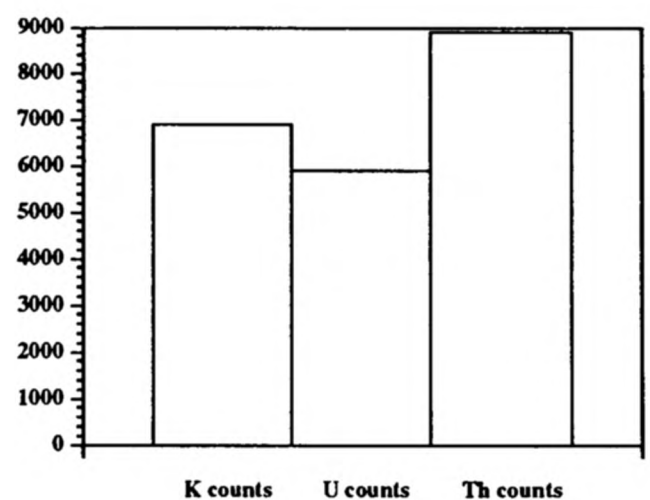
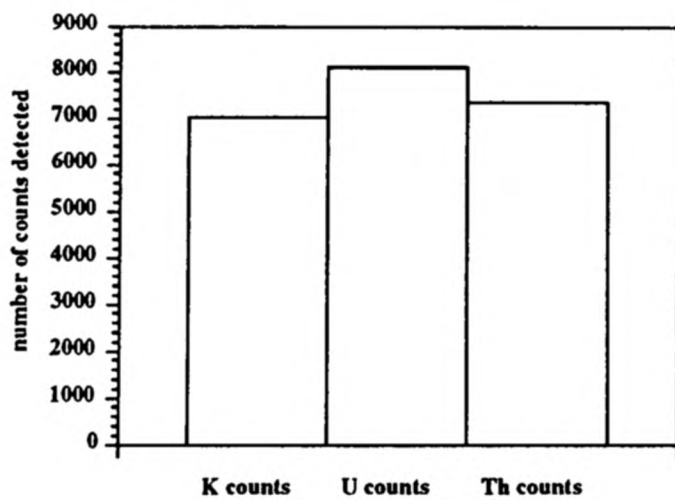


FIGURE 2.05 Calibration results with temperature drift are compared to calibration results collected when the GR-410 gamma-ray spectrometer was stable. The results were collected over a ten minute time interval on the BGS calibration pads. During temperature drift on the K pad, the number of counts received by the K window are lower than the number received by the U window. Similarly on the U pad the number of counts received by the K window are larger than the number of counts received by the U window. These results would not be expected considering the K and U concentrations of the K3-88 and U8-89 pad.

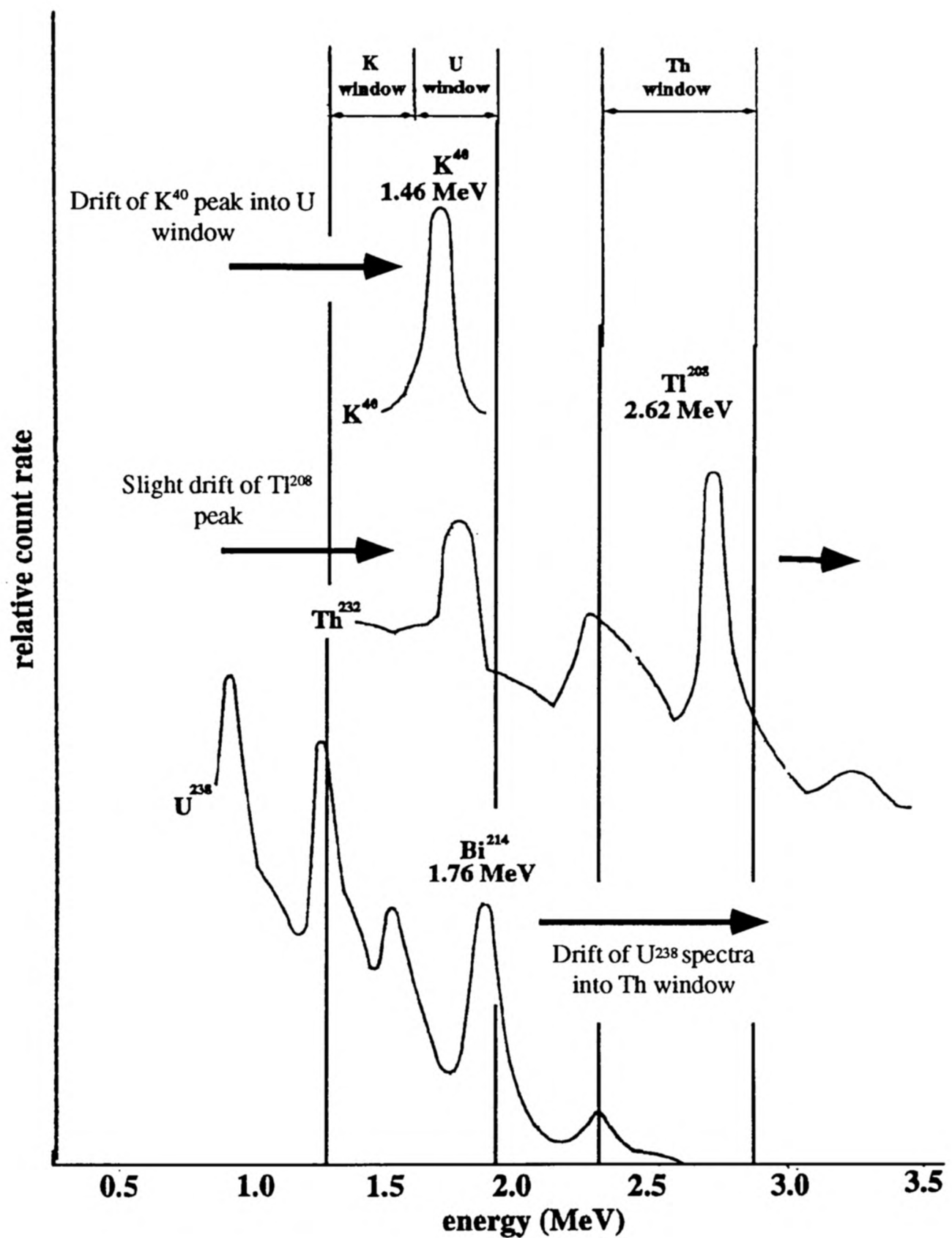


FIGURE 2.06 Temperature drift. Temperature drift is an important source of unpredictable error within the gamma-ray data-set collected with the GR-410 spectrometer. The under-sensitivity towards K shown by the machine used in this investigation can be explained by drift of the K^{40} gamma-ray spectrum into the U window. This would deplete the number of counts detected in the K window but increase the number of counts received in the U window and so elevate the calculated U concentration. The slight over sensitivity towards Th can be explained movement of the higher portion of the U gamma-ray spectrum into the Th window. This is not accounted for by stripping factors and hence the calculated Th concentration would be elevated.

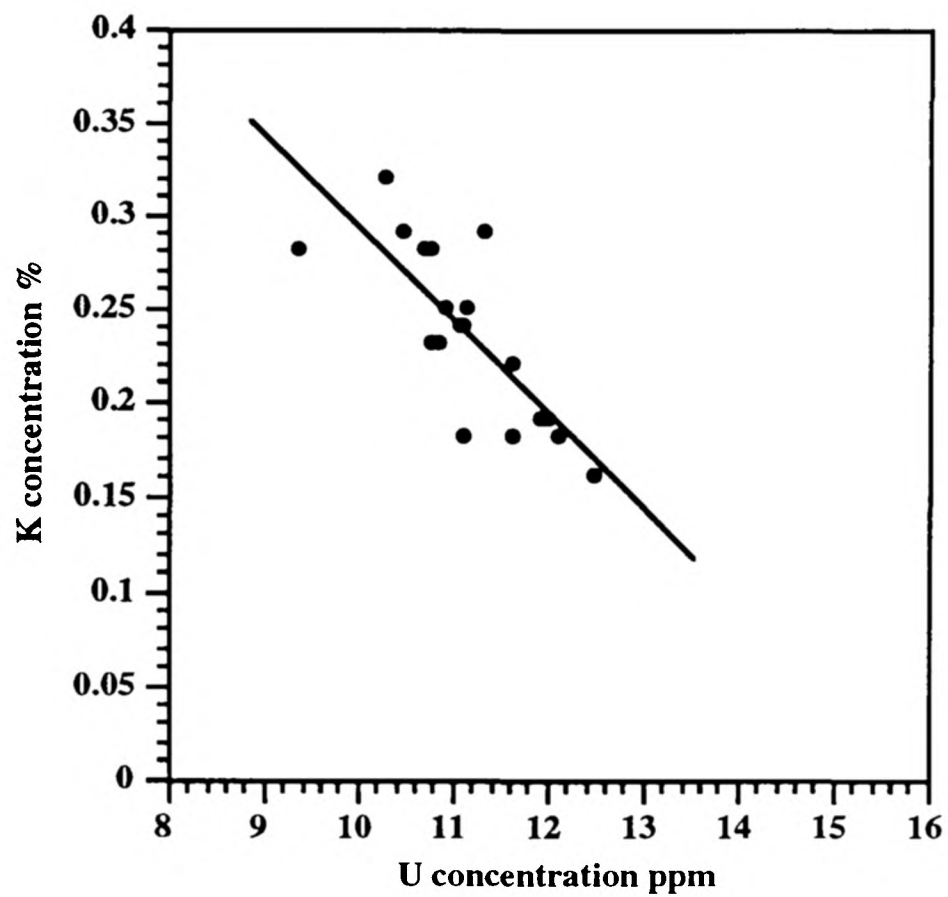


FIGURE 2.07 A Negative covariant relationship between calculated K and U concentration from total counts measured with the GR-410 spectrometer. The data-set represents twenty repeated readings from a single point that were taken on Iron Ledge in the horizontal plane.

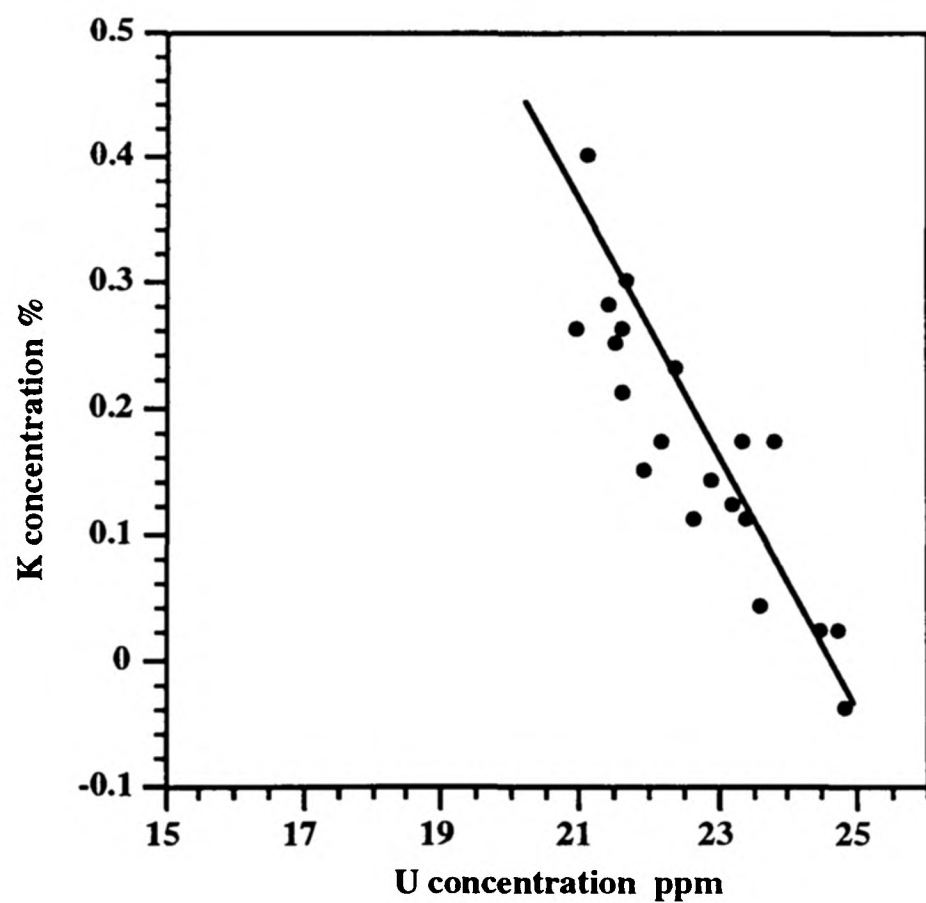


FIGURE 2.07 B Negative covariant relationship between calculated K and U concentration from total counts measured with the GR-410 spectrometer. The data-set represents twenty repeated readings from a single point that were taken on Belemnite Bed in the horizontal plane.

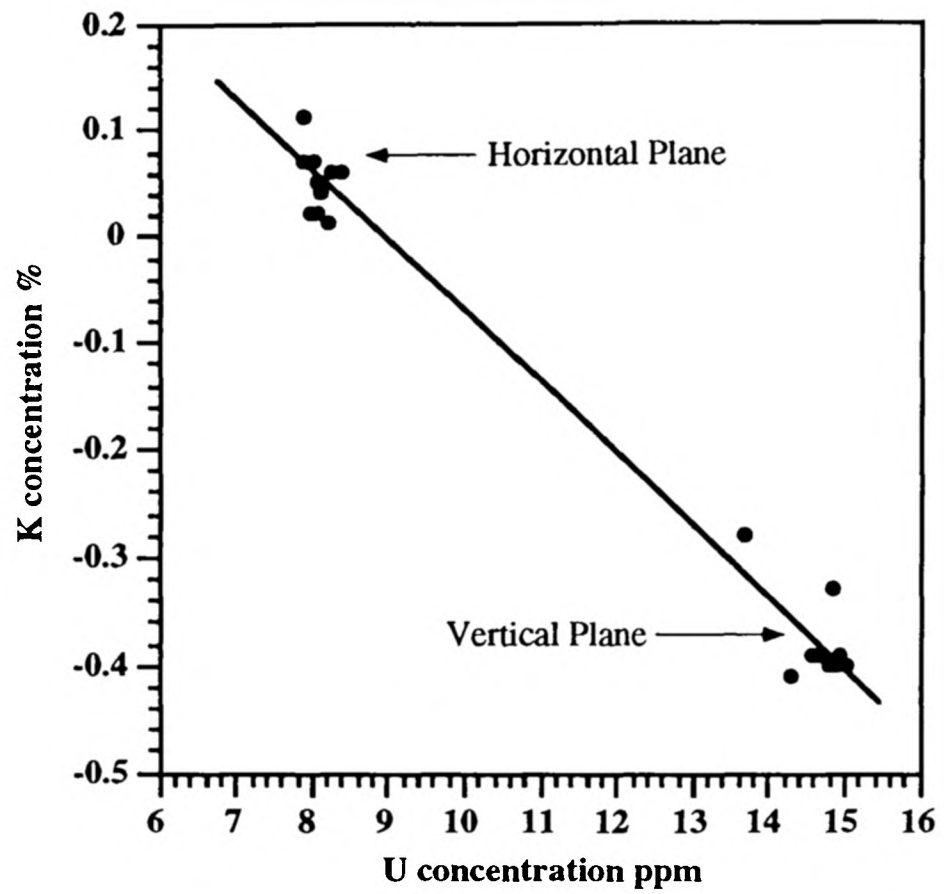


FIGURE 2.07 C Negative covariant relationship between calculated K and U concentration from total counts measured with the GR-410 spectrometer. The data-set represents twenty repeated readings from a single point that were taken on the Lower Cement Bed in the horizontal and vertical plane.

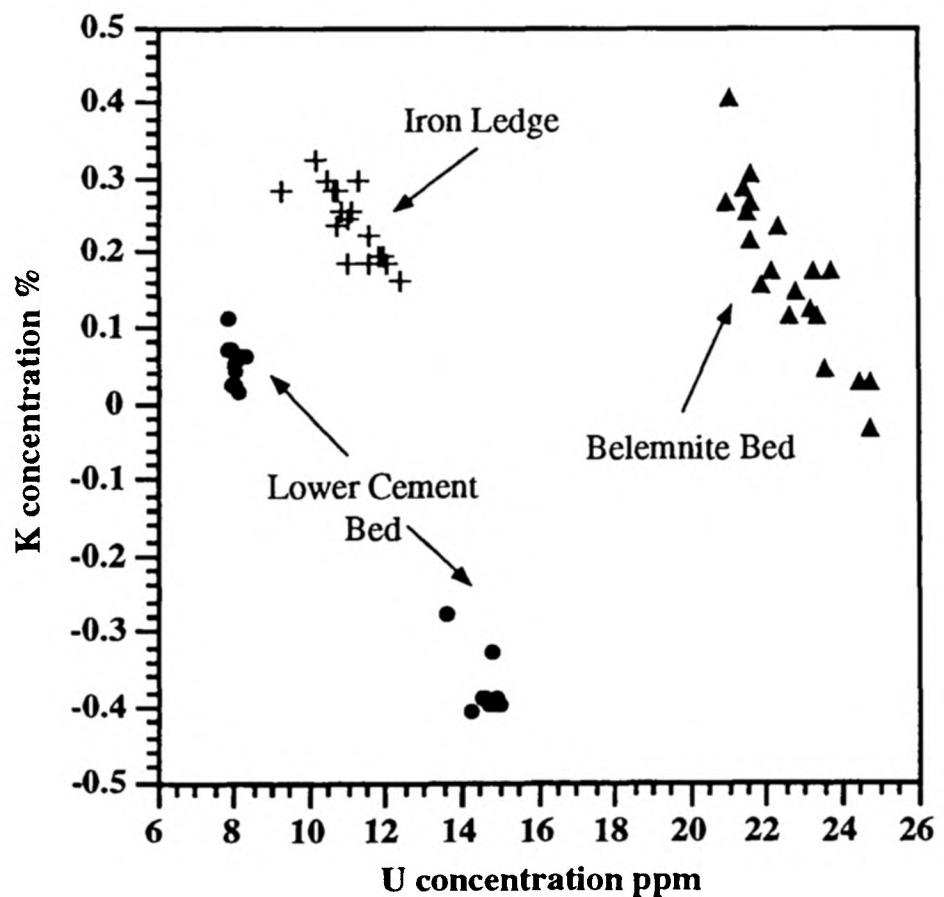


FIGURE 2.07 D Relationship between calculated K and U concentration from total counts measured with the GR-410 spectrometer for the three data-sets (60 samples)

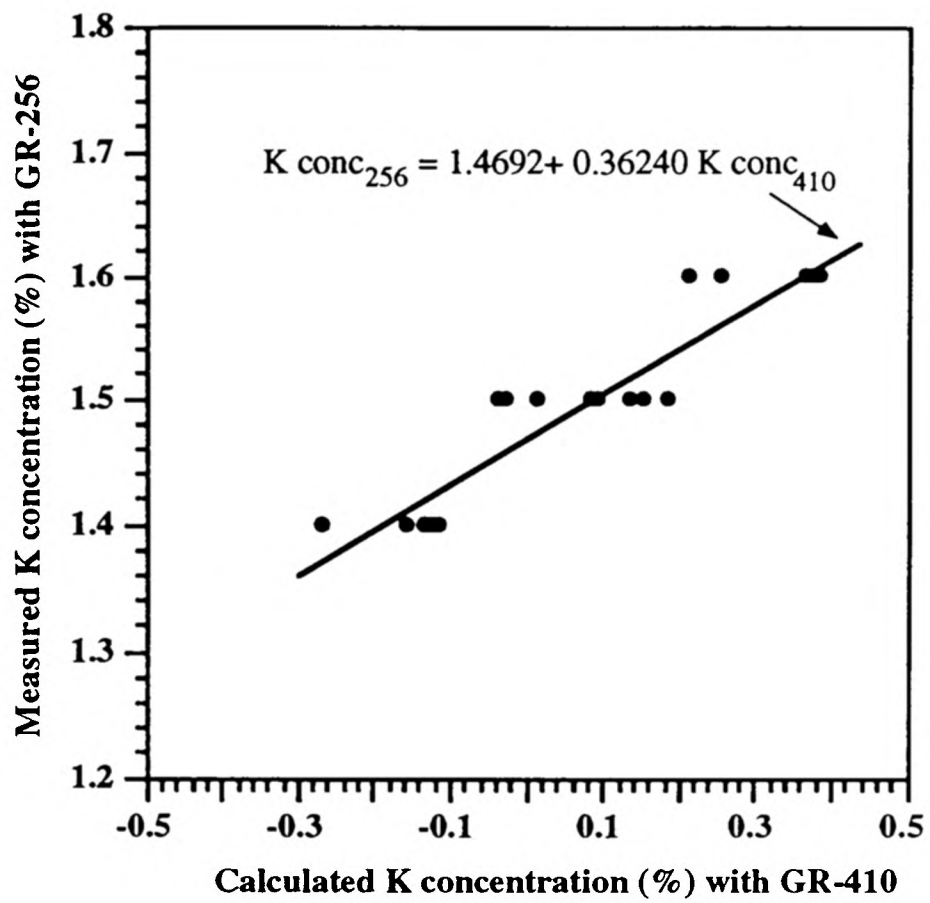


FIGURE 2.08 A Numerical relationship between K concentration calculated from total counts detected with the GR-410 and K concentration detected by the GR-256. Readings were taken in the horizontal plane on the Belemnite Bed. (Correlation significant at the 95 % level for a coefficient of 0.866)

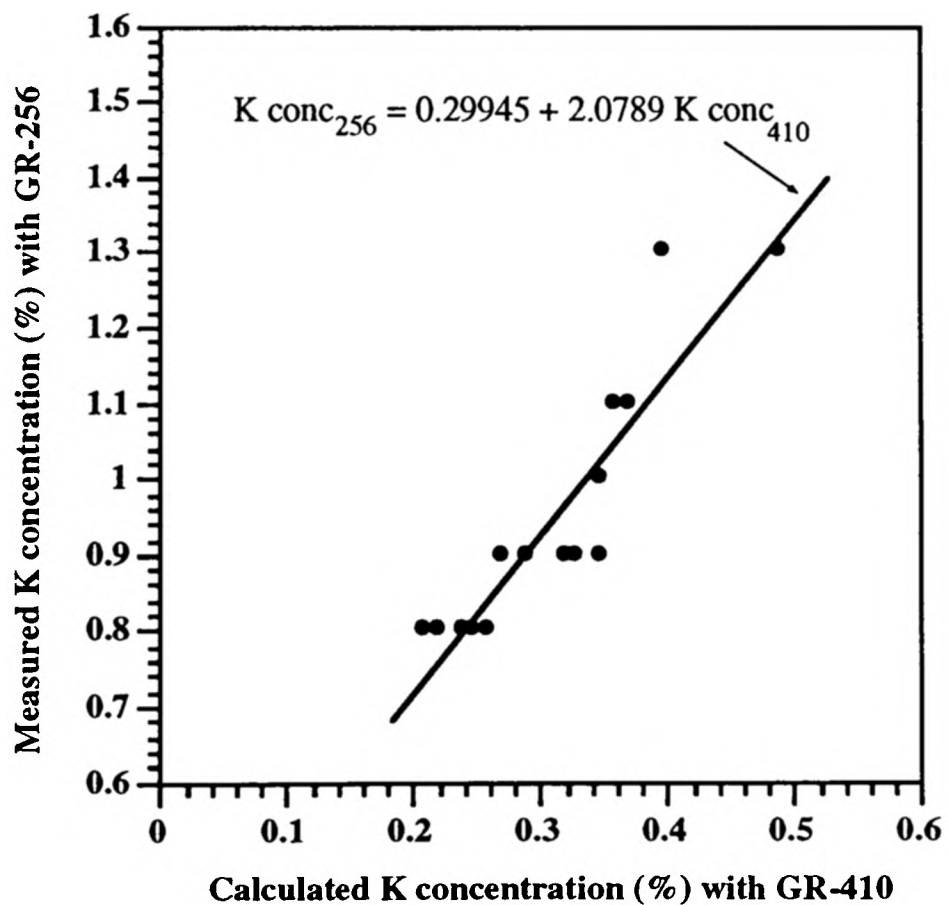


FIGURE 2.08 B Numerical relationship between K concentration calculated from total counts detected with the GR-410 and K concentration detected by the GR-256. Readings were taken in the horizontal plane on Iron Ledge. (Correlation significant at the 95 % level for a coefficient of 0.856)

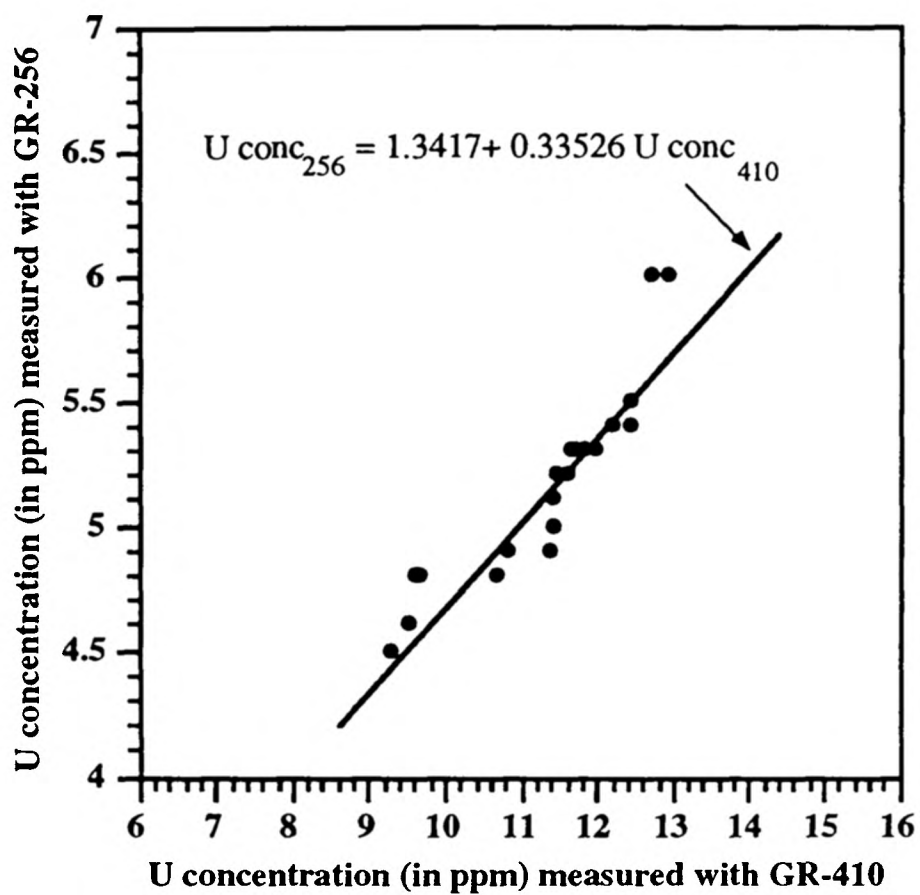


FIGURE 2.09 A Positive covariant relationship between U concentration calculated from total counts detected with the GR-410 and U concentration detected by the GR-256. Readings were taken in the horizontal plane on the Belemnite Bed. (Correlation significant at the 95 % level for a coefficient of 0.835)

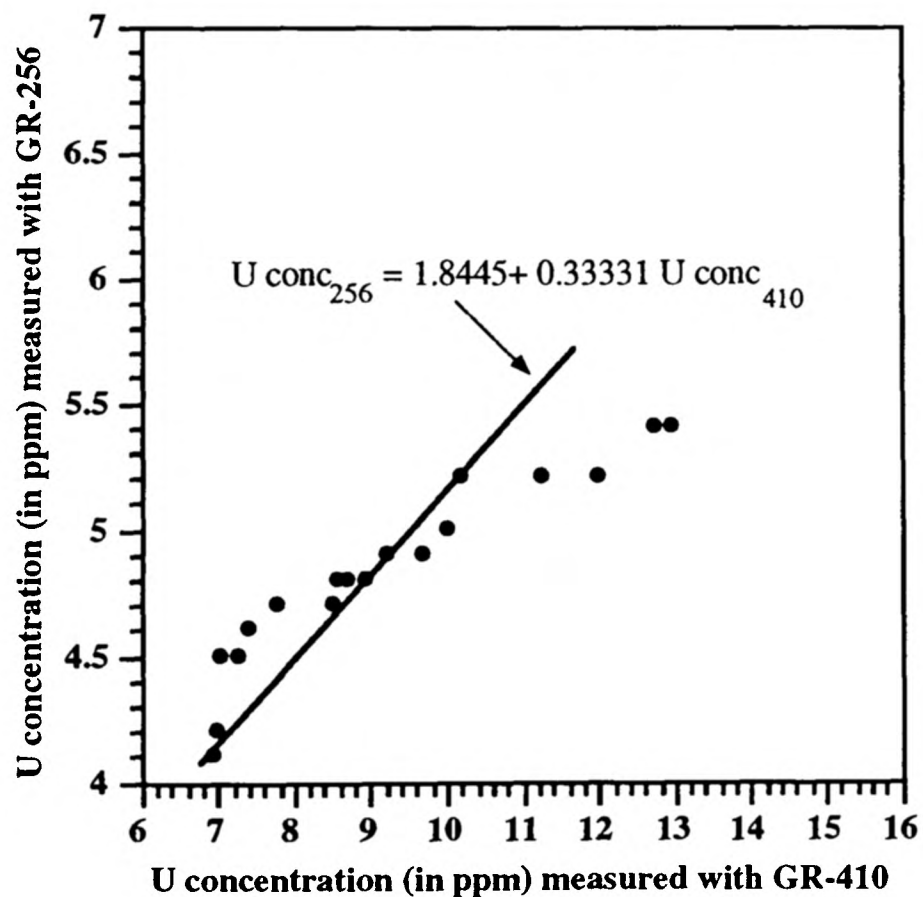


FIGURE 2.09 B Positive covariant relationship between U concentration calculated from total counts detected with the GR-410 and U concentration detected by the GR-256. Readings were taken in the horizontal plane on Iron Ledge. (Correlation significant at the 95 % level for a coefficient of 0.628)

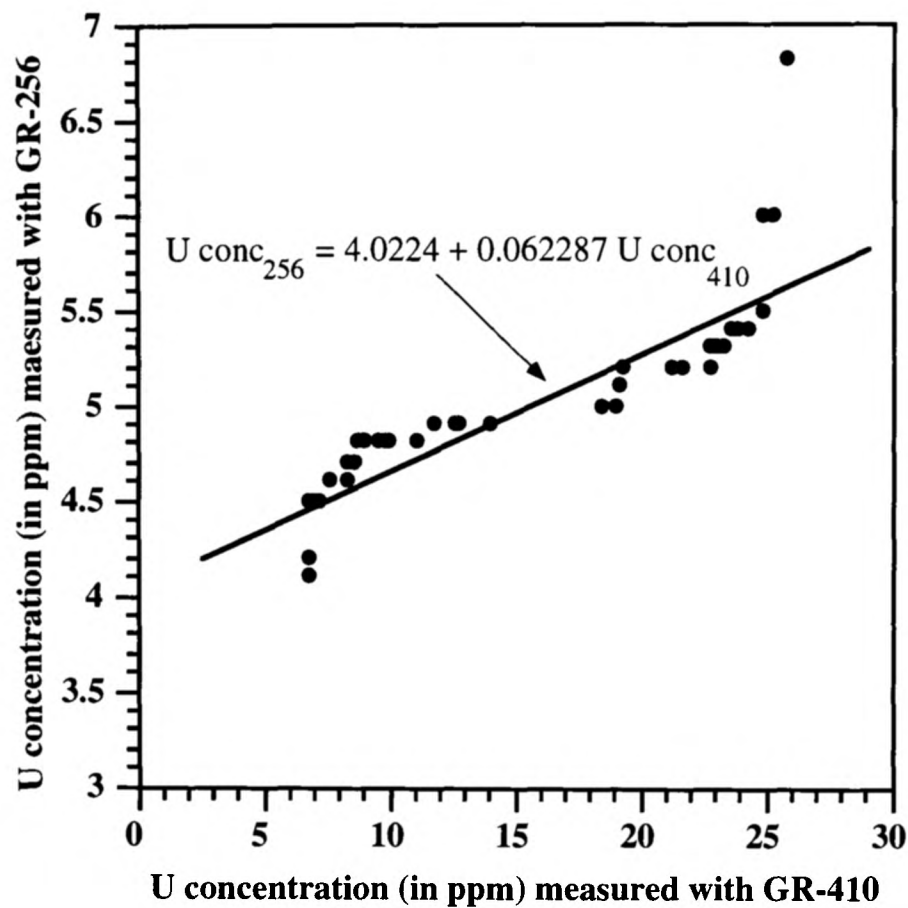


FIGURE 2.09 C Positive covariant linear relationship between U concentration calculated from total counts detected with the GR-410 and U concentration detected by the GR-256. The data-set of 40 measurements represents readings taken on both Iron Ledge and the Belemnite Bed. (Correlation significant at the 95 % level for a coefficient of 0.741)

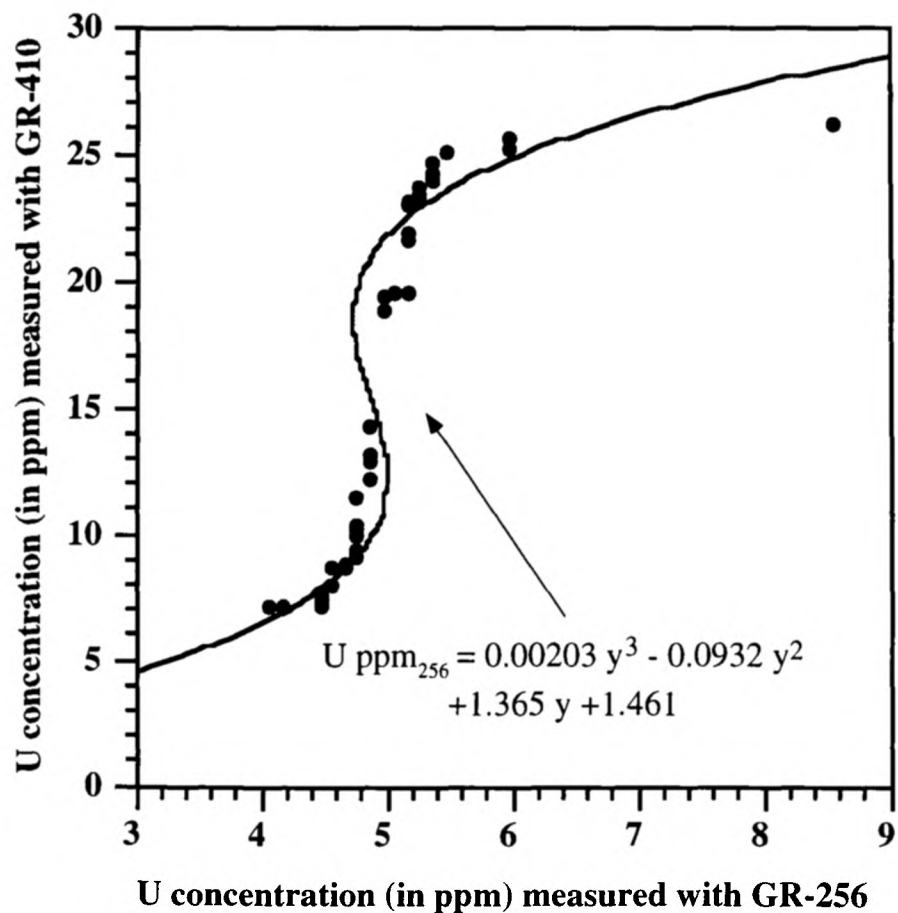


FIGURE 2.09 D Three degree polynomial relationship between U concentration calculated from total counts detected with the GR-410 and U concentration detected by the GR-256. The relationship is given as U ppm₂₅₆ as a function of U ppm₄₁₀. The data-set of 40 measurements represents readings taken on both Iron Ledge and the Belemnite Bed. The best-fit curve shows a backward trend over the mid-field which is not supported by the individual data points.

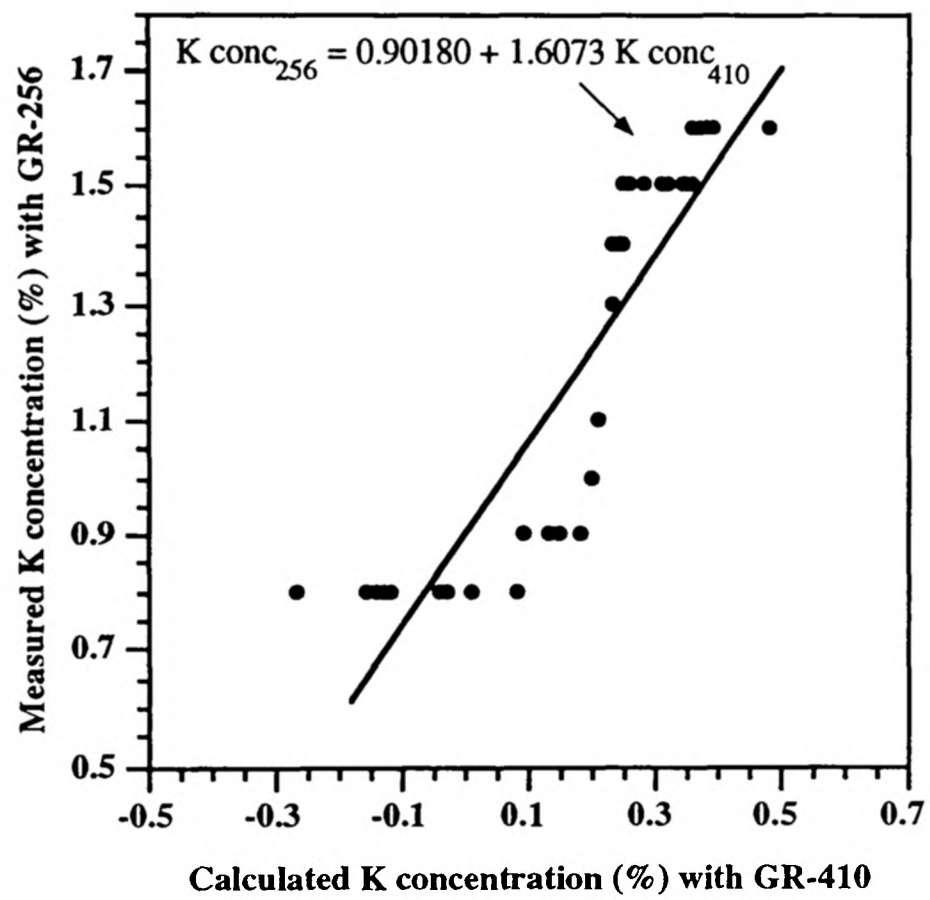


FIGURE 2.10 Positive covariant linear relationship between K concentration calculated from total counts detected with the GR-410 and K concentration detected by the GR-256. The data-set of 40 measurements represents readings taken on both Iron Ledge and the Belemnite Bed. (Correlation significant at the 95 % level for a coefficient of 0.792)

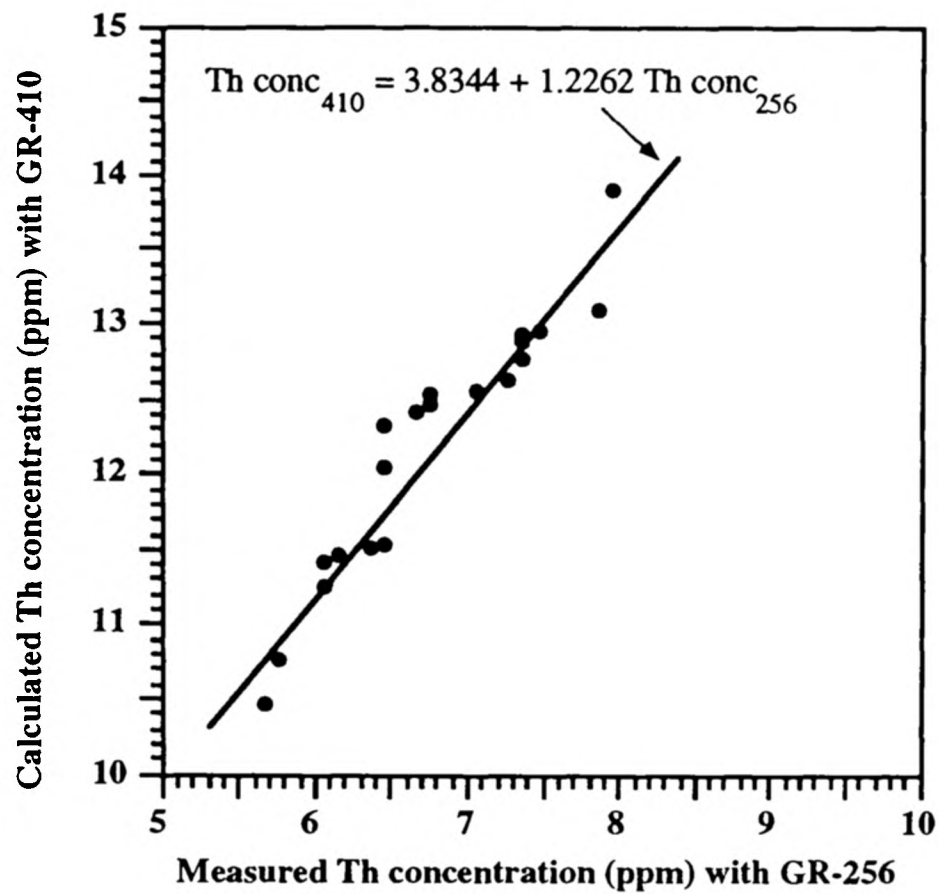


FIGURE 2.11 A Positive covariant linear relationship between Th concentration calculated from total counts detected with the GR-410 and Th concentration detected by the GR-256. Readings were taken in the horizontal plane on the Belemnite Bed. (Correlation significant at the 95 % level for a coefficient of 0.913)

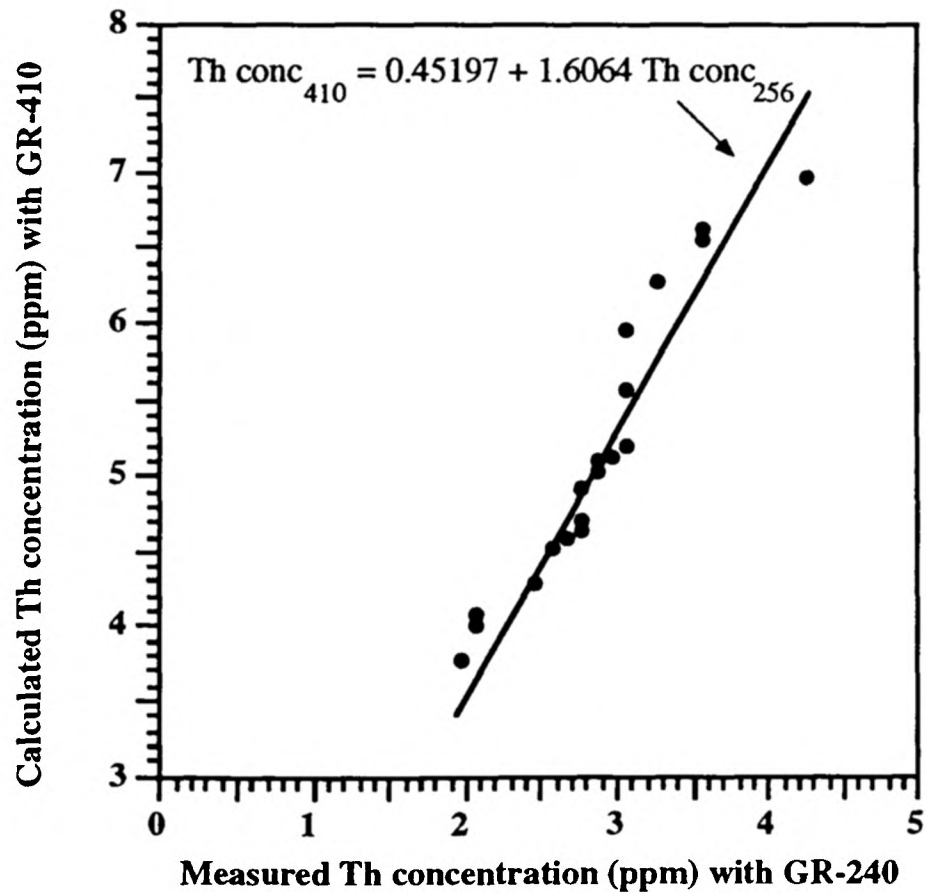


FIGURE 2.11 B Positive covariant linear relationship between Th concentration calculated from total counts detected with the GR-410 and Th concentration detected by the GR-256. Readings were taken in the horizontal plane on Iron Ledge. (Correlation significant at the 95 % level for a coefficient of 0.954)

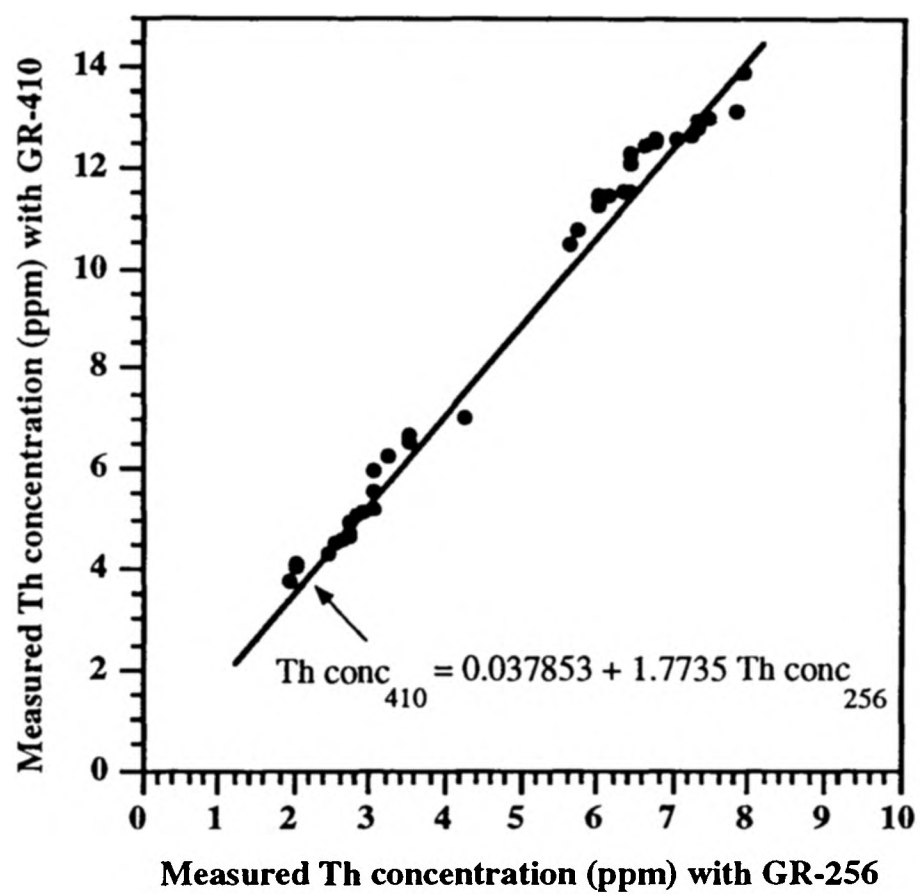
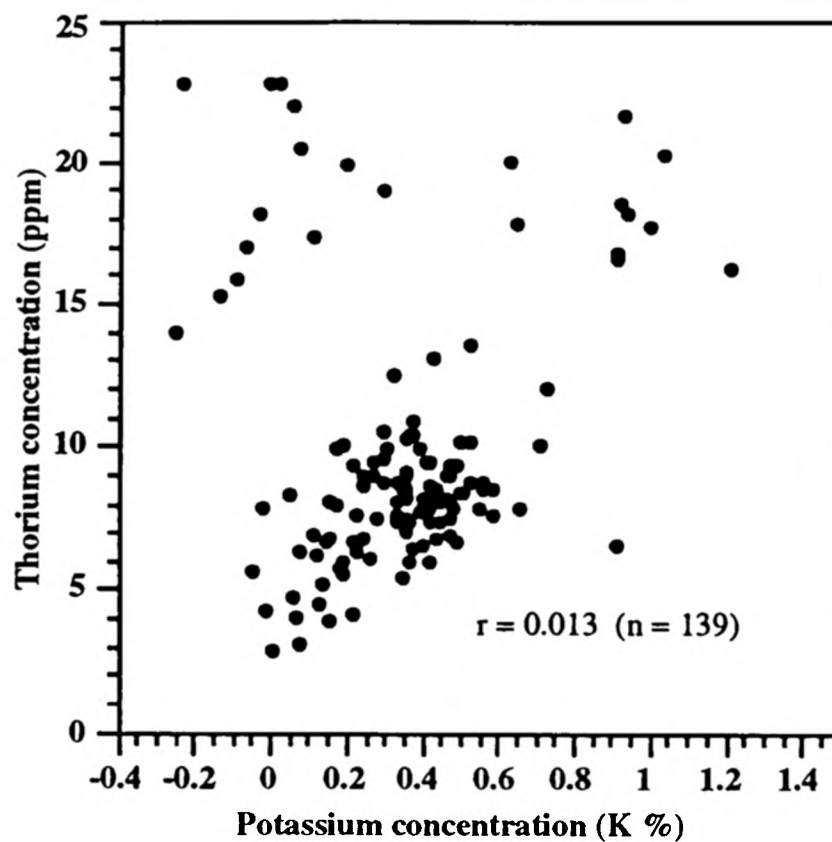


FIGURE 2.12 Positive covariant linear relationship between Th concentration calculated from total counts detected with the GR-410 and Th concentration detected by the GR-256. The data-set of 40 measurements represents readings taken on both Iron Ledge and the Belemnite Bed. (Correlation significant at the 95 % level for a coefficient of 0.792)

Raw GR-410 Data



Realigned GR-410 Data

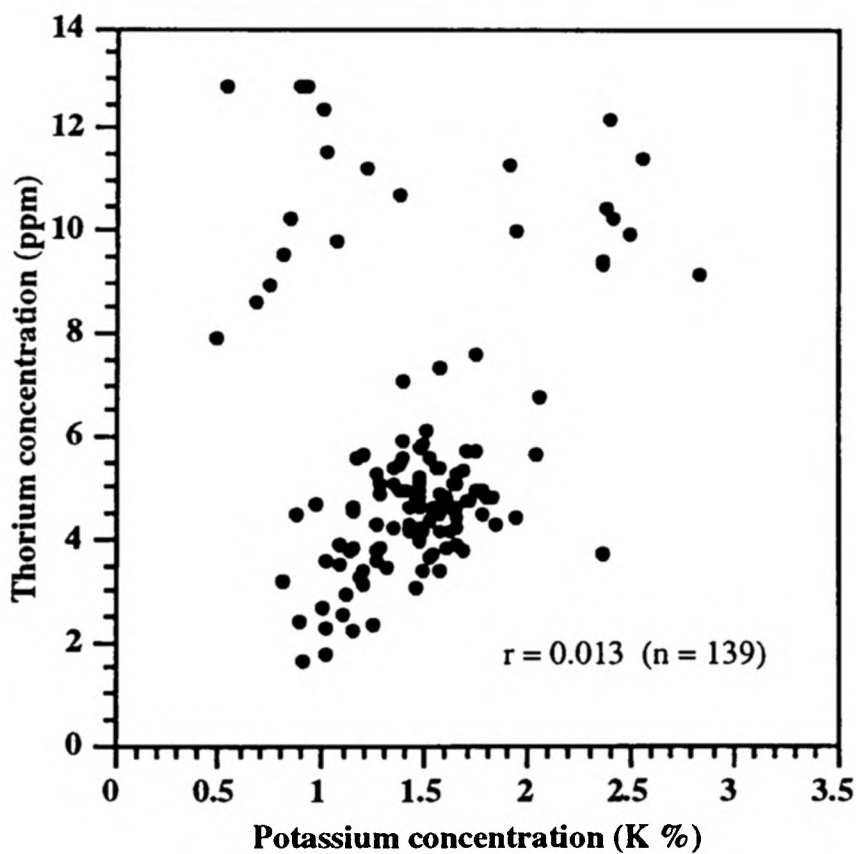


FIGURE 2.13 Part of the Unreliable GR-410 Data-Set.

ABOVE Numerical relationship between calculated K and Th concentration and calculated U and Th concentration from raw data collected with the GR-410. A positive covariant relationship between Th and K is not shown, as would be expected. This indicates that the data-set is not robust.

BELOW Numerical relationship between realigned K and Th concentration and realigned U and Th concentration using realignment formulae given in Chapter 2, Section 2.05. Again a positive covariant relationship between Th and K is not shown, as would be expected.

The data-set comprises 139 measured samples from west of Kilve Pylle, Somerset (*bucklandi* Zone, *bucklandi* Subzone, to *semicostatum* Zone, *lyra* Subzone).

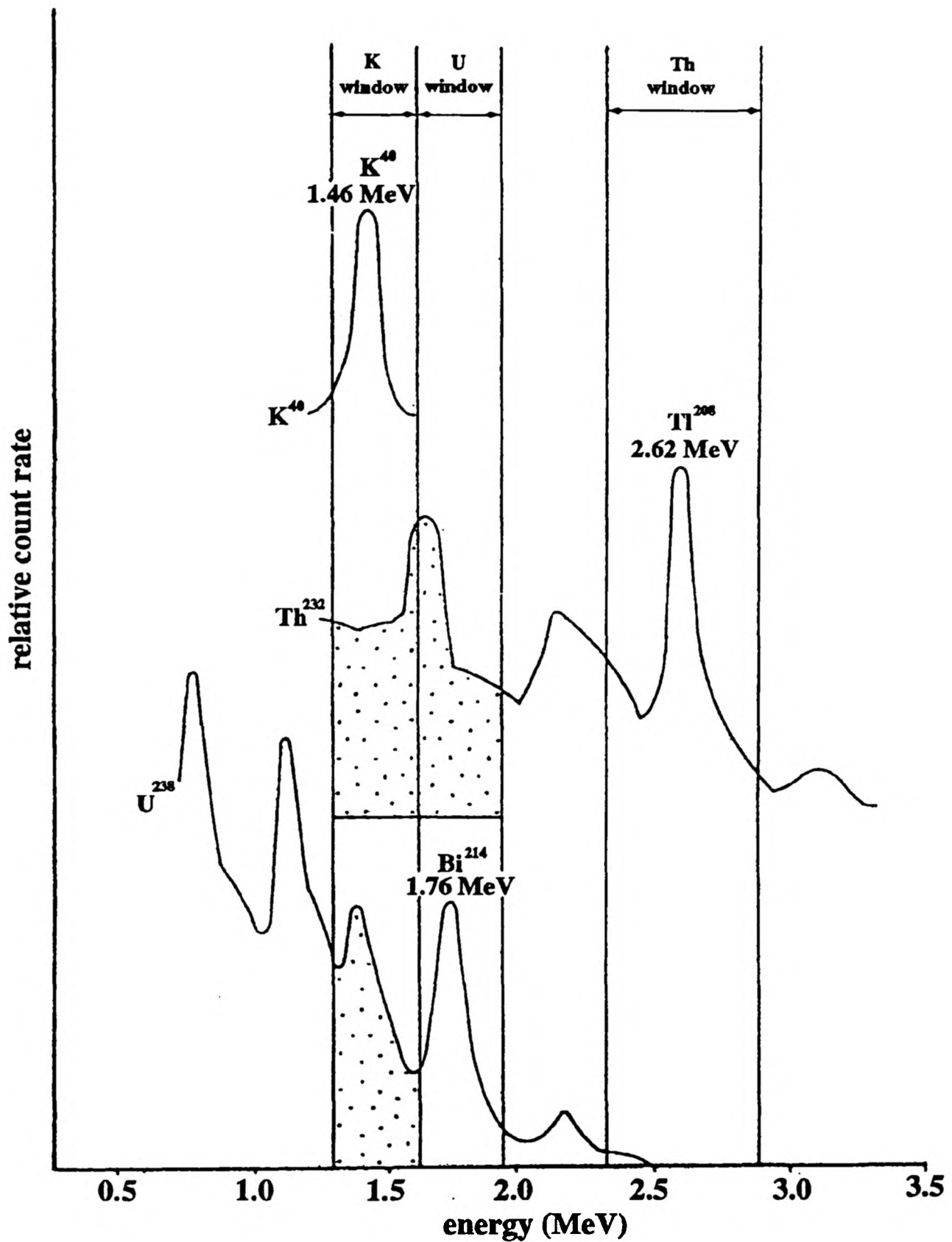


FIGURE 2.14 The individual energy windows used in the determination of K, U and Th concentrations in portable gamma-ray spectrometers. The use of broad energy windows (In order to take account of energy spreading away from the discrete peak) results in an overlapping of energy spectra measured from the different decay series. This phenomenon can be removed by the accurate determination of stripping constants. The stripping constant represent the ratio of counts detected in one window to those in another from pure sources of U and Th.

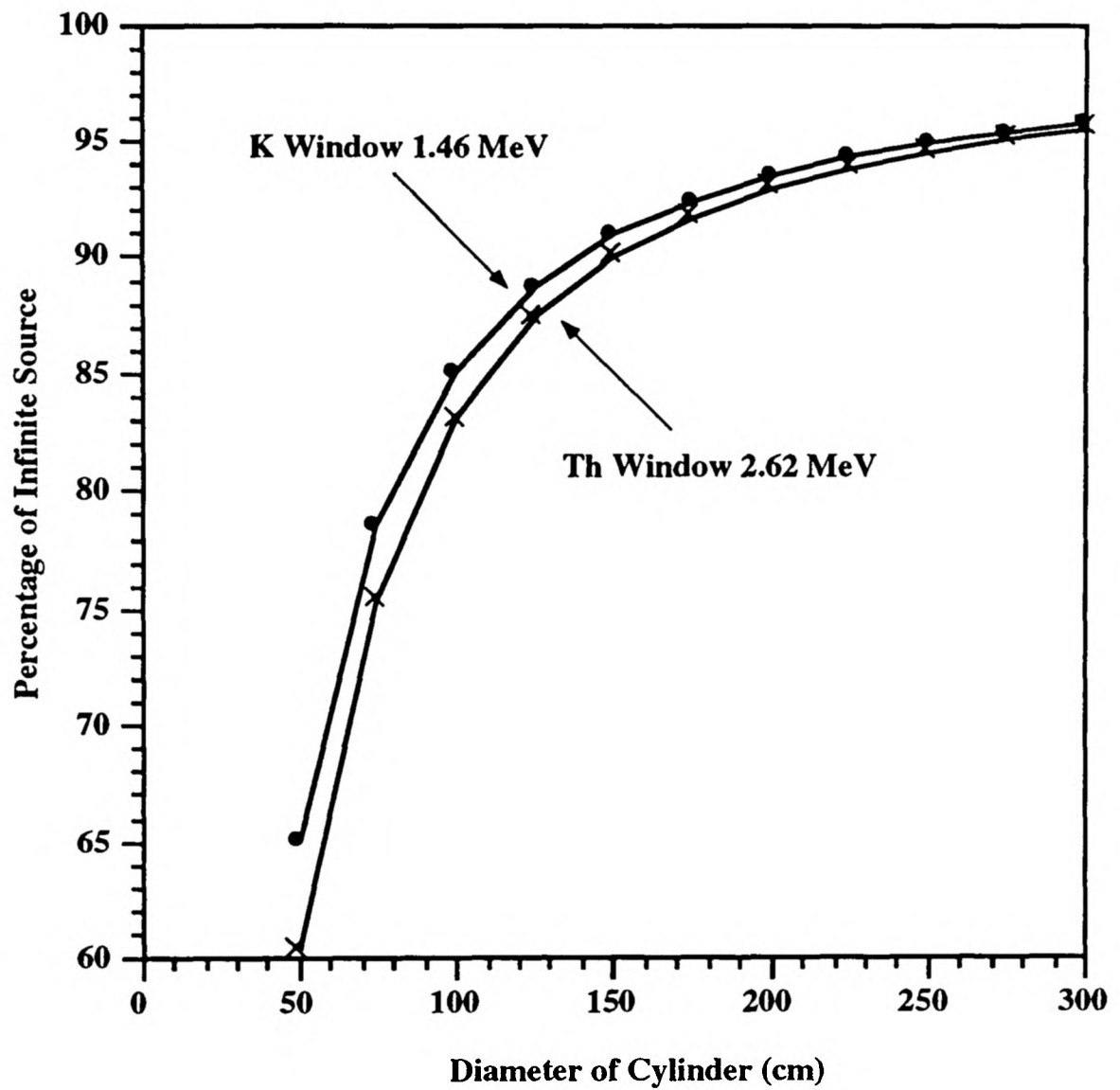


FIGURE 2.15 Response of a typical portable gamma-ray spectrometer to cylindrical calibration pads of varying diameter. the diameter is increased by 25 cm for each data point from 50 cm at the base of the curve to 300 cm at the top of the curve. The pads conform to the specifications outlined in Appendix 1, Table 1.17. Data are plotted from Grasty *et al.* (1991).

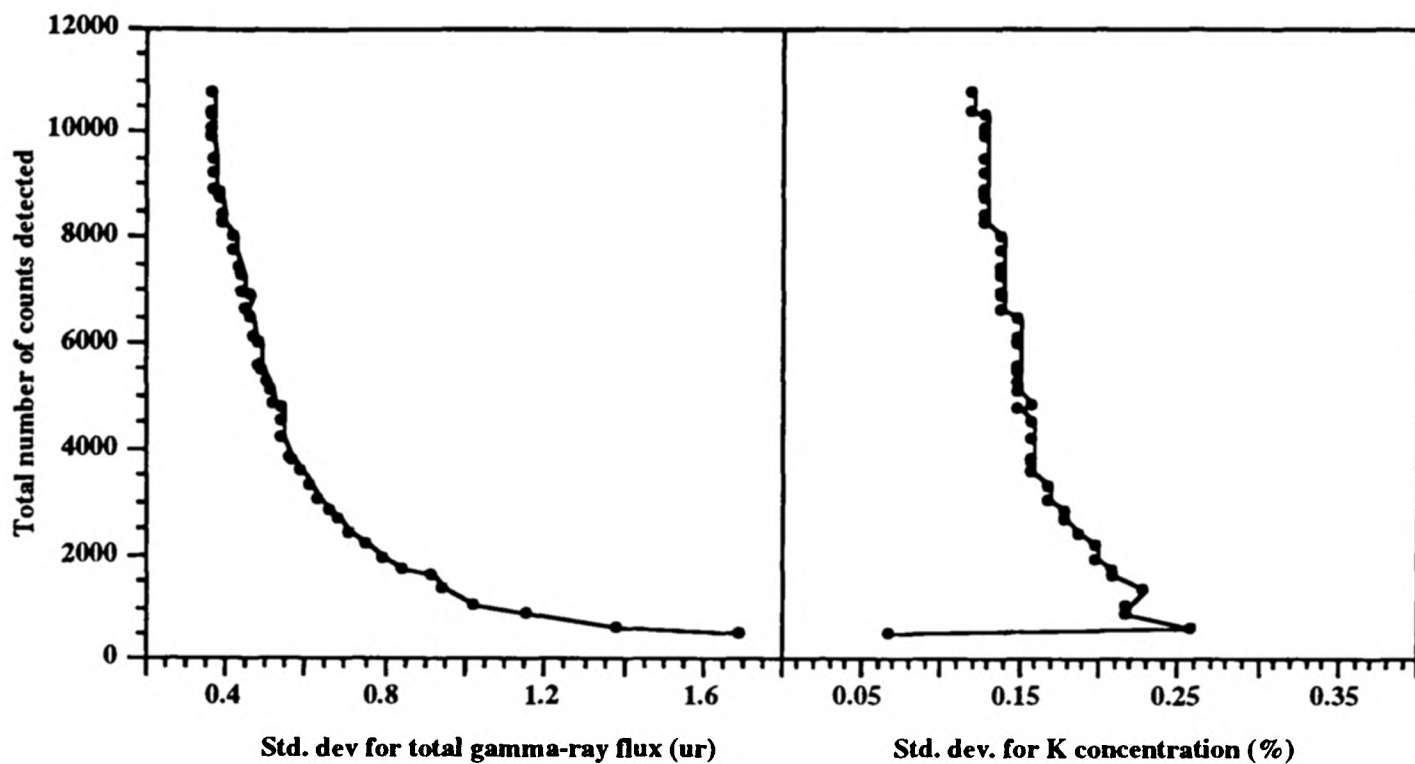
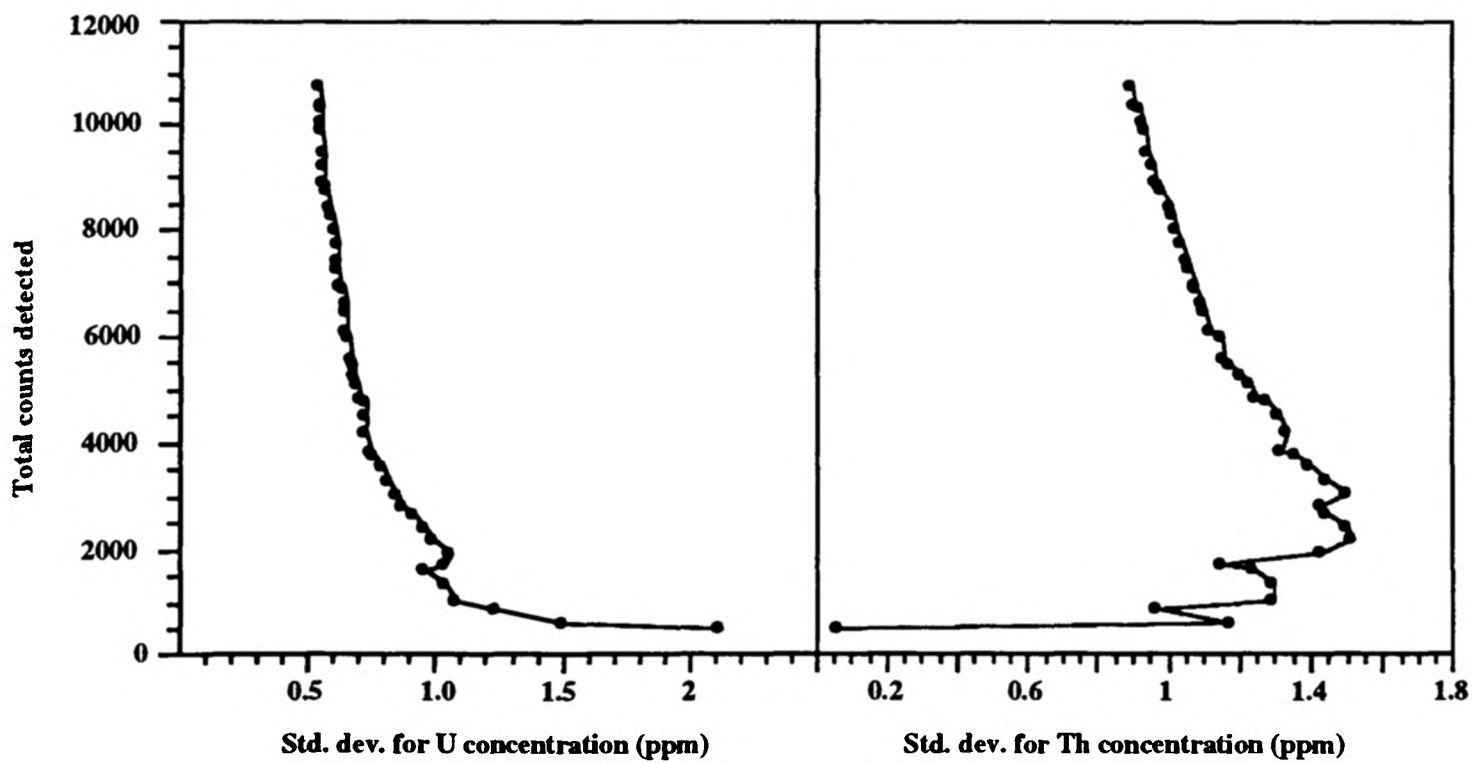


FIGURE 2.16 Standard deviation curves for 48 repeated readings taken from a single point on the Belemnite Bed. The measurements were taken with the GR-256 gamma-ray spectrometer in the horizontal plane with 5-second increments in measurement time up to a maximum of 240 seconds.



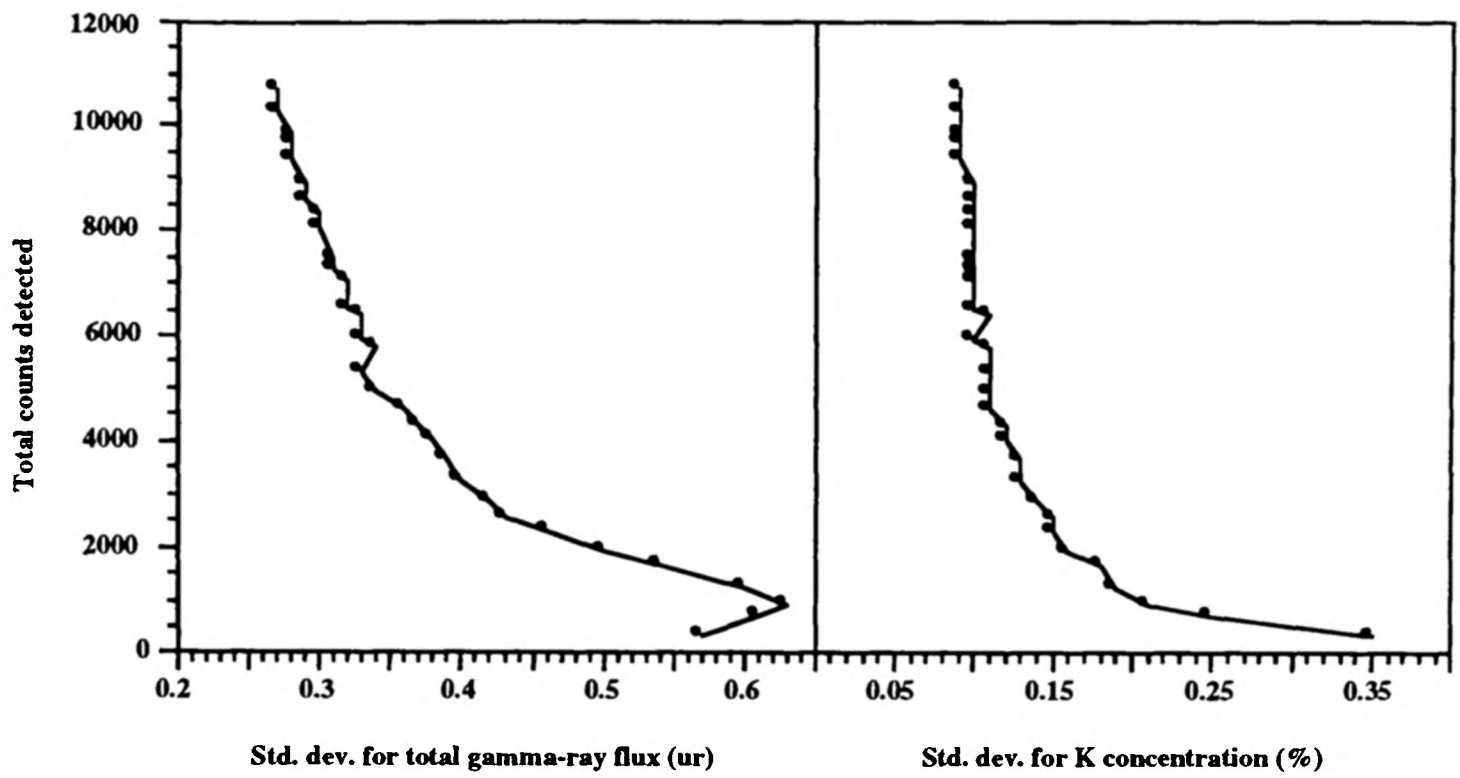
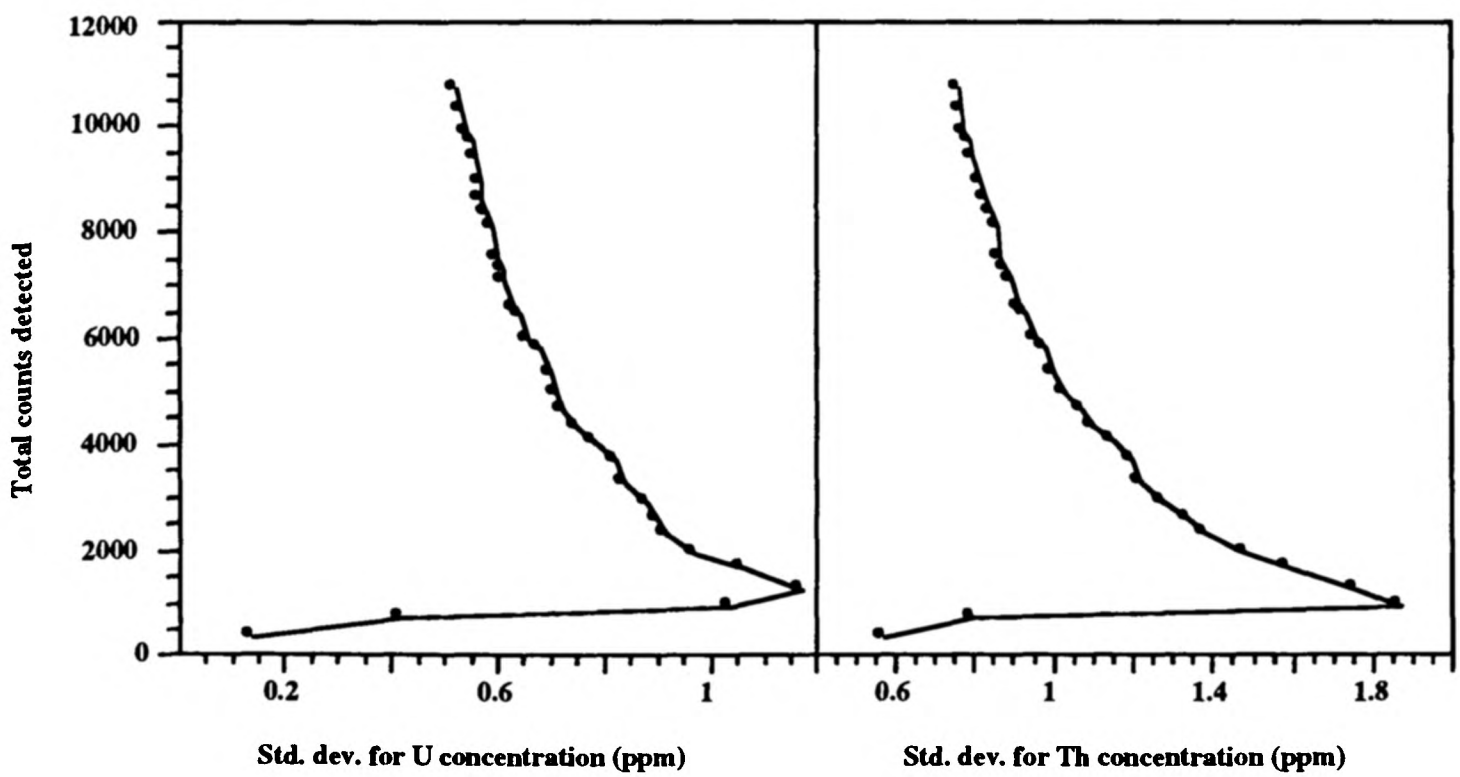


FIGURE 2.17 Standard deviation curves for 33 repeated readings taken from a single point on Iron Ledge. The measurements were taken with the GR-256 gamma-ray spectrometer in the horizontal plane with 10-second increments in measurement time up to a maximum of 320 seconds.



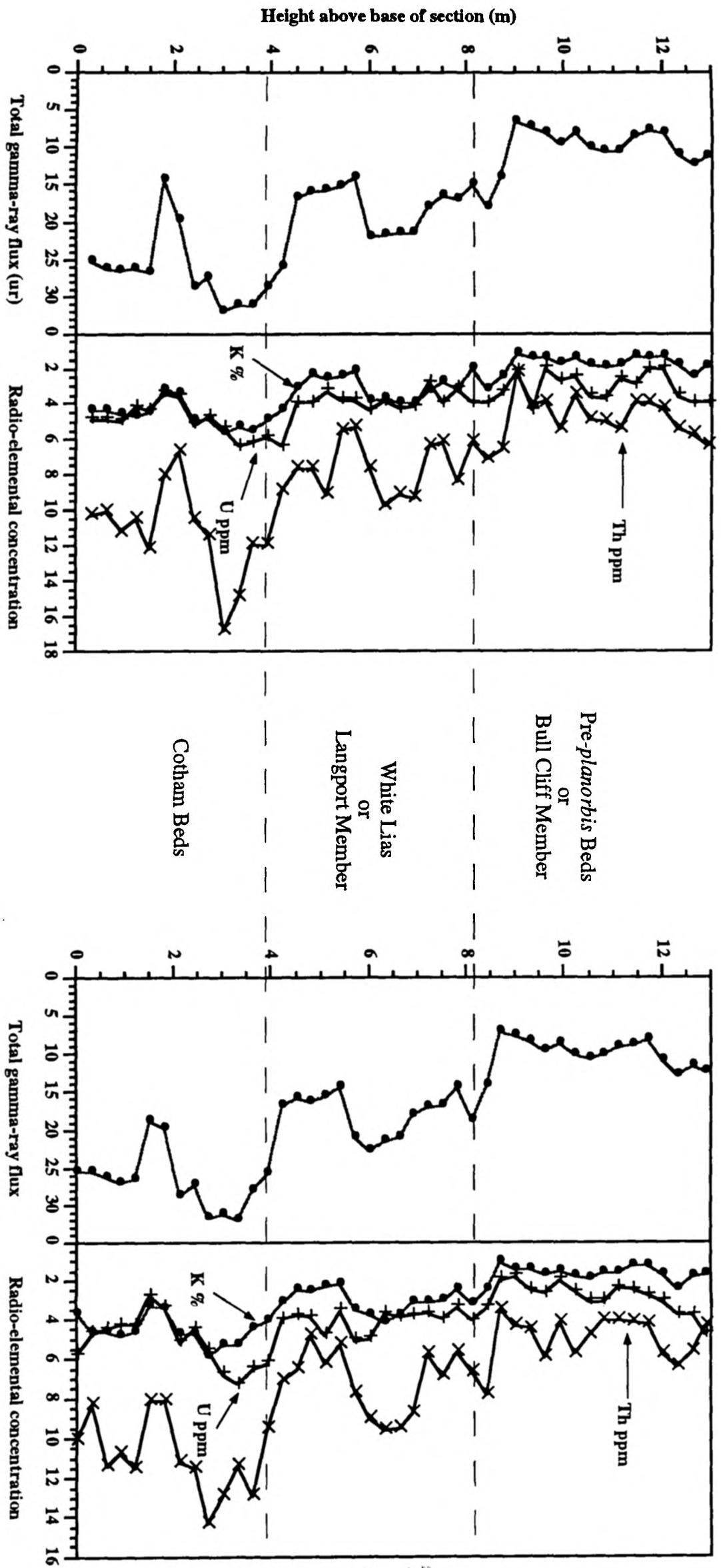


FIG 2.18

FIGURE 2.18

FIGURE 2.18 Comparison of gamma-ray measurements collected from identical points exactly five hours apart from each other. The measurements were taken from the Rhætan succession exposed in St. Mary's Well Bay, South Glamorgan (ST 180630). All data collected with the GR-256 spectrometer on the 11 th and 12th September 1995.

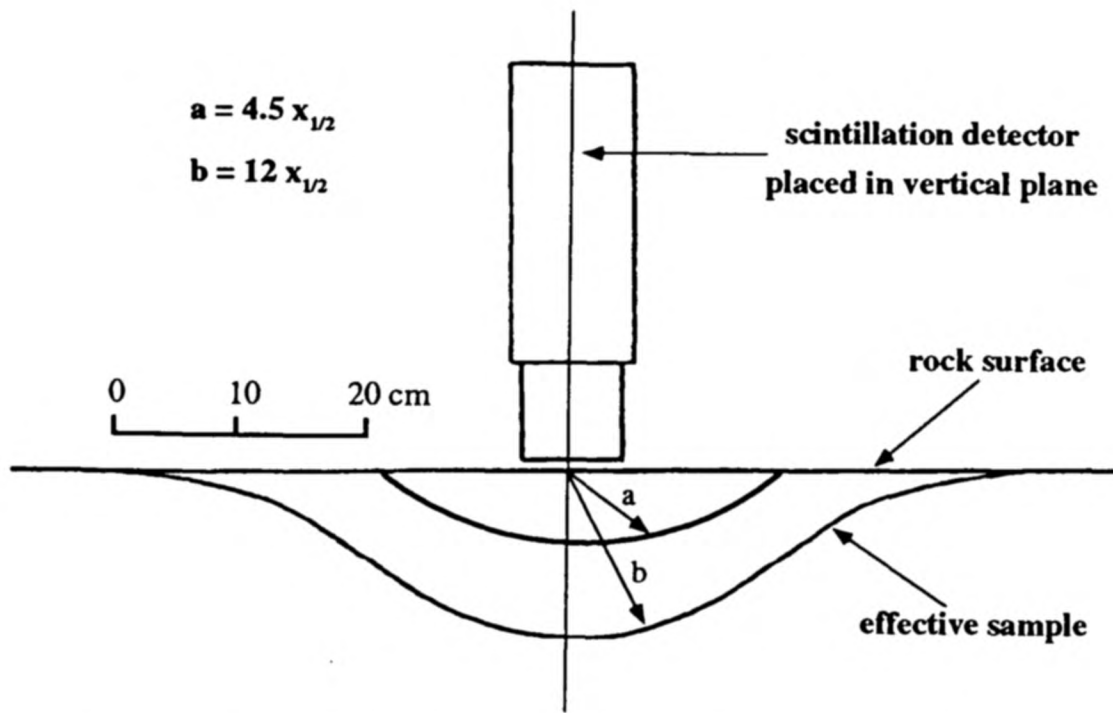


FIGURE 2.19 A Sample geometry for an uncollimated GR-256 or GR-410 gamma-ray spectrometer. Hemispheres a and b provide 60 % and 99 % of the sample. Half-thickness ($x_{1/2}$) is given by $0.639/\mu p$ where μ is mass absorption coefficient and p is the density. (Adapted from Heath 1982).

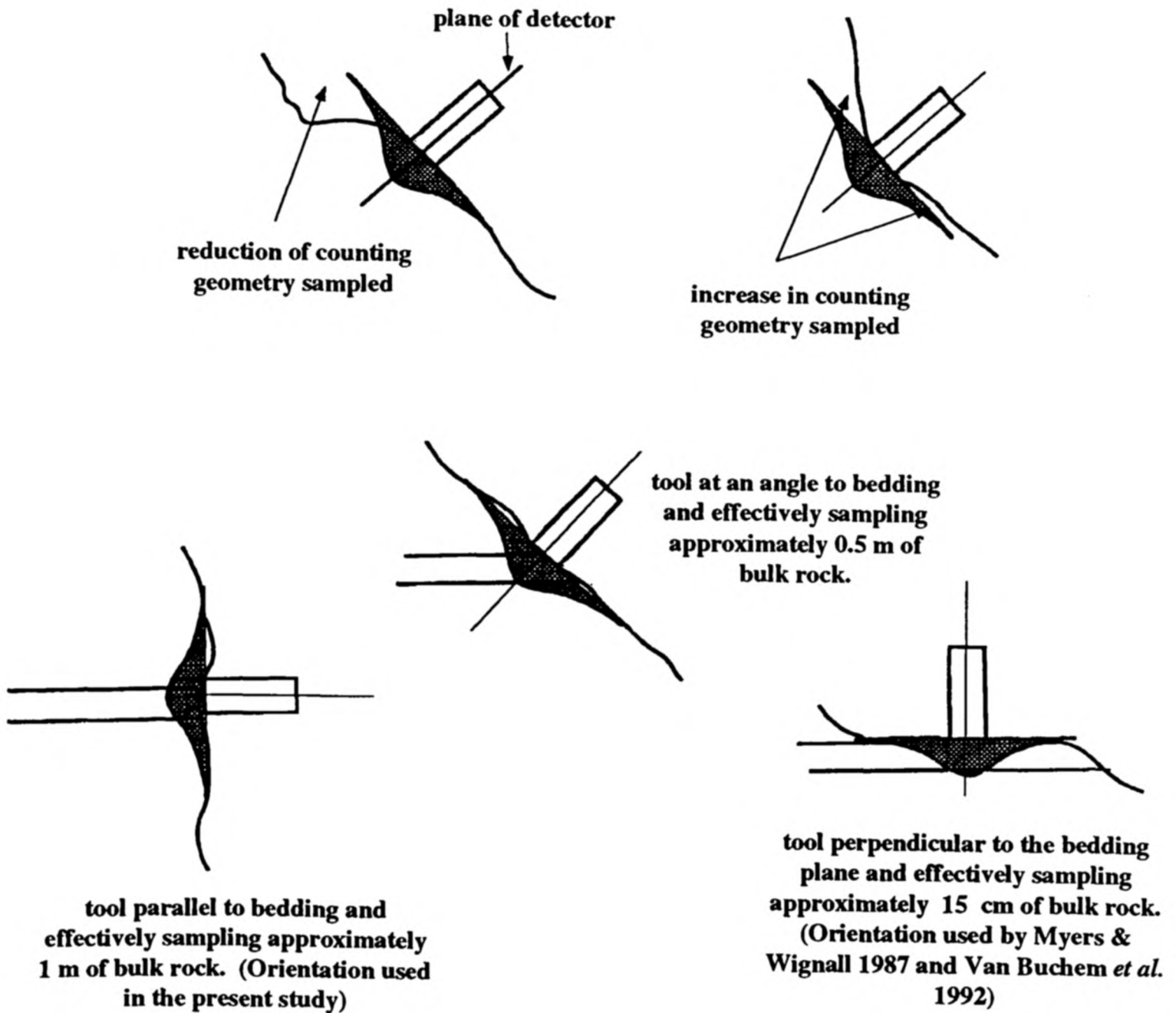


FIGURE 2.19 Relationship between counting geometry and stratigraphical bedding surfaces. Tool resolution is greatly effected by the orientation at which the scintillation detector is placed upon the fresh outcrop surface. (Modified from Parkinson 1994).

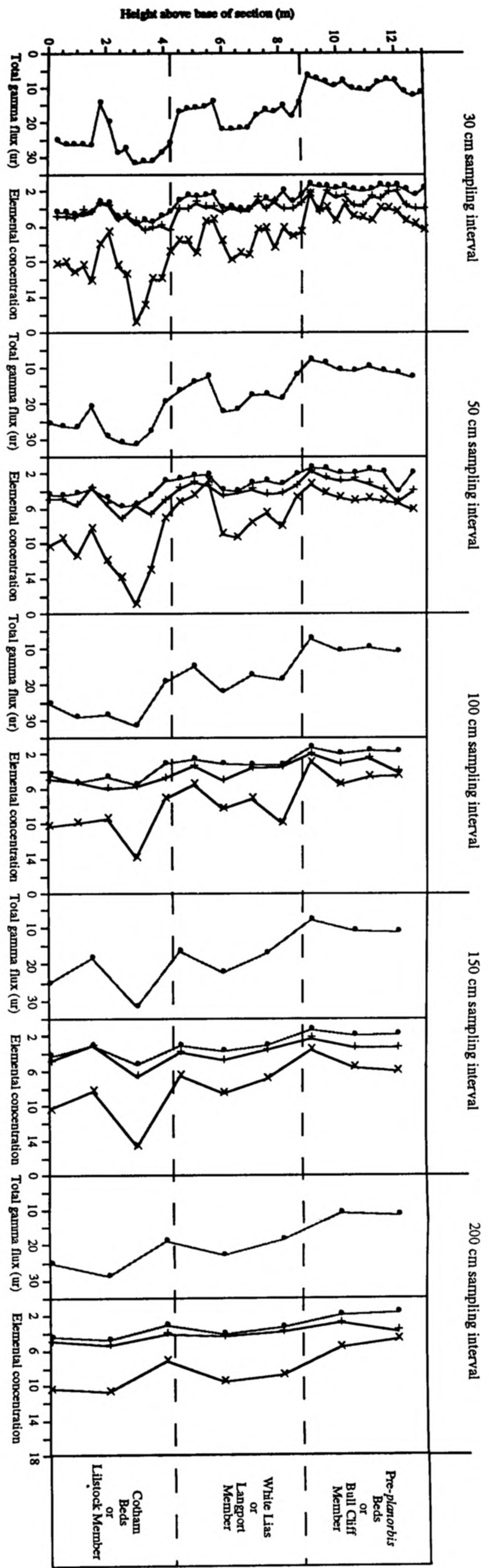


FIGURE 2.20 Loss of high-frequency information with successive increases in sampling interval. The trends that are developed within the 30 cm sampled gamma-ray logs can be convincingly identified in the 50 cm, 100 cm and 150 cm sampled logs. The 200 cm sampled gamma-ray logs do not accurately reflect the stratigraphic gamma-ray trends demonstrated at a higher frequency of scale. Each set of gamma-ray readings were measured from St. Mary's Well Bay, Glamorgan (ST 180680) and are of Rhaetian (Upper Triassic) age.

Figure 2.20

Chapter 3
Figure 3.01 to Figure 3.60

**The Gamma-Ray Characteristics of the Lower Lias
in Southern Britain**

BIOSTRATIGRAPHY		LITHOSTRATIGRAPHY		
Zone	Subzone	Dorset Coast	Somerset Coast	Glamorgan Coast
SINEMURIAN	<i>Arnioceras semicostatum</i>	Blue Lias Formation	Doniford Shales	Porthkerry Formation
	<i>Arietites bucklandi</i>		Quantocks Beds	
			<i>Vermiceras conybeari</i>	
<i>Schlotheimia angulata</i>	<i>Schlotheimia complanata</i>	Blue Lias <i>sensu stricto</i>		
	<i>Schlotheimia extranodosa</i>			
<i>Alsatites liasicus</i>	<i>Alsatites laqueus</i>	St Audrie's Shales		
	<i>Waehneroceras portlocki</i>			
<i>Psiloceras planorbis</i>	<i>Caloceras johnstoni</i>	Aldergrove Beds		
	<i>Psiloceras planorbis</i>			
RHAETIAN	Pre- <i>planorbis</i> Beds			Bull Cliff Member

FIGURE 3.01 A comparison of the lithostratigraphic and biostratigraphic divisions of the Rhaetian - Lower Sinemurian succession in southern Britain. Based upon Trueman (1920), Lang (1924), Dean *et al.* (1961), Palmer (1972) and Ivimey-Cook & Donovan (1983). The informal term "Blue Lias" typically refers to high frequency limestone-marl alternations that characterise the exposure at Lyme Regis, Dorset (SY 328910). In this present study the term "Blue Lias" is used for all Lower Lias sedimentary rocks in southern Britain of pre-*planorbis* to *semicostatum* Zone (*lyra* Subzone) age.

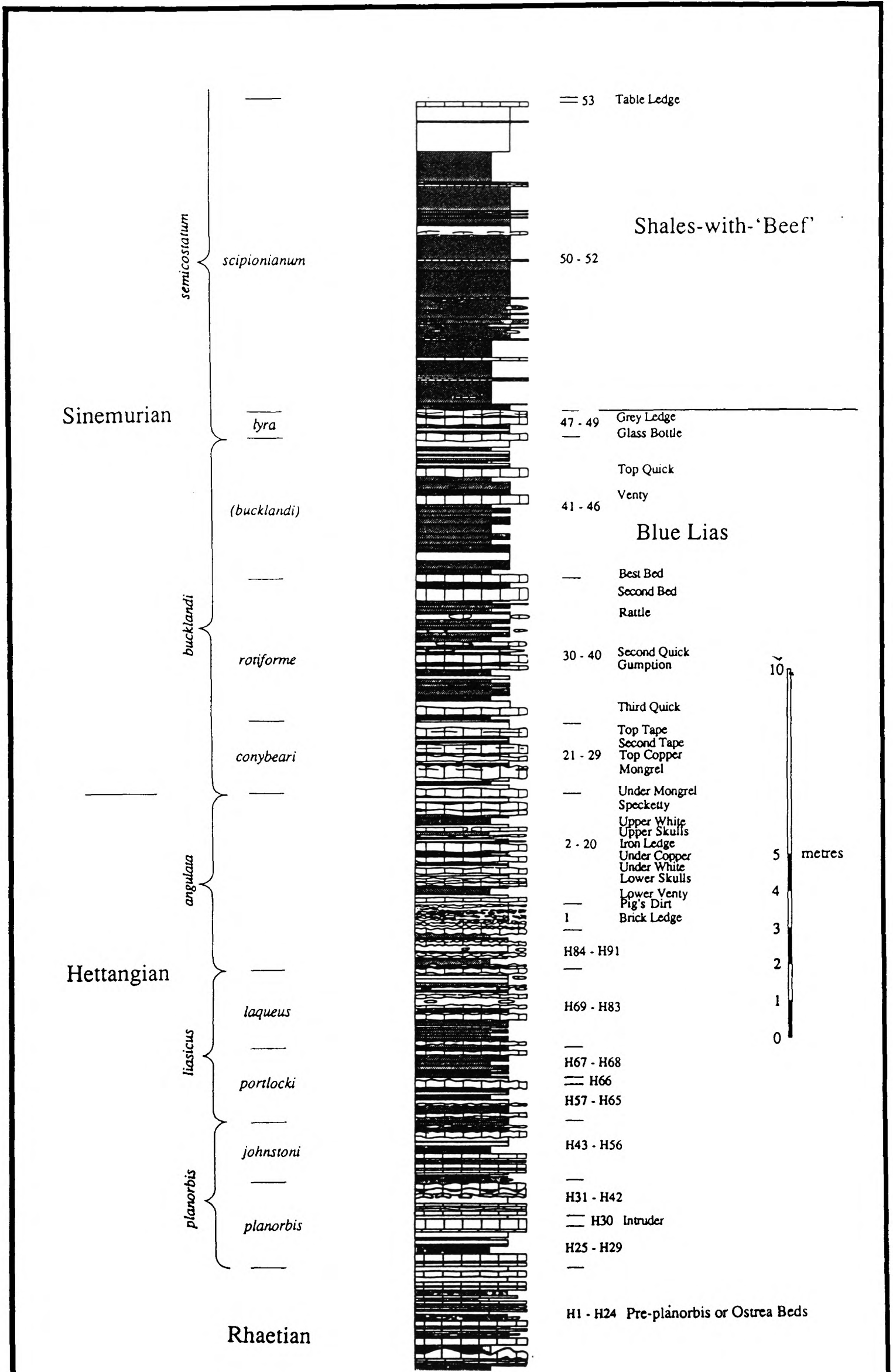


FIGURE 3.02 Stratigraphic log for the Blue Lias and lower part of the Shales-with-Beef (from Hesselbo & Jenkyns 1995a). Bed numbers are taken from Lang *et al.* (1922) and Lang (1924). Biostratigraphy based on Lang *et al.* (1922), Lang (1924), Dean *et al.* (1961) and Ivimey-Cook & Donovan (1983). Section measured between Pinhay Bay (SY 318908) and Seven Rock Point, Lyme Regis, Dorset (SY 328910).

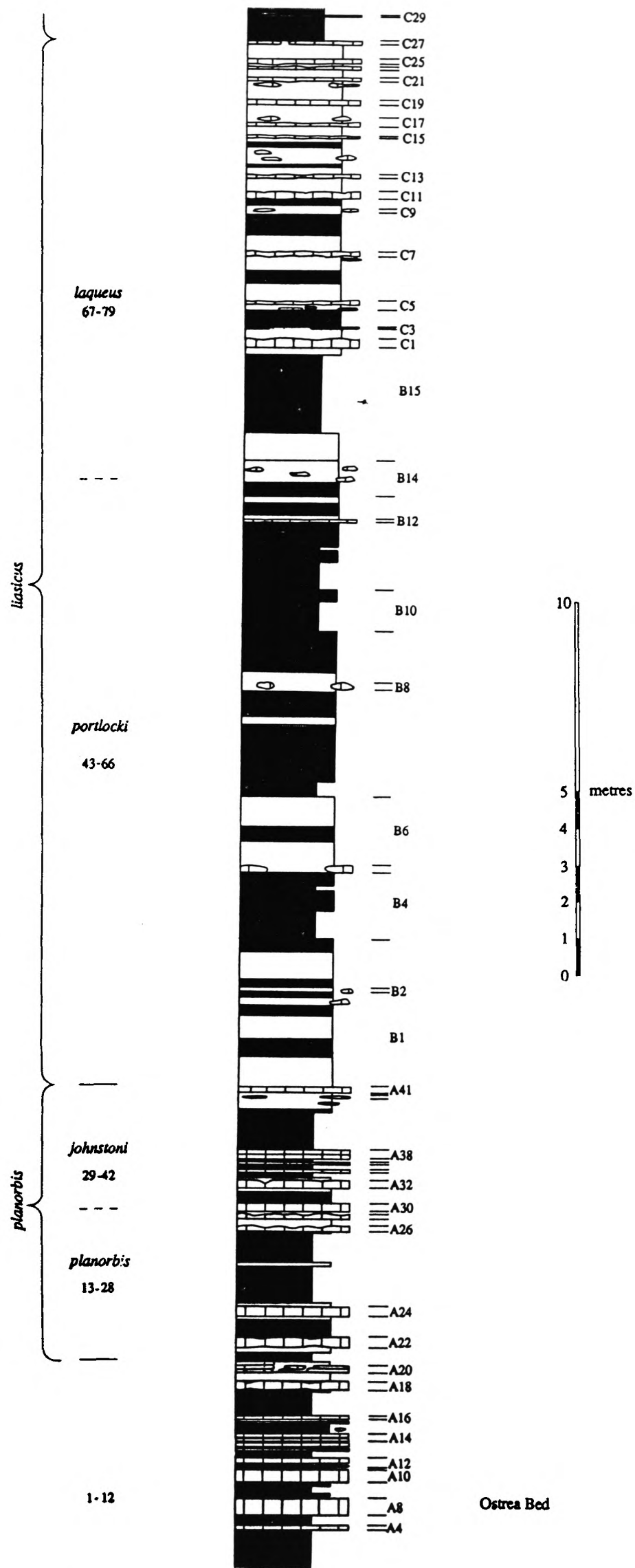


FIGURE 3.03 Stratigraphic log for the Blue Lias at St Audrie's Bay, Somerset ST 102433 (Unpublished, courtesy of Hesselbo & Jenkyns.) Bed numbers are taken from Palmer (1972). Biostratigraphy based upon Dean *et al.* (1961) and Ivimey-Cook & Donovan (1983).

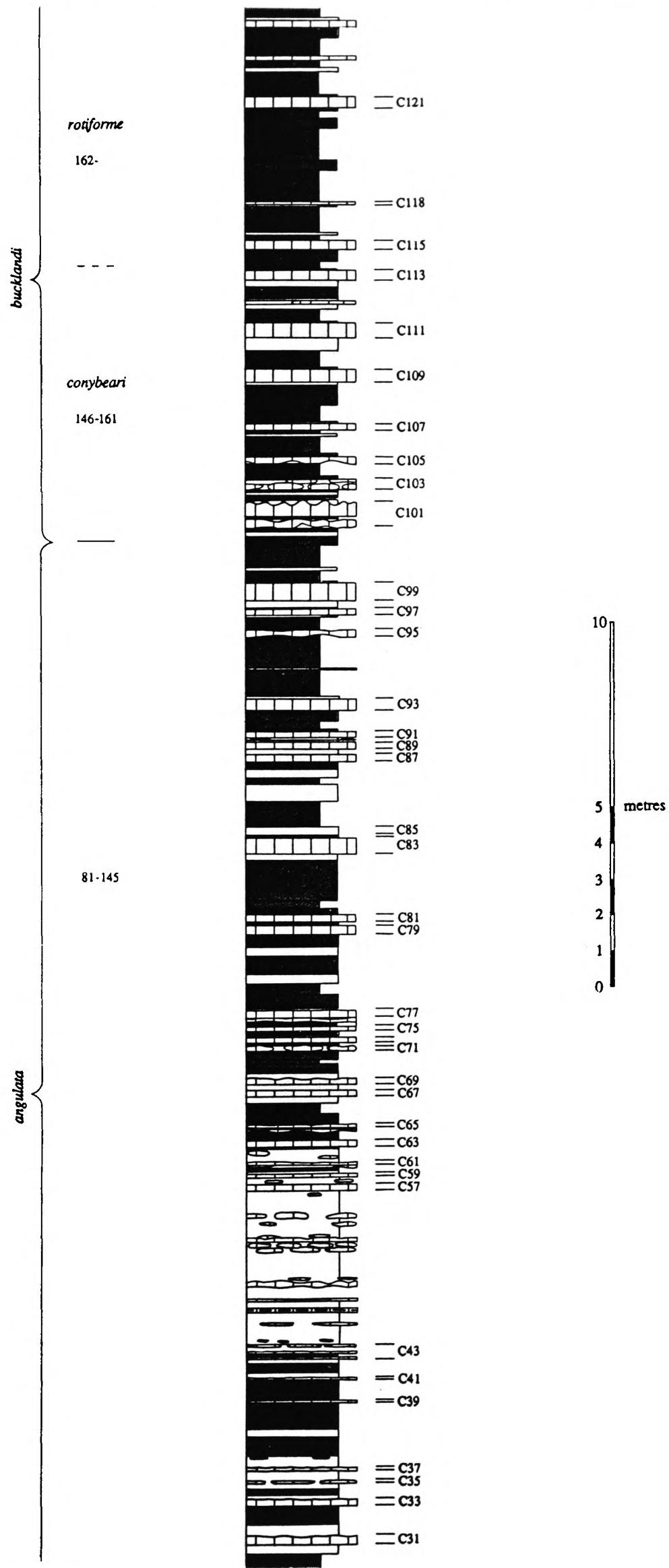


FIGURE 3.04 Stratigraphic log for the Blue Lias at Kilve Pill, Somerset.
 (Unpublished, courtesy of Hesselbo & Jenkyns.) Bed numbers are taken from Palmer (1972).
 Biostratigraphy based upon Dean *et al.* (1961) and Ivimey-Cook & Donovan (1983).
 Measured from ST144455 to ST 153452.

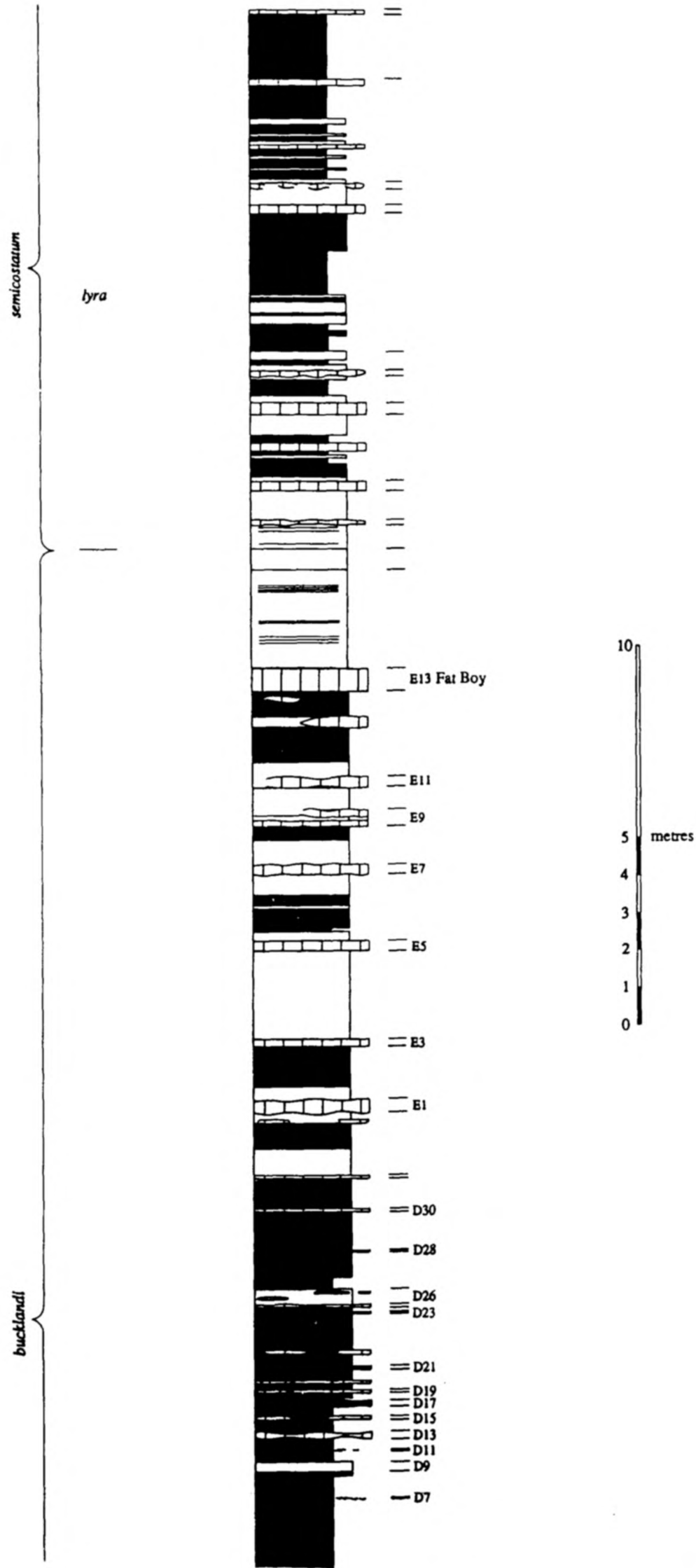


FIGURE 3.05 Stratigraphic log for the Blue Lias at Kilve Pill, Somerset (ST 139457 - ST 144455) and Hinkley Point, Somerset (ST 210465). (Unpublished, courtesy of Hesselbo & Jenkyns). Bed numbers are taken from Palmer (1972). Biostratigraphy based upon Dean *et al.* (1961) and Ivimey-Cook & Donovan (1983).

St Mary's Well Bay, Glamorgan

Bed numbers from Trueman (1920)

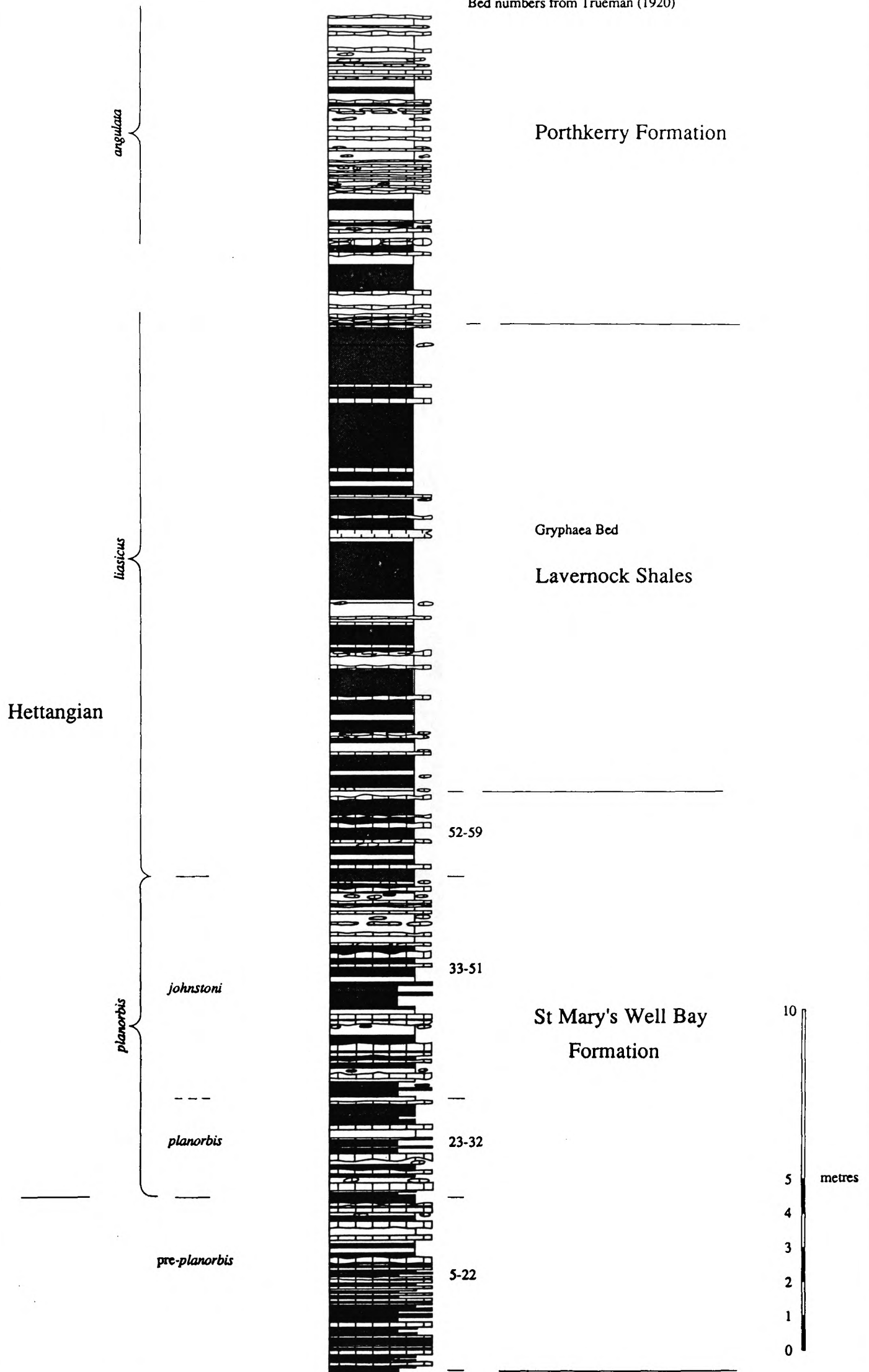


FIGURE 3.06 Stratigraphic log for the Blue Lias at St. Mary's Well Bay, Glamorgan (ST 176677 to ST 187681). (Unpublished, courtesy of Hesselbo & Jenkyns). Bed numbers are taken from Trueman (1920). Biostratigraphy based upon Trueman (1920), Cope *et al.* (1980), Waters & Lawrence (1987) and Wilson *et al.* (1990).

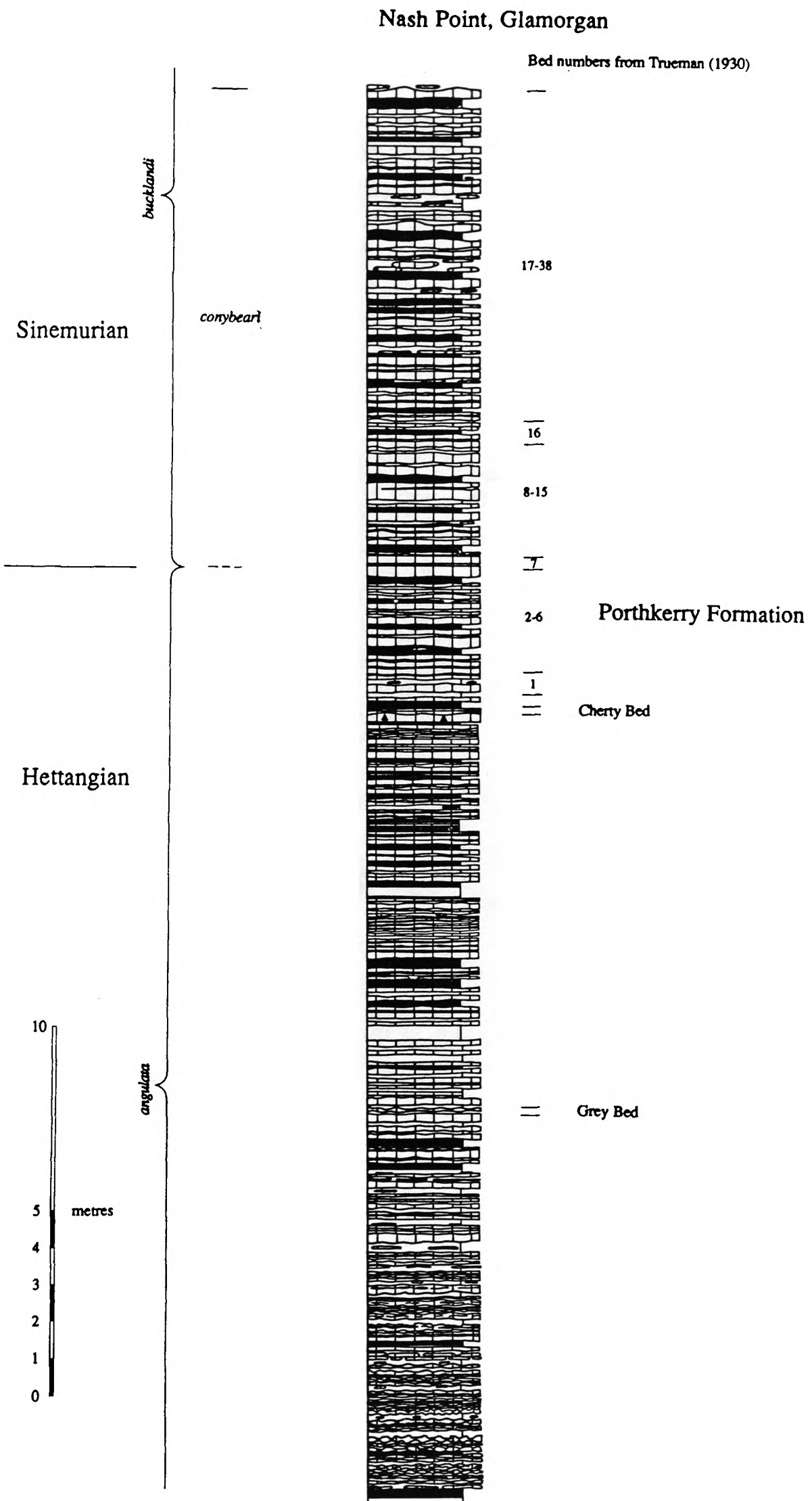


FIGURE 3.07 Stratigraphic log for the Blue Lias at Nash Point, Glamorgan (SS 914684). (Unpublished, courtesy of Hesselbo & Jenkyns). Bed numbers are taken from Trueman (1930). Biostratigraphy based upon Trueman (1930), Cope *et. al.* (1980), Waters & Lawrence (1987) and Wilson *et al.* (1990).

Charmouth - foreshore and cliff below Black Ven

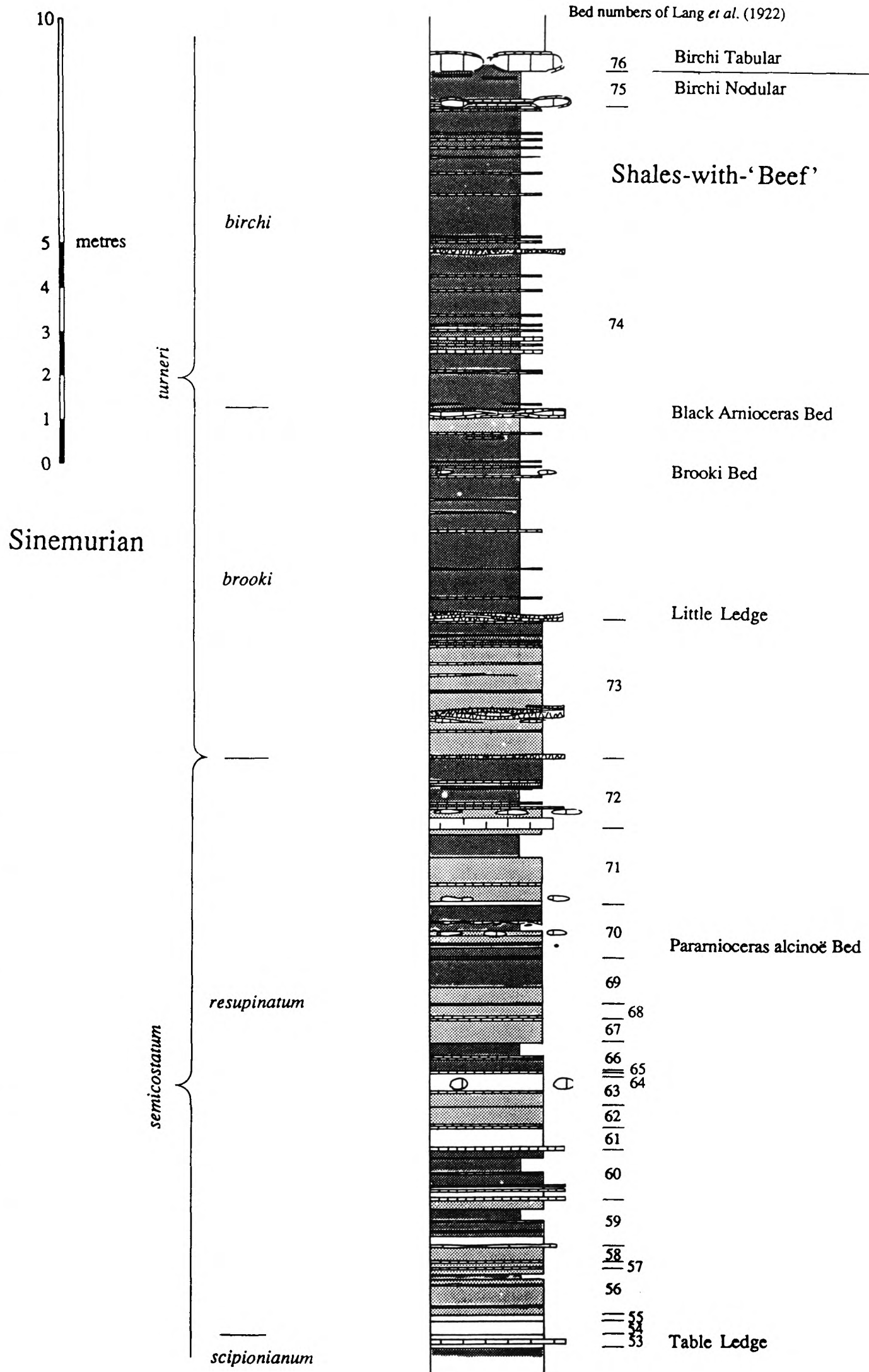


FIGURE 3.08 A Stratigraphic log for the upper Shales-with-'Beef' (from Hesselbo & Jenkyns 1995a). Bed numbers are taken from Lang *et al.* (1922) and biostratigraphy based on Lang *et al.* (1922) and Dean *et al.* (1961).

Charmouth - cliff below Stonebarrow

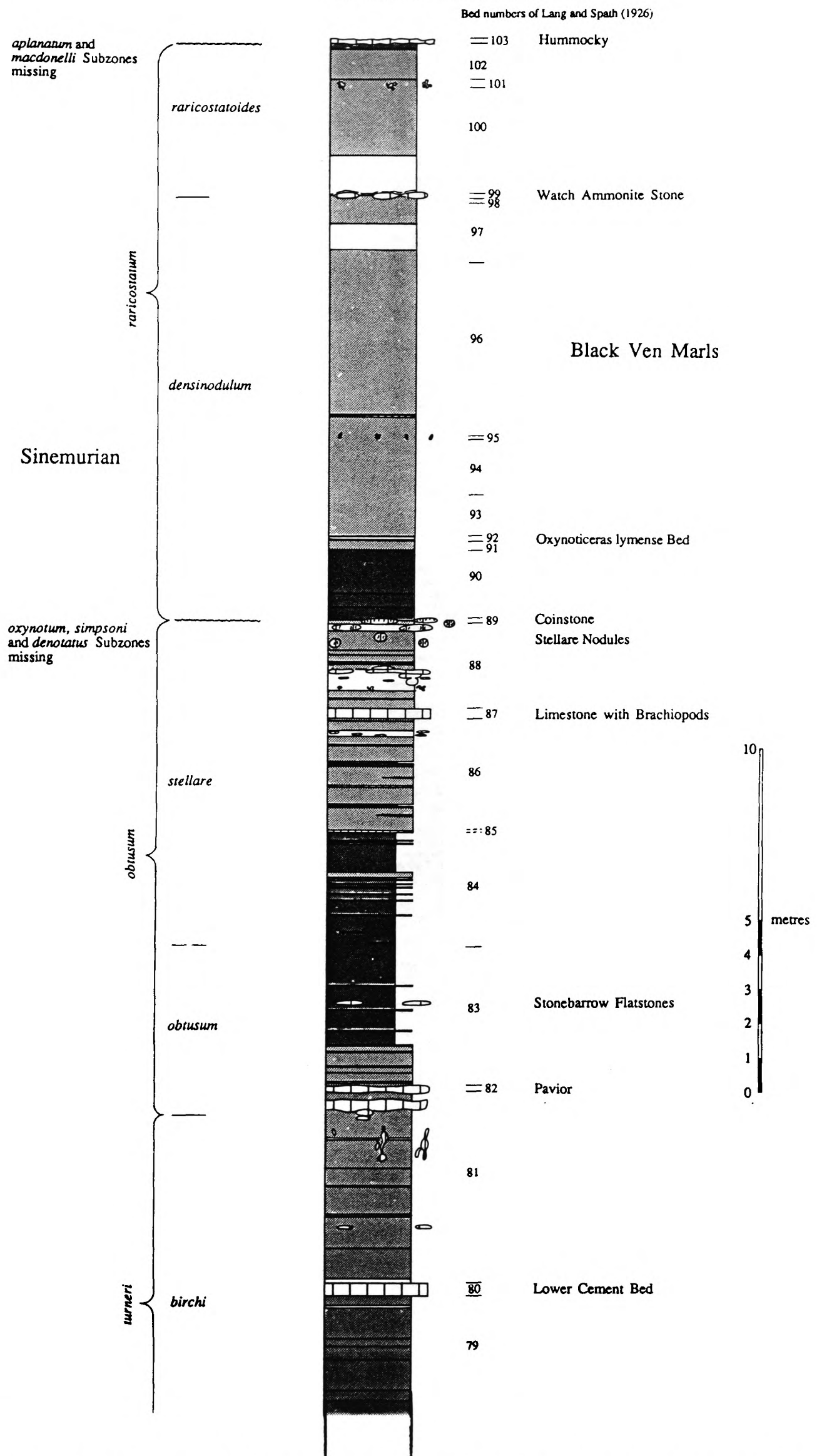


FIGURE 3.08 B Stratigraphic log for the Black Ven Marls (from Hesselbo & Jenkyns 1995a). Bed numbers are taken from Lang & Spath (1926) and biostratigraphy based on Lang & Spath (1926) and Dean *et al.* (1961).

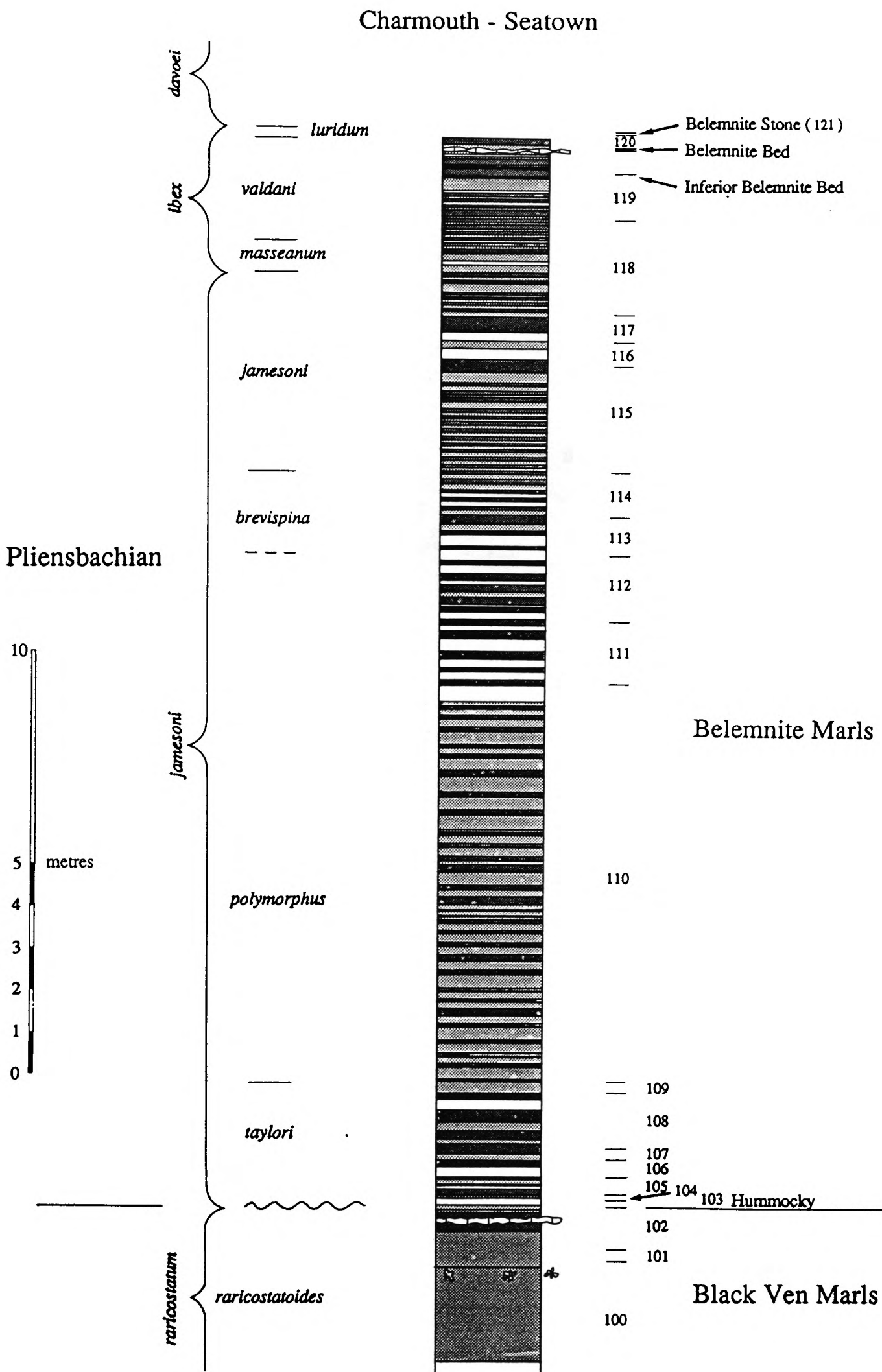


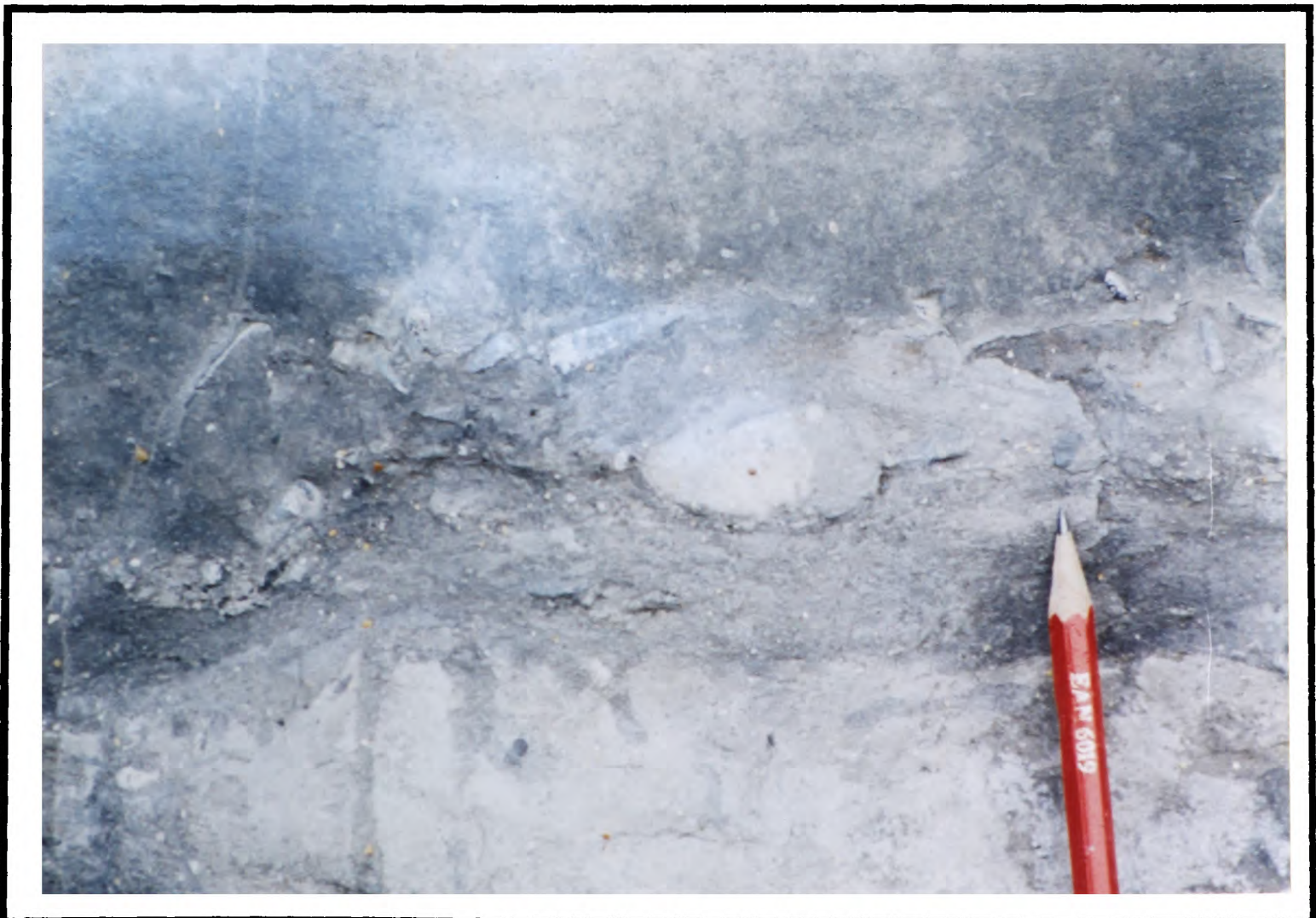
FIGURE 3.09 Stratigraphic log for the Belemnite Marls based on a number of exposures along the Dorset coast, stretching from beneath Stonebarrow in the west (SY 380927) to Seatown in the east (SY 415918). Bed numbers are taken from Lang *et al.* (1928) with biostratigraphy based mainly upon the work of on Lang *et al.* (1928) and Dean *et al.* (1961). (Taken from Hesselbo & Jenkyns 1995a).



FIGURE 3.10 Sinemurian - Pliensbachian Stage boundary, Dorset (SY 380927)

(ABOVE) The top of the Hummocky limestone (bed 103) , an erosional disconformity at which the two highest subzones of the *raricostatum* Zone are absent; it represents the boundary between the Sinemurian and Pliensbachian Stages in Dorset. There is a distinct change in depositional style in the Lower Pliensbachian away from dominantly argillaceous style of deposition (typified by the Black Ven Marls) to a more pelagic style of deposition and the development of light marl - dark marl couplets. Geological hammer is 35 cm in length.

(BELOW) *Skolithos* in the Hummocky limestone. The base of the Hummocky limestone is probably the deepest level to which Pliensbachian burrowers penetrated (Hesselbo & Jenkyns 1995a). Pencil is 6 cm in length.



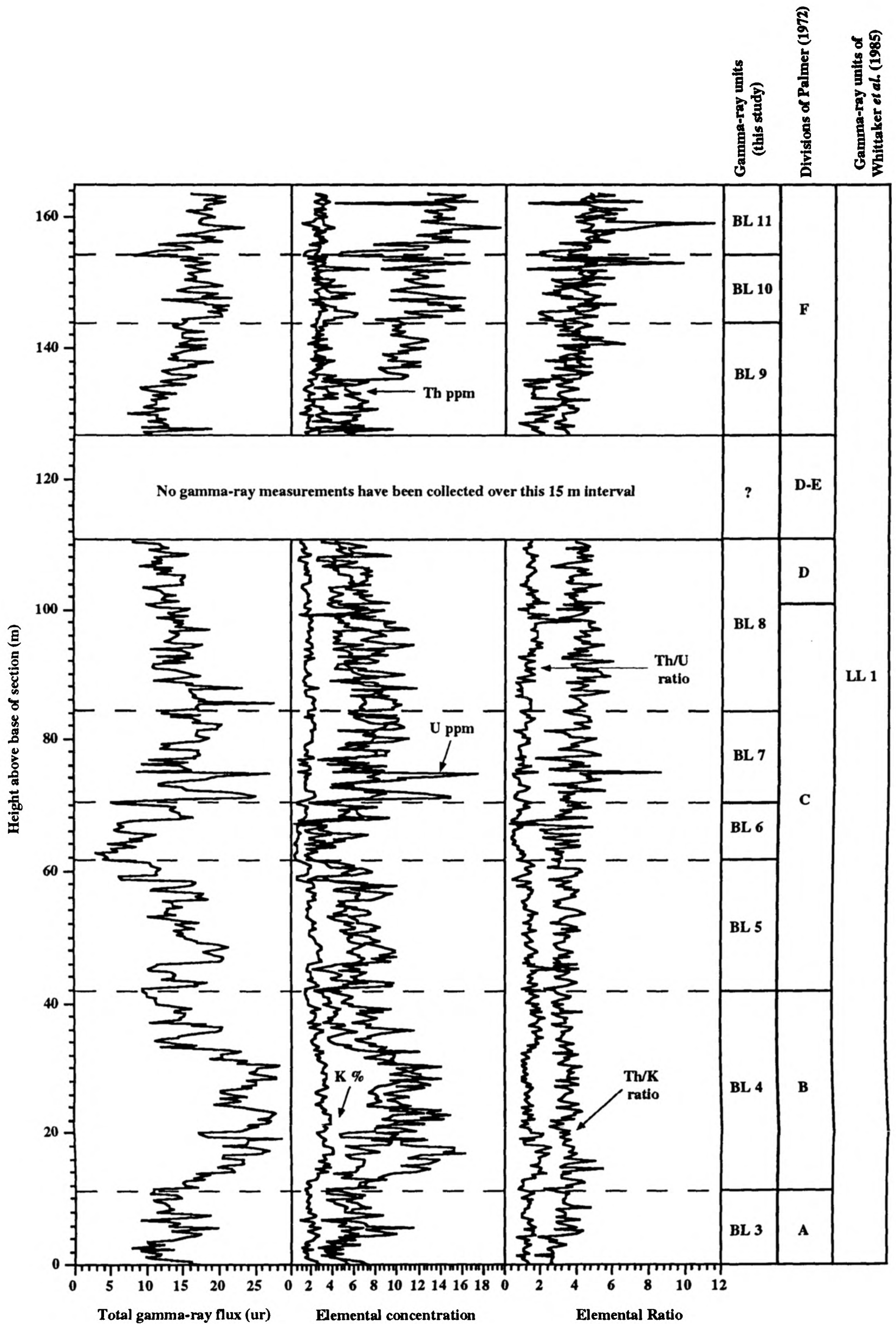


FIGURE 3.11 Gamma-ray logs for the Lower Lias of the Somerset coast based on 501 individual measurements. The Blue Lias has been subdivided on the basis of total gamma-ray signature and elemental log signature into 9 gamma-ray units, BL 3 to BL 11. These gamma-ray units are at an equal or higher resolution than the lithostratigraphic divisions proposed by Palmer (1972). The units of Whittaker *et al.* (1985), identified from the same sequence from the Burton Row borehole in Somerset, are also shown. Clearly, much finer subdivision of the Whittaker *et al.* gamma-ray units is possible.

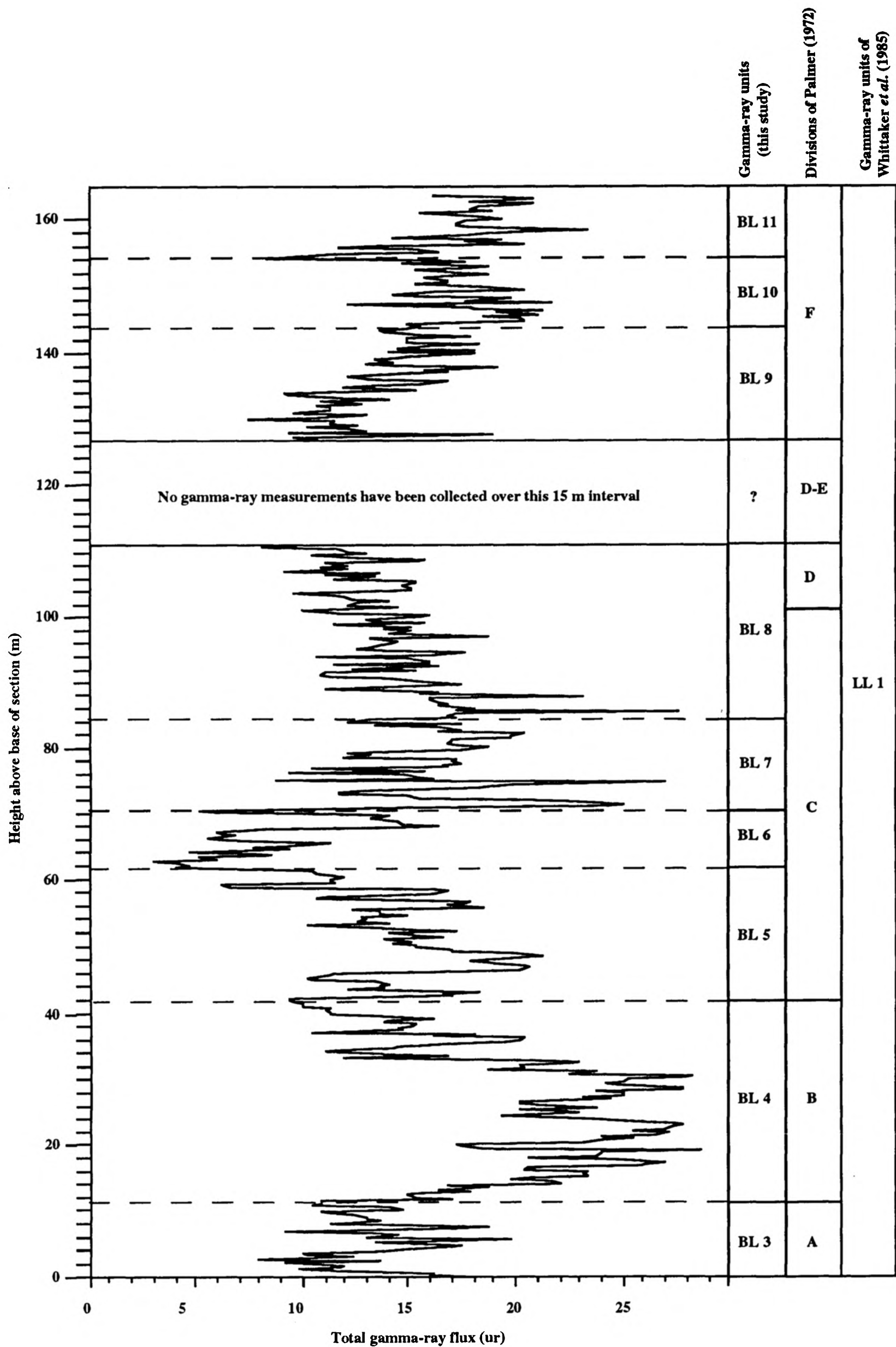


FIGURE 3.12 Stratigraphic packaging within the Lower Lias of the Somerset coast based on total gamma-ray signature. The gamma-ray units, defined in this study, can be enhanced by altering the aspect ratio of the total gamma-ray flux scale to exaggerate the low frequency component of the total gamma-ray signature. The units of Whittaker *et al.* (1995), identified for the same sequence from the Burton Row borehole in Somerset, are also shown.

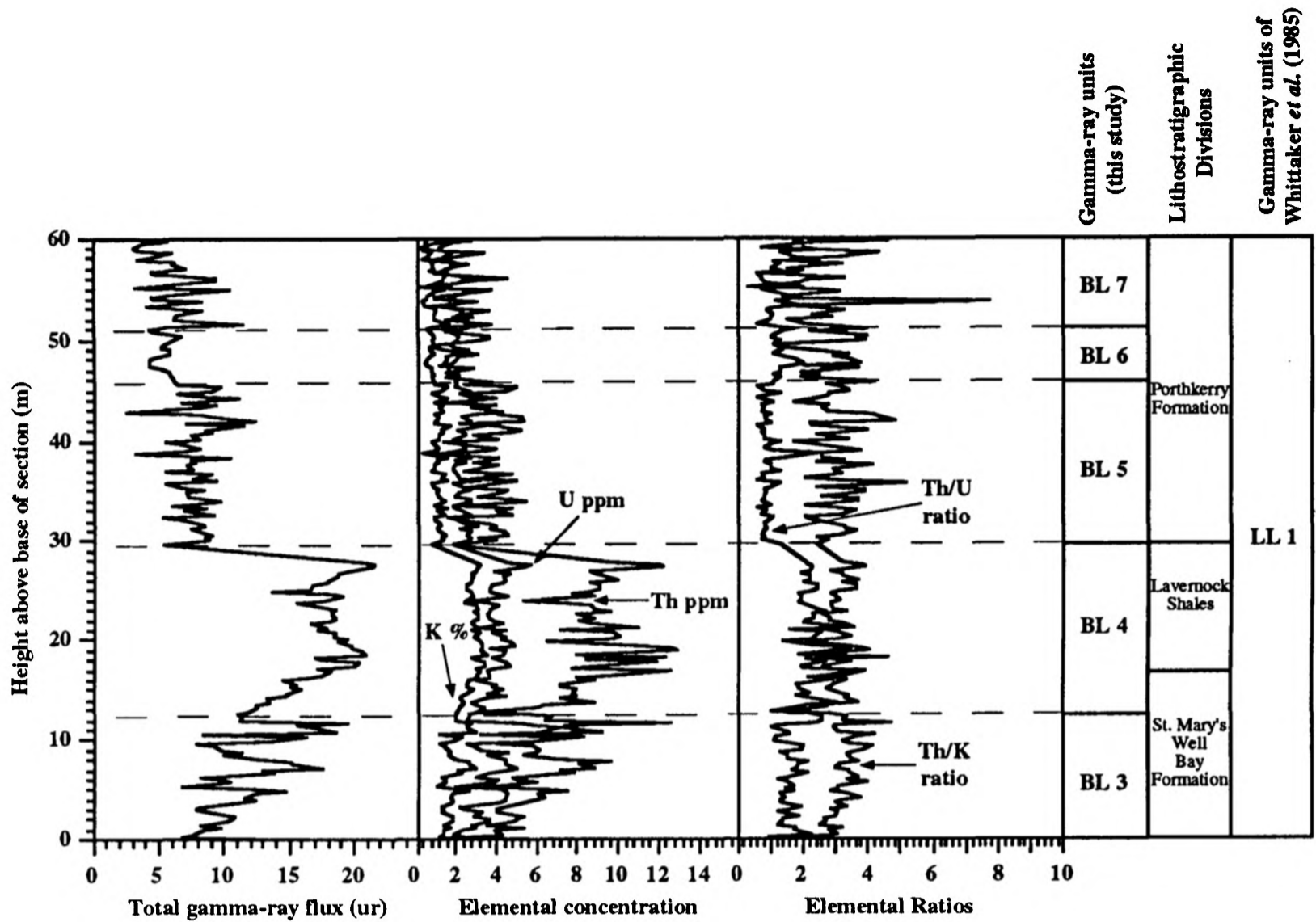


FIGURE 3.13A Gamma-ray logs for the Lower Lias succession of the Glamorgan coast based upon 196 sets of measurements. The St. Mary's Well Bay Formation, Lavernock Shales and Porthkerry Formation have been subdivided on the basis of total gamma-ray signature and elemental-log signature into 5 gamma-ray units. These are equivalent to the single unit identified by Whittaker *et al.* (1995) for the same sequence from the Burton Row borehole in Somerset. Clearly, finer subdivision of the Lower Lias gamma-ray signature is possible. The vertical scale is identical to that used in Figures 3.11 and 3.12.

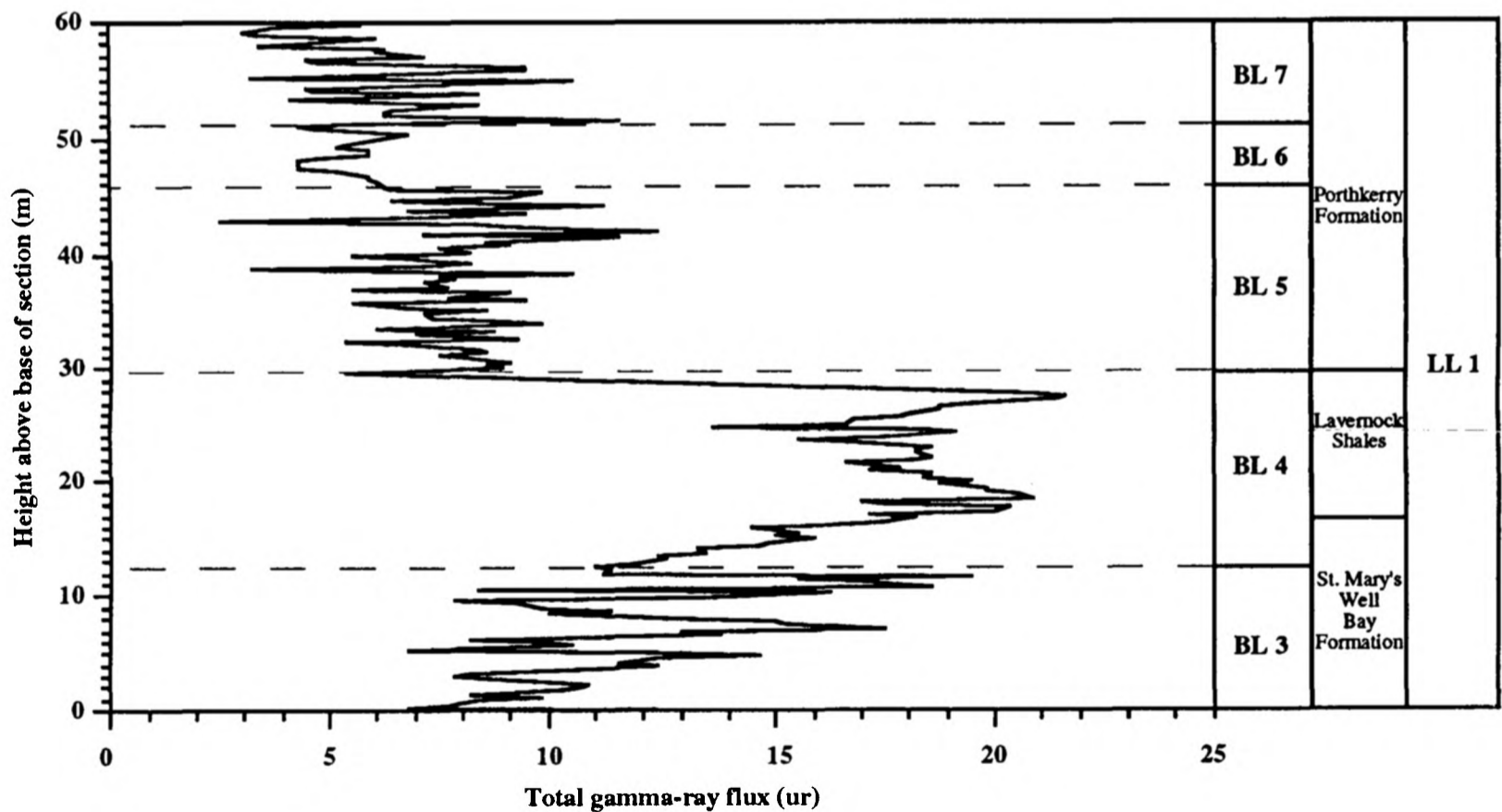


FIGURE 3.13B Stratigraphic packaging within the Lower Lias of the Somerset coast based on total gamma-ray signature. The gamma-ray units, defined in this study, can be enhanced by altering the aspect ratio of the total gamma-ray flux scale to exaggerate the low frequency component of the total gamma-ray signature. The vertical scale is identical to that used in Figures 3.11 and 3.12.



FIGURE 3.14 The Blue Lias, St Audrie's Bay, Somerset

(ABOVE) The yellow field notebook is placed at the horizon currently recognised at which ammonites of the genus *Psiloceras* first appear and which delineate the boundary between the Rhaetian (Triassic) and Hettangian (Jurassic). The first appearance occurs six metres above the base of the Blue Lias. The section (ST 102433) has been recently proposed as a candidate Global Stratotype Section for the base of the Jurassic System (Warrington *et al.* 1994). (Dimensions of notebook 20 cm x 13 cm).

(BELOW) Field aspect of the *liasicus* Zone at St Audrie's Cliff (St. Audrie's Shales of Palmer 1972). The *liasicus* Zone is dominantly argillaceous, a consistent character over southern Britain. The series of limestones in the middle of the cliff are Palmer's beds C1 to C29. (Cliff approximately 18 m in height).





FIGURE 3.15 The Blue Lias, East of Kilve Pylle, Somerset

(ABOVE) Field aspect of the *angulata* Zone and lowermost *bucklandi* Zone exposed east of Kilve Pylle (ST 153452). The section is typified by high-frequency alternations between limestone and marl and is equivalent to beds C31 to C121 of Palmer (1972). The boundary between the *angulata* Zone and *conybeari* Subzone (*bucklandi* Zone) is located just below the base of limestone C101 as indicated. (Cliff is approximately 40 m in height)

(BELOW) The *bucklandi* Zone at Kilve Pylle (ST 144455). The section represents the *rotiforme* Subzone with the thick limestone above the dark marl unit being C121 of Palmer 1972. (Field assistant is 1.82 m high).



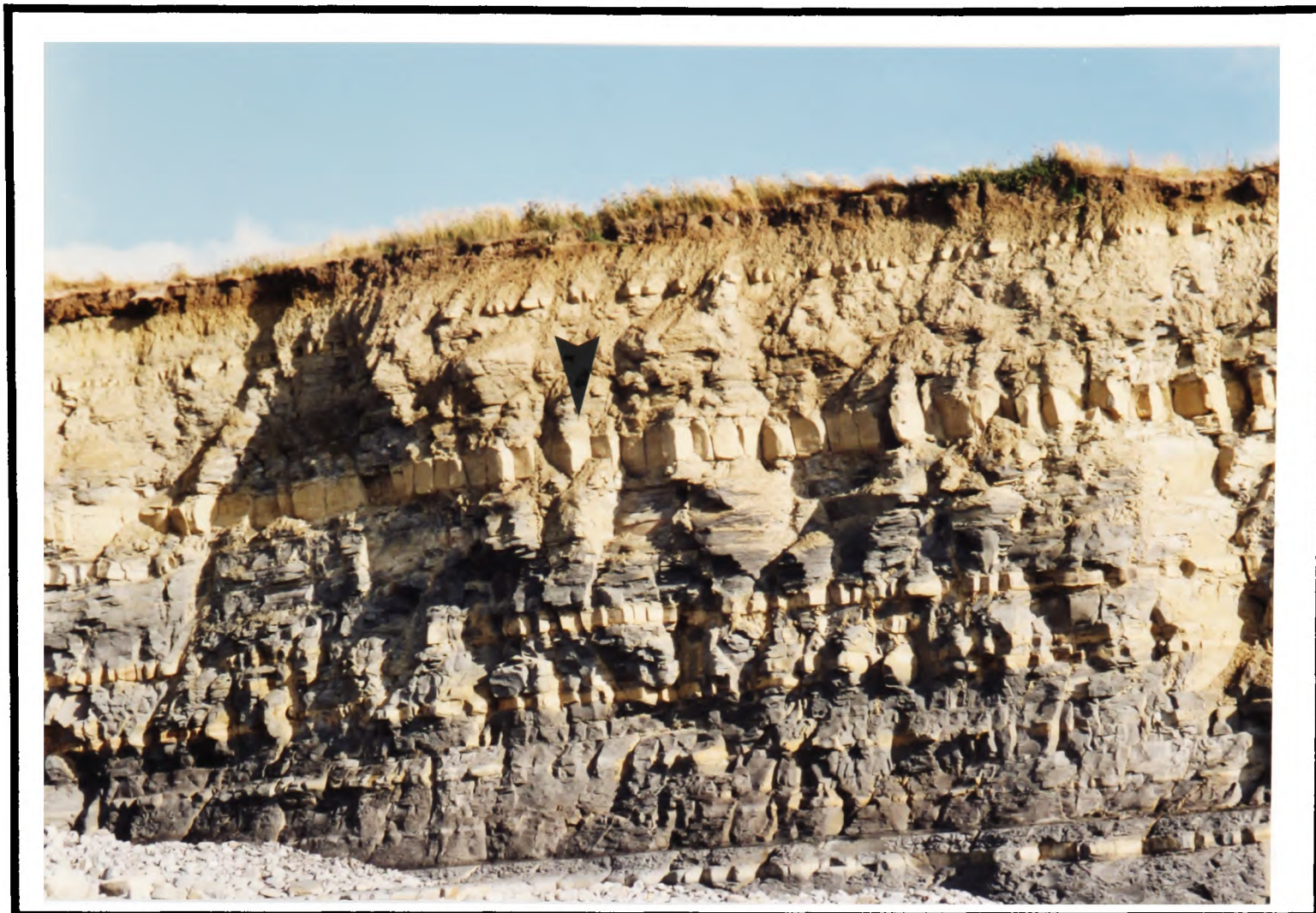


FIGURE 3.16 The Blue Lias, West of Kilve Pylle and at Hinkley Point, Somerset

(ABOVE) Field aspect of the *bucklandi* Subzone of the *bucklandi* Zone, west of Kilve Pylle (ST 139457 - ST 14455). The section corresponds to Division D of Palmer (1972). The thick prominent limestone running through the cliff is known as Fat Boy (bed number E13). Cliff is 8.6 m in height.

(BELOW) Field aspect at Hinkley Point (ST 210465) of the *lyra* Subzone of the *semicostatum* Zone. The section is entirely exposed as foreshore and corresponds to the Doniford Shales of Palmer (1972).





Figure 3.17 The Blue Lias at Doniford Bay, Somerset

Field aspect of the *lyra* Subzone of the *semicostatum* Zone at the west end of Doniford Bay (ST 079433 to ST 082430). The section exposed corresponds to the Doniford Shales of Palmer (1972). The *lyra* Subzone is dominantly argillaceous and is expanded by a factor of 38.3 relative to the time equivalent strata exposed at Seven Rock Point, Lyme Regis (ST 328910). Dimensions of yellow field-notebook are 20 cm x 13 cm.



FIGURE 3.18 The Blue Lias at St. Mary's Well Bay and Lavernock Point, Glamorgan

(ABOVE) The yellow field notebook is placed at the horizon at which ammonites of the genus *Psiloceras* first appear and which therefore delineates the boundary between the Rhaetian (Triassic) and Hettangian (Jurassic). The first appearance is 5 m above the base of the Blue Lias (St. Mary's Well Bay Formation of Richardson 1905). Dimensions of notebook 20 cm x 13 cm. Grid Reference ST 176677.

(BELOW) The yellow field notebook is placed on the boundary between the underlying argillaceous Langport Member (Lilstock Formation) and the Bull Cliff Member of the Blue Lias. The Bull Cliff Member (*pre-planorbis*) is characterised by a 4 m sequence of planar bedded limestones with minor mudstone horizons. Section exposed at Lavernock Point (ST 187681).





FIGURE 3.19 The Blue Lias at St. Mary's Well Bay , Glamorgan

(ABOVE) Field aspect of the *liasicus* Zone (Lavernock Shales of Strahan & Cantrill 1902) at the designated type locality (Waters & Lawrence 1987) between St. Mary's Well Bay and Lavernock Point (ST 176677 - ST 187681). The *liasicus* Zone is characterised by a series of dark grey, calcareous, bioturbated mudstones with subordinate beds of nodular limestone and correspond in Somerset to the St. Audrie's Shales of Palmer (1972). Cliff is approximately 37 m in height.

(BELOW) The yellow field notebook is placed above the boundary between the underlying St Mary's Well Bay Formation and the overlying Lavernock Shales. The lithostratigraphic contact occurs within the *liasicus* Zone. (Dimensions of field notebook 20 cm x 13 cm).

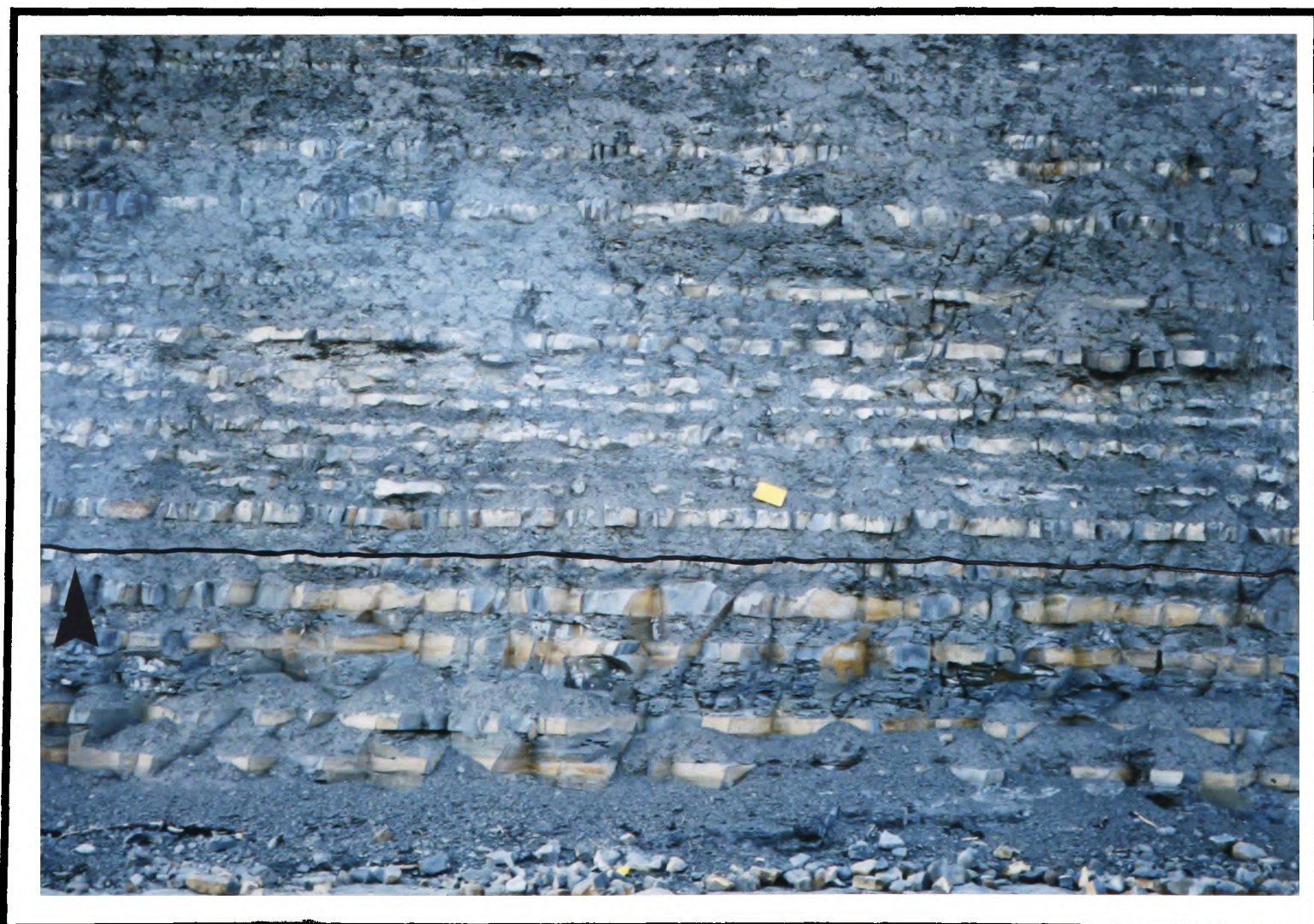
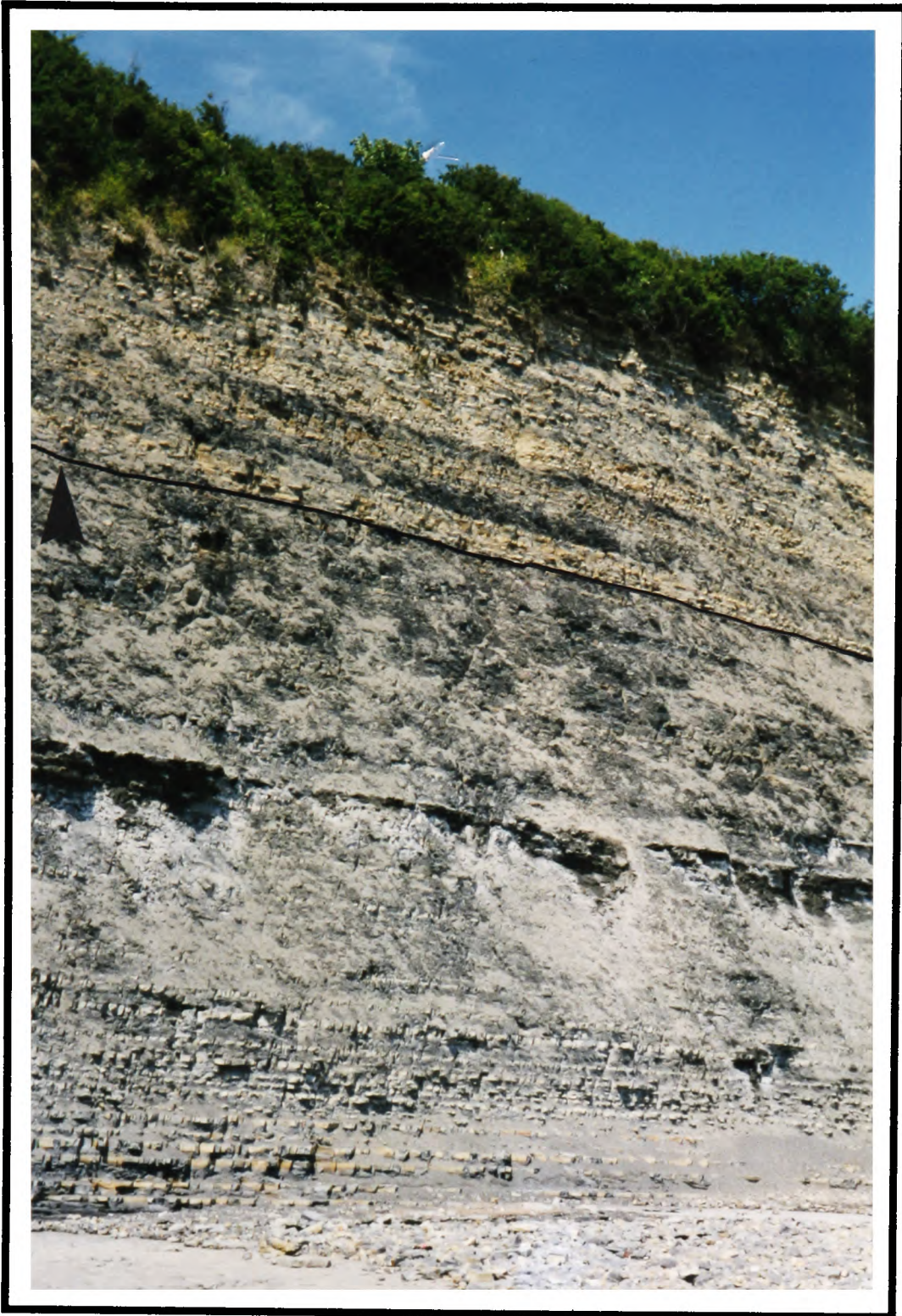


FIGURE 3.20

The Blue Lias at St. Mary's Well Bay and Nash Point, Glamorgan



(LEFT) Contact between the Lavernock Shales (*liasicus* Zone) and the Porthkerry Formation (*angulata* Zone) between St Mary's Well Bay and Lavernock Point (ST 176677 - ST 187681). The boundary is taken at the base of the first continuous group of limestone beds which contrast with the argillaceous nature to the underlying Lavernock Shales. The high - frequency alternations between limestone and marl are typical of the *angulata* Zone in the Bristol Channel Basin and correspond in Somerset to the Blue Lias (*sensu stricto*) of Palmer (1972). Cliff is approximately 37 m high.

(BELOW) The Porthkerry Formation (Trueman 1920) at Nash Point (SS 914684). The section is biostratigraphically equivalent to the *angulata* Zone and *conybeari* Subzone of the *bucklandi* Zone. The boundary between the two ammonite Zones runs mid-way through the cliff, above which the limestone beds become markedly thicker and less concretionary. Cliff is 38 m high.



Stratigraphic log (unpublished, courtesy of Hesselbo & Jenkyns)

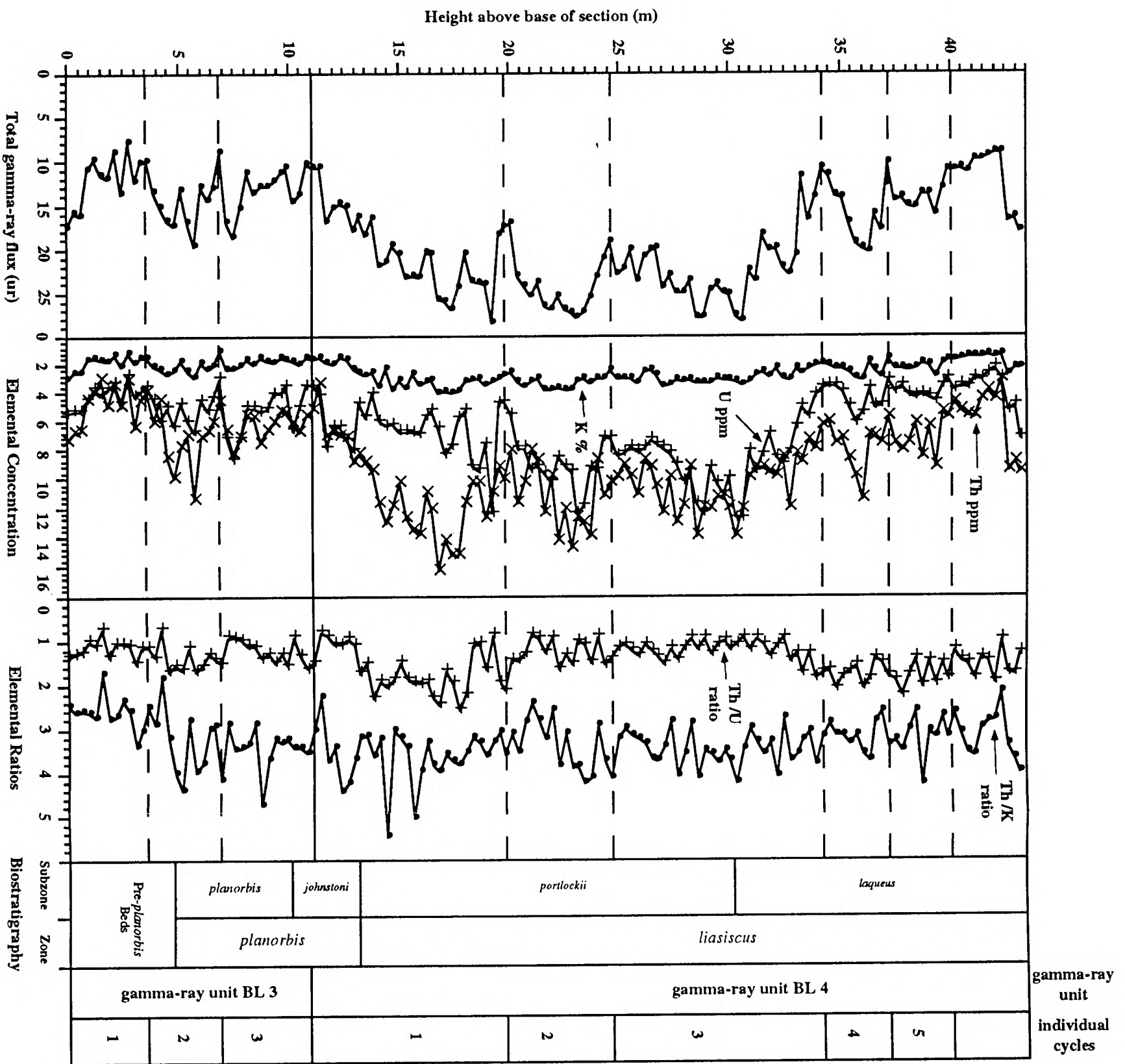


FIGURE 3.21 Total gamma-ray log, elemental concentration logs and elemental ratio curves for the Blue Lias exposed at St. Audrie's Bay, Somerset (ST 102433). Biostratigraphic boundaries are indicated. The gamma-ray logs are based on 145 sets of measurements.

Figure 3.21

East of Kilve Pylle, Somerset.

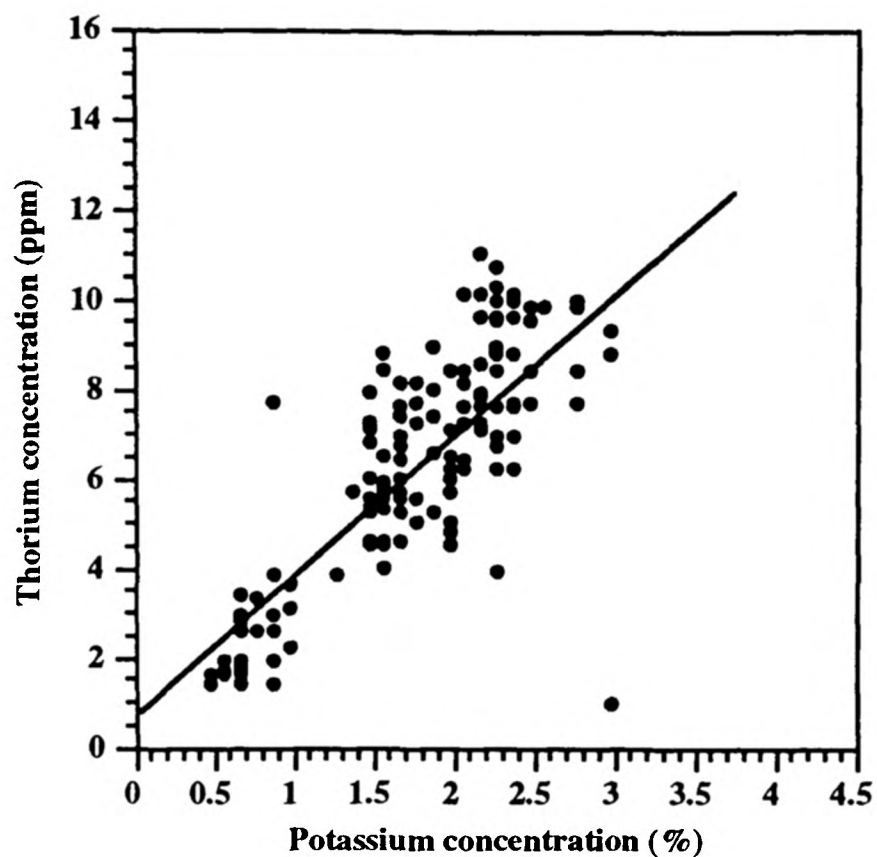


FIGURE 3.24A Linear regression correlation between Th concentration and K concentration. A correlation coefficient of 0.63 suggests a statistically robust correlation at the 95 % significance level (n = 154). The relationship between the two elements can be described by the linear equation : $\text{Th ppm} = 3.17 \text{ K \%} + 0.066$

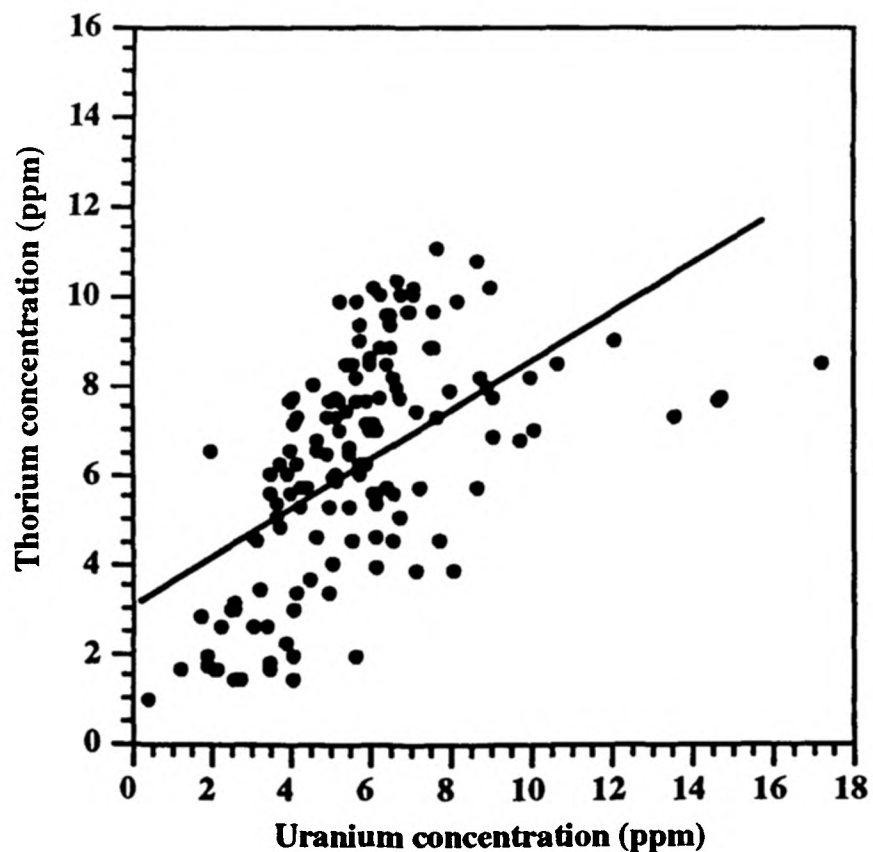
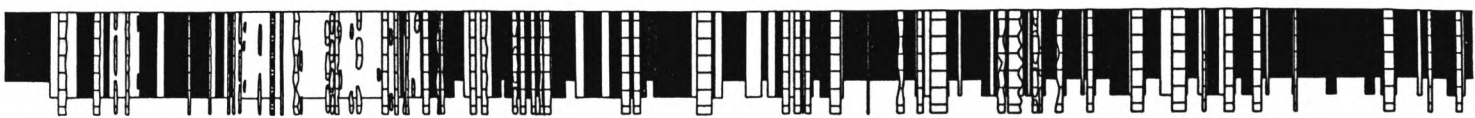


FIGURE 3.24B Linear regression correlation between Th concentration and U concentration. A correlation coefficient of 0.36 suggests a weak but statistically robust correlation at the 95 % significance level (n = 154). The relationship between the two elements can be described by the linear equation : $\text{Th ppm} = 0.550 \text{ U ppm} + 3.051$



Stratigraphic log (unpublished, courtesy of Hesselbo & Jenkins)

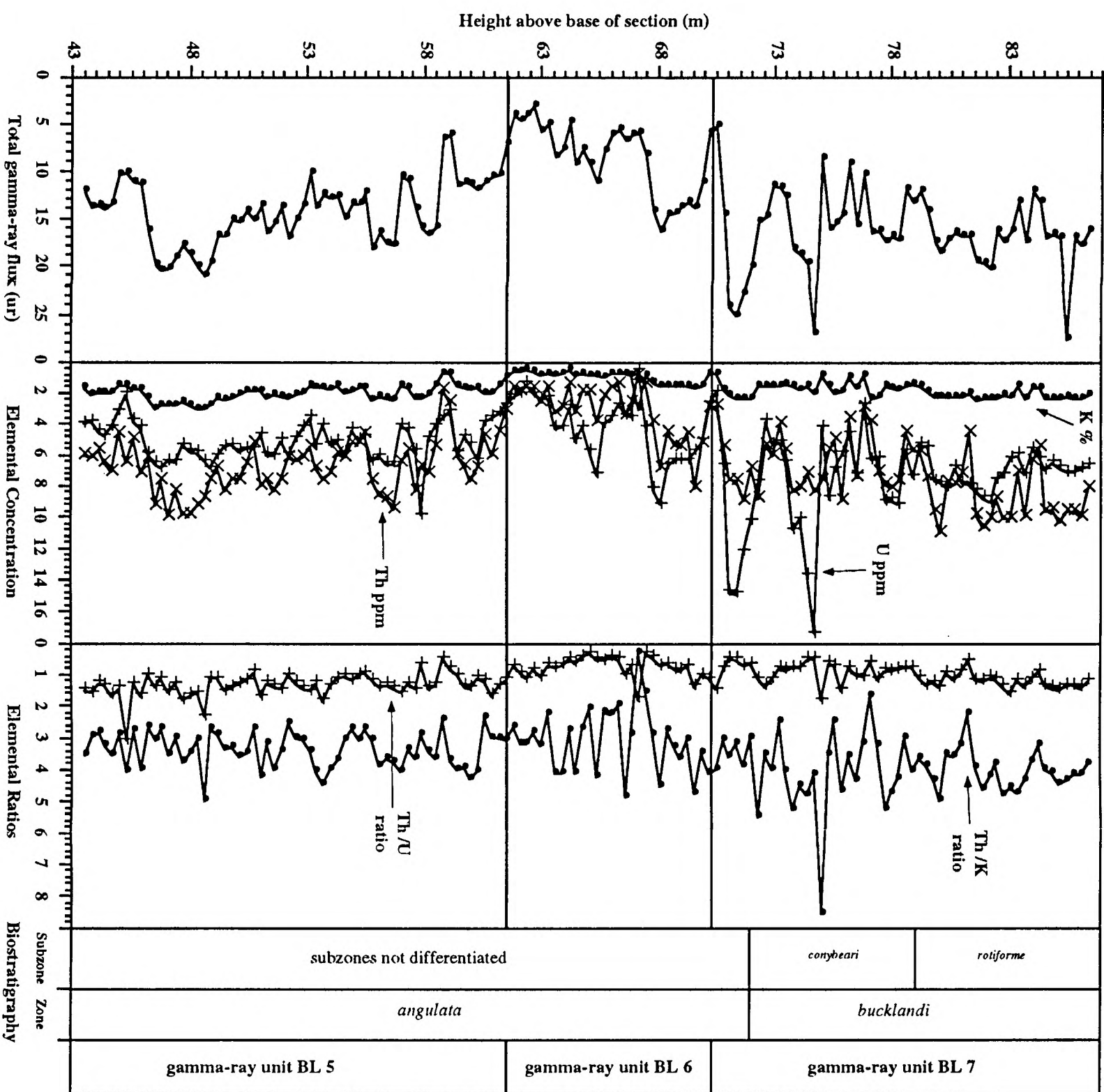


FIGURE 3.23 Total gamma-ray log, elemental concentration logs and elemental ratio curves for the Blue Lias exposed east of Kilve Pyllle, Somerset (ST 144455 to ST 153452). Biostratigraphic boundaries are indicated. The gamma-ray logs are based on 154 sets of measurements.

Figure 3.23

West of Kilve Pylle, Somerset.

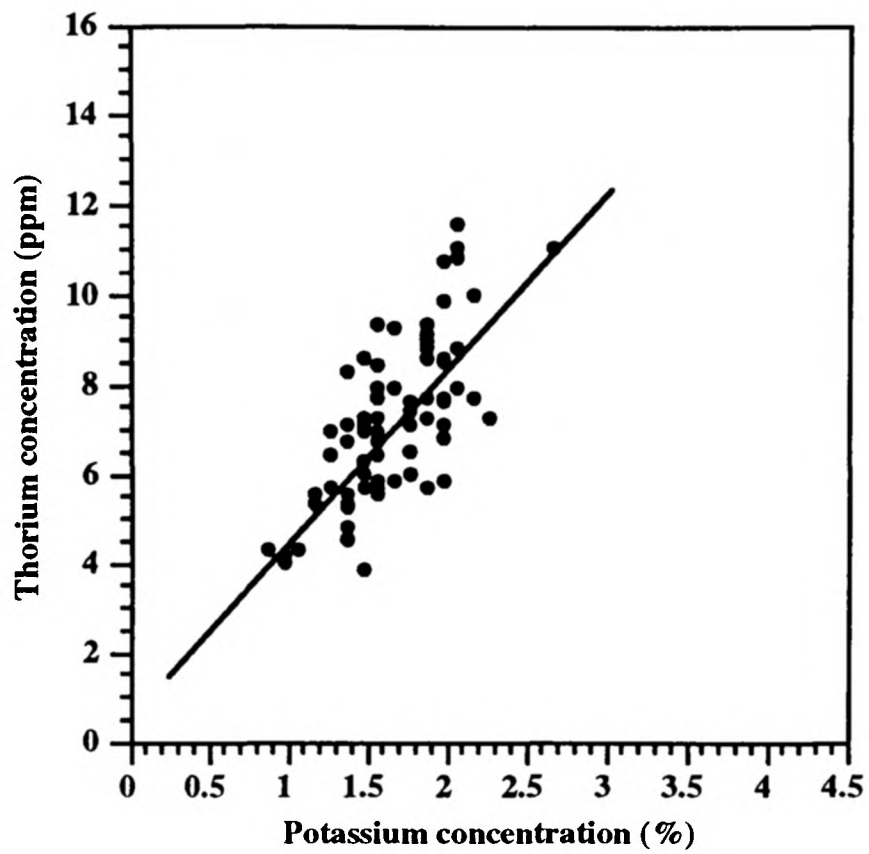


FIGURE 3.26A Linear regression correlation between Th concentration and K concentration. A correlation coefficient of 0.59 suggests a statistically robust correlation at the 95 % significance level (n = 80). The relationship between the two elements can be described by the linear equation : $\text{Th ppm} = 3.916 \text{ K \%} + 0.567$

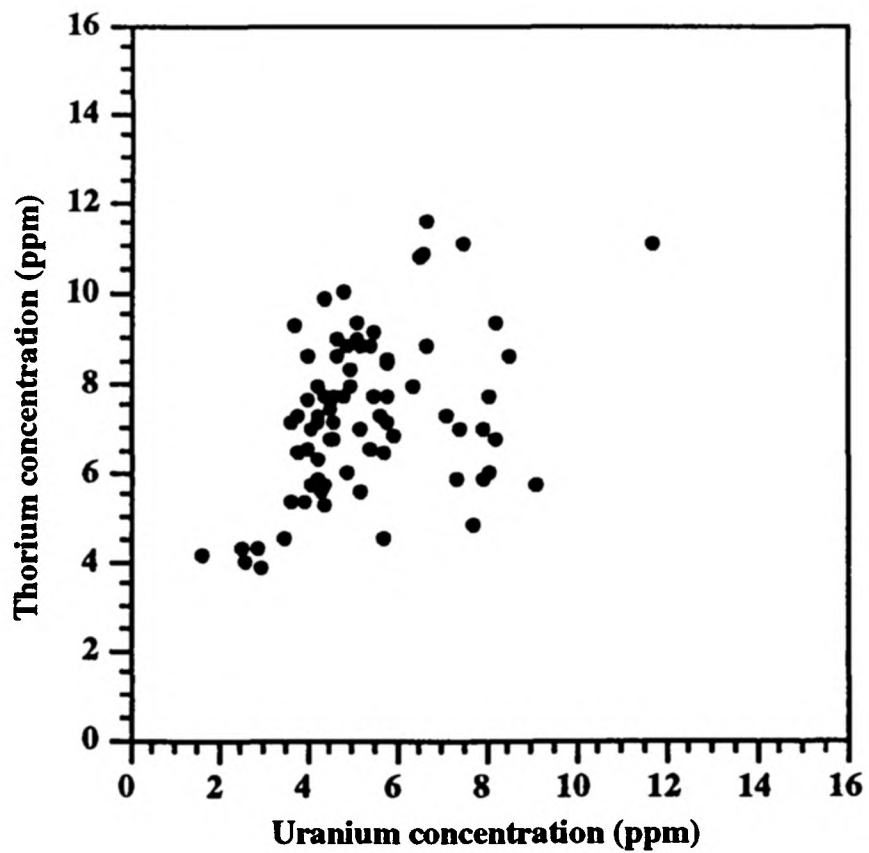


FIGURE 3.26B Linear regression correlation between Th concentration and U concentration. A correlation coefficient of 0.15 indicates that no statistically robust relationship is between the two elements (n=80).

Stratigraphic log (unpublished, courtesy of Hesselbo & Jenkins)

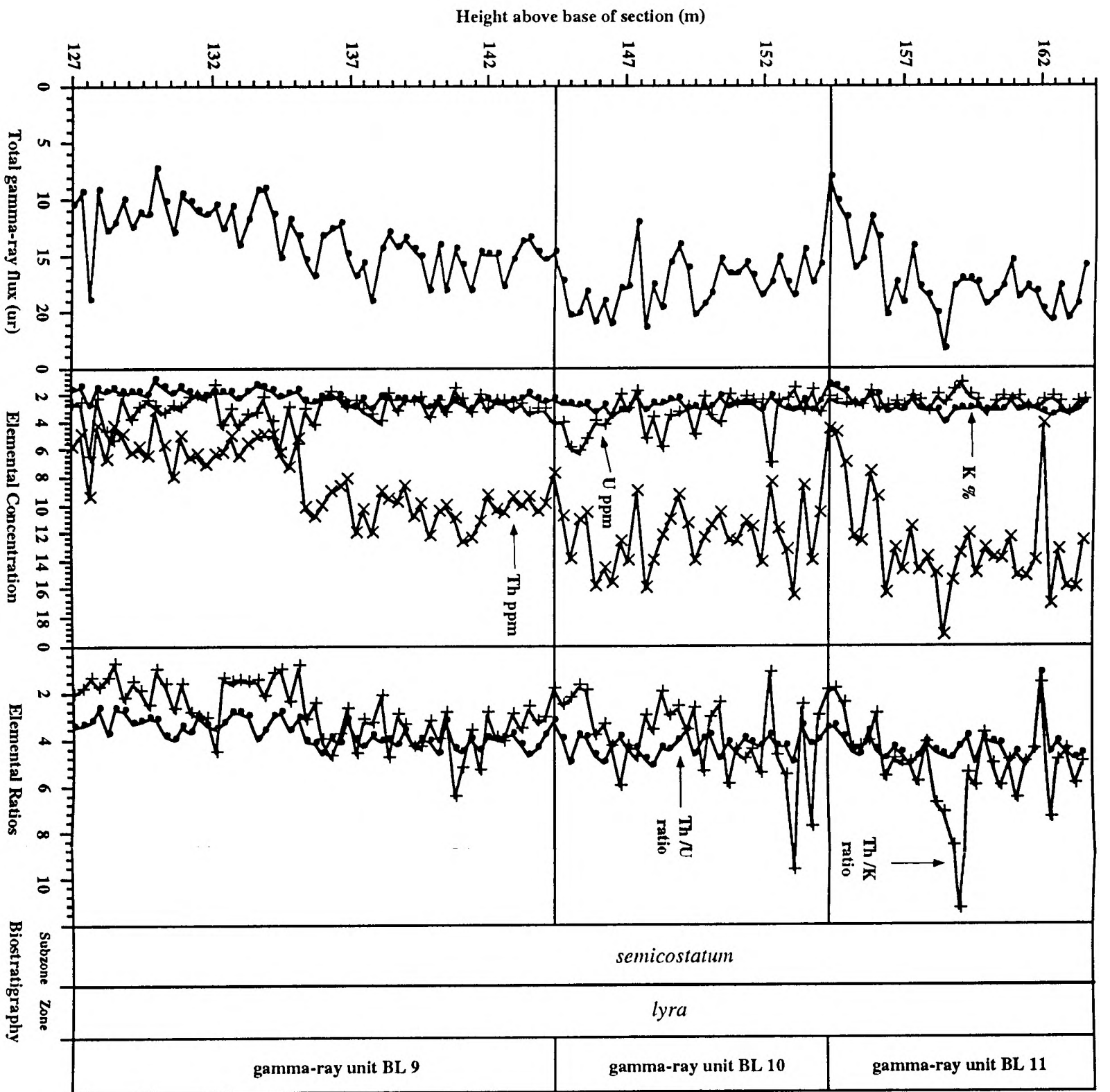
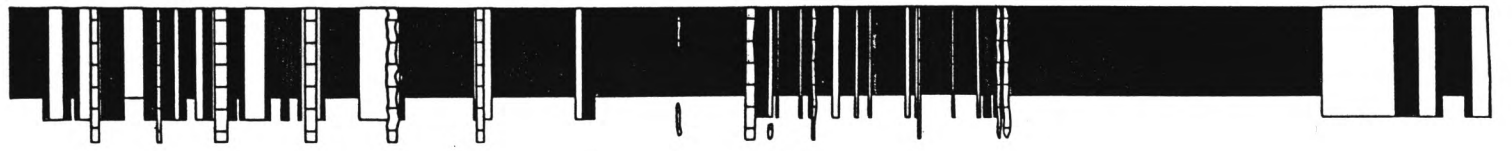


FIGURE 3.27 Total gamma-ray log, elemental concentration logs and elemental ratio curves for the Blue Lias exposed on the foreshore and as cliff section at the west end of Doniford Bay (Helwell Bay), Somerset (ST 079433 to ST 082430). Biostratigraphic boundaries are indicated. The gamma-ray logs are based on 123 measured samples.

Figure 3.27

Doniford Bay, Somerset.

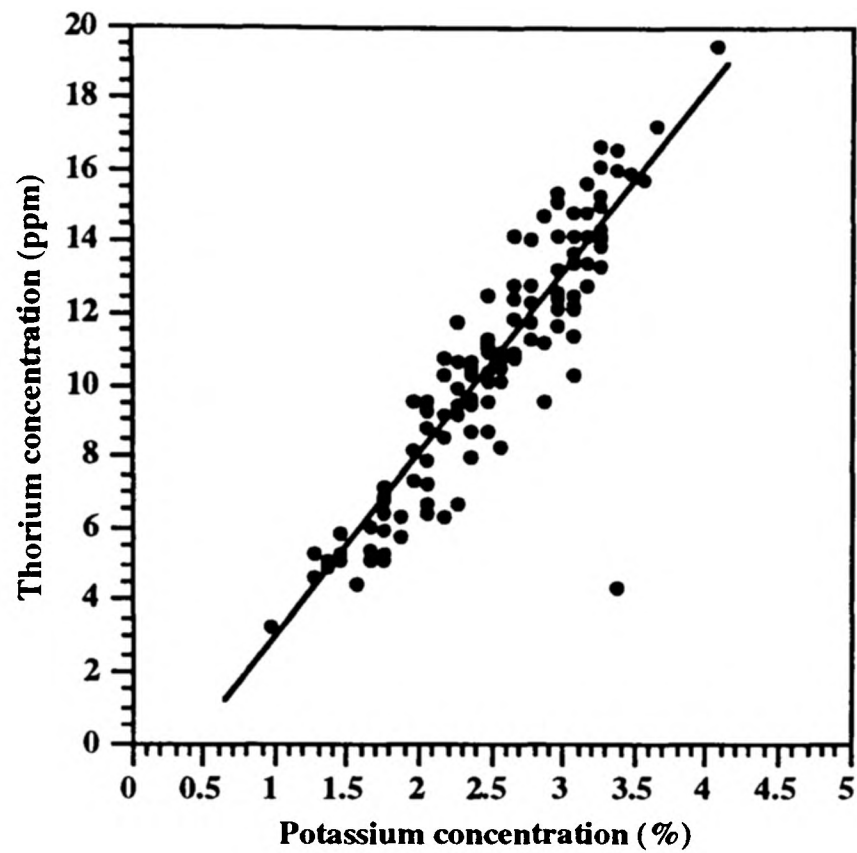


FIGURE 3.28A Linear regression correlation between Th concentration and K concentration. A correlation coefficient of 0.81 suggests a strong, statistically robust correlation at the 95 % significance level (n = 123). The relationship between the two elements can be described by the linear equation : $\text{Th ppm} = 5.190 \text{ K \%} - 2.727$

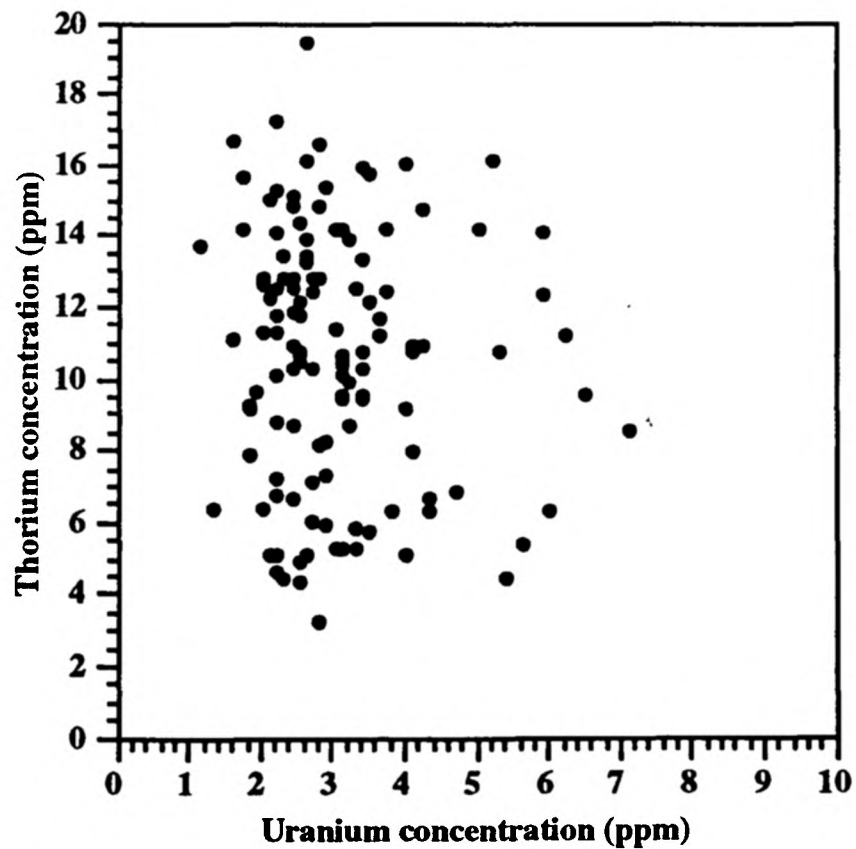
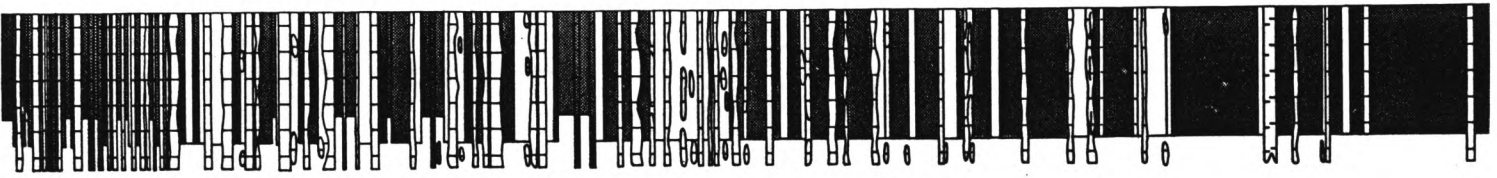


FIGURE 3.28B Linear regression correlation between Th concentration and U concentration. A correlation coefficient of 0.01 indicates that there is no linear covariant relationship between the two elements.



Stratigraphic log (unpublished, courtesy of Hesselbo & Jenkyns)

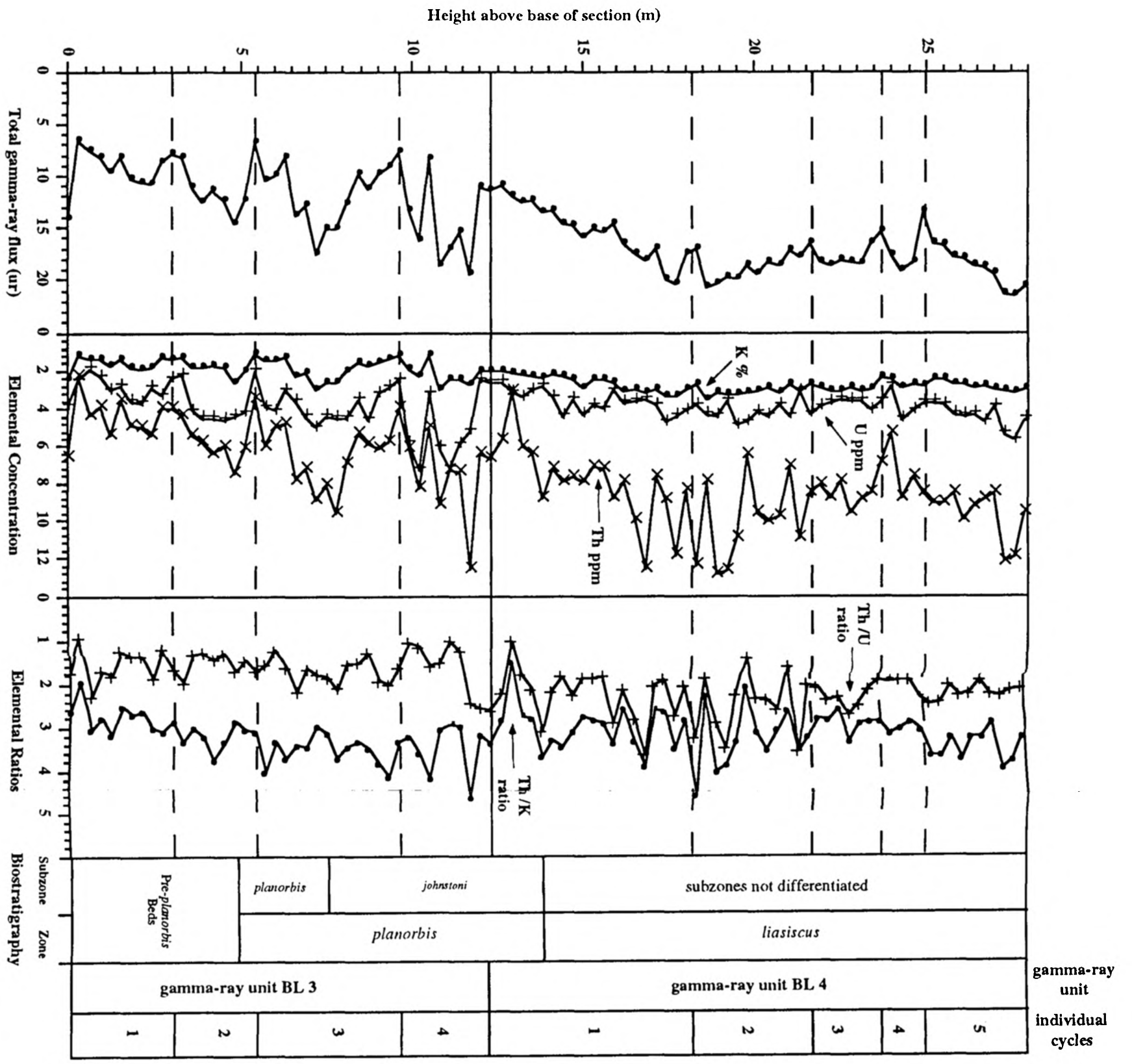


FIGURE 3.29 Total gamma-ray log, elemental concentration logs and elemental ratio curves for the Blue Lias Formation (St. Mary's Well Bay Formation and Lavernock Shales) exposed at St. Mary's Well Bay, Glamorgan (ST 176677 - ST 187681). Biostratigraphic boundaries are indicated. The gamma-ray logs are based on 96 sets of measurements.

Figure 3.29

St. Mary's Well Bay, South Glamorgan.

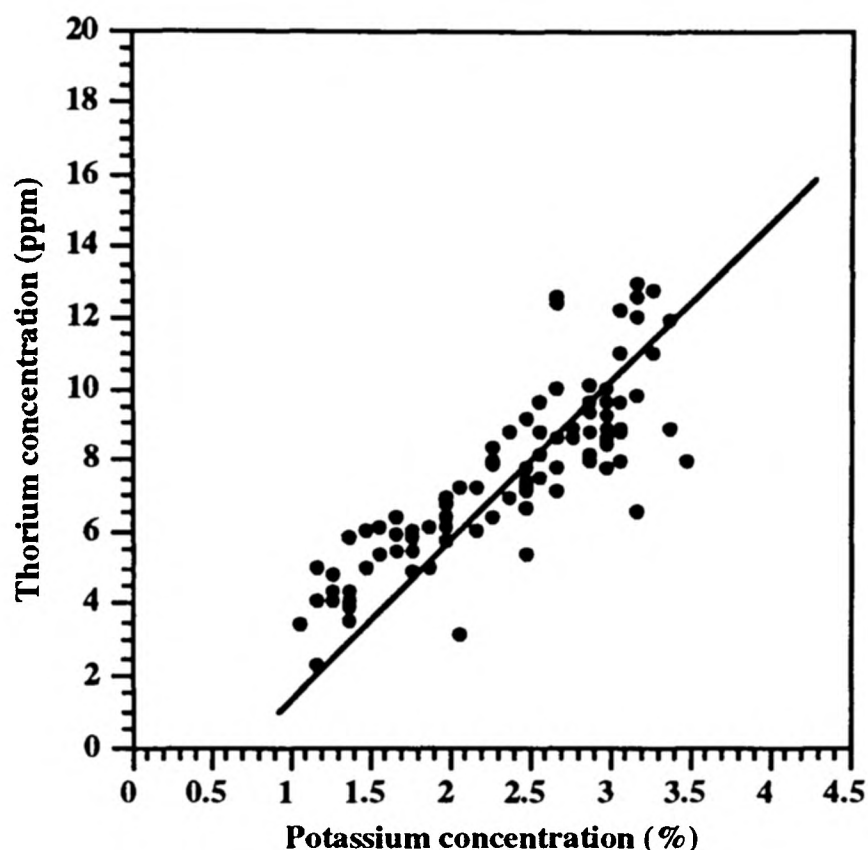


FIGURE 3.30A Linear regression correlation between Th concentration and K concentration. A correlation coefficient of 0.73 suggests a statistically robust correlation at the 95 % significance level (n = 96). The relationship between the two elements can be described by the linear equation : $\text{Th ppm} = 3.061 \text{ K\%} - 0.225$

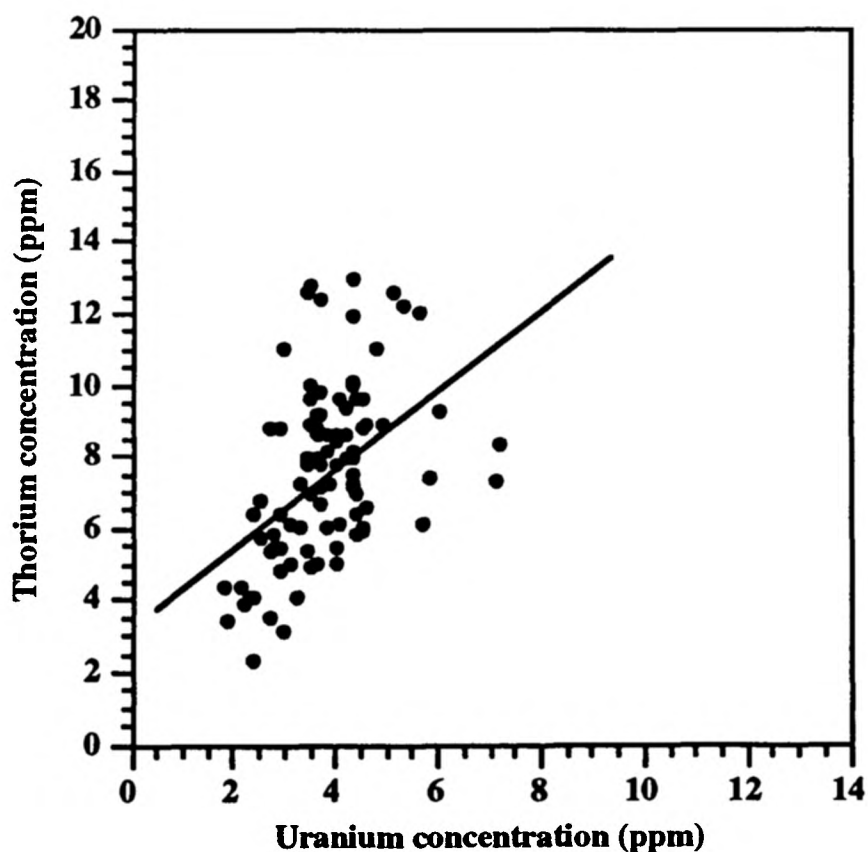


FIGURE 3.30B Linear regression correlation between Th concentration and U concentration. A correlation coefficient of 0.25 indicates that there is no covariant linear relationship between the two elements. A correlation coefficient of 0.30 or more is required for a statistically robust correlation at the 95 % significance level for n =96.

Stratigraphic log (unpublished, courtesy of Hesselbo & Jenkyns)

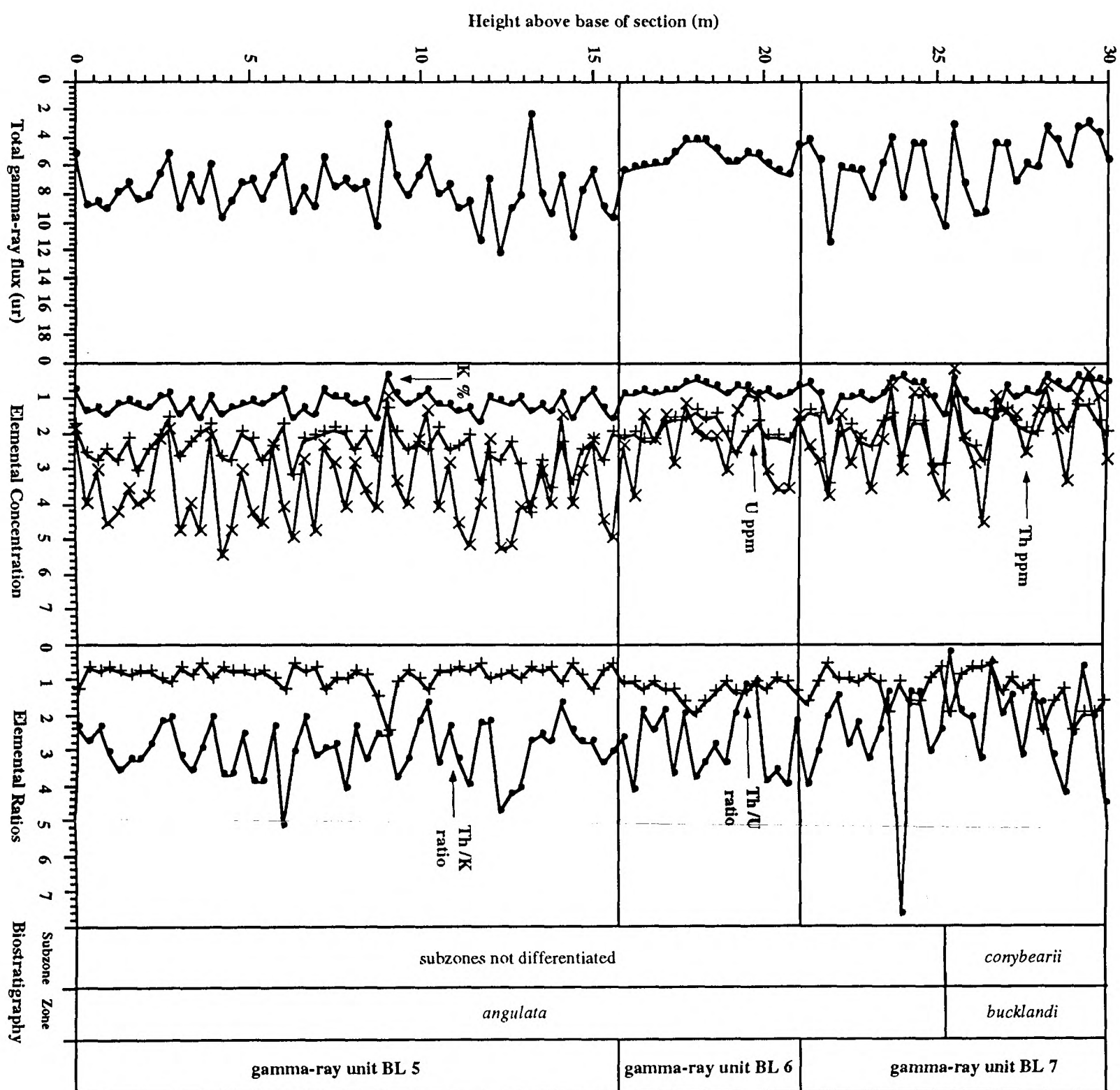
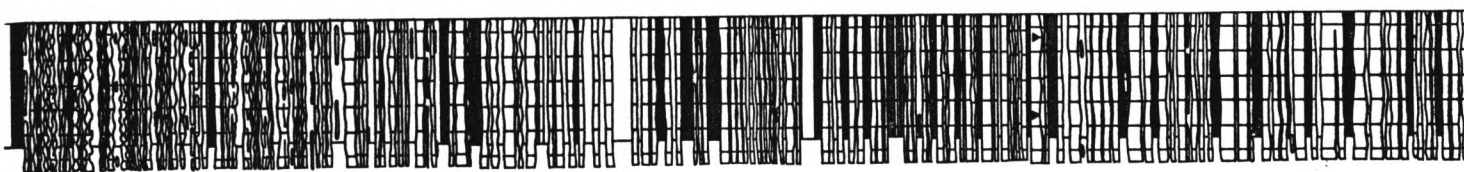


FIGURE 3.31 Total gamma-ray log, elemental concentration logs and elemental ratio curves for the Blue Lias (Porthkerry Formation) exposed at Nash Point, Glamorgan (ST 914684). Biostratigraphic boundaries are indicated. The gamma-ray logs are based on 100 sets of measurements.

Figure 3.31

Nash Point, South Glamorgan.

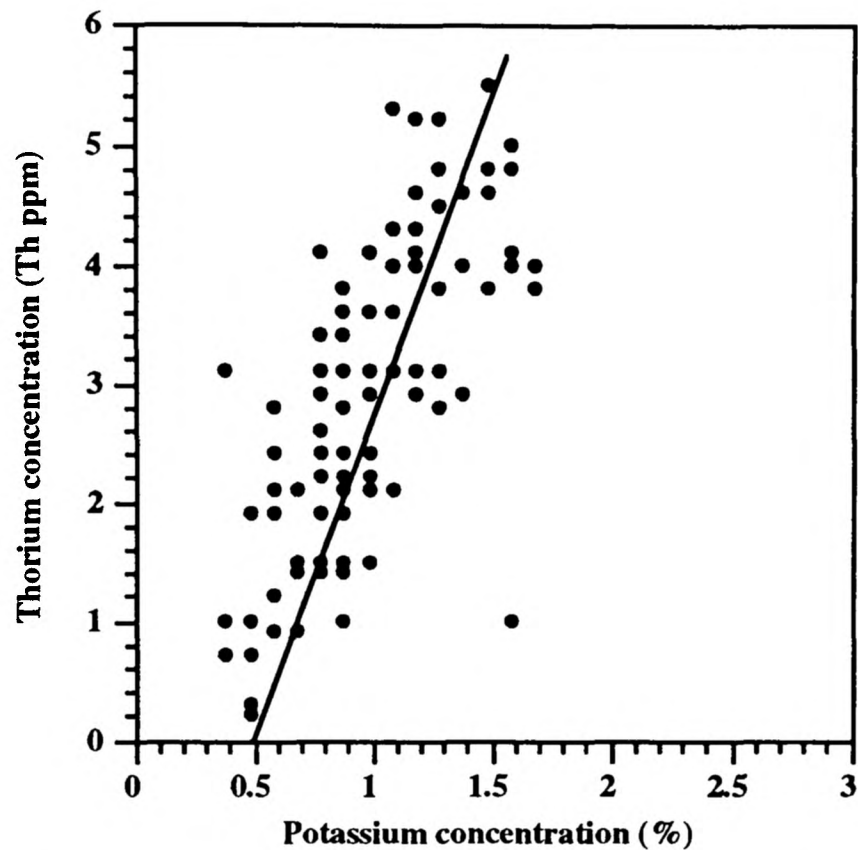


FIGURE 3.32A Linear regression correlation between Th concentration and U concentration. A correlation coefficient of 0.54 suggests a weak but statistically robust correlation at the 95 % significance level (n = 100). The relationship between the two elements can be described by the linear equation : $\text{Th ppm} = 2.93 \text{ K \%} - 0.067$

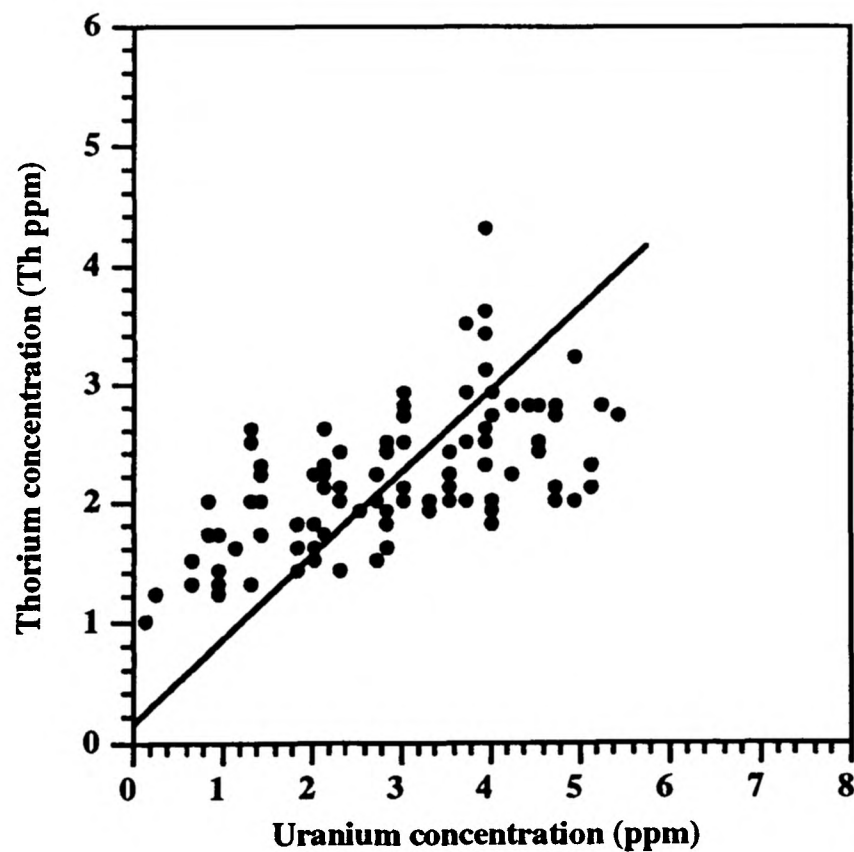


FIGURE 3.32B Linear regression correlation between Th concentration and K concentration. A correlation coefficient of 0.62 suggests a weak but statistically robust correlation at the 95 % significance level (n = 100). The relationship between the two elements can be described by the linear equation :
 $\text{Th ppm} = 1.42 \text{ U ppm} + 0.195$

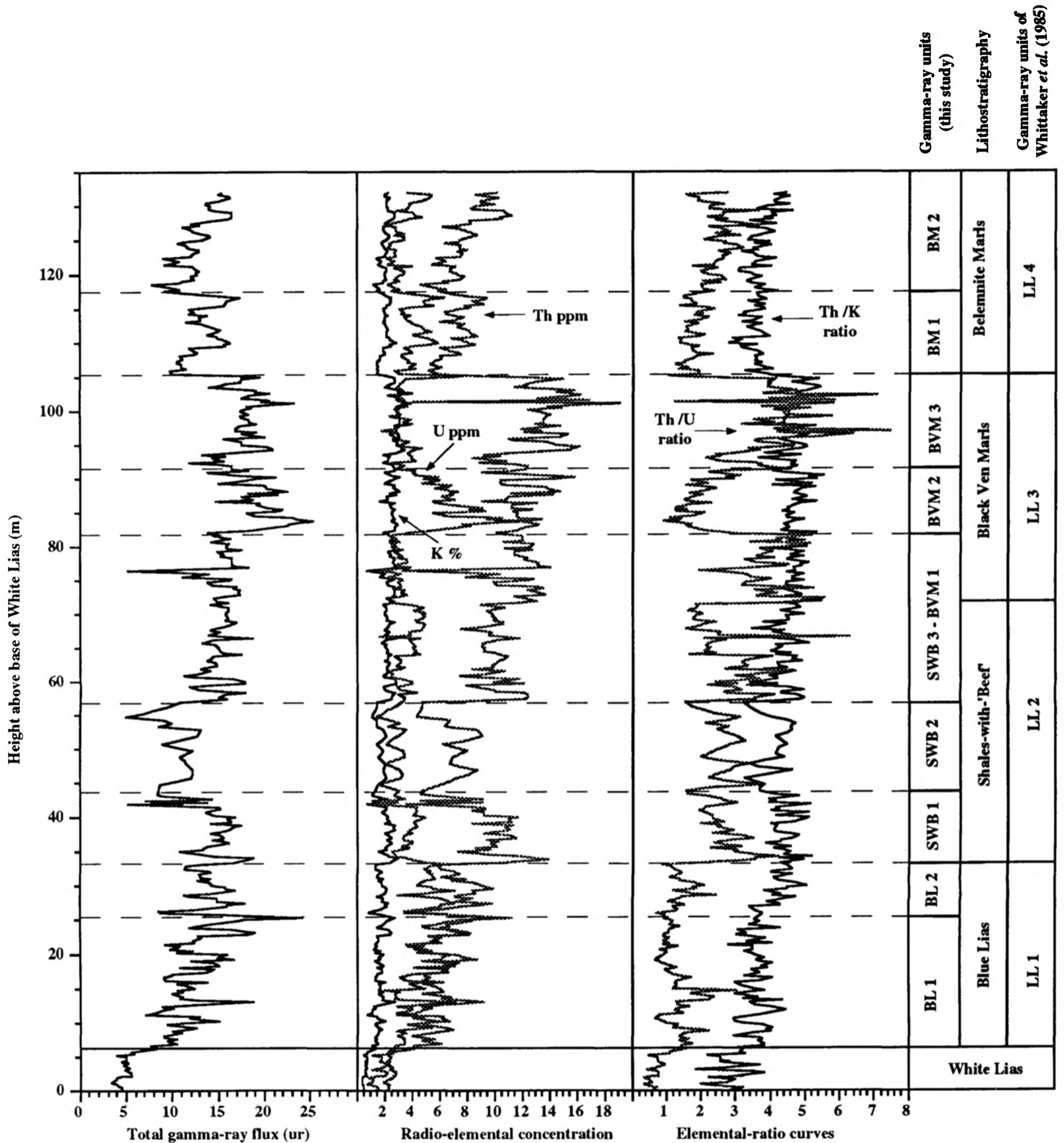


FIGURE 3.33 Gamma-ray logs for the Lower Lias succession of the Dorset coast based upon 421 measurements. The Blue Lias to Belemnite Marls have been subdivided on the basis of total gamma-ray signature and elemental-log signature into 10 gamma-ray units. Gamma-ray units SWB 3 and BVM 1 can be viewed as a single gamma-ray unit since there is essentially little difference in total gamma-ray signature between the Shales-with-'Beef' and Black Ven Marls over this interval. However, there is a very great change in Th/U ratio at the boundary between these two formations. The pronounced increase in Th/U ratio in the Black Ven marls arises from a decrease in U concentration and an increase in Th concentration. These two logs destructively interfere and result in essentially little change in total gamma-ray flux across the boundary between the Shales-with-'Beef' and Black Ven Marls. The units of Whittaker *et al.* (1985), identified for the same sequence from the Burton Row borehole in Somerset, are also shown. Clearly, finer sub-division of the Whittaker *et al.* gamma-ray units is possible.

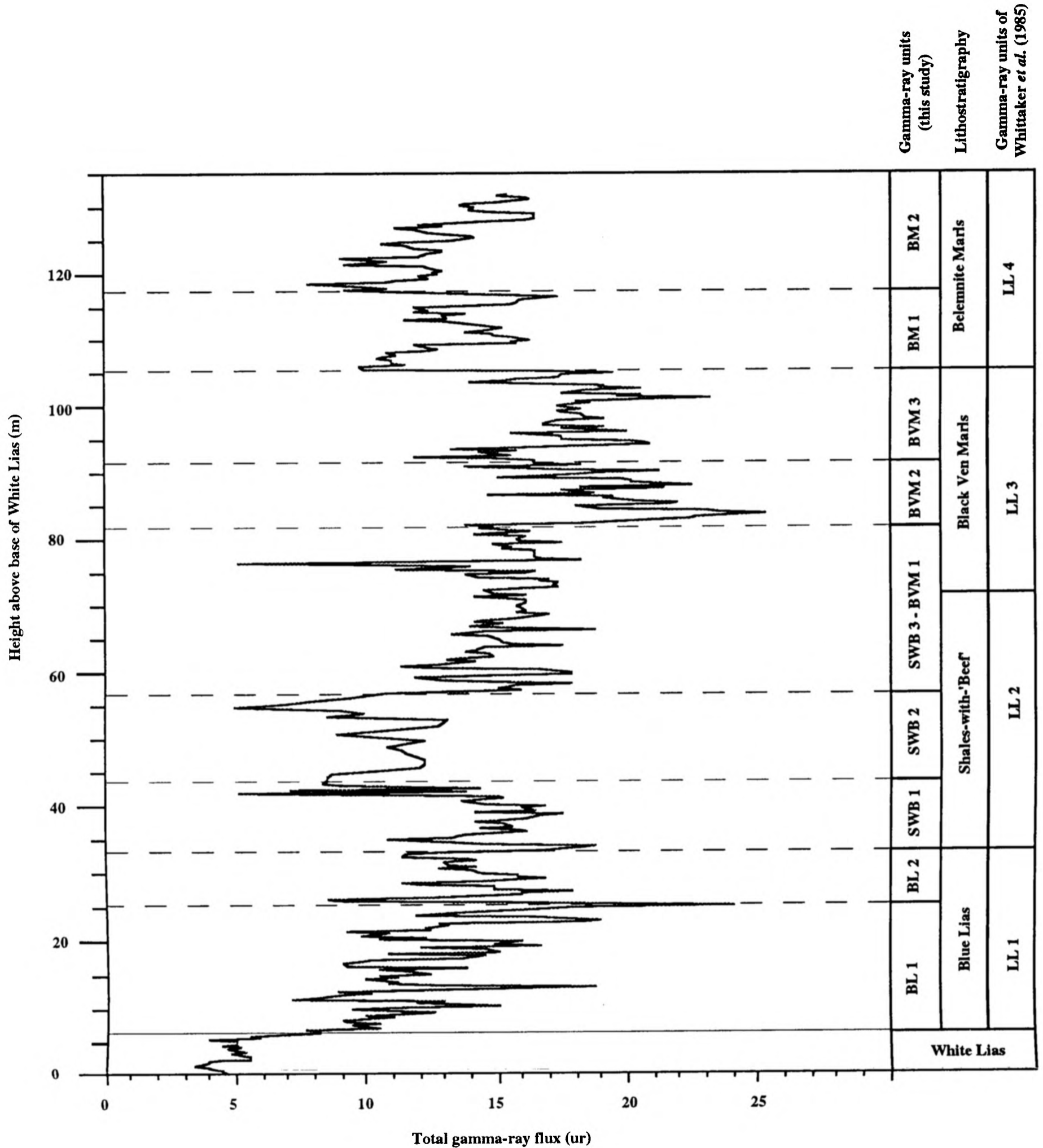


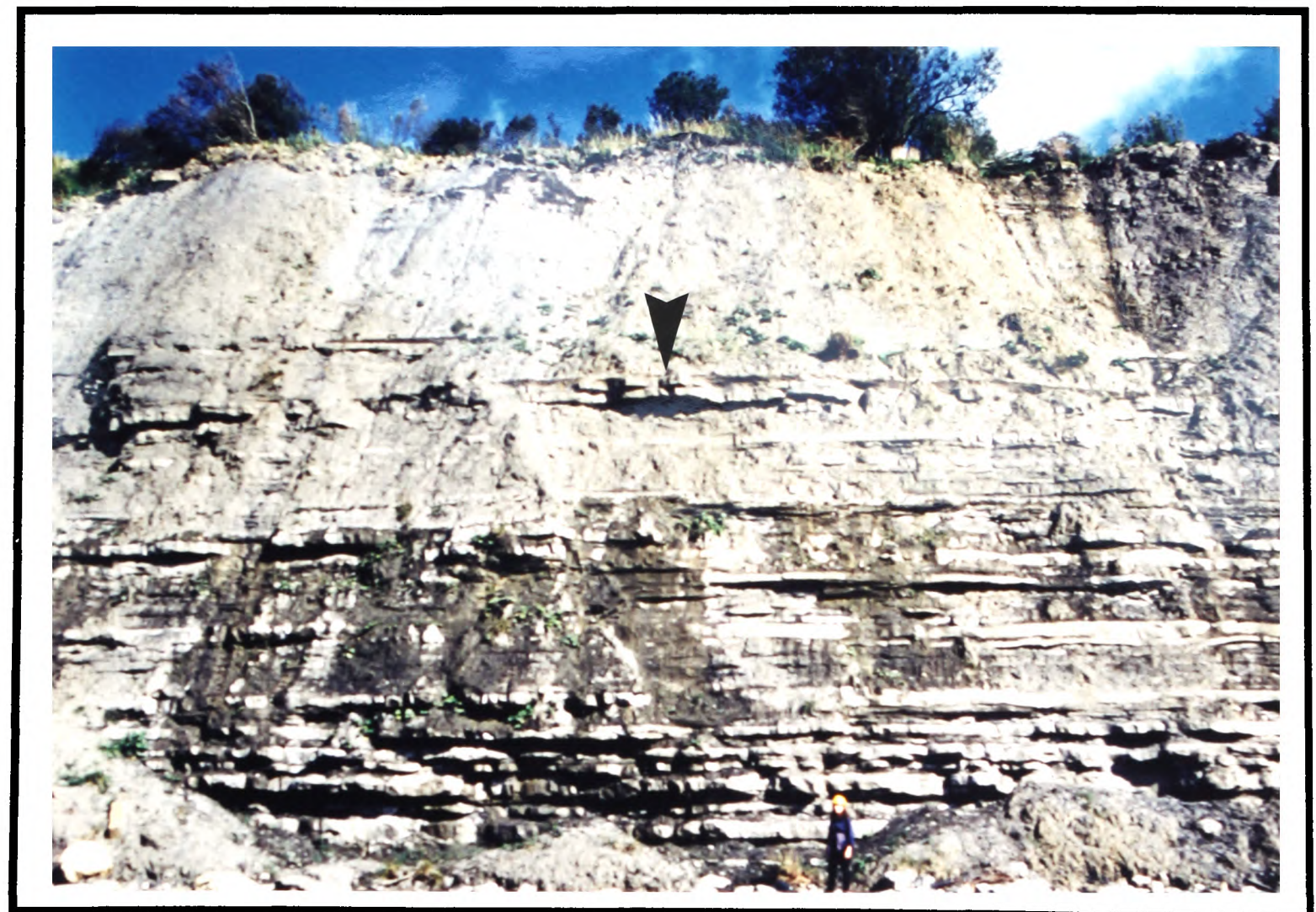
FIGURE 3.34 Stratigraphic packaging within the Lower Lias of the Dorset coast based upon total gamma-ray signature. The gamma-ray units defined in this study can be enhanced by altering the aspect ratio of the gamma-ray flux scale. The gamma-ray units can clearly be identified by enhancing the low frequency component of the total gamma-ray signature in this way. The units of Whittaker *et al.* (1985), identified for the same sequence from the Burton Row borehole in Somerset, are also shown.



FIGURE 3.35 The Blue Lias Formation, Dorset.

(ABOVE) Boundary between the White Lias and the *Pre-planorbis* Beds of the Blue Lias at Pinhay Bay (SY 318908). The White Lias is composed of a series of redeposited carbonate-mud flows as inferred from the matrix-supported intraclastic nature of most beds. These contrast with the high-frequency limestone-marl alternations characteristic of the Blue Lias. Height of cliff approximately 16 m.

(BELOW) Contact between the Blue Lias and the Shales-with-Beef at Seven Rock Point, Lyme Regis (SY 328910). In contrast to the Blue Lias, the Shales-with-Beef are dominantly argillaceous with minor concretionary or tabular limestones. The prominent uppermost limestone in the foreground is Grey Ledge which represents the boundary between the two formations. Height of cliff approximately 17 m.



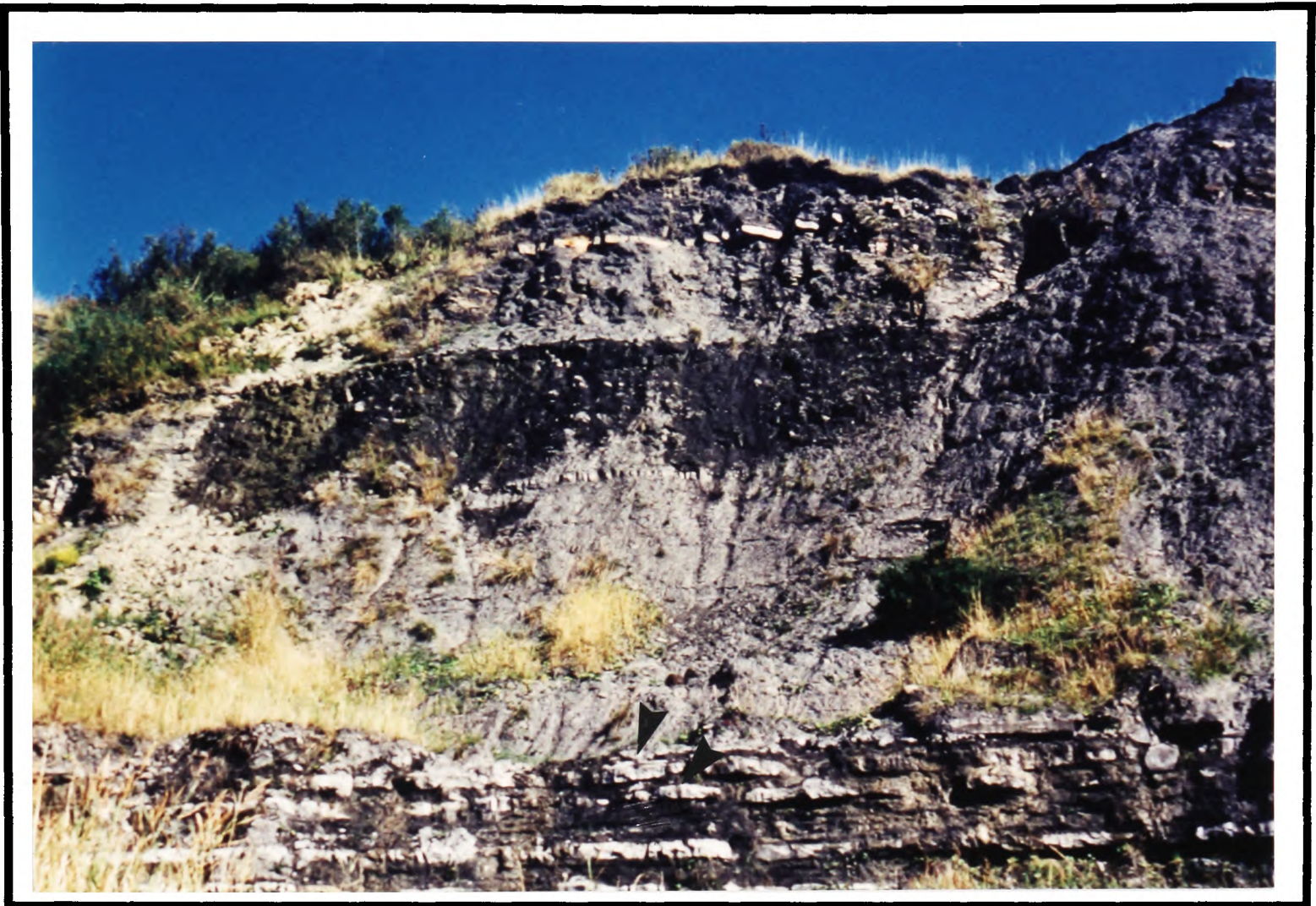


FIGURE 3.36 Shales-with-'Beef' at Seven Rock Point, Lyme Regis, Dorset

Field aspect of the lower Shales-with-'Beef' at Seven Rock Point, Lyme Regis (SY 328910). The exposure is representative of the *scipionianum* Subzone of the *semicostatum* Zone. The argillaceous nature of the Shales-with-'Beef' contrasts with the limestone-marl cycles developed in the Blue Lias. In the foreground, the top two limestones of the Blue Lias (known as Grey Ledge, and Glass Bottle) are biostratigraphically equivalent to the condensed *lyra* Subzone of the *semicostatum* Zone. The condensed *lyra* Subzone of the Blue Lias clearly contrasts with the expanded *scipionianum* Subzone of the Shales-with-'Beef'. (Height of cliff is approximately 12 m).



FIGURE 3.37 The Black Ven Marls, Charmouth, Dorset

(ABOVE) Field aspect of the Black Ven Marls west of Charmouth at Black Ven (SY 364930). The formation, together with the Shales-with-'Beef' below, comprises a package of predominantly dark laminated shales and dark marls with occasional concretionary and tabular limestone horizons. The Belemnite Marls are exposed towards the top of the cliff. (Cliff approximately 50 m in height).

(BELOW) Black Ven Marls below Stonebarrow cliff, east of Charmouth (SY 380927). The lowermost limestone is known as the Lower Cement Bed (bed 80). The Black Ven Marls at Stonebarrow are slightly condensed with respect to the section exposed on Black Ven and the first recorded *Asteroceras* (Lang & Spath 1926) occurs slightly lower at Stonebarrow. These observations are compatible with syndepositional activity on the intervening Char Fault during the late Sinemurian. (Cliff approximately 30 m in height).

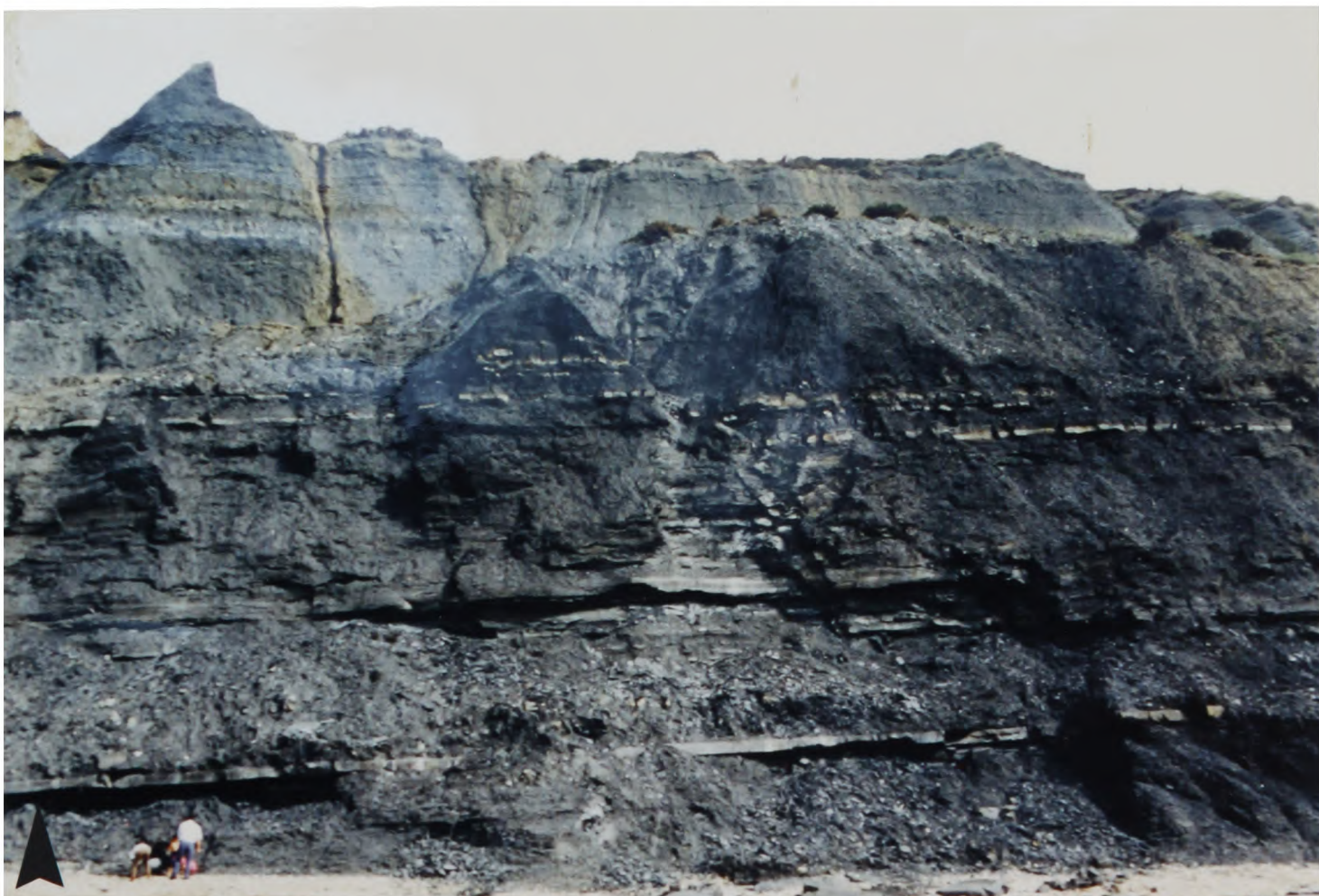




FIGURE 3.38 Belemnite Marls exposed east of Charmouth, Dorset (SY 380927-SY 415918)

(ABOVE) The Belemnite Marls that outcrop beneath Stonebarrow, east of the village of Charmouth (SY 380927). The series of light marl - dark marl couplets are a striking feature of the formation and less strongly overprinted by diagenesis than comparable cycles developed in the Blue Lias. The formation as a whole can be considered as a sedimentary cycle of first progressively increasing and then progressively decreasing bed-couplet thickness. (Height of cliff approximately 23 m).

(BELOW) The Belemnite Stone (SY 415918). Biostratigraphic condensation at the top of the Belemnite Marls culminates in a condensed 5 cm light grey-brown concretionary horizon known as the Belemnite Stone. (bed 121) The nodular limestone contains abundant belemnites, bivalves and *Chondrites*. Above bed 121, the strata belong to the Green Ammonite Beds (*davoei* Zone). Hammer is 35 cm in length.



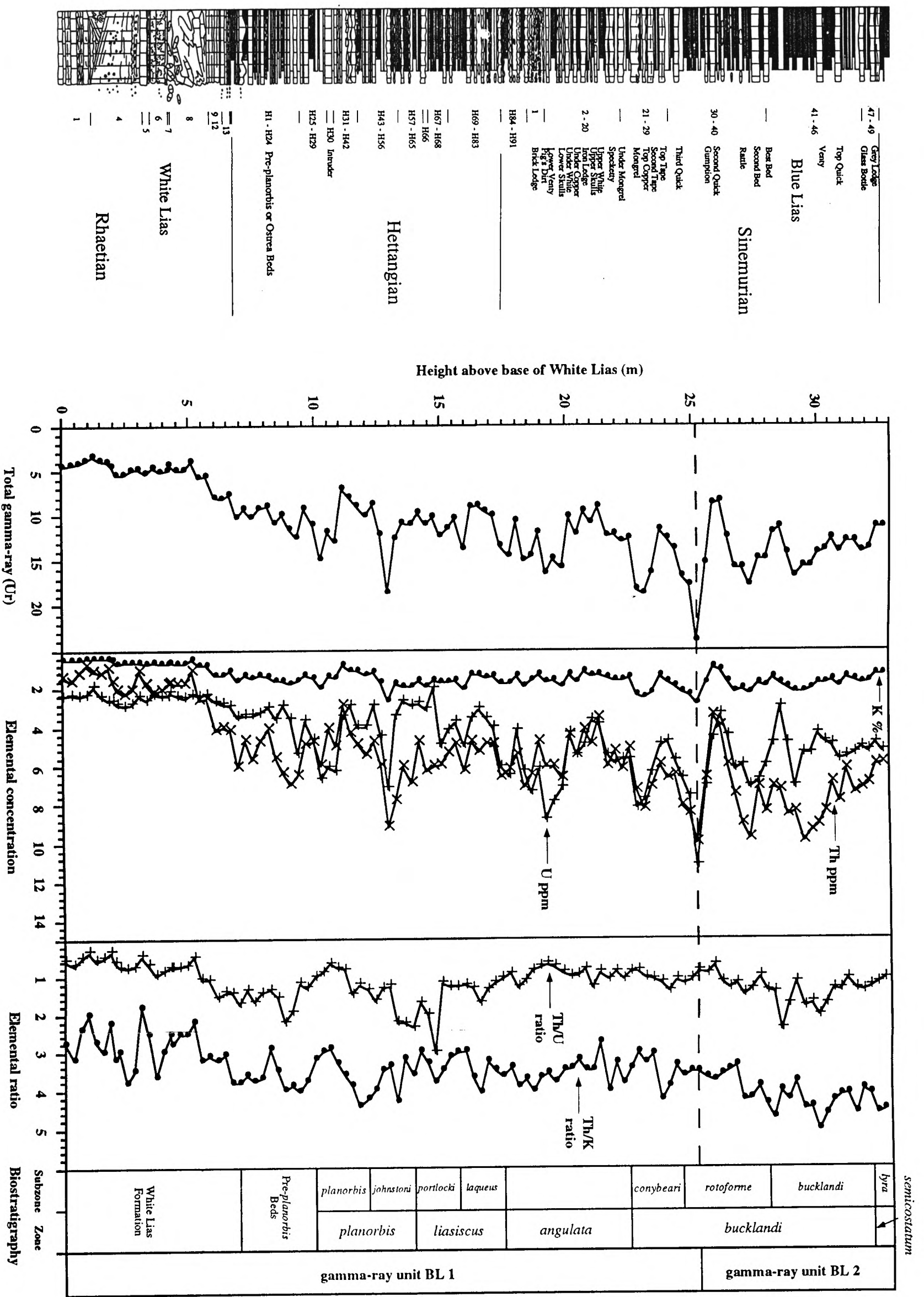


FIGURE 3.39

Total gamma-ray log, elemental concentration logs and elemental ratio curves for the Blue Lias Formation. Biostratigraphic boundaries are indicated. The gamma-ray logs are based on 87 sets of measurements that were collected between Pinhay Bay, Devon (SY 318908) and Seven Rock Point, Dorset (SY 328910). The underlying White Lias (Langport Member of the Llistock Formation) is also shown.

Blue Lias, Lyme Regis, Dorset.

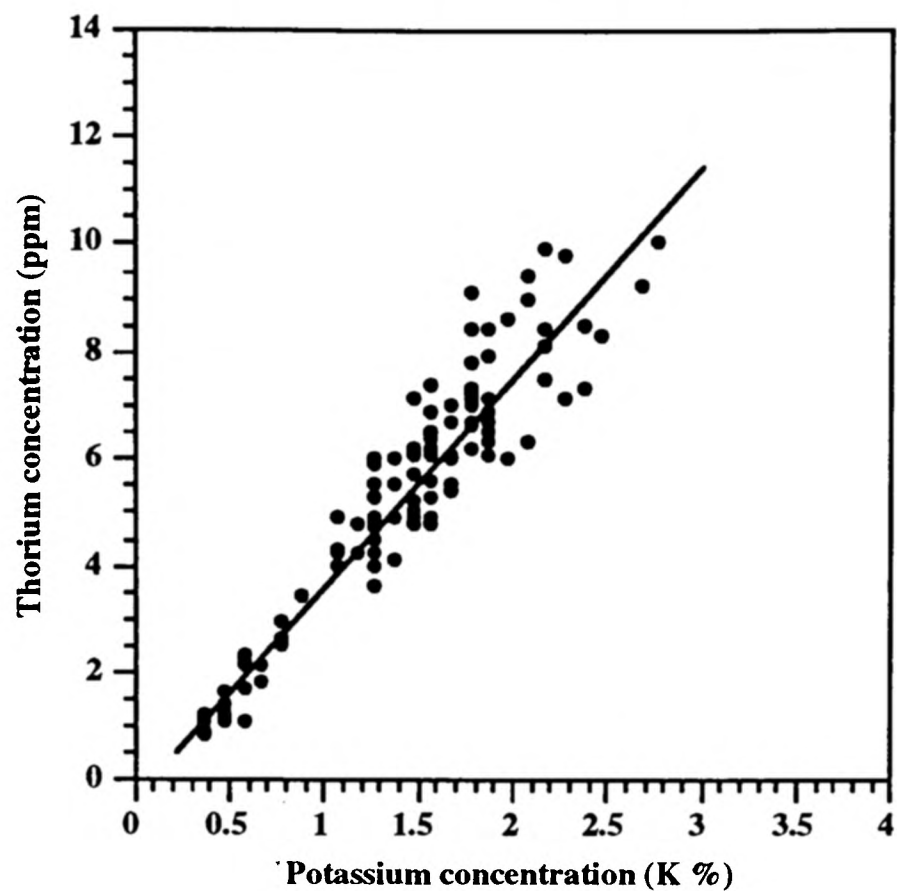


FIGURE 3.40A Linear regression correlation between Th concentration and K concentration. A correlation coefficient of 0.889 suggests a statistically robust correlation at the 95 % significance level (n = 87). The relationship between the two elements can be described by the linear equation : $\text{Th ppm} = 3.9485 \text{ K \%} - 0.40727$

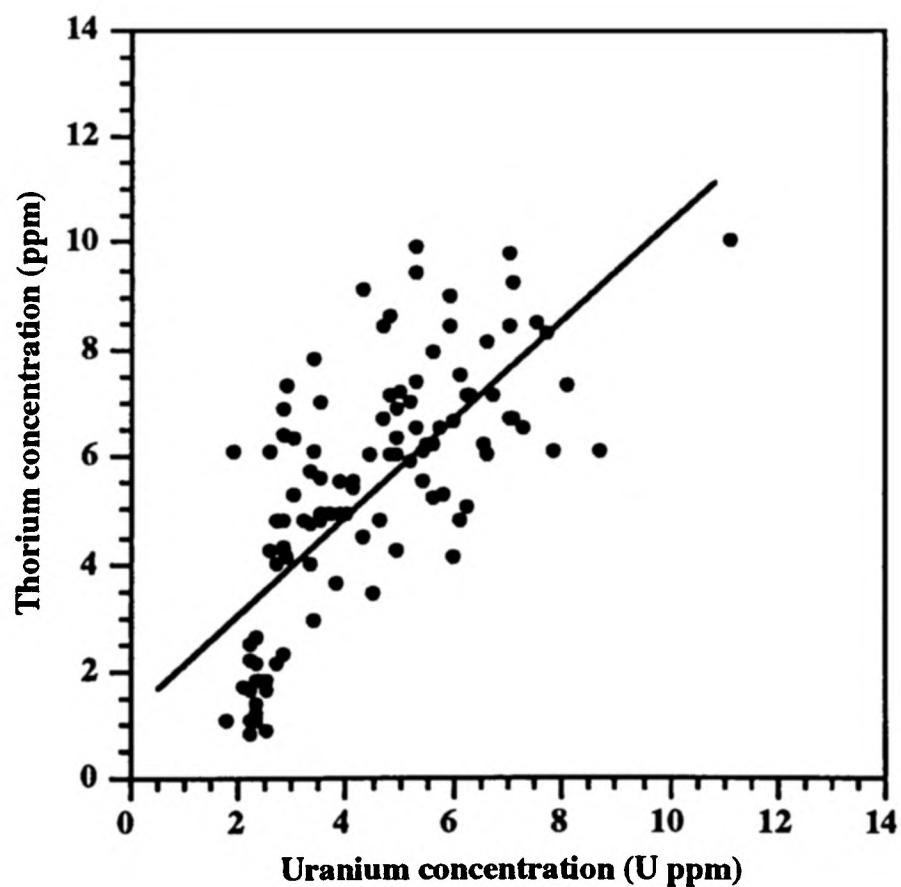
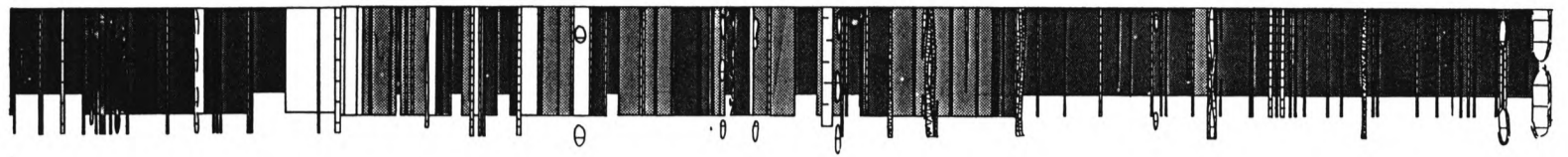


FIGURE 3.40B Linear regression correlation between Th concentration and U concentration. A correlation coefficient of 0.509 suggests a weak but statistically robust correlation at the 95 % significance level (n = 87). The relationship between the two elements can be described by the linear equation : $\text{Th ppm} = 0.9119 \text{ U ppm} + 1.2337$

Stratigraphic log of Hesselbo & Jenkyns (1995a)



Height above base of white Lias (metres)

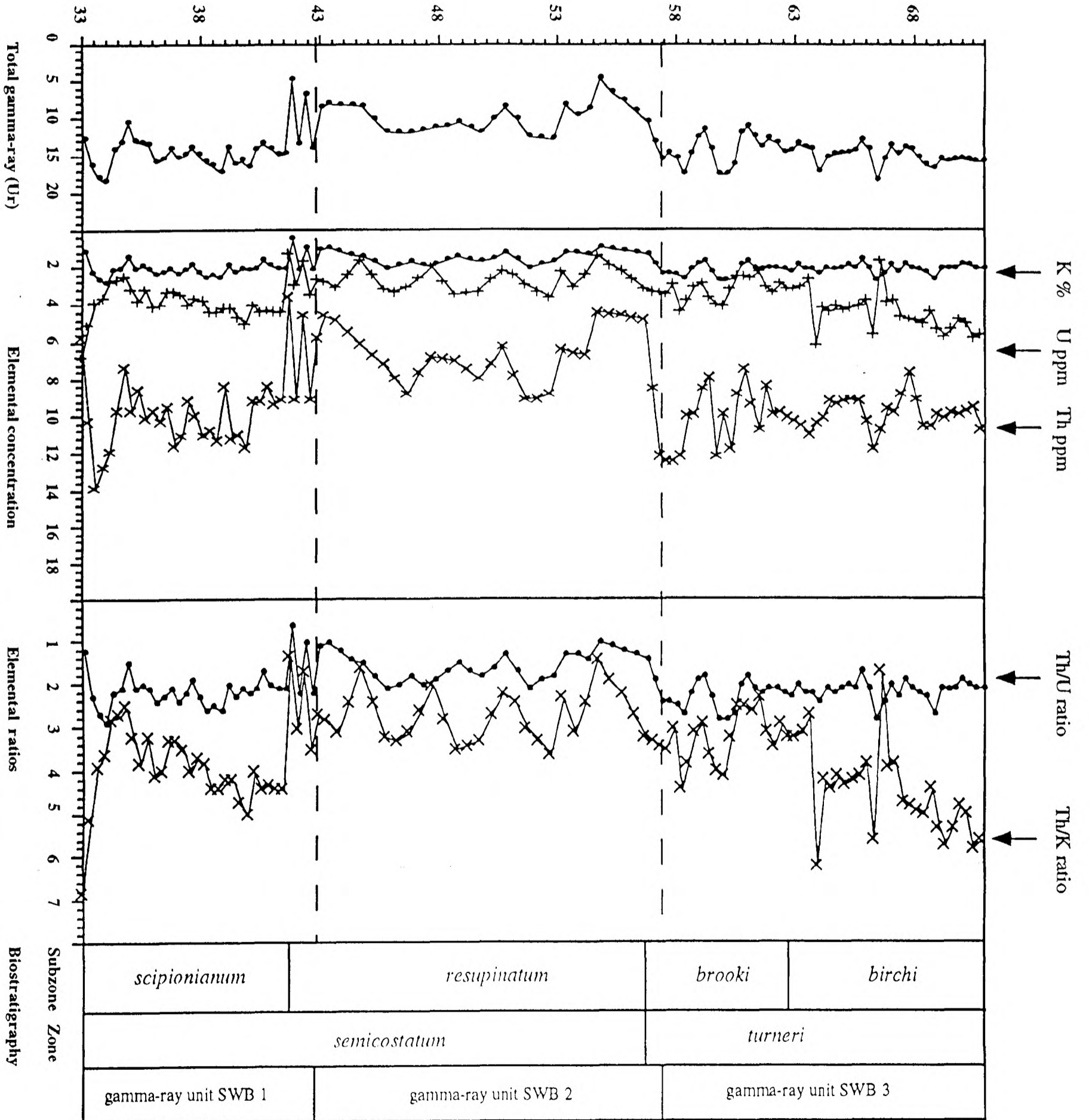


FIGURE 3.41 Total gamma-ray log, elemental concentration logs and elemental ratio curves for the Shales-with-Beef. Biostratigraphic boundaries are indicated. The gamma-ray logs are based on 108 sets of measurements.

FIGURE 3.41

Shales-with-'Beef', Charmouth, Dorset.

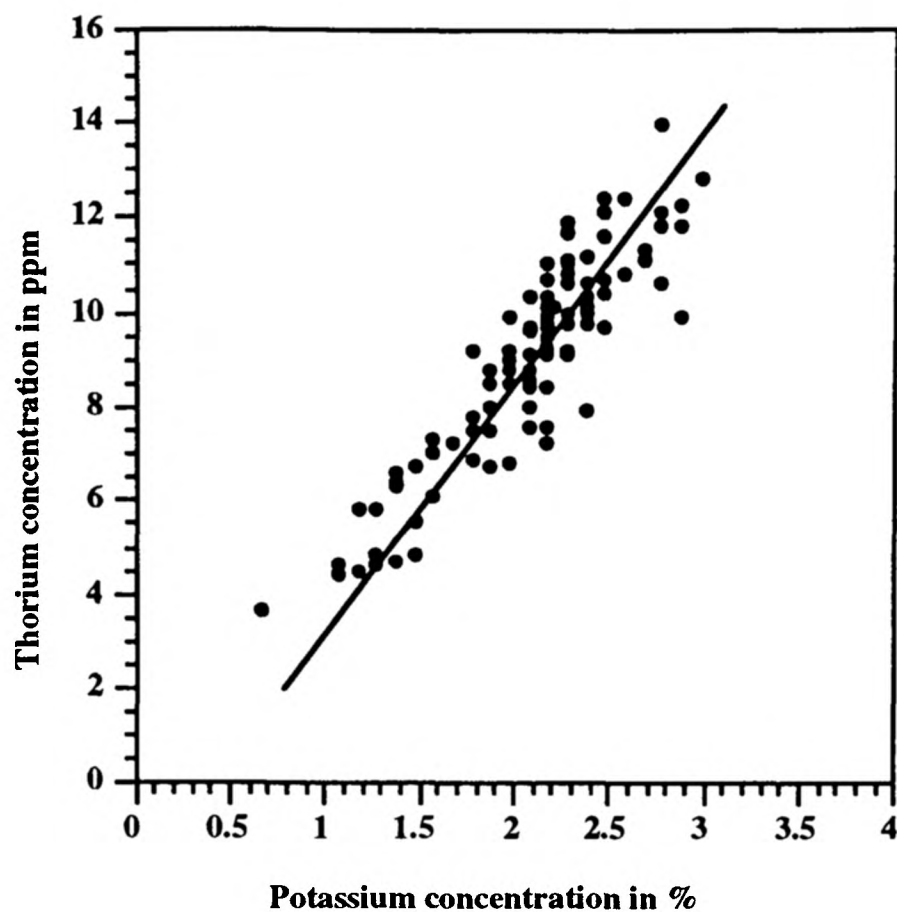


FIGURE 3.42A Linear-regression correlation between Th concentration and K concentration. A correlation coefficient of 0.87 suggests a statistically robust correlation at the 95 % significance level (n = 108). The relationship between the two elements can be described by the linear equation :

$$\text{Th ppm} = 3.95 \text{ K \%} + 0.943$$

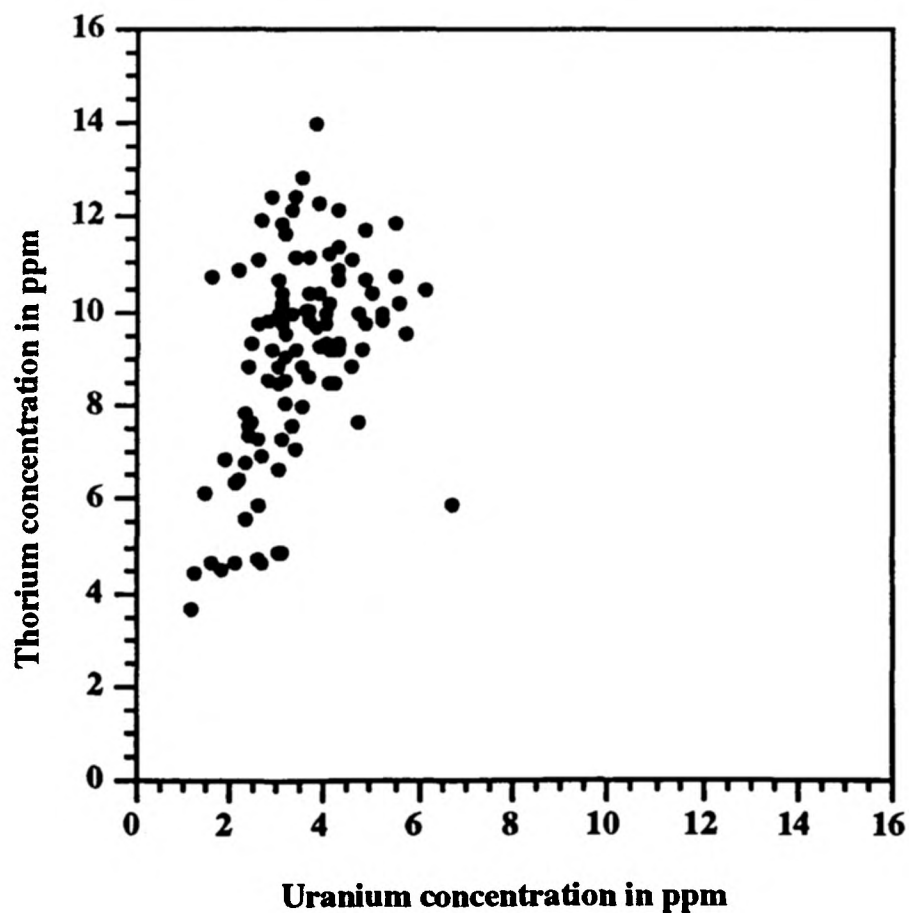


FIGURE 3.42B Linear-regression correlation between Th concentration and U concentration. A correlation coefficient of 0.14 indicates that no statistically robust relationship is shown by the two elements (n = 108).

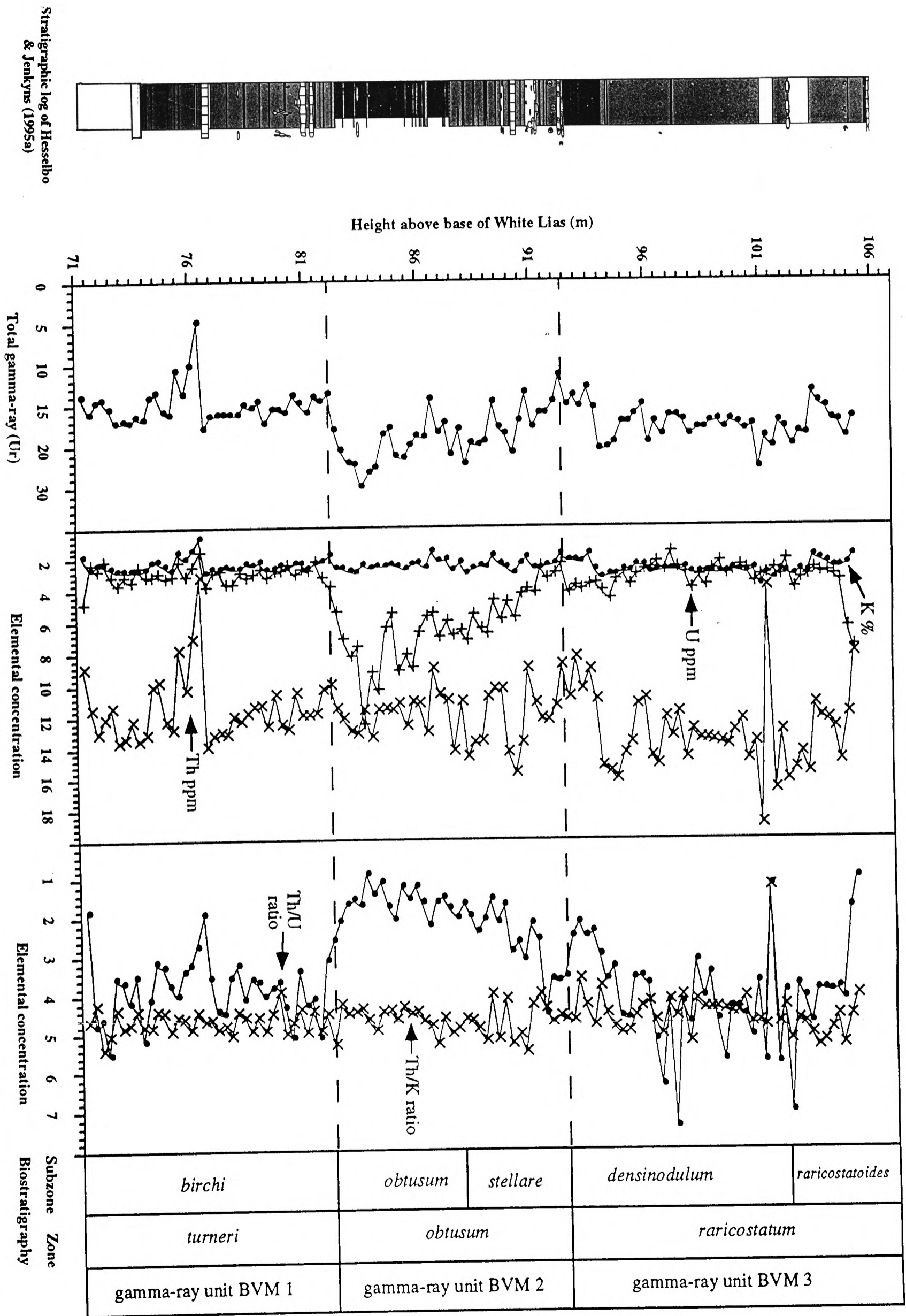


FIGURE 3.43 Total gamma-ray log, elemental concentration logs and elemental ratio curves for the Black Ven Marls. Biostratigraphic boundaries are indicated. The gamma-ray logs are based on 114 sets of measurements.

FIGURE 3.43

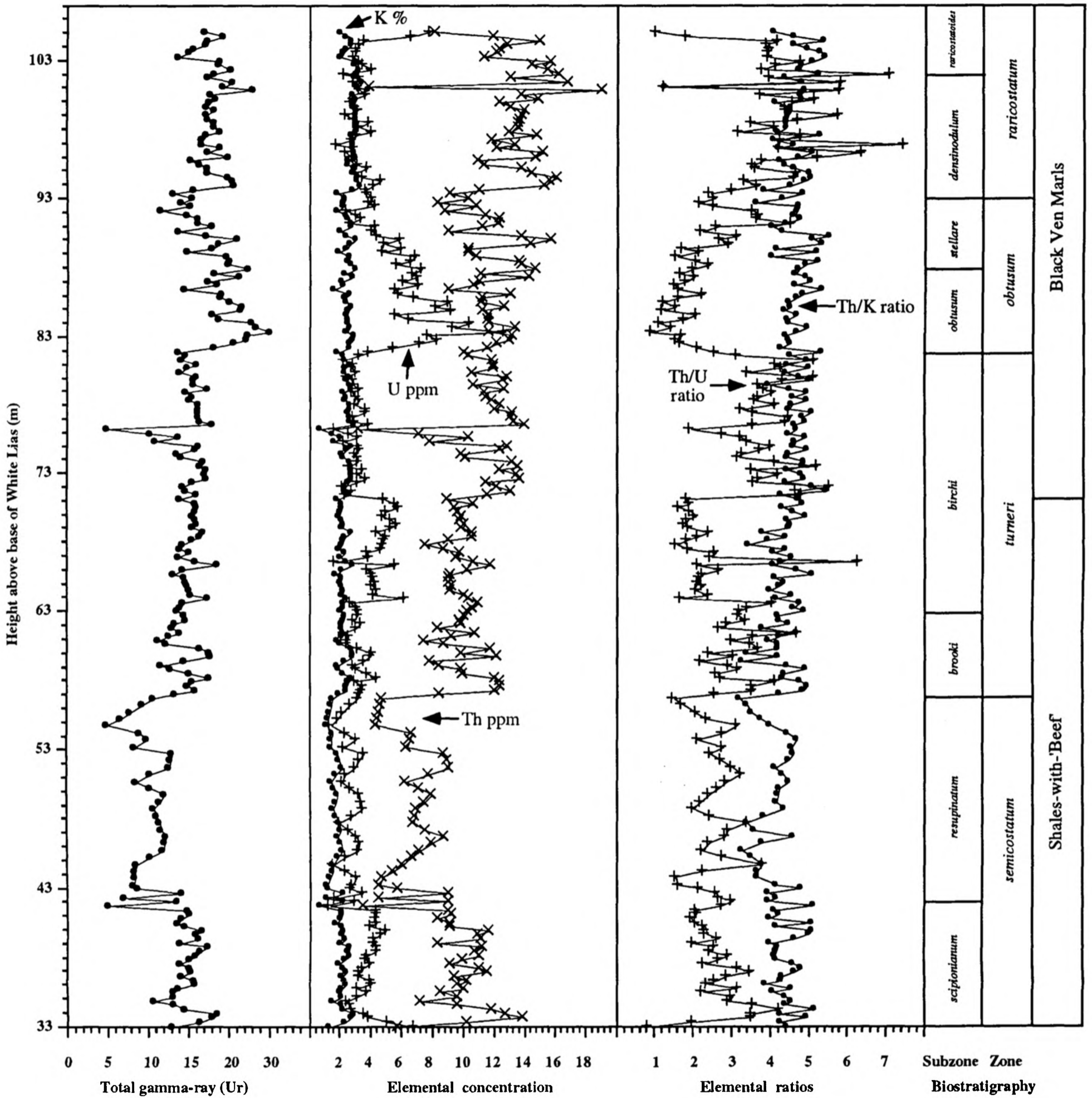


FIGURE 3.44 Total gamma-ray log, elemental-concentration logs and elemental-ratio curves for Shales-with-'Beef' and Black Ven Marls. Biostratigraphic boundaries are indicated. The gamma-ray logs are based on 222 sets of gamma-ray measurements.

Black Ven Marls, Charmouth, Dorset.

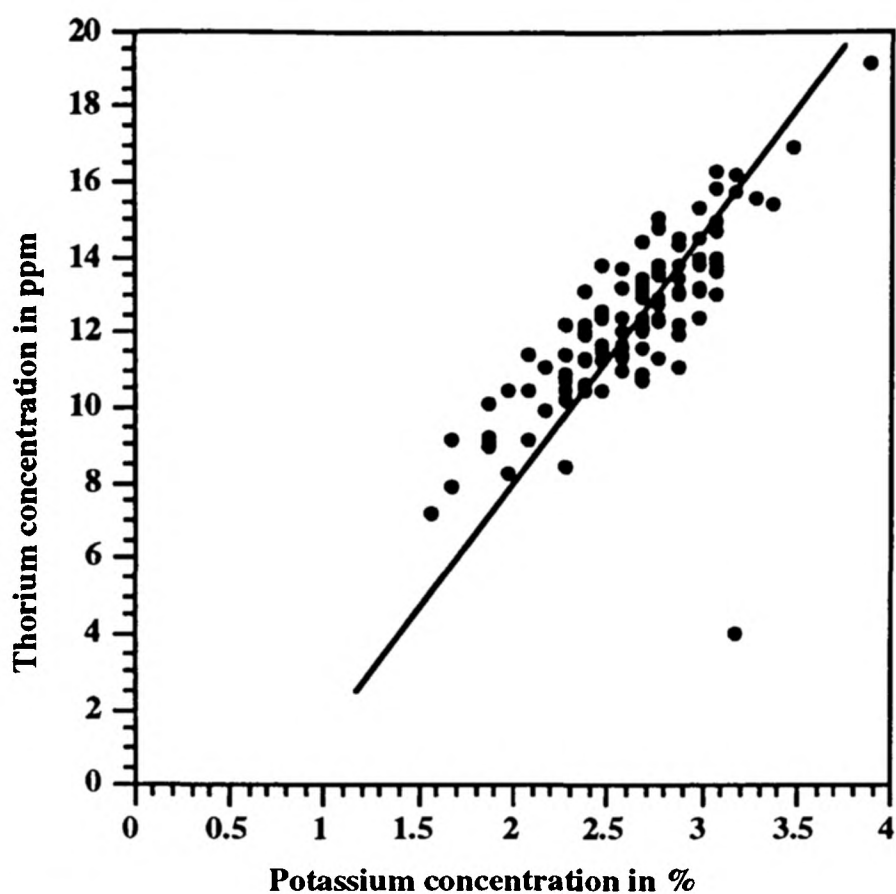


FIGURE 3.45A Linear-regression correlation between Th concentration and K concentration. A correlation coefficient of 0.64 suggests a statistically robust correlation at the 95 % significance level (n = 114). The relationship between the two elements can be described by the linear equation :

$$\text{Th ppm} = 4.24 \text{ K \%} + 1.083$$

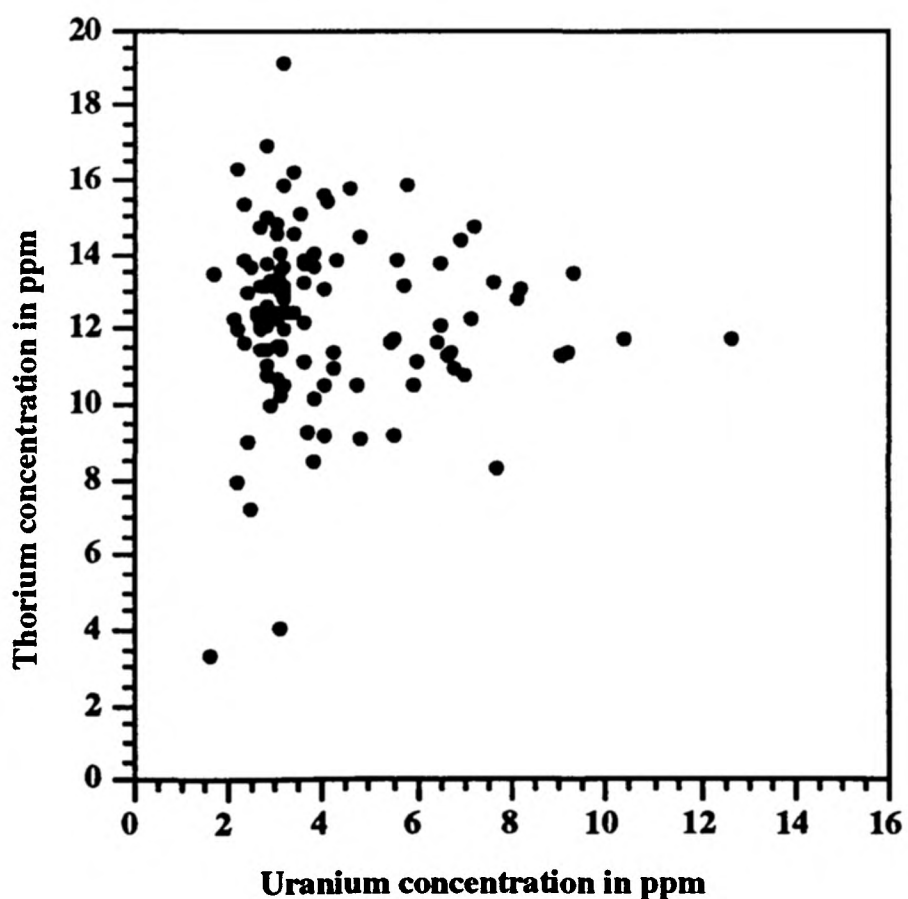


FIGURE 3.45B Linear-regression correlation between Th concentration and U concentration. A correlation coefficient of 0.01 indicates that no statistically robust relationship is shown by the two elements (n = 114).

Stratigraphic log of
Hesselbo & Jenkyns (1995a)

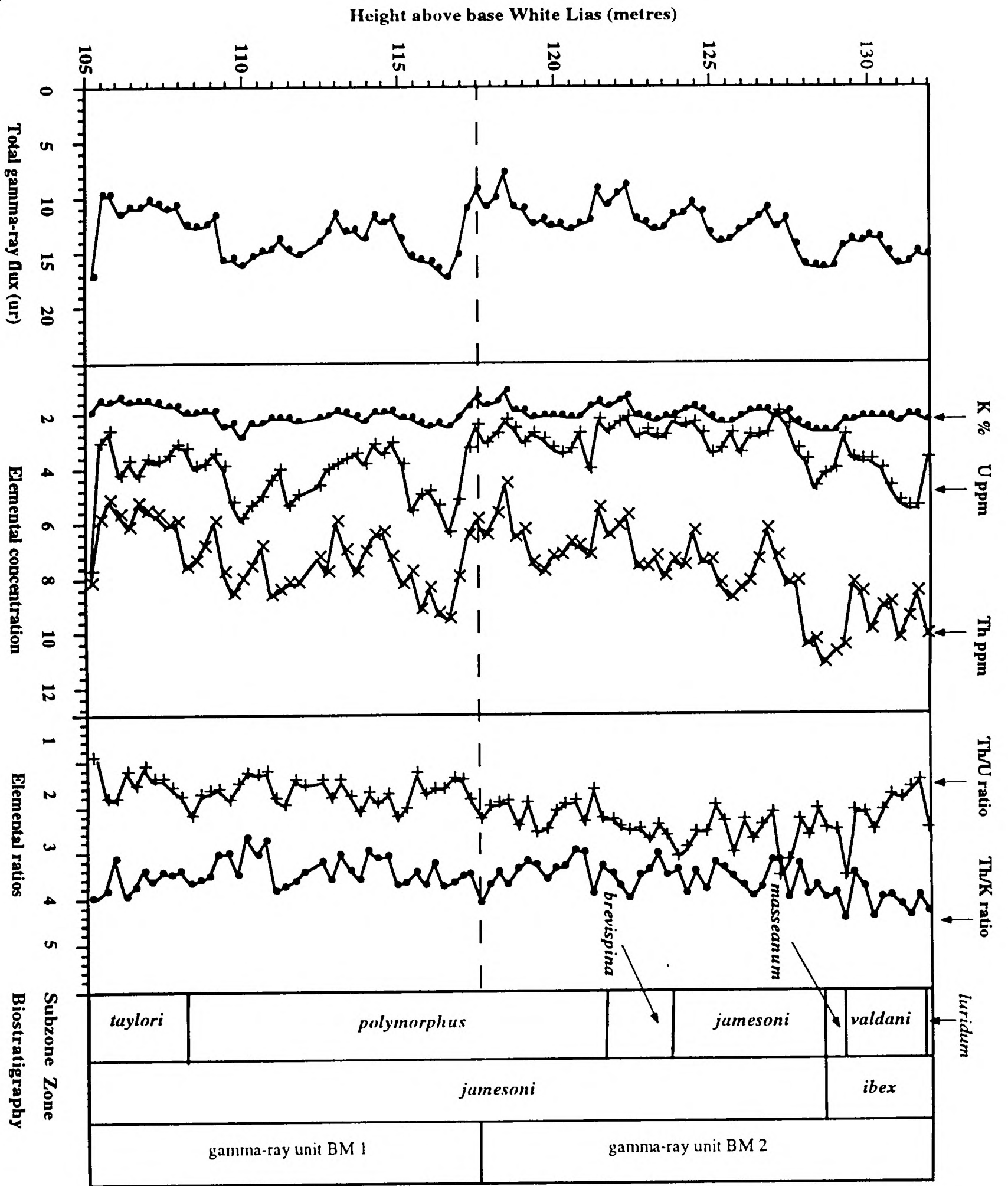


FIGURE 3.46 Total gamma-ray log, elemental concentration logs and elemental ratio curves for the Belemnite Marls. Biostratigraphic boundaries are indicated. The gamma-ray logs are based on 89 sets of measurements.

FIGURE 3.46

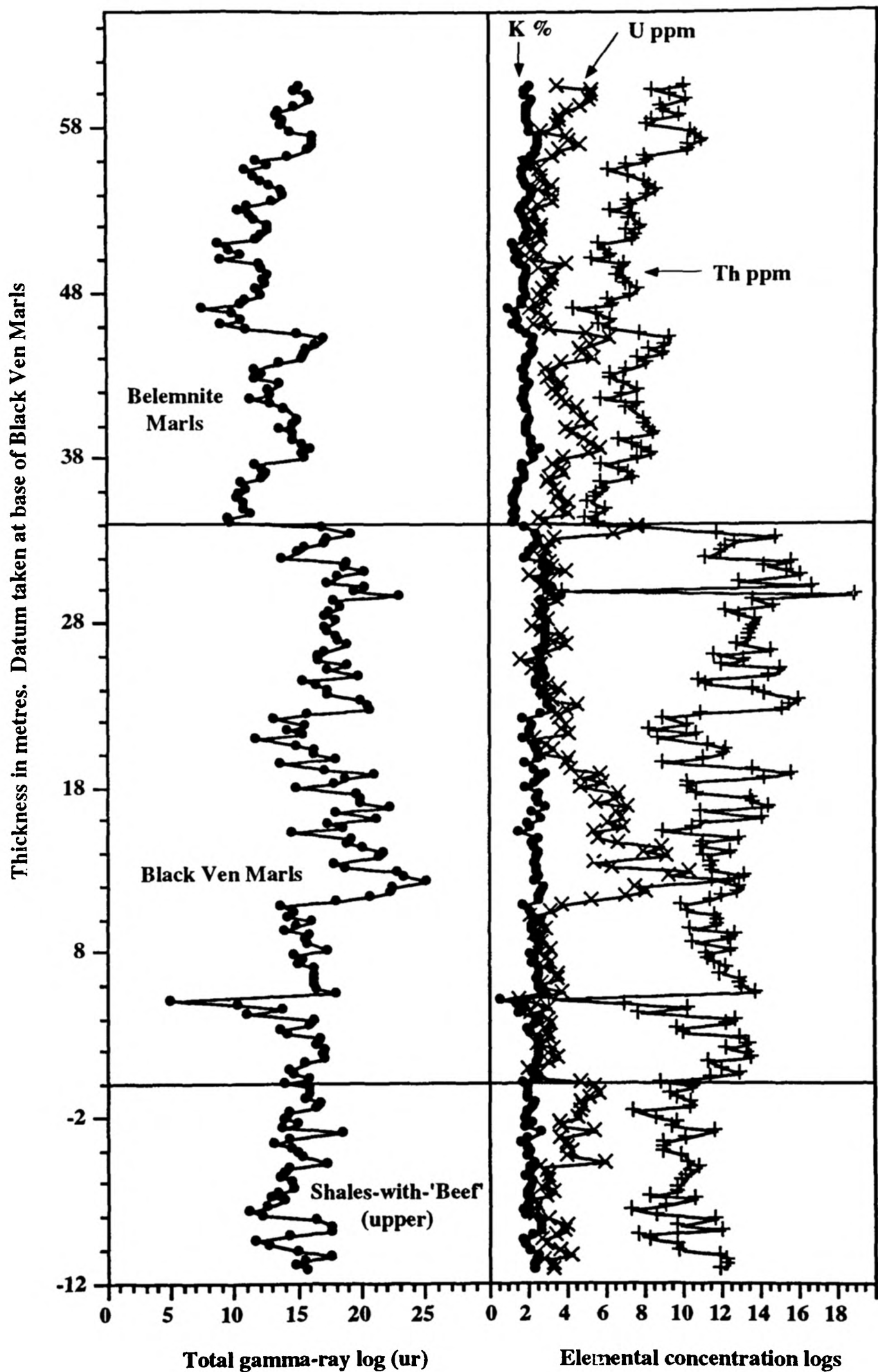


FIGURE 3.47 Total gamma-ray logs and elemental-concentration logs for the Shales-with-'Beef' and the entire Black Ven Marls and Belemnite Marls. The reduction in total gamma-ray flux and Th concentration within the Belemnite Marls (in contrast to the formations below) is clearly displayed.



FIGURE 3.48 Stratigraphic packaging within the Belemnite Marls. Each gamma-ray unit is characterised by a trend in the low frequency component of the signature. This can be enhanced by either altering the aspect ratio of the X and Y axis, as in case B, or by normalising the horizontal axis to a range of log values, as in case C.

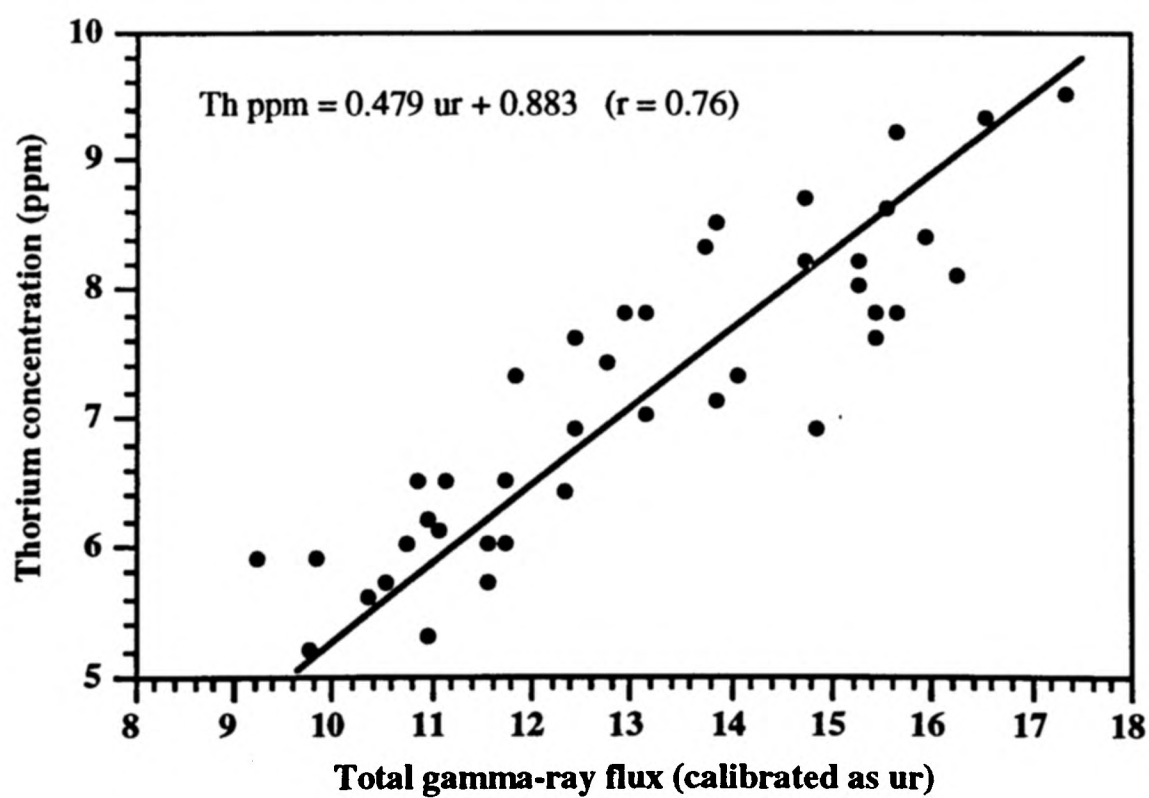
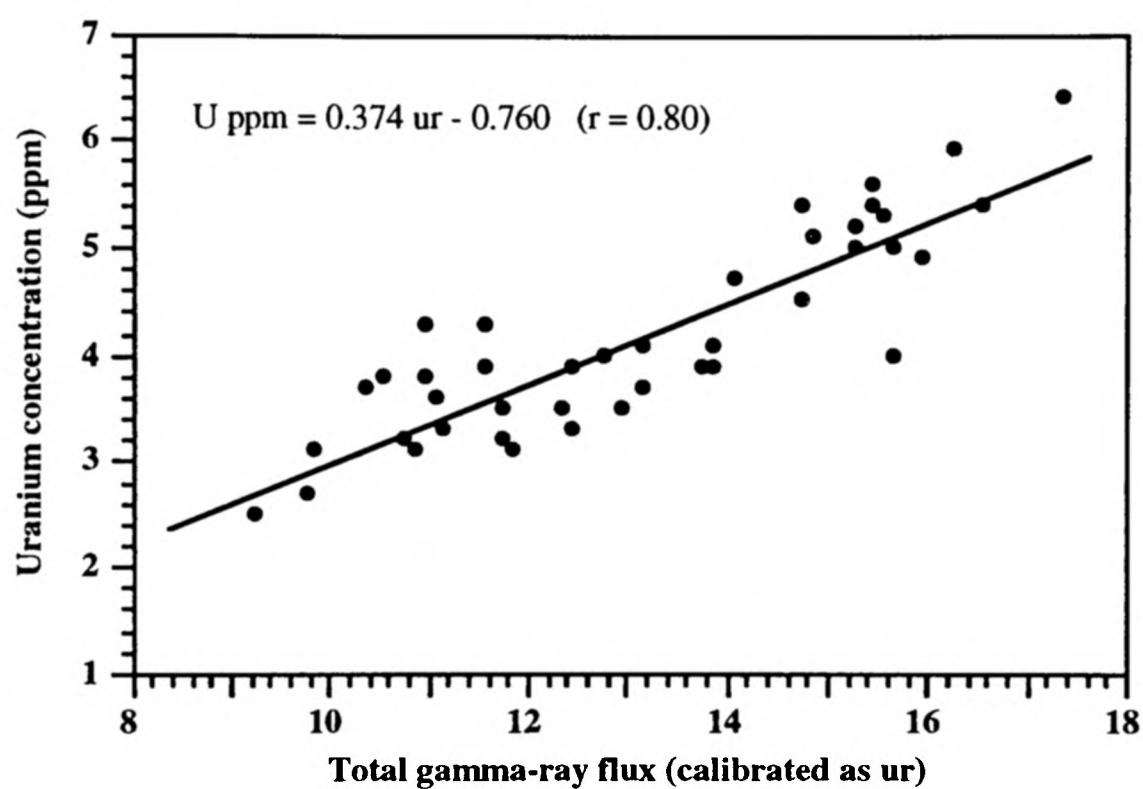
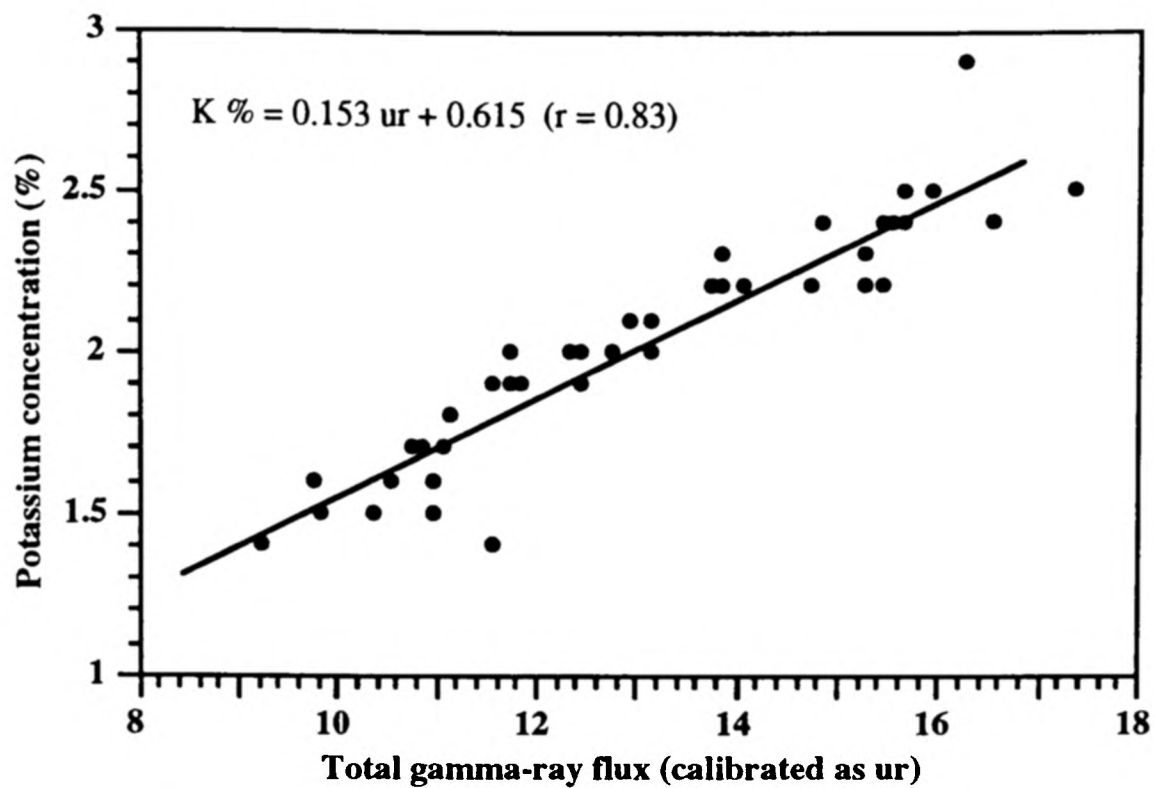


FIGURE 3.49 Positive linear regression between total gamma-ray flux and radioelemental concentration within gamma-ray unit BM 1. Correlation coefficients are indicated.

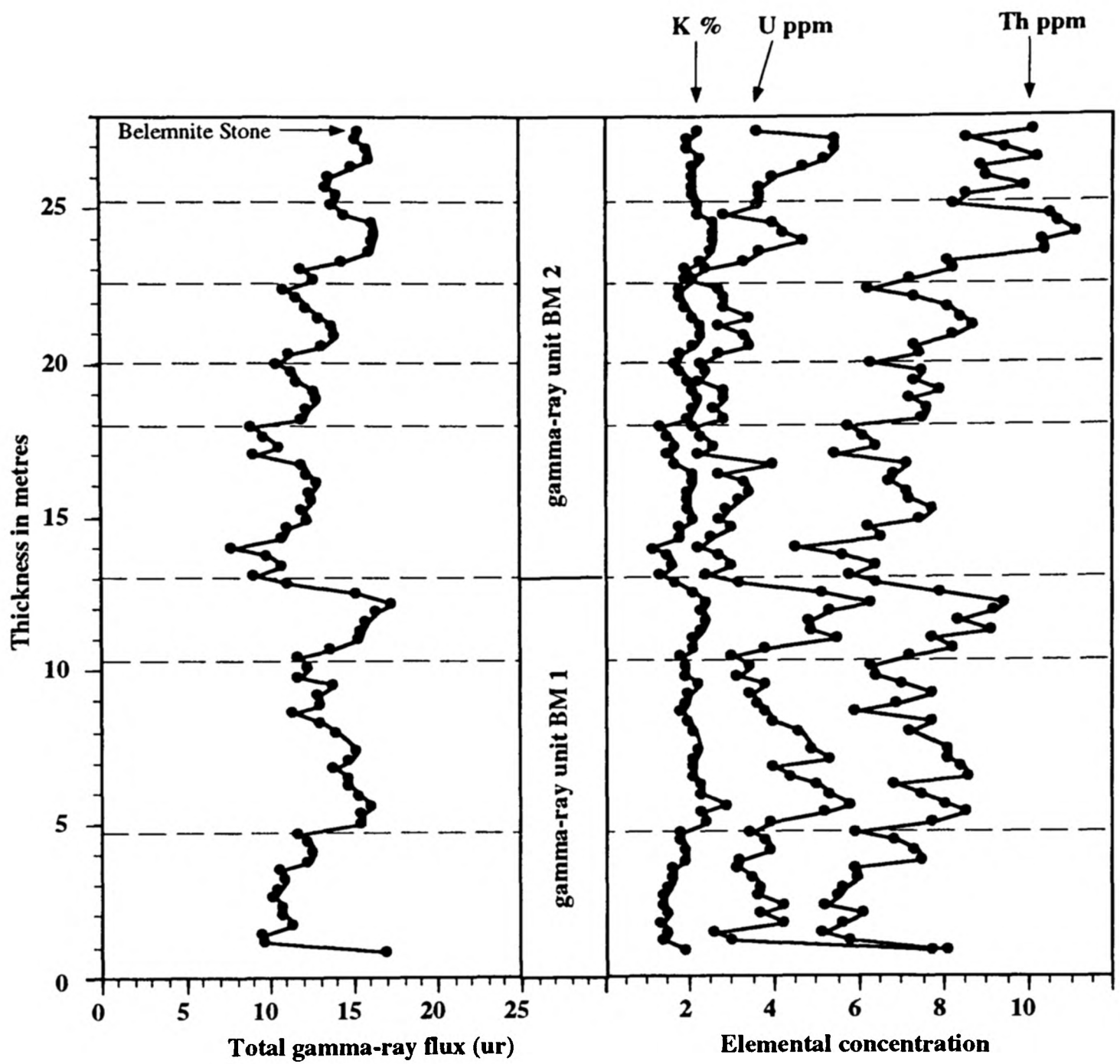


FIGURE 3.50 Discrete carbonate cycles evident in the gamma-ray signature for the Belemnite Marls. These cycles are strongly mirrored in the Th concentration log. Total gamma-ray signature lacks the high-frequency variation evident within the Black Ven Marls and Shales-with-'Beef'. The lack of high-frequency variation allows these cycles to be clearly identified.

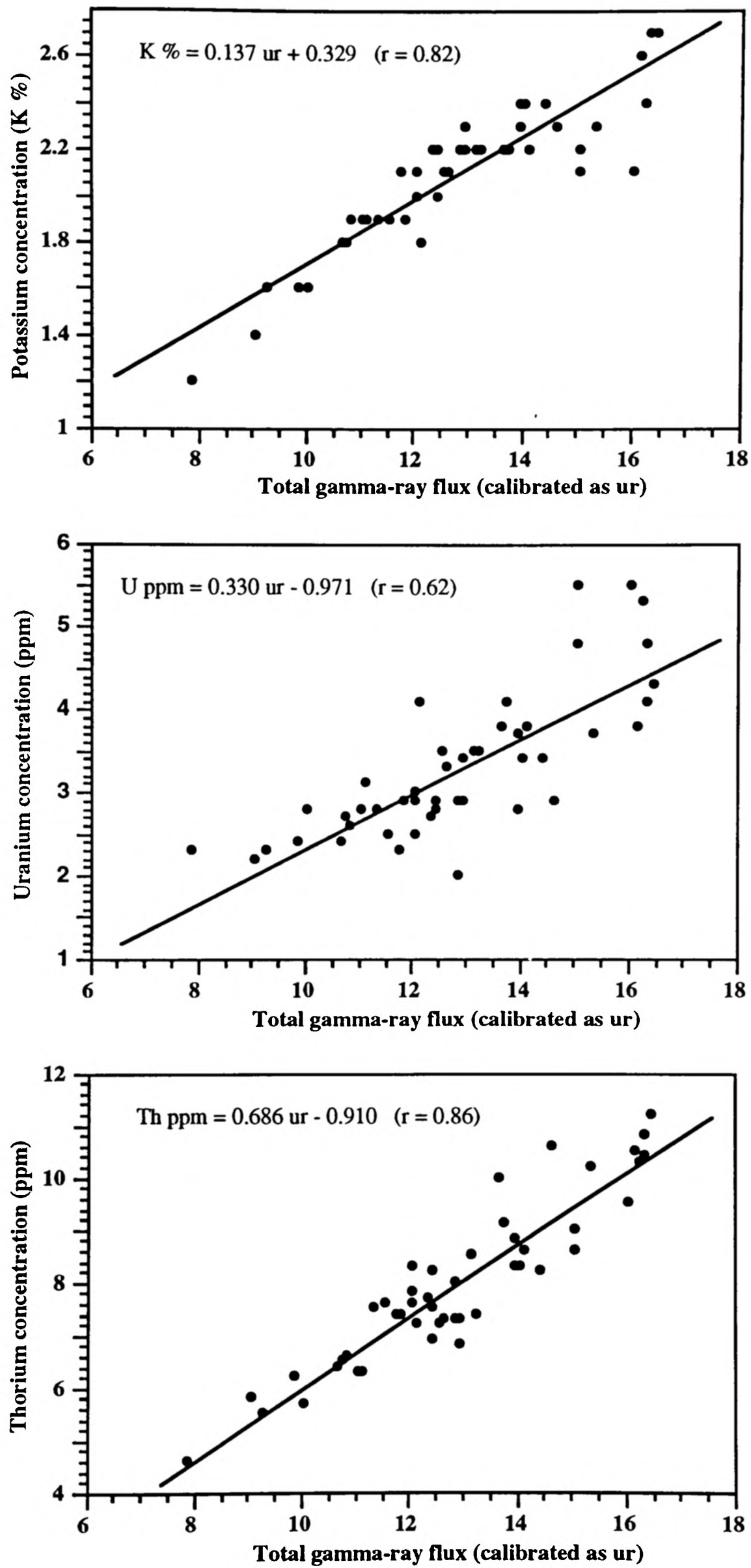


FIGURE 3.51 Positive linear regression between total gamma-ray flux and radioelemental concentration within gamma-ray unit BM 2. Correlation coefficients are indicated.

Belemnite Marls, Seatown, Dorset.

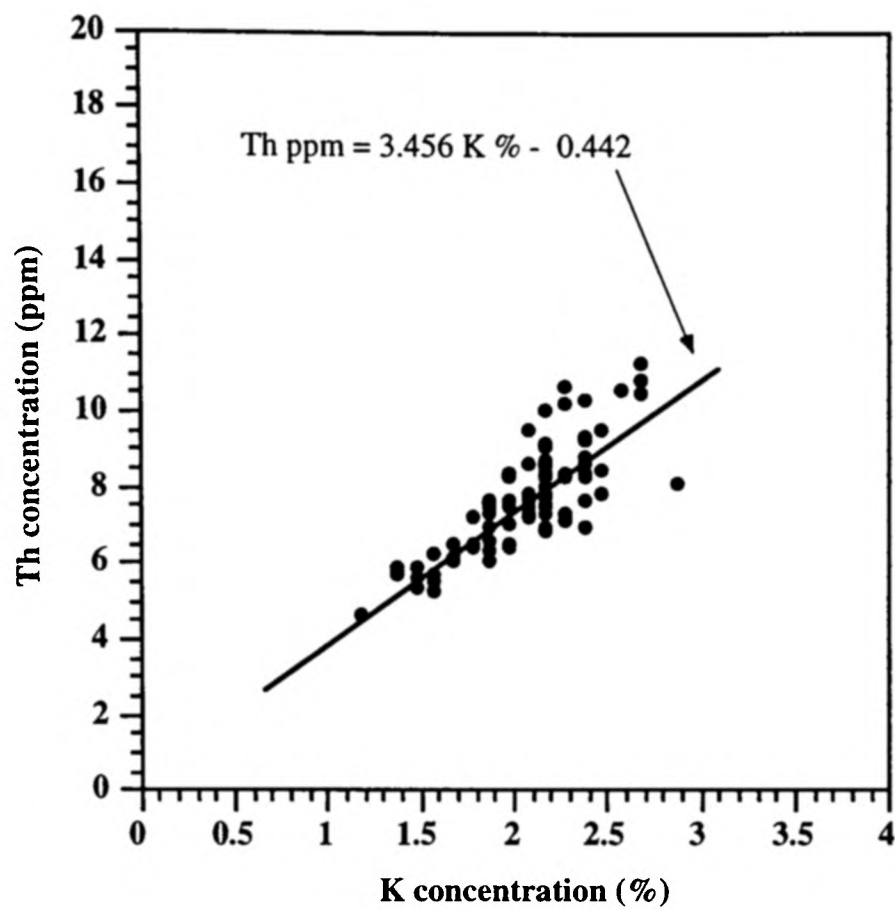


FIGURE 3.52A Positive linear regression between Th concentration and K concentration. A correlation coefficient of 0.66 suggests a statistically robust relationship at the 95 % significance level ($n = 89$). The relationship between the two elements is given with reference to the formula of the linear regression.

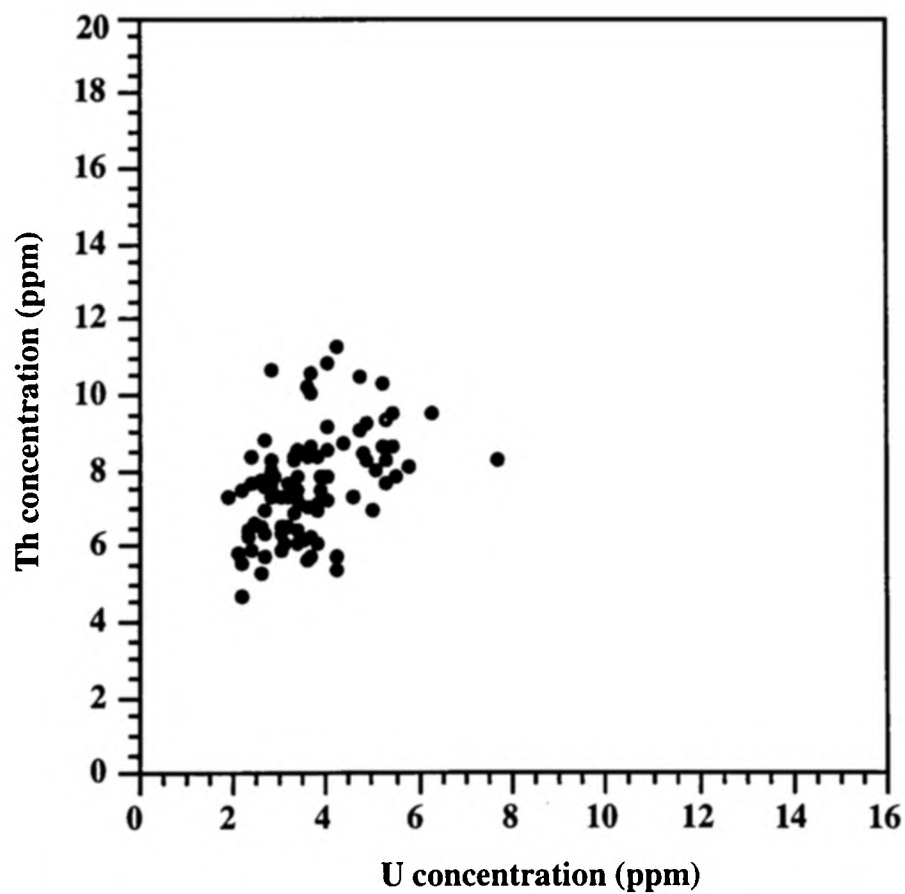


FIGURE 3.52B Positive linear regression between Th concentration and U concentration. A correlation coefficient of 0.19 indicates that no statistically robust relationship is shown between the two elements ($n = 89$).



FIGURE 3.53
The *luridum* Subzone at
Blockley Pit, Gloucestershire
(SP 182369).

(ABOVE) Field aspect of Blockley Pit, currently owned and managed by Northcot Brick Co.

(LEFT) The lowermost 4.2 m thick fresh section exposed at the SE end of the pit. The section is argillaceous in character and shows no evidence for the development of light marl - dark marl couplets that are clearly displayed within the Belemnite Marls at Stonebarrow, Dorset (SY 380927). Lithologically, the section exposed at Blockley Pit shows more similarities to the Shales-with-'Beef' and Black Ven Marls, in Dorset, than the time-equivalent Belemnite Marls. The thickness of the *luridum* Subzone is expanded by a factor of 324 at Blockley Pit relative to the Belemnite Stone in Dorset.

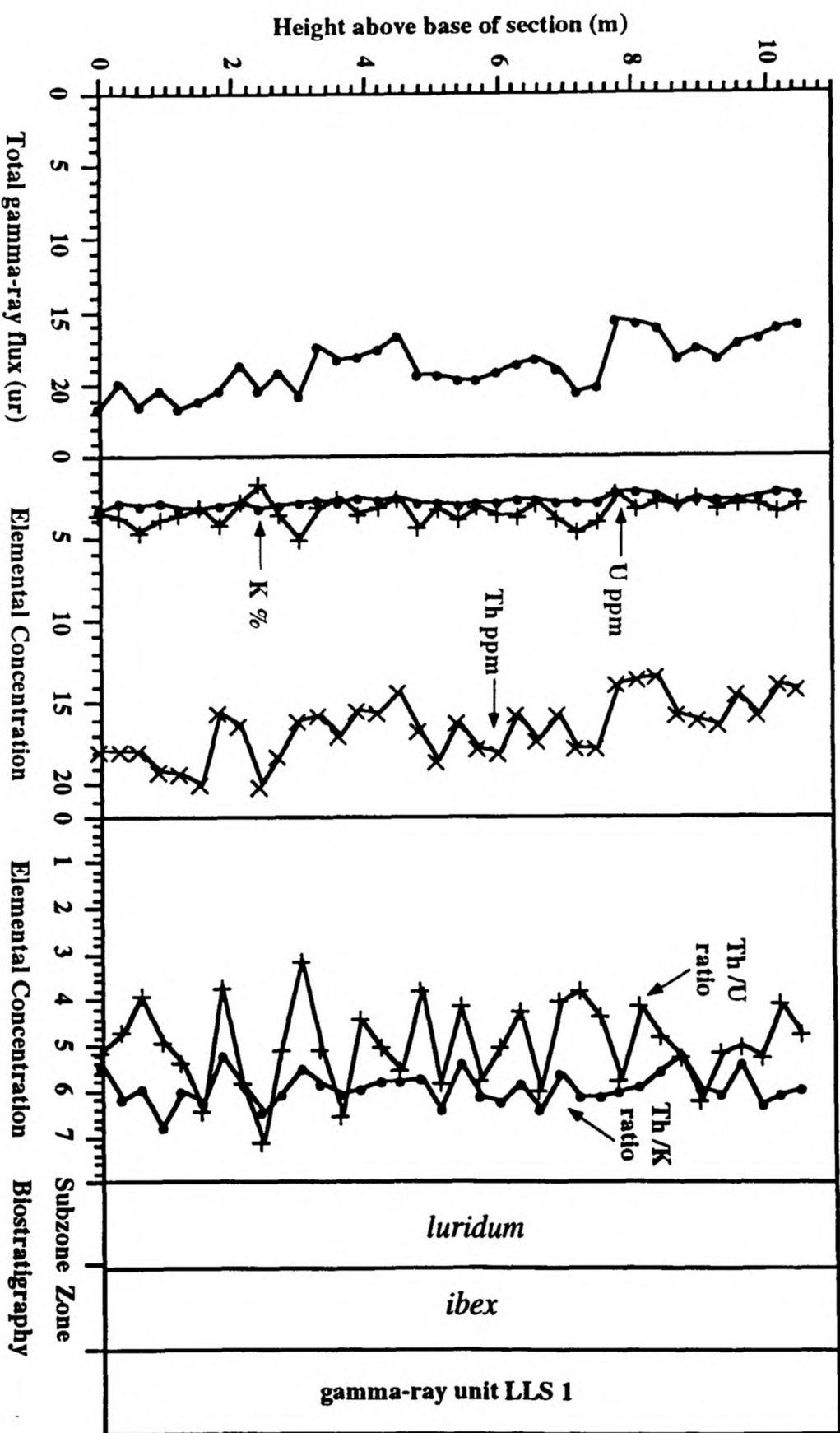


FIGURE 3.54 Total gamma-ray log, elemental concentration logs and elemental ratio curves for the series of sections exposed at Blockley Pit, Gloucestershire (SP 182369). The argillaceous expanded section is the lateral time equivalent of the Belemnite Stone found at the top of the Belemnite Marls at Seatown, Dorset (SY 415918). Biostratigraphic boundaries are indicated. The gamma-ray logs are based on 36 measured samples. (LLS = Lower Lias shale).

Blockley Pit, Gloucestershire.

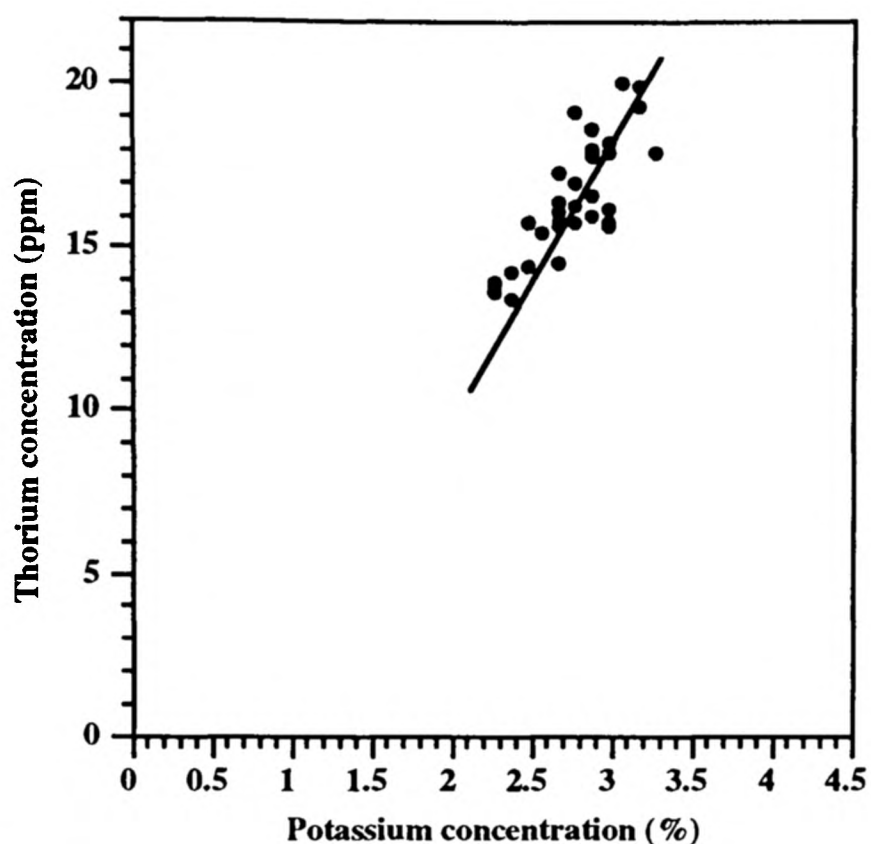


FIGURE 3.55A Linear regression correlation between Th concentration and K concentration. A correlation coefficient of 0.75 suggests a strong, statistically robust correlation at the 95 % significance level (n = 36). The relationship between the two elements can be described by the linear equation : $\text{Th ppm} = 5.695 \text{ K \%} + 0.649$

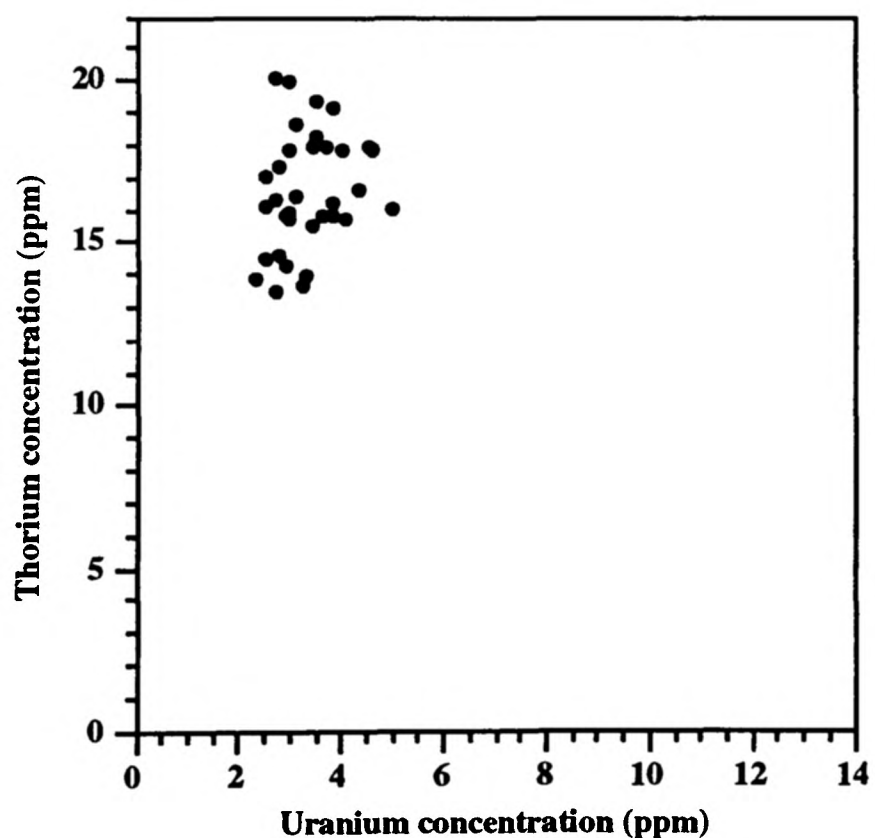
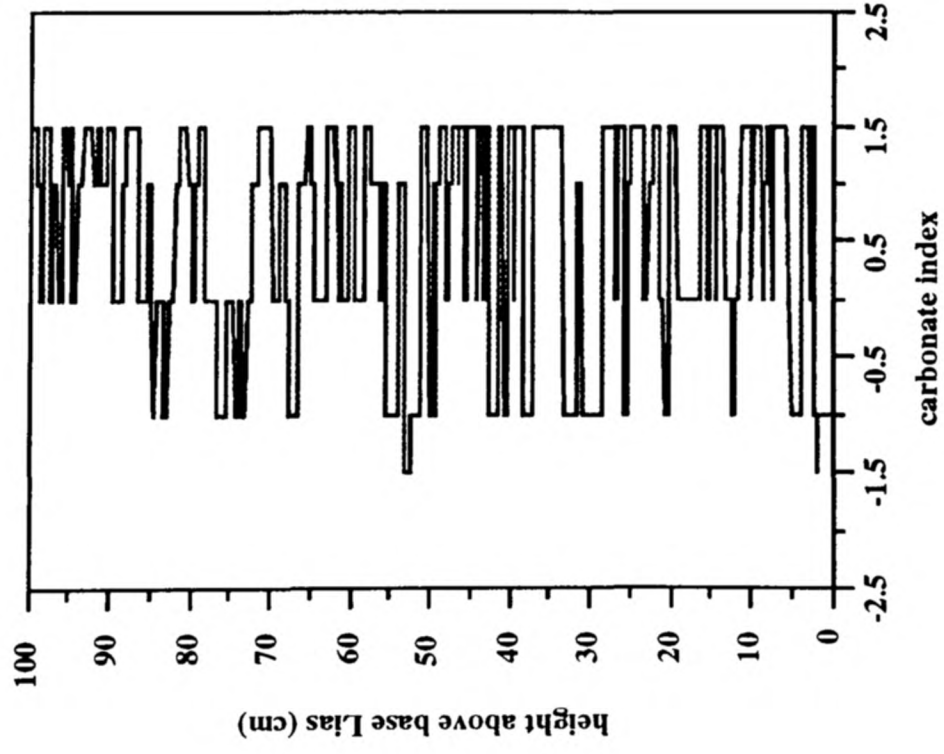


FIGURE 3.55B Linear regression correlation between Th concentration and U concentration. A correlation coefficient of 0.02 indicates that there is no linear covariant relationship between the two elements.

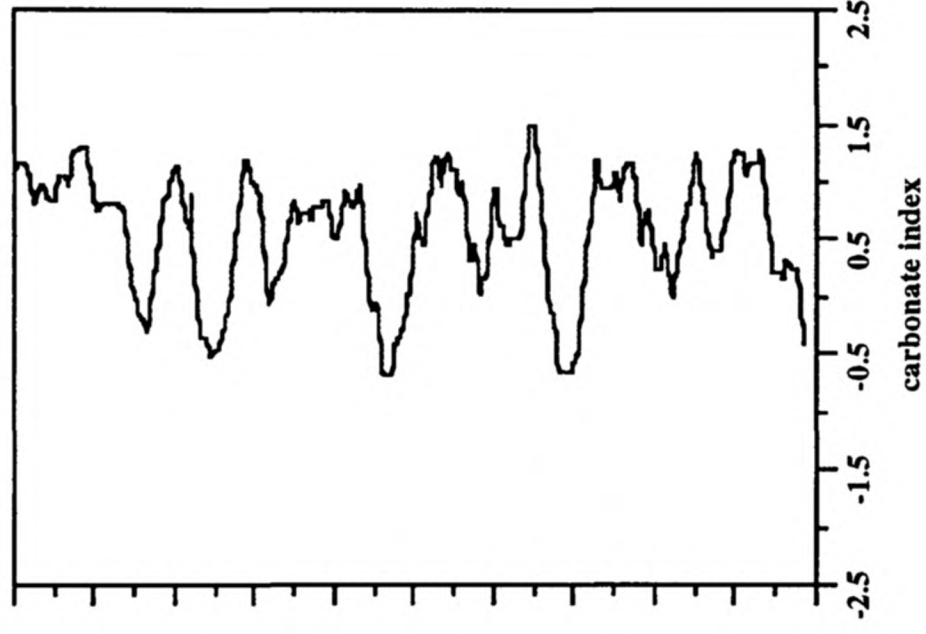
Stage 1

Square wave with high-frequency noise



Stage 2

Noise filtered out over a 30-point running mean



Stage 3

Inverse carbonate index for direct comparison with gamma-ray logs

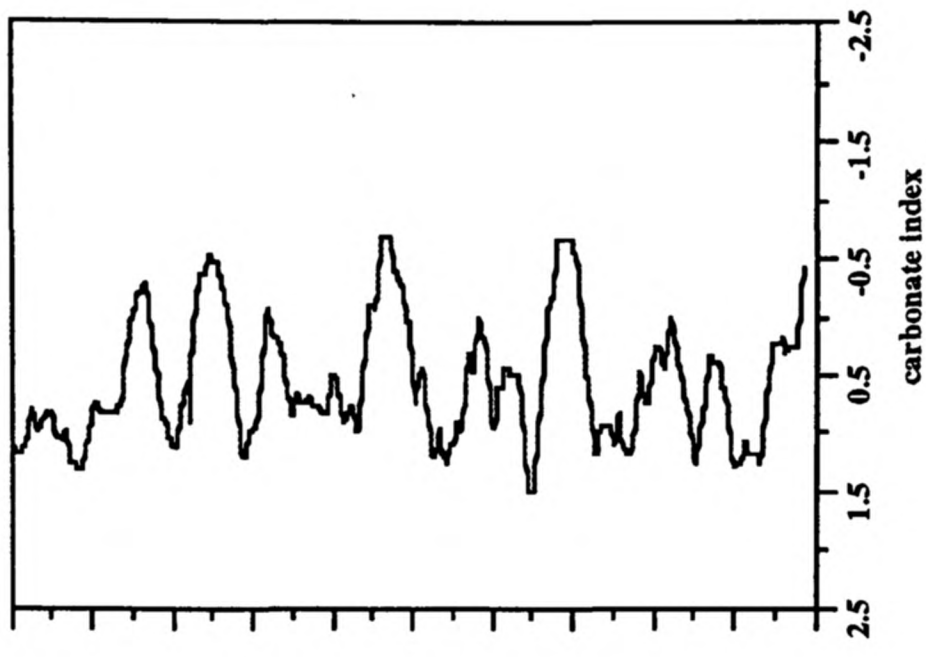


FIGURE 3.56 The production of a synthetic gamma-ray log using bed thickness data from measured stratigraphic sections.

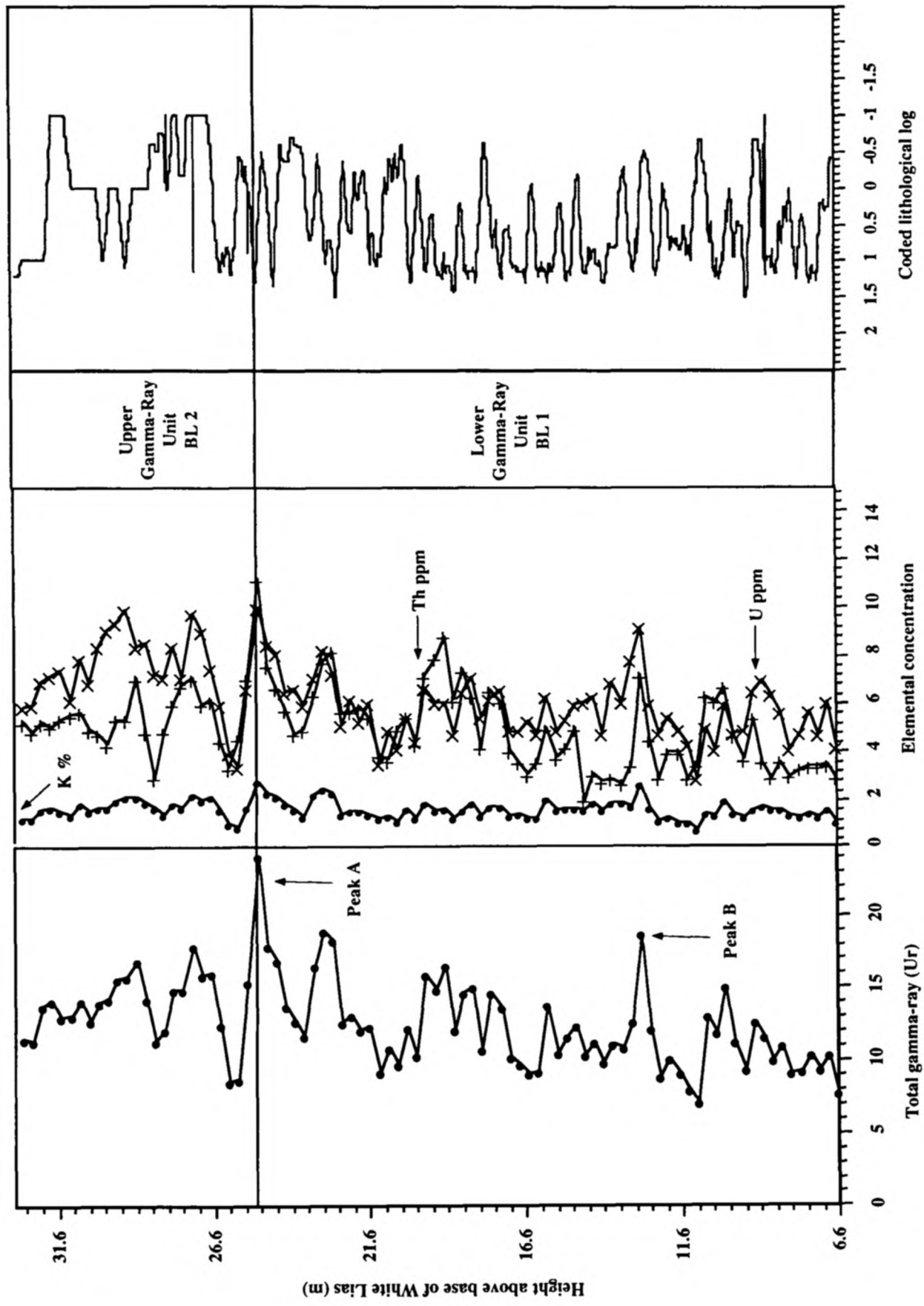


FIGURE 3.57 Comparison of the outcrop gamma-ray log with the coded-lithological log for the Blue Lias of the Dorset coast. Important information shown by the gamma-ray log cannot be obtained from the synthetic coded lithological log. For the coded lithological-log to be used as a proxy gamma-ray log, identical concentrations of K, U and Th have to be assumed for each horizon of the same lithology. The outcrop gamma-ray log clearly shows that this is an invalid assumption, with fluctuations in each of the radio-elemental logs (for an identical lithology) evident.

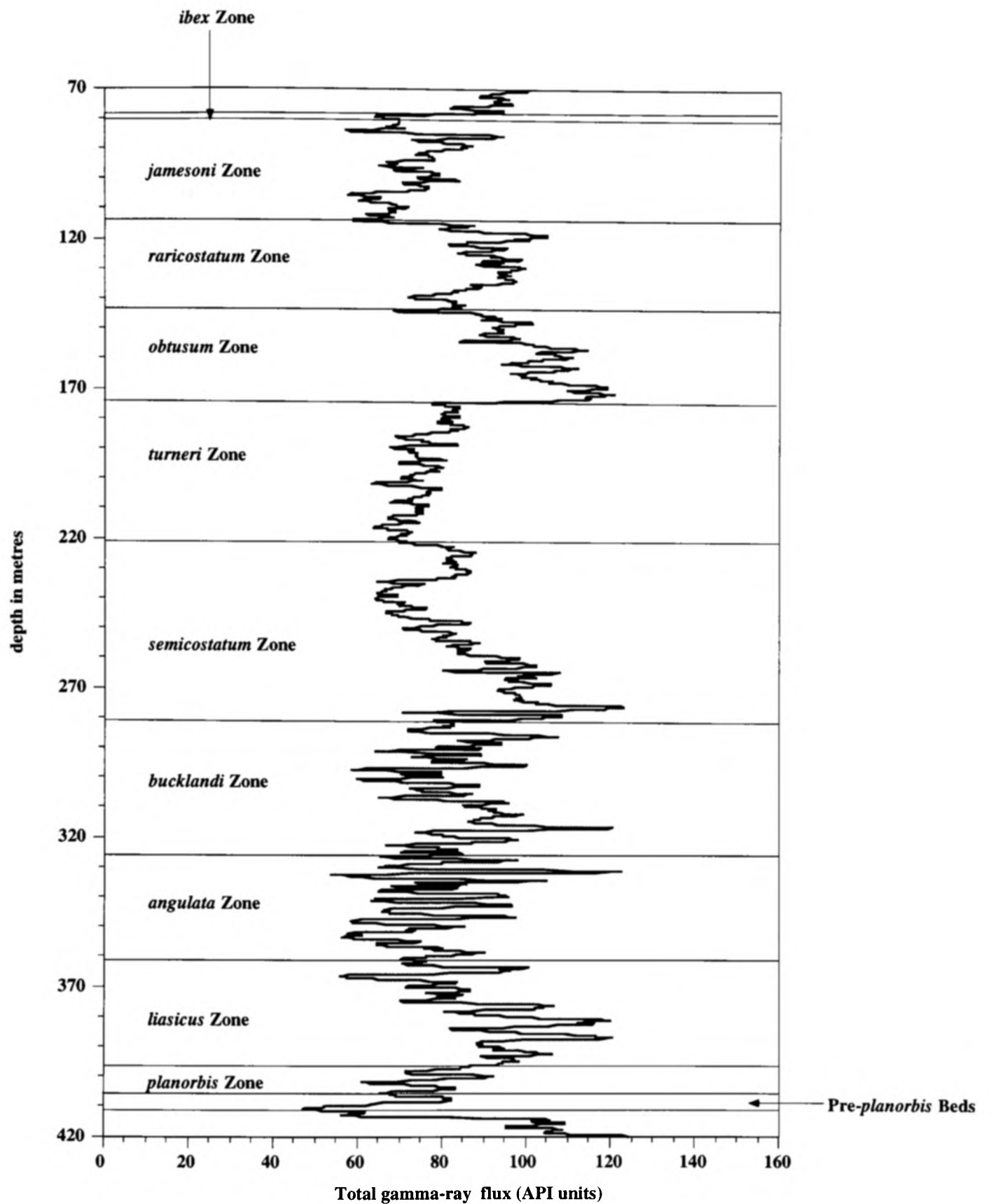


FIGURE 3.58 A Biostratigraphic divisions of the Burton Row borehole at the zonal level of resolution. The biostratigraphy in Burton Row is accurately known to the resolution of ammonite subzones between 404.68 m and 232.87 m, base *planorbis* Subzone to top *scipionianum* Subzone (Whittaker 1983). Thereafter, resolution is at the level of the ammonite zone (see Ivimey-Cook & Donovan 1983).

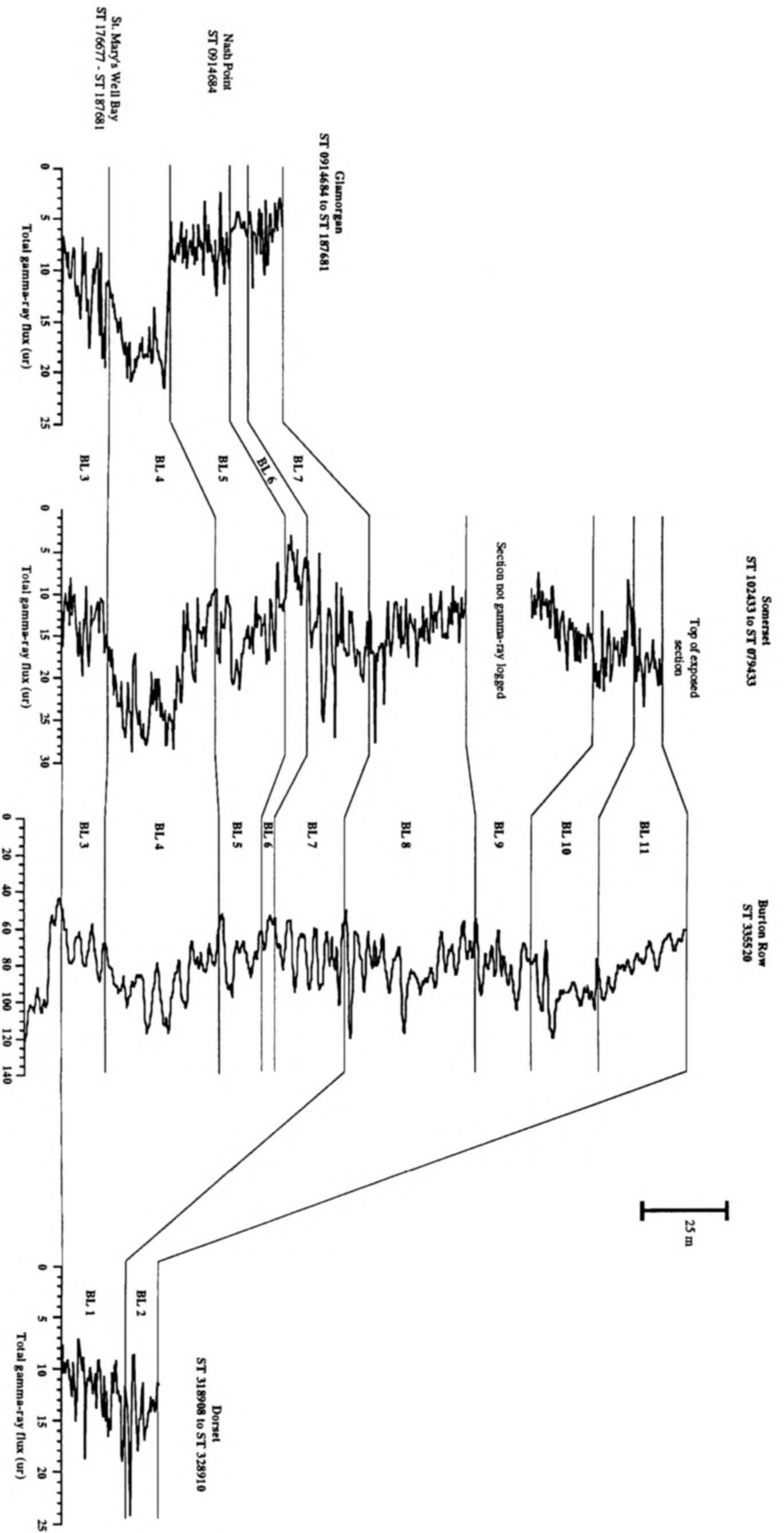


FIGURE 3.58 B Correlation of the Hettangian to Lower Sinemurian succession across southern Britain.

The outcrop total gamma-ray log for the Glamorgan coast was collected from St. Mary's Well Bay to Lavernock Point (ST 176677 to ST 187681) for the *Pre-planorbis* Beds to basal 12.3 m of the *luscicus* Zone and at Nash Point, ST 102433, for the *angulata* and *bucklandi* Zones. Total gamma-ray logs for the Somerset coast were collected from St. Audrie's Bay, ST 102433, for the *Pre-planorbis* Beds to *angulata* Zone, east of Klive Pill, ST 144455 to ST 153452, for the *angulata* and *bucklandi* Zones, west of Klive Pill, ST 139457 to ST 144455, for the *bucklandi* Zone and lowermost 5.4 m of the *semicostatum* Zone and from the west end of Doniford Bay, ST 079433 to 082430, for the remainder of the *semicostatum* Zone. The section measured from Hinkley Point, ST 210465, was found to be artificially contaminated with radionuclides. The total gamma-ray log for the Dorset coast was collected from sections exposed between Pinhay Bay (SY 318908) and Seven Rock Point, Lyme Regis (SY 328910).

Figure 3.58 B

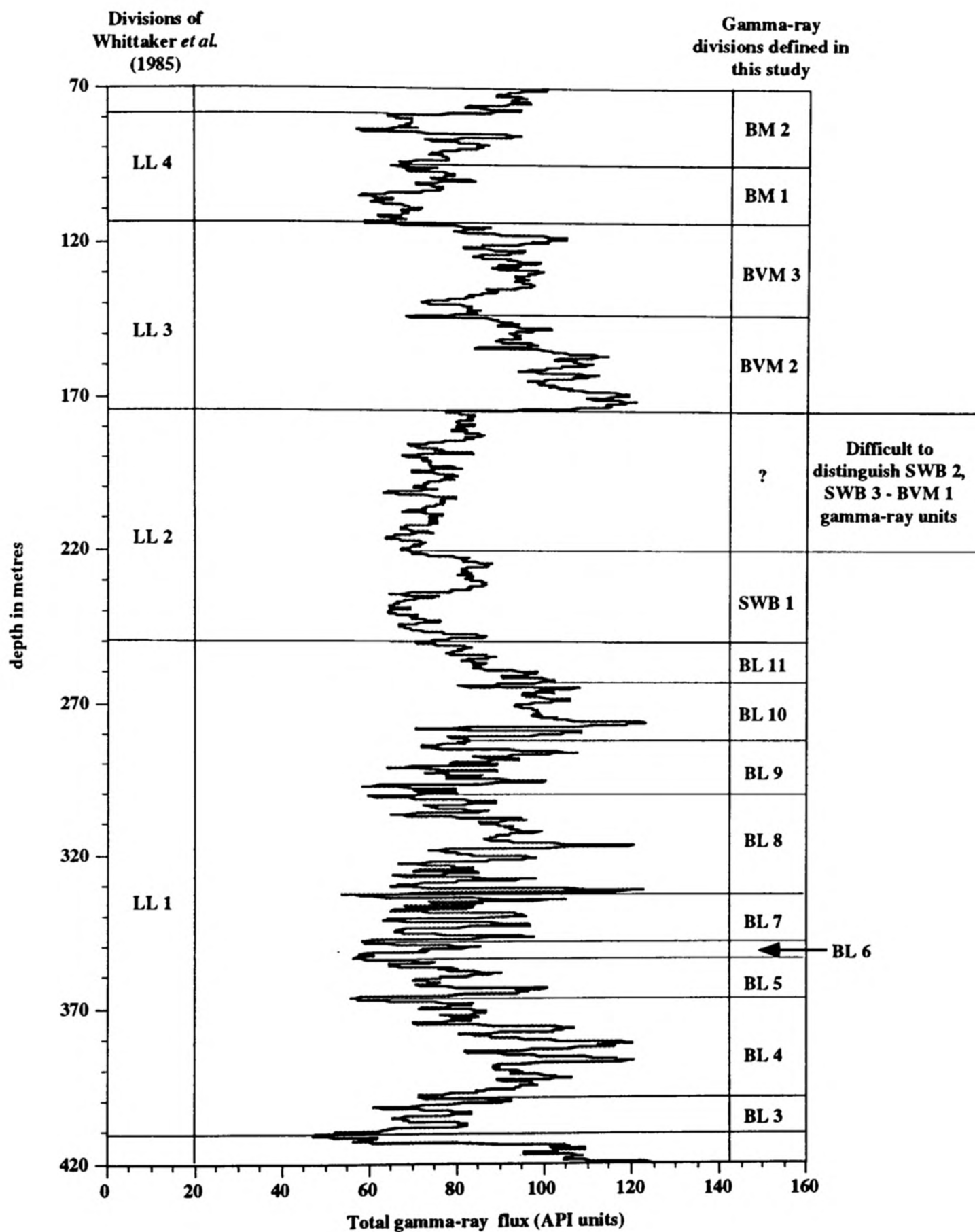


FIGURE 3.59 Divisions of the Burton Row borehole. The gamma-ray units originally identified by Whittaker *et al.* (1985) from this borehole are shown. Comparison with the gamma-ray units defined in this study are shown. Gamma-ray units BL 3 to BL 11, defined from coastal exposure in the Bristol Channel Basin, can be identified in Burton Row. Gamma-ray units BVM 2 to BM 2, defined from the exposure along the Dorset coast in the Wessex Basin, can also be identified in the Burton Row borehole. It is difficult to distinguish gamma-ray units SWB 2 and SWB 3-BVM 1 in Burton Row between the depths 199.8 m and 154.63 m. It is probable that the Black Ven Marls are thicker than Whittaker's (1985) division would suggest.

Biostratigraphy in Burton Row is accurately known to the resolution of ammonite subzones between 404.68 m and 232.87 m (base *planorbis* Subzone to top *sciponianum* Subzone). Thereafter, resolution is at the level of the ammonite zone (see Ivimey-Cook & Donovan 1983). Within Burton Row, the gamma-ray unit BVM 2 additionally includes the *oxynotum* Zone that is represented by the Coinstone disconformity in Dorset. The *oxynotum* Zone is represented between the depths 137.50 m and 154.63 m (Whittaker 1983).

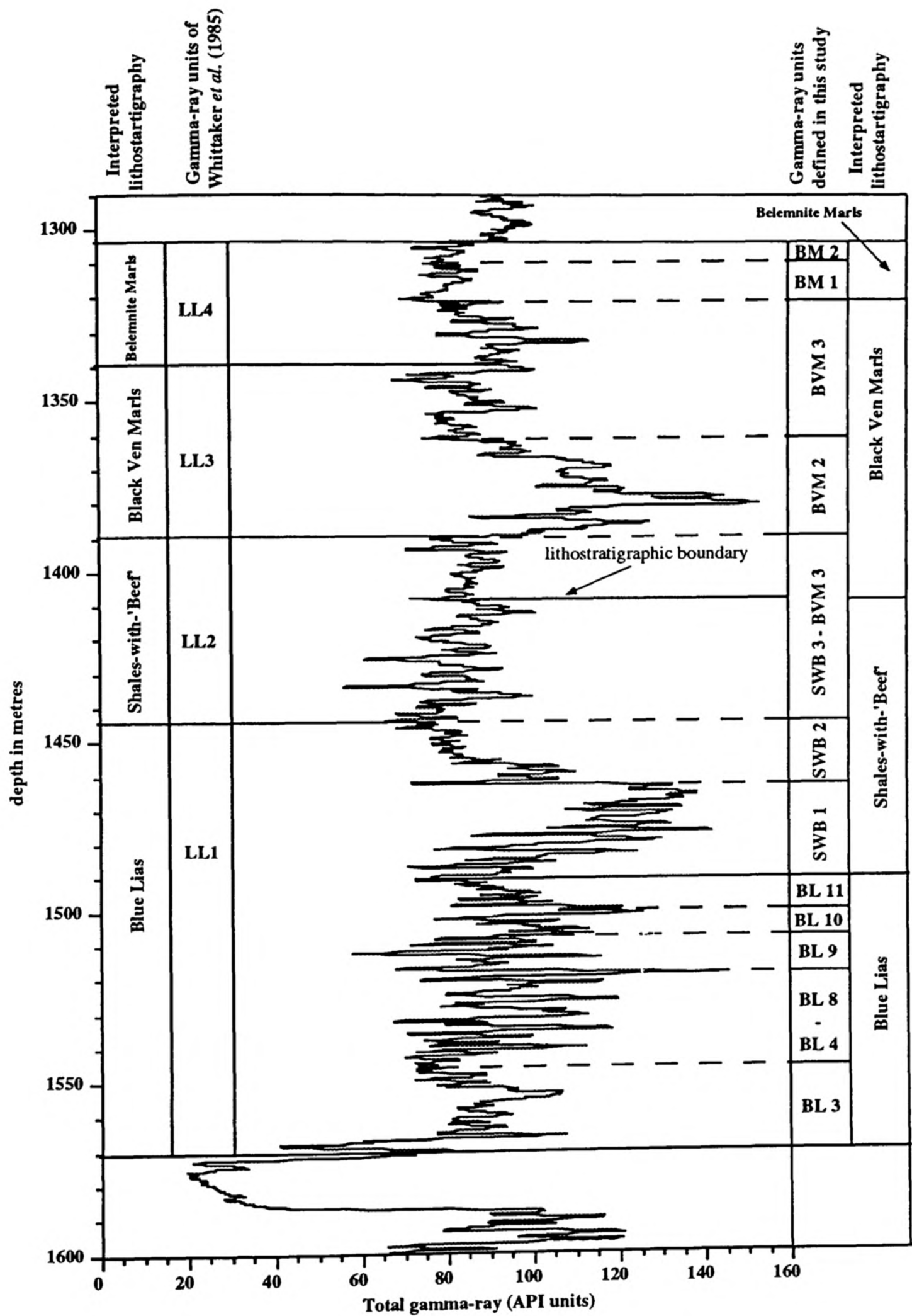


FIGURE 3.60 Division of the uncored Winterborne Kingston borehole into total gamma-ray units. A comparison of the divisions made by Whittaker *et al.* (1985) and those based on this study is shown. There are considerable differences in the identification of formation boundaries and the thickness of the recognised formations. All the gamma-ray units defined from the Dorset outcrop gamma-ray log can be identified in the Winterborne Kingston borehole.

Chapter 4
Figure 4.01 to Figure 4.22

**Interpretation of the Gamma-Ray Characteristics shown
by the Lower Lias in Southern Britain**

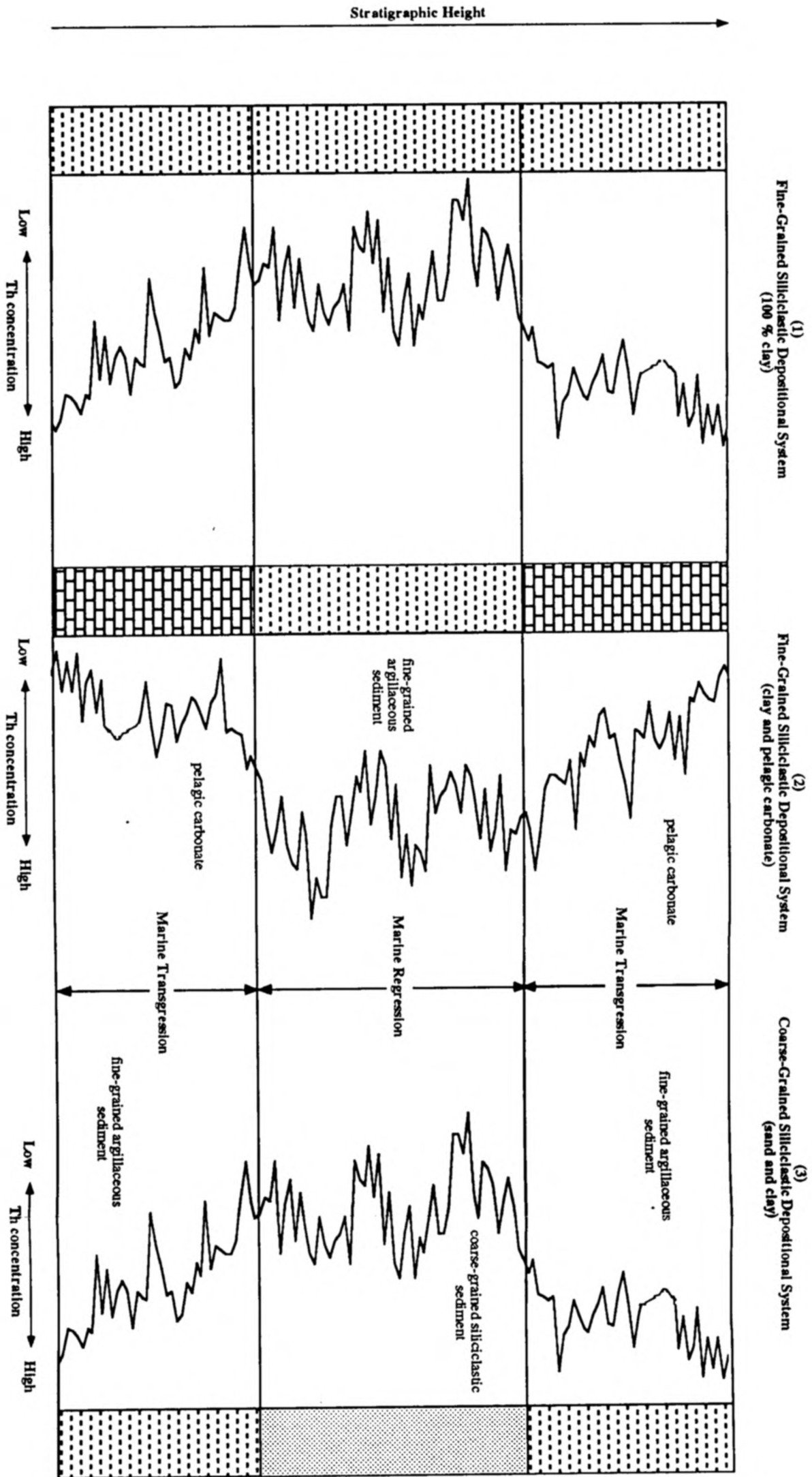


FIGURE 4.01 A Typical signatures that would be expected to be shown by the Th gamma-ray log for (1) a fine-grained depositional system of 100% clay, (2) a fine-grained depositional system characterized by clay and pelagic carbonate and, (3) a coarse-grained depositional system. The Th concentration log for the 100% clay depositional system is theoretical, whereby Th concentration increases with decreasing particle size due to the higher surface area-to-volume ratio shown by smaller grains. In the mixed pelagic carbonate and clay depositional system (2), during conditions of marine regression, the deposition of clay correlate with the deposition of sand in the coarse-grained depositional system. A high Th concentration in the former therefore equates with a low Th concentration in the latter(3). During marine transgression pelagic carbonate may be the dominant component of marine sediment in the fine-grained clay-pelagic carbonate depositional system giving rise to a low Th concentration. In contrast during periods of transgression, argillaceous material may be the dominant component of marine sediment which gives rise to high Th concentrations on the gamma-ray log for the coarse-grained depositional system.

Figure 4.01 A

B

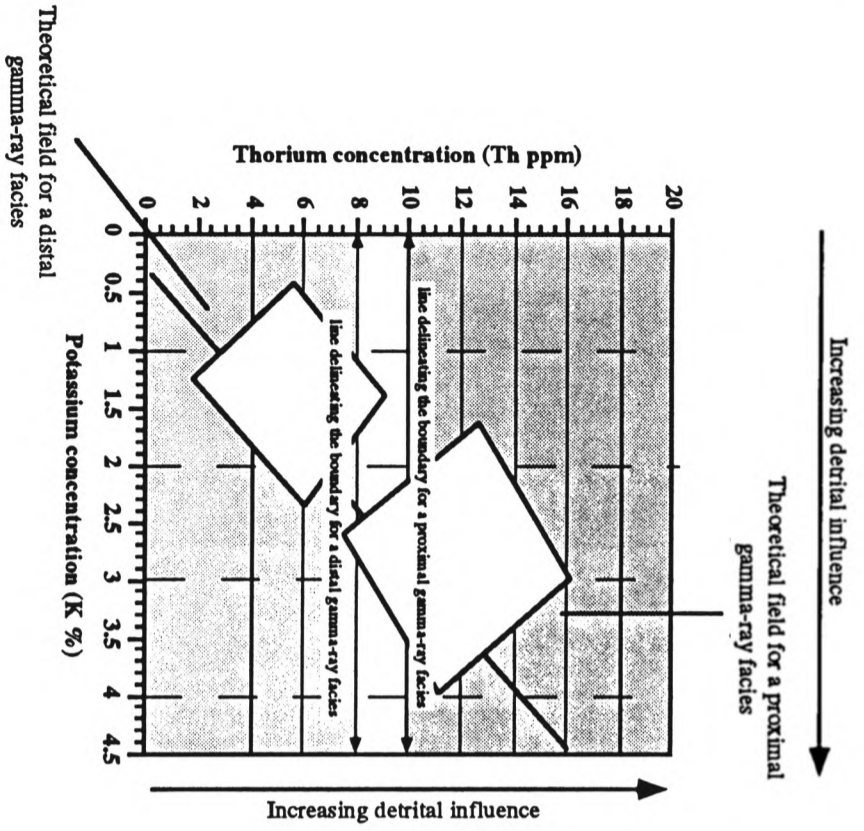


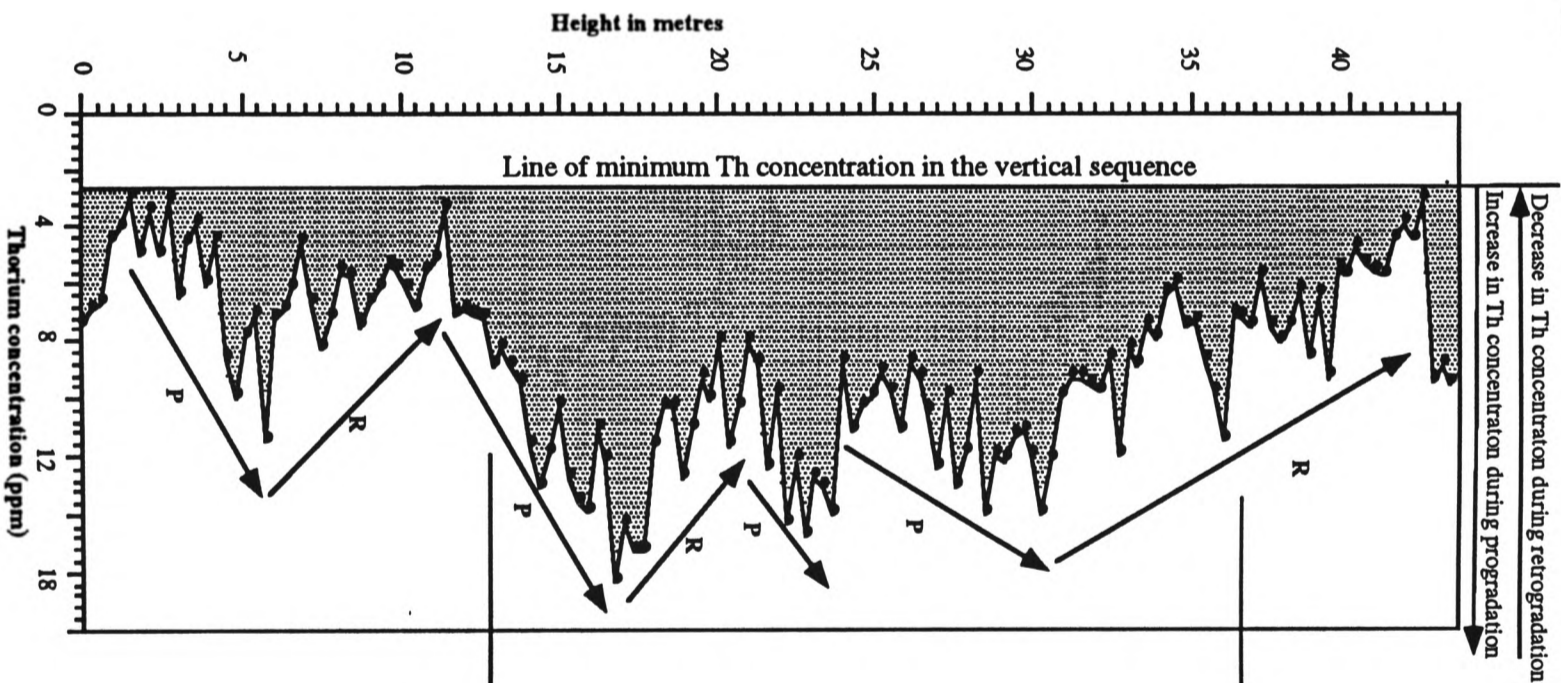
FIGURE 4.01 Facies Analysis Using the Th Gamma-Ray Log

ABOVE (A) For all sets of measurements that have been collected in this study there is a strong linear positive correlation between soluble K and insoluble Th. The delineation between a proximal and a distal facies is taken at a Th concentration of 8 ppm to 10 ppm which commonly coincides with a K concentration of 2.25, although the actual K concentration will be determined by fluctuations within the detrital clay mineralogy. Distal mudrock facies, defined by low detrital elemental concentrations, ($Th < 8\text{ppm}$) will fall in the lower left hand corner of the regression plot and a proximal mudrock facies ($Th > 10\text{ppm}$) will fall in the upper right hand corner of the regression plot. Allowance has to be made for the degree of scatter away from the regression line, which is probably an indication of diagenetic alteration (*i.e.* degree of K mobility).

RIGHT (B) The Th concentration log, collected from a marine mudrock sequence can also be used to determine intervals of mudrock progradation (denoted P on the curve) and intervals of mudrock retrogradation (denoted R on the curve). Increases in Th concentration, over a sufficient vertical interval, indicate the progressive clastic dilution of hemipelagic carbonate as fine-grained clastics prograde basinward. Conversely, decreases in Th concentration would therefore represent periods of retrogradation when deposition would become increasingly dominated by hemipelagic carbonate as fine-grained clastic deposition is confined to the basin margin.

This argument assumes that pelagic carbonate productivity does not increase during periods of regression but productivity may increase during periods of transgression or highstand. This is in accordance with Berger (1976) for coccolith distribution in the Recent and Schlager (1990).

C



Retrogradational Stacking Pattern:
Decrease in fine-grained sediment supply. Hemipelagic carbonate dilution leads to an decrease in the concentration of Th within a vertical sequence.

These trends are denoted by the letter R.

Progradational Stacking Pattern: Increase in fine-grained sediment supply. Clastic dilution of hemipelagic carbonate leads to an increase in the concentration of Th within a vertical sequence.

These trends are denoted by the letter P.

FIGURE 4.01 B and C

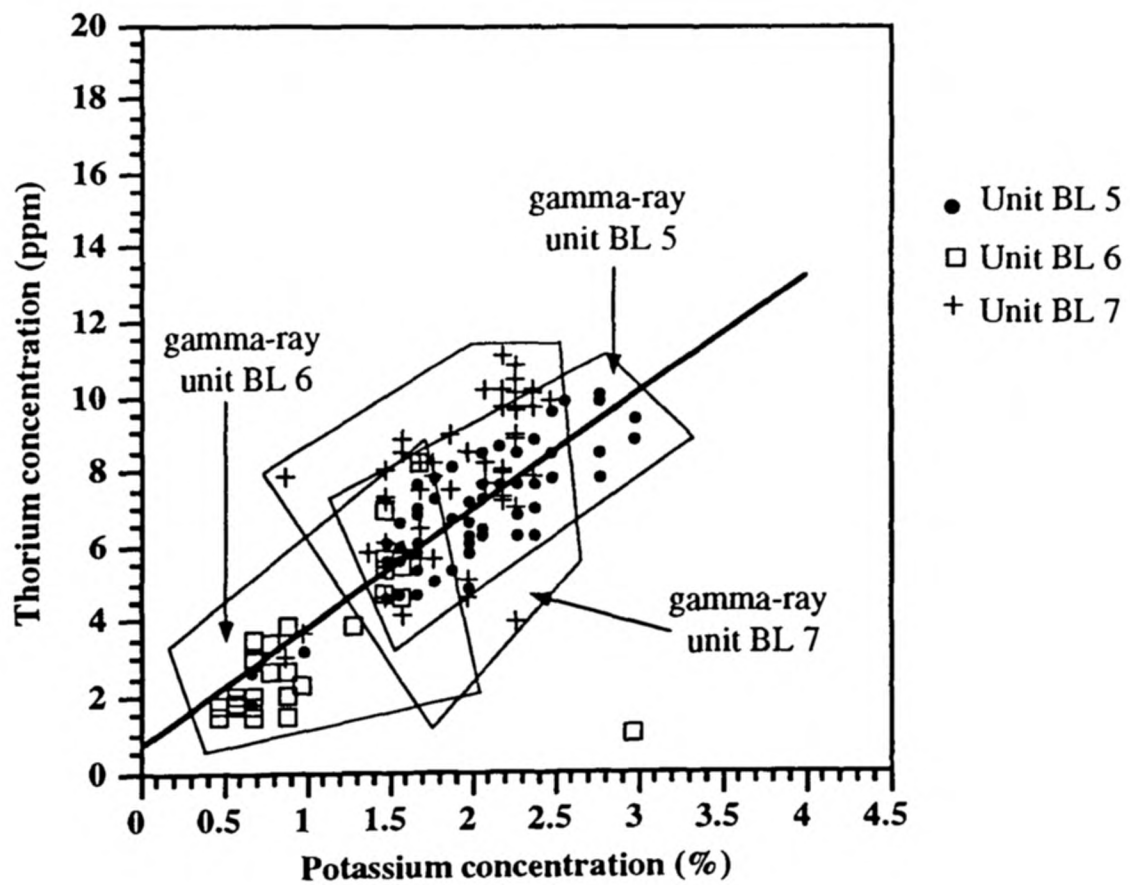
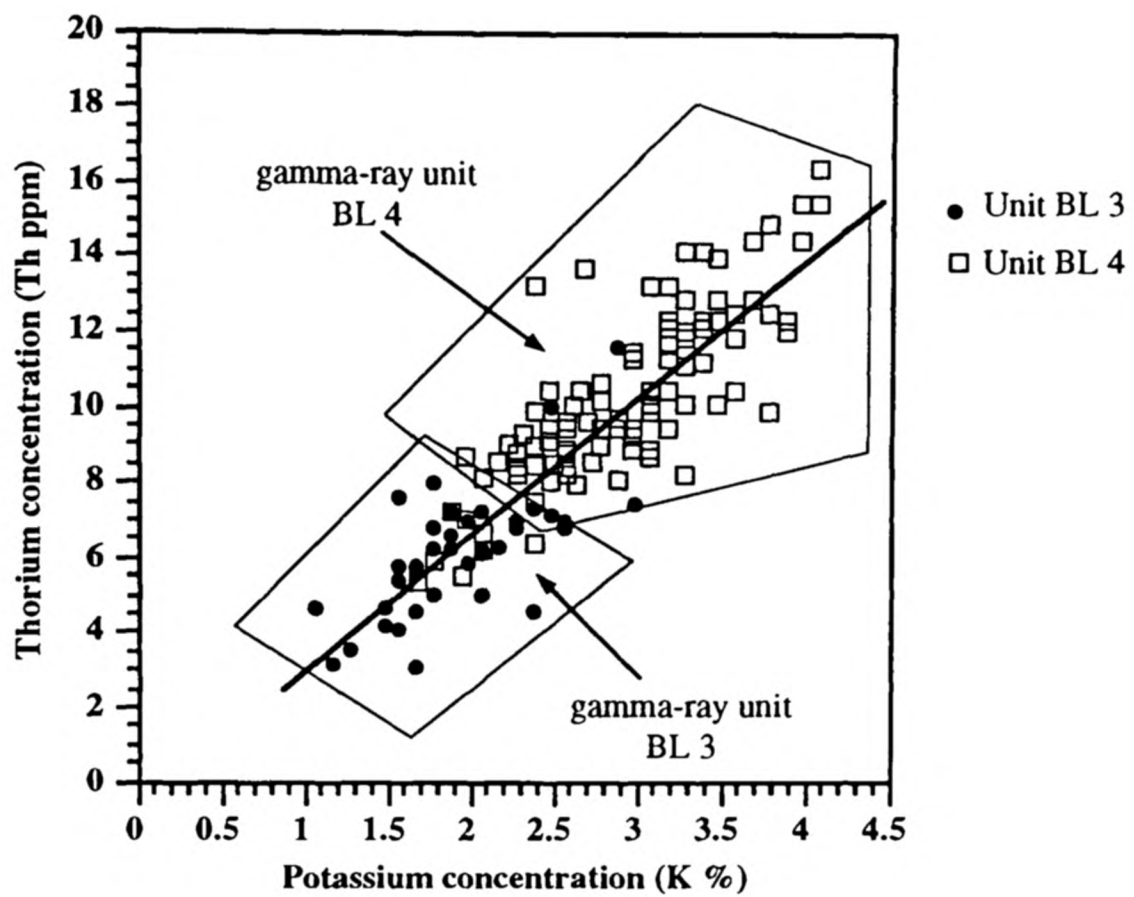


FIGURE 4.02 Th-K fields shown by each gamma-ray unit for the Pre-*planorbis* Beds to *bucklandi* Zone in Somerset. Units BL 3 and BL 6 have Th-K concentrations that are characteristic of a distal gamma-ray facies in contrast to unit BL 4 that has Th-K concentrations that are characteristic of a proximal gamma-ray facies. The other units that are shown have detrital element concentrations that are typical of both gamma-ray facies.

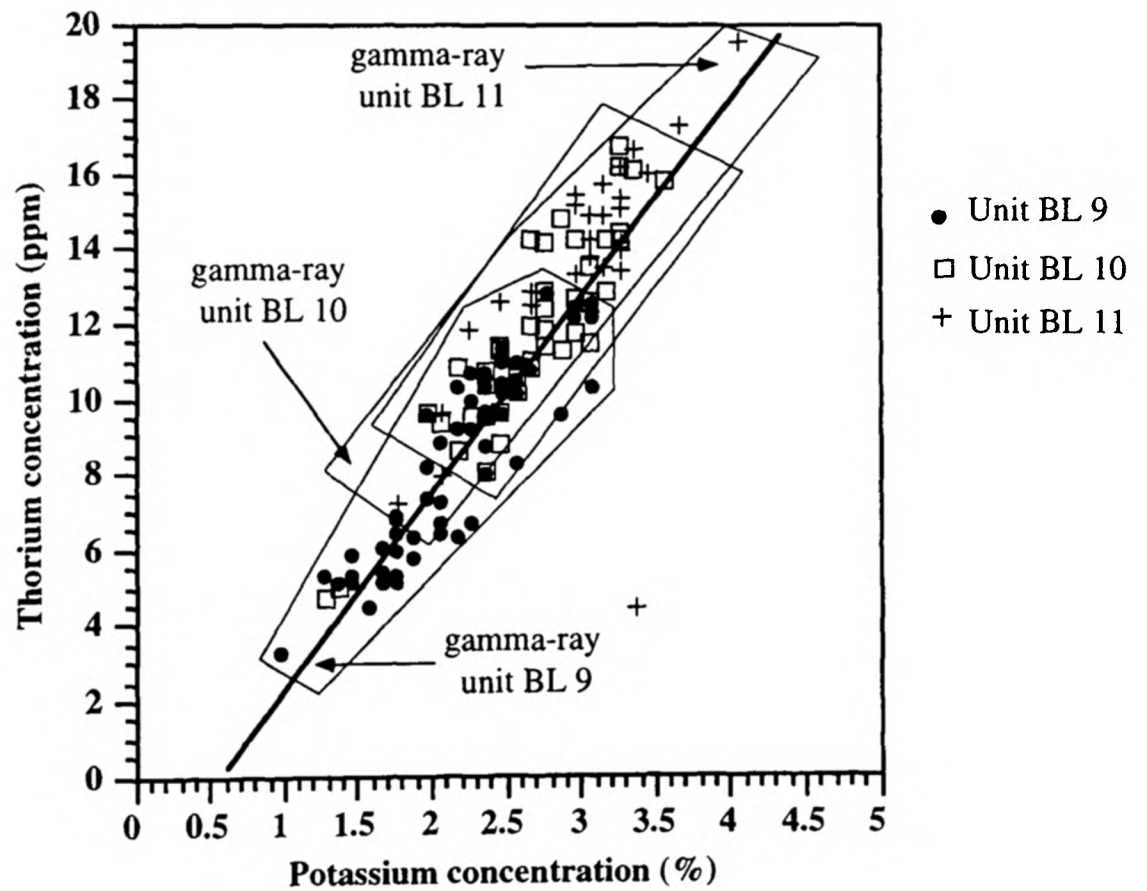
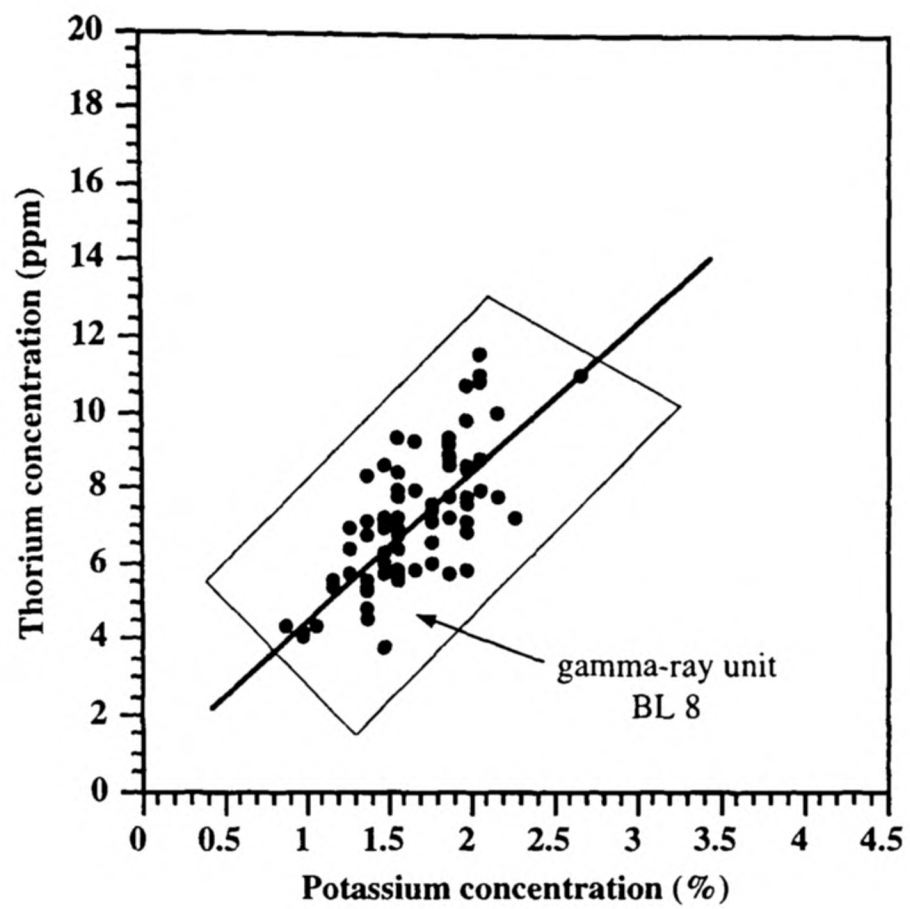


FIGURE 4.03 Th-K fields shown by each gamma-ray unit for the upper *bucklandi* Zone and lower *semicostatum* Zone in Somerset. Units BL 10 and BL 11 have Th-K concentrations that are characteristic of a proximal gamma-ray facies. The other units that are shown have detrital element concentrations that are typical of both gamma-ray facies.

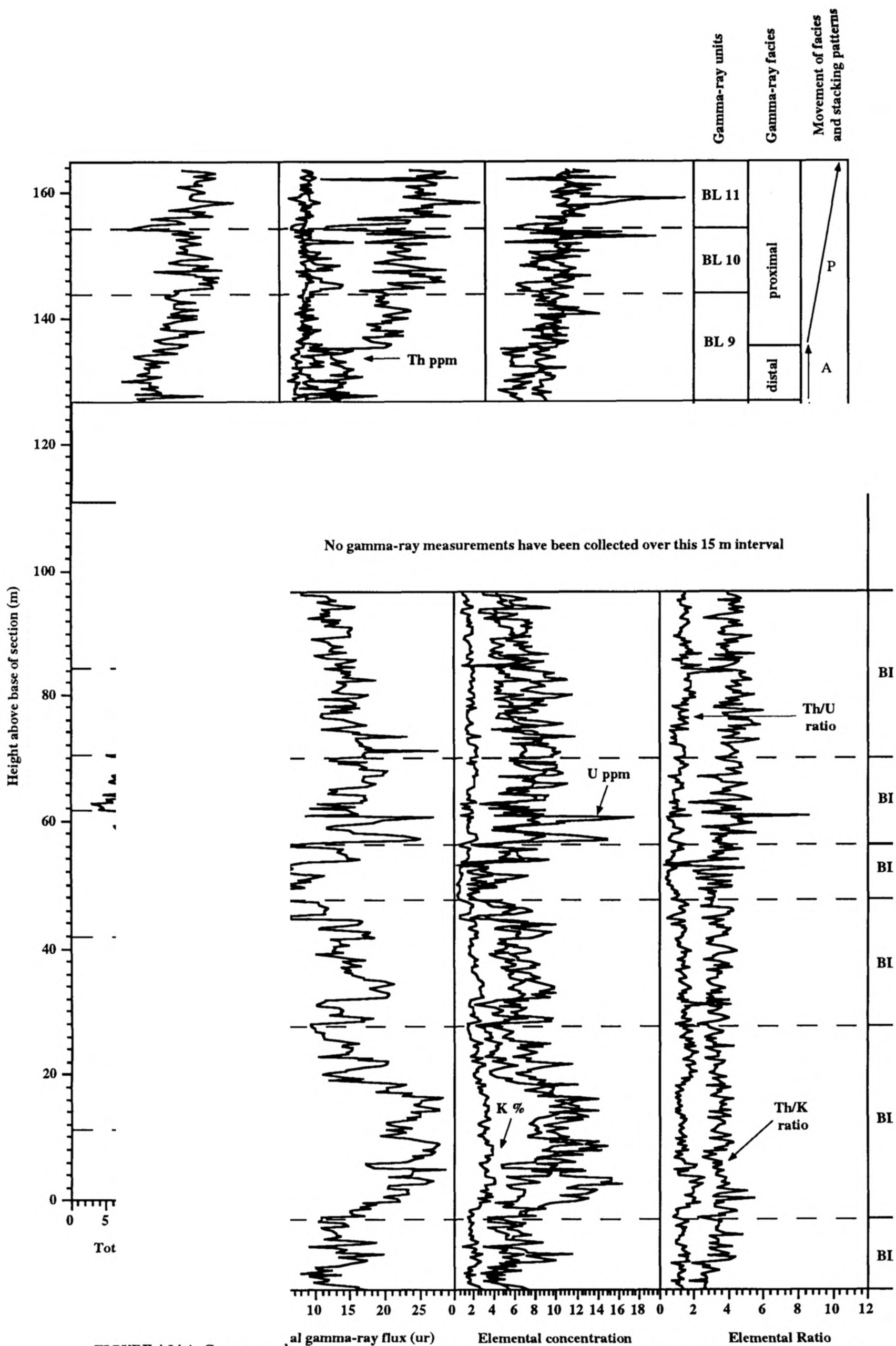


FIGURE 4.04 A Gamma-ray logs for the Lower Liass succession of the Connecticut coast divided into gamma-ray units. The direction of detrital influence and migration of facies, as inferred from the Th concentration log, is shown for each gamma-ray unit. Stacking patterns within each gamma-ray unit are also indicated (P = progradation, A = aggradation and R = retrogradation).

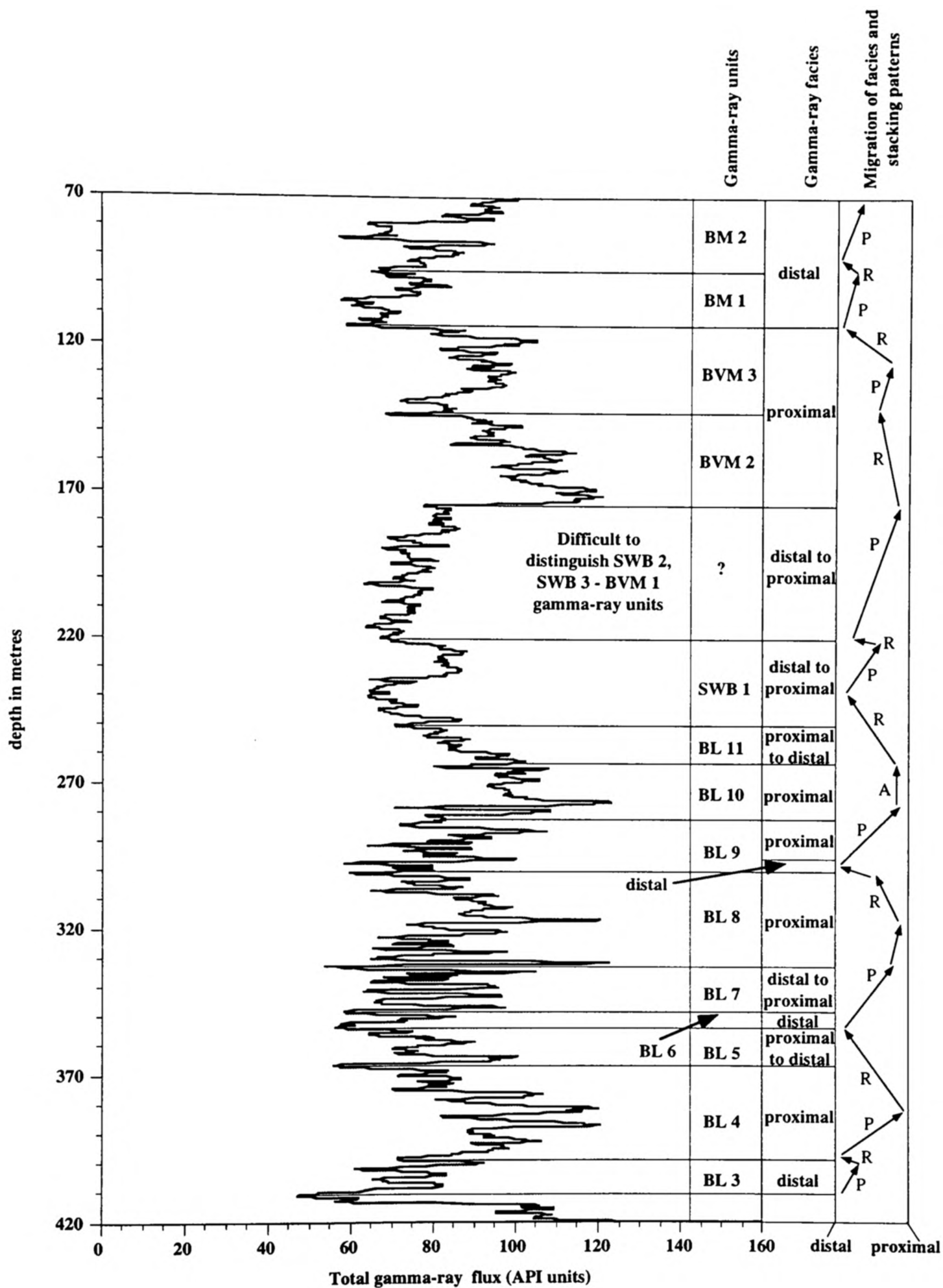


FIGURE 4.04 B The total gamma-ray log of the Burton Row borehole divided into gamma-ray facies based on the spectral gamma-ray data collected from the Dorset and Somerset coasts. The direction of detrital influence and migration of facies is shown for each gamma-ray unit. Stacking patterns within each gamma-ray unit are also indicated (P = progradation, A = aggradation and R = retrogradation).

This interpretation assumes that the total gamma-ray log for Burton Row reflects Th content. This assumption is only valid by comparison with the outcrop spectral gamma-ray log data and cannot be made on the basis of total gamma-ray flux alone.

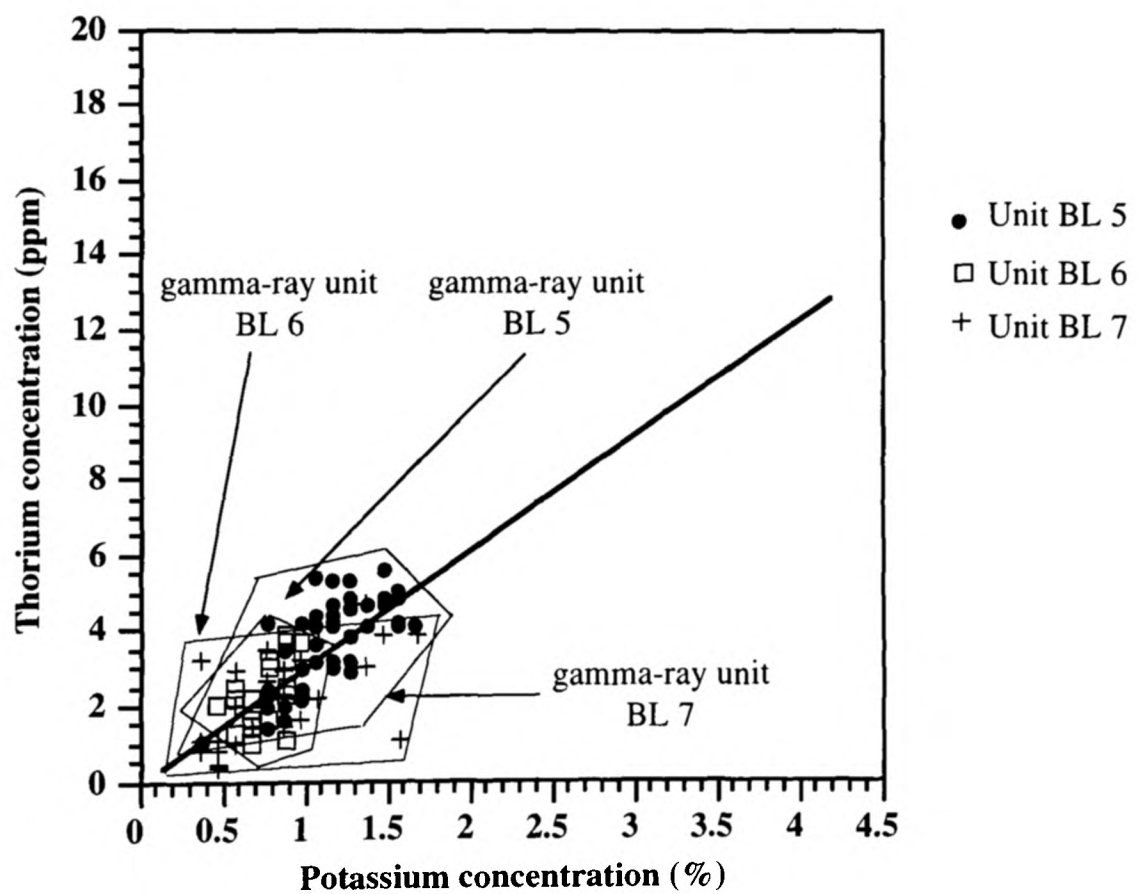
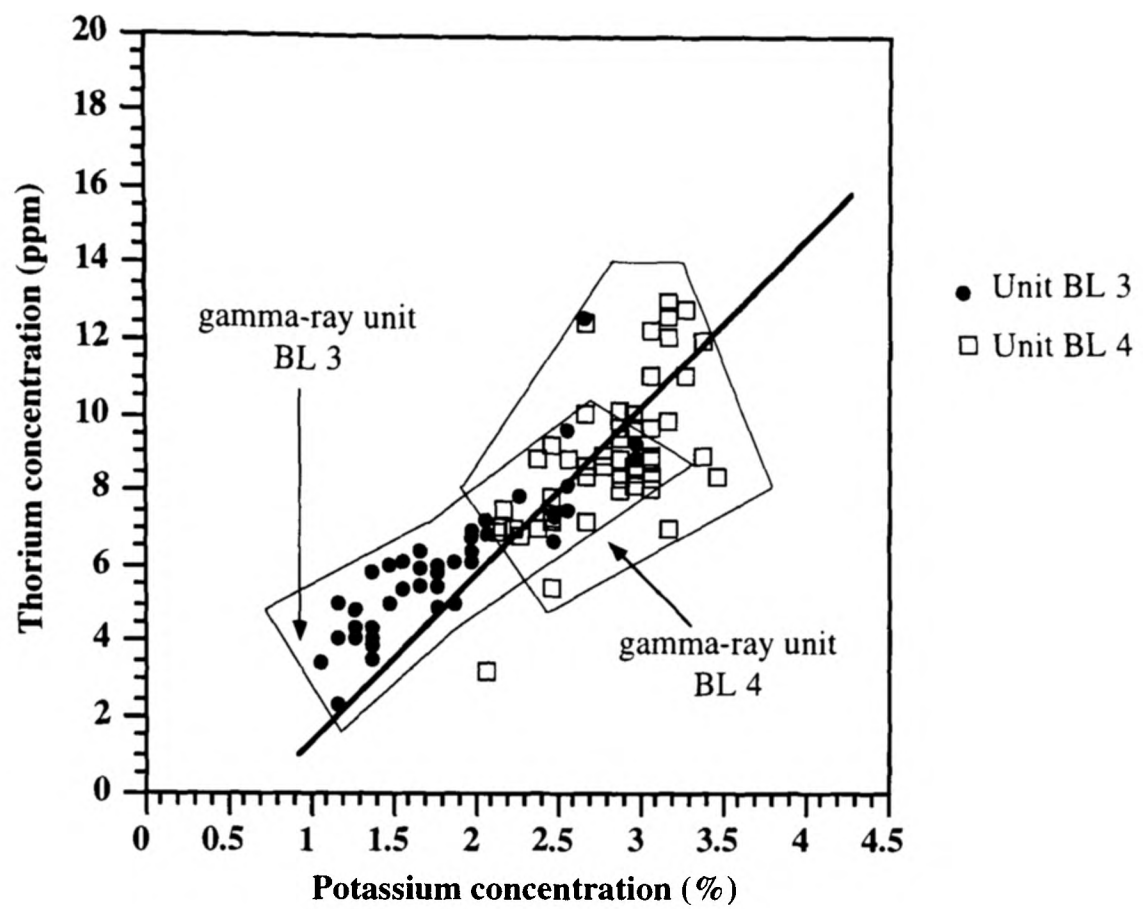


FIGURE 4.05 Th-K fields shown by each gamma-ray unit for the Pre-*planorbis* Beds to *bucklandi* Zone in Glamorgan. Units BL 3, BL 5, BL 6 and BL 7 have Th-K concentrations that are characteristic of a distal gamma-ray facies in contrast to unit BL 4 that has Th-K concentrations that are characteristic of a proximal gamma-ray facies.

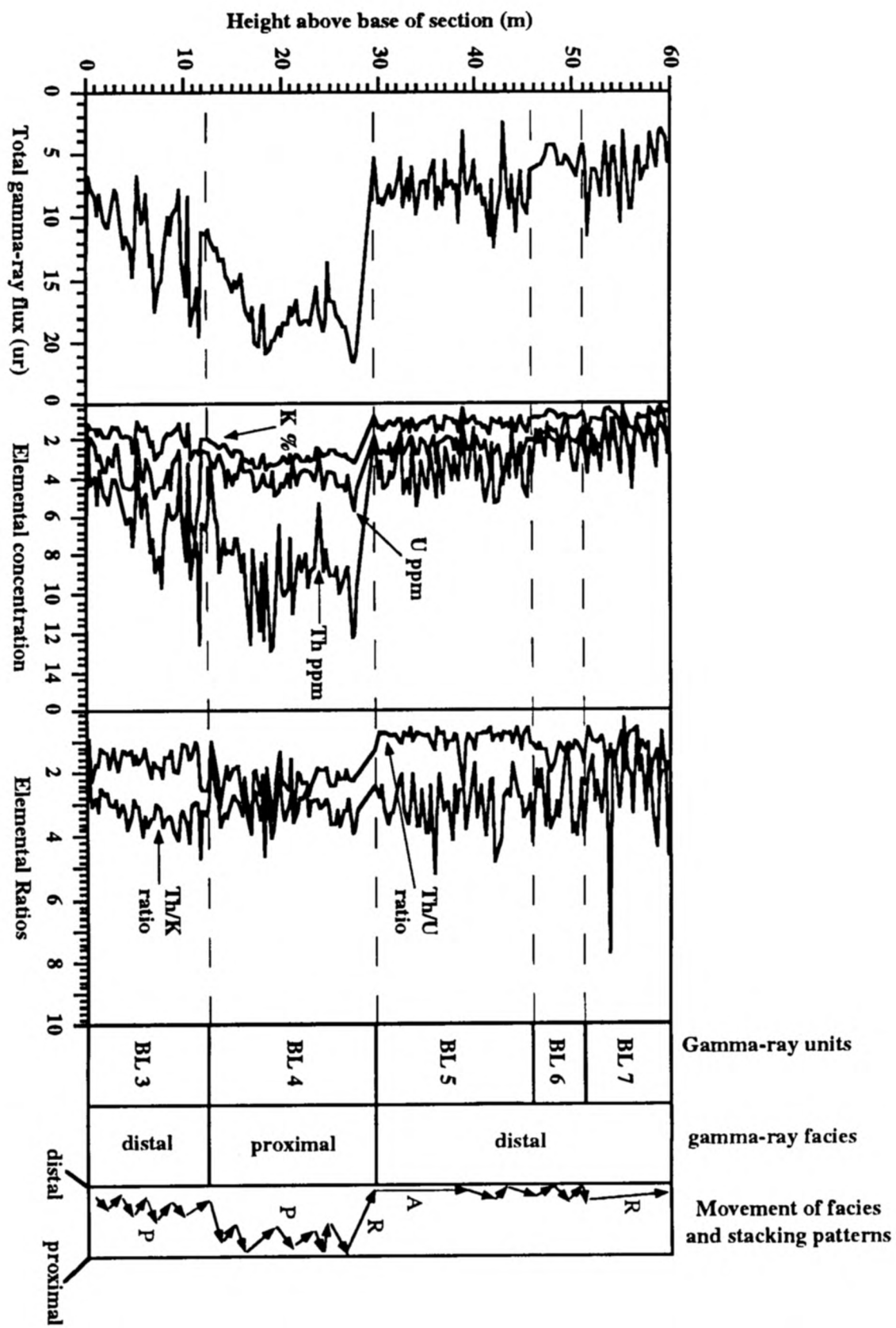


FIGURE 4.06

FIGURE 4.06 Gamma-ray logs for the Lower Lias succession of the Glamorgan coast divided into gamma-ray facies. The direction of detrital influence and migration of facies, as inferred from the Th concentration log, is shown for each gamma-ray unit. Stacking patterns within each gamma-ray unit are also indicated (P = progradation, A = aggradation and R = retrogradation).

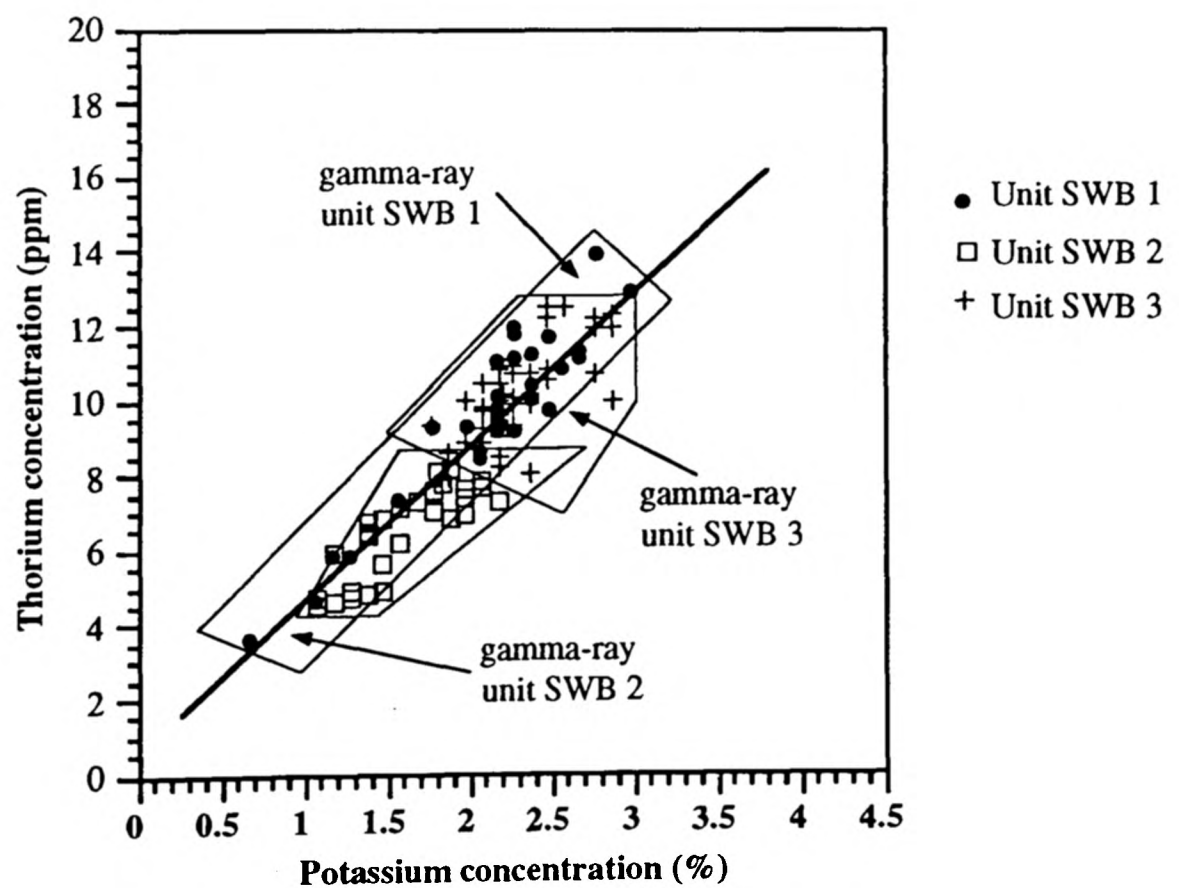
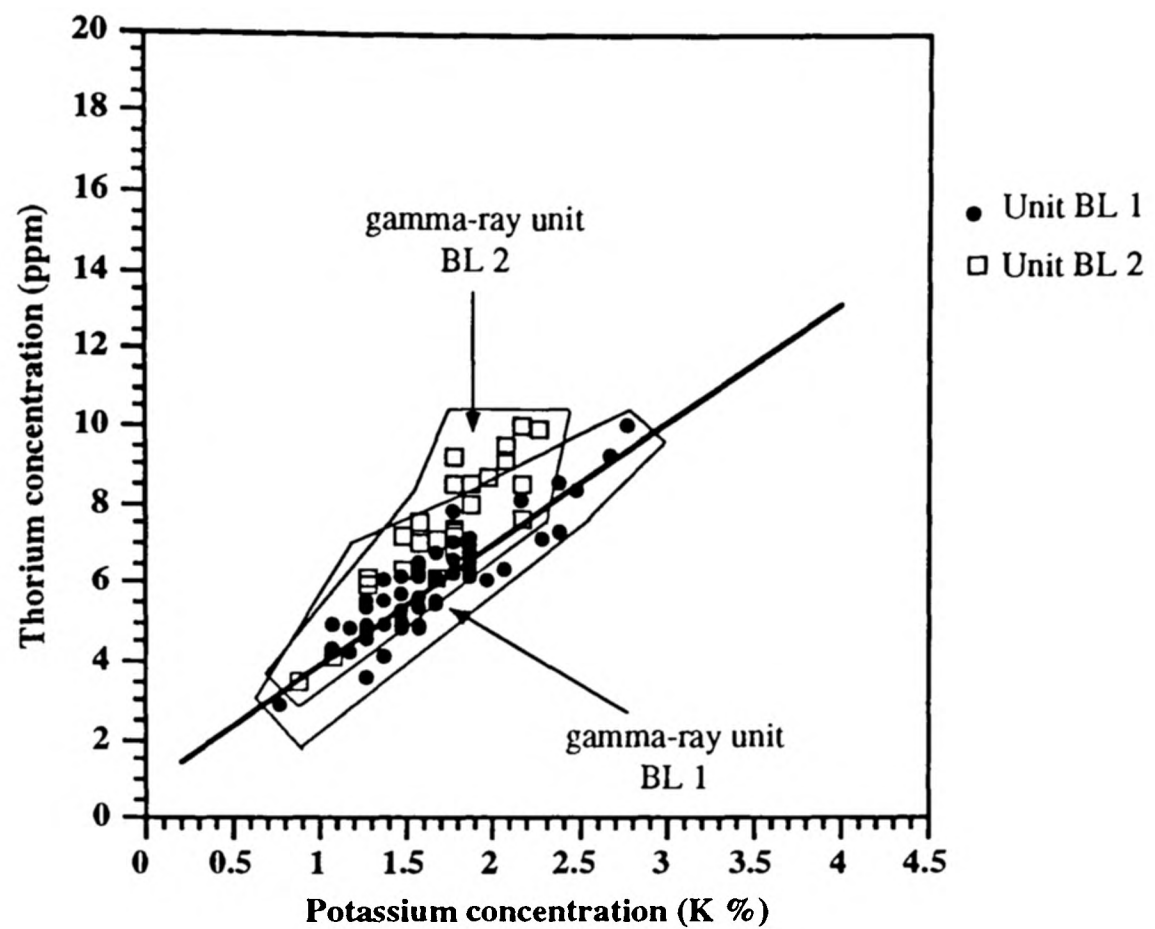


FIGURE 4.07 Th-K fields shown by each gamma-ray unit for the *Pre-planorbis* Beds to the *turneri* Zone in Dorset. Units BL 1, BL 2 and SWB 2 have Th-K concentrations that are characteristic of a distal gamma-ray facies in contrast to units SWB 1 and SWB 3 that have Th-K concentrations that are characteristic of a proximal gamma-ray facies.

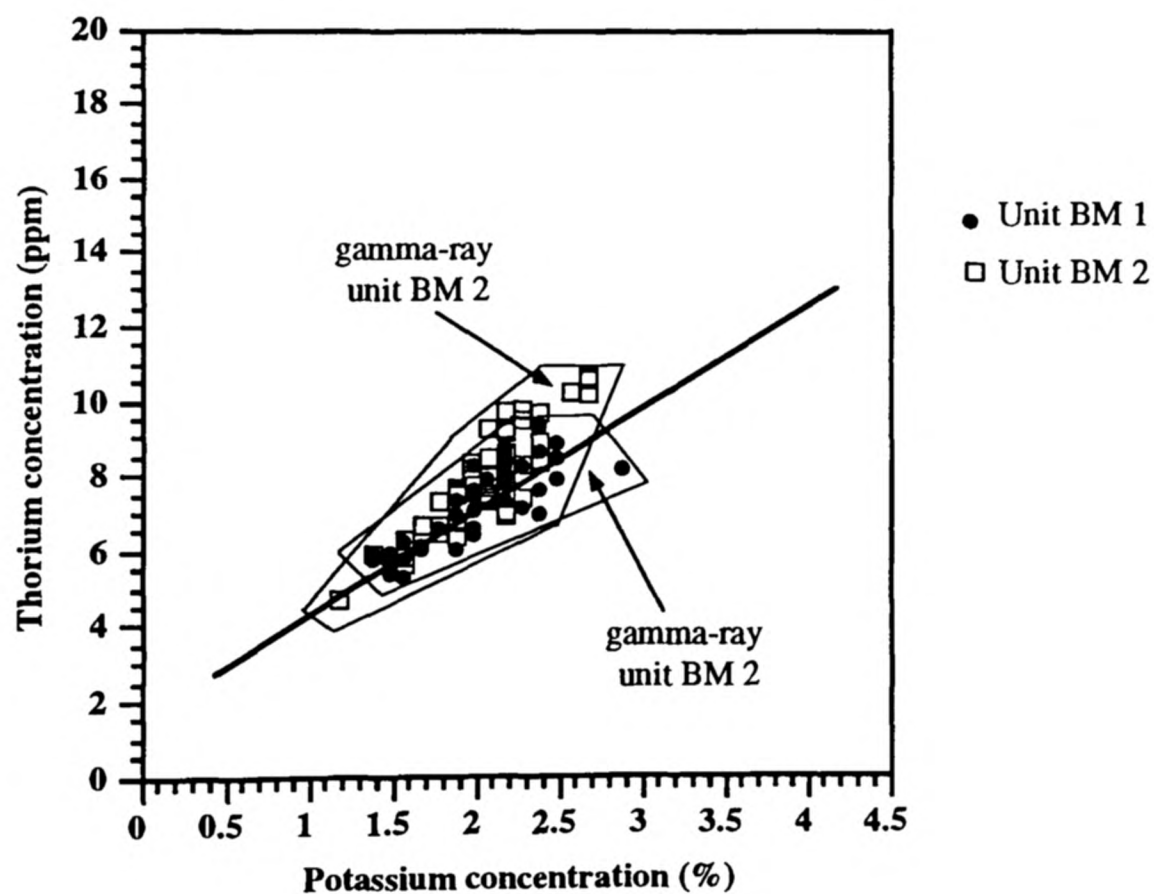
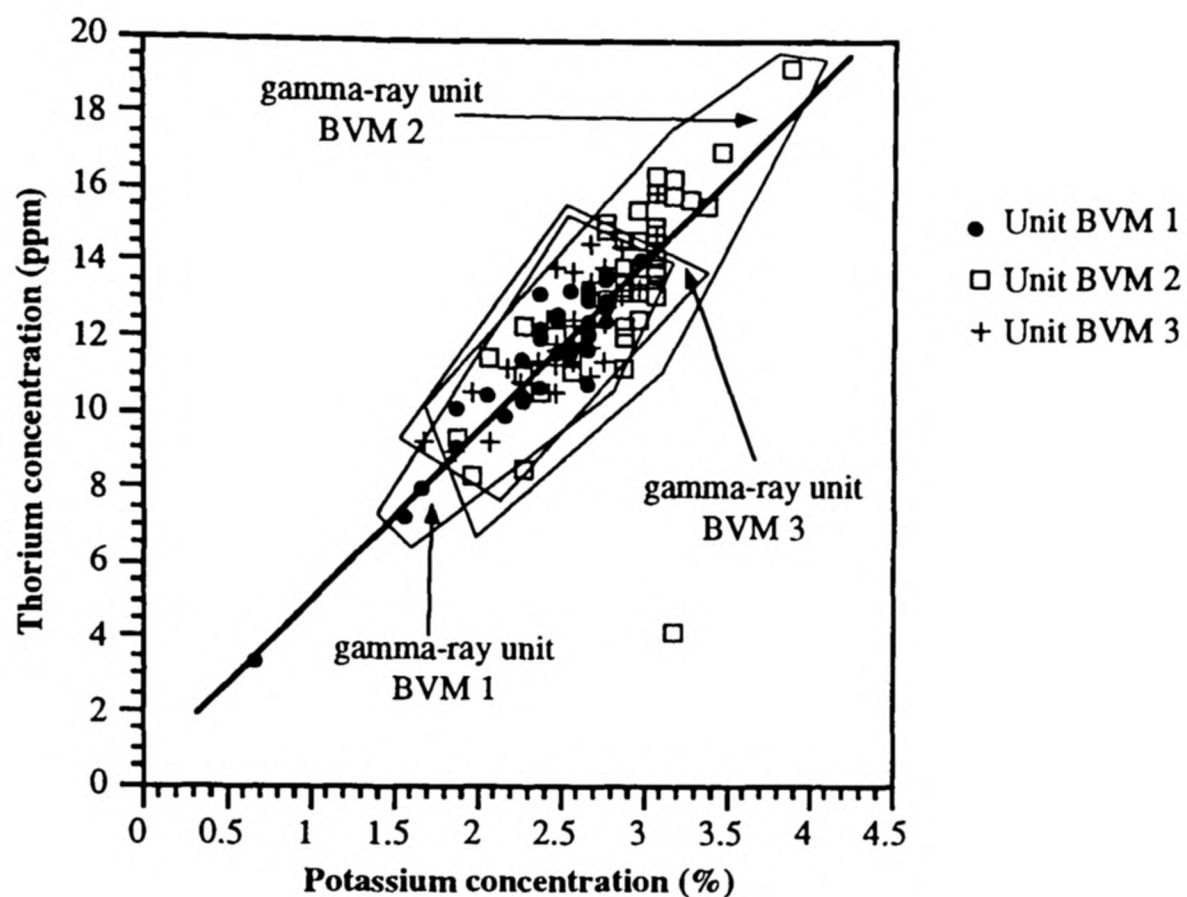
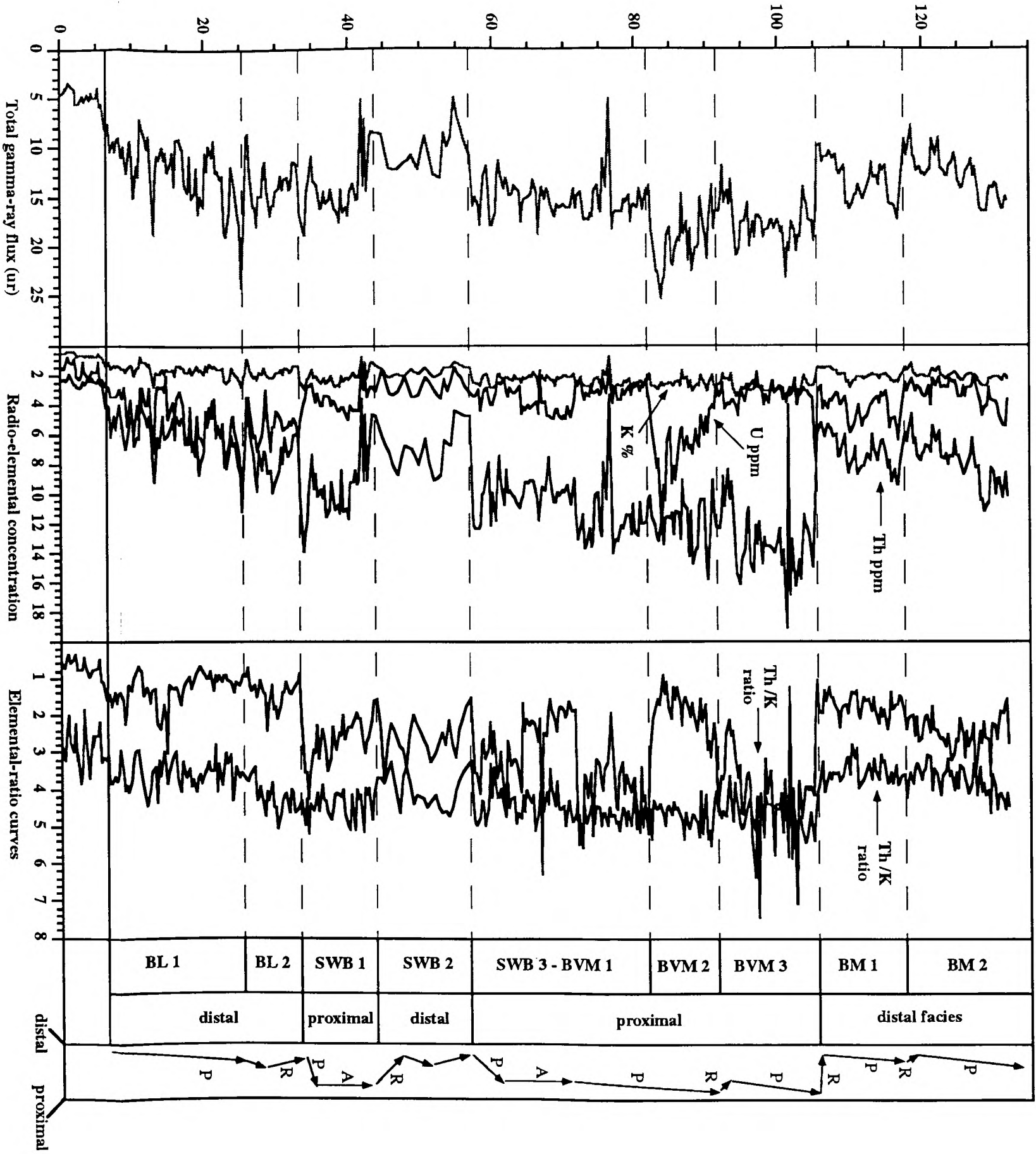


FIGURE 4.08 Th-K fields shown by each gamma-ray unit for the *turneri* Zone to *ibex* Zone in Dorset. Units BM 1 and BM 2 have Th-K concentrations that are characteristic of a distal gamma-ray facies in contrast to units BVM 1, BVM 2 and BVM 3 that have Th-K concentrations that are characteristic of a proximal gamma-ray facies.

Height above base of White Lias (m)



Gamma-ray units

Gamma-ray facies

Movement of facies and stacking patterns

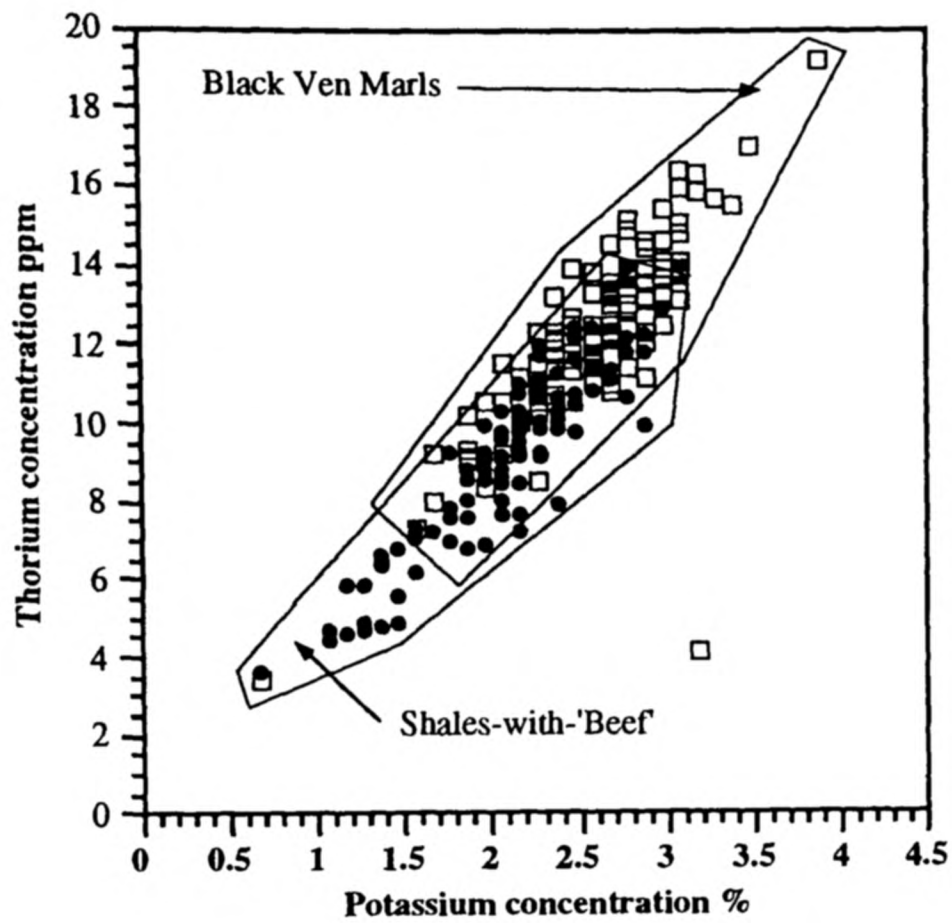


FIGURE 4.10 A Linear regression between Th concentration and K concentration for the Shales-with-'Beef' and Black Ven Marls. The Black Ven Marls are characterised by higher Th and K concentrations and are interpreted as the most proximal of the two formations.

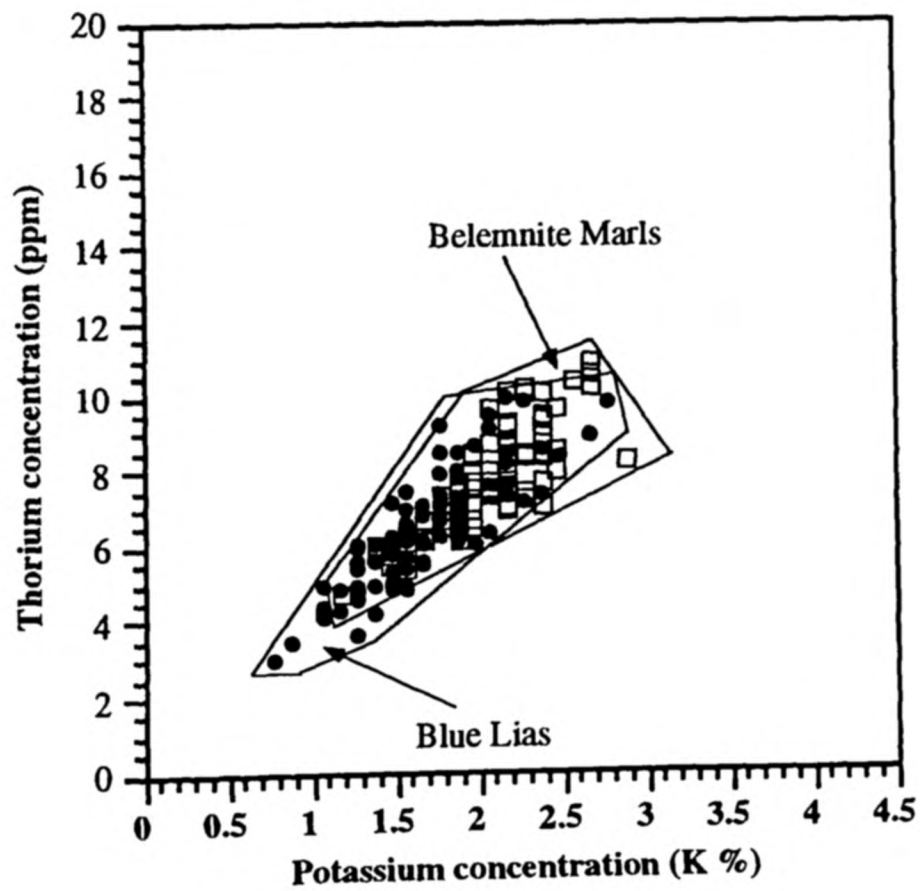


FIGURE 4.10 B Linear regression between Th concentration and K concentration for the Blue Lias and Belemnite Marls.



FIGURE 4.11 The *obtusum* Shales (gamma-ray unit BVM 2) at Stonebarrow, Charmouth, Dorset.

(ABOVE) Field aspect of the *obtusum* Shales that outcrop at Stonebarrow (SY 3780927). The *obtusum* Shales form a distinctive stratal package that comprises organic-rich 'paper shales' with a maximum TOC of 11.68 %. Maximum measured U concentration is 12.7 ppm. In the photograph, the *obtusum* Shales are the sediment package that runs mid-way through the cliff above the scree slope and are bound by two concretionary limestone horizons. The lowermost, bed 82, is known as Pavior (P) and the uppermost, bed 89, is known as the Coinstone (C). Cliff is approximately 30 m in height.

(BELOW) The laminated nature of the *obtusum* Shales can clearly be seen in the small headlands below Stonebarrow (SY 384926). The yellow field notebook rests on the Pavior limestone (P) at which there is evidence for a small stratal gap (e.g. *Diplocraterion* and *Thalassinoides*). Notebook is 20 cm x 13 cm.



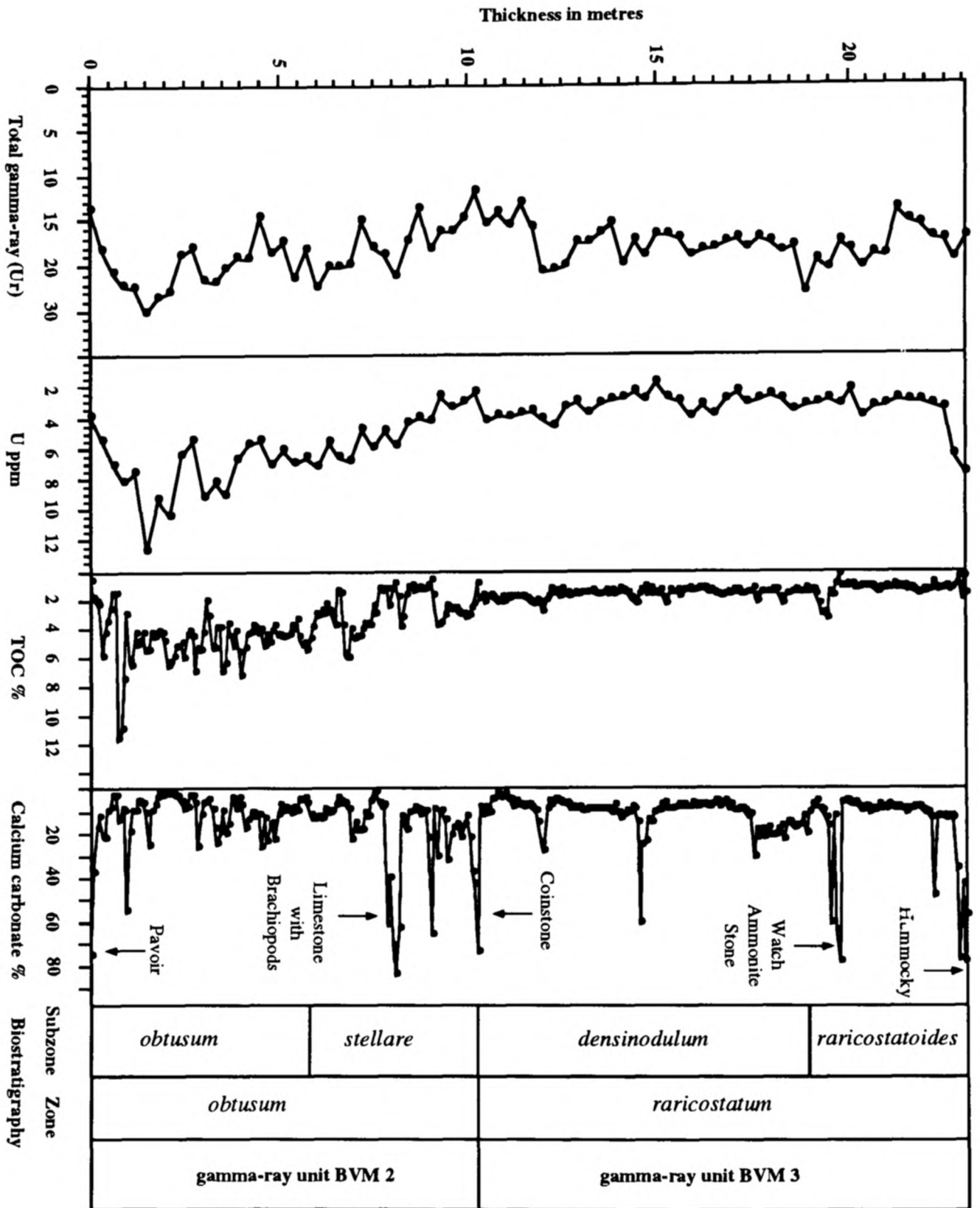


FIGURE 4.12 Comparison between total gamma-ray flux and U concentration for the *obtusum* Shales. Calcium carbonate data is also given. (Unpublished TOC and calcium carbonate data is reproduced courtesy of Jenkins & Weedon).

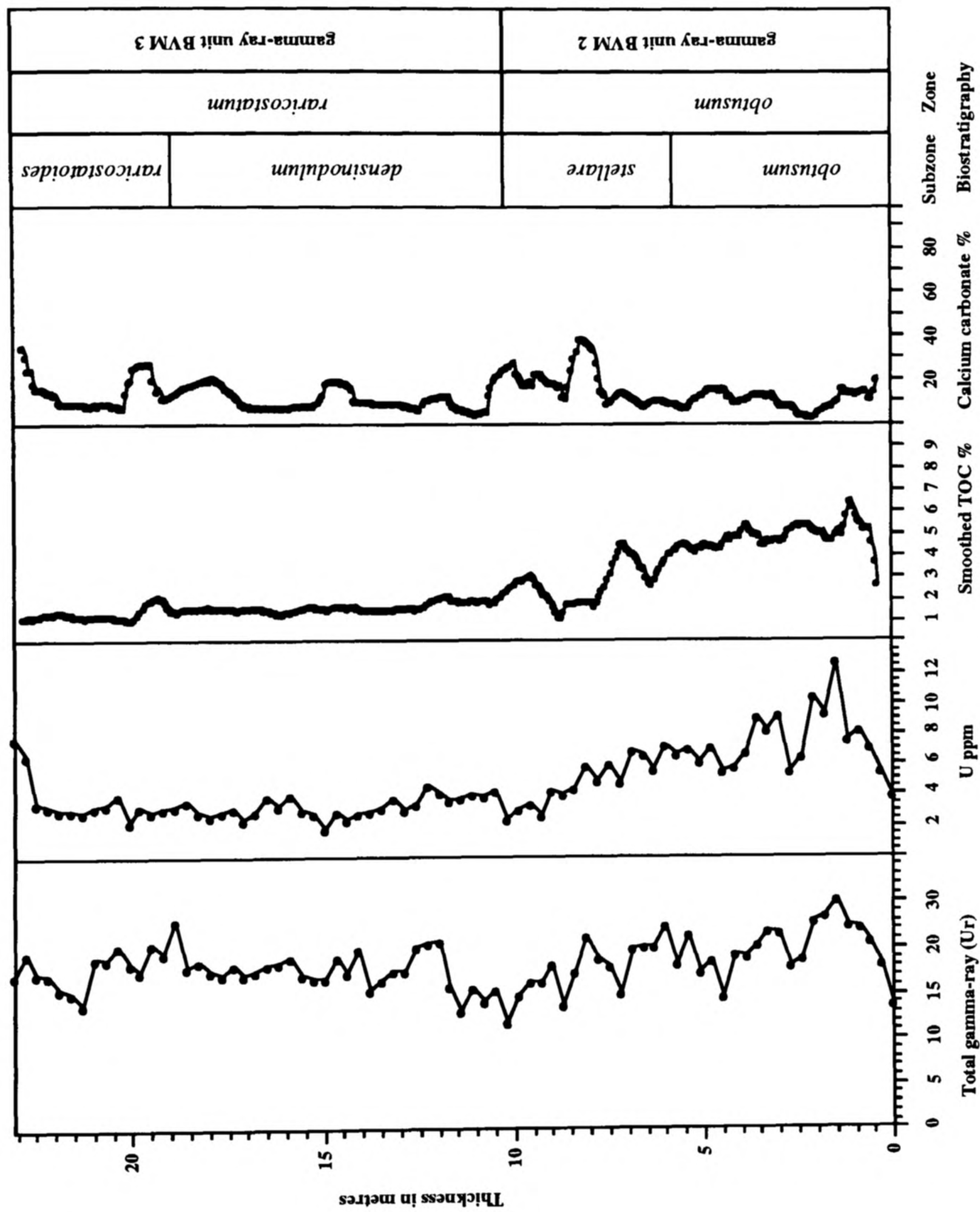


FIGURE 4.13 Comparison between total gamma-ray flux and U concentration for the *obtusum* Shales with TOC and calcium carbonate data. The latter two data-sets were collected using a 30 cm sampling interval. Thus for direct comparison with the gamma-ray data the TOC and calcium carbonate data-sets have to be smoothed over a 10 cm sampling interval. The U log signature closely resembles the TOC profile for the same interval. (Unpublished TOC and calcium carbonate data is reproduced courtesy of Jenkyns & Weedon).

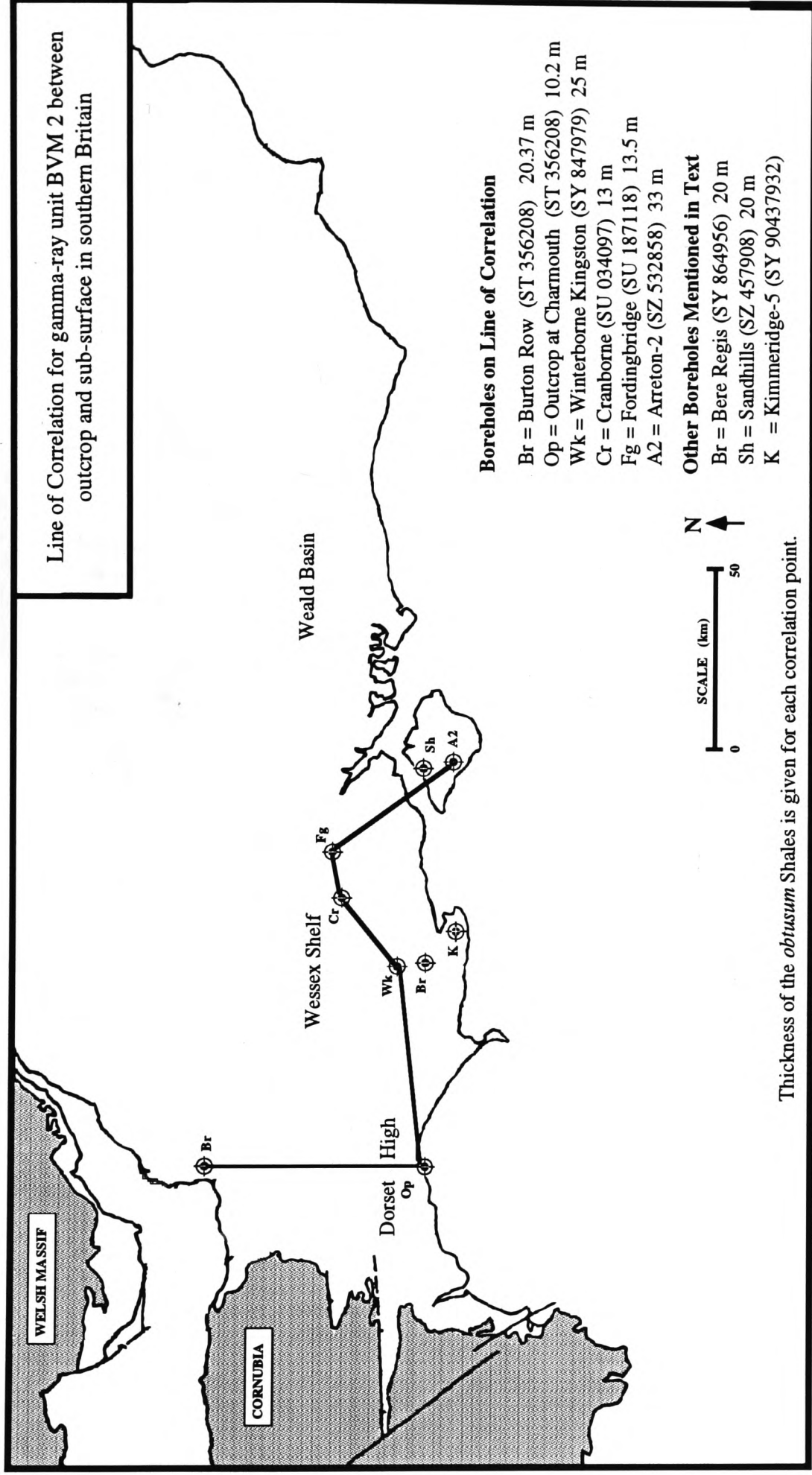


FIGURE 4.14 The *obtusum* Shales exposed along the coastline of south Dorset (SY 3780927) were deposited on the Mid-Dorset High on the northern footwall side of the major Abbotsbury-Ridgeway Fault System. Faults with an east-west orientation were characterised by an early to Mid-Late Jurassic downthrow to the south, an inference based on evidence of syndimentary fissures in sandstones and limestones or changes in stratal thickness and facies (Jenkyns & Senior 1991, Hesselbo & Jenkyns 1995a). Faults with an approximate north-south orientation generally had an Early to Mid Jurassic downthrow to the west, evidenced by stratal thinning and the development of hiatus-concretions on fault-block crests (Hesselbo & Palmer 1992).

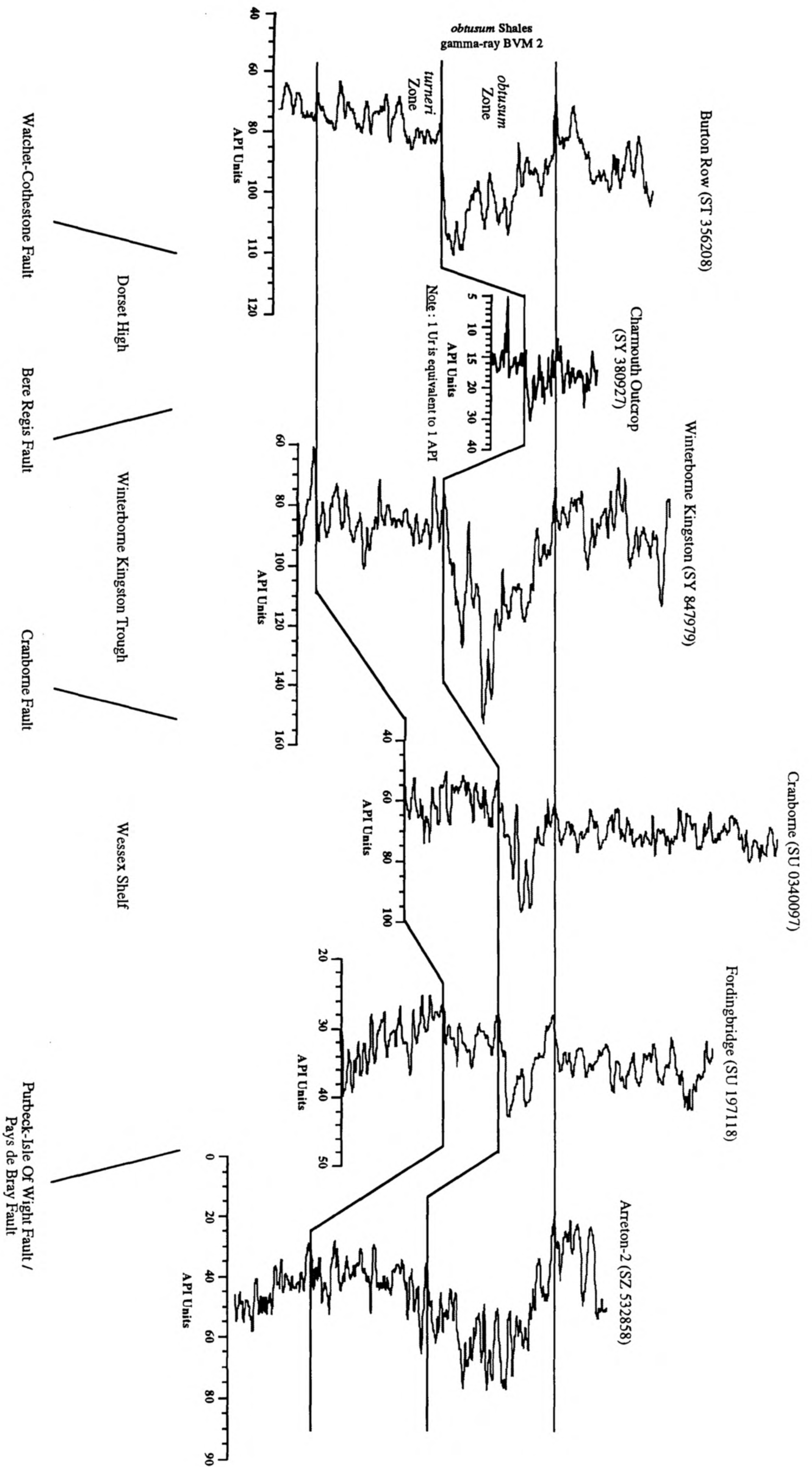


FIGURE 4.15 A correlation of the *obtusum* Shales (gamma-ray unit BVM 2) from outcrop into the subsurface away from the coastal area. At outcrop the *obtusum* Shales represent the *stellare* and the *obtusum* Subzones of the *obtusum* Zone. In the fully cored Burton Row borehole, the organic-rich shales also include the *denotatus* Subzone of the *obtusum* Zone. Correlation in the other boreholes shown on the line of section can only be made upon the basis of total gamma-ray signature.

FIGURE 4.15

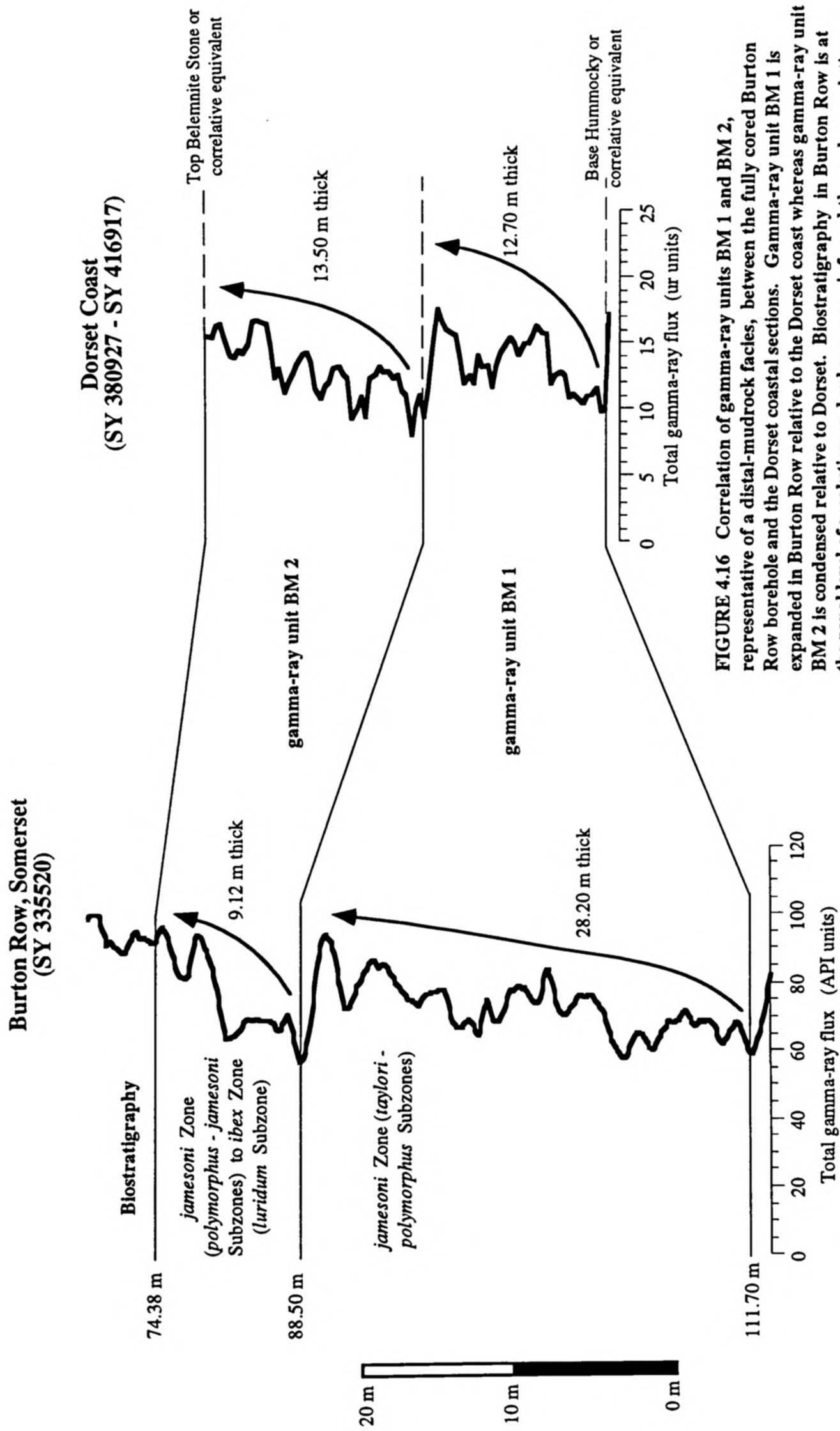


FIGURE 4.16 Correlation of gamma-ray units BM 1 and BM 2, representative of a distal-mudrock facies, between the fully cored Burton Row borehole and the Dorset coastal sections. Gamma-ray unit BM 1 is expanded in Burton Row relative to the Dorset coast whereas gamma-ray unit BM 2 is condensed relative to Dorset. Biostratigraphy in Burton Row is at the zonal level of resolution and subzones are inferred through correlation with the outcrop gamma-ray log.

Distal Gamma-Ray Facies
 (Belemnite Marls, Dorset, SY 380927 - SY 415918)

Proximal Gamma-Ray Facies
 (Blockley Pit, Gloucestershire, SP182369)

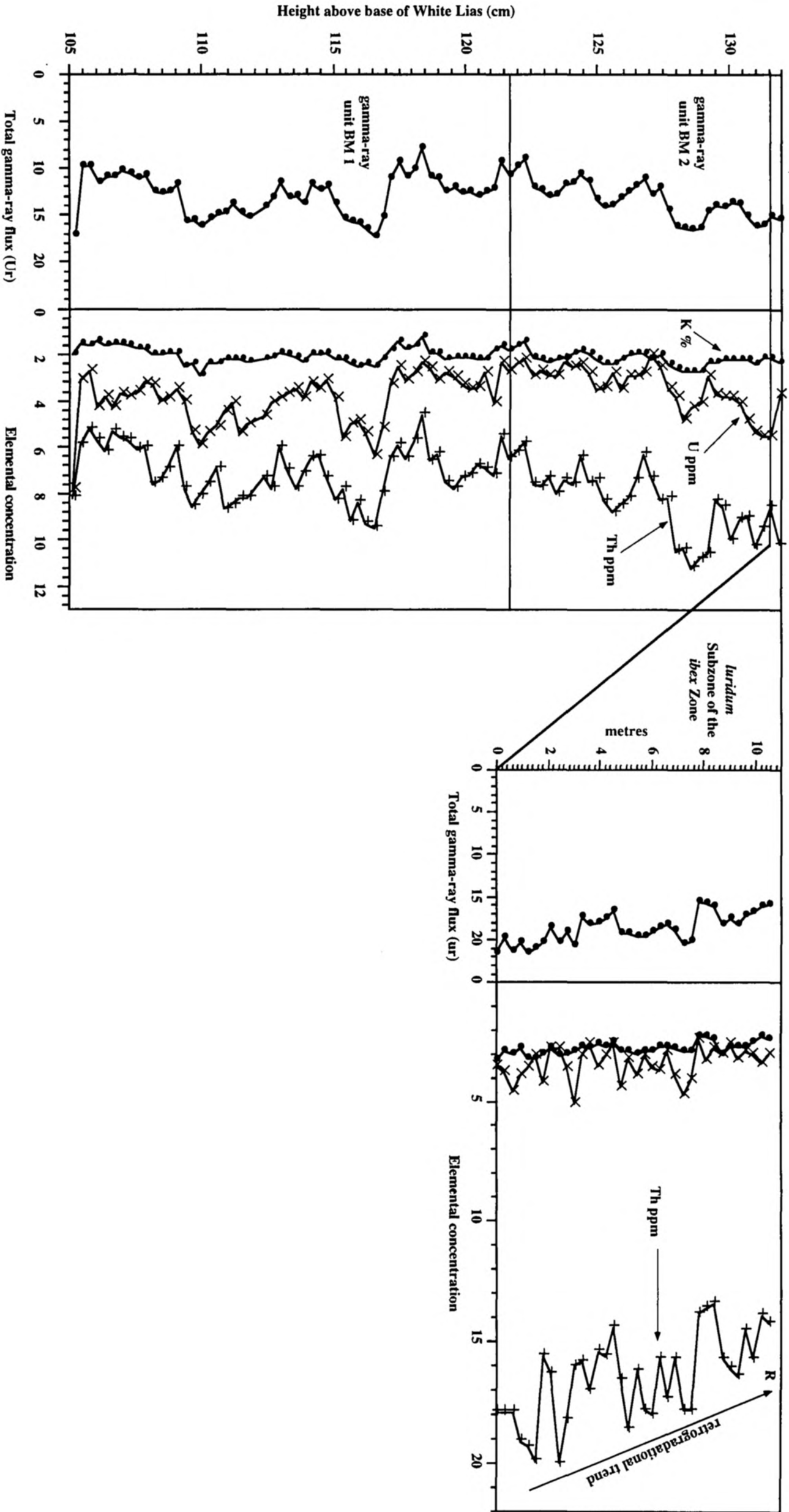


FIGURE 4.17

FIGURE 4.17 Comparison of the gamma-ray signatures for a distal gamma-ray facies and a proximal gamma-ray facies. Stratigraphic condensation of the distal facies in the *luridium* Subzone coincides with stratigraphic expansion of the proximal facies at the basin margin. The x-axis for radio-element concentration is scaled.

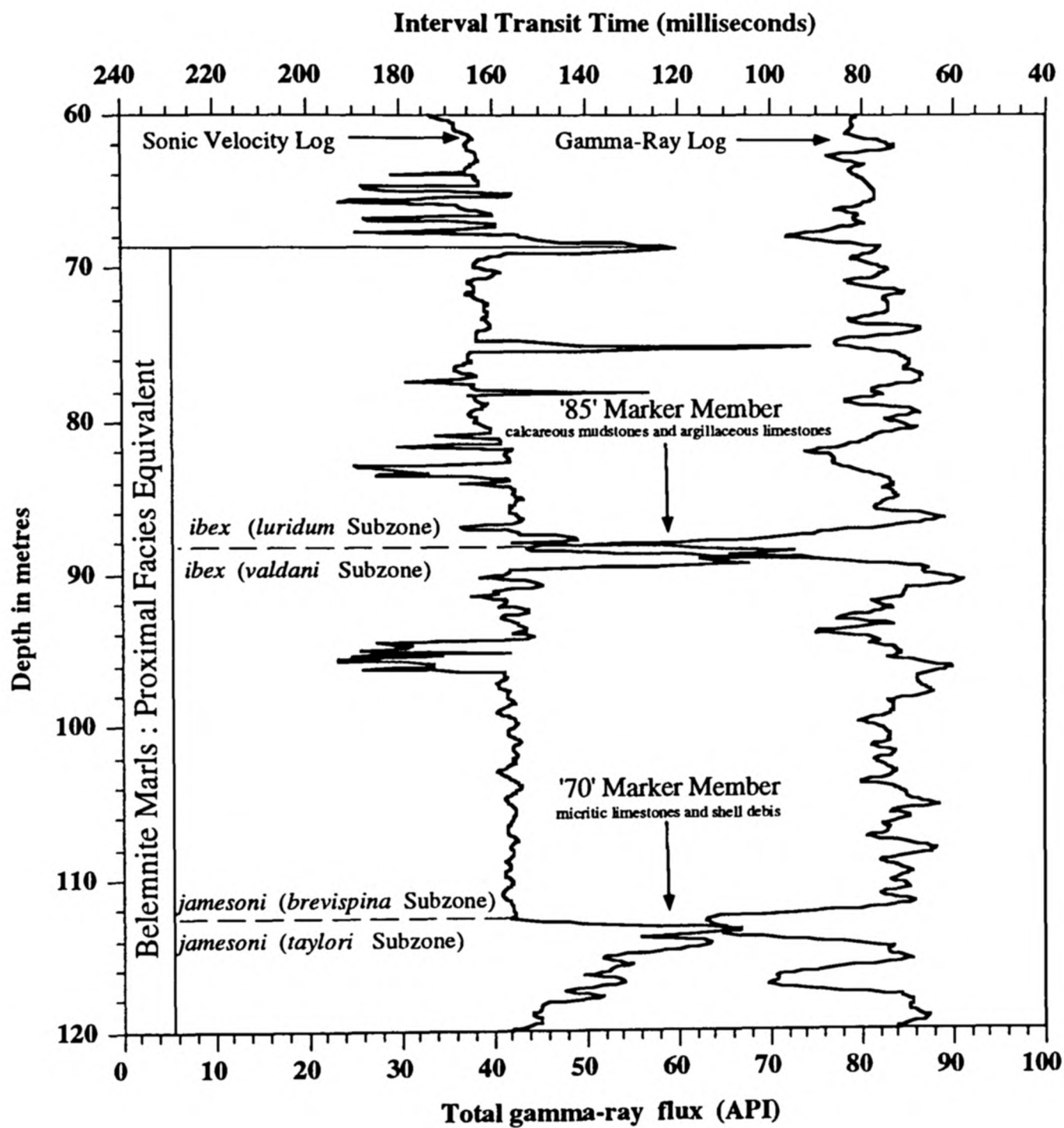


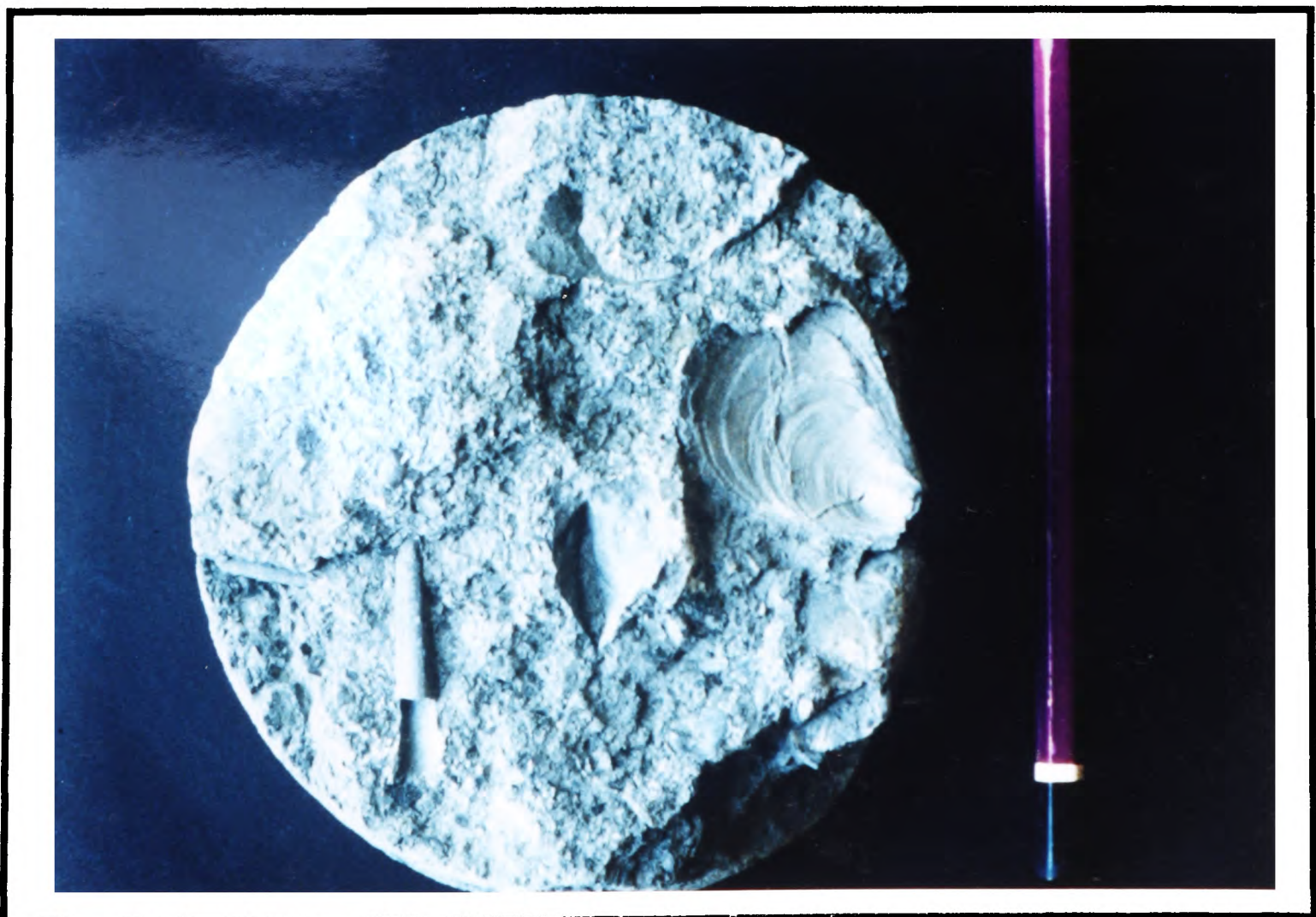
FIGURE 4.18 The wireline-log trace of two laterally persistent geophysical marker horizons recognised within the Lower Lias of Oxfordshire. The '70' and '85' Markers are considered to be sufficiently distinct to be defined as lithological members within the Lias sequence (Horton & Poole 1977) and can easily be distinguished using the sonic-velocity and total-gamma-ray logs. The '70' Marker Member is a moderate to low gamma-ray radioactive feature and lies within the *jamesoni* Zone. The '85' Marker Member is a low-radioactive feature of between 35-45 API on the total gamma-ray log and lies within the *ibex* Zone.



FIGURE 4.19 The '70' and '85' Marker Member, East Midland Shelf.

(ABOVE) Core representative of the '70' Marker Member from the Steeple Aston borehole (depth 114.45 m). The '70' Marker Member comprises micritic limestones and bioclastic (bivalve) debris and is a moderate to low radioactive feature on the total gamma-ray log. The marker is taken to represent the boundary between the *brevispina* Subzone and the *taylori* Subzone (*jamesoni* Zone). Pencil is 16 cm long.

(BELOW) Core representative of the '85' Marker Member from the Steeple Aston borehole (depth 89.35 m). The '85' Marker Member comprises calcareous mudstones and argillaceous limestones and is taken to represent the boundary between the *valdani* and *luridum* Subzones (*ibex* Zone). The marker is a distinctive low radioactive feature of 35-45 API on the total gamma-ray log. Pencil is 16 cm in length.



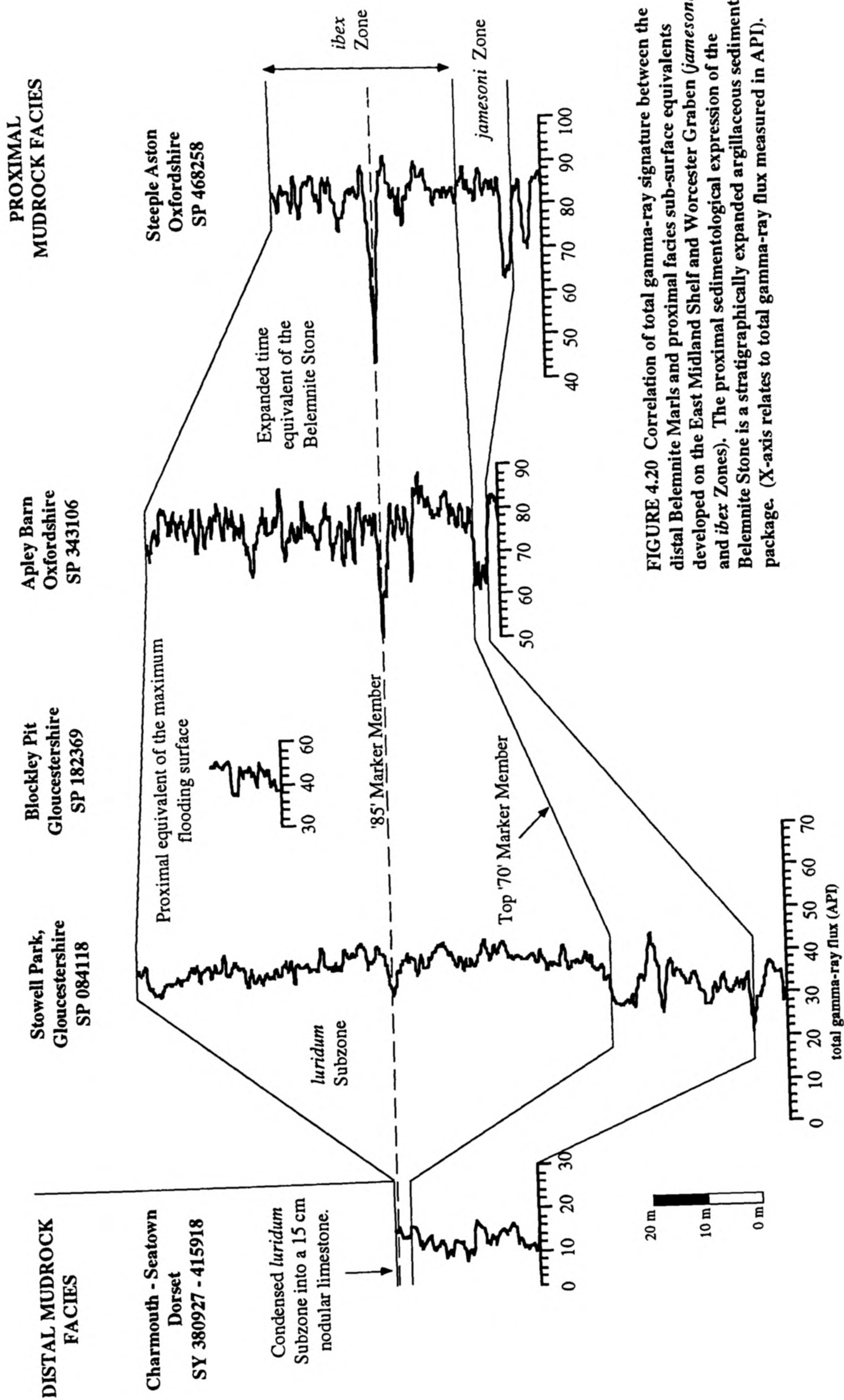


FIGURE 4.20 Correlation of total gamma-ray signature between the distal Belemnite Marls and proximal facies sub-surface equivalents developed on the East Midland Shelf and Worcester Graben (*jamesoni* and *ibex* Zones). The proximal sedimentologically expanded argillaceous sediment Belemnite Stone is a stratigraphically expanded argillaceous sediment package. (X-axis relates to total gamma-ray flux measured in API).

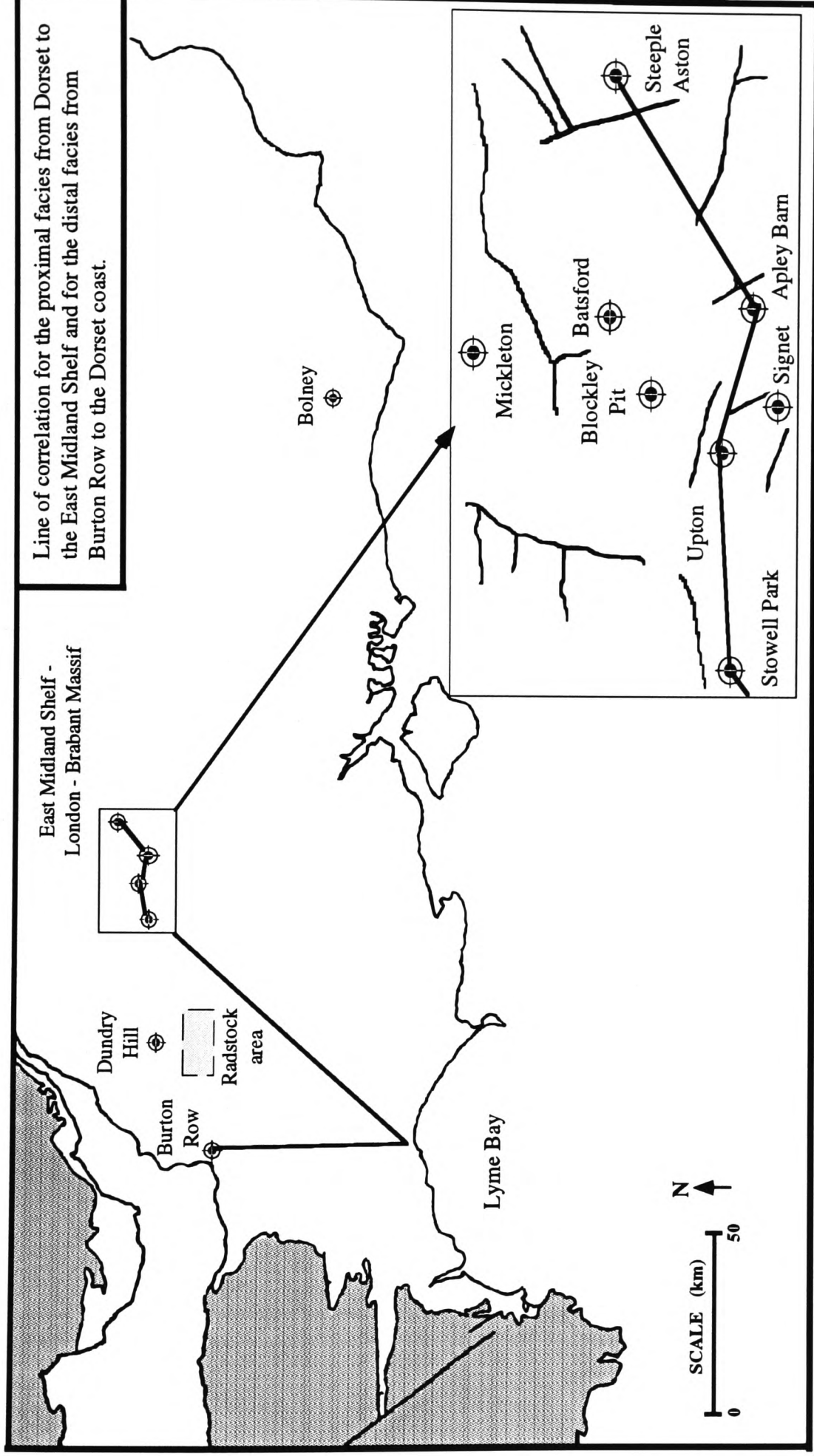


FIGURE 4.21 The Belemnite Marls and lateral time equivalents elsewhere in southern Britain (*jamesoni* to *ibex* Zones). A proximal mudrock facies is identified in the Stowell Park, Apley Barn and Steeple Aston boreholes on the basis of total gamma-ray signature and inferred in the Dundry Hill and Upton boreholes. The proximal facies outcrops at Blockley Pit Gloucestershire. A distal facies is identified in the Burton Row borehole and on the Dorset Coast. Locally, within the Radstock area the sequence becomes considerably condensed. Grid References for localities : Apley Barn (SP 343106), Burton Row, Brent Knoll (ST 335520), Elton Farm, Dundry Hill (ST 563658), Steeple Aston (SP 468258), Stowell Park (SP 084118), Upton, Witney (SP 231131), Blockley Pit section (SP 182369), Dorset coastal sections (SY 380927 - SY 415918), Bolney borehole, Sussex (TQ 280442).

Zone	Subzone	Distal Mudrock Facies			Condensed Facies		Proximal Mudrock Facies				
		DORSET COAST	BURTON ROW	RADSTOCK AREA	ELTON FARM DUNDY HILL	STOWELL PARK	UPTON	APLEY BARN	STEEPLE ASTON		
<i>Tragophlyoceras ibex</i>	<i>Beaniceras luridum</i>	Belemnite Stone (4-5 cm thick)	Total gamma-ray log suggests a limestone-type lithology of low total gamma-ray flux.	mudstone sequence 20 m thick	22.10 m thick '85' Marker Member	37 m thick '85' Marker Member	UPTON Biostratigraphy is at best at the zonal level of resolution. <i>ibex</i> Zone 9.75 m thick	36.58 m thick '85' Marker Member	16.47 m thick '85' Marker Member		
	<i>A. valdani</i>	Belemnite Marls Formation. Cyclic Sedimentation	Condensed into 1.28 m of section.	<i>Valdani</i> Limestone coarse-grained crystalline limestone 0.4 m thick.	Grey micaceous and massive mudstones. <i>valdani</i> and <i>masseanum</i> Subzones are 16.18 m in thickness	8.23 m thick Grey calcareous to silty mudstones 2.74 m thick Grey calcareous to silty mudstones				14.66 m thick micaceous mudstones	micaceous mudstones with occasional bioclastic limestones 19.22 m thick
	<i>Tropidoceras masseanum</i>	High frequency alternations displayed by light marl - dark marl couplets <i>Chondrites</i> common.	Evidence for cyclic sedimentation		grey, micaceous mudstone. Finely laminated. High pyrite content. (<i>Jamesoni</i> , <i>brevispina</i> and <i>polymorphus</i> Subzones not individually differentiated. Equivalent to 16.61 m of strata)	3.35 m thick Calcareous mudstones and foraminiferal shales	silty mudstone and fine-grained argillaceous limestones <i>Jamesoni</i> Zone 23.77 m thick	9.75 m thick micaceous mudstones and occasional limestone non-sequence	micaceous mudstones and prominent bioclastic limestones. <i>polymorphus</i> & <i>brevispina</i> Subzones 12.72 m thick non-sequence		
	<i>Uptonia Jamesoni</i>	Gamma-ray package BM 2 coincides with stratigraphic condensation	Grey calcareous mudstones with limestone nodules. <i>Chondrites</i> is common within the calcareous mudstones units	<i>Jamesoni</i> Limestone bioclastic limestone. High iron content 0.7 m thick.	37.32 m Abundance of Belemnites						
<i>Uptonia Jamesoni</i>	<i>P. brevispina</i>	Gamma-ray package BM 1 coincides with stratigraphic expansion			'70' Marker Member 3.08 m thick	'70' Marker Member 14.02 m thick			'70' Marker Member		
	<i>Polymorphites polymorphus</i>										
	<i>Phricodoceras taylori</i>	Hummocky Limestone 0.20 m		<i>Arriagus</i> Bed 50 cm							

FIGURE 4.22

FIGURE 4.22 Correlation panel for the Lower Pliensbachian in southern Britain. Data from Green & Melville 1956, Worssam 1963, Poole 1977, Whitaker & Green 1983 and Donovan & Kellaway 1984. Disconformities are shown. Thickness of ammonite subzones are given where possible.

Chapter 5
Figure 5.01 to Figure 5.15

**A Sequence Stratigraphic Synthesis for the Lower Lias
in Southern Britain and Final Conclusions**

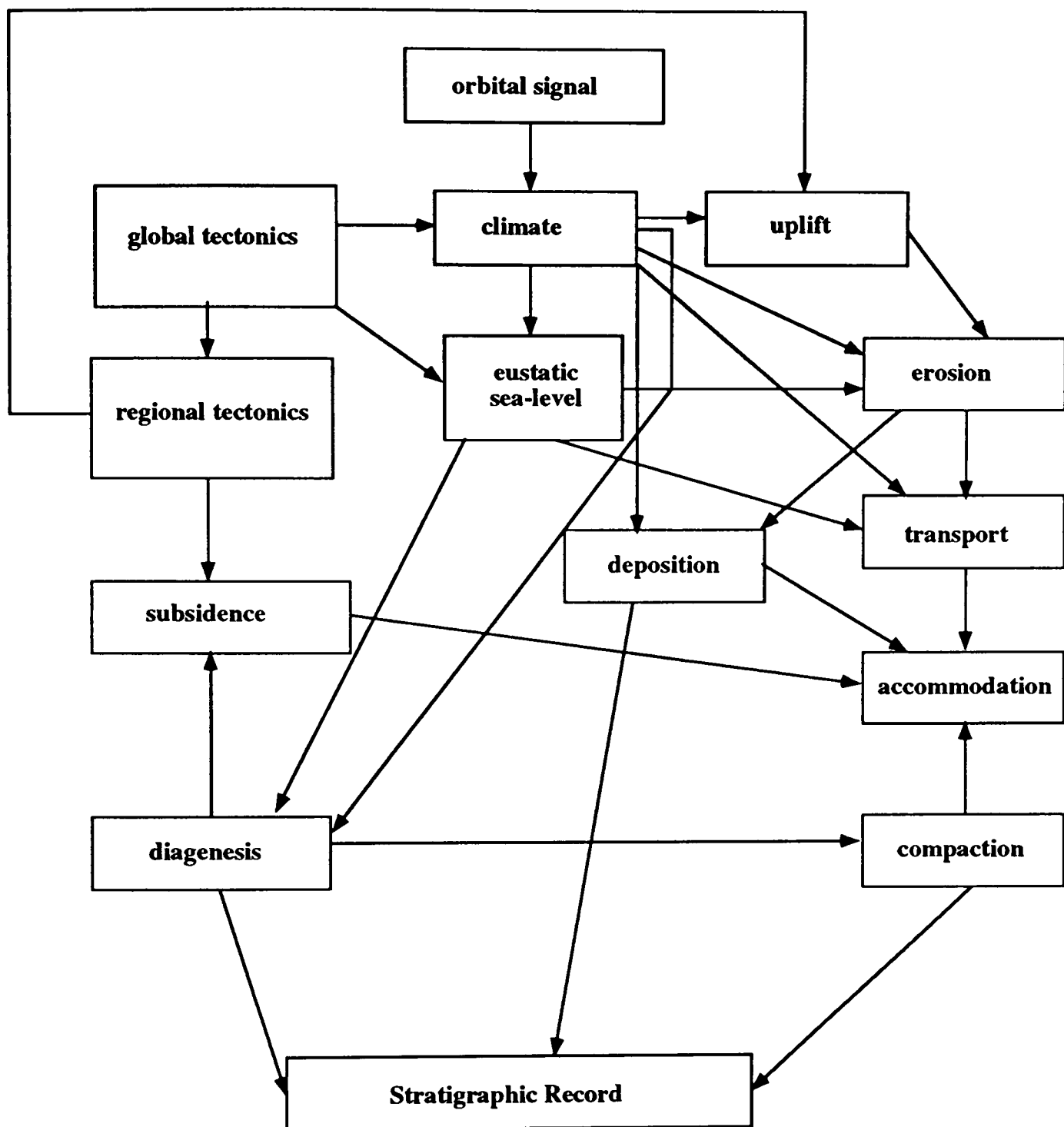


FIGURE 5.01 The complex system of interactions and feedbacks which influence the stratigraphic record. Sea-level is influenced by climate and global or regional tectonics. Deposition is influenced by accommodation space (the space available beneath base level which may be sea-level itself or storm wave-base). There is a negative feedback loop between accommodation and deposition but a positive feedback loop involving sediment compaction as a result of loading. Loading also acts to increase subsidence and hence accommodation. (Based on Smith 1994.)

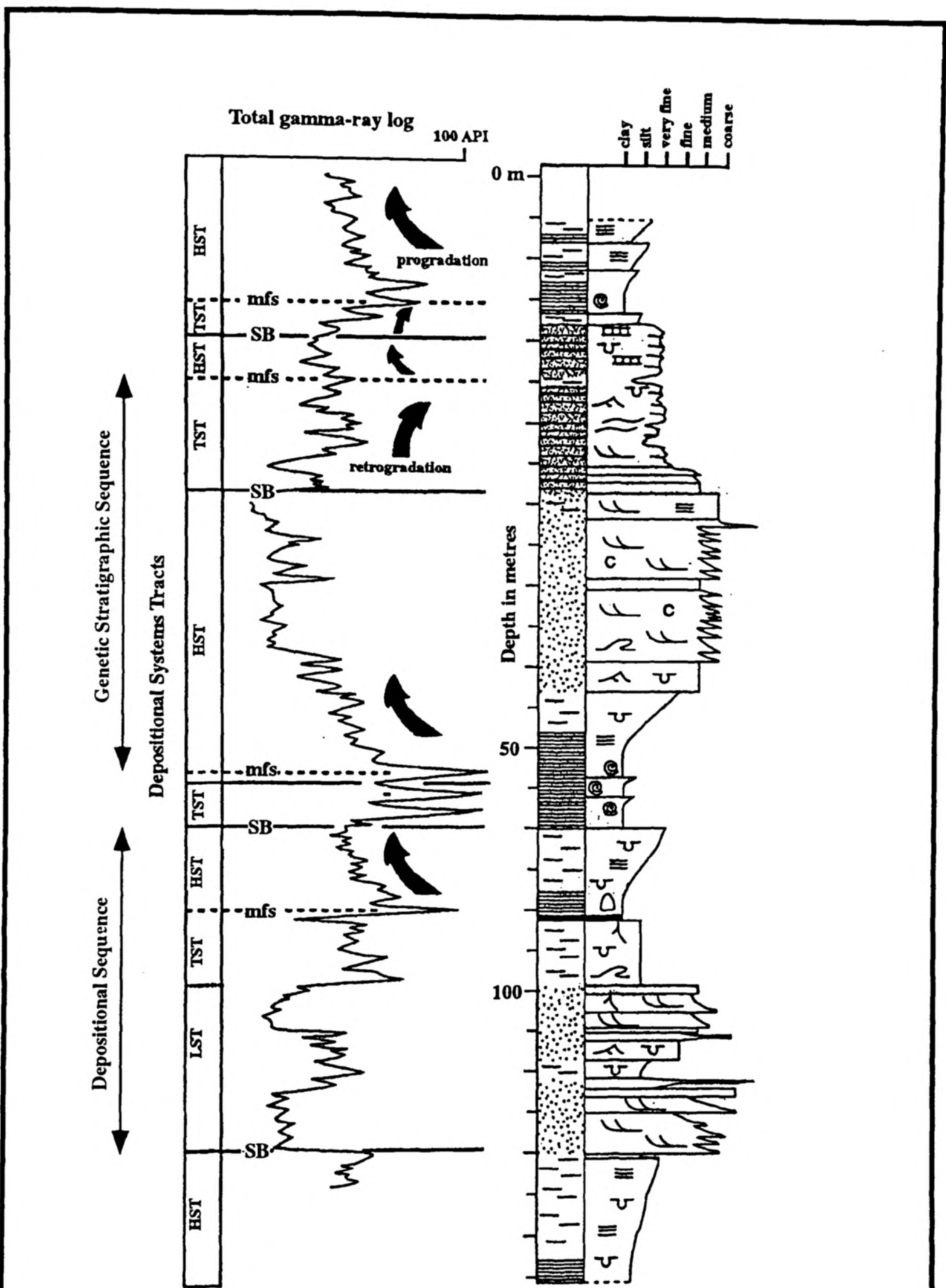
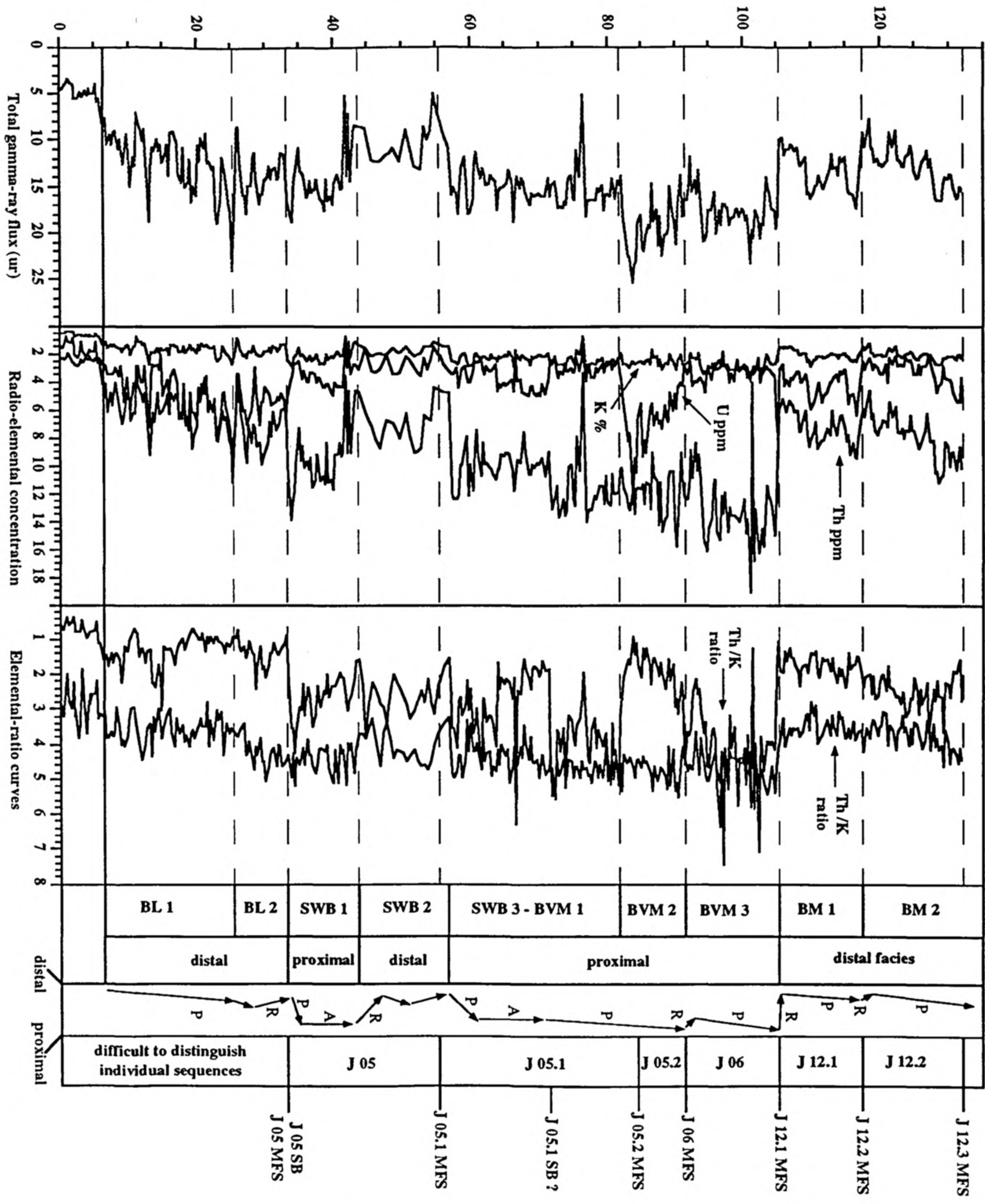


FIGURE 5.02 Depositional sequence stratigraphic interpretation of a total gamma-ray log for a coarse-grained siliciclastic system. The associated lithological log is also given. The inferred maximum flooding surface is denoted mfs and the inferred sequence boundary SB. Inferred depositional systems tracts are also given although system tract terminology is not applicable to the Lower Lias of southern Britain as there is no pronounced change in depositional system away from the open marine environment. (Based upon Gawthorpe *et al.* 1994)

Height above base of White Lias (m)



Gamma-ray uni
 Gamma-ray facies
 Movement of facies and stacking patterns
 Genetic stratigraphic sequences
 Sequence stratigraphic surfaces

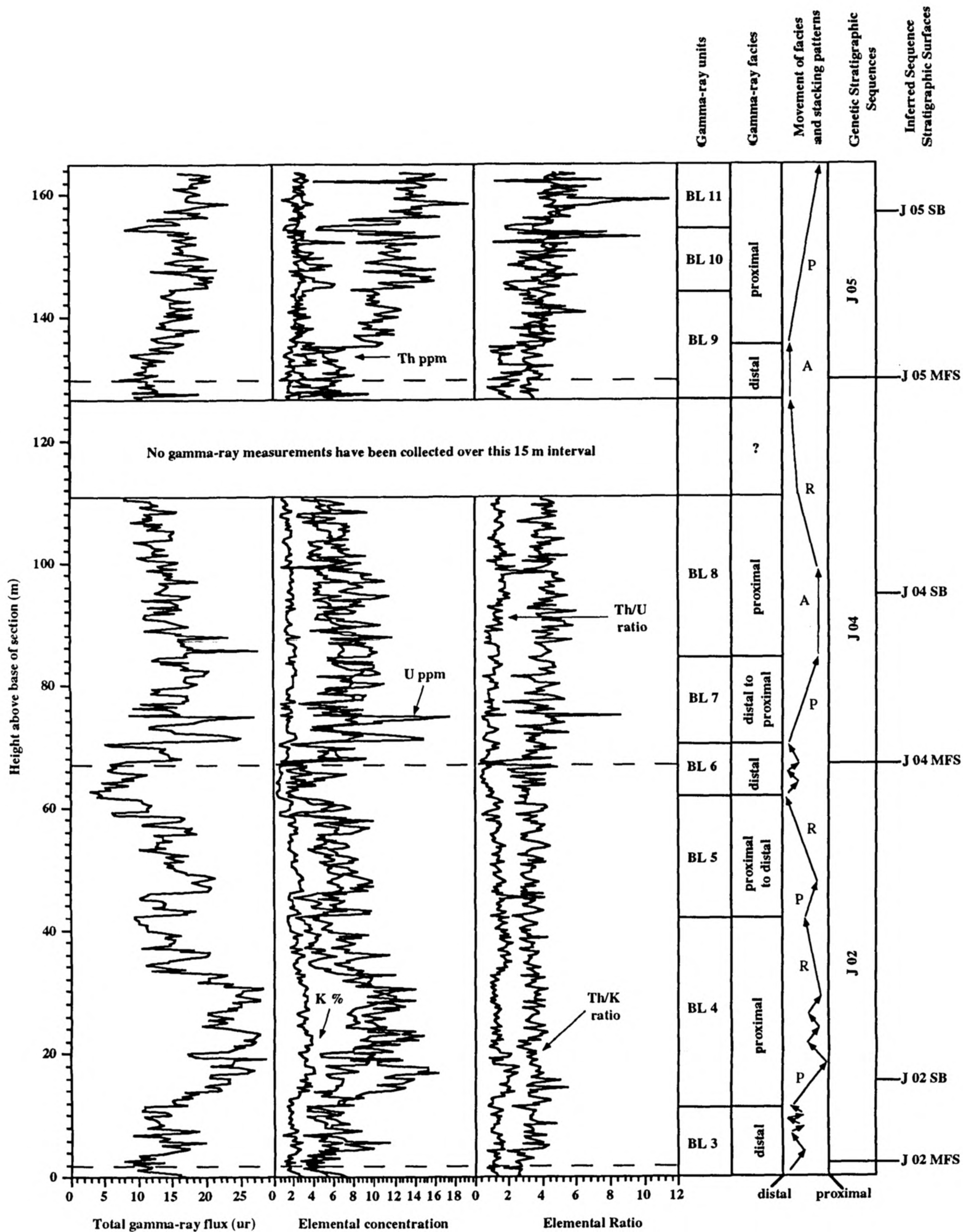


FIGURE 5.03 Gamma-ray logs for the Lower Lias succession of the Somerset coast divided into genetic stratigraphic sequences (*sensu* Galloway 1989). Inferred maximum flooding surfaces are denoted MFS and inferred sequence boundaries are denoted SB.

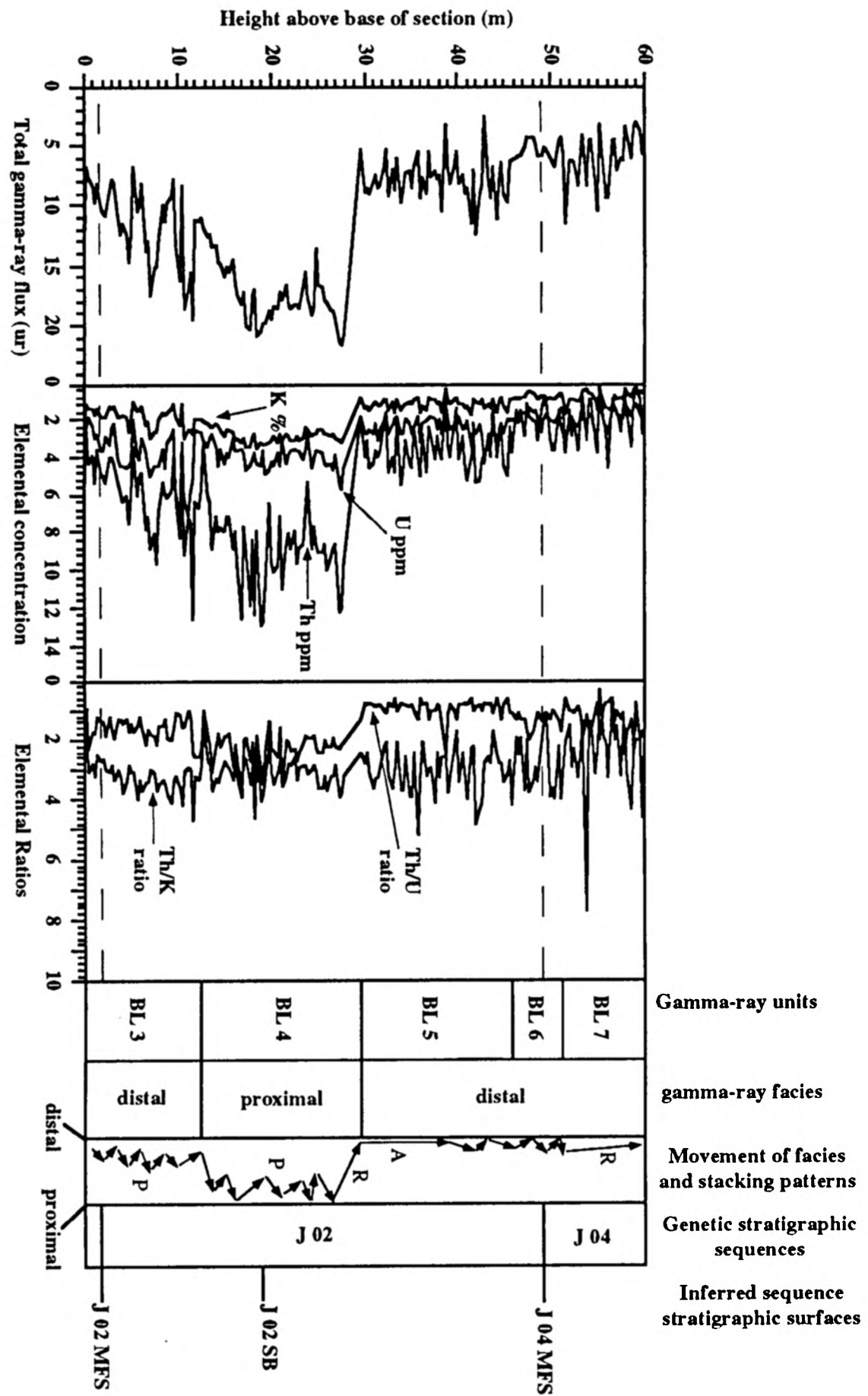
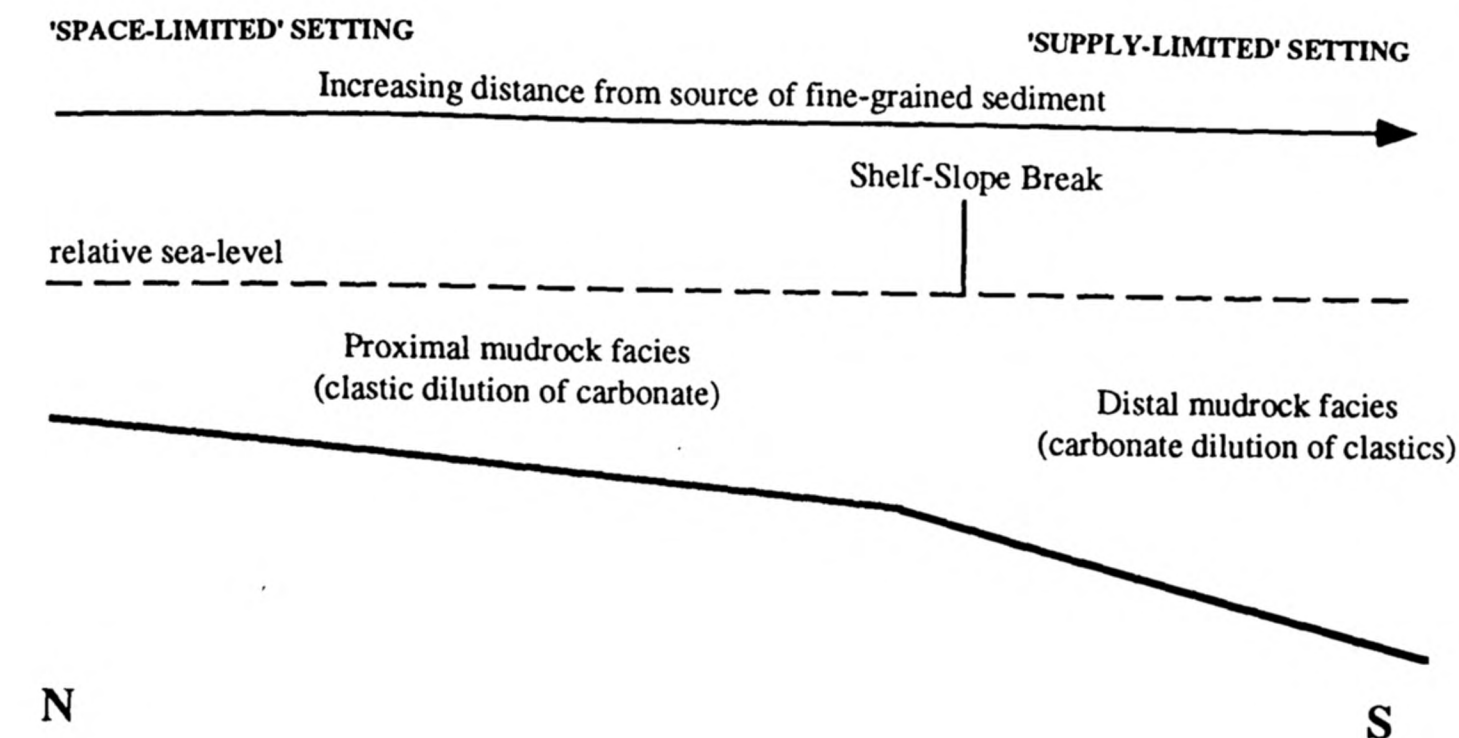
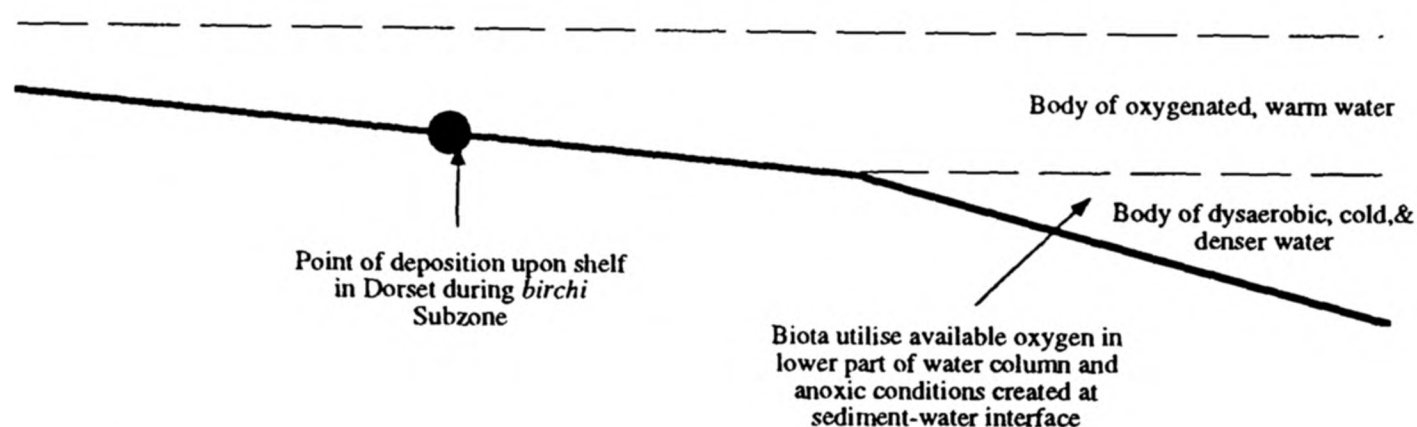


FIGURE 5.04 Gamma-ray logs for the Lower Lias succession of the Glamorgan coast divided into genetic stratigraphic sequences (*sensu* Galloway 1989). Inferred maximum flooding surfaces are denoted MFS and inferred sequence boundaries are denoted SB.

FIGURE 5.04



A) Water-Mass Stratification Developed (*birchi* Subzone)



B) Relative Sea-Level Rise (*obtusum* Subzone)

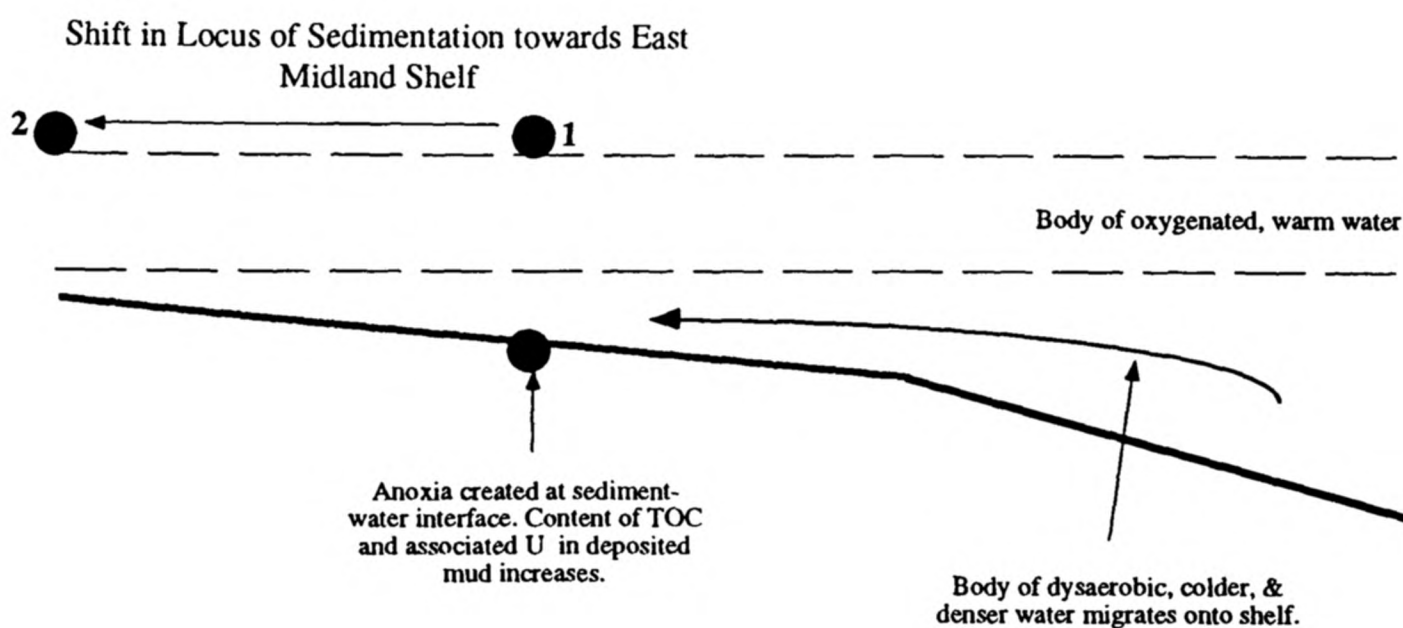


FIGURE 5.06 Possible interpretation of the *obtusum* Shales (gamma-ray unit BVM 2). The development of regional anoxia during the *obtusum* Zone is attributed to migration of dense, dysaerobic water onto the shelf during relative sea-level rise. Anoxic conditions persist on the shelf during subsequent progradation but are destroyed by mixing of the water masses, possibly during the associated relative sea-level fall. Immediately following relative sea-level rise, the shelf may have become starved (below the resolution of the ammonite subzone) to create the stratal gap at the horizon known as Pavior, prior to sediment progradation back into Dorset.



FIGURE 5.07 The Coinstone at Stonebarrow, Charmouth, Dorset.

(ABOVE) Field aspect of the Coinstone, which consists of a horizon of bored and encrusted early diagenetic, clay-hosted septarian concretions coincident with a biostratigraphic gap of three ammonite subzones. Several types of concretion of variable complexity have been distinguished (Hesselbo & Palmer 1992), of which two, probably derived from slightly different stratigraphic levels, have been juxtaposed by condensation at the erosion surface. (Field assistant is 1.62 m in height).

(BELOW) Exhumation above the sediment-water interface is evident in several Coinstone concretions due to intense surface boring. A mechanism of stratal erosion has been proposed by Hesselbo & Palmer (1992) in which burrowing by crustaceans is inferred to have caused resuspension and increased bed roughness, thus facilitating erosion by relatively weak bottom currents.



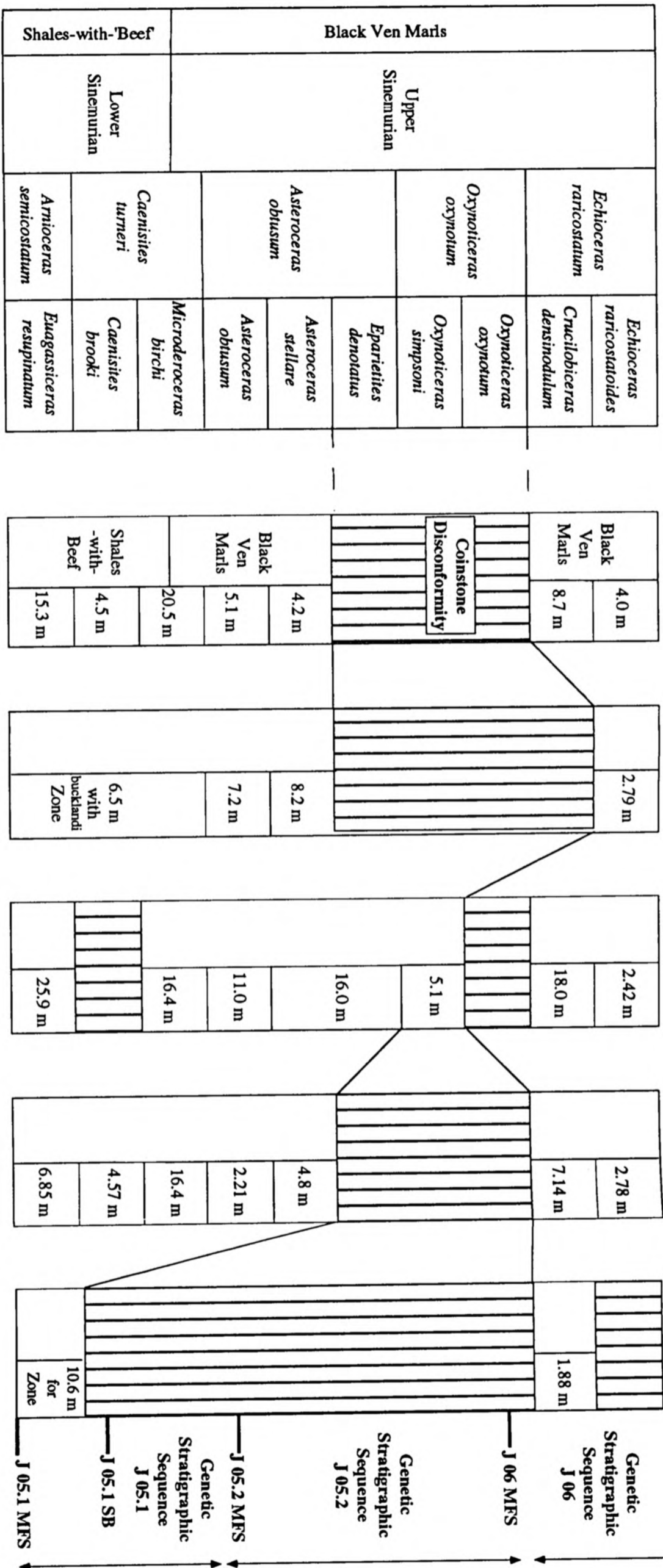
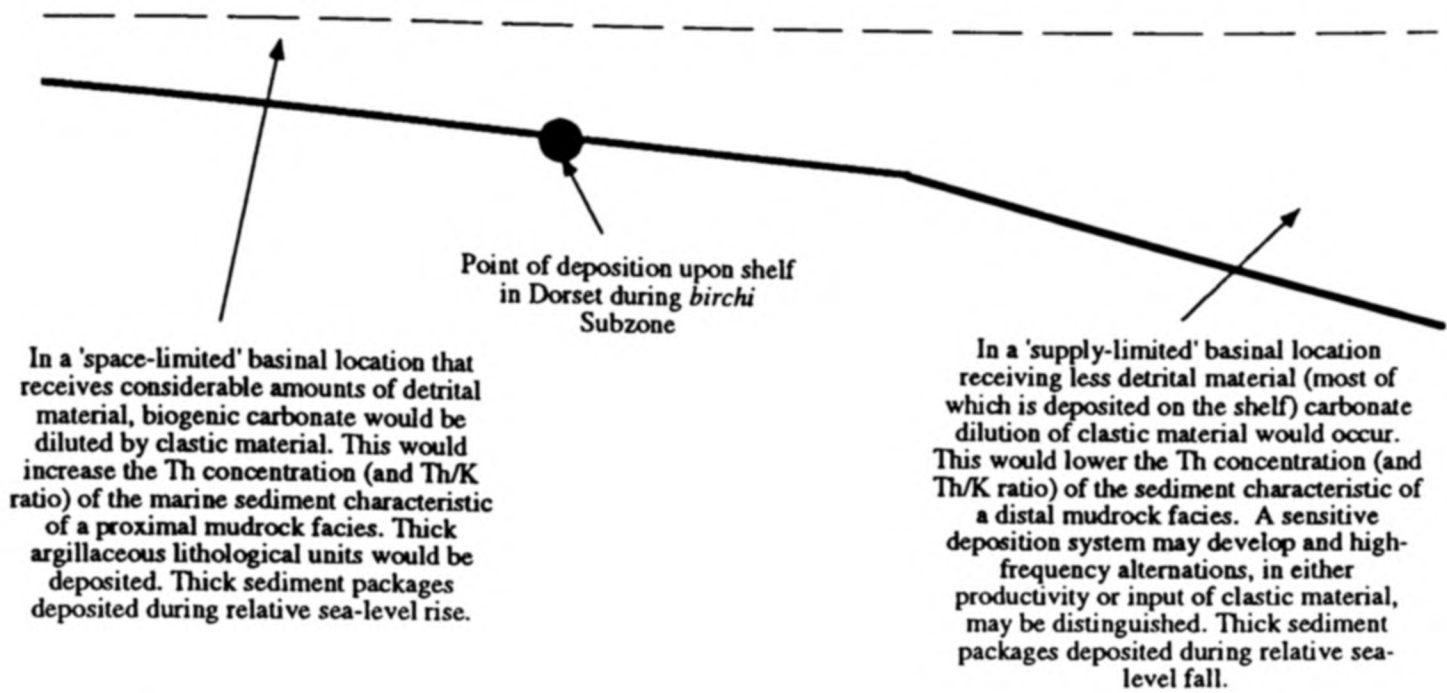


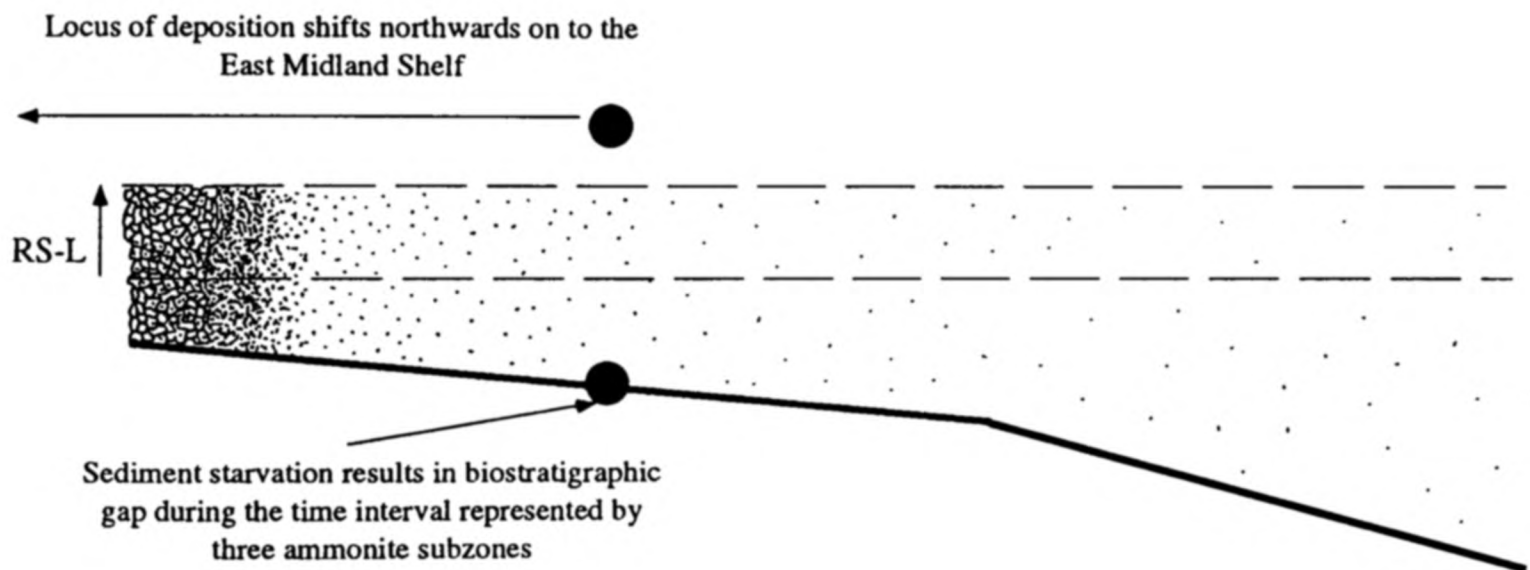
FIGURE 5.08

FIGURE 5.08 The Coinstone disconformity as evident at outcrop in Dorset (SY 380927) shows a variation in ammonite subzonal duration across southern Britain. Only surface exposure and sub-surface data with a subzonal biostratigraphic resolution is shown. The disconformity developed within the Shales-with-'Beef' is extremely local in geographical extent and is likely to be independent of processes that produced the Coinstone disconformity and may be due to erosion from waves impinging upon the shallow East Midland Shelf. Based upon Green & Melville (1956), Worsam (1963), Poole (1969), Cope *et al.* (1981) and Donovan & Kellaway (1984). The Coinstone disconformity cannot be identified from outcrop or subsurface gamma-ray data without a corresponding ammonite subzonal biostratigraphic data-set. Inferred candidate maximum-flooding surfaces (MSF) and candidate correlative conformities of sequence boundaries (SB) are shown. Subzonal thicknesses are indicated.

A) DEPOSITIONAL STYLE PRIOR TO RELATIVE SEA-LEVEL RISE



B) DEPOSITION DURING RELATIVE SEA-LEVEL RISE



C) DEPOSITION DURING HIGHSTAND AND RELATIVE SEA-LEVEL FALL

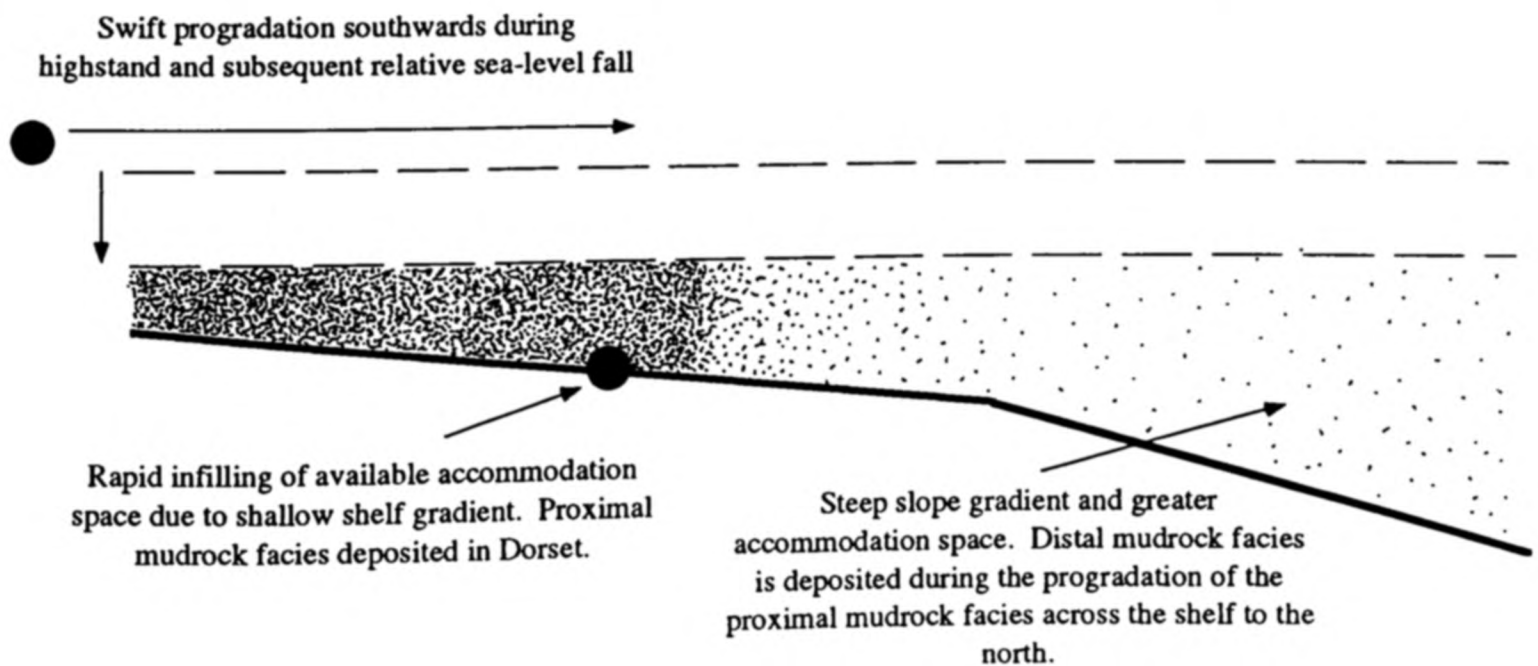
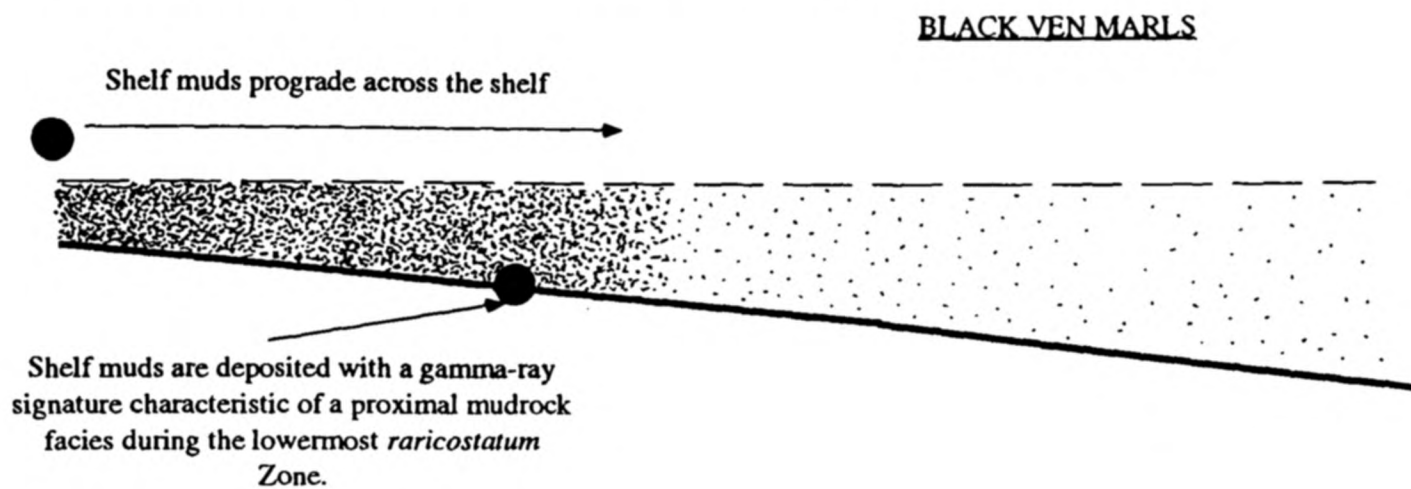


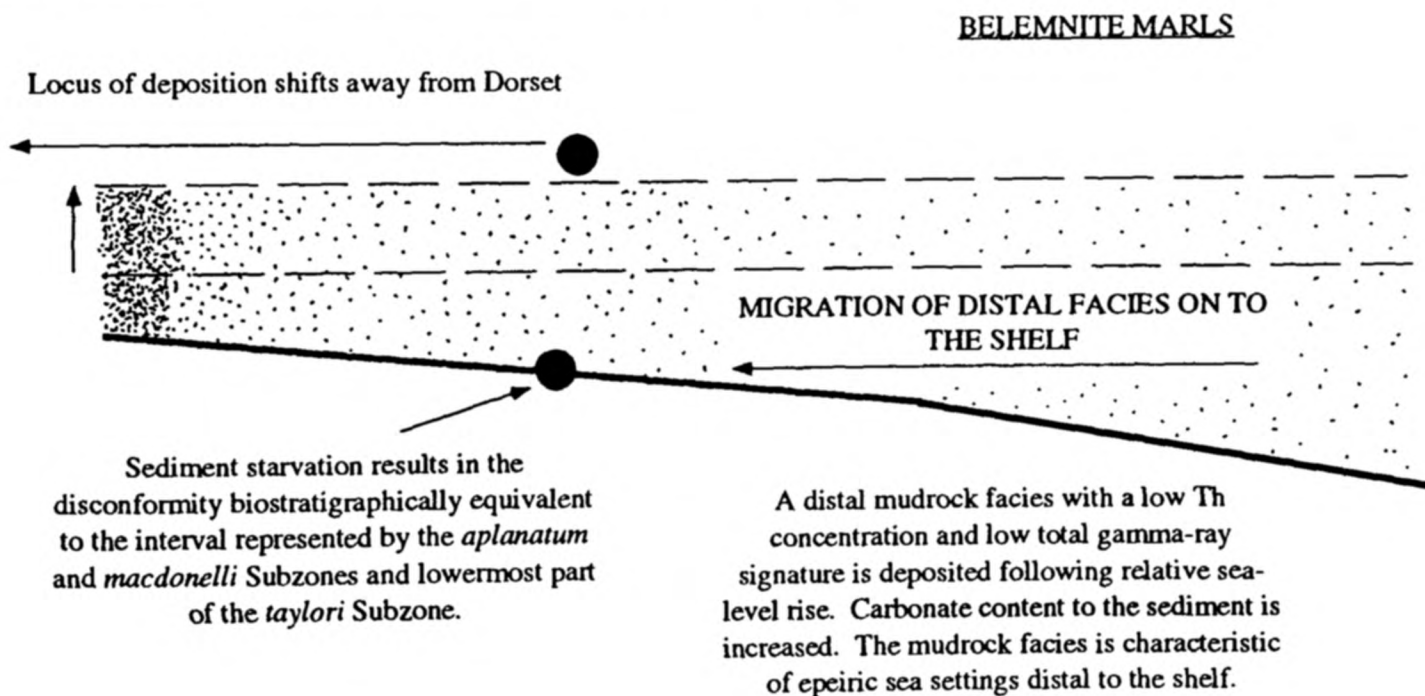
FIGURE 5.09 Possible interpretation of the Coinstone in terms of relative sea-level change.

FIGURE 5.10
Migration of mudrock facies at the Sinemurian - Pliensbachian boundary

A) DEPOSITION DURING UPPER SINEMURIAN STAGE



B) DEPOSITION DURING THE LOWER PLIENSBAICHIAN STAGE



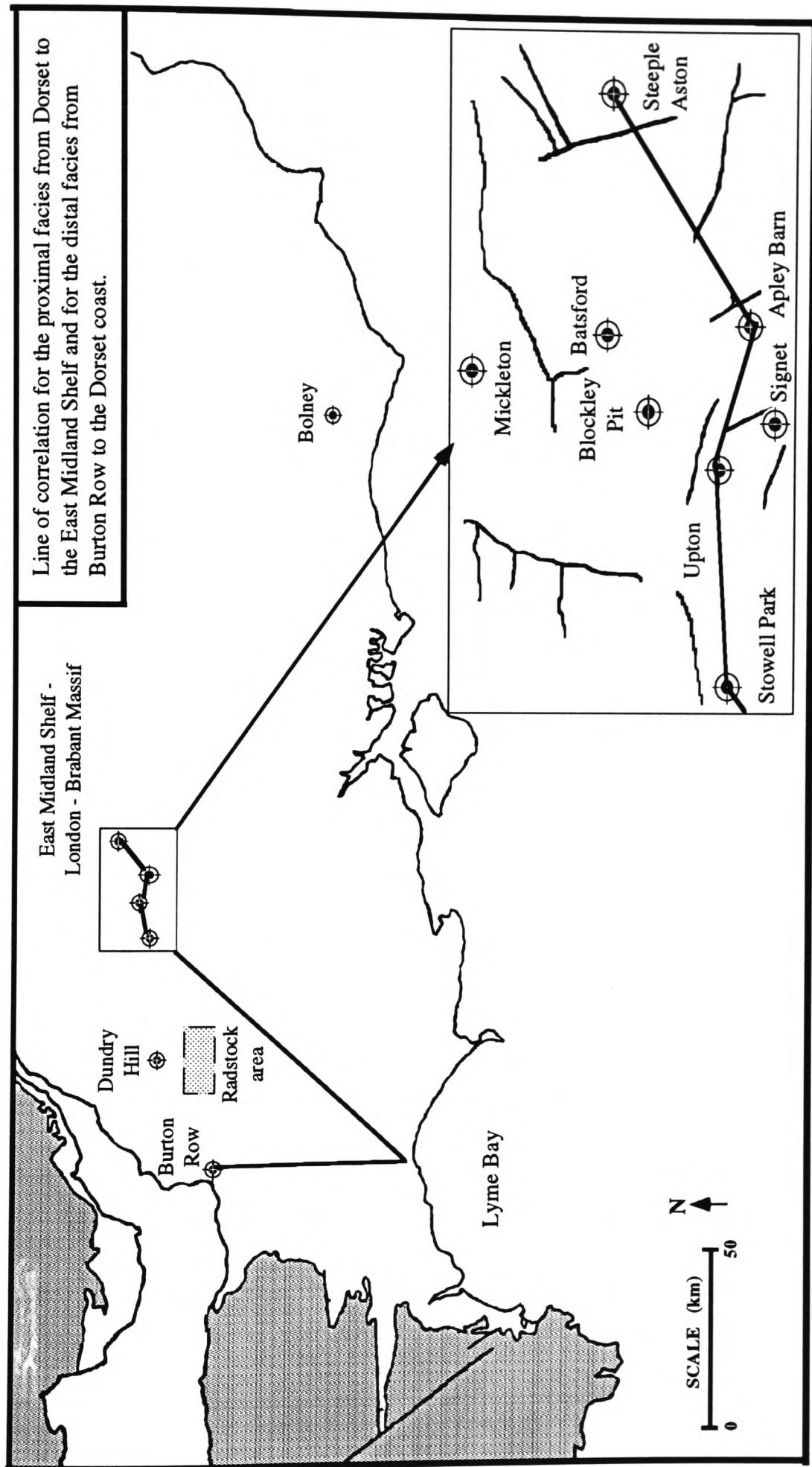


FIGURE 5.11 The Belemnite Marls and lateral time equivalents elsewhere in southern Britain (*jamesoni* to *ibex* Zones). A proximal mudrock facies is identified in the Stowell Park, Apley Barn and Steeple Aston boreholes on the basis of total gamma-ray signature and inferred in the Dundry Hill and Upton boreholes. The proximal facies outcrops at Blockley Pit Gloucestershire. A distal facies is identified in the Burton Row borehole and on the Dorset Coast. Locally, within the Radstock area the sequence becomes considerably condensed. Grid References for localities: Apley Barn (SP 343106), Burton Row, Brent Knoll (ST 335520), Elton Farm, Dundry Hill (ST 563658), Steeple Aston (SP 468258), Stowell Park (SP 084118), Upton, Witney (SP 231131), Blockley Pit section (SP 182369), Dorset coastal sections (SY 380927 - SY 415918), Bolney borehole, Sussex (TQ 280442).

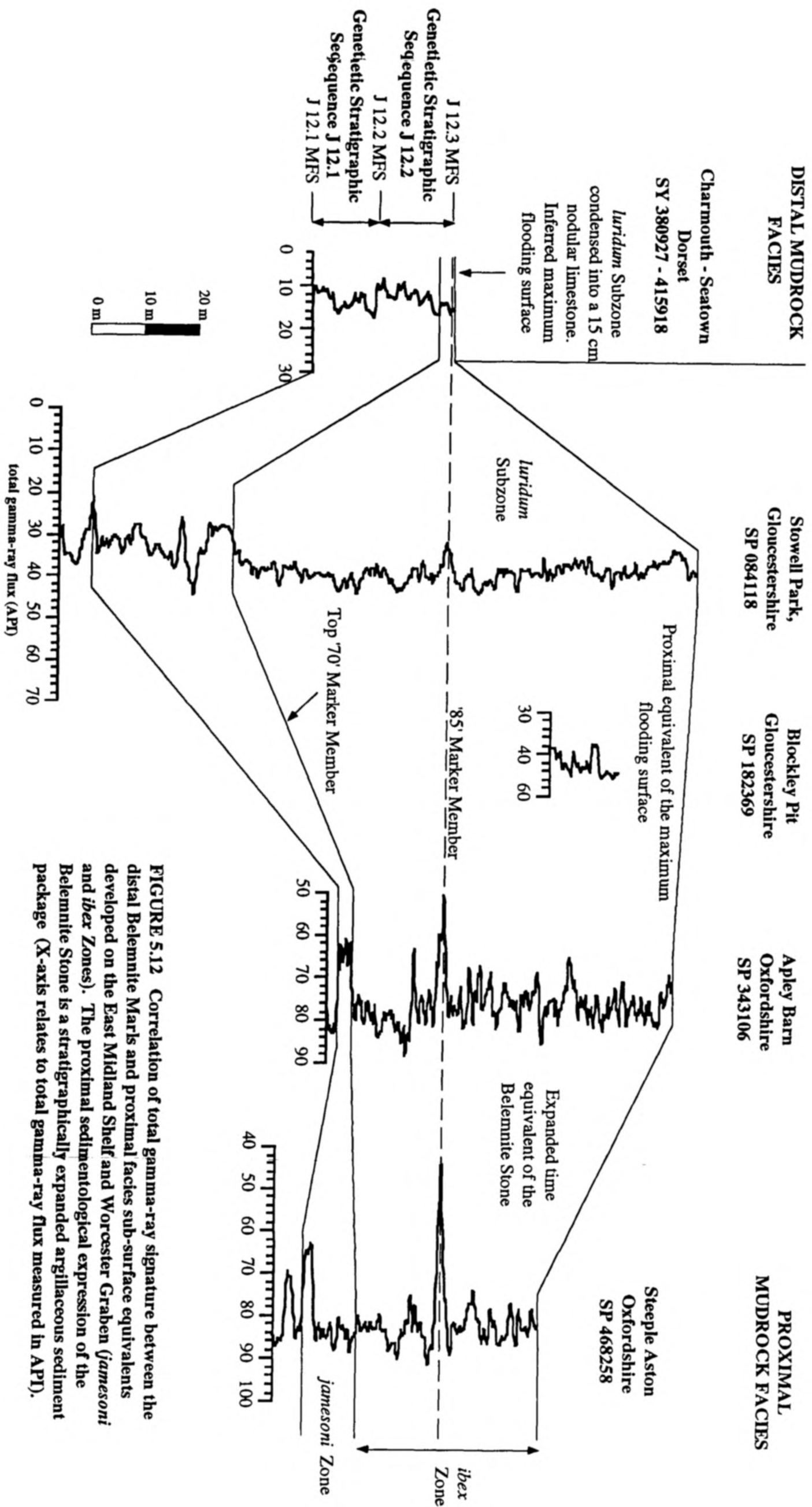


FIGURE 5.12 Correlation of total gamma-ray signature between the distal Belemnite Marls and proximal facies sub-surface equivalents developed on the East Midland Shelf and Worcester Graben (*Jamesoni* and *iber* Zones). The proximal sedimentological expression of the Belemnite Stone is a stratigraphically expanded argillaceous sediment package (X-axis relates to total gamma-ray flux measured in APF).

FIGURE 5.12

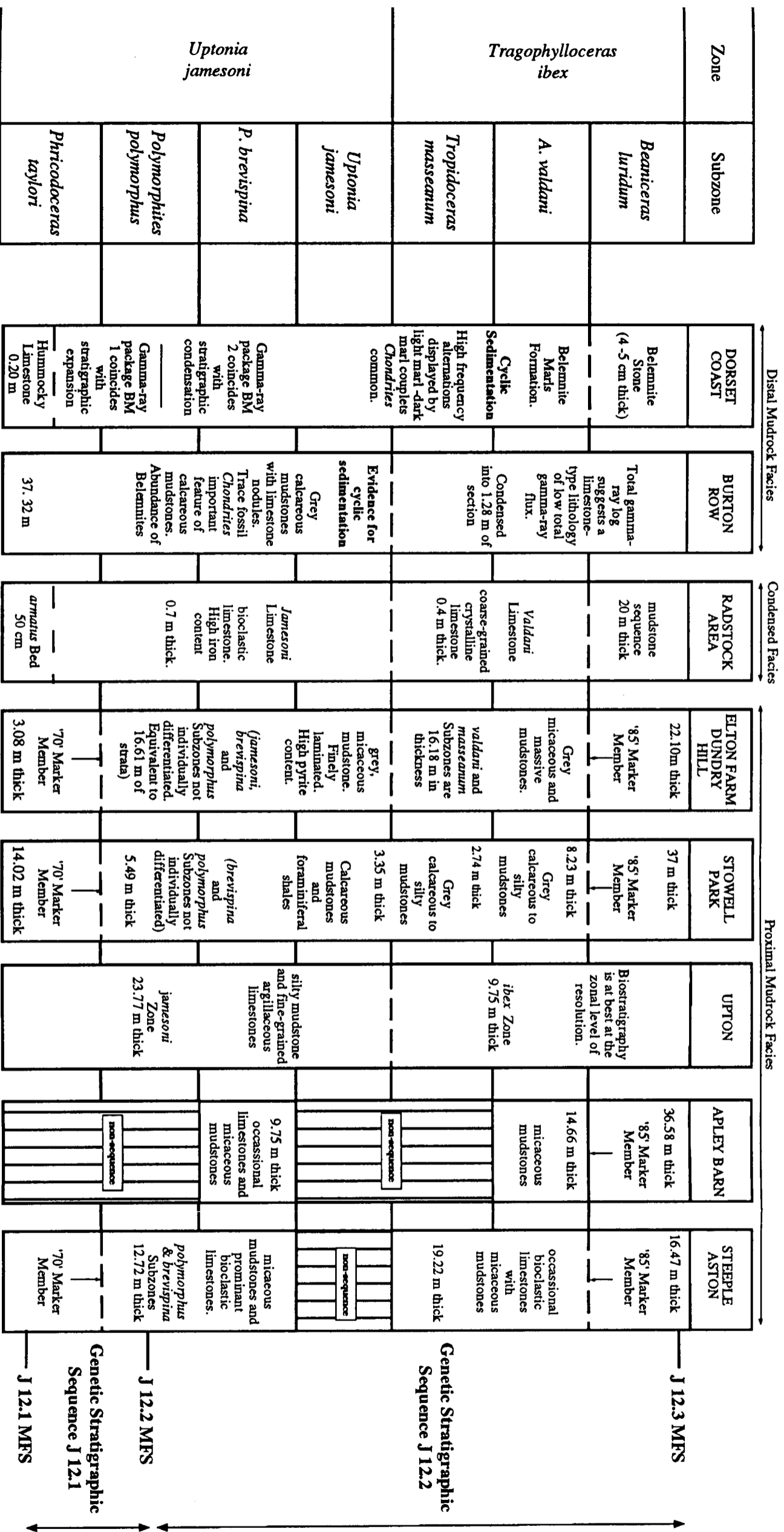


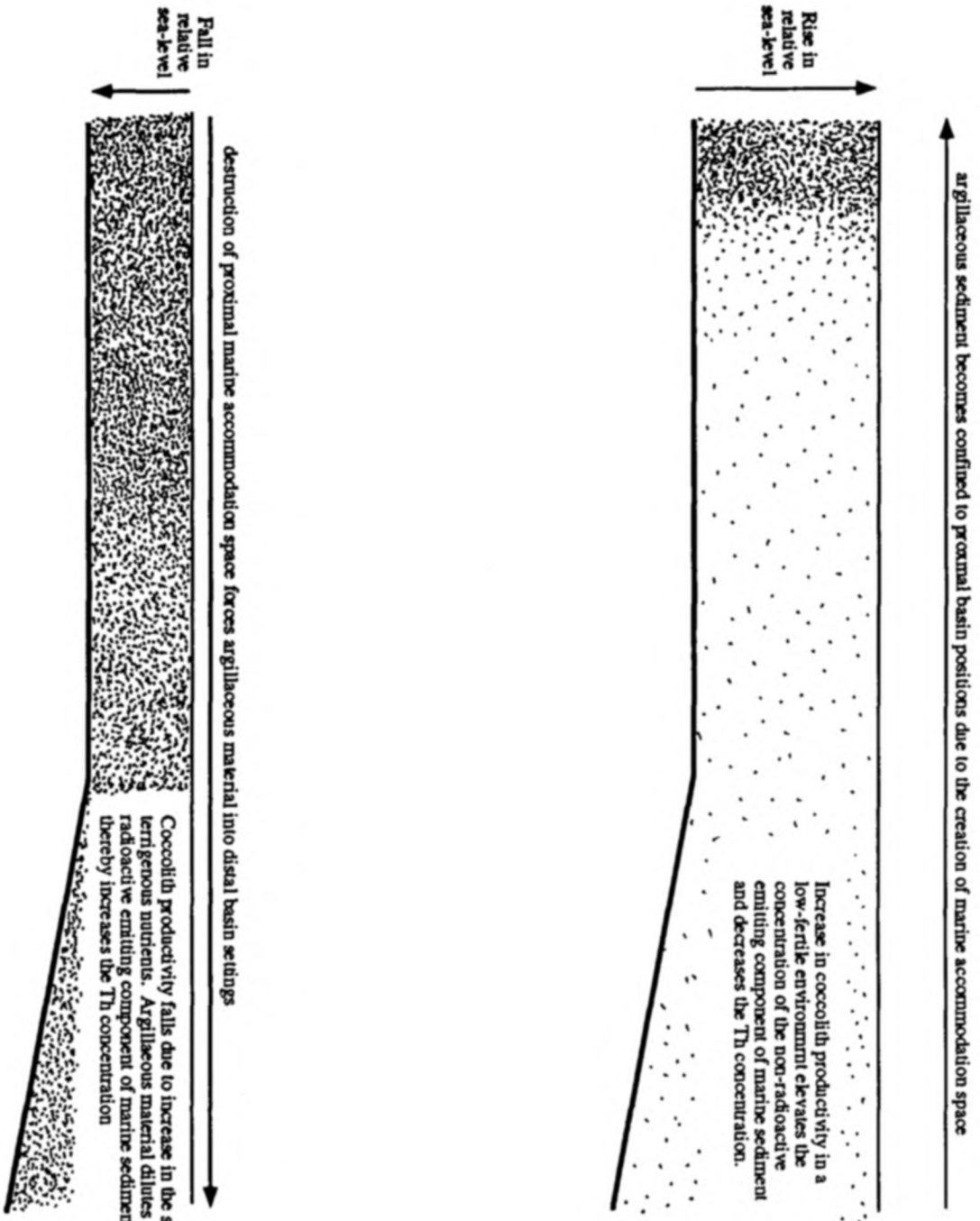
FIGURE 5.13 Sequence stratigraphic correlation panel for the Lower Pliensbachian in southern Britain. Data from Green & Melville 1956, Worssam 1963, Poole 1977, Whitaker & Green 1983 and Onovan & Kellaway 1984. Disconformities are shown. Thickness of ammonite subzones are given where possible. Inferred maximum-flooding surfaces and genetic stratigraphic sequences are shown.

FIGURE 5.13

A

PROXIMAL BASIN SETTING
(Space-limited *sensu* Galloway & Williams 1991)

DISTAL BASIN SETTING
(Supply-limited *sensu* Galloway & Williams 1991)



B

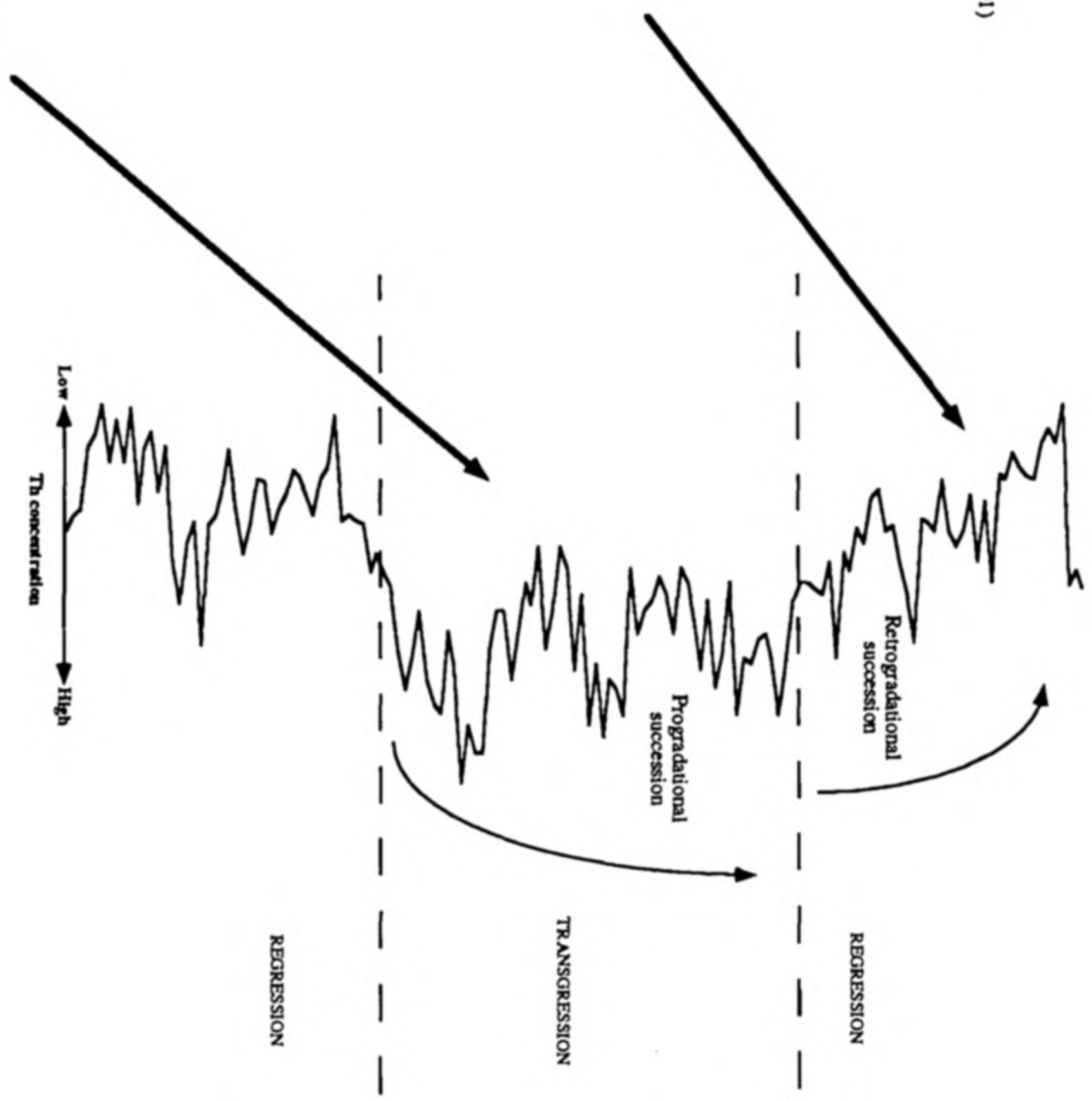
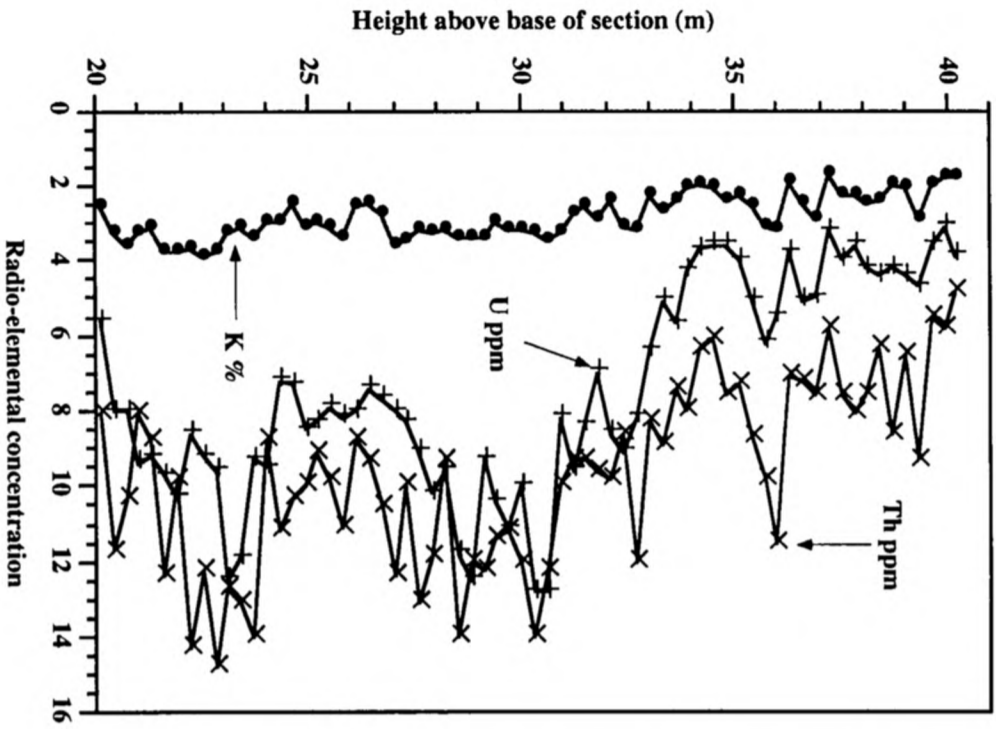


FIGURE 5.14

FIGURE 5.14 A model for the deposition of the Lower Lias and the influence of sediment supply on the Th gamma-ray log. The argillaceous intervals are principally regressive in character and the carbonate-rich intervals are principally transgressive in character.

A

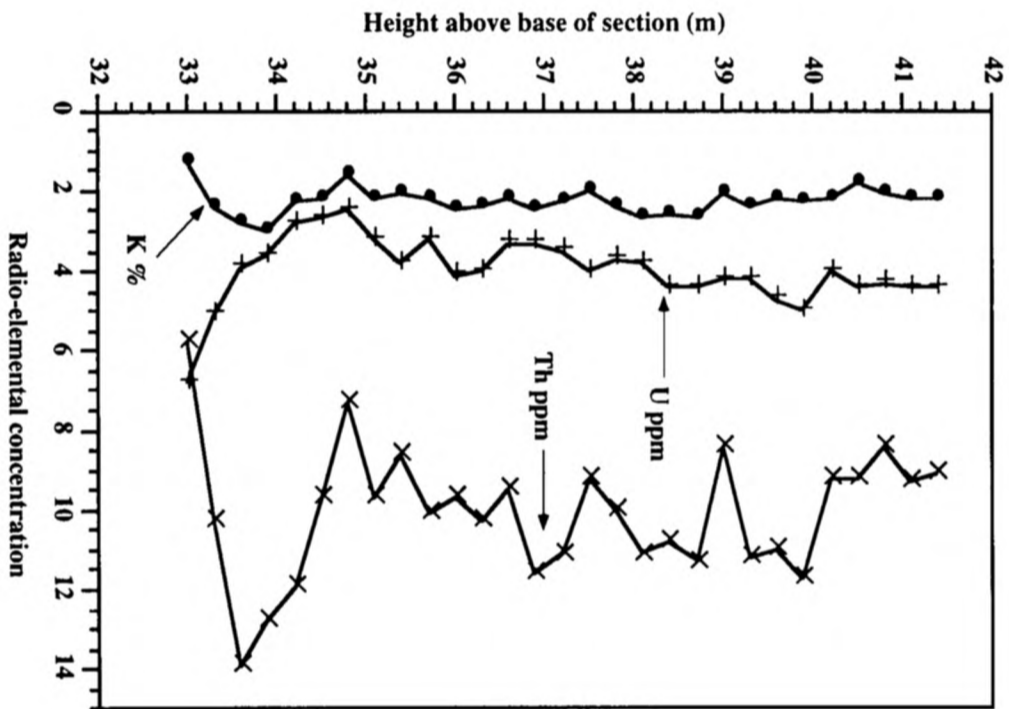
liasicus Shales, Bristol Channel Basin.
Gamma-ray unit BL 4



High U - High Th
(positive covariant relationship between U and Th at 95 % significance level)

B

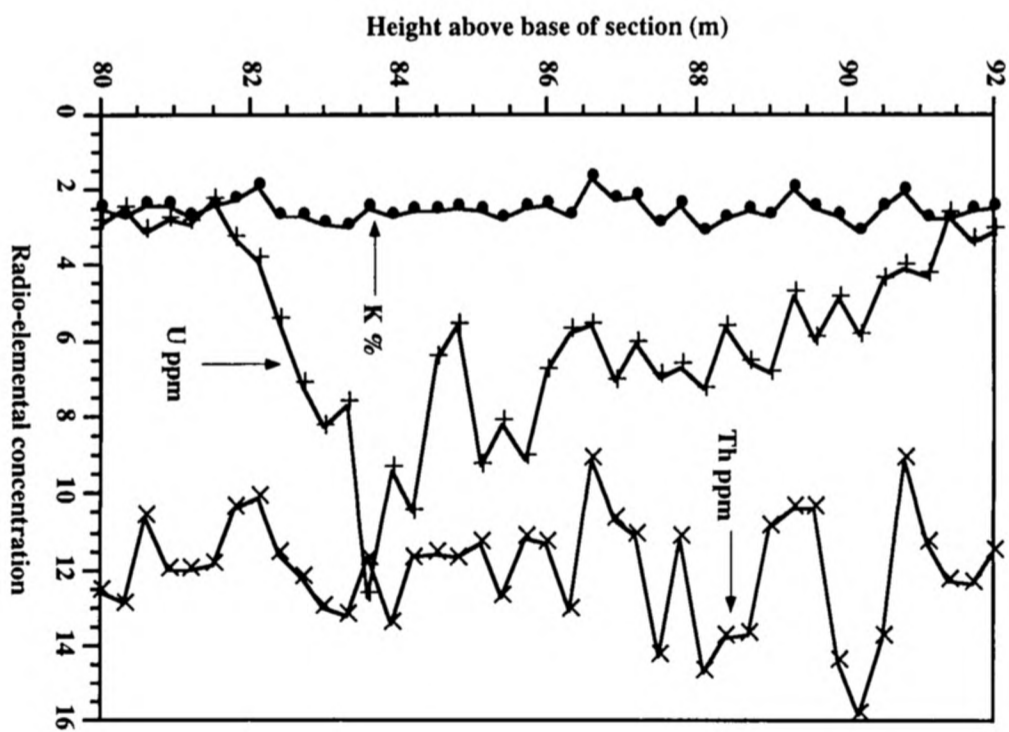
scipionianum Shales, Wessex Basin.
Gamma-ray unit SWB 1



Low U - High Th
(no covariant relationship between U and Th at 95 % significance level)

C

obtusum Shales, Wessex Basin.
Gamma-ray unit BVM 2



Increasing, then decreasing U - High Th
(no covariant relationship between U and Th at 95 % significance level)

FIGURE 5.15

FIGURE 5.15 Three types of shale can be distinguished in the Lower Lias in southern Britain, primarily based on the U concentration log as Th concentration for all argillaceous intervals is high. In case A anoxia appears to have developed during a fall in relative sea-level as the supply of terrigenous nutrients to the marine environment increased. This may have led to an increase in productivity and oxygen-depletion of the water column, resulting in bottom-water anoxia. In case B, the *scipionianum* Shales are also interpreted as having been deposited during a fall in relative sea-level, but anoxia appears to have not been extensively developed, as indicated by a low concentration of U. In case C, the U concentration log shows an increase followed by a progressive decrease in U, which is interpreted as the result of a rise in relative sea-level with the migration of anoxic basinal-waters on to the shelf. The development of anoxia in the Lower Lias is not diagnostic of any one particular part of the relative sea-level curve.

Appendix 1

**Methodology and Experimentation Data Required for
Outcrop Based Gamma-Ray Spectrometry.**

<u>Plane Taken</u>	<u>Horizon</u>	<u>Sample time</u> Secs	<u>Total Number of Counts Recorded</u> Total	<u>Total Number of Counts Recorded</u>			<u>Elemental Concentrations</u>			<u>Total ur</u>	
				<u>K</u>	<u>U</u>	<u>Th</u>	<u>K %</u>	<u>U ppm</u>	<u>Th ppm</u>		
Vertical Plane	Iron Ledge	280	9073	1402	558	127	0.90	4.50	2.80	08.40	
Vertical Plane	Iron Ledge	280	9104	1409	594	132	0.80	4.90	2.90	08.50	
Vertical Plane	Iron Ledge	280	9043	1384	588	141	0.80	4.80	3.10	08.40	
Vertical Plane	Iron Ledge	280	9237	1409	598	140	0.80	4.80	3.10	08.60	
Vertical Plane	Iron Ledge	280	8905	1307	500	106	0.80	4.10	2.10	07.60	
Vertical Plane	Iron Ledge	280	8910	1374	520	127	0.90	4.10	2.00	08.20	
Vertical Plane	Iron Ledge	280	8863	1393	556	105	0.90	4.70	2.10	08.20	
Vertical Plane	Iron Ledge	280	9549	1511	626	125	0.90	5.20	2.60	09.00	
Vertical Plane	Iron Ledge	280	9288	1383	626	127	0.80	5.20	2.70	08.70	
Vertical Plane	Iron Ledge	280	9008	1383	582	139	0.80	4.70	3.00	08.90	
Vertical Plane	Iron Ledge	280	8785	1340	557	129	0.80	4.50	2.80	08.10	
Vertical Plane	Iron Ledge	280	8981	1401	566	133	0.90	4.60	2.90	08.30	
Vertical Plane	Iron Ledge	280	8907	1378	579	118	0.80	4.80	2.50	08.20	
Vertical Plane	Iron Ledge	280	8895	1384	526	130	0.90	4.20	2.80	08.20	
Vertical Plane	Iron Ledge	280	11975	1729	783	141	0.80	6.80	2.90	12.10	
Vertical Plane	Iron Ledge	280	10359	1717	656	145	1.10	5.40	3.30	10.10	
Vertical Plane	Iron Ledge	280	9951	1558	639	140	1.00	5.20	3.10	09.50	
Vertical Plane	Iron Ledge	280	11331	1941	726	186	1.30	5.00	4.30	11.30	
Vertical Plane	Iron Ledge	280	10282	1649	616	166	1.10	4.90	3.60	10.00	
Vertical Plane	Iron Ledge	280	11191	1920	670	161	1.30	5.40	3.60	11.10	
							Mean	0.92	4.98	2.91	9.07

Table 1.10 Data-set representing 20 samples taken at different locations on the Iron Ledge limestone (Blue Lias Formation) that outcrops at Seven Rock Point, Lyme Regis, Dorset (SY 335916). The data were collected with the B.P. GR-256 gamma-ray spectrometer on October 25th 1993 with the detector placed perpendicular to bedding (*i.e.* in the vertical plane). All field calibration and experimental data in this study were collected with the detector placed in the vertical plane, unless otherwise stated, to be consistent with the data collected from the calibration facility at the British Geological Survey, Keyworth.

<u>Plane Taken</u>	<u>Horizon</u>	<u>Sample Time</u>		<u>Total Number of Counts Recorded</u>			<u>Calculated Elemental Concentrations</u>			
		<u>Secs</u>	<u>Total</u>	<u>K</u>	<u>U</u>	<u>Th</u>	<u>K %</u>	<u>U ppm</u>	<u>Th ppm</u>	<u>Total ur</u>
Vertical Plane	Iron Ledge	360	41360	1685	1641	312	0.21	12.02	6.25	24.29
Vertical Plane	Iron Ledge	360	38390	1507	1393	258	0.25	10.23	5.17	22.55
Vertical Plane	Iron Ledge	360	39240	1481	1357	234	0.49	10.06	4.69	23.04
Vertical Plane	Iron Ledge	360	41820	1689	1519	253	0.32	11.30	5.07	24.56
Vertical Plane	Iron Ledge	360	45480	1883	1754	347	0.29	12.77	6.96	26.71
Vertical Plane	Iron Ledge	360	47280	2046	1913	330	0.33	14.18	6.61	27.77
Vertical Plane	Iron Ledge	360	44060	1802	1768	326	0.22	13.00	6.53	25.88
Vertical Plane	Iron Ledge	360	50490	1638	1356	296	0.36	09.74	5.93	29.65
Vertical Plane	Iron Ledge	360	48530	1478	1191	253	0.35	08.59	5.07	28.50
Vertical Plane	Iron Ledge	360	48190	1560	1271	250	0.37	09.26	5.01	28.30
Vertical Plane	Iron Ledge	360	47700	1431	1234	244	0.29	08.99	4.89	28.01
Vertical Plane	Iron Ledge	360	49690	1575	1224	276	0.40	08.74	5.53	29.18
Vertical Plane	Iron Ledge	360	48770	1480	1191	254	0.35	08.58	5.09	28.64
Vertical Plane	Iron Ledge	360	45770	1191	1022	224	0.24	07.33	4.49	26.88
Vertical Plane	Iron Ledge	360	50980	1202	0990	230	0.26	07.04	4.61	29.94
Vertical Plane	Iron Ledge	360	44590	1157	0969	202	0.25	07.01	4.05	26.19
Vertical Plane	Iron Ledge	360	45030	1151	0973	213	0.24	06.98	4.27	26.44
Vertical Plane	Iron Ledge	360	44320	1143	0974	199	0.24	07.06	3.99	26.03
Vertical Plane	Iron Ledge	360	45410	1234	1056	187	0.27	07.80	3.75	26.67
Vertical Plane	Iron Ledge	360	46400	1292	1040	228	0.24	07.46	4.57	27.25
						Mean	0.30	9.41	5.13	26.82

Table 1.11 Data-set representing 20 samples taken at different locations on the limestone horizon known as Iron Ledge of the Blue Lias Formation that outcrops at Seven Rock Point, Lyme Regis, Dorset (SY 335916). Data collected with the GR-410 gamma-ray spectrometer. Raw data shown. Realignment formulae for comparison with radio-elemental concentration data collected with the GR-256 gamma-ray spectrometer are given in Chapter 2 (Section 2.05). The data were collected on July 17th 1994. The radio-elemental data were retrospectively found to be unreliable and cannot be used for interpretation.

<u>Plane Taken</u>	<u>Horizon</u>	<u>Sample Time</u> Secs	<u>Total Number of Counts Recorded</u>			<u>Elemental Concentrations</u>				
			<u>Total</u>	<u>K</u>	<u>U</u>	<u>Th</u>	<u>K %</u>	<u>U ppm</u>	<u>Th ppm</u>	<u>Total ur</u>
Vertical Plane	Belemnite Bed	215	9450	1677	547	182	1.50	5.30	5.70	12.50
Vertical Plane	Belemnite Bed	215	9487	1704	608	202	1.50	6.00	6.50	12.60
Vertical Plane	Belemnite Bed	215	9564	1666	546	202	1.50	5.20	6.50	12.70
Vertical Plane	Belemnite Bed	215	9506	1667	561	204	1.50	5.40	6.50	12.60
Vertical Plane	Belemnite Bed	215	9183	1574	569	195	1.40	5.50	6.20	12.10
Vertical Plane	Belemnite Bed	215	9576	1634	557	208	1.50	5.30	6.80	12.70
Vertical Plane	Belemnite Bed	215	9748	1748	542	229	1.60	4.90	7.50	13.00
Vertical Plane	Belemnite Bed	215	9650	1724	524	238	1.60	4.60	7.90	12.90
Vertical Plane	Belemnite Bed	215	9098	1593	543	223	1.40	5.00	7.30	11.90
Vertical Plane	Belemnite Bed	215	9407	1657	521	191	1.50	4.90	6.10	12.50
Vertical Plane	Belemnite Bed	215	9520	1656	560	227	1.50	5.20	7.40	12.60
Vertical Plane	Belemnite Bed	215	9436	1645	548	209	1.50	5.10	6.80	12.50
Vertical Plane	Belemnite Bed	215	9680	1725	576	226	1.60	5.40	7.40	12.90
Vertical Plane	Belemnite Bed	215	9248	1538	502	181	1.40	4.80	5.80	12.20
Vertical Plane	Belemnite Bed	215	9223	1564	524	216	1.40	4.80	7.10	12.20
Vertical Plane	Belemnite Bed	215	9340	1580	548	190	1.40	5.30	6.10	12.40
Vertical Plane	Belemnite Bed	215	9506	1647	493	199	1.60	4.50	6.40	12.60
Vertical Plane	Belemnite Bed	215	9406	1640	570	227	1.50	5.30	7.40	12.50
Vertical Plane	Belemnite Bed	215	9804	1722	612	208	1.50	6.00	6.70	13.10
Vertical Plane	Belemnite Bed	215	9617	1693	540	241	1.60	4.80	8.00	12.80
						Mean	1.50	5.17	6.81	12.57

Table 1.12 Data-set representing 20 samples taken at different locations on the dark laminated-shale horizon known as the Belemnite Bed (Belemnite Marls Formation) that outcrops west of Seatown, Dorset (SY 318908). The data were collected with the B.P. GR-256 gamma-ray spectrometer on May 16th 1993. The detector was placed perpendicular to bedding (*i.e.* in the vertical plane).

<u>Plane Taken</u>	<u>Horizon</u>	<u>Sample Time</u> Secs	<u>Total Number of Counts Recorded</u>			<u>Calculated Elemental Concentrations</u>			<u>Total ur</u>	
			<u>Total</u>	<u>K</u>	<u>U</u>	<u>Th</u>	<u>K %</u>	<u>U ppm</u>		<u>Th ppm</u>
Vertical Plane	Belemnite Bed	240	43360	2035	2266	414	0.10	25.02	12.45	38.20
Vertical Plane	Belemnite Bed	240	43870	1936	2141	400	0.10	23.57	12.03	38.65
Vertical Plane	Belemnite Bed	240	44650	1895	2013	424	0.16	21.80	12.75	39.33
Vertical Plane	Belemnite Bed	240	45580	1921	1982	419	0.22	21.45	12.60	40.15
Vertical Plane	Belemnite Bed	240	47200	1887	1788	374	0.39	19.38	11.24	41.58
Vertical Plane	Belemnite Bed	240	48120	1820	1814	409	0.26	19.44	12.30	42.39
Vertical Plane	Belemnite Bed	240	48580	1832	1739	379	0.37	18.73	11.40	42.79
Vertical Plane	Belemnite Bed	240	48250	1871	1779	382	0.38	19.21	11.49	42.50
Vertical Plane	Belemnite Bed	240	40610	1806	2132	358	-0.02	23.78	10.76	35.77
Vertical Plane	Belemnite Bed	240	41490	1793	2109	383	-0.03	23.30	11.52	36.55
Vertical Plane	Belemnite Bed	240	42310	1945	2076	381	0.19	22.91	11.46	37.27
Vertical Plane	Belemnite Bed	240	41780	1793	2140	462	-0.11	23.09	13.89	36.80
Vertical Plane	Belemnite Bed	240	43940	2017	2239	435	0.09	24.52	13.08	38.71
Vertical Plane	Belemnite Bed	240	44940	2019	2316	430	0.02	25.52	12.93	39.59
Vertical Plane	Belemnite Bed	240	42350	1806	2194	417	-0.12	24.10	12.54	37.31
Vertical Plane	Belemnite Bed	240	42260	1940	2098	412	0.14	22.94	12.39	37.23
Vertical Plane	Belemnite Bed	240	42000	1915	2105	416	0.10	23.00	12.51	37.00
Vertical Plane	Belemnite Bed	240	40080	1825	2358	429	-0.26	26.05	12.90	35.31
Vertical Plane	Belemnite Bed	240	40420	1789	2224	348	-0.13	24.99	10.46	35.61
Vertical Plane	Belemnite Bed	240	40440	1819	2237	428	-0.15	24.55	12.87	35.62
						Mean	0.09	22.87	12.18	38.42

Table 1.13 Data-set representing 20 samples taken at different locations on the dark laminated-shale horizon known as the Belemnite Bed (Belemnite Marls Formation) that outcrops west of Seatown, Dorset (SY 318908). Data collected with the GR-410 gamma-ray spectrometer. Raw data shown. Realignment formulae for comparison with radio-elemental concentration data collected with the GR-256 gamma-ray spectrometer are given in Chapter 2 (Section 2.05). The data were collected on July 24th 1994. The radio-elemental data were retrospectively found to be unreliable and cannot be used for interpretation.

A) Readings for a single point on Belemnite Bed on high voltage

Plane	Horizon	Sample Time Secs	Total Number of Counts Recorded			Th	Total μr	Calculated Elemental Concentrations		
			Total	K	U			K %	U ppm	Th ppm
Vertical	Belemnite Bed	240	43360	2035	2266	414	38.20	0.10	25.02	12.45
Vertical	Belemnite Bed	240	43870	1936	2141	400	38.65	0.10	23.5	12.03
Vertical	Belemnite Bed	240	44650	1895	2013	424	39.33	0.16	21.80	12.75
Vertical	Belemnite Bed	240	45580	1921	1982	419	40.15	0.22	21.45	12.60
Vertical	Belemnite Bed	240	47200	1887	1788	374	41.58	0.39	19.38	11.24
Vertical	Belemnite Bed	240	48120	1820	1814	409	42.39	0.26	19.44	12.30
Vertical	Belemnite Bed	240	48580	1832	1739	379	42.79	0.37	18.73	11.40
Vertical	Belemnite Bed	240	40610	1806	2132	358	35.77	-0.02	23.78	10.76
Vertical	Belemnite Bed	240	41490	1793	2109	383	36.55	-0.03	23.30	11.52
Vertical	Belemnite Bed	240	42310	1945	2076	381	37.27	0.19	22.91	11.46
Vertical	Belemnite Bed	240	41780	1793	2140	462	36.80	-0.11	23.09	13.89
Vertical	Belemnite Bed	240	43940	2017	2229	435	38.71	0.10	24.40	13.08
Vertical	Belemnite Bed	240	44940	2019	2316	430	39.59	0.02	25.52	12.93
Vertical	Belemnite Bed	240	42350	1806	2194	417	37.31	-0.12	24.10	12.54
Vertical	Belemnite Bed	240	42260	1940	2098	412	37.23	0.14	22.94	12.39
Vertical	Belemnite Bed	240	48250	1871	1779	382	42.50	0.38	19.21	11.49
Vertical	Belemnite Bed	240	42000	1915	2105	416	37.00	0.10	23.00	12.51
Vertical	Belemnite Bed	240	40080	1873	2250	381	35.31	-0.07	25.07	11.46
Vertical	Belemnite Bed	240	40420	1789	2224	348	35.61	-0.13	24.99	10.46
Vertical	Belemnite Bed	240	40440	1819	2237	428	35.62	0.15	24.55	12.87
					Mean		38.42	0.09	22.81	12.10

Table 1.14 Comparison between data collected under conditions of high battery voltage (11 V) and low battery voltage (below 11 V) with the GR-410 gamma-ray spectrometer. Data collected on the dark laminated-shale horizon known as the Belemnite Bed (Belemnite Marls Formation) that outcrops west of Seatown, Dorset (SY 318908). Raw data are shown. Realignment formulae for comparison with radio-elemental concentration data collected with the GR-256 gamma-ray spectrometer are given in Chapter 2 (Section 2.05). Collected on July 23rd 1993. (1 of 2).

B) Readings for a single point on Belemnite Bed on low voltage

<u>Plane</u>	<u>Horizon</u>	<u>Sample Time</u> <u>Secs</u>	<u>Total Number of Counts Recorded</u>			<u>Calculated Elemental Concentrations</u>				
			<u>Total</u>	<u>K</u>	<u>U</u>	<u>Th</u>	<u>Total ur</u>	<u>K %</u>	<u>U ppm</u>	<u>Th ppm</u>
Vertical	Belemnite Bed	240	51590	1983	1782	384	45.45	0.51	19.23	11.55
Vertical	Belemnite Bed	240	53730	1964	1812	379	47.33	0.46	19.64	11.40
Vertical	Belemnite Bed	240	50030	1916	1742	359	44.07	0.48	18.92	10.79
Vertical	Belemnite Bed	240	51160	1955	1733	355	45.07	0.54	18.84	10.67
Vertical	Belemnite Bed	240	50970	1949	1684	374	44.90	0.57	18.09	11.24
Vertical	Belemnite Bed	240	51280	1991	1692	366	45.17	0.62	18.25	11.00
Vertical	Belemnite Bed	240	51160	1907	1712	405	45.07	0.47	18.20	12.18
Vertical	Belemnite Bed	240	51840	1954	1640	405	45.67	0.60	17.31	12.18
Vertical	Belemnite Bed	240	51850	1932	1630	391	45.67	0.59	17.29	11.76
Vertical	Belemnite Bed	240	54080	1947	1606	387	47.64	0.63	17.02	11.64
						Mean	45.60	0.55	18.28	11.44
						Percentage Difference	18.70	474.51	-19.87	-5.49

Table 1.14 (2 of 2). The radio-elemental data that were collected with the GR-410 was retrospectively found to be unreliable. Only total gamma-ray flux can therefore be confidently used for interpretation (see Section 2.05).

<u>Calibration Pad</u>	<u>Sample Time</u>	<u>Total counts</u>	<u>K counts</u>	<u>U counts</u>	<u>Th counts</u>
K3-88	120 seconds	16180	772	1200	66
K3-88	120 seconds	16520	776	1404	84
K3-88	120 seconds	16530	775	1537	44
K3-88	120 seconds	16180	772	1200	66
K3-88	60 seconds	8050	386	417	40
K3-88	60 seconds	8370	385	878	44
U8-89	120 seconds	30050	1816	1353	183
U8-89	120 seconds	28820	2032	1632	211
U8-89	120 seconds	30400	1735	1183	167
U8-89	120 seconds	31070	1649	1221	208
U8-89	60 seconds	15500	795	591	84
U8-89	60 seconds	15760	814	624	118
T3-88	120 seconds	38680	1151	2103	1473
T3-88	120 seconds	33690	1435	1439	1499
T3-88	120 seconds	36380	1304	1818	1274
T3-88	120 seconds	33740	1473	1462	1458
T3-88	60 seconds	16390	854	661	823
T3-88	60 seconds	15480	819	635	816
B3-88	120 seconds	7320	270	575	67
B3-88	120 seconds	7360	333	664	99
B3-88	120 seconds	7760	334	767	74
B3-88	120 seconds	7570	316	768	80
B3-88	60 seconds	3850	174	406	52
B3-88	60 seconds	3820	179	419	54
Summed Results					
K3-88	600 seconds	82160	3882	6490	369
U8-89	600 seconds	151600	8841	6604	971
T3-88	600 seconds	174360	7040	8118	7343
B3-88	600 seconds	37680	1606	3599	426

Table 1.15 Temperature drift during calibration of the GR-410 gamma-ray spectrometer. The number of U counts on U8-89 pad are only approximately double those detected on the background radiation pad B3-88. Similarly the number of K counts on U8-89 pad are actually greater than the number of U counts detected on the same pad. This indicates drift of the gamma-ray spectra with the K-energy window recording a significant proportion of counts from a pure U source. On the K3-88 pad the number of U counts are actually greater than the number of K counts indicating drift of the K gamma-ray spectra into the U energy window. In this case the U window is recording a significant proportion of gamma-ray counts from a pure K source. (See Chapter 2, Section 2.03).

The calibration data were collected on the 9th January 1995.

Plane Taken	Horizon	Sample Time Secs	Total Number of Counts Recorded		Calculated Elemental Concentrations				Total µr	
			Total	K	U	Th	K %	U ppm		Th ppm
Horizontal (S)	Lower Cement Bed	480	35940	1671	2712	466	-0.40	15.08	7.01	15.83
Horizontal (S)	Lower Cement Bed	480	37560	1727	2657	424	-0.33	14.90	6.37	16.54
Horizontal (S)	Lower Cement Bed	480	38020	1623	2641	443	-0.39	14.73	6.66	16.75
Horizontal (S)	Lower Cement Bed	480	37990	1650	2462	412	-0.28	13.73	6.19	16.73
Horizontal (S)	Lower Cement Bed	480	37650	1622	2643	434	-0.39	14.77	6.52	16.58
Horizontal (S)	Lower Cement Bed	480	37390	1574	2626	389	-0.40	14.84	5.85	16.47
Horizontal (S)	Lower Cement Bed	480	36540	1575	2603	410	-0.39	14.62	6.16	16.09
Horizontal (S)	Lower Cement Bed	480	37170	1606	2661	415	-0.40	14.96	6.24	16.37
Horizontal (S)	Lower Cement Bed	480	37250	1508	2559	414	-0.41	14.33	6.22	16.41
Horizontal (S)	Lower Cement Bed	480	37780	1627	2663	409	-0.39	14.99	6.15	16.64
Horizontal (D)	Lower Cement Bed	480	37810	1643	2510	428	-0.31	13.97	6.43	16.65
Horizontal (D)	Lower Cement Bed	480	39540	1679	2383	437	-0.23	13.15	6.57	17.42
Horizontal (D)	Lower Cement Bed	480	44480	1870	2567	485	-0.22	14.11	7.29	19.59
Horizontal (D)	Lower Cement Bed	480	44240	1759	2439	470	-0.22	13.37	7.07	19.49
Horizontal (D)	Lower Cement Bed	480	43330	1653	2327	423	-0.22	12.85	6.36	19.08
Horizontal (D)	Lower Cement Bed	480	44320	1744	2366	433	-0.18	13.06	6.51	19.52
Horizontal (D)	Lower Cement Bed	480	44250	1715	2342	403	-0.18	13.02	6.06	19.49
Horizontal (D)	Lower Cement Bed	480	47410	1785	2023	457	0.00	10.84	6.87	20.88
Horizontal (D)	Lower Cement Bed	480	46830	1704	1966	421	-0.01	10.62	6.33	20.63
Horizontal (D)	Lower Cement Bed	480	48310	1760	1962	455	0.01	10.46	6.84	21.28
Vertical (S)	Lower Cement Bed	480	46100	1495	1577	355	0.06	8.45	5.34	20.30
Vertical (S)	Lower Cement Bed	480	47470	1434	1488	342	0.07	7.95	5.14	20.91

Table 1.16 Comparison between data collected with the detector of the gamma-ray spectrometer placed in the horizontal plane (parallel to bedding) and the detector placed in the vertical plane (perpendicular to bedding). The data were collected on the limestone known as the Lower Cement Bed (Black Ven Marls Formation) that outcrops east of Charmouth, Dorset (SY 368930) with the GR-410 gamma-ray spectrometer. Raw data shown. Same location denoted as (S) and different locations as (D). The data were collected on July 15th 1994. Only total gamma-ray flux can be reliably interpreted. (1 of 2.)

Plane Taken	Horizon	Sample Time		Total Number of Counts Recorded			Calculated Elemental Concentrations				Total μ
		Secs	Th	K	U	Th	K %	U ppm	Th ppm		
Vertical (S)	Lower Cement Bed	480		1510	1496	350	0.11	7.97	5.26	20.66	
Vertical (S)	Lower Cement Bed	480		1405	1530	382	0.02	8.06	5.74	20.47	
Vertical (S)	Lower Cement Bed	480		1463	1548	336	0.06	8.34	5.05	20.43	
Vertical (S)	Lower Cement Bed	480		1443	1526	356	0.05	8.13	5.35	20.44	
Vertical (S)	Lower Cement Bed	480		1446	1544	366	0.04	8.20	5.50	20.49	
Vertical (S)	Lower Cement Bed	480		1434	1501	323	0.07	8.10	4.86	20.49	
Vertical (S)	Lower Cement Bed	480		1406	1545	378	0.02	8.17	5.68	20.49	
Vertical (S)	Lower Cement Bed	480		1414	1562	373	0.01	8.29	5.60	20.52	
Vertical (D)	Lower Cement Bed	480		1017	999	256	0.07	05.24	3.85	17.49	
Vertical (D)	Lower Cement Bed	480		1087	1176	249	0.03	06.36	3.74	17.00	
Vertical (D)	Lower Cement Bed	480		1085	1100	280	0.06	05.77	4.21	16.92	
Vertical (D)	Lower Cement Bed	480		1743	2089	460	-0.06	11.23	6.92	22.32	
Vertical (D)	Lower Cement Bed	480		1518	1600	364	0.06	08.56	5.47	19.64	
Vertical (D)	Lower Cement Bed	480		1999	1945	448	0.17	10.38	6.73	25.19	
Vertical (D)	Lower Cement Bed	480		1484	1418	340	0.14	07.52	5.11	21.59	
Vertical (D)	Lower Cement Bed	480		1572	1426	380	0.17	07.42	5.71	23.73	
Vertical (D)	Lower Cement Bed	480		1151	945	261	0.18	04.88	3.92	22.64	
Vertical (D)	Lower Cement Bed	480		1250	1811	425	-0.22	09.64	6.39	24.26	
					Mean horizontal		-0.27	13.62	6.49	17.92	
					Mean vertical		0.06	07.93	5.28	20.76	

Table 1.16 (2 of 2). Realignment formulae for comparison with radio-elemental concentration data collected with the GR-256 gamma-ray spectrometer are given in Chapter 2 (Section 2.05).

Specifications Of Transportable Calibration Pads

Dimensions 1 m x 1 m x 0.3 m

Weight	B-Pad	(B3-88) 680 Kg
	K-Pad	(K3-88) 670 Kg
	U-Pad	(U8-89) 670 Kg
	T-Pad	(T3-88) 680 Kg

Density	B-Pad	2.28 g/cm ³
	K-Pad	2.23 g/cm ³
	U-Pad	2.24 g/cm ³
	T-Pad	2.28 g/cm ³

Composition	B-Pad	Standard concrete with 3/8 inch limestone aggregate
	K-Pad	Feldspar crushed to 3/4 inch with cement in the ratio 4 feldspar to 1 cement
	U-Pad	Concrete with 3/8 inch limestone aggregate + phosphate slag crushed to 1/4 inch
	T-Pad	Concrete with 3/8 inch limestone aggregate + thorium ore crushed

Percentage of infinite source

K-Pad	86.5 % for 1.46 MeV potassium gamma-rays
U-Pad	85.8 % for 1.76 MeV uranium gamma-rays
T-Pad	84.2 % for 2.62 MeV thorium gamma-rays

Concentration of Transportable Pads

	K (%)	U (ppm)	Th (ppm)
B-Pad	1.43 +/- 0.01	0.94 +/- 0.02	2.32 +/- 0.06
K-Pad	7.57 +/- 0.05	1.22 +/- 0.09	1.40 +/- 0.12
U-Pad	1.07 +/- 0.01	46.93 +/- 0.32	2.75 +/- 0.07
T-Pad	1.43 +/- 0.02	1.74 +/- 0.16	121.6 +/- 1.66

(errors are at the one sigma level)

Table 1.17 Specifications of the calibration pads used at the British Geological Survey, Keyworth to determine stripping ratios and sensitivity constants for portable gamma-ray spectrometers.

Program PADWIN

The calibration program called PADWIN was originally written by Leif Lovborg and his associates at the Riso National Laboratory in Denmark. The program has been modified by the British Geological Survey to allow for the non-infinite size of the transportable pads. Calibration constants and associated errors are calculated. These errors take into consideration Poisson counting errors as well as uncertainties in the concentration of the pads.

The program is in executable form for an IBM-PC or AT compatible computer and will run with or without a math coprocessor. The program assumes that the gamma-ray spectrometer has a typical 7.6 cm x 7.6 cm sodium iodide scintillation crystal within the detector assembly.

The following data are input into the program for any new calibration being processed :

- 1) number of pads
- 2) counting time in minutes on the Blank Pad
- 3) accumulated counts in the K-window on the Blank Pad
- 4) accumulated counts in the U-window on the Blank Pad
- 5) accumulated counts in the Th-window on the Blank Pad

The sequence is repeated for counting time and window counts for the potassium, uranium and thorium pads. The count time needs to be the same for each pad but can be a summation of separate count times. The program automatically determines, from the known radioelemental concentrations of the four pads, the errors in concentration and the geometric correction factors.

PADWIN first calculates the potassium, uranium and thorium window sensitivities for small pad-size sources from the total count and pad-concentration data. The geometric correction factors are then applied to these small source sensitivities to give infinite source sensitivities.

Table 1.18 Details of the BGS gamma spectrometer software program known as PADWIN (v1.1). The program is used determine stripping ratios and sensitivity constants for portable gamma-ray spectrometers from raw data obtained on transportable calibration pads.

(A) Calibration of GR-256 S/No. 1560 owned by B.P.

<u>11th January 1991</u>	<u>Test 1</u>	<u>Test 2</u>	<u>Channels</u>
Total counts	2829	2822	70 - 255
K counts	410	443	110 - 124
U counts	158	164	131 - 149
Th counts	63	66	194 - 216

<u>25th March 1992</u>	<u>Test 1</u>	<u>Test 2</u>	<u>Channels</u>
Total counts	2947	2927	70 - 255
K counts	461	469	111 - 125
U counts	249	255	133 - 151
Th counts	87	77	197 - 219

<u>13th May 1992</u>	<u>Test 1</u>	<u>Test 2</u>	<u>Channels</u>
Total counts 2826	2927	2846	70 - 255
K counts	426	407	110 - 124
U counts	269	183	113 - 149
Th counts	99	51	194 - 216

<u>19th October 1992</u>	<u>Test 1</u>	<u>Test 2</u>	<u>Channels</u>
Total counts	2744	2709	70 - 255
K counts	431	423	110 - 124
U counts	143	157	113 - 149
Th counts	84	86	194 - 216

(B) Calibration of GR-256 S/No. 1521 owned by Leeds University

<u>16th August 1995</u>	<u>Test 1</u>	<u>Test 2</u>	<u>Channels</u>
Total counts	2951	3083	70 - 255
K counts	447	453	110 - 124
U counts	172	205	113 - 149
Th counts	45	51	194 - 216

<u>31st August 1995</u>	<u>Test 1</u>	<u>Test 2</u>	<u>Channels</u>
Total counts	2885	2991	70 - 255
K counts	428	424	116 - 130
U counts	169	169	140 - 189
Th counts	71	74	210 - 232

Table 1.19 Calibration data for the GR-256 gamma-ray spectrometer owned by Leeds University using identical count rates and constants to those previously used by the B.P. machine. The Leeds University machine was subject to spectral drift which often brought the machine out of tolerance (as shown by the channels on the 31st August 1995). No measurements could be taken with the machine when this occurred and the spectrometer had to be sent away in order for the problem to be rectified.

Data supplied by David Skinner & Partners Ltd.

CALIBRATION OF TRANSPORTABLE PADS
(Data Processed and Obtained from PADWIN Program)

WINDOW COUNTS

	<u>Time (minutes)</u>	<u>K counts</u>	<u>U counts</u>	<u>Th counts</u>
B Pad	10.0	4808	691	551
K Pad	10.0	15622	942	517
U Pad	10.0	6213	8603	701
T Pad	10.0	6903	5916	8888

A-MATRIX FROM NONLINEAR REGRESSION

176.0	(2.7570)	13.33	(0.3257)	3.377	(0.11470)
3.943	(0.7142)	17.19	(0.3000)	4.265	(0.04265)
0.4812	(0.5545)	0.2646	(0.3023)	6.988	(0.12690)

INVERSE A-MATRIX

0.005782	(2.7570)	-0.004480	(0.0001142)	-0.00005969	(-0.0001019)
-0.001239	(-0.0002646)	0.05967	(0.0008612)	-0.3582	(0.0008875)
-0.0003512	(0.0004591)	-0.001951	(0.002569)	-0.1445	(0.003043)

WINDOW SENSITIVITIES FOR SMALL SOURCES

K Sensitivity	=	217.00	(2.757) counts per minute per % K
U Sensitivity	=	19.74	(0.3007) counts per minute per ppm U
Th Sensitivity	=	8.32	(0.1269) counts per minute per ppm Th

WINDOW SENSITIVITIES FOR INFINITE SOURCES

K Sensitivity	=	265.20	(3.213) counts per minute per % K
U Sensitivity	=	22.60	(0.3518) counts per minute per ppm U
Th Sensitivity	=	9.21	(0.1510) counts per minute per ppm Th

Table 1.20 Calculated window sensitivities and stripping ratios for the Edinburgh University GR-256 gamma-ray spectrometer using the PADWIN (BGS gamma spectrometer software v1.1) program and CAL-256 program. Individual counts times have been summed into a single measurement taken over a 10 minute interval. This is the input into the program. The data were collected on the 10th October 1995. (1 of 2.)

STRIPPING RATIOS

Th into U (alpha)	=	0.6104	(0.0125)
Th into K (beta)	=	0.4833	(0.0160)
U into K (gamma)	=	0.7751	(0.0188)
U into Th (A)	=	0.0154	(0.0174)
K into Th (B)	=	0.0027	(0.0031)
K into U (C)	=	0.0224	(0.0041)

(numbers in parentheses are estimated standard deviations).

Table 1.20 (2 of 2). The forward stripping ratios (alpha, beta, gamma) should be less than 1 whilst the backward stripping ratios (A, B, C) should be near to 0.

	<u>Time seconds</u>	<u>Total counts</u>	<u>5.68 CPS/ur</u>	<u>4.14 CPS/ur</u>	<u>4.73 CPS/ur</u>	<u>Range in ur</u>
Iron Ledge	300	36420	21.37	29.322	5.67	3.66
Iron Ledge	300	37650	22.10	30.31	26.53	3.78
Iron Ledge	300	38030	22.32	30.62	26.80	3.82
Iron Ledge	300	38360	22.51	30.89	27.24	3.88
Iron Ledge	300	38410	22.54	30.93	27.07	3.86
Iron Ledge	300	37880	22.23	30.50	26.69	3.80
Iron Ledge	300	38410	22.54	30.93	27.07	3.86
Iron Ledge	300	37840	22.21	30.47	26.67	3.80
Iron Ledge	300	37510	22.01	30.20	26.43	3.77
Iron Ledge	300	38340	22.50	30.87	27.02	3.85
Iron Ledge	300	39320	23.08	31.66	27.71	3.95
Iron Ledge	300	39540	23.20	31.84	27.86	3.97
Iron Ledge	300	40100	23.53	32.29	28.26	4.03
Iron Ledge	300	40380	23.70	32.51	28.46	4.06
Iron Ledge	300	40670	23.87	32.75	28.66	4.08
Iron Ledge	300	40810	23.95	32.86	28.76	4.10
Iron Ledge	300	41090	24.11	33.08	28.96	4.13
Iron Ledge	300	39910	23.42	32.13	28.13	4.01
Iron Ledge	300	39290	23.06	31.63	27.69	3.95
Lower Cement Bed	480	35940	21.09	18.09	15.83	2.26
Lower Cement Bed	480	37560	22.04	18.90	16.54	2.36
Lower Cement Bed	480	38020	22.31	19.13	16.75	2.39
Lower Cement Bed	480	37990	22.29	19.12	16.73	2.38
Lower Cement Bed	480	37650	22.10	18.95	16.58	2.36
Lower Cement Bed	480	37390	21.94	18.82	16.47	2.35
Lower Cement Bed	480	36540	21.44	18.39	16.09	2.29
Lower Cement Bed	480	37170	21.81	18.70	16.37	2.33
Lower Cement Bed	480	37250	21.86	18.74	16.41	2.34
Lower Cement Bed	480	37780	22.17	19.01	16.64	2.37
Lower Cement Bed	480	37810	22.19	19.03	16.65	2.37
Lower Cement Bed	480	39540	23.20	19.90	17.42	2.48
Lower Cement Bed	480	44480	26.10	22.38	19.59	2.79
Lower Cement Bed	480	44240	25.96	22.26	19.49	2.78
Lower Cement Bed	480	43330	25.43	21.80	19.08	2.72
Lower Cement Bed	480	44320	26.01	22.30	19.52	2.78
Lower Cement Bed	480	44250	25.97	22.27	19.49	2.78
Lower Cement Bed	480	47410	27.82	23.86	20.88	2.98
Lower Cement Bed	480	46830	27.48	23.57	20.63	2.94
Lower Cement Bed	480	48310	28.35	24.31	21.28	3.03
Belemnite Bed	240	43990	25.82	44.27	38.75	5.52
Belemnite Bed	240	43170	25.33	43.45	38.03	5.42
Belemnite Bed	240	43670	25.63	43.95	38.47	5.48
Belemnite Bed	240	43650	2.56	4.39	3.85	0.55
Belemnite Bed	240	44270	25.98	44.56	39.00	5.56
Belemnite Bed	240	44320	26.01	44.61	39.04	5.56
Belemnite Bed	240	44210	25.94	44.49	38.94	5.55
Belemnite Bed	240	44450	26.09	44.74	39.16	5.58
Belemnite Bed	240	45420	26.65	45.71	40.01	5.70
Belemnite Bed	240	45670	26.80	45.96	40.23	5.73
Belemnite Bed	240	45990	26.99	46.29	40.51	5.77
Belemnite Bed	240	46000	27.00	46.30	40.52	5.77
Belemnite Bed	240	46400	27.23	46.70	40.87	5.83
Belemnite Bed	240	46510	27.29	46.81	40.97	5.84
Belemnite Bed	240	46640	27.37	46.94	41.09	5.86
Belemnite Bed	240	46350	27.20	46.65	40.83	5.82
Belemnite Bed	240	47070	27.62	47.37	41.46	5.91
Belemnite Bed	240	47280	27.75	47.58	41.65	5.94
Belemnite Bed	240	47300	27.76	47.60	41.67	5.94

Table 1.21 Calibration of total gamma-ray flux to ur using each of the total gamma ray sensitivity constants determined from the BGS transportable calibration pads. Range in total gamma-ray flux (ur units) between each of the constants is given.

The Mann-Whitney Statistical Test (Procedure for Calculation)

Step 1

Rank the data (taking both data-sets together) giving rank 1 to the lowest score and so on. If there are tied observations the mean rank is given to each of the tied observations.

Step 2

Find the sum of the ranks for the smaller sample or if both samples are the same size find the sum of the ranks of sample A. Call this value T.

Step 3

Find U where :

$$U = N_A N_B + (N_A(N_A+1) / 2) - T$$

where N_A is the number of scores in the smaller sample or if both samples are the same size the sample for which ranks were totalled to find T.

Step 4

Find the standard deviation of U where :

$$SD_U = [N_A N_B (N_A + N_B + 1) / 12]^{0.5}$$

Step 5

Find the Z-score :

$$Z = [(U - (N_A N_B / 2)) / SD_U]$$

For a two-tailed non-directional test, the alternative hypothesis (*i.e.* there is a difference) is significant at the 95 % level if the observed Z if it exceeds 1.96. For a one-tailed directional test 95 % significance is attained if Z exceeds 1.64

Reference

Mann, H.B. & Whitney, D.R. 1947 On a test of whether one or two random variables is stochastically larger than the other, *Annals of Mathematical Statistics* , 18, 52-54.

TABLE 1.22 Mathematical Execution of the Mann-Whitney Statistical Test.

Sample time Secs	Total Number of Counts Recorded			Total µr	Elemental Concentrations			Standard Deviations				
	Total	K	U		Th	K %	U ppm	Th ppm	µr	K	U	Th
5	206	37	10	5	11.6	1.6	3.6	7.1	1.70	0.07	0.07	2.12
10	482	81	31	10	14	1.5	6.6	7.0	1.39	0.26	1.18	1.50
15	620	94	36	11	11.6	1.1	5.2	5	1.16	0.22	0.97	1.24
20	846	140	53	19	11.9	1.3	5.5	6.6	1.03	0.22	1.30	1.08
25	1048	198	57	16	11.8	1.6	4.9	4.2	0.95	0.23	1.30	1.04
30	1342	244	67	31	12.8	1.7	4.2	7.4	0.92	0.21	1.24	0.96
35	1598	270	85	35	13.1	1.5	4.7	7.1	0.85	0.21	1.15	1.04
40	1735	284	120	38	12.3	1.2	6.5	6.6	0.80	0.20	1.43	1.06
45	1928	313	102	57	12.1	1.4	3.9	9.2	0.76	0.20	1.52	1.00
50	2209	395	131	62	12.6	1.6	4.9	8.9	0.72	0.19	1.50	0.96
55	2408	375	139	44	12.5	1.3	5.4	5.5	0.69	0.18	1.45	0.92
60	2648	444	144	63	12.6	1.5	4.6	7.5	0.67	0.18	1.43	0.88
65	2802	506	154	53	12.2	1.6	4.9	5.5	0.64	0.17	1.50	0.85
70	3038	541	178	88	12.3	1.5	4.6	9.0	0.62	0.17	1.45	0.82
75	3295	579	186	72	12.5	1.5	5.0	6.7	0.60	0.16	1.40	0.80
80	3543	610	191	75	12.7	1.5	4.8	6.6	0.58	0.16	1.36	0.77
85	3763	683	214	87	12.6	1.6	5.0	7.2	0.57	0.16	1.32	0.75
90	3841	708	232	86	12.5	1.6	5.2	6.7	0.55	0.16	1.34	0.73
95	4205	754	229	73	12.6	1.6	5.1	5.2	0.55	0.16	1.31	0.73
100	4508	766	281	106	12.9	1.4	5.7	7.4	0.55	0.15	1.28	0.73
105	4759	757	290	102	13	1.3	5.7	6.8	0.53	0.16	1.25	0.71
110	4836	858	287	99	12.5	1.5	5.4	6.3				

Table 1.23 Data-set representing 48 samples taken at a single point on the Belemnite Bed (Belemnite Marls Formation) that outcrops west of Seatown, Dorset (SY 318908). The data were collected with the B.P. GR-256 gamma-ray spectrometer placed perpendicular to bedding with 5 second increments in measurement time up to a maximum of 240 seconds. The data were collected on October 23rd 1993. (1 of 2.)

<u>Sample time</u> <u>Secs</u>	<u>Total Number of Counts Recorded</u>			<u>Total</u> <u>µr</u>	<u>Elemental Concentrations</u>			<u>Standard Deviations</u>				
	<u>Total</u>	<u>K</u>	<u>U</u>		<u>Th</u>	<u>K%</u>	<u>U ppm</u>	<u>Th ppm</u>	<u>µr</u>	<u>K</u>	<u>U</u>	<u>Th</u>
115	5099	903	297	117	12.7	1.6	5.1	7.2	0.52	0.15	1.23	0.70
120	5264	946	278	125	12.5	1.6	4.4	7.4	0.51	0.15	1.21	0.69
125	5480	886	334	123	12.5	1.3	5.5	6.9	0.50	0.15	1.18	0.69
130	5594	985	352	128	12.2	1.6	5.6	6.9	0.49	0.15	1.16	0.68
135	6011	1063	327	119	12.7	1.6	5.0	6.0	0.49	0.15	1.15	0.67
140	6133	1105	355	134	12.5	1.6	5.2	6.7	0.48	0.15	1.12	0.66
145	6487	1192	397	134	12.8	1.6	5.8	6.4	0.47	0.15	1.11	0.66
150	6615	1177	359	128	12.6	1.6	4.9	5.9	0.46	0.14	1.10	0.65
155	6912	1210	398	153	12.8	1.5	5.2	6.9	0.47	0.14	1.08	0.64
160	6957	1174	402	178	12.4	1.4	4.8	7.9	0.45	0.14	1.08	0.63
165	7289	1199	412	146	12.6	1.4	5.1	6.1	0.45	0.14	1.07	0.62
170	7429	1254	472	178	12.4	1.4	5.7	7.3	0.44	0.14	1.06	0.62
175	7752	1375	481	171	12.7	1.5	5.7	6.8	0.43	0.14	1.04	0.62
180	8007	1326	455	176	12.7	1.4	5.1	6.8	0.43	0.14	1.03	0.61
185	8282	1365	484	191	12.8	1.4	5.2	7.2	0.40	0.13	1.02	0.60
190	8445	1442	473	172	12.7	1.5	5.1	6.3	0.40	0.13	1.01	0.59
195	8729	1575	478	187	12.8	1.6	4.9	6.7	0.39	0.13	0.99	0.58
200	8841	1525	496	197	12.6	1.5	4.9	6.9	0.39	0.13	0.98	0.58
205	8889	1561	532	187	12.3	1.5	5.4	6.3	0.38	0.13	0.97	0.57
210	9236	1605	550	222	12.5	1.5	5.2	6.8	0.38	0.13	0.96	0.57
215	9513	1646	598	204	12.6	1.4	5.8	6.5	0.38	0.13	0.95	0.57
220	9914	1702	537	213	12.9	1.6	4.8	6.8	0.37	0.13	0.94	0.56
225	10093	1779	592	207	12.9	1.6	5.4	6.4	0.37	0.13	0.93	0.56
230	10319	1826	561	209	12.9	1.6	5.0	6.3	0.37	0.13	0.92	0.55
235	10380	1766	608	220	12.6	1.4	5.2	6.8	0.37	0.12	0.91	0.55
240	10764	1917	639	225	12.9	1.6	5.5	6.5	0.37	0.12	0.9	0.54

Table 1.23 (2 of 2).

Sample time Secs	Total Number of Counts Recorded			Total µr	Elemental Concentrations			Standard Deviations			
	Total	K	U		Th	K %	U ppm	Th ppm	µr	K	U
5	170	31	12	2	1.1	5.7	2.3	0.57	0.35	0.14	0.57
10	319	47	25	5	0.6	5.9	3.1	0.61	0.25	0.42	0.80
20	702	96	42	6	0.8	5.1	1.5	0.63	0.21	1.04	1.87
30	943	140	57	25	0.8	3.6	5.8	0.60	0.19	1.17	1.76
40	1255	209	60	12	1.0	3.4	1.6	0.54	0.18	1.06	1.59
50	1659	254	112	27	0.8	5.1	3.4	0.50	0.16	0.97	1.48
60	1950	301	123	34	0.9	4.5	3.7	0.46	0.15	0.92	1.38
70	2287	365	158	32	0.9	5.3	2.7	0.43	0.15	0.90	1.34
80	2582	429	154	50	1.0	4.0	4.1	0.42	0.14	0.88	1.28
90	2856	445	161	37	0.9	4.0	2.4	0.40	0.13	0.84	1.22
100	3271	482	200	46	0.8	4.6	2.8	0.39	0.13	0.82	1.20
110	3678	575	214	67	0.9	4.1	4.0	0.38	0.12	0.78	1.15
120	4019	643	246	56	0.9	4.7	2.9	0.37	0.12	0.75	1.10
130	4327	678	272	71	0.9	4.6	3.4	0.36	0.11	0.72	1.07
140	4609	729	285	74	0.9	4.5	3.3	0.34	0.11	0.71	1.03
150	4950	762	338	75	0.8	5.2	3.1	0.33	0.11	0.70	1.00
160	5323	830	355	87	0.9	5.0	3.4	0.34	0.11	0.68	0.98
170	5786	820	364	98	0.8	4.7	3.7	0.33	0.10	0.66	0.96
180	5928	912	371	79	0.9	4.7	2.6	0.33	0.11	0.64	0.93
190	8411	1044	383	92	1.0	4.5	3.0	0.32	0.10	0.63	0.92
200	6513	1049	414	117	0.9	4.5	3.8	0.32	0.10	0.63	0.92
210	7057	1061	461	115	0.8	4.9	3.4	0.32	0.10	0.61	0.90

Table 1.24 Data-set representing 33 samples taken at a single point on Iron Ledge (Blue Lias Formation) that outcrops at Seven Rock Point, Lyme Regis, Dorset (SY 335916). The data were collected with the B.P. GR-256 gamma-ray spectrometer with the detector placed perpendicular to bedding using 10 second increments in measurement time up to a maximum of 360 seconds. The data were collected on October 23rd 1993. (1 of 2.)

<u>Sample time</u> <u>Secs</u>	<u>Total Number of Counts Recorded</u>				<u>Total</u> <u>ur</u>	<u>Elemental Concentrations</u>				<u>Standard Deviations</u>			
	<u>Total</u>	<u>K</u>	<u>U</u>	<u>Th</u>		<u>K %</u>	<u>U ppm</u>	<u>Th ppm</u>	<u>ur</u>	<u>K</u>	<u>U</u>	<u>Th</u>	
220	7296	1154	495	105	8.7	0.9	5.2	2.8	0.31	0.10	0.61	0.88	
230	7495	1227	433	101	8.5	1.0	4.2	2.6	0.31	0.10	0.60	0.87	
240	8042	1253	501	101	8.8	0.9	4.8	2.5	0.30	0.10	0.59	0.86	
250	8339	1367	510	114	8.8	1.0	4.6	2.8	0.30	0.10	0.58	0.85	
260	8590	1362	516	132	8.7	0.9	4.4	3.2	0.29	0.10	0.57	0.83	
270	8904	1379	509	131	8.6	0.9	4.2	3.0	0.29	0.10	0.57	0.82	
280	9373	1496	583	140	8.8	0.9	4.7	3.1	0.28	0.09	0.56	0.80	
290	9726	1566	620	152	8.8	0.9	4.8	3.3	0.28	0.09	0.55	0.79	
300	9879	1550	613	170	8.6	0.9	4.5	3.7	0.28	0.09	0.54	0.78	
310	10312	1649	630	145	8.7	0.9	4.6	2.9	0.27	0.09	0.53	0.77	
320	10693	1663	681	177	8.8	0.9	4.7	3.5	0.27	0.09	0.52	0.76	

Table 1.24 (2 of 2).

Plane	Horizon	Sample Time Secs	Total Number of Counts Recorded			Calculated Elemental Concentrations				
			Total	K	U	Th	K %	U ppm	Th ppm	Total ur
Vertical Plane	Belemnite Stone	240	9513	1646	598	204	1.40	5.80	6.50	12.60
Vertical Plane	Belemnite Stone	240	9467	1589	554	183	1.40	5.40	5.90	12.60
Vertical Plane	Belemnite Stone	240	9360	1670	520	193	1.60	4.90	6.10	12.40
Vertical Plane	Belemnite Stone	240	9577	1743	545	224	1.60	5.00	7.30	12.70
Vertical Plane	Belemnite Stone	240	9485	1702	557	219	1.60	5.20	7.20	12.60
Vertical Plane	Belemnite Stone	240	9505	1634	513	201	1.50	4.80	6.60	12.60
Vertical Plane	Belemnite Stone	240	9556	1631	559	194	1.50	5.40	6.20	12.70
Vertical Plane	Belemnite Stone	240	9417	1681	528	184	1.60	5.10	5.90	12.50
Vertical Plane	Belemnite Stone	240	9591	1701	530	192	1.60	5.00	6.10	12.80
Vertical Plane	Belemnite Stone	240	9378	1659	537	207	1.50	5.00	6.70	12.40
Vertical Plane	Belemnite Stone	240	9403	1657	556	199	1.50	5.30	6.40	12.50
Vertical Plane	Belemnite Stone	240	9512	1602	549	204	1.40	5.20	6.50	12.60
Vertical Plane	Belemnite Stone	240	9539	1693	529	239	1.60	4.70	7.90	12.70
Vertical Plane	Belemnite Stone	240	9379	1634	522	201	1.50	4.90	6.50	12.40
Vertical Plane	Belemnite Stone	240	9455	1633	541	169	1.50	5.30	5.30	12.50
Vertical Plane	Belemnite Stone	240	9570	1657	512	209	1.60	4.70	6.80	12.70
Vertical Plane	Belemnite Stone	240	9669	1674	547	218	1.50	5.10	7.10	12.90
Vertical Plane	Belemnite Stone	240	9527	1633	547	205	1.50	5.20	6.70	12.70
Vertical Plane	Belemnite Stone	240	9558	1729	541	213	1.60	5.00	6.90	12.70
Vertical Plane	Belemnite Stone	240	9344	1674	558	197	1.50	5.40	6.30	12.40
						Mean	1.53	5.12	6.55	12.60

Table 1.25 Data-set representing 20 repeated samples taken for the same point (*i.e.* constant counting geometry) on the dark laminated-shale horizon known as the Belemnite Bed (Belemnite Marls Formation) that outcrops west of Seatown, Dorset (SY 318908). The data were collected with the B.P. GR-256 gamma-ray spectrometer with the detector placed perpendicular to bedding (*i.e.* in the vertical plane) The data were collected on October 25th 1993.

<u>Plane Taken</u>	<u>Horizon</u>	<u>Sample time</u>		<u>Total Number of Counts Recorded</u>			<u>Elemental Concentrations</u>			
		<u>Secs</u>	<u>Total</u>	<u>K</u>	<u>U</u>	<u>Th</u>	<u>K %</u>	<u>U ppm</u>	<u>Th ppm</u>	<u>Total ur</u>
Vertical Plane	Iron Ledge	280	9248	1440	590	145	0.90	4.70	3.30	8.60
Vertical Plane	Iron Ledge	280	9492	1467	598	136	0.90	4.90	3.00	9.00
Vertical Plane	Iron Ledge	280	9415	1515	614	147	0.90	5.00	3.30	8.90
Vertical Plane	Iron Ledge	280	9391	1523	578	151	1.00	4.60	3.40	8.80
Vertical Plane	Iron Ledge	280	9494	1489	584	158	0.90	3.40	3.50	9.00
Vertical Plane	Iron Ledge	280	9370	1436	613	142	0.80	5.00	3.10	8.80
Vertical Plane	Iron Ledge	280	9498	1523	591	159	1.00	4.60	3.70	9.00
Vertical Plane	Iron Ledge	280	9418	1457	605	149	0.90	4.90	3.30	8.90
Vertical Plane	Iron Ledge	280	9330	1472	610	157	0.90	4.90	3.50	8.80
Vertical Plane	Iron Ledge	280	9417	1483	582	147	0.90	4.60	3.30	8.90
Vertical Plane	Iron Ledge	280	9307	1492	589	138	0.90	4.80	3.00	8.70
Vertical Plane	Iron Ledge	280	9336	1418	570	146	0.90	4.50	3.30	8.90
Vertical Plane	Iron Ledge	280	9282	1467	587	140	0.90	4.70	3.10	8.70
Vertical Plane	Iron Ledge	280	9282	1436	600	134	0.90	4.90	2.90	8.70
Vertical Plane	Iron Ledge	280	9455	1523	594	116	1.00	5.00	2.30	8.90
Vertical Plane	Iron Ledge	280	9438	1472	602	128	0.90	5.00	2.70	8.90
Vertical Plane	Iron Ledge	280	9556	1525	599	128	1.00	4.90	2.70	9.00
Vertical Plane	Iron Ledge	280	9403	1462	616	163	0.90	4.90	3.70	8.80
Vertical Plane	Iron Ledge	280	9352	1423	614	130	0.80	5.10	2.70	8.80
Vertical Plane	Iron Ledge	280	9298	1467	541	144	1.00	4.20	3.30	8.70
						Mean	0.92	4.73	3.16	8.84

Table 1.26 Data-set representing 20 repeated samples taken at the same point (*i.e.* constant counting geometry) on the Iron Ledge limestone (Blue Lias Formation) that outcrops at Seven Rock Point, Lyme Regis, Dorset (SY 335916). The data were collected with the B.P. GR-256 gamma-ray spectrometer on October 26th 1993 with the detector placed perpendicular to bedding in the vertical plane.

<u>Total (ur)</u>	<u>K %</u>	<u>U ppm</u>	<u>Th ppm</u>
<u>(A) Multiple readings at the same location</u>			
0.00	-8.50	+13.28	-0.76
0.00	-8.50	+5.47	-9.92
-1.59	+4.58	-4.30	-6.87
+0.79	+4.58	-2.34	+11.45
0.00	+4.58	+1.56	+9.92
0.00	-1.96	-6.25	+0.76
+0.79	-1.96	+5.47	-5.34
-0.79	+4.58	-0.39	-9.92
+1.59	+4.58	-2.34	-6.87
-1.59	-1.96	-2.34	+2.29
-0.79	-1.96	+3.52	-2.29
0.00	-8.50	+1.56	-0.76
+0.79	+4.58	-8.20	+20.61
-1.59	-1.96	-4.30	-0.76
-0.79	-1.96	+3.52	-19.08
+0.79	+4.58	-8.20	+3.82
+2.38	-1.96	-0.39	+8.40
+0.79	-1.96	+1.56	+2.29
+0.79	+4.58	-2.34	+5.34
-1.59	-1.96	+5.47	-3.82

(B) Readings taken at different locations

-0.56	0.00	+2.51	-16.30
+0.24	0.00	+16.05	-4.55
+1.03	0.00	+0.58	-4.55
+0.24	0.00	+4.45	-4.55
-3.74	-6.67	+6.38	-8.96
+1.03	0.00	+2.51	-0.15
+3.42	+6.67	-5.22	+10.13
+2.63	+6.67	-11.03	+16.01
-5.33	-6.67	-3.29	+7.20
-0.56	0.00	-5.22	-10.43
+0.24	0.00	+0.58	+8.66
-0.56	0.00	-1.35	-0.15
+2.63	+6.67	+4.45	+8.66
-2.94	-6.67	-7.16	-14.83
-2.94	-6.67	-7.16	+4.26
-1.35	-6.67	+2.51	-10.43
+0.24	+6.67	-12.96	-6.02
-0.56	0.00	+2.51	+8.66
+4.22	0.00	+16.05	-1.62
+1.83	+6.67	-7.16	+17.47

Table 1.27 The percentage error calculated for total gamma-ray flux and radio-elemental concentration for measurements collected at the same location and different locations on the Belemnite Bed. The Belemnite Bed outcrops west of Seatown, Dorset (SY 318908). The percentage error is calculated from the data given in Tables 1.12 and 1.25.

<u>Total (ur)</u>	<u>K %</u>	<u>U ppm</u>	<u>Th ppm</u>
<u>(A) Multiple readings at the same location</u>			
-2.71	-2.2	-0.63	+4.43
+1.81	-2.2	+3.59	-5.06
+0.68	-2.2	+5.71	+4.43
-0.45	+8.7	-2.75	+7.59
+1.81	-2.2	-28.12	+10.76
-0.45	-13.0	+5.71	-1.90
+1.81	+8.7	-2.75	+17.09
+0.68	-2.2	+3.59	+4.43
-0.45	-2.2	+3.59	+10.76
+0.68	-2.2	-2.75	+4.43
-1.58	-2.2	+1.48	-5.06
+0.68	-2.2	-4.86	+4.43
-1.58	-2.2	-0.63	-1.90
-1.58	-2.2	+3.59	-8.23
+0.68	+8.7	+5.71	-27.22
+0.68	-2.2	+5.71	-14.56
+1.81	+8.7	+3.59	-14.56
-0.45	-2.2	+3.59	+17.09
-0.45	-13.0	+7.82	-14.56
-1.58	+8.7	-11.21	+4.43
<u>(B) Readings taken at different locations</u>			
-7.39	-2.17	-9.64	-3.78
-6.28	-13.04	-1.61	-0.34
-7.39	-13.04	-3.61	+6.53
-5.18	-13.04	-3.61	+6.53
-16.21	-13.04	-17.67	-27.84
-9.59	-2.17	-17.67	-31.27
-9.59	-2.17	-5.62	-27.84
-0.77	-2.17	+4.42	-10.65
-4.08	-13.04	+4.42	-7.22
-1.87	-13.04	-5.62	+3.09
-10.69	-13.04	-9.64	-3.78
-8.49	+2.17	-7.63	-0.34
-9.59	-13.04	-3.61	-14.09
-9.59	-2.17	-15.66	-3.78
+33.41	-13.04	+72.69	-0.34
+11.36	+19.57	+8.43	+13.40
+4.74	+8.70	+4.42	+6.53
+24.59	+41.30	+0.40	+47.77
+10.25	+19.57	-1.61	+23.71
+22.38	+41.30	+8.43	+23.71

Table 1.28 The percentage error calculated for total gamma-ray flux and radio-elemental concentration for measurements collected at the same location and different locations on the Iron Ledge. The Iron Ledge limestone outcrops at Seven Rock Point, Lyme Regis, Dorset (SY 335916). The percentage error is calculated from the data given in Tables 1.11 and 1.26.

Lithostratigraphy	Height m	Time Secs	Total Number of Counts			Th	Ur	Elemental Concentration		
			Total	K	U			K %	U ppm	Th ppm
First Set of Measurements (first reading taken at 9 a.m.)										
Cotham Beds	0.0	120	9720	2255	348	157	25.2	4.4	4.9	10.3
Cotham Beds	0.3	120	10067	2236	347	153	26.3	4.4	4.9	10.1
Cotham Beds	0.6	120	10101	2312	350	168	26.4	4.6	5.0	11.2
Cotham Beds	0.9	120	10052	2327	315	156	26.2	4.7	4.2	10.5
Cotham Beds	1.2	120	10239	2271	337	177	26.8	4.5	4.4	12.2
Cotham Beds	1.5	240	15462	3334	518	256	14.3	3.2	3.4	8.1
Cotham Beds	1.8	240	15848	3532	524	222	19.9	3.4	3.6	6.7
Cotham Beds	2.1	120	10929	2441	365	160	28.8	4.9	5.2	10.5
Cotham Beds	2.4	120	10513	2425	349	169	27.6	4.9	4.7	11.5
Cotham Beds	2.7	120	11950	2830	415	232	31.9	5.7	5.4	16.9
Cotham Beds	3.0	120	11646	2648	408	213	31.3	5.3	6.4	15.0
Cotham Beds	3.3	120	11776	2757	424	177	31.3	5.5	6.2	12.0
Cotham Beds	3.6	120	10907	2478	409	177	28.8	4.9	5.9	12.0
Cotham Beds	3.9	120	9761	2295	417	144	26.0	4.4	6.4	8.9
White Lias	4.2	240	13872	2814	568	248	17.0	3.1	4.0	7.7
White Lias	4.5	240	13344	2728	568	251	16.2	2.4	4.0	7.7
White Lias	4.8	240	13079	2814	520	280	15.9	2.6	3.3	9.1
White Lias	5.1	240	12834	2734	512	198	15.4	2.5	3.8	5.5
White Lias	5.4	240	11940	2496	524	195	14.1	2.2	3.8	5.3
White Lias	5.7	240	17222	3832	638	290	22.0	3.8	4.4	7.7
White Lias	6.0	120	9106	2984	294	148	21.9	3.7	3.9	9.8
White Lias	6.3	240	16972	5308	620	280	21.6	4	4.3	9.1
White Lias	6.6	240	16724	3900	616	285	21.6	4	4.2	9.3

Table 1.29 Collection of data from identical positions within the Rhaetian succession exposed in St. Mary's Well Bay, Glamorgan (ST 18060) that includes the Cotham Beds (Lilstock Member), the White Lias (Langport Member) and the Pre-planorbis Beds (Bull Cliff Member). The first and second set of gamma-ray measurements were collected exactly five hours apart on the 16th September 1995 using the Edinburgh University GR-256. (1 of 4.)

Lithostratigraphy	Height m	Time Secs	Total Number of Counts			Th	Ur	Elemental Concentration		
			Total	K	U			K%	U ppm	Th ppm
White Lias	6.9	240	14572	3396	500	216	18.0	3.3	2.8	6.4
White Lias	7.2	240	13600	3052	558	211	16.6	2.8	4.0	6.2
White Lias	7.5	240	13852	3342	502	264	17.1	3.2	3.2	8.4
White Lias	7.8	240	12680	2904	552	214	15.2	2	4.0	6.2
White Lias	8.1	240	14694	3392	590	259	18.2	3.2	4.0	7.1
Pre-planorbis	8.4	240	12382	1465	520	293	14.2	2.5	3.4	6.6
Pre-planorbis	8.7	360	10677	1170	465	182	6.7	1.2	2.2	2.3
Pre-planorbis	9.0	360	15658	1303	453	301	7.6	1.4	4.4	4.1
Pre-planorbis	9.3	360	12341	1357	492	281	8.3	1.4	2.0	3.9
Pre-planorbis	9.6	360	13896	1679	630	372	9.7	1.7	2.7	5.4
Pre-planorbis	9.9	240	12189	1340	549	238	8.2	1.4	2.5	3.5
Pre-planorbis	10.2	240	9594	1160	464	230	10.3	1.8	3.6	4.9
Pre-planorbis	10.5	240	9950	1208	468	232	10.7	1.9	3.7	5.0
Pre-planorbis	10.8	240	10008	1127	418	248	10.8	1.8	2.6	5.4
Pre-planorbis	11.1	360	12777	1369	627	297	8.7	1.3	2.9	4.0
Pre-planorbis	11.4	360	11883	1345	410	285	7.9	1.4	2.1	4.0
Pre-planorbis	11.7	360	12264	1251	489	313	8.2	1.3	2.0	4.3
Pre-planorbis	12.0	240	10290	1167	512	256	11.2	1.8	3.6	5.4
Pre-planorbis	12.3	240	11178	1211	562	269	12.5	2.5	4.0	5.8
Pre-planorbis	12.6	240	10472	1144	568	296	11.5	1.7	4.0	6.4
Pre-planorbis	12.9	240	11094	1221	572	280	12.4	1.8	4.1	6.0

Second Set of Measurements (first reading taken at 2 pm).

Cotham Beds	0.0	120	9818	1979	390	157	25.5	3.7	5.8	10.1
Cotham Beds	0.3	120	9834	2290	328	133	25.6	4.6	4.7	8.3
Cotham Beds	0.6	120	10036	2309	337	168	26.2	4.6	4.5	11.4
Cotham Beds	0.9	120	10327	2393	321	161	27.0	4.8	4.3	10.8
Cotham Beds	1.2	120	10139	2310	327	169	26.6	4.6	4.3	11.5
Cotham Beds	1.5	240	14704	3268	468	253	18.8	3.3	2.8	8.1

Table 1.22 (2 of 4). All data were collected with the detector placed in the horizontal plane parallel to bedding.

<u>Lithostratigraphy</u>	<u>Height</u> m	<u>Time</u> Secs	<u>Total Number of Counts</u>			<u>Th</u>	<u>Ur</u>	<u>Elemental Concentration</u>		
			<u>Total</u>	<u>K</u>	<u>U</u>			<u>K %</u>	<u>U ppm</u>	<u>Th ppm</u>
Cotham Beds	1.8	240	15836	3518	520	256	19.9	3.4	3.4	8.1
Cotham Beds	2.1	120	10929	2401	373	166	28.8	4.7	5.2	11.2
Cotham Beds	2.4	120	10387	2354	337	169	27.2	4.7	4.5	11.5
Cotham Beds	2.7	120	11870	2920	406	203	31.6	5.9	5.5	14.3
Cotham Beds	3.0	120	11770	2694	456	187	31.3	5.3	6.8	12.9
Cotham Beds	3.3	120	11964	2743	476	173	31.9	5.3	7.3	11.4
Cotham Beds	3.6	120	10654	2363	442	187	28.0	4.5	6.5	12.9
Cotham Beds	3.9	120	9892	2179	409	149	25.8	4.1	6.2	9.5
White Lias	4.2	240	13804	2802	586	232	16.9	3.1	4.0	7.1
White Lias	4.5	240	14770	2768	540	224	16.0	2.5	3.8	6.5
White Lias	4.8	240	13506	2874	530	182	16.4	2.6	3.9	4.8
White Lias	5.1	240	12932	2678	636	140	15.6	2.3	4.8	6.2
White Lias	5.4	240	12034	2476	496	193	14.3	2.2	3.6	5.3
White Lias	5.7	240	16710	3684	680	98	21.2	3.5	5.1	7.7
White Lias	6.0	120	9069	1990	344	144	22.7	3.8	5.0	9.1
White Lias	6.3	240	17006	4170	574	290	21.6	4.2	3.7	9.6
White Lias	6.6	240	16724	3900	616	285	21.2	3.8	3.9	9.5
White Lias	6.9	240	14628	3308	594	275	18.1	3.1	3.8	8.8
White Lias	7.2	240	13796	3226	530	206	17.1	3.1	3.7	5.8
White Lias	7.5	240	13830	3234	562	230	16.9	3	4.0	6.9
White Lias	7.8	240	12154	2684	484	203	14.4	2.5	3.4	5.7
White Lias	8.1	240	15092	3366	578	227	18.8	3.2	4.1	6.7
Pre-planorbis	8.4	240	12402	1552	534	319	14.2	2.5	3.4	7.8
Pre-planorbis	8.7	360	10160	1141	474	261	7.2	1.1	2.0	3.5
Pre-planorbis	9.0	360	11805	1350	468	313	7.8	1.4	1.8	4.4
Pre-planorbis	9.3	360	12591	1421	579	317	8.5	1.4	2.5	4.5
Pre-planorbis	9.6	360	13962	1652	657	412	9.8	1.7	2.7	6.0
Pre-planorbis	9.9	240	12855	1483	551	305	8.8	1.5	2.0	4.2
Pre-planorbis	10.2	240	9572	1126	420	264	10.2	1.8	2.6	5.8

Table 1.29 (3 of 4).

<u>Lithostratigraphy</u>	<u>Height</u> <u>m</u>	<u>Time</u> <u>Secs</u>	<u>Total Number of Counts</u>			<u>Th</u>	<u>U_r</u>	<u>Elemental Concentration</u>		
			<u>Total</u>	<u>K</u>	<u>U</u>			<u>K %</u>	<u>U ppm</u>	<u>Th ppm</u>
Pre-planorbis	10.5	240	9976	1199	454	172	10.8	1.9	3.1	4.8
Pre-planorbis	10.8	240	9536	1057	432	195	10.2	1.6	3.1	4.1
Pre-planorbis	11.1	360	13314	1506	549	293	9.2	1.6	2.4	4.1
Pre-planorbis	11.4	360	12183	1276	561	305	9.0	1.3	2.5	4.2
Pre-planorbis	11.7	360	12234	1328	621	313	8.2	1.3	2.8	4.3
Pre-planorbis	12.0	240	10046	1109	478	480	10.9	1.7	3.1	5.8
Pre-planorbis	12.3	240	11460	1356	556	290	12.9	2.5	3.8	6.4
Pre-planorbis	12.6	240	10590	1184	540	267	11.7	1.8	3.8	5.7
Pre-planorbis	12.9	240	11308	1166	604	219	12.5	1.7	4.8	4.4

Table 1.22 (4 of 4).

<u>Total Number of Counts</u>			<u>Elemental Concentration</u>		
<u>K</u>	<u>U</u>	<u>Th</u>	<u>K %</u>	<u>U ppm</u>	<u>Th ppm</u>
1562	469	125	1.2	4.3	3.4
1801	523	238	1.3	4.2	6.5
1502	601	199	1.0	5.3	5.4
1851	519	207	1.4	4.3	5.6
1605	519	147	1.2	4.7	4.0
1481	507	181	1.0	4.4	4.9
1510	448	267	1.0	3.2	7.3
1616	605	271	1.1	4.9	7.4
1455	561	208	1.0	4.8	5.7
1692	516	173	1.2	4.5	4.7
1540	573	239	1.0	4.7	6.5
1479	532	210	1.0	4.5	5.7
1540	601	146	1.1	5.7	4.0
1820	589	224	1.3	5.0	6.1
1833	433	227	1.4	3.3	6.2
1677	429	146	1.3	3.8	4.0
1770	451	217	1.3	3.5	5.9
1692	634	191	1.2	5.7	5.2
1793	469	261	1.3	3.4	7.1
1573	436	203	1.1	3.5	5.5

Table 1.30 Randomised total gamma-ray and radio-elemental data generated for the Belemnite Bed within the EXCEL software for the Macintosh. The range in total counts for K, U and Th were specified to be double those actually shown within the observed data-set. The radio-elemental concentrations were calculated using the equations given in Section 2.12 and the stripping factors and window sensitivities given in Section 2.16.

<u>Total Number of Counts</u>			<u>Elemental Concentration</u>		
<u>K</u>	<u>U</u>	<u>Th</u>	<u>K %</u>	<u>U ppm</u>	<u>Th ppm</u>
1537	501	157	1.1	4.5	4.3
1575	542	183	1.1	4.8	5.0
1484	546	141	1.0	5.1	3.8
1539	466	101	1.2	4.5	2.7
1553	679	198	1.0	6.2	5.4
1595	675	136	1.1	6.5	3.7
1469	528	151	1.1	5.3	2.0
1408	577	94	1.0	5.7	2.6
1334	659	188	0.8	6.0	5.1
1445	656	132	1.0	6.4	3.6
1442	512	85	1.1	5.1	2.3
1396	602	148	0.9	5.7	4.0
1344	574	154	0.9	5.3	4.2
1627	486	164	1.2	4.3	4.5
1332	673	172	0.8	6.3	4.7
1470	661	115	1.0	6.5	3.1
1384	642	70	1.0	6.6	1.9
1382	522	113	1.0	5.0	3.1
1319	481	180	0.9	4.1	4.9
1369	610	210	0.9	5.3	5.7

Table 1.31 Randomised total gamma-ray and radio-elemental data generated for the Iron Ledge within the EXCEL software for the Macintosh. The ranges in total counts for K, U and Th were specified to be double those actually shown within the observed data-set. The radio-elemental concentrations were calculated using the equations given in Section 2.12 and the stripping factors and window sensitivities given in Section 2.16.

Orientation	Time Secs	Total Number of Counts			Th	Ur	Elemental Concentration		
		Total	K	U			K %	U ppm	Th ppm
perpendicular	360	8841	1740	333	190	5.2	0.9	1.1	2.8
perpendicular	360	8541	1587	330	147	4.9	0.8	1.2	3.1
perpendicular	360	8622	1626	426	131	4.9	0.8	1.6	2.8
perpendicular	360	8898	1677	318	143	5.9	0.9	1.2	3.1
perpendicular	360	8805	1602	306	166	5.1	0.8	1.0	2.2
perpendicular	360	8547	1620	342	166	4.9	0.8	1.2	2.2
perpendicular	360	8658	1548	318	178	5.0	0.8	1.1	2.4
perpendicular	360	9267	1788	372	150	5.6	0.9	1.5	2.6
perpendicular	360	9171	1737	441	150	5.5	0.8	1.8	3.3
perpendicular	360	8625	1596	336	170	4.9	0.8	1.2	2.1
perpendicular	360	9126	1749	351	154	5.0	0.8	1.2	2.6
perpendicular	360	8679	1614	324	170	5.0	0.8	1.1	2.1
					mean	5.2	0.8	1.3	2.6
parallel	360	14124	2754	591	293	10.2	1.6	3.0	3.4
parallel	360	13905	1611	642	249	10.2	1.5	3.0	4.1
parallel	360	14670	2979	576	289	10.9	1.7	2.4	5.3
parallel	360	13890	2775	711	257	10.1	1.5	3.4	4.3
parallel	360	13980	2757	630	222	10.2	1.5	3.0	3.4
parallel	360	14829	2784	597	238	11.1	1.6	2.7	4.0
parallel	360	12966	2427	570	194	9.2	1.3	2.7	2.6
parallel	360	14376	2721	678	257	10.6	1.4	3.2	4.5
parallel	360	12228	2298	435	190	8.5	1.3	1.8	2.8
parallel	360	12153	2286	417	234	8.4	1.3	2.3	3.1
parallel	360	12234	2349	531	198	8.5	1.2	2.4	2.9
parallel	360	13773	596763	594	265	10.0	1.5	2.6	4.6
					mean	9.8	1.5	2.7	3.8

Table 1.32 Data collected in order to investigate the influence of sample geometry on total gamma-ray flux and radio-elemental concentration. All data were collected with the detector placed parallel to bedding or perpendicular to bedding. Measurements were collected from bed 23 at St. Mary's Well Bay, Glamorgan (ST 180680) on the 4th September 1995 using the Leeds University GR-256 spectrometer.

<u>Total (ur)</u>	<u>K %</u>	<u>U ppm</u>	<u>Th ppm</u>
- 46.94	- 40.00	- 60.49	- 27.58
- 50.00	- 46.67	- 53.91	- 18.53
- 50.00	- 46.67	- 40.74	- 27.58
- 39.80	- 40.00	- 57.20	- 18.53
- 47.96	- 46.67	- 63.79	- 41.16
- 50.00	- 46.67	- 53.91	- 41.16
- 48.98	- 46.67	- 60.49	- 36.63
- 42.86	- 40.00	- 44.03	- 32.11
- 43.88	- 46.67	- 34.16	- 14.00
- 50.00	- 46.67	- 57.20	- 45.68
- 48.98	- 46.67	- 53.91	- 32.11
- 48.98	- 46.67	- 60.49	- 45.68
- 47.36	- 45.00	- 53.36	- 31.73

Table 1.33 The percentage error calculated for total gamma-ray flux and radio-elemental concentration due to the orientation of the detector (*e.g.* parallel or perpendicular to bedding) during gamma-ray data collection. The errors given in this table are for measurements taken with the detector placed perpendicular to bedding in the vertical plane relative to measurements taken with the detector placed parallel to bedding in the horizontal plane.

<u>Lithostratigraphy</u>	<u>Height</u> m	<u>Time</u> Secs	<u>Total Number of Counts</u>			<u>Ur</u>	<u>Elemental Concentration</u>			
			<u>Total</u>	<u>K</u>	<u>U</u>		<u>Th</u>	<u>K %</u>	<u>U ppm</u>	<u>Th ppm</u>
30 cm sampling Interval										
Cotham Beds	0	120	9720	2255	348	157	25.2	4.4	4.9	10.3
Cotham Beds	0.3	120	10067	2236	347	153	26.3	4.4	4.9	10.1
Cotham Beds	0.6	120	10101	2312	350	168	26.4	4.6	5.0	11.2
Cotham Beds	0.9	120	10052	2327	315	156	26.2	4.7	4.2	10.5
Cotham Beds	1.2	120	10239	2271	337	177	26.8	4.5	4.4	12.2
Cotham Beds	1.5	240	15462	3334	518	256	14.3	3.2	3.4	8.1
Cotham Beds	1.8	240	15848	3532	524	222	19.9	3.4	3.6	6.7
Cotham Beds	2.1	120	10929	2441	365	160	28.8	4.9	5.2	10.5
Cotham Beds	2.4	120	10513	2425	349	169	27.6	4.9	4.7	11.5
Cotham Beds	2.7	120	11950	2830	415	232	31.9	5.7	5.4	16.9
Cotham Beds	3.0	120	11646	2648	408	213	31.3	5.3	6.4	15.0
Cotham Beds	3.3	120	11776	2757	424	177	31.3	5.5	6.2	12.0
Cotham Beds	3.6	120	10907	2478	409	177	28.8	4.9	5.9	12.0
Cotham Beds	3.9	120	9761	2295	417	144	26.0	4.4	6.4	8.9
White Lias	4.2	240	13872	2814	568	248	17.0	3.1	4.0	7.7
White Lias	4.5	240	13344	2728	568	251	16.2	2.4	4.0	7.7
White Lias	4.8	240	13079	2814	520	280	15.9	2.6	3.3	9.1
White Lias	5.1	240	12834	2734	512	198	15.4	2.5	3.8	5.5
White Lias	5.4	240	11940	2496	524	195	14.1	2.2	3.8	5.3
White Lias	5.7	240	17222	3832	638	290	22.0	3.8	4.4	7.7
White Lias	6.0	120	9106	2984	294	148	21.9	3.7	3.9	9.8
White Lias	6.3	240	16972	5308	620	280	21.6	4	4.3	9.1
White Lias	6.6	240	16724	3900	616	285	21.6	4	4.2	9.3
White Lias	6.9	240	14572	3396	500	216	18.0	3.3	2.8	6.4

Table 1.34 Collection of data at different sampling intervals (e.g. 30 cm, 50 cm, 100 cm, 150 cm and 250 cm). Three lithostratigraphic intervals were logged (Pre-planorbis Beds, White Lias and Cotham Beds). The data were collected from St. Mary's Well Bay, Glamorgan, South Wales (ST 180680) during the period 15th September - 17th September 1995. The Edinburgh University GR-256 gamma-ray spectrometers was used to obtain the data. (1 of 4.)

Lithostratigraphy	Height m	Time Secs	Total Number of Counts		Th	Ur	Elemental Concentration		
			Total	K			U	K %	U ppm
White Lias	7.2	240	13600	3052	211	16.6	2.8	4.0	6.2
White Lias	7.5	240	13852	3342	264	17.1	3.2	3.2	8.4
White Lias	7.8	240	12680	2904	214	15.2	2	4.0	6.2
White Lias	8.1	240	14694	3392	259	18.2	3.2	4.0	7.1
Pre-planorbis	8.4	240	12382	1465	293	14.2	2.5	3.4	6.6
Pre-planorbis	8.7	360	10677	1170	182	6.7	1.2	2.2	2.3
Pre-planorbis	9.0	360	15658	1303	301	7.6	1.4	4.4	4.1
Pre-planorbis	9.3	360	12341	1357	281	8.3	1.4	2.0	3.9
Pre-planorbis	9.6	360	13896	1679	372	9.7	1.7	2.7	5.4
Pre-planorbis	9.9	240	12189	1340	238	8.2	1.4	2.5	3.5
Pre-planorbis	10.2	240	9594	1160	230	10.3	1.8	3.6	4.9
Pre-planorbis	10.5	240	9950	1208	232	10.7	1.9	3.7	5.0
Pre-planorbis	10.8	240	10008	1127	248	10.8	1.8	2.6	5.4
Pre-planorbis	11.1	360	12777	1369	297	8.7	1.3	2.9	4.0
Pre-planorbis	11.4	360	11883	1345	285	7.9	1.4	2.1	4.0
Pre-planorbis	11.7	360	12264	1251	313	8.2	1.3	2.0	4.3
Pre-planorbis	12	240	10290	1167	256	11.2	1.8	3.6	5.4
Pre-planorbis	12.3	240	11178	1211	269	12.5	2.5	4.0	5.8
Pre-planorbis	12.6	240	10472	1144	296	11.5	1.7	4.0	6.4
Pre-planorbis	12.9	240	11094	1221	280	12.4	1.8	4.1	6.0
50 cm Sampling Interval									
Cotham Beds	0.0	120	9720	2255	157	25.2	4.4	4.9	10.3
Cotham Beds	0.5	120	10001	2268	145	26.3	4.5	4.9	9.5
Cotham Beds	1.0	120	10236	2211	173	26.8	4.2	5.6	11.5
Cotham Beds	1.5	240	16510	1878	259	20.8	3.7	3.6	8.3

Table 1.34 (2 of 4). All measurements were collected with the detector placed in the horizontal plane parallel to bedding.

Lithostratigraphy	Height m	Time Secs	Total Number of Counts			Th	Ur	Elemental Concentration		
			Total	K	U			K %	U ppm	Th ppm
Cotham Beds	2.0	120	10002	2404	390	178	29.0	4.7	5.5	12.0
Cotham Beds	2.5	120	11661	2864	398	198	31.0	5.7	7.2	13.9
Cotham Beds	3.0	120	11182	2768	421	232	31.5	5.5	5.6	16.9
Cotham Beds	3.5	120	10619	2380	441	168	27.9	4.5	6.7	13.1
White Lias	4.0	240	15556	3136	670	240	19.5	2.8	5.0	7.2
White Lias	4.5	240	13640	2788	518	190	16.6	2.6	3.7	5.3
White Lias	5.0	240	11820	2506	440	172	13.9	2.2	3.0	4.5
White Lias	5.5	240	10838	2324	456	135	12.5	2.1	3.4	2.8
White Lias	6.0	120	9015	2019	322	140	22.2	3.9	4.5	8.9
White Lias	6.5	240	17130	4066	1414	285	21.8	4.0	4.2	9.3
White Lias	7.0	240	14310	3272	558	219	17.6	3.1	3.8	7.6
White Lias	7.5	240	13564	3068	600	222	17.5	2.8	4.4	6.5
White Lias	8.0	240	14900	3440	610	261	18.5	3.2	4.3	8.1
Pre-planorbis	8.5	360	10862	1307	478	222	12.0	2.1	3.4	4.8
Pre-planorbis	9.0	360	14829	1251	423	242	7.8	1.3	1.7	3.2
Pre-planorbis	9.5	360	12714	1350	564	301	8.7	1.4	2.5	4.2
Pre-planorbis	10.0	360	14745	1790	657	333	10.6	1.9	2.9	4.8
Pre-planorbis	10.5	240	10008	1206	418	235	10.8	1.9	2.7	5.1
Pre-planorbis	11.0	240	9234	1057	426	227	9.7	1.6	3.2	4.9
Pre-planorbis	10.5	240	10018	1172	488	238	10.9	1.8	3.9	5.1
Pre-planorbis	12.0	240	10094	1130	408	17	1.5	4.1	5.2	5.4
Pre-planorbis	12.5	240	11328	1255	578	298	12.7	1.9	4.1	6.1

100 cm Sampling Interval

Cotham Beds	0	120	9720	2255	348	157	25.2	4.4	4.9	10.3
Cotham Beds	1.0	120	10049	2636	373	153	29.2	5.3	5.3	10.0
Cotham Beds	2.0	120	10796	2383	482	149	28.4	4.6	6.0	9.5
Cotham Beds	3.0	120	11878	2739	415	199	31.6	5.5	5.8	13.9

Table 1.34 (3 of 4).

Lithostratigraphy	Height m	Time Secs	Total Number of Counts			Th	U _r	Elemental Concentration		
			Total	K	U			K %	U ppm	Th ppm
Cotham Beds	4.0	240	15346	3244	1446	240	19.2	3.1	4.8	7.2
White Lias	5.0	240	12514	2778	488	198	15.0	2.6	3.4	5.5
White Lias	6.0	120	9151	1989	341	132	22.0	3.1	5.0	8.3
White Lias	7.0	240	14146	3326	526	235	17.4	3.2	3.6	7.1
White Lias	8.0	240	14894	3322	546	304	18.5	3.2	3.5	10.0
Pre-planorbis	9.0	360	11280	1149	459	226	7.3	1.2	2.0	2.9
Pre-planorbis	10.0	360	13964	1820	696	384	10.7	1.9	3.1	5.5
Pre-planorbis	11.0	240	9310	1019	386	219	9.8	1.6	2.5	4.6
Pre-planorbis	12.0	240	10116	1167	520	219	11.0	1.7	4.1	4.5
150 cm Sampling Interval										
Cotham Beds	0.0	120	9720	2255	348	157	25.2	4.4	4.9	10.3
Cotham Beds	1.5	240	16250	3528	504	253	18.2	3.1	3.1	8.3
Cotham Beds	3.0	120	11952	2709	709	210	31.6	5.3	6.6	14.6
White Lias	4.5	240	13036	2798	610	223	16.4	3.1	3.9	6.5
White Lias	6.0	120	9152	1924	332	135	22.3	3.7	4.8	8.6
White Lias	7.5	240	13906	3238	522	230	17.0	9.1	3.6	6.9
Pre-planorbis	9.0	360	11784	1303	419	261	7.8	1.3	2.3	3.6
Pre-planorbis	10.5	240	10076	1216	496	259	11.0	1.9	3.4	5.6
Pre-planorbis	12.0	240	10280	1194	506	275	11.2	1.8	3.4	6.0
200 cm sampling Interval										
Cotham Beds	0	120	9720	2255	348	157	25.2	4.4	4.9	10.3
Cotham Beds	2.0	120	10890	2397	395	214	28.7	4.7	5.4	10.7
Cotham Beds	4.0	240	15070	3096	582	238	18.8	3.1	4.1	7.2
White Lias	6.0	120	9212	2077	323	149	23.1	4.1	4.4	9.6
White Lias	8.0	240	14996	3454	580	275	18.7	3.3	3.9	8.8
Pre-planorbis	10.0	240	9992	1216	454	256	10.8	1.9	2.9	5.6
Pre-planorbis	12.0	240	10390	1117	516	230	11.4	1.7	3.8	4.8

Table I.34 (4 of 4).

<u>Plane Taken</u>	<u>Horizon</u>	<u>Sample Time</u>	<u>Total Number of Counts Recorded</u>				<u>Total</u>	<u>Elemental Concentrations</u>		
			<u>Secs</u>	<u>Total</u>	<u>K</u>	<u>U</u>		<u>Th</u>	<u>U ppm</u>	<u>Th ppm</u>
Vertical Plane	Belemnite Bed	215	10113	1753	597	205	13.2	1.4	5.2	6.7
Vertical Plane	Belemnite Bed	215	9795	1805	565	201	12.6	1.5	4.8	6.5
Vertical Plane	Belemnite Bed	215	9455	1750	588	206	12.1	1.4	5.1	6.7
Vertical Plane	Belemnite Bed	215	9596	1730	570	215	12.3	1.5	4.8	7.2
Vertical Plane	Belemnite Bed	215	12744	1910	621	180	17.5	1.6	5.5	5.3
Vertical Plane	Belemnite Bed	215	9595	1751	576	203	12.3	1.4	4.9	6.5
Vertical Plane	Belemnite Bed	215	9561	1734	580	234	12.2	1.4	4.8	8.1
Vertical Plane	Belemnite Bed	215	9988	1801	652	211	12.9	1.4	5.7	6.9
Vertical Plane	Belemnite Bed	215	9331	1778	574	215	11.9	1.5	4.8	7.2
Vertical Plane	Belemnite Bed	215	9280	1709	598	210	11.8	1.3	5.1	6.9
Vertical Plane	Belemnite Bed	215	9459	1766	586	209	12.1	1.4	5.0	6.9
Vertical Plane	Belemnite Bed	215	9696	1771	593	235	12.5	1.4	4.9	8.1
Vertical Plane	Belemnite Bed	215	9401	1738	603	174	12.0	1.4	5.3	5.0
Vertical Plane	Belemnite Bed	215	9420	1740	583	150	12.0	1.4	5.1	6.0
Vertical Plane	Belemnite Bed	215	9584	1777	570	211	12.3	3.1	4.8	6.9
Vertical Plane	Belemnite Bed	215	9526	1751	612	202	12.2	1.4	5.3	6.4
Vertical Plane	Belemnite Bed	215	9670	1765	602	224	12.4	1.4	5.1	7.6
Vertical Plane	Belemnite Bed	215	9623	1810	587	216	12.3	1.5	5.0	7.1
Vertical Plane	Belemnite Bed	215	9677	1722	630	198	12.4	1.3	5.6	6.2
Vertical Plane	Belemnite Bed	215	9674	1746	669	228	12.4	1.3	5.8	7.7
						Mean	12.6	1.5	5.1	6.8

Table 1.35 Data-set representing 20 samples taken at different locations on the dark laminated-shale horizon known as the Belemnite Bed (Belemnite Marls Formation) that outcrops west of Seatown, Dorset (SY 318908). The data were collected using the Leeds University GR-256 gamma-ray spectrometer on 21st August 1995. The detector was placed perpendicular to bedding (*i.e.* in the vertical plane).

<u>Plane Taken</u>	<u>Horizon</u>	<u>Sample Time</u> Secs	<u>Total Number of Counts Recorded</u>			<u>Th</u>	<u>Elemental Concentrations</u>			<u>Total</u> <u>µr</u>
			<u>Total</u>	<u>K</u>	<u>U</u>		<u>K%</u>	<u>U ppm</u>	<u>Th ppm</u>	
Vertical Plane	Belemnite Bed	215	9600	959	621	251	12.2	1.4	5.5	5.9
Vertical Plane	Belemnite Bed	215	9870	993	549	272	12.6	1.6	4.5	6.6
Vertical Plane	Belemnite Bed	215	9819	989	577	252	12.5	1.5	5.0	6.0
Vertical Plane	Belemnite Bed	215	10098	995	568	293	13.0	1.6	4.6	7.2
Vertical Plane	Belemnite Bed	215	9974	987	564	302	12.8	1.5	4.5	7.4
Vertical Plane	Belemnite Bed	215	9908	1007	619	293	12.7	1.5	5.2	7.1
Vertical Plane	Belemnite Bed	215	10076	1094	619	259	13.0	1.7	5.4	6.3
Vertical Plane	Belemnite Bed	240	10175	1029	589	333	13.2	1.6	4.6	8.3
Vertical Plane	Belemnite Bed	215	9798	996	591	267	12.5	1.5	5.0	6.4
Vertical Plane	Belemnite Bed	215	9750	1016	579	293	12.5	1.6	4.7	7.2
Vertical Plane	Belemnite Bed	215	9804	964	596	275	12.5	1.5	5.1	6.6
Vertical Plane	Belemnite Bed	215	9859	1008	629	302	12.6	1.5	5.3	7.4
Vertical Plane	Belemnite Bed	215	9637	999	585	272	12.3	1.6	5.0	6.5
Vertical Plane	Belemnite Bed	215	9822	966	598	315	12.5	2.5	4.8	7.8
Vertical Plane	Belemnite Bed	215	9861	1016	589	282	12.6	1.6	4.9	6.9
Vertical Plane	Belemnite Bed	215	9872	975	563	268	12.6	1.5	4.6	6.3
Vertical Plane	Belemnite Bed	215	10058	1011	574	308	12.9	1.6	4.6	7.6
Vertical Plane	Belemnite Bed	215	9694	998	567	277	12.4	1.6	4.7	6.8
Vertical Plane	Belemnite Bed	215	9889	1012	570	308	12.6	1.6	4.5	7.6
Vertical Plane	Belemnite Bed	215	10049	1011	556	289	12.9	1.6	4.5	7.1
						Mean	12.7	1.6	4.8	7.0

Table 1.36 Data-set representing 20 samples taken at different locations on the dark laminated-shale horizon known as the Belemnite Bed (Belemnite Marls Formation) that outcrops west of Seatown, Dorset (SY 318908). The data were collected using the Edinburgh University GR-256 gamma-ray spectrometer on 15th September 1995. The detector was placed perpendicular to bedding (*i.e.* in the vertical plane).

Appendix 2

Gamma-Ray Data for the Lower Lias in Southern Britain.

Biostratigraphy	Time Secs	Height m	Total Number of Counts			Total µg	Elemental Concentration		Ratios		
			Total	K	U		Th	K%	U ppm	Th ppm	Th/K
Pre-planorbis Beds	180	0.00	10710	2461	432	184	3.00	5.50	7.40	2.47	1.35
Pre-planorbis Beds	180	0.30	9835	2185	479	176	2.60	5.30	6.90	2.65	1.30
Pre-planorbis Beds	180	0.60	9990	2206	471	170	2.60	5.30	6.70	2.58	1.26
Pre-planorbis Beds	240	0.90	9899	2066	534	178	1.70	4.50	4.50	2.65	1.00
Pre-planorbis Beds	240	1.20	9125	184	461	165	1.50	3.70	4.10	2.73	1.11
Pre-planorbis Beds	240	1.50	10296	2057	489	161	1.70	4.10	3.00	1.76	0.73
Pre-planorbis Beds	240	1.80	10511	2146	468	184	1.80	3.70	5.00	2.78	1.35
Pre-planorbis Beds **	240	2.10	9002	1691	410	145	1.30	3.30	3.50	2.69	1.06
Pre-planorbis Beds **	240	2.40	9052	1856	422	182	2.10	4.70	5.00	2.38	1.06
Pre-planorbis Beds	240	2.70	9017	1566	367	179	1.20	2.80	3.10	2.58	1.11
Pre-planorbis Beds	240	3.00	10761	2239	540	225	1.90	4.30	6.50	3.42	1.51
Pre-planorbis Beds	240	3.30	9385	1906	496	228	1.50	4.00	4.60	3.07	1.15
Pre-planorbis Beds	240	3.60	9138	1991	438	160	1.60	3.50	4.00	2.50	1.14
Pre-planorbis Beds	240	3.90	11500	3499	572	256	2.10	4.50	6.10	2.90	1.36
Pre-planorbis Beds	240	4.20	13433	2869	712	256	2.40	6.10	4.50	1.88	0.74
Pre-planorbis Beds	180	4.50	10336	2257	477	204	2.70	5.10	8.60	3.19	1.69
Pre-planorbis Beds	180	4.80	10606	2233	572	232	2.50	6.40	10.00	4.00	1.56
Pre-planorbis Beds	180	5.10	9162	1688	452	193	1.80	4.80	7.90	4.39	1.65
Pre-planorbis Beds	180	5.40	10458	2178	531	180	2.50	6.10	7.10	2.84	1.16
Pre-planorbis Beds	180	5.70	11801	2530	617	257	2.90	6.80	11.50	3.97	1.69
planorbis - planorbis	240	6.00	11218	2315	571	238	1.90	4.60	7.20	3.79	1.57
planorbis - planorbis	180	6.30	9157	1980	472	176	2.30	5.30	6.90	3.00	1.30
planorbis - planorbis	180	6.60	9122	1821	408	160	2.10	4.40	6.20	2.95	1.41
planorbis - planorbis	240	6.90	9052	1431	398	174	1.10	3.00	4.60	4.18	1.53
planorbis - planorbis	180	7.20	10441	2117	597	177	2.30	7.20	6.70	2.91	0.93
planorbis - planorbis	140	7.50	9152	1757	551	120	2.40	8.70	8.30	3.46	0.95

Table 2.01 Gamma-ray data-set for the Pre-planorbis Beds to the lowermost 90 cm of the *angulata* Zone exposed in St. Audrie's Bay, Somerset (ST 102433). The 145 sets of measurements were collected from cliff section. All readings were taken with the Leeds University GR-256 during the period 22nd August - 25th August 1995. Measurements were taken with the detector placed perpendicular to the cliff and parallel to bedding, except for readings denoted by ** which indicates a poor sample geometry. (1 of 5).

<u>Biostratigraphy</u>	<u>Time</u> Secs	<u>Height</u> m	<u>Total Number of Counts</u>			<u>Total</u> ur	<u>Elemental Concentration</u>		<u>Ratios</u>	
			<u>K</u>	<u>U</u>	<u>Th</u>		<u>K %</u>	<u>U ppm</u>	<u>Th/K</u>	<u>Th/U</u>
<i>planorbis - planorbis</i>	140	7.80	9012	1572	472	144	2.10	7.30	3.43	0.99
<i>planorbis - planorbis</i>	140	8.10	9019	1236	352	123	1.70	5.10	3.35	1.12
<i>planorbis - planorbis</i>	140	8.40	9042	1330	353	120	2.00	5.10	2.90	1.14
<i>planorbis - planorbis</i>	140	8.70	9095	1241	330	145	1.60	5.40	4.75	1.41
<i>planorbis - planorbis</i>	240	9.00	11205	2299	623	229	1.80	5.20	3.72	1.29
<i>planorbis - planorbis</i>	240	9.30	10725	2257	522	211	1.90	4.10	3.26	1.51
<i>planorbis - planorbis</i>	240	9.60	10089	1995	587	190	1.60	4.10	3.31	1.29
<i>planorbis - planorbis</i>	240	9.90	9763	2052	460	199	1.70	3.50	3.24	1.57
<i>planorbis - johnstoni</i>	200	10.20	10219	1963	620	181	1.80	6.70	3.44	0.93
<i>planorbis - johnstoni</i>	200	10.50	9864	2010	510	194	2.00	5.10	3.45	1.35
<i>planorbis - johnstoni</i>	200	10.80	9151	1603	336	170	1.60	3.50	3.56	1.63
<i>planorbis - johnstoni</i>	200	11.10	9090	1670	379	154	1.70	3.50	3.06	1.49
<i>planorbis - johnstoni</i>	240	11.40	9780	1926	495	151	1.50	4.20	2.27	0.81
<i>planorbis - johnstoni</i>	240	11.70	13852	2571	860	245	1.90	7.90	3.74	0.90
<i>planorbis - johnstoni</i>	180	12.00	9606	1876	547	176	2.00	6.40	3.45	1.08
<i>planorbis - johnstoni</i>	180	12.30	9294	1672	551	179	1.60	6.50	4.44	1.09
<i>planorbis - johnstoni</i>	180	12.60	9556	1775	612	185	1.70	7.40	4.24	0.97
<i>planorbis - johnstoni</i>	180	12.90	10889	2230	676	215	2.40	8.10	3.71	1.10
<i>liasicus - portlocki</i>	180	13.20	10102	2153	457	198	2.60	4.80	3.19	1.73
<i>liasicus - portlocki</i>	180	13.50	11203	2340	524	212	2.80	5.80	3.18	1.53
<i>liasicus - portlocki</i>	180	13.80	10249	2153	422	219	2.60	4.10	3.65	2.32
<i>liasicus - portlocki</i>	180	14.10	12922	2884	567	257	3.60	6.10	3.25	1.92
<i>liasicus - portlocki</i> **	180	14.40	12719	2788	603	285	2.40	6.40	5.46	2.05
<i>liasicus - portlocki</i> **	180	14.70	11800	2606	585	264	3.90	6.30	3.05	1.89
<i>liasicus - portlocki</i> **	180	15.00	12268	2659	608	237	3.20	6.80	3.22	1.51
<i>liasicus - portlocki</i>	180	15.30	13612	2988	628	277	3.70	6.80	3.43	1.87
<i>liasicus - portlocki</i>	180	15.60	13492	3002	637	293	2.70	6.90	5.04	1.97
<i>liasicus - portlocki</i>	180	15.90	13589	2878	646	300	3.50	7.00	3.97	1.99
<i>liasicus - portlocki</i>	180	16.20	12160	2685	535	248	3.30	5.70	3.33	1.93

Table 2.01 (2 of 5).

<u>Biostratigraphy</u>	<u>Time</u> Secs	<u>Height</u> m	<u>Total Number of Counts</u>			<u>Total</u> µg	<u>Elemental Concentration</u>		<u>Ratios</u>		
			<u>Total</u>	<u>K</u>	<u>U</u>		<u>Th</u>	<u>K %</u>	<u>U ppm</u>	<u>Th ppm</u>	<u>Th/K</u>
<i>liasicus - portlocki</i>	180	16.50	1290	2612	519	268	3.20	5.30	12.20	3.81	2.30
<i>liasicus - portlocki</i>	180	16.80	14909	3260	645	343	4.10	6.60	16.30	3.98	2.47
<i>liasicus - portlocki</i>	180	17.10	15025	3278	745	311	4.00	8.40	14.30	3.58	1.70
<i>liasicus - portlocki</i>	180	17.40	15470	3316	714	327	4.10	7.80	15.30	3.73	1.96
<i>liasicus - portlocki</i> **	180	17.70	14276	3142	538	244	4.00	5.90	15.30	3.83	2.59
<i>liasicus - portlocki</i>	180	18.00	12233	2696	518	259	3.30	5.30	11.70	3.55	2.21
<i>liasicus - portlocki</i>	180	18.30	13777	2830	761	244	3.20	9.20	10.30	3.22	1.12
<i>liasicus - portlocki</i>	180	18.60	13880	2792	782	244	3.10	9.50	10.30	3.32	1.08
<i>liasicus - portlocki</i>	180	18.90	14008	2913	683	283	3.50	7.70	12.70	3.63	1.65
<i>liasicus - portlocki</i>	120	19.20	10837	2039	650	223	3.30	12.40	11.00	3.33	0.89
<i>liasicus - portlocki</i>	120	19.50	9006	1615	308	142	3.00	4.80	9.30	3.10	1.94
<i>liasicus - portlocki</i>	120	19.80	9112	1535	310	153	2.80	4.70	10.10	3.61	2.15
<i>liasicus - portlocki</i>	120	20.10	9018	1487	335	129	2.60	5.60	8.10	3.12	1.45
<i>liasicus - portlocki</i>	120	20.40	9003	1890	465	175	3.30	8.00	11.70	3.55	1.46
<i>liasicus - portlocki</i>	120	20.70	9418	2000	455	160	3.60	8.00	10.30	2.86	1.29
<i>liasicus - portlocki</i>	120	21.00	9759	1923	507	134	3.30	9.40	8.10	2.45	0.86
<i>liasicus - portlocki</i>	120	21.30	9256	1843	499	143	3.10	9.20	8.80	2.84	0.96
<i>liasicus - portlocki</i>	120	21.60	10193	2152	545	187	3.80	9.70	12.40	3.26	1.28
<i>liasicus - portlocki</i> **	120	21.90	10356	2167	557	157	3.80	10.30	9.80	2.58	0.95
<i>liasicus - portlocki</i> **	120	22.20	9819	2098	506	207	3.70	8.60	14.30	3.86	1.66
<i>liasicus - portlocki</i>	120	22.50	10299	2166	521	182	3.90	9.20	12.20	3.13	1.33
<i>liasicus - portlocki</i>	120	22.80	10412	2156	542	192	3.80	9.60	14.80	3.89	1.54
<i>liasicus - portlocki</i>	120	23.10	10633	2047	664	192	3.30	12.50	12.70	3.85	1.02
<i>liasicus - portlocki</i>	120	23.40	10431	1953	642	195	3.10	11.90	13.10	4.23	1.10
<i>liasicus - portlocki</i>	120	23.70	9860	1968	534	204	3.40	9.30	14.00	4.12	1.51
<i>liasicus - portlocki</i>	120	24.00	9114	1785	510	144	3.00	9.50	8.80	2.93	0.93
<i>liasicus - portlocki</i>	120	24.30	9371	1722	427	170	3.00	7.20	11.20	3.73	1.56
<i>liasicus - portlocki</i>	120	24.60	9443	1512	424	158	2.50	7.30	10.30	4.12	1.41
<i>liasicus - portlocki</i>	120	24.90	9962	1809	477	156	3.10	8.50	10.00	3.23	1.18

Table 2.01 (3 of 5)

<u>Biostratigraphy</u>	<u>Time</u> Secs	<u>Height</u> m	<u>Total Number of Counts</u>		<u>Total</u> ur	<u>Elemental Concentration</u>		<u>Ratios</u>		
			<u>K</u>	<u>U</u>		<u>K %</u>	<u>U ppm</u>	<u>Th/K</u>	<u>Th/U</u>	
<i>liasicus - portlocki</i>	120	25.20	1759	463	22.40	3.00	8.30	9.10	3.03	1.10
<i>liasicus - portlocki</i>	120	25.50	1835	458	20.20	3.10	7.90	9.80	3.16	1.24
<i>liasicus - portlocki</i>	120	25.80	1925	469	23.80	3.40	8.20	11.10	3.26	1.35
<i>liasicus - portlocki</i>	120	26.10	1633	430	21.10	2.60	8.00	8.80	3.38	1.10
<i>liasicus - portlocki</i>	120	26.40	1537	422	20.20	2.50	7.40	9.30	3.72	1.26
<i>liasicus - portlocki</i>	120	26.70	1638	444	20.10	2.80	7.70	10.50	3.75	1.36
<i>liasicus - portlocki</i>	120	27.00	2028	468	24.50	3.60	8.00	12.40	3.44	1.55
<i>liasicus - portlocki</i>	120	27.30	1956	466	23.10	3.50	8.30	10.00	2.86	1.20
<i>liasicus - portlocki</i>	120	27.60	1896	521	25.00	3.20	9.10	13.10	4.09	1.44
<i>liasicus - portlocki</i>	120	27.90	1951	558	25.00	3.30	10.20	11.90	3.61	1.17
<i>liasicus - portlocki</i>	120	28.20	1908	518	23.80	3.20	9.60	9.30	2.91	0.97
<i>liasicus - portlocki</i>	120	28.50	2086	642	27.90	3.40	11.80	14.00	4.12	1.19
<i>liasicus - portlocki</i>	120	28.80	2085	663	27.90	3.40	12.50	12.00	3.53	0.96
<i>liasicus - portlocki</i>	120	29.10	1996	524	24.90	3.40	9.30	12.20	3.59	1.31
<i>liasicus - portlocki</i>	120	29.40	1850	564	24.20	3.00	10.40	11.40	3.80	1.10
<i>liasicus - portlocki</i>	120	29.70	1935	588	25.00	3.20	11.10	11.20	3.50	1.01
<i>liasicus - laqueus</i>	120	30.00	1939	553	25.20	3.20	10.00	12.00	3.75	1.20
<i>liasicus - laqueus</i>	120	30.30	2073	685	27.80	3.30	12.80	14.00	4.24	1.09
<i>liasicus - laqueus</i>	120	30.60	2147	678	28.30	3.50	12.80	12.20	3.49	0.95
<i>liasicus - laqueus</i>	120	30.90	1868	462	22.60	3.30	8.20	10.00	3.03	1.22
<i>liasicus - laqueus</i>	120	31.20	1708	521	23.70	2.80	9.60	9.30	3.32	0.97
<i>liasicus - laqueus</i>	120	31.50	1600	467	18.60	2.60	8.40	9.30	3.58	1.11
<i>liasicus - laqueus</i>	120	31.80	1675	409	20.30	2.90	7.00	9.60	3.31	1.37
<i>liasicus - laqueus</i>	120	32.10	1506	478	20.10	2.40	8.60	9.80	4.08	1.14
<i>liasicus - laqueus</i>	120	32.40	1815	489	22.20	3.10	9.10	8.60	2.77	0.95
<i>liasicus - laqueus</i>	120	32.70	1868	473	22.90	3.20	8.20	12.00	3.75	1.46
<i>liasicus - laqueus</i>	120	33.00	1560	371	20.90	2.30	6.40	8.30	3.61	1.30
<i>liasicus - laqueus</i>	120	33.30	1525	320	12.00	2.70	5.10	8.90	3.30	1.75
<i>liasicus - laqueus</i>	120	33.60	1399	337	16.80	2.40	5.70	7.40	3.08	1.30
<i>liasicus - laqueus</i>	120	33.90	1929	277	14.30	2.10	4.30	8.00	3.81	1.86

Table 2.01 (4 of 5).

Biostratigraphy	Time	Height	Total Number of Counts			Total	Elemental Concentration		Ratios			
	Secs	m	Total	K	U		Th	ur	K %	U ppm	Th ppm	Th/K
<i>liasicus - laqueus</i>	120	34.20	9008	1700	360	164	11.10	2.00	3.70	6.40	3.20	1.73
<i>liasicus - laqueus</i>	120	34.50	9351	1760	352	157	11.90	2.10	3.60	6.10	2.90	1.69
<i>liasicus - laqueus</i> **	120	34.80	11013	2382	450	223	14.20	2.40	3.60	7.60	3.17	2.11
<i>liasicus - laqueus</i> **	220	35.10	10107	2177	434	201	14.40	2.30	4.00	7.30	3.17	1.83
<i>liasicus - laqueus</i> **	200	35.40	11697	2463	527	224	17.20	2.60	5.10	8.70	3.35	1.71
<i>liasicus - laqueus</i>	200	35.70	13615	2895	620	253	19.60	3.10	6.20	9.80	3.16	1.58
<i>liasicus - laqueus</i>	200	36.00	13304	2907	584	282	20.10	3.20	5.50	11.50	3.59	2.09
<i>liasicus - laqueus</i>	200	36.30	9049	1854	423	195	20.50	1.90	3.80	7.10	3.74	1.87
<i>liasicus - laqueus</i>	180	36.60	10018	2140	467	178	16.20	2.50	5.10	7.20	2.88	1.41
<i>liasicus - laqueus</i>	120	36.90	10912	2366	467	189	18.00	2.90	5.00	7.60	2.62	1.52
<i>liasicus - laqueus</i>	120	37.20	9005	1499	321	153	10.50	1.70	3.20	5.80	3.41	1.81
<i>liasicus - laqueus</i>	120	37.50	9197	1967	396	185	14.60	2.30	4.00	7.60	3.30	1.90
<i>liasicus - laqueus</i>	120	37.80	9108	1946	373	193	14.40	2.30	3.60	8.10	3.52	2.25
<i>liasicus - laqueus</i>	120	38.10	9497	2103	409	185	15.20	2.50	4.20	7.60	3.04	1.81
<i>liasicus - laqueus</i>	120	38.40	9594	2023	414	166	15.40	2.40	4.40	6.30	2.63	1.43
<i>liasicus - laqueus</i>	120	38.70	9049	1793	413	205	13.90	2.00	4.20	8.60	4.30	2.05
<i>liasicus - laqueus</i>	120	39.00	9036	1827	407	168	14.00	2.10	4.40	6.50	3.10	1.48
<i>liasicus - laqueus</i>	120	39.30	10526	2341	468	215	16.20	2.90	4.70	9.30	3.21	1.98
<i>liasicus - laqueus</i>	120	39.60	9006	3486	680	149	13.30	2.00	3.60	5.50	2.75	1.53
<i>liasicus - laqueus</i>	360	39.90	15030	3172	636	304	11.30	1.80	3.10	5.80	3.22	1.87
<i>liasicus - laqueus</i>	360	40.20	14966	3262	722	272	11.20	1.80	3.90	4.80	2.67	1.23
<i>liasicus - laqueus</i>	360	40.50	14788	2998	700	290	11.00	1.70	3.60	5.30	3.12	1.47
<i>liasicus - laqueus</i>	360	40.80	15120	2986	514	301	11.40	1.60	3.70	5.70	3.56	1.54
<i>liasicus - laqueus</i>	360	41.10	13694	2890	638	230	10.00	1.60	3.10	5.80	3.63	1.87
<i>liasicus - laqueus</i>	360	41.40	13736	2792	634	256	10.00	1.50	3.20	4.50	3.00	1.41
<i>liasicus - laqueus</i>	360	41.70	13294	2632	684	238	9.60	1.40	2.70	4.00	2.86	1.48
<i>liasicus - laqueus</i>	360	42.00	13180	2720	510	256	9.40	1.60	2.30	4.50	2.81	1.96
<i>liasicus - laqueus</i>	240	42.30	9126	1618	396	140	9.40	1.40	3.10	3.10	2.21	1.00
<i>angulata</i>	240	42.60	13174	3086	652	304	17.10	2.80	5.40	9.50	3.39	1.76
<i>angulata</i>	240	42.90	13478	2786	634	280	16.60	2.40	5.00	8.90	3.71	1.78
<i>angulata</i>	120	43.20	9136	1431	419	152	18.20	2.40	7.30	9.60	4.00	1.32

Table 2.01 (5 of 5)

Biostratigraphy	Time Secs	Height m	Total Number of Counts			Total µg	Elemental Concentration		Ratios	
			Total	K	U		Th	K%	U ppm	Th/K
<i>angulata</i> Zone	240	43.50	10558	2098	500	208	1.70	4.00	3.53	1.50
<i>angulata</i> Zone	240	43.80	10812	1280	500	214	2.10	3.90	2.95	1.59
<i>angulata</i> Zone	240	44.10	11660	1250	450	203	2.00	4.50	2.85	1.27
<i>angulata</i> Zone	240	44.40	11940	2418	594	224	2.00	4.80	3.25	1.35
<i>angulata</i> Zone	240	44.70	10540	2356	536	232	2.00	4.20	3.55	1.69
<i>angulata</i> Zone	240	45.00	9432	1898	422	177	1.60	3.20	2.88	1.44
<i>angulata</i> Zone	240	45.30	9992	1914	428	219	1.60	2.10	4.06	3.10
<i>angulata</i> Zone	240	45.60	10048	2112	480	185	1.80	3.80	2.78	1.32
<i>angulata</i> Zone	240	45.90	10876	2190	546	238	1.80	4.30	4.00	1.67
<i>angulata</i> Zone	240	46.20	13508	2728	686	219	2.30	6.00	2.70	1.03
<i>angulata</i> Zone	240	46.50	15980	3396	778	290	3.00	6.60	3.10	1.41
<i>angulata</i> Zone	120	46.80	9175	1625	390	127	2.80	6.90	2.75	1.12
<i>angulata</i> Zone	120	47.10	9100	1592	385	154	2.80	6.40	3.57	1.56
<i>angulata</i> Zone	240	47.40	15428	3088	758	272	2.80	6.50	3.00	1.29
<i>angulata</i> Zone	240	47.70	14474	2956	676	156	2.60	5.40	3.77	1.81
<i>angulata</i> Zone	240	48.00	15224	3202	714	167	2.80	5.80	3.50	1.69
<i>angulata</i> Zone	120	48.30	9005	1670	354	145	3.00	5.90	3.10	1.58
<i>angulata</i> Zone	120	48.60	9102	1693	408	213	3.00	6.40	5.00	2.34
<i>angulata</i> Zone	240	48.90	15780	3892	780	256	2.80	6.90	2.75	1.12
<i>angulata</i> Zone	240	49.20	13936	2804	700	232	2.40	6.10	2.88	1.13
<i>angulata</i> Zone	240	49.50	13920	2842	666	272	2.50	5.50	3.36	1.53
<i>angulata</i> Zone	240	49.80	12740	2562	650	251	2.30	5.40	3.30	1.41
<i>angulata</i> Zone	240	50.10	12812	2568	686	255	2.10	5.80	3.62	1.31
<i>angulata</i> Zone	240	50.40	12792	2396	670	222	1.90	5.60	3.47	1.18
<i>angulata</i> Zone	240	50.70	12000	3546	640	190	1.90	5.60	2.74	0.93

Table 2.02 Gamma-ray data-set for the *angulata* Zone and *bucklandi* Zone (*conybeari* and *rotiforme* Subzones) exposed east of Kilve Pylle, Somerset (ST 144455 to ST 153452). The 154 sets of measurements were collected from cliff section apart from the stratigraphic interval represented between 51.90 m and 63.30 m, which was measured on the foreshore. All readings were taken with the Leeds University GR-256 during the period 26th August - 30th August 1995. Measurements were taken with the detector parallel to bedding except for readings taken on the foreshore where the detector was placed perpendicular to bedding. Sets of measurements denoted by ** indicate a poor sample geometry. (1 of 5).

<u>Biostratigraphy</u>	<u>Time</u> Secs	<u>Height</u> m	<u>Total Number of Counts</u>			<u>Total</u> µg	<u>Elemental Concentration</u>		<u>Ratios</u>		
			<u>K</u>	<u>U</u>	<u>Th</u>		<u>K %</u>	<u>U ppm</u>	<u>Th/K</u>	<u>Th/U</u>	
<i>angulata</i> Zone	240	51.00	12304	2326	590	256	1.90	4.70	8.00	4.21	1.70
<i>angulata</i> Zone	240	51.30	13596	2804	696	248	2.40	6.00	7.60	3.17	1.27
<i>angulata</i> Zone	240	51.60	12944	2596	720	204	2.10	6.10	8.40	4.00	1.38
<i>angulata</i> Zone **	240	51.90	12540	2568	624	248	2.20	5.10	7.60	3.45	1.49
<i>angulata</i> Zone **	240	52.20	14018	2836	790	219	2.40	6.00	6.20	2.58	1.03
<i>angulata</i> Zone	240	52.50	12696	2476	602	219	2.10	5.00	6.40	3.05	1.28
<i>angulata</i> Zone **	240	52.80	11650	2340	534	214	2.00	4.30	6.20	3.10	1.44
<i>angulata</i> Zone **	240	53.10	10028	1932	460	195	1.60	3.60	5.50	3.44	1.53
<i>angulata</i> Zone **	240	53.40	11872	2230	640	232	1.70	5.40	6.90	4.06	1.28
<i>angulata</i> Zone	240	53.70	10828	2104	430	243	1.70	4.10	7.60	4.47	1.85
<i>angulata</i> Zone	240	54.00	11894	2246	618	201	1.80	5.30	7.20	4.00	1.36
<i>angulata</i> Zone	240	54.30	11060	2078	608	206	1.60	5.20	5.90	3.69	1.13
<i>angulata</i> Zone	240	54.60	12532	2408	418	219	2.00	5.90	6.20	3.10	1.05
<i>angulata</i> Zone	240	54.90	11578	2286	536	193	1.90	4.40	5.20	2.74	1.18
<i>angulata</i> Zone	240	55.20	11614	2110	592	193	1.70	5.10	5.20	3.06	1.02
<i>angulata</i> Zone	240	55.50	10758	2086	566	182	1.70	4.80	4.60	2.71	0.96
<i>angulata</i> Zone	240	55.80	14816	29190	738	243	2.50	6.40	7.70	3.08	1.20
<i>angulata</i> Zone	240	56.10	13652	2686	722	278	2.20	6.10	8.60	3.91	1.41
<i>angulata</i> Zone	240	56.40	14378	2878	766	280	2.40	6.60	8.80	3.67	1.33
<i>angulata</i> Zone **	240	57.00	10274	1958	516	224	1.60	4.10	6.50	4.06	1.59
<i>angulata</i> Zone **	240	57.30	10592	2112	538	201	1.70	4.40	5.70	3.35	1.30
<i>angulata</i> Zone **	240	57.60	13302	2761	682	269	2.30	5.70	8.40	3.65	1.47
<i>angulata</i> Zone **	240	57.90	13276	2714	640	177	2.30	9.90	6.70	2.91	0.68
<i>angulata</i> Zone **	240	58.20	12365	2522	304	240	2.10	5.00	7.20	3.43	1.44
<i>angulata</i> Zone	240	58.50	9916	1938	508	195	1.50	4.10	5.50	3.67	1.34
<i>angulata</i> Zone	360	58.80	10317	1770	633	158	0.70	3.60	1.72	2.46	0.48
<i>angulata</i> Zone	360	59.10	9981	1704	570	182	0.70	3.20	2.60	3.71	0.81
<i>angulata</i> Zone	240	59.40	11572	4064	340	427	1.50	5.90	6.00	4.00	1.02
<i>angulata</i> Zone	240	59.70	14274	2512	1022	240	1.70	4.80	6.70	3.94	1.40
<i>angulata</i> Zone	240	60.00	16156	2766	1168	266	1.80	5.30	7.70	4.28	1.45

Table 2.02 (2 of 5)

<u>Biostratigraphy</u>	<u>Time</u> Secs	<u>Height</u> m	<u>Total Number of Counts</u>			<u>Total</u> ur	<u>Elemental Concentration</u>			<u>Ratios</u>		
			<u>Total</u>	<u>K</u>	<u>U</u>		<u>Th</u>	<u>K %</u>	<u>U ppm</u>	<u>Th ppm</u>	<u>Th/K</u>	<u>Th/U</u>
angulata Zone	240	60.30	15918	2692	246	248	12.00	1.70	6.30	6.90	4.06	1.10
angulata Zone	240	60.60	14314	2680	946	190	11.30	2.00	3.90	4.80	2.40	1.23
angulata Zone	240	60.90	14006	2638	882	224	10.60	2.00	3.60	6.00	3.00	1.67
angulata Zone	240	61.20	10846	1998	802	176	10.50	1.50	3.30	4.50	3.00	1.36
angulata Zone	360	61.50	10821	2049	528	268	7.10	1.00	2.70	3.10	3.10	1.15
angulata Zone	480	61.80	10532	1632	548	132	4.20	0.60	2.20	1.60	2.67	0.73
angulata Zone **	480	62.10	11184	1864	560	200	4.70	0.60	2.00	1.90	3.17	0.95
angulata Zone **	480	62.40	10552	1700	432	174	4.20	0.50	1.40	1.60	3.20	1.14
angulata Zone **	480	62.70	10396	1876	552	195	3.10	0.60	2.00	1.70	2.83	0.85
angulata Zone	360	63.00	9576	1701	480	174	5.90	0.80	2.40	2.60	3.25	1.08
angulata Zone	480	63.30	11804	2064	596	233	5.10	0.70	2.30	1.60	2.29	0.70
angulata Zone	240	63.60	9043	1346	494	145	8.50	0.80	4.30	3.30	4.13	0.77
angulata Zone	360	63.90	9261	1800	720	206	7.70	0.70	4.20	2.90	4.14	0.69
angulata Zone	480	64.20	11264	1824	688	158	4.80	0.50	2.90	1.40	2.80	0.48
angulata Zone	240	64.50	9006	1266	474	301	9.40	0.80	5.10	3.30	4.13	0.65
angulata Zone	360	64.80	11445	1779	705	170	7.70	0.70	4.20	1.90	2.71	0.45
angulata Zone	240	65.10	9009	1478	618	119	9.30	0.90	5.80	1.90	2.11	0.33
angulata Zone	240	65.40	10040	1640	768	166	11.30	0.90	7.30	3.80	4.22	0.52
angulata Zone	360	65.70	11655	2118	687	182	7.90	1.00	4.00	2.20	2.20	0.55
angulata Zone	360	66.00	9984	1719	621	150	6.30	0.70	3.60	1.60	2.29	0.44
angulata Zone	360	66.30	9306	1620	495	139	5.60	0.70	2.70	1.40	2.00	0.52
angulata Zone	360	66.60	10500	1743	612	226	6.80	0.70	3.40	3.40	4.86	1.00
angulata Zone	360	66.90	11028	192	627	194	6.30	0.90	3.50	2.60	2.89	0.74
angulata Zone	360	67.20	9816	1650	531	115	6.10	3.00	0.50	0.90	0.30	1.80
angulata Zone	360	67.50	11985	2016	705	154	8.30	0.90	4.20	1.40	1.56	0.33
angulata Zone	240	67.80	12114	2026	844	163	14.40	1.30	8.20	3.80	2.92	0.46
angulata Zone	240	68.10	13454	2330	960	216	16.40	1.50	9.20	6.80	4.53	0.74
angulata Zone **	240	68.40	12324	2198	730	182	14.70	1.60	6.70	4.50	2.81	0.67
angulata Zone **	240	68.70	12174	2172	702	195	14.50	1.60	6.30	5.30	3.31	0.84
angulata Zone **	240	69.00	11810	2114	698	198	13.90	1.50	6.30	5.50	3.67	0.87

Table 2.02 (3 of 5).

Biostratigraphy	Time Secs	Height m	Total Number of Counts			Total µr	Elemental Concentration		Ratios			
			Total	K	U		Th	K %	U ppm	Th ppm	Th/K	Th/U
<i>angulata</i> Zone **	240	69.30	11410	2082	692	180	13.30	1.50	6.30	4.60	3.07	0.73
<i>angulata</i> Zone **	240	69.60	12536	2256	690	259	14.00	1.70	5.80	8.10	4.76	1.40
<i>angulata</i> Zone	240	69.90	10720	2014	588	193	11.30	1.50	5.10	5.20	3.47	1.02
<i>angulata</i> Zone	480	70.20	13096	2244	1088	204	6.10	0.70	2.60	2.90	4.14	1.12
<i>angulata</i> Zone	480	70.50	11868	2152	560	196	5.20	0.70	1.90	2.80	4.00	1.47
<i>angulata</i> Zone	240	70.80	13322	3596	732	203	14.70	1.80	6.70	5.50	3.06	0.82
<i>angulata</i> Zone	120	71.10	9362	1649	735	267	24.20	2.10	14.80	7.60	3.62	0.51
<i>angulata</i> Zone	120	71.40	9665	1756	740	271	25.10	2.40	14.90	7.70	3.21	0.52
<i>angulata</i> Zone	120	71.70	9006	1602	632	285	22.80	2.30	12.20	8.90	3.87	0.73
<i>angulata</i> Zone	120	72.00	9015	1543	530	251	20.30	2.30	10.20	6.90	3.00	0.68
<i>angulata</i> Zone	240	72.30	12892	2310	852	293	15.50	1.60	7.70	8.80	5.50	1.14
<i>bucklandi</i> - <i>conybeari</i>	240	72.60	12278	2234	908	198	14.80	1.50	3.80	5.30	3.53	1.39
<i>bucklandi</i> - <i>conybeari</i>	240	72.90	10312	2020	620	214	11.70	1.50	5.30	6.00	4.00	1.13
<i>bucklandi</i> - <i>conybeari</i>	240	73.20	10378	2024	584	166	11.80	1.60	5.20	4.00	2.50	0.77
<i>bucklandi</i> - <i>conybeari</i>	240	73.50	11038	2038	720	206	12.80	1.40	6.50	5.70	4.07	0.88
<i>bucklandi</i> - <i>conybeari</i>	240	73.80	14736	2564	1128	280	18.30	1.60	10.80	8.40	5.25	0.78
<i>bucklandi</i> - <i>conybeari</i>	240	74.10	15260	2568	1064	270	19.00	1.80	10.10	8.10	4.50	0.80
<i>bucklandi</i> - <i>conybeari</i>	240	74.40	15788	2676	1344	238	19.80	1.50	13.70	7.20	4.80	0.53
<i>bucklandi</i> - <i>conybeari</i>	240	74.70	10298	1690	854	148	27.00	2.00	17.40	8.40	4.20	0.48
<i>bucklandi</i> - <i>conybeari</i>	240	75.00	9254	1410	886	127	8.70	0.90	4.20	7.70	8.56	1.83
<i>bucklandi</i> - <i>conybeari</i>	240	75.30	13352	2360	926	211	16.20	1.60	8.80	5.70	3.56	0.65
<i>bucklandi</i> - <i>conybeari</i>	240	75.60	12964	2550	750	193	15.60	2.00	6.90	5.00	2.50	0.72
<i>bucklandi</i> - <i>conybeari</i>	240	75.90	12272	2394	690	282	14.60	1.90	5.90	8.90	4.68	1.51
<i>bucklandi</i> - <i>conybeari</i>	240	76.20	9122	1518	402	156	9.30	1.00	4.60	3.60	3.60	0.78
<i>bucklandi</i> - <i>conybeari</i>	240	76.50	13080	2382	812	221	15.80	1.70	7.30	7.40	4.35	1.01
<i>bucklandi</i> - <i>conybeari</i>	240	76.80	9692	1260	356	134	10.40	0.90	2.70	2.90	3.22	1.07
<i>bucklandi</i> - <i>conybeari</i>	240	77.10	13684	2666	678	224	16.70	2.30	6.30	3.90	1.70	0.62
<i>bucklandi</i> - <i>conybeari</i>	240	77.40	13468	2686	714	240	16.50	2.20	6.20	7.10	3.23	1.15
<i>bucklandi</i> - <i>conybeari</i>	240	77.70	14358	2614	1022	348	17.50	1.50	9.00	7.90	5.27	0.88

Table 2.02 (4 of 5)

<u>Biostratigraphy</u>	<u>Time</u> <u>Secs</u>	<u>Height</u> <u>m</u>	<u>Total Number of Counts</u>			<u>Total</u> <u>ur</u>	<u>Elemental Concentration</u>		<u>Ratios</u>	
			<u>K</u>	<u>U</u>	<u>Th</u>		<u>K %</u>	<u>U ppm</u>	<u>Th/K</u>	<u>Th/U</u>
<i>bucklandi - conybeari</i>	240	78.00	14178	2570	1048	275	1.70	8.90	4.76	0.91
<i>bucklandi - conybeari</i>	240	78.30	14052	2598	978	259	1.80	9.20	4.28	0.84
<i>bucklandi - conybeari</i>	240	78.60	10512	2036	632	177	1.50	5.70	3.00	0.79
<i>bucklandi - conybeari</i>	240	78.90	11379	2089	796	206	1.40	7.40	4.07	0.77
<i>bucklandi - conybeari</i>	240	79.20	10652	2070	622	210	1.60	5.30	3.63	1.09
<i>bucklandi - conybeari</i>	240	79.50	12134	2337	725	246	1.90	5.50	3.89	1.35
<i>bucklandi - conybeari</i>	240	79.80	14210	2830	871	304	2.20	7.70	4.36	1.25
<i>bucklandi - conybeari</i>	240	80.10	15031	2831	892	335	2.20	7.80	5.00	1.41
<i>bucklandi - conybeari</i>	240	80.40	14143	2806	889	263	2.20	8.10	3.55	0.96
<i>bucklandi - conybeari</i>	240	80.70	13683	2732	777	263	2.20	6.80	3.59	1.16
<i>bucklandi - conybeari</i>	240	81.00	13930	2719	845	236	2.20	7.80	3.27	0.92
<i>bucklandi - conybeari</i>	240	81.30	13853	2677	869	260	2.00	7.90	2.25	0.57
<i>bucklandi - conybeari</i>	240	81.60	15709	3087	925	306	2.50	8.30	3.92	1.18
<i>bucklandi - conybeari</i>	240	81.90	15752	2962	976	329	2.30	8.80	4.65	1.22
<i>bucklandi - conybeari</i>	240	82.20	16153	3120	996	308	2.40	9.10	4.21	1.11
<i>bucklandi - conybeari</i>	240	82.50	10615	2132	640	213	2.30	7.60	3.83	1.16
<i>bucklandi - conybeari</i>	240	82.80	10674	2042	626	234	2.10	7.20	4.81	1.40
<i>bucklandi - conybeari</i>	240	83.10	10103	2030	559	236	2.20	6.20	4.59	1.63
<i>bucklandi - conybeari</i>	240	83.40	9009	1575	517	181	1.50	6.00	4.73	1.18
<i>bucklandi - conybeari</i>	240	83.70	10682	2155	624	259	2.30	7.20	4.35	1.39
<i>bucklandi - conybeari</i>	240	84.00	9433	1639	491	166	1.70	5.60	3.76	1.14
<i>bucklandi - conybeari</i>	240	84.30	11410	2257	696	203	1.70	6.20	3.24	0.89
<i>bucklandi - conybeari</i>	240	84.60	14021	2898	610	304	2.40	7.00	4.00	1.37
<i>bucklandi - conybeari</i>	240	84.90	13828	2738	771	297	2.30	6.50	4.13	1.46
<i>bucklandi - conybeari</i>	240	85.20	13993	2863	800	319	2.30	6.80	4.48	1.51
<i>bucklandi - conybeari</i>	240	85.50	14264	2782	621	302	2.20	7.10	4.36	1.35
<i>bucklandi - conybeari</i>	240	85.80	10493	2137	613	227	2.30	7.10	4.17	1.35
<i>bucklandi - conybeari</i>	240	86.10	10925	2172	606	232	2.40	6.90	4.17	1.45
<i>bucklandi - conybeari</i>	240	86.40	10111	1989	575	198	2.10	6.70	3.86	1.21

Table 2.02 (5 of 5)

Biostratigraphy	Time Secs	Height m	Total Number of Counts			Total µr	Elemental Concentration		Ratios		
			Total	K	U		K %	U ppm	Th/K	Th/U	
<i>bucklandi - bucklandi</i>	240	86.70	13702	2352	962	214	1.60	9.20	5.70	3.56	0.62
<i>bucklandi - bucklandi</i>	240	87.00	13480	2340	888	261	1.60	8.20	7.70	4.81	0.94
<i>bucklandi - bucklandi</i>	240	87.30	13224	2314	934	282	1.50	8.60	8.60	5.73	1.00
<i>bucklandi - bucklandi</i> **	240	87.60	13182	2388	848	211	1.60	8.00	5.80	3.63	0.73
<i>bucklandi - bucklandi</i>	240	87.90	9005	1543	624	172	2.70	11.80	11.00	4.07	0.93
<i>bucklandi - bucklandi</i>	240	88.20	13934	2214	864	82	1.50	8.00	6.90	4.60	0.86
<i>bucklandi - bucklandi</i>	240	88.50	13406	2356	894	235	1.60	8.30	6.70	4.19	0.81
<i>bucklandi - bucklandi</i>	240	88.80	10944	2130	824	190	1.40	7.80	4.80	3.43	0.62
<i>bucklandi - bucklandi</i>	240	89.10	9844	1722	502	219	1.30	3.90	6.40	4.92	1.64
<i>bucklandi - bucklandi</i>	240	89.40	12822	2200	870	219	1.50	8.20	6.00	4.00	0.73
<i>bucklandi - bucklandi</i>	240	89.70	14166	2370	920	298	1.60	8.30	9.30	5.81	1.12
<i>bucklandi - bucklandi</i>	240	90.00	13490	2532	790	296	2.00	6.60	10.70	5.35	1.62
<i>bucklandi - bucklandi</i>	240	90.30	12258	2144	700	272	1.60	5.90	8.40	5.25	1.42
<i>bucklandi - bucklandi</i>	240	90.60	11838	2140	668	222	1.60	5.80	6.40	4.00	1.10
<i>bucklandi - bucklandi</i>	240	90.90	10072	1868	556	220	1.40	4.30	7.10	5.07	1.65
<i>bucklandi - bucklandi</i>	240	91.20	9770	1884	532	195	1.40	4.40	5.50	3.93	1.25
<i>bucklandi - bucklandi</i> **	240	91.50	9926	1890	536	193	1.40	4.50	5.20	3.71	1.16
<i>bucklandi - bucklandi</i>	240	91.80	12798	2228	748	261	1.60	6.50	7.90	4.94	1.22
<i>bucklandi - bucklandi</i>	240	92.10	10746	1866	628	264	1.40	5.10	8.30	5.93	1.63
<i>bucklandi - bucklandi</i>	240	92.40	13474	2824	804	243	2.30	7.20	7.20	3.13	1.00
<i>bucklandi - bucklandi</i>	240	92.70	10898	1982	648	177	1.40	5.80	4.50	3.21	0.78
<i>bucklandi - bucklandi</i>	240	93.00	13120	2424	770	285	1.90	5.60	9.10	4.79	1.63
<i>bucklandi - bucklandi</i>	240	93.30	13108	2618	692	253	2.20	5.90	7.70	3.50	1.31
<i>bucklandi - bucklandi</i>	240	93.60	12410	2366	650	277	1.90	5.30	8.80	4.63	1.66
<i>bucklandi - bucklandi</i>	240	93.90	9626	1944	516	200	1.50	4.20	5.70	3.80	1.36
<i>bucklandi - bucklandi</i>	240	94.20	13264	2568	632	301	2.20	4.90	10.00	4.55	2.04

Table 2.03 Gamma-ray data-set for the *bucklandi* Zone (*bucklandi* Subzone) exposed west of Kilve Pylle, Somerset (ST 139457 - ST 144455). The 80 sets of measurements were collected from cliff section. All readings were taken with the Leeds University GR-256 during the period 1st September - 3rd September 1995. Measurements were taken with the detector placed perpendicular to the cliff and parallel to bedding, except for readings denoted by ** which indicates a poor sample geometry. (1 of 3).

<u>Biostratigraphy</u>	<u>Time</u> <u>Secs</u>	<u>Height</u> <u>m</u>	<u>Total Number of Counts</u>			<u>Total</u> <u>ur</u>	<u>Elemental Concentration</u>			<u>Ratios</u>	
			<u>K</u>	<u>U</u>	<u>Th</u>		<u>K %</u>	<u>U ppm</u>	<u>Th ppm</u>	<u>Th/K</u>	<u>Th/U</u>
<i>bucklandi - bucklandi</i>	240	94.50	14254	2644	810	346	2.10	6.80	11.50	5.48	1.69
<i>bucklandi - bucklandi</i>	240	94.80	10764	2320	542	269	2.00	4.10	8.60	4.30	2.10
<i>bucklandi - bucklandi</i>	240	95.10	10876	2108	556	256	1.70	4.30	7.90	4.65	1.84
<i>bucklandi - bucklandi</i>	240	95.40	11296	2054	578	230	1.60	4.70	6.70	4.19	1.43
<i>bucklandi - bucklandi</i>	240	95.70	11752	2308	532	243	2.00	4.10	7.60	3.80	1.85
<i>bucklandi - bucklandi</i>	240	96.00	12040	2342	614	283	1.90	4.80	8.90	4.68	1.85
<i>bucklandi - bucklandi</i>	240	96.30	12168	2346	608	272	1.90	4.80	8.60	4.53	1.79
<i>bucklandi - bucklandi</i>	240	96.60	11226	2192	534	246	1.80	4.10	7.60	4.22	1.85
<i>bucklandi - bucklandi</i>	240	96.90	15012	2726	882	333	2.10	7.60	11.00	5.24	1.45
<i>bucklandi - bucklandi</i>	240	97.20	14388	2798	802	330	2.10	6.70	10.80	5.14	1.61
<i>bucklandi - bucklandi</i>	240	97.50	11956	2328	640	282	1.90	5.20	8.90	4.68	1.71
<i>bucklandi - bucklandi</i>	240	97.80	12702	2338	664	277	1.90	5.50	8.80	4.63	1.60
<i>bucklandi - bucklandi</i>	240	98.10	11786	2354	590	298	2.00	4.50	9.80	4.90	2.18
<i>bucklandi - bucklandi</i>	240	98.40	12650	2504	628	277	2.10	5.00	5.80	2.80	1.16
<i>bucklandi - bucklandi</i>	240	98.70	10876	2250	528	201	1.90	4.30	5.70	3.00	1.33
<i>bucklandi - bucklandi</i>	240	99.00	13016	2538	624	253	2.10	5.10	7.90	3.76	1.55
<i>bucklandi - bucklandi</i>	240	99.30	11158	1356	423	249	1.00	1.70	4.10	4.10	2.41
<i>bucklandi - bucklandi</i>	240	99.60	10146	2098	638	232	1.60	5.30	6.90	4.31	1.30
<i>bucklandi - bucklandi</i>	240	99.90	12838	2848	657	150	1.90	6.80	8.80	4.63	1.29
<i>bucklandi - bucklandi</i>	240	100.20	13118	2556	806	162	2.00	7.40	5.80	2.90	0.78
<i>bucklandi - bucklandi</i>	240	100.50	10252	1918	544	238	1.50	4.30	7.20	4.80	1.67
<i>bucklandi - bucklandi</i>	240	100.80	9198	1794	452	172	1.40	3.60	4.50	3.21	1.25
<i>bucklandi - bucklandi</i>	240	101.10	10760	2084	522	283	1.70	3.80	9.20	5.41	2.42
<i>bucklandi - bucklandi</i>	240	101.40	12214	2406	602	251	2.00	4.90	7.70	3.85	1.57
<i>bucklandi - bucklandi</i>	240	101.70	10540	2104	488	232	1.80	3.70	7.10	3.94	1.92
<i>bucklandi - bucklandi</i>	240	102.00	10914	2138	526	222	1.80	4.10	6.50	3.61	1.59
<i>bucklandi - bucklandi</i>	240	102.30	11904	2306	586	251	1.90	4.70	7.70	4.05	1.64
<i>bucklandi - bucklandi</i>	240	102.60	11398	226	592	211	1.80	5.00	6.00	3.33	1.20

Table 2.03 (2 of 3).

<u>Biostratigraphy</u>	<u>Time</u> Secs	<u>Height</u> m	<u>Total Number of Counts</u>			<u>Total</u> µr	<u>Elemental Concentration</u>			<u>Ratios</u>		
			<u>Total</u>	<u>K</u>	<u>U</u>		<u>Th</u>	<u>K %</u>	<u>U ppm</u>	<u>Th ppm</u>	<u>Th/K</u>	<u>Th/U</u>
<i>bucklandi - bucklandi</i>	240	102.90	10504	2006	514	237	12.00	1.60	3.90	7.20	4.50	1.85
<i>bucklandi - bucklandi</i>	240	103.20	9872	1778	492	191	11.10	1.40	4.00	5.30	3.79	1.33
<i>bucklandi - bucklandi</i>	240	103.50	8978	776	470	193	9.70	1.20	3.70	5.30	4.42	1.43
<i>bucklandi - bucklandi</i>	240	103.80	10935	2994	516	356	15.20	1.30	7.50	6.90	5.31	0.92
<i>bucklandi - bucklandi</i>	240	104.10	12634	2292	644	221	15.10	1.80	5.50	6.50	3.61	1.18
<i>bucklandi - bucklandi</i>	240	104.40	12464	2466	688	230	14.90	2.00	6.00	6.80	3.40	1.13
<i>bucklandi - bucklandi</i>	240	104.70	12390	2304	576	238	14.70	1.90	5.70	7.20	3.79	1.26
<i>bucklandi - bucklandi</i>	240	105.00	12772	2248	684	238	15.40	2.00	5.90	7.10	3.55	1.20
<i>bucklandi - bucklandi</i>	240	105.30	12796	2470	664	253	15.40	2.00	5.60	7.70	3.85	1.38
<i>bucklandi - bucklandi</i>	240	105.60	10142	1888	568	227	11.50	1.40	4.60	6.70	4.79	1.46
<i>bucklandi - bucklandi</i>	240	105.90	11514	2260	570	248	13.50	1.90	4.50	7.70	4.05	1.71
<i>bucklandi - bucklandi</i>	240	106.20	9076	1932	530	227	11.10	1.50	4.20	6.90	4.60	1.64
<i>bucklandi - bucklandi</i>	240	106.50	10356	2236	578	245	13.60	1.80	4.60	7.40	4.11	1.61
<i>bucklandi - bucklandi</i>	240	106.80	12882	2658	594	235	9.20	1.50	3.10	3.80	2.53	1.23
<i>bucklandi - bucklandi</i>	240	107.10	10580	2086	528	203	12.10	1.70	4.30	5.80	3.41	1.35
<i>bucklandi - bucklandi</i>	240	107.40	9738	1928	532	216	10.90	1.50	4.30	6.30	4.20	1.47
<i>bucklandi - bucklandi</i>	240	107.70	11508	2160	402	226	12.20	0.90	2.60	4.30	4.78	1.65
<i>bucklandi - bucklandi</i>	240	108.00	9908	213	555	238	11.10	1.00	2.70	4.00	4.00	1.48
<i>bucklandi - bucklandi</i>	240	108.30	12764	2634	734	293	15.30	1.90	5.20	9.30	4.89	1.79
<i>bucklandi - bucklandi</i>	240	108.60	13104	2634	634	240	15.80	2.00	5.90	8.50	4.25	1.44
<i>bucklandi - bucklandi</i>	240	108.90	10960	2010	474	214	12.70	1.50	5.00	6.00	4.00	1.20
<i>bucklandi - bucklandi</i>	240	109.20	9514	1646	430	198	10.50	1.20	4.40	5.50	4.58	1.25
<i>bucklandi - bucklandi</i>	240	109.50	11134	2198	618	200	12.90	1.60	5.30	5.50	3.44	1.04
<i>bucklandi - bucklandi</i> **	240	109.80	10564	2038	578	232	12.10	1.50	4.70	7.10	4.73	1.51
<i>bucklandi - bucklandi</i> **	240	110.10	10356	1784	544	201	11.80	1.30	4.50	5.70	4.38	1.27
<i>bucklandi - bucklandi</i> **	240	110.40	11922	2166	591	250	8.10	1.10	3.00	4.30	3.91	1.43

Table 2.03 (3 of 3).

Biostratigraphy	Time Secs	Height m	Total Number of Counts			Total µ	Elemental Concentration		Ratios			
			Total	K	U		Th	K %	U ppm	Th/K	Th/U	
<i>semicosatum-lyra</i>	240	127.0	11335	2105	523	271	10.7	1.7	2.8	6.0	3.53	2.14
<i>semicosatum-lyra</i>	240	127.3	10360	1847	493	234	9.6	1.5	2.7	5.1	3.40	1.89
<i>semicosatum-lyra</i>	240	127.6	21942	4479	1235	489	19.0	2.9	6.6	9.5	3.28	1.44
<i>semicosatum-lyra</i>	240	127.9	10224	1862	448	229	9.4	1.6	2.4	4.4	2.75	1.83
<i>semicosatum-lyra</i>	240	128.2	13184	2407	760	303	12.9	1.8	4.8	6.8	3.78	1.42
<i>semicosatum-lyra</i>	240	128.5	12561	2225	778	217	12.2	1.6	5.5	4.4	2.75	0.80
<i>semicosatum-lyra</i>	240	128.8	13062	2533	533	277	10.2	1.8	2.2	5.1	2.83	2.32
<i>semicosatum-lyra</i>	240	129.1	15404	2862	786	336	12.5	1.9	3.9	6.3	3.32	1.62
<i>semicosatum-lyra</i>	240	129.4	11780	2222	546	265	11.3	1.8	3.0	5.9	3.28	1.97
<i>semicosatum-lyra</i>	240	129.7	14350	2935	612	346	11.5	2.1	2.5	6.6	3.14	2.64
<i>semicosatum-lyra</i>	240	130.0	10232	1593	562	191	7.4	1.0	2.9	3.2	3.20	1.10
<i>semicosatum-lyra</i> **	240	130.3	13305	2322	712	314	10.4	1.5	3.4	5.8	3.87	1.71
<i>semicosatum-lyra</i> **	240	130.6	15883	2955	703	413	13.0	2.0	2.9	8.1	4.05	2.79
<i>semicosatum-lyra</i>	240	130.9	10482	1852	538	240	9.7	1.5	3.1	5.2	3.47	1.68
<i>semicosatum-lyra</i>	240	131.2	10935	2140	486	294	10.3	1.8	2.3	6.7	3.72	2.91
<i>semicosatum-lyra</i>	240	131.5	14138	2933	556	340	11.2	2.1	2.1	6.4	3.05	3.05
<i>semicosatum-lyra</i>	240	131.8	14319	3002	605	373	11.4	2.1	2.3	7.2	3.43	3.13
<i>semicosatum-lyra</i>	240	132.1	13584	2623	575	336	10.7	1.8	1.4	6.4	3.56	4.57
<i>semicosatum-lyra</i>	240	132.4	15605	2916	856	339	12.7	1.9	4.4	6.3	3.32	1.43
<i>semicosatum-lyra</i>	240	132.7	9117	1538	435	198	10.8	1.8	3.2	5.2	2.89	1.63
<i>semicosatum-lyra</i>	240	133.0	12788	2571	643	269	14.1	2.3	4.4	6.6	2.87	1.50
<i>semicosatum-lyra</i>	240	133.3	11111	2129	544	235	11.9	1.9	3.6	5.7	3.00	1.58
<i>semicosatum-lyra</i>	240	133.6	12254	2091	679	281	9.4	1.3	3.4	5.2	4.00	1.53

Table 2.04 Gamma-ray data-set for the *semicosatum* Zone (*lyra* Subzone) exposed at the west end of Doniford Bay, Somerset (ST 1079433 - ST 082430). The 122 sets of measurements were collected from cliff section. All readings were taken with the Edinburgh University GR-256 during the period 19th September - 21st September 1995. Measurements were taken with the detector placed perpendicular to the cliff and parallel to bedding, except for readings denoted by ** which indicates a poor sample geometry. (1 of 5).

<u>Biostratigraphy</u>	<u>Time</u> Secs	<u>Height</u> m	<u>Total Number of Counts</u>			<u>Total</u> µr	<u>Elemental Concentration</u>		<u>Ratios</u>			
			<u>Total</u>	<u>K</u>	<u>U</u>		<u>Th</u>	<u>K %</u>	<u>U ppm</u>	<u>Th ppm</u>	<u>Th/K</u>	<u>Th/U</u>
<i>semicosatum-lyra</i>	240	133.9	12021	2086	544	277	9.2	1.4	2.3	5.1	3.64	2.22
<i>semicosatum-lyra</i>	240	134.2	11972	2175	649	239	11.5	1.7	4.1	5.1	3.00	1.24
<i>semicosatum-lyra</i>	240	134.5	15190	2958	897	291	15.3	2.2	6.1	6.3	2.86	1.03
<i>semicosatum-lyra</i>	240	134.8	12339	2426	572	321	11.9	2.0	3.0	7.3	3.65	2.43
<i>semicosatum-lyra</i>	240	135.1	13487	2335	828	248	13.3	1.7	5.7	5.3	3.12	0.93
<i>semicosatum-lyra</i> **	240	135.4	12260	2374	534	353	15.5	2.5	3.2	10.3	4.12	3.22
<i>semicosatum-lyra</i> **	200	135.7	11024	2148	477	316	16.9	2.6	4.3	10.9	4.19	2.53
<i>semicosatum-lyra</i> **	240	136.0	10753	2115	469	348	13.3	2.2	2.5	10.2	4.64	4.08
<i>semicosatum-lyra</i>	240	136.3	10415	2118	393	312	12.7	2.3	1.9	9.1	3.96	4.79
<i>semicosatum-lyra</i>	240	136.6	10076	2016	423	303	12.2	2.1	2.3	8.8	4.19	3.83
<i>semicosatum-lyra</i>	200	136.9	9875	2047	394	243	14.9	2.6	3.0	8.2	3.15	2.73
<i>semicosatum-lyra</i> **	240	137.2	13216	2784	514	405	16.9	3.0	2.6	12.1	4.03	4.65
<i>semicosatum-lyra</i>	200	137.5	10407	2000	475	313	15.8	2.4	3.2	10.4	4.33	3.25
<i>semicosatum-lyra</i> **	200	137.8	12261	2544	483	344	19.1	3.1	3.6	12.1	3.90	3.36
<i>semicosatum-lyra</i> **	200	138.1	9649	1861	488	268	14.5	2.2	4.1	9.1	4.14	2.22
<i>semicosatum-lyra</i> **	240	138.4	10597	2195	418	329	13.0	2.4	2.0	9.6	4.00	4.80
<i>semicosatum-lyra</i>	200	138.7	9534	1891	443	287	14.3	2.3	3.3	9.9	4.30	3.00
<i>semicosatum-lyra</i>	180	139.0	9086	1854	366	256	13.5	2.4	2.5	8.7	3.63	3.48
<i>semicosatum-lyra</i>	180	139.3	9660	1962	401	310	14.5	2.5	2.5	10.9	4.36	4.36
<i>semicosatum-lyra</i>	180	139.6	9998	1935	372	292	15.1	2.5	2.3	10.1	4.04	4.39
<i>semicosatum-lyra</i>	240	139.9	14032	2883	625	416	18.1	3.0	3.8	12.4	4.13	3.26
<i>semicosatum-lyra</i>	180	140.2	9430	1797	397	306	14.1	2.3	2.6	10.6	4.61	4.08
<i>semicosatum-lyra</i>	240	140.5	13996	2962	557	350	18.1	3.1	3.5	10.2	3.29	2.91
<i>semicosatum-lyra</i>	180	140.8	9651	1934	344	314	14.5	2.5	1.7	11.1	4.44	6.53
<i>semicosatum-lyra</i>	180	141.1	9428	1933	373	324	16.0	2.8	2.4	12.7	4.54	5.29
<i>semicosatum-lyra</i>	180	141.4	10529	2197	444	322	18.2	3.1	3.4	12.5	4.03	3.68
<i>semicosatum-lyra</i>	180	141.7	9840	1956	378	321	14.8	2.5	2.1	11.3	4.52	5.38
<i>semicosatum-lyra</i>	200	142.0	9928	1983	458	273	15.0	2.4	3.2	9.4	3.92	2.94

Table 2.04 (2 of 5)

<u>Biostratigraphy</u>	<u>Time</u> <u>Secs</u>	<u>Height</u> <u>m</u>	<u>Total Number of Counts</u>			<u>Total</u> <u>µg</u>	<u>Elemental Concentration</u>			<u>Ratios</u>	
			<u>Total</u>	<u>K</u>	<u>U</u>		<u>Th</u>	<u>K %</u>	<u>U ppm</u>	<u>Th ppm</u>	<u>Th/K</u>
<i>semicosatum-lyra</i>	180	142.3	9908	2006	400	297	2.6	2.6	10.4	4.00	4.00
<i>semicosatum-lyra</i>	180	142.6	10366	2040	444	282	2.7	2.6	10.7	3.96	4.12
<i>semicosatum-lyra</i>	200	142.9	10206	2009	476	278	2.5	3.2	9.5	3.80	2.97
<i>semicosatum-lyra</i>	180	143.2	9294	1880	408	295	2.4	2.8	10.2	4.25	3.64
<i>semicosatum-lyra</i>	200	143.5	9147	1694	449	279	2.0	3.5	9.5	4.75	2.71
<i>semicosatum-lyra</i>	200	143.8	9809	1910	446	306	2.4	3.2	10.6	4.42	3.31
<i>semicosatum-lyra</i>	200	144.1	10228	2073	440	292	2.6	3.2	10.1	3.88	3.16
<i>semicosatum-lyra</i>	200	144.4	9803	1950	476	239	2.4	4.2	7.9	3.29	1.88
<i>semicosatum-lyra</i>	200	144.7	11251	2200	525	315	2.7	4.2	10.9	4.04	2.60
<i>semicosatum-lyra</i>	180	145.0	11689	2175	631	356	2.8	6.0	14.0	5.00	2.33
<i>semicosatum-lyra</i>	180	145.3	11549	2246	615	293	2.9	6.3	11.2	3.86	1.78
<i>semicosatum-lyra</i>	180	145.6	10651	2056	546	282	2.7	5.4	10.7	3.96	1.98
<i>semicosatum-lyra</i>	180	145.9	13292	2751	597	445	3.4	4.1	16.0	4.71	3.90
<i>semicosatum-lyra</i>	180	146.2	11074	2138	529	371	2.9	4.3	14.7	5.07	3.42
<i>semicosatum-lyra</i>	180	146.5	16140	3399	671	517	3.6	3.6	15.7	4.36	4.36
<i>semicosatum-lyra</i>	180	146.8	10452	2228	363	323	3.2	2.1	12.7	3.97	6.05
<i>semicosatum-lyra</i>	180	147.1	10423	2267	442	349	3.2	3.2	14.1	4.41	4.41
<i>semicosatum-lyra</i> **	180	147.4	17610	3401	705	538	2.1	1.9	9.2	4.38	4.84
<i>semicosatum-lyra</i>	180	147.7	12295	2451	614	406	3.3	5.3	16.1	4.88	3.04
<i>semicosatum-lyra</i>	180	148.0	13742	2661	659	467	2.7	3.8	14.1	5.22	3.71
<i>semicosatum-lyra</i>	180	148.3	11351	2155	609	318	2.8	6.0	12.3	4.39	2.05
<i>semicosatum-lyra</i>	180	148.6	10385	2045	489	321	2.5	3.7	11.2	4.48	3.03
<i>semicosatum-lyra</i>	180	148.9	11423	2267	540	325	2.3	3.5	9.4	4.09	2.69
<i>semicosatum-lyra</i>	180	149.2	12767	2624	552	384	3.1	3.1	11.4	3.68	3.68
<i>semicosatum-lyra</i>	180	149.5	11685	2239	574	359	3.0	5.1	14.1	4.70	2.76
<i>semicosatum-lyra</i>	180	149.8	11227	2174	372	318	3.1	2.3	12.5	4.03	5.43
<i>semicosatum-lyra</i>	180	150.1	10715	2150	449	301	3.0	3.7	11.6	3.87	3.14
<i>semicosatum-lyra</i>	180	150.4	9112	1648	462	280	2.2	4.2	10.7	4.86	2.55

Table 2.04 (3 of 5)

<u>Biostratigraphy</u>	<u>Time</u> Secs	<u>Height</u> m	<u>Total Number of Counts</u>			<u>Total</u> ur	<u>Elemental Concentration</u>		<u>Ratios</u>			
			<u>Total</u>	<u>K</u>	<u>U</u>		<u>Th</u>	<u>K %</u>	<u>U ppm</u>	<u>Th ppm</u>	<u>Th/K</u>	<u>Th/U</u>
<i>semicosatum-lyra</i>	180	150.7	9796	2047	359	320	16.7	3.0	2.1	12.6	4.20	6.00
<i>semicosatum-lyra</i>	180	151.0	9771	2015	401	324	16.7	2.8	2.8	12.7	4.54	4.54
<i>semicosatum-lyra</i>	180	151.3	9317	1923	350	290	15.8	2.8	2.3	11.3	4.04	4.91
<i>semicosatum-lyra</i>	180	151.6	9899	1997	381	304	16.9	2.8	2.6	11.7	4.18	4.50
<i>semicosatum-lyra</i>	180	151.9	10735	2322	417	361	18.6	3.3	2.6	14.3	4.33	5.50
<i>semicosatum-lyra</i>	180	152.2	10172	1803	631	235	17.5	2.2	7.2	8.5	3.86	1.18
<i>semicosatum-lyra</i>	180	152.5	11138	2331	454	366	15.3	2.7	2.5	11.8	4.37	4.72
<i>semicosatum-lyra</i>	180	152.8	10221	2175	385	339	17.6	3.1	2.4	13.4	4.32	5.58
<i>semicosatum-lyra</i>	180	153.1	10828	2290	389	412	18.7	3.3	1.7	16.6	5.03	9.76
<i>semicosatum-lyra</i>	180	153.4	9711	1989	425	261	14.6	2.5	3.3	8.7	3.48	2.64
<i>semicosatum-lyra</i>	180	153.7	10260	2239	360	355	17.6	3.3	1.8	14.1	4.27	7.83
<i>semicosatum-lyra</i>	180	154.0	10472	2114	472	309	16.0	2.6	3.5	10.7	4.12	3.06
<i>semicosatum-lyra</i>	360	154.3	9258	1547	433	213	8.3	1.3	2.3	4.6	3.54	2.00
<i>semicosatum-lyra</i>	360	154.6	9994	1568	498	243	10.4	1.4	2.6	4.9	3.50	1.88
<i>semicosatum-lyra</i>	360	154.9	12240	2281	527	310	11.7	1.8	2.8	7.1	3.94	2.54
<i>semicosatum-lyra</i>	180	155.2	9562	1889	397	318	16.3	2.7	2.8	12.4	4.59	4.43
<i>semicosatum-lyra</i>	180	155.5	9133	1921	409	324	15.4	2.7	2.9	12.7	4.70	4.38
<i>semicosatum-lyra</i>	240	155.8	9708	1952	374	273	11.7	2.1	1.9	7.8	3.71	4.11
<i>semicosatum-lyra</i>	180	156.1	9142	1748	427	278	13.6	2.1	3.2	9.5	4.52	2.97
<i>semicosatum-lyra</i>	180	156.4	11671	2426	463	410	20.4	3.4	2.9	16.5	4.85	5.69
<i>semicosatum-lyra</i>	180	156.7	10234	2118	403	336	17.6	3.0	2.7	13.2	4.40	4.89
<i>semicosatum-lyra</i>	180	15.07	12357	2511	492	411	19.3	3.2	2.9	14.8	4.63	5.10
<i>semicosatum-lyra</i>	180	157.3	9521	1790	397	332	14.3	2.3	2.3	11.7	5.09	5.09
<i>semicosatum-lyra</i>	180	157.6	10393	2159	413	373	17.9	3.1	2.5	14.8	4.77	5.92
<i>semicosatum-lyra</i>	180	157.9	10770	2321	451	352	18.6	3.3	3.3	13.9	4.21	4.21
<i>semicosatum-lyra</i>	180	158.2	11620	2315	395	376	20.3	3.3	2.2	15.0	4.55	6.82
<i>semicosatum-lyra</i>	180	158.5	13164	2834	493	476	23.4	4.1	2.7	19.4	4.73	7.19
<i>semicosatum-lyra</i>	180	158.8	10341	2199	379	391	17.8	3.2	1.8	15.6	4.88	8.67

Table 2.04 (4 of 5)

<u>Biostratigraphy</u>	<u>Time</u> Secs	<u>Height</u> m	<u>Total Number of Counts</u>			<u>Total</u> µr	<u>Elemental Concentration</u>			<u>Ratios</u>	
			<u>K</u>	<u>U</u>	<u>Th</u>		<u>K %</u>	<u>U ppm</u>	<u>Th ppm</u>	<u>Th/K</u>	<u>Th/U</u>
<i>semicosatum-lyra</i>	180	159.1	2122	310	345	17.2	3.1	1.2	13.7	4.42	11.42
<i>semicosatum-lyra</i>	180	159.4	2134	356	313	17.2	3.1	2.2	12.2	3.94	5.55
<i>semicosatum-lyra</i> **	180	159.7	2118	419	377	17.6	3.0	2.5	15.1	5.03	6.04
<i>semicosatum-lyra</i>	180	160.0	2344	462	340	19.4	3.3	3.5	13.3	4.03	3.80
<i>semicosatum-lyra</i>	180	160.3	2282	412	351	18.7	3.3	2.7	13.9	4.21	5.15
<i>semicosatum-lyra</i>	180	160.6	2258	390	353	17.9	3.3	2.3	14.0	4.24	6.09
<i>semicosatum-lyra</i> **	180	160.9	1993	422	352	15.6	2.5	2.5	12.5	5.00	5.00
<i>semicosatum-lyra</i> **	180	161.2	2294	406	381	18.9	3.3	2.3	15.2	4.61	6.61
<i>semicosatum-lyra</i> **	180	161.5	2127	452	384	17.8	3.0	3.0	15.3	5.10	5.10
<i>semicosatum-lyra</i> **	180	161.8	2209	444	357	18.3	3.1	3.1	14.1	4.55	4.55
<i>semicosatum-lyra</i>	180	162.1	2362	426	378	19.9	3.4	2.6	4.3	1.26	1.65
<i>semicosatum-lyra</i>	180	162.4	2559	434	427	20.9	3.7	2.3	17.2	4.65	7.48
<i>semicosatum-lyra</i>	180	162.7	2228	408	338	17.9	3.2	2.7	13.4	4.19	4.96
<i>semicosatum-lyra</i>	180	163.0	2796	558	440	20.8	3.5	3.5	15.9	4.54	4.54
<i>semicosatum-lyra</i>	180	163.3	2564	500	545	19.5	3.3	2.7	16.1	4.88	5.96
<i>semicosatum-lyra</i>	180	163.6	1890	383	323	16.1	2.7	2.5	12.7	4.70	5.08

Table 2.04 (5 of 5)

Biostratigraphy	Height m	Time Secs	Total Number of Counts			Th	Total µr	Elemental Concentration		Ratios		
			Total	K	U			K.%	U ppm	Th/K	Th/U	
Pre-planorbis Beds	0.0	240	12382	1465	520	222	14.2	2.5	3.8	6.6	2.64	1.74
Pre-planorbis Beds	0.3	360	10677	1170	465	138	6.7	1.2	2.5	2.3	1.92	0.92
Pre-planorbis Beds	0.6	360	15658	1303	453	228	7.6	1.4	1.9	4.3	3.07	2.26
Pre-planorbis Beds	0.9	360	12341	1357	492	213	8.3	1.4	2.3	3.9	2.79	1.70
Pre-planorbis Beds	1.2	360	13896	1679	630	282	9.7	1.7	3.0	5.4	3.18	1.80
Pre-planorbis Beds	1.5	360	12189	1340	549	180	8.2	1.4	2.8	3.5	2.50	1.25
Pre-planorbis Beds	1.8	240	9594	1160	464	174	10.3	1.8	3.6	4.9	2.72	1.36
Pre-planorbis Beds	2.1	240	9950	1208	468	176	10.7	1.9	3.7	5.0	2.63	1.35
Pre-planorbis Beds	2.4	240	10008	1127	418	188	10.8	1.8	2.9	5.4	3.00	1.86
Pre-planorbis Beds	2.7	360	12777	1369	627	225	8.7	1.3	3.3	4.0	3.08	1.21
Pre-planorbis Beds	3.0	360	11883	1345	410	216	7.9	1.4	2.4	4.0	2.86	1.67
Pre-planorbis Beds	3.3	360	12264	1251	489	237	8.2	1.3	2.2	4.3	3.31	1.95
Pre-planorbis Beds	3.6	240	10290	1167	512	194	11.2	1.8	4.1	5.4	3.00	1.32
Pre-planorbis Beds	3.9	240	11178	1211	562	204	12.5	1.8	4.5	5.8	3.22	1.29
Pre-planorbis Beds	4.2	240	10472	1144	568	224	11.5	1.7	4.5	6.4	3.76	1.42
Pre-planorbis Beds	4.5	240	11094	1221	572	212	12.4	1.8	4.6	6.0	3.33	1.30
Pre-planorbis Beds	4.8	240	12768	1608	590	252	14.7	2.6	4.4	7.5	2.88	1.70
planorbis - planorbis	5.1	240	11100	1301	536	212	12.4	2.0	4.2	6.1	3.05	1.45
planorbis - planorbis	5.4	360	10815	1101	441	192	6.8	1.1	2.0	3.4	3.09	1.70
planorbis - planorbis	5.7	240	9826	1011	508	214	10.5	1.5	3.9	6.0	4.00	1.54
planorbis - planorbis	6.0	240	9406	1051	506	180	10.0	1.5	4.1	5.0	3.33	1.22
planorbis - planorbis	6.3	240	9006	890	408	174	8.2	1.3	3.0	4.8	3.69	1.60

Table 2.05 Gamma-ray data-set for the Pre-planorbis Beds to the *Iiasicus* Zone exposed in St. Mary's Well Bay, Glamorgan (ST 176677 - ST 187681). The 96 sets of measurements were collected from cliff section. All readings were taken with the Edinburgh University GR-256 during the period 23rd September - 27th September 1995. Measurements were taken with the detector placed perpendicular to the cliff and parallel to bedding, except for readings denoted by ** which indicates a poor sample geometry. (1 of 4).

<u>Biostratigraphy</u>	<u>Height</u> m	<u>Time</u> Secs	<u>Total Number of Counts</u>		<u>Th</u>	<u>Total</u> ur	<u>Elemental Concentration</u>			<u>Ratios</u>		
			<u>Total</u>	<u>K</u>			<u>U</u>	<u>K %</u>	<u>U ppm</u>	<u>Th ppm</u>	<u>Th/K</u>	<u>Th/U</u>
<i>planorbis - planorbis</i>	6.6	240	12198	1471	528	262	13.9	2.3	3.6	7.8	3.39	2.17
<i>planorbis - planorbis</i>	6.9	240	11468	1374	582	246	12.9	2.1	4.4	7.2	3.43	1.64
<i>planorbis - planorbis</i>	7.2	240	14722	1873	682	294	17.5	3.0	5.0	8.9	2.97	1.78
<i>planorbis - planorbis</i>	7.5	240	13040	1654	600	268	15.2	2.6	4.4	8.1	3.12	1.84
<i>planorbis - johnstoni</i>	7.8	240	12980	1645	644	316	15.1	2.6	4.5	9.6	3.69	2.13
<i>planorbis - johnstoni</i>	8.1	240	11392	1345	582	236	12.8	2.0	4.5	6.9	3.45	1.53
<i>planorbis - johnstoni</i>	8.4	240	9352	1057	464	188	9.9	1.6	3.5	5.3	3.31	1.51
<i>planorbis - johnstoni</i>	8.7	240	10338	1158	566	210	11.3	1.7	4.6	5.9	3.47	1.28
<i>planorbis - johnstoni</i>	9.0	240	9326	1054	454	212	9.8	1.6	3.2	6.1	3.81	1.91
<i>planorbis - johnstoni</i>	9.3	360	13323	1448	639	306	9.2	1.4	2.9	5.8	4.14	2.00
<i>planorbis - johnstoni</i>	9.6	360	11844	1217	519	225	7.8	1.2	2.5	4.0	3.33	1.60
<i>planorbis - johnstoni</i>	9.9	240	11832	1300	672	216	13.4	1.9	5.8	6.1	3.21	1.05
<i>planorbis - johnstoni</i>	10.2	240	13902	1602	852	294	16.3	2.3	7.3	8.3	3.61	1.14
<i>planorbis - johnstoni</i>	10.5	360	12447	1288	642	270	8.4	1.2	3.2	5.0	4.17	1.56
<i>planorbis - johnstoni</i>	10.8	240	15484	1913	774	356	18.6	3.0	6.1	9.2	3.07	1.51
<i>planorbis - johnstoni</i>	11.1	240	14370	1671	820	254	17.0	2.5	7.2	7.3	2.92	1.01
<i>planorbis - johnstoni</i>	11.4	240	13334	1618	718	254	15.5	7.5	5.9	7.4	0.99	1.25
<i>planorbis - johnstoni</i>	11.7	240	13764	3046	702	327	19.4	2.7	5.2	12.6	4.65	2.44
<i>planorbis - johnstoni</i>	12.0	240	9968	2202	404	214	11.2	2.0	2.5	6.4	3.18	2.56
<i>planorbis - johnstoni</i>	12.3	240	10820	2354	416	224	11.4	2.0	2.6	6.7	3.35	2.60
<i>planorbis - johnstoni</i>	12.6	240	9684	2210	408	195	11.0	2.0	2.6	5.7	2.84	2.20
<i>planorbis - johnstoni</i>	12.9	240	10454	2350	434	140	11.9	2.1	3.1	3.1	1.47	1.00
<i>planorbis - johnstoni</i>	13.2	240	10924	2562	490	209	12.6	2.2	3.4	6.0	2.74	1.78
<i>planorbis - johnstoni</i>	13.5	240	10786	2538	460	214	12.4	2.3	3.0	6.4	2.77	2.11
<i>planorbis - johnstoni</i>	13.8	240	11522	2624	466	269	13.5	2.4	2.8	8.8	3.66	3.08
<i>planorbis - johnstoni</i>	14.1	240	11378	2482	510	240	13.3	2.2	3.4	7.2	3.28	2.14
<i>liasicus Zone</i>	14.4	240	12340	2666	604	253	14.7	2.3	4.4	7.9	3.44	1.82
<i>liasicus Zone</i>	14.7	240	12368	2736	538	251	14.8	2.5	3.5	7.7	3.10	2.23

Table 2.05 (2 of 4)

<u>Biostratigraphy</u>	<u>Height</u> m	<u>Time</u> Secs	<u>Total Number of Counts</u>			<u>Total</u> ur	<u>Elemental Concentration</u>			<u>Ratios</u>	
			<u>Total</u>	<u>K</u>	<u>U</u>		<u>K %</u>	<u>U ppm</u>	<u>Th ppm</u>	<u>Th/K</u>	<u>Th/U</u>
<i>liasicus</i> Zone	15.0	240	13202	3154	606	16.0	2.9	4.3	7.9	2.73	1.85
<i>liasicus</i> Zone	15.3	240	12634	2614	546	15.1	2.5	3.8	7.1	2.82	1.85
<i>liasicus</i> Zone	15.6	240	12884	2792	570	15.5	2.5	4.0	7.2	2.89	1.81
<i>liasicus</i> Zone	15.9	240	12264	2824	484	14.6	2.6	3.0	8.8	3.37	2.90
<i>liasicus</i> Zone	16.2	240	13532	3240	550	16.5	3.1	3.7	7.9	2.55	2.12
<i>liasicus</i> Zone	16.5	240	14204	3214	558	17.5	3.0	3.6	10.0	3.33	2.81
<i>liasicus</i> Zone	16.8	240	14676	3368	574	18.2	3.2	3.5	12.6	3.92	3.62
<i>liasicus</i> Zone	17.1	240	13980	3054	556	17.1	3.0	3.8	7.7	2.58	2.03
<i>liasicus</i> Zone	17.4	240	15906	3612	658	20.0	3.4	4.7	8.9	2.63	1.90
<i>liasicus</i> Zone	17.7	240	16154	3624	658	20.4	3.4	4.4	11.9	3.49	2.72
<i>liasicus</i> Zone	18.0	240	14312	3236	588	17.6	3.0	4.1	8.4	2.81	2.06
<i>liasicus</i> Zone	18.3	240	13900	2972	606	17.0	2.7	3.8	12.4	4.59	3.24
<i>liasicus</i> Zone	18.6	240	16426	3646	644	20.8	3.5	4.3	7.9	2.26	1.85
<i>liasicus</i> Zone	18.9	240	16274	3470	798	20.5	3.2	4.4	12.9	4.03	2.90
<i>liasicus</i> Zone	19.2	240	15792	3434	592	19.8	3.3	3.6	12.7	3.86	3.49
<i>liasicus</i> Zone	19.5	240	15824	3540	700	19.9	3.3	4.9	11.0	3.34	2.25
<i>liasicus</i> Zone	19.8	240	15062	3394	632	18.7	3.2	4.7	6.5	2.04	1.39
<i>liasicus</i> Zone	20.1	240	15534	3292	616	19.4	3.1	4.2	9.6	3.11	2.31
<i>liasicus</i> Zone	20.4	240	14836	3190	632	18.4	2.9	4.4	10.1	3.50	2.33
<i>liasicus</i> Zone	20.7	240	14964	3338	578	18.6	3.2	3.8	9.8	3.06	2.57
<i>liasicus</i> Zone	21.0	240	14032	2876	612	17.2	2.7	4.4	7.1	2.61	1.59
<i>liasicus</i> Zone	21.3	240	14400	3364	524	17.8	3.1	3.1	11.0	3.55	3.54
<i>liasicus</i> Zone	21.6	240	13608	2990	606	16.6	2.7	4.3	8.6	3.19	2.02
<i>liasicus</i> Zone	21.9	240	14742	3138	572	18.3	2.9	3.9	8.1	2.79	2.07
<i>liasicus</i> Zone	22.2	240	14966	3280	564	18.6	3.1	3.7	8.8	2.83	2.35
<i>liasicus</i> Zone	22.5	240	14684	3248	506	18.2	3.1	3.5	7.9	2.55	2.28
<i>liasicus</i> Zone	22.8	240	14664	3096	544	18.3	2.9	3.6	9.6	3.32	2.71
<i>liasicus</i> Zone	23.1	240	14862	3230	550	18.5	3.1	3.6	8.9	2.89	2.45

Table 2.05 (3 of 4)

<u>Biostratigraphy</u>	<u>Height</u> m	<u>Time</u> Secs	<u>Total Number of Counts</u>			<u>Th</u>	<u>Total</u> µr	<u>Elemental Concentration</u>			<u>Ratios</u>	
			<u>Total</u>	<u>K</u>	<u>U</u>			<u>K %</u>	<u>U ppm</u>	<u>Th ppm</u>	<u>Th/K</u>	<u>Th/U</u>
<i>liasicus</i> Zone	23.4	240	14948	3206	596	285	16.6	3.0	4.1	8.6	2.87	2.10
<i>liasicus</i> Zone	23.7	240	12846	2698	524	227	15.5	2.4	3.6	6.9	2.87	1.89
<i>liasicus</i> Zone	24.0	240	15660	2930	592	198	17.7	2.5	2.8	5.3	2.13	1.94
<i>liasicus</i> Zone	24.3	240	15296	3156	646	275	19.1	2.9	4.6	8.8	3.02	1.90
<i>liasicus</i> Zone	24.6	240	14832	2980	584	251	18.4	2.7	4.1	7.7	2.87	1.89
<i>liasicus</i> Zone	24.9	240	14972	3026	558	272	13.6	2.8	3.7	8.6	3.07	2.30
<i>liasicus</i> Zone	25.2	240	13600	2802	556	282	16.6	2.5	3.7	9.1	3.65	2.44
<i>liasicus</i> Zone **	25.5	240	13748	2768	564	280	16.8	2.5	3.8	9.1	3.65	2.39
<i>liasicus</i> Zone **	25.8	240	14442	3010	608	269	17.8	2.7	4.3	8.6	3.19	2.02
<i>liasicus</i> Zone **	26.1	240	14538	3048	644	301	18.0	2.7	4.4	10.0	3.69	2.24
<i>liasicus</i> Zone **	26.4	240	15048	3120	618	285	18.7	2.9	4.3	9.3	3.20	2.18
<i>liasicus</i> Zone **	26.7	240	15070	3072	658	280	18.8	2.8	4.7	8.9	3.19	1.90
<i>liasicus</i> Zone **	27.0	120	9405	1596	288	135	19.4	3.0	3.9	8.6	2.87	2.20
<i>liasicus</i> Zone **	27.3	120	9126	1736	381	180	21.4	3.1	5.4	12.2	3.94	2.25
<i>liasicus</i> Zone **	27.6	120	9126	1777	396	177	21.5	3.2	5.7	12.0	3.76	2.12
<i>liasicus</i> Zone **	27.9	120	9010	1648	328	149	20.8	3.0	4.6	9.6	3.21	2.08

Table 2.05 (4 of 4)

Biostratigraphy	Height m	Time Secs	Total Number of Counts			Th	Total µg	Elemental Concentration		Ratios		
			Total	K	U			K %	U ppm	Th ppm	Th/K	Th/U
<i>angulata</i> Zone	0.0	400	9966	1918	472	177	5.3	0.8	1.8	1.9	2.4	1.1
<i>angulata</i> Zone	0.3	400	14024	2886	652	267	8.9	1.4	2.6	4.0	2.8	1.5
<i>angulata</i> Zone	0.6	400	13748	2730	674	230	8.6	1.3	2.8	3.1	2.4	1.1
<i>angulata</i> Zone	0.9	360	14262	2982	648	293	9.1	1.5	2.5	4.6	3.1	1.9
<i>angulata</i> Zone	1.2	360	11732	2344	604	251	8.0	1.2	2.8	4.3	3.6	1.6
<i>angulata</i> Zone	1.5	360	11140	2196	520	224	7.4	1.1	2.2	3.6	3.3	1.6
<i>angulata</i> Zone	1.8	360	13076	2678	680	238	8.5	1.2	3.1	4.0	3.3	1.3
<i>angulata</i> Zone	2.1	360	12018	2424	568	235	8.3	1.3	2.5	3.8	2.9	1.5
<i>angulata</i> Zone	2.4	360	10350	2040	486	185	6.7	1.0	2.1	2.2	2.2	1.0
<i>angulata</i> Zone	2.7	360	9006	1762	390	158	5.3	0.9	1.6	1.9	2.1	1.2
<i>angulata</i> Zone	3.0	360	12898	2728	616	275	9.2	1.5	2.7	4.8	3.2	1.8
<i>angulata</i> Zone	3.3	360	10608	2122	536	243	6.9	1.1	2.3	4.0	3.6	1.7
<i>angulata</i> Zone	3.6	360	12470	2748	506	267	8.7	1.6	2.0	4.8	3.0	2.5
<i>angulata</i> Zone	3.9	360	9826	1902	430	158	6.1	1.0	1.8	2.1	2.1	1.2
<i>angulata</i> Zone	4.2	360	13526	2758	616	298	9.8	1.5	2.7	5.5	3.7	2.1
<i>angulata</i> Zone	4.5	360	12410	2435	628	272	8.7	1.3	2.8	4.8	3.7	1.7
<i>angulata</i> Zone	4.8	360	11032	2182	474	211	7.3	1.2	2.0	3.1	2.6	1.6
<i>angulata</i> Zone	5.1	360	10826	2194	524	246	7.1	1.1	2.2	4.3	3.9	1.9
<i>angulata</i> Zone **	5.4	360	12206	2382	618	261	8.5	1.2	2.8	4.6	3.9	1.7
<i>angulata</i> Zone **	5.7	360	10548	2060	522	187	6.8	1.0	2.4	2.4	2.4	1.0
<i>angulata</i> Zone **	6.0	360	9340	1782	450	243	5.6	0.8	1.8	4.1	5.2	2.3
<i>angulata</i> Zone	6.3	360	13150	2904	694	282	9.4	1.6	3.2	5.0	3.1	1.6
<i>angulata</i> Zone	6.6	360	11406	2348	500	195	7.7	1.3	2.2	2.8	2.1	1.2
<i>angulata</i> Zone	6.9	360	12744	2667	522	261	9.0	1.5	2.1	4.8	3.2	2.3
<i>angulata</i> Zone	7.2	360	9324	1788	462	182	5.6	0.8	2.0	2.4	3.0	1.2

Table 2.06 Gamma-ray data-set for the *angulata* Zone and *bucklandi* Zone (*conybeari* Subzone) exposed at Nash Point, South Glamorgan (SS 914684). The 100 sets of measurements were collected from cliff section. All readings were taken with the Leeds University GR-256 during the period 7th September - 10th September 1995. Measurements were taken with the detector placed perpendicular to the cliff and parallel to bedding, except for readings denoted by ** which indicates a poor sample geometry. (1 of 4.)

<u>Biostratigraphy</u>	<u>Height</u> <u>m</u>	<u>Time</u> <u>Secs</u>	<u>Total Number of Counts</u>		<u>Th</u>	<u>Total</u> <u>ur</u>	<u>Elemental Concentration</u>		<u>Ratios</u>			
			<u>Total</u>	<u>K</u>			<u>U</u>	<u>K %</u>	<u>U ppm</u>	<u>Th ppm</u>	<u>Th/K</u>	<u>Th/U</u>
<i>angulata</i> Zone	7.5	360	10344	2019	486	242	7.6	1.0	1.9	2.9	2.9	1.6
<i>angulata</i> Zone	7.8	360	10785	2043	498	242	7.1	1.0	2.0	4.1	4.1	2.0
<i>angulata</i> Zone	8.1	360	11550	2328	543	198	7.8	1.2	2.5	2.9	2.4	1.2
<i>angulata</i> Zone	8.4	360	11118	2130	504	226	7.4	1.1	2.0	3.6	3.3	1.8
<i>angulata</i> Zone	8.7	360	14358	2898	717	313	10.4	1.6	2.7	4.1	2.6	1.5
<i>angulata</i> Zone	9.0	480	9284	1432	452	169	3.3	0.4	1.3	1.0	2.6	0.8
<i>angulata</i> Zone	9.3	360	10617	1926	486	214	6.9	0.9	2.0	3.4	3.8	1.7
<i>angulata</i> Zone	9.6	360	11728	2277	561	242	8.2	1.2	2.5	4.0	3.3	1.6
<i>angulata</i> Zone	9.9	360	10455	2010	510	174	6.8	1.0	2.3	2.2	2.2	1.0
<i>angulata</i> Zone	10.2	360	9297	1755	516	147	5.6	0.8	2.5	1.4	1.7	0.6
<i>angulata</i> Zone	10.5	360	11862	2268	474	242	8.1	1.2	1.9	4.1	3.4	2.2
<i>angulata</i> Zone	10.8	360	11160	2298	546	202	7.5	1.2	2.5	2.9	2.4	1.2
<i>angulata</i> Zone	11.1	360	12831	2547	567	261	9.1	1.4	2.4	4.6	3.3	1.9
<i>angulata</i> Zone	11.4	360	12312	2448	528	281	8.6	1.3	2.1	5.2	4.0	2.4
<i>angulata</i> Zone	11.7	240	10174	2056	470	161	11.5	1.7	3.4	4.0	2.3	1.2
<i>angulata</i> Zone	12.0	360	10803	2061	549	178	7.1	1.0	2.6	2.2	2.2	0.9
<i>angulata</i> Zone	12.3	240	10750	2148	430	193	12.4	1.1	2.8	5.3	4.8	1.9
<i>angulata</i> Zone	12.6	360	12813	2364	558	281	9.1	1.2	2.3	5.2	4.3	2.2
<i>angulata</i> Zone	12.9	360	11898	2067	630	246	8.2	1.0	2.9	4.1	4.1	1.4
<i>angulata</i> Zone	13.2	240	9470	1818	504	158	2.5	1.4	4.3	4.0	2.8	0.9
<i>angulata</i> Zone	13.5	360	11976	2388	582	210	8.1	1.2	2.8	3.1	2.6	1.1
<i>angulata</i> Zone	13.8	240	9502	1824	500	158	9.5	1.4	3.6	4.0	2.8	1.1
<i>angulata</i> Zone	14.1	360	10443	1866	501	154	6.8	0.9	2.3	1.5	1.7	0.7
<i>angulata</i> Zone	14.4	240	9946	1982	462	161	11.2	1.6	3.4	4.0	2.5	1.2
<i>angulata</i> Zone	14.7	360	11604	2187	552	140	7.9	1.1	2.5	3.1	2.8	1.2
<i>angulata</i> Zone	15.0	360	11298	1764	498	174	6.4	0.8	2.2	2.2	2.8	1.0
<i>angulata</i> Zone	15.3	240	9005	1720	472	172	9.0	1.3	2.8	4.5	3.4	1.6
<i>angulata</i> Zone	15.6	240	9030	1822	334	180	9.8	1.6	2.0	5.0	3.1	2.6

Table 2.06 (2 of 4).

<u>Biostratigraphy</u>	<u>Height</u> m	<u>Time</u> Secs	<u>Total Number of Counts</u>			<u>Total</u> µr	<u>Elemental Concentration</u>			<u>Ratios</u>		
			<u>Total</u>	<u>K</u>	<u>U</u>		<u>Th</u>	<u>K %</u>	<u>U ppm</u>	<u>Th ppm</u>	<u>Th/K</u>	<u>Th/U</u>
<i>angulata</i> Zone	15.9	360	10095	954	486	182	6.4	0.9	2.1	2.4	2.7	1.1
<i>angulata</i> Zone	16.2	360	9432	1720	490	158	6.2	0.9	2.0	3.8	4.2	1.9
<i>angulata</i> Zone	16.5	360	9758	1790	484	150	6.1	0.8	2.2	1.5	1.9	0.7
<i>angulata</i> Zone	16.8	360	9610	1874	496	177	5.9	0.9	2.2	2.2	2.5	1.0
<i>angulata</i> Zone	17.1	360	9530	1676	213	209	5.8	0.8	1.7	1.5	1.9	0.9
<i>angulata</i> Zone	17.4	540	13251	2460	612	297	5.2	0.8	1.6	2.9	3.7	1.8
<i>angulata</i> Zone	17.7	540	11976	2208	576	202	4.3	0.6	1.6	1.2	2.0	0.8
<i>angulata</i> Zone	18.0	540	11919	1944	546	242	4.3	0.5	1.4	1.9	3.8	1.3
<i>angulata</i> Zone	18.3	540	11943	2196	588	249	4.3	0.6	1.6	2.1	3.4	1.3
<i>angulata</i> Zone	18.6	540	12894	2361	552	202	4.9	0.7	1.5	2.1	2.9	1.4
<i>angulata</i> Zone	18.9	360	9486	1802	462	209	5.8	0.9	2.0	3.1	3.4	1.6
<i>angulata</i> Zone	19.2	360	9502	1722	522	143	5.8	0.7	2.6	1.4	2.0	0.5
<i>angulata</i> Zone	19.5	360	89067	1644	438	108	5.2	0.7	2.0	0.9	1.2	0.4
<i>angulata</i> Zone	19.8	360	9006	1794	392	129	5.3	0.9	1.7	1.0	1.1	0.6
<i>angulata</i> Zone	20.1	360	9702	1802	502	209	6.0	0.8	2.1	3.1	3.9	1.5
<i>angulata</i> Zone	20.4	360	10230	2052	508	222	6.5	1.0	2.1	3.6	3.6	1.7
<i>angulata</i> Zone	20.7	360	10414	1930	518	224	6.7	0.9	2.2	3.6	4.0	1.6
<i>angulata</i> Zone	21.0	540	12639	2403	606	230	4.7	0.7	1.7	1.5	2.2	0.9
<i>angulata</i> Zone	21.3	540	11571	2019	486	226	4.3	0.6	1.4	2.4	4.0	1.7
<i>angulata</i> Zone	21.6	360	9364	1784	404	190	5.7	0.9	1.5	2.8	3.1	1.8
<i>angulata</i> Zone	21.9	360	15340	3116	760	338	11.6	1.7	3.5	3.9	2.3	1.1
<i>angulata</i> Zone	22.2	360	9946	1986	438	150	6.2	1.0	2.0	1.5	1.5	0.8
<i>angulata</i> Zone	22.5	360	9966	1916	438	201	6.3	1.0	1.8	2.9	2.9	1.6
<i>angulata</i> Zone	22.8	360	10182	1912	486	169	6.5	0.9	2.2	2.1	2.3	0.9
<i>angulata</i> Zone	23.1	360	12156	2122	428	222	8.4	1.1	2.4	3.6	3.3	1.5
<i>angulata</i> Zone	23.4	540	14405	2661	612	261	6.0	0.9	1.7	2.2	2.5	1.3
<i>angulata</i> Zone	23.7	540	11640	1848	534	186	4.1	0.5	1.5	0.7	1.4	0.5

Table 2.06 (3 of 4).

Biostratigraphy	Height m	Time Secs	Total Number of Counts			Total µr	Elemental Concentration			Ratios	
			Total	K	U		Th	K %	U ppm	Th ppm	Th/K
<i>angulata</i> Zone	24.0	360	12120	2354	576	8.4	0.4	2.7	3.1	7.7	1.2
<i>angulata</i> Zone	24.3	540	12450	2142	300	4.6	0.6	1.7	0.9	1.4	0.5
<i>angulata</i> Zone	24.6	540	12186	2091	594	4.5	0.6	1.7	0.9	1.4	0.5
<i>bucklandi</i> - <i>conybeari</i>	24.9	360	12092	2168	612	8.4	1.0	2.9	3.1	3.1	1.1
<i>bucklandi</i> - <i>conybeari</i>	25.2	360	14168	2726	630	10.4	1.5	2.9	3.8	2.5	1.3
<i>bucklandi</i> - <i>conybeari</i>	25.5	540	10296	1728	408	3.2	0.5	1.0	0.2	0.3	0.2
<i>bucklandi</i> - <i>conybeari</i>	25.8	360	11036	2176	486	7.3	1.1	2.2	2.1	1.9	0.9
<i>bucklandi</i> - <i>conybeari</i>	26.1	360	13200	2604	544	9.5	1.4	2.4	2.9	2.1	1.2
<i>bucklandi</i> - <i>conybeari</i>	26.4	360	13154	2566	634	9.4	1.4	2.8	4.6	3.3	1.6
<i>bucklandi</i> - <i>conybeari</i>	26.7	540	12357	2139	222	4.6	1.6	1.4	1.0	0.6	0.7
<i>bucklandi</i> - <i>conybeari</i>	27.0	540	12318	2301	525	4.5	0.7	1.3	1.4	2.0	1.0
<i>bucklandi</i> - <i>conybeari</i>	27.3	360	9884	1986	404	7.2	1.0	1.7	1.5	1.5	0.9
<i>bucklandi</i> - <i>conybeari</i> **	27.6	360	9642	1764	438	6.0	0.8	1.9	2.6	3.2	1.4
<i>bucklandi</i> - <i>conybeari</i> **	27.9	360	9920	1852	490	6.2	0.9	2.0	1.4	1.5	0.7
<i>bucklandi</i> - <i>conybeari</i> **	28.2	540	10620	1731	471	3.4	0.4	1.3	0.7	1.7	0.5
<i>bucklandi</i> - <i>conybeari</i> **	28.5	540	11937	2175	552	4.3	0.6	1.4	1.9	3.2	1.3
<i>bucklandi</i> - <i>conybeari</i> **	28.8	360	9808	1750	460	6.1	0.8	1.9	3.4	4.3	1.8
<i>bucklandi</i> - <i>conybeari</i> **	29.1	540	10539	1752	477	3.4	0.4	1.2	1.0	2.6	0.8
<i>bucklandi</i> - <i>conybeari</i> **	29.4	540	10062	1782	477	3.0	0.5	1.2	0.3	0.7	0.3
<i>bucklandi</i> - <i>conybeari</i> **	29.7	540	11262	1875	576	3.8	0.5	1.7	1.0	2.1	0.6
<i>bucklandi</i> - <i>conybeari</i> **	30.0	360	9430	1548	474	5.7	0.6	2.0	2.8	4.6	1.3

Table 2.06 (4 of 4).

Biostratigraphy	Horizon	Thick. (m)	Time Secs	Total Number of Counts Recorded			Total µ	Elemental Concentrations			Ratios		
				Total	K	U		Th	U ppm	Th ppm	Th/K	Th/U	
Langport Member	Bed1	0.0	480	10377	1427	526	130	4.6	0.5	2.4	1.4	2.80	0.58
Langport Member	Bed1	0.3	480	10122	1473	514	138	4.4	0.5	2.3	1.6	3.20	0.70
Langport Member	Bed1	0.6	480	9835	1403	512	115	4.2	0.5	2.4	1.2	2.40	0.50
Langport Member	Bed1	0.9	480	9461	1303	489	93	3.9	0.4	2.3	0.8	2.00	0.35
Langport Member	Bed1	1.2	500	9067	1216	451	116	3.4	0.4	1.9	1.1	2.75	0.58
Langport Member	Bed1	1.5	540	10702	1425	589	130	3.9	0.4	2.4	1.2	3.00	0.50
Langport Member	Bed1	1.8	540	10829	1498	605	113	4.0	0.4	2.6	0.9	2.25	0.35
Langport Member	Bed1	1.9	540	11471	1627	642	155	4.5	0.5	2.6	1.6	3.20	0.62
Langport Member	Bed 4	2.1	520	12631	1986	672	189	5.5	0.7	2.8	2.1	3.00	0.75
Langport Member	Bed 4	2.4	500	12085	1830	676	199	5.5	0.6	2.9	2.3	3.83	0.79
Langport Member	Bed 4	2.7	480	11134	1615	616	168	5.1	0.6	2.8	2.1	3.50	0.75
Langport Member	Bed 4	3.0	480	10639	1583	540	148	4.8	0.6	2.4	1.1	1.83	0.46
Langport Member	Bed 5	3.3	480	11540	1763	586	156	5.4	0.7	2.6	1.8	2.57	0.69
Langport Member	Bed 6	3.6	480	10569	1614	549	178	4.7	0.6	2.3	2.2	3.67	0.96
Langport Member	Bed 6	3.9	480	11258	1734	561	175	5.2	0.7	2.4	2.1	3.00	0.88
Langport Member	Bed 6	4.2	480	10983	1722	639	153	5.0	0.7	2.4	1.8	2.57	0.75
Langport Member	Bed 6	4.2	480	10164	1500	503	147	4.4	0.6	2.2	1.7	2.83	0.77
Langport Member	Bed 8	4.5	480	10983	1722	539	153	5.0	0.7	2.4	1.8	2.57	0.75
Langport Member	Bed 8	4.8	480	10928	1720	571	158	5.0	0.7	2.5	1.8	2.57	0.72
Langport Member	Bed 8	5.1	480	9569	1358	491	108	4.0	0.5	2.3	1.1	2.20	0.48
Langport Member	Bed 8	5.4	480	11964	1936	579	204	5.8	0.8	2.4	2.6	3.25	1.08
Langport Member	Bed 8	5.7	480	11801	1900	555	198	5.6	0.8	2.3	2.5	3.13	1.09
Langport Member **	Bed 8	6.0	360	15079	2855	695	297	8.1	1.3	2.7	4.2	3.23	1.56
Langport Member **	Bed 8	6.3	360	15252	2831	707	288	8.2	1.3	2.8	4.0	3.08	1.43
Pre-Planorbis Beds		6.6	360	10925	1933	542	225	7.7	1.1	2.9	4.2	3.82	1.45

Table 2.07 Gamma-ray data-set for the White Lias and Blue Lias Formations that outcrop between Pinhay Bay, Devon and Seven Rock Point, Lyme Regis, Dorset (SY 318908 - SY 328910). A total number of 109 sets of measurements were collected. All readings were taken with the B.P. GR-256. The White Lias (Langport Member) was measured during the period 10th February - 12th February 1992. The remaining sets of measurements were collected during the period February 15th - March 4th 1993. Measurements denoted by ** indicate a poor sample geometry on cliff section. (1 of 4.)

Biostratigraphy	Horizon	Thick. (m)	Time Secs	Total Number of Counts Recorded				Total µg	Elemental Concentrations			Ratios	
				Total	K	U	Th		K %	U ppm	Th ppm	Th/K	Th/U
Pre-Planorbis Beds		6.9	330	13714	2684	684	315	10.4	1.6	3.5	6.1	3.81	1.74
Pre-Planorbis Beds		7.2	300	11567	2058	582	227	9.4	1.3	3.4	4.7	3.62	1.38
Pre-Planorbis Beds		7.5	300	11411	2139	546	248	10.4	1.5	3.4	5.7	3.80	1.68
Pre-Planorbis Beds		7.8	300	10436	1881	516	211	9.3	1.3	3.3	4.8	3.69	1.45
Pre-Planorbis Beds		8.1	300	10300	1896	471	206	9.1	1.4	3.0	4.1	2.93	1.37
Pre-Planorbis Beds		8.4	300	11856	2256	569	242	11.0	1.6	3.6	5.6	3.50	1.56
Pre-Planorbis Beds		8.7	300	11011	2174	509	271	10.0	1.6	2.9	6.4	4.00	2.21
Pre-Planorbis Beds		9.0	300	12415	2460	595	298	11.6	1.8	3.6	7.0	3.89	1.94
Pre-Planorbis Beds		9.3	300	13260	2441	783	280	12.6	1.6	5.4	6.5	4.06	1.20
Pre-Planorbis Beds		9.6	300	10558	1886	561	217	9.4	1.3	3.7	4.9	3.77	1.32
planorbis - planorbis	H25-H29	9.9	300	12048	2209	672	216	11.2	1.5	4.7	4.8	3.20	1.02
planorbis - planorbis	H25-H29	10.2	300	15266	2992	920	268	15.0	2.0	6.7	6.0	3.00	0.90
planorbis - planorbis	H30	10.5	300	12637	2259	801	194	11.9	1.4	6.1	4.1	2.93	0.67
planorbis - planorbis	H31-H42	10.8	300	13563	2369	851	225	13.0	1.5	6.3	5.0	3.33	0.79
planorbis - planorbis	H31-H42	11.1	360	10308	1627	585	168	7.1	0.8	3.5	2.9	3.63	0.83
planorbis - planorbis	H31-H42	11.4	300	9334	1581	456	190	8.0	1.1	2.9	4.3	3.91	1.48
planorbis - planorbis	H31-H42	11.7	300	12330	2125	702	258	9.1	1.1	4.0	4.9	4.45	1.23
planorbis - johnstoni	H31-H42	12.0	300	13381	2356	735	291	10.1	1.3	4.0	5.5	4.23	1.38
planorbis - johnstoni	H43-H56	12.3	300	12097	2120	567	254	8.9	1.2	2.9	4.8	4.00	1.66
planorbis - johnstoni	H43-H56	12.6	300	15480	2896	809	313	12.2	1.7	4.5	6.0	3.53	1.33
planorbis - johnstoni	H43-H56	12.9	300	22018	4513	1258	466	18.7	2.7	7.2	9.2	3.41	1.28
planorbis - johnstoni	H43-H56	13.2	300	15959	2989	726	390	12.7	1.8	3.5	7.8	4.33	2.23
planorbis - johnstoni	H43-H56	13.5	300	14214	2967	579	317	10.9	1.9	2.7	6.1	3.21	2.26
planorbis - johnstoni	H43-H56	13.8	300	14395	3036	628	350	11.1	1.9	2.9	6.9	3.63	2.38
planorbis - johnstoni	H43-H56	14.1	300	13138	2567	556	254	9.9	1.6	2.8	4.8	3.00	1.71
liasicus - portlocki	H57-H65	14.4	300	14426	2969	635	323	11.2	1.9	3.1	6.3	3.32	2.03
liasicus - portlocki	H57-H65	14.7	300	13660	2657	598	313	10.4	1.6	2.0	6.1	3.81	3.05
liasicus - portlocki	H57-H65	15.0	300	15681	2950	879	316	12.4	1.7	5.0	6.0	3.53	1.20
liasicus - portlocki	H57-H65	15.3	370	11187	2163	567	212	11.6	1.7	4.2	5.4	3.18	1.29

Table 2.07 (2 of 4).

<u>Biostratigraphy</u>	<u>Horizon</u>	<u>Thick.</u> (m)	<u>Time</u> Secs	<u>Total Number of Counts Recorded</u>				<u>Total</u> µr	<u>Elemental Concentrations</u>			<u>Ratios</u>	
				<u>Total</u>	<u>K</u>	<u>U</u>	<u>Th</u>		<u>K %</u>	<u>U ppm</u>	<u>Th ppm</u>	<u>Th/K</u>	<u>Th/U</u>
<i>liasicus - portlocki</i>	H66	15.6	370	9193	1572	458	175	10.5	1.6	3.8	4.9	3.06	1.29
<i>liasicus - portlocki</i>	H67-H68	15.9	270	12864	2605	666	246	13.8	2.1	5.0	6.3	3.00	1.26
<i>liasicus - laqueus</i>	H69-H83	16.2	270	9332	1679	491	193	9.2	1.3	3.6	4.8	3.69	1.33
<i>liasicus - laqueus</i>	H69-H83	16.5	300	10290	1834	501	234	9.1	1.3	3.1	5.3	4.08	1.71
<i>liasicus - laqueus</i>	H69-H83	16.8	300	10777	2062	550	216	9.7	1.5	3.6	4.9	3.27	1.36
<i>liasicus - laqueus</i>	H69-H83	17.1	270	10130	1826	547	197	10.2	1.4	4.1	4.9	3.50	1.20
<i>liasicus - laqueus</i>	H69-H83	17.4	270	12687	2404	176	260	13.6	1.8	6.1	6.6	3.67	1.08
<i>angulata Zone</i>	H84-H91	17.7	270	13441	2508	815	245	14.6	1.8	6.6	6.2	3.44	0.94
<i>angulata Zone</i>	H84-H91	18.0	270	10513	1890	560	216	10.8	1.4	4.2	5.5	3.93	1.31
<i>angulata Zone</i>	H84-H91	18.3	270	13812	2561	808	276	15.1	1.9	6.3	7.1	3.74	1.13
<i>angulata Zone</i>	H84-H91	18.6	240	11969	2119	804	229	14.6	1.6	7.4	6.5	4.06	0.88
<i>angulata Zone</i>	1	18.9	240	10246	1763	663	174	12.1	1.3	6.2	4.8	3.69	0.77
<i>angulata Zone</i>	1	19.2	240	13280	2285	923	218	16.6	1.7	8.8	6.1	3.59	0.69
<i>angulata Zone</i>	1	19.5	200	10144	1766	698	181	14.9	1.6	7.9	6.1	3.81	0.77
<i>angulata Zone</i>	Lower Venty	19.8	200	10676	1964	661	195	15.9	1.9	7.2	6.7	3.53	0.93
<i>angulata Zone</i>	Lower Venty	20.1	300	11368	1957	631	201	10.4	1.3	4.4	4.5	3.46	1.02
<i>angulata Zone</i>	Lower Skulls	20.4	300	12993	2487	771	242	12.3	1.7	5.5	5.5	3.24	1.0
<i>angulata Zone</i>	Under White	20.7	300	10779	1894	625	191	9.7	1.2	5.0	4.2	3.50	0.84
<i>angulata Zone</i>	2-20	21.0	300	11008	2044	562	219	10.9	1.4	3.7	4.9	3.50	1.32
<i>angulata Zone</i>	Iron Ledge	21.3	300	10366	1855	549	166	9.2	1.3	3.9	3.6	2.77	0.92
<i>angulata Zone</i>	Upper Skulls	21.6	300	13030	2353	783	265	12.4	1.5	5.5	6.1	4.07	1.11
<i>angulata Zone</i>	2-20	21.9	270	11602	2193	737	215	12.2	1.6	5.9	5.3	3.31	0.90
<i>angulata Zone</i>	Speckety	22.2	270	12270	2180	731	245	13.1	1.6	5.7	6.2	3.88	1.09
<i>angulata Zone</i>	Speckety	22.5	270	12003	2132	708	210	12.7	1.5	5.7	5.2	3.47	0.91
<i>bucklandi - conybeari</i>	21-29	22.8	270	16217	3142	1000	285	18.3	2.4	8.2	7.3	3.04	0.89
<i>bucklandi - conybeari</i>	21-29	23.1	270	16693	3257	988	320	18.9	2.5	7.8	8.3	3.32	1.06
<i>bucklandi - conybeari</i>	21-29	23.4	240	13215	2588	730	247	16.5	2.3	6.4	7.1	3.09	1.11
<i>bucklandi - conybeari</i>	Second Tape	23.7	240	10031	1756	583	208	11.8	1.4	5.0	6.0	4.29	1.20
<i>bucklandi - conybeari</i>	21-29	24.0	240	10749	1979	581	229	12.8	1.7	4.8	6.7	3.94	1.40
<i>bucklandi - rotiforme</i>	21-29	24.3	240	11378	2237	664	224	13.8	1.9	5.8	6.5	3.42	1.12

Table 2.07 (3 of 4).

<u>Biostratigraphy</u>	<u>Horizon</u>	<u>Thick.</u> (m)	<u>Time</u> Secs	<u>Total Number of Counts Recorded</u>				<u>Total</u> µg	<u>Elemental Concentrations</u>			<u>Ratios</u>	
				<u>Total</u>	<u>K</u>	<u>U</u>	<u>Th</u>		<u>K %</u>	<u>U ppm</u>	<u>Th ppm</u>	<u>Th/K</u>	<u>Th/U</u>
<i>bucklandi - rotiforme</i>	Third Quack	24.6	240	13513	2574	777	277	16.9	2.2	6.7	8.1	3.68	1.21
<i>bucklandi - rotiforme</i>	21-29	24.9	240	14163	2773	867	290	17.9	2.4	7.6	8.5	3.54	1.12
<i>bucklandi - rotiforme</i>	30-40	25.2	240	18341	3398	1204	343	24.1	2.8	11.2	10	3.57	0.89
<i>bucklandi - rotiforme</i>	30-40	25.5	240	12450	2267	785	235	15.4	1.8	7.1	6.7	3.72	0.94
<i>bucklandi - rotiforme</i>	Gumpton	25.8	360	11057	1751	690	176	8.8	0.9	4.6	3.4	3.78	0.74
<i>bucklandi - rotiforme</i>	Second Quick	26.1	330	10836	1871	551	203	8.6	1.1	3.4	4.0	3.64	1.18
<i>bucklandi - rotiforme</i>	30-40	26.4	240	10524	1939	538	209	12.5	1.7	4.5	6.0	3.53	1.33
<i>bucklandi - rotiforme</i>	30-40	26.7	240	12918	2518	723	257	16.0	2.2	6.2	7.5	3.41	1.21
<i>bucklandi - rotiforme</i>	30-40	27.0	240	12832	2474	731	301	15.9	2.1	6.0	9.0	4.29	1.50
<i>bucklandi - rotiforme</i>	30-40	27.3	240	14145	2694	844	329	17.9	2.3	7.1	9.8	4.26	1.38
<i>bucklandi - rotiforme</i>	Second Bed	27.6	240	12132	2187	763	247	14.9	1.8	6.8	7.1	3.94	1.04
<i>bucklandi - rotiforme</i>	30-40	27.9	240	12174	2242	720	287	14.9	1.9	6.0	8.4	4.42	1.40
<i>bucklandi - rotiforme</i>	Best Bed	28.2	240	10287	1796	598	241	12.1	1.5	4.9	7.1	4.73	1.45
<i>bucklandi - rotiforme</i>	41-45	28.5	300	12197	2356	541	308	11.4	1.8	3.0	7.3	4.06	2.43
<i>bucklandi - bucklandi</i>	41-46	28.8	240	11720	2248	627	288	14.3	2.0	4.9	8.6	4.30	1.76
<i>bucklandi - bucklandi</i>	41-46	29.1	240	13521	2574	817	284	16.9	2.2	7.1	8.4	3.82	1.18
<i>bucklandi - bucklandi</i>	41-46	29.4	200	10623	2044	580	274	15.8	2.2	5.4	9.9	4.50	1.83
<i>bucklandi - bucklandi</i>	41-46	29.7	200	10558	2021	574	260	15.7	2.1	5.4	9.4	4.48	1.74
<i>bucklandi - bucklandi</i>	41-46	30.0	200	9783	1752	494	253	14.3	1.8	4.4	9.1	5.06	2.07
<i>bucklandi - bucklandi</i>	41-46	30.3	240	11507	2109	615	280	14.0	1.8	4.8	8.4	4.67	1.75
<i>bucklandi - bucklandi</i>	41-46	30.6	240	10749	1892	604	239	12.8	1.6	5.0	6.9	4.31	1.38
<i>bucklandi - bucklandi</i>	41-46	30.9	240	11658	2197	686	268	14.2	1.9	5.7	7.9	4.16	1.39
<i>bucklandi - bucklandi</i>	Top Quick	31.2	240	10922	1830	643	217	13.1	1.5	5.6	6.2	4.13	1.11
<i>bucklandi - bucklandi</i>	41 - 46	31.5	240	10878	1974	646	254	13.0	1.6	5.4	7.4	4.63	1.37
<i>bucklandi - bucklandi</i>	41 - 46	31.8	240	11591	2120	615	244	14.1	1.8	5.1	7.2	4.00	1.41
<i>bucklandi - bucklandi</i>	41 - 46	32.1	240	11394	2008	635	242	13.8	1.7	5.3	7.0	4.12	1.32
<i>semicostatium - lyra</i>	47 - 49	32.4	240	9803	1627	579	211	11.4	1.3	4.9	6.0	4.62	1.22
<i>semicostatium - lyra</i>	Grey Ledge	32.7	240	9846	1659	605	206	11.5	1.3	5.3	5.9	4.54	1.11

Table 2.07 (4 of 4).

Biostratigraphy	Horizon	Thick. (m)	Time Secs	Total Number of Counts Recorded			Total µr	Elemental Concentrations			Ratios		
				Total	K	U		Th	K %	U ppm	Th ppm	Th/K	Th/U
<i>semicostatium-scipionianum</i>	50 - 52	33.00	240	10966	1777	738	205	13.2	1.3	6.8	5.8	4.46	0.85
<i>semicostatium-scipionianum</i>	50 - 52	33.30	240	11075	2181	567	286	16.6	2.4	5.1	10.3	4.29	2.02
<i>semicostatium-scipionianum</i>	50 - 52	33.60	240	11982	2418	538	376	18.2	2.8	3.9	13.9	4.96	3.56
<i>semicostatium-scipionianum</i>	50 - 52	33.90	240	11908	2536	497	346	18.7	3.0	3.6	12.8	4.27	3.56
<i>semicostatium-scipionianum</i>	50 - 52	34.20	240	9963	1997	417	321	14.6	2.3	2.8	11.9	5.17	4.25
<i>semicostatium-scipionianum</i>	50 - 52	34.50	240	9293	1873	380	265	13.4	2.2	2.7	9.7	4.41	3.59
<i>semicostatium-scipionianum</i>	50 - 52	34.80	240	9388	1743	395	247	10.8	1.6	2.5	7.3	4.56	2.92
<i>semicostatium-scipionianum</i>	50 - 52	35.10	240	9198	1897	412	265	13.3	2.2	3.2	9.7	4.41	3.03
<i>semicostatium-scipionianum</i>	50 - 52	35.40	240	9272	1883	440	237	13.4	2.1	3.8	8.6	4.10	2.26
<i>semicostatium-scipionianum</i>	50 - 52	35.70	240	9546	1933	418	276	13.9	2.2	3.2	10.1	4.59	3.16
<i>semicostatium-scipionianum</i>	50 - 52	36.00	240	10805	2209	483	267	16.1	2.5	4.1	9.7	3.88	2.37
<i>semicostatium-scipionianum</i>	50 - 52	36.30	240	10599	2110	482	251	15.8	2.4	4.0	10.3	4.29	2.58
<i>semicostatium-scipionianum</i>	50 - 52	36.60	240	9860	1930	419	261	14.4	2.2	3.3	9.5	4.32	2.88
<i>semicostatium-scipionianum</i>	50 - 52	36.90	240	10480	2193	455	314	15.5	2.5	3.3	11.6	4.64	3.52
<i>semicostatium-scipionianum</i>	50 - 52	37.20	240	10345	2043	463	300	15.3	2.3	3.5	11.1	4.83	3.17
<i>semicostatium-scipionianum</i>	50 - 52	37.50	240	9740	1862	464	256	14.2	2.0	4.0	9.2	4.60	2.30
<i>semicostatium-scipionianum</i>	50 - 52	37.80	240	10330	2140	462	274	15.3	2.4	3.7	10.0	4.17	2.70
<i>semicostatium-scipionianum</i>	50 - 52	38.10	240	10805	2290	483	303	16.1	2.7	3.8	11.1	4.11	2.92
<i>semicostatium-scipionianum</i>	50 - 52	38.40	240	11075	2265	525	294	16.6	2.6	4.4	10.8	4.15	2.45
<i>semicostatium-scipionianum</i>	50 - 52	38.70	240	11642	2362	530	308	17.6	2.7	4.4	11.3	4.19	2.57
<i>semicostatium-scipionianum</i>	50 - 52	39.00	240	9656	1917	470	234	14.1	2.1	4.2	8.4	4.00	2.00
<i>semicostatium-scipionianum</i>	50 - 52	39.30	240	11019	2173	512	304	16.5	2.4	4.2	11.2	4.67	2.67
<i>semicostatium-scipionianum</i>	50 - 52	39.60	240	10710	2065	548	300	16.0	2.2	4.7	11.0	5.00	2.34
<i>semicostatium-scipionianum</i>	50 - 52	39.90	240	11185	2134	576	318	16.8	2.3	5.0	11.7	5.09	2.34
<i>semicostatium-scipionianum</i>	50 - 52	40.20	240	9941	1940	469	256	14.6	2.2	4.0	9.2	4.18	2.30

Table 2.08 Gamma-ray data-set for the Shales-with-'Beef' that outcrop between Seven Rock Point, Lyme Regis and Stonebarrow, Charmouth (SY 328910 - SY 364390). A total number of 109 sets of measurements were collected. All readings were taken with the B.P. GR-256. The *scipionianum* Subzone was measured during the period 20th March - March 23rd 1993. The remaining sets of measurements were collected during the period April 24th - April 27th 1993 (41.70 m to 61.20 m) and 19th May - 24th May 1993 (61.50 m to 70.80 m). Measurements denoted by ** indicate a poor sample geometry. (1 of 4.)

Biostratigraphy	Horizon	Thick. (m)	Time Secs	Total Number of Counts Recorded			Total wt	Elemental Concentrations			Ratios		
				Total	K	U		Th	K %	U ppm	Th ppm	Th/K	Th/U
<i>semicostatum-scipionianum</i>	50 - 52	40.50	240	9469	1695	490	235	13.7	1.8	4.4	9.2	5.11	2.09
<i>semicostatum-scipionianum</i>	50 - 52	40.80	240	9762	1881	474	236	14.3	2.1	4.3	8.4	4.00	1.95
<i>semicostatum-scipionianum</i>	50 - 52	41.10	240	10372	2008	498	258	15.3	2.2	4.4	9.3	4.23	2.11
<i>semicostatum-scipionianum</i>	50 - 52	41.40	240	10222	1999	493	251	15.1	2.2	4.4	9.1	4.14	2.07
<i>semicostatum-resupinatum</i>	53 - 73	41.70	420	9815	1518	377	228	5.2	0.7	1.3	3.6	5.14	2.77
<i>semicostatum-resupinatum</i>	53 - 73	42.00	420	20004	4187	478	531	13.8	2.3	3.0	9.1	3.96	3.03
<i>semicostatum-resupinatum</i>	53 - 73	42.30	420	12095	2154	469	283	7.1	1.1	1.7	4.6	4.18	2.71
<i>semicostatum-resupinatum</i>	53 - 73	42.60	420	20526	4198	499	527	14.3	2.3	3.5	9.1	3.96	2.60
<i>semicostatum-resupinatum</i>	53 - 73	42.90	300	10080	1770	469	245	8.9	1.2	2.7	5.8	4.83	2.15
<i>semicostatum-resupinatum</i> **	53 - 73	43.20	300	9696	1634	454	204	8.4	1.1	2.8	4.6	4.18	1.64
<i>semicostatum-resupinatum</i> **	53 - 73	43.70	300	9890	1931	502	212	8.5	1.3	3.1	4.8	3.69	1.55
<i>semicostatum-resupinatum</i> **	53 - 73	44.20	300	9995	2234	389	243	8.6	1.5	2.4	5.5	3.67	2.29
<i>semicostatum-resupinatum</i> **	53 - 73	44.70	300	10100	1931	259	270	8.7	1.6	1.6	6.1	3.81	3.81
<i>semicostatum-resupinatum</i> **	53 - 73	45.20	300	11023	2234	389	297	10.4	1.9	2.4	6.7	3.53	2.79
<i>semicostatum-resupinatum</i> **	53 - 73	45.70	300	13980	2376	518	319	12.0	2.2	3.2	7.2	3.27	2.25
<i>semicostatum-resupinatum</i> **	53 - 73	46.20	240	13996	2822	534	354	12.2	2.1	3.3	8.0	3.81	2.42
<i>semicostatum-resupinatum</i> **	53 - 73	46.70	240	13965	3276	502	390	12.3	1.9	3.1	8.8	4.63	2.84
<i>semicostatum-resupinatum</i> **	53 - 73	47.20	240	13876	2829	421	337	11.9	2.1	2.6	7.6	3.62	2.92
<i>semicostatum-resupinatum</i> **	53 - 73	47.70	240	13862	3127	324	301	11.6	2.0	2.0	6.8	3.40	3.40
<i>semicostatum-resupinatum</i> **	53 - 73	48.20	240	13823	2814	453	305	11.3	1.8	2.8	6.9	3.83	2.46
<i>semicostatum-resupinatum</i> **	53 - 73	48.70	240	11054	2501	567	310	10.9	1.6	3.5	7.0	4.38	2.00
<i>semicostatum-resupinatum</i> **	53 - 73	49.20	240	9152	2820	551	333	11.6	1.8	3.4	7.5	4.17	2.21
<i>semicostatum-resupinatum</i> **	53 - 73	49.70	240	13954	1563	534	355	12.2	1.9	3.3	8.0	4.21	2.42
<i>semicostatum-resupinatum</i> **	53 - 73	50.20	240	11065	1398	437	319	10.5	1.7	2.7	7.2	4.24	2.67
<i>semicostatum-resupinatum</i> **	53 - 73	50.70	240	9987	1287	356	279	8.8	1.4	2.2	6.3	4.50	2.86
<i>semicostatum-resupinatum</i> **	53 - 73	51.20	240	10980	1654	388	345	10.5	1.8	2.4	7.8	4.33	3.25
<i>semicostatum-resupinatum</i> **	53 - 73	51.70	240	13054	2022	486	403	12.8	2.2	3.0	9.1	4.14	3.03
<i>semicostatum-resupinatum</i> **	53 - 73	52.20	240	11056	2045	534	399	13.0	2.0	3.3	9.0	4.50	2.73

Table 2.08 (2 of 4).

Biostratigraphy	Horizon	Thick. (m)	Time Secs	Total Number of Counts Recorded			Total µ	Elemental Concentrations		Ratios			
				Total	K	U		Th	K%	U ppm	Th ppm	Th/K	Th/U
<i>semicostatum-resupinatum</i> **	53 - 73	52.70	240	12270	1745	583	390	13.2	1.9	3.6	8.8	4.63	2.44
<i>semicostatum-resupinatum</i> **	53 - 73	53.20	240	9965	1286	372	283	8.6	1.4	2.3	6.4	4.57	2.78
<i>semicostatum-resupinatum</i> **	53 - 73	53.70	240	1067	1290	502	292	10.0	1.4	3.1	6.6	4.71	2.13
<i>semicostatum-resupinatum</i> **	53 - 73	54.20	240	11040	1378	388	297	9.1	1.5	2.4	6.7	4.47	2.79
<i>semicostatum-resupinatum</i> **	53 - 73	54.70	240	9779	1010	226	195	5.0	1.1	1.0	4.4	4.00	3.14
<i>semicostatum-resupinatum</i> **	53 - 73	55.20	240	9876	1101	307	199	6.9	1.2	1.9	4.5	3.75	2.37
<i>semicostatum-resupinatum</i> **	53 - 73	55.70	240	9976	1193	356	204	8.0	1.3	2.2	4.6	3.54	2.09
<i>semicostatum-resupinatum</i> **	53 - 73	56.20	180	10980	1285	437	208	9.5	1.4	2.7	4.7	3.40	1.74
<i>semicostatum-resupinatum</i> **	53 - 73	56.70	180	11070	1713	518	208	10.9	1.5	3.2	4.8	3.20	1.50
<i>semicostatum-resupinatum</i>	53 - 73	57.00	180	9272	2002	534	369	13.5	2.0	3.3	8.5	4.25	2.58
<i>semicostatum-resupinatum</i>	53 - 73	57.30	180	10296	1923	420	295	16.0	2.5	3.4	12.1	4.84	3.56
<i>turneri - brooki</i>	Bed 74	57.60	180	10202	1955	432	301	15.1	2.5	3.5	12.4	4.96	3.54
<i>turneri - brooki</i>	Bed 74	57.90	180	10504	1967	396	301	15.7	2.6	3.0	12.4	4.77	4.13
<i>tunneri - brooki</i>	Bed 74	58.20	240	14108	2917	648	393	17.8	2.8	4.4	12.1	4.32	2.75
<i>turneri - brooki</i>	Bed 74	58.50	240	12336	2408	557	330	15.2	2.3	3.8	10.0	4.35	2.63
<i>turneri - brooki</i>	Bed 74	58.80	240	9289	2149	492	325	13.0	2.0	3.1	9.9	4.95	3.19
<i>turneri - brooki</i>	Bed 74	59.10	240	9152	2050	446	280	11.9	1.9	2.9	8.5	4.47	2.93
<i>turneri - brooki</i>	Bed 74	59.40	200	9951	2081	417	220	14.6	2.4	3.6	7.9	3.29	2.19
<i>turneri - brooki</i>	Bed 74	59.70	180	10605	2231	467	299	17.9	2.9	4.0	12.2	4.21	3.05
<i>turneri - brooki</i>	Bed 74	60.00	200	14072	2996	580	327	17.8	2.9	4.1	9.9	3.41	2.41
<i>turneri - brooki</i>	Bed 74	60.30	200	13292	2818	537	382	16.6	2.8	3.2	11.8	4.21	3.69
<i>turneri - brooki</i>	Bed 74	60.60	200	10491	2152	416	289	12.4	2.1	2.5	8.0	4.19	3.52
<i>turneri - brooki</i>	Bed 74	60.90	200	9784	1986	397	250	11.4	1.9	2.5	7.5	3.95	3.00
<i>turneri - brooki</i>	Bed 74	61.20	200	10673	2229	441	306	12.7	2.2	2.6	9.3	4.23	3.58
<i>turneri - birchi</i>	Bed 74	61.50	200	9727	1968	367	291	14.2	2.3	2.3	10.8	4.70	4.70
<i>turneri - birchi</i>	Bed 74	61.80	200	9162	1888	389	233	13.2	2.2	3.1	8.4	3.82	2.71
<i>turneri - birchi</i>	Bed 74	62.10	200	9370	1914	431	272	13.6	2.2	3.4	9.9	4.50	2.91
<i>turneri - birchi</i>	Bed 74	62.40	200	10074	1969	395	269	14.0	2.3	2.9	9.8	4.26	3.38
<i>turneri - birchi</i>	Bed 74	62.70	200	9984	2040	423	274	14.7	2.4	3.2	10.1	4.21	3.16

Table 2.08 (3 of 4).

Biostratigraphy	Horizon	Thick. (m)	Time Secs	Total Number of Counts Recorded			Total µg	Elemental Concentrations			Ratios		
				Total	K	U		Th	K %	U ppm	Th ppm	Th/K	Th/U
<i>turneri - birchi</i>	Bed 74	63.00	200	9506	1831	420	283	13.8	2.1	3.2	10.3	4.90	3.22
<i>turneri - birchi</i>	Bed 74	63.30	200	9736	1996	424	287	14.2	2.3	3.1	10.6	4.61	3.42
<i>turneri - birchi</i>	Bed 74	63.60	200	9916	1990	401	298	14.5	2.3	2.7	11.0	4.78	4.07
<i>turneri - birchi</i>	Bed 74	63.90	180	10442	2074	582	259	17.5	2.5	6.2	10.4	4.16	1.68
<i>turneri - birchi</i>	Bed 74	64.20	200	10483	2034	506	290	15.5	2.2	4.2	10.1	4.59	2.40
<i>turneri - birchi</i>	Bed 74	64.50	200	10282	2043	499	255	15.2	2.3	4.4	9.2	4.00	2.09
<i>turneri - birchi</i>	Bed 74	64.80	200	10176	487	469	265	15.1	2.2	4.1	9.3	4.23	2.27
<i>turneri - birchi</i>	Bed 74	65.10	200	9972	1917	392	251	14.9	2.1	4.3	9.2	4.36	2.13
<i>turneri - birchi</i>	Bed 74	65.40	200	10004	2017	481	250	14.7	2.2	4.2	9.1	4.14	2.17
<i>turneri - birchi</i>	Bed 74	65.70	200	9223	1728	472	256	13.3	1.8	4.1	9.2	5.11	2.24
<i>turneri - birchi</i>	Bed 74	66.00	200	9885	1944	469	283	14.5	2.2	3.8	10.3	4.68	2.71
<i>turneri - birchi</i>	Bed 74	66.30	200	12337	2578	629	321	18.8	2.9	5.6	11.8	4.07	2.11
<i>turneri - birchi</i>	Bed 74	66.60	200	10730	2117	620	292	16.0	2.5	1.7	10.7	4.28	6.29
<i>turneri - birchi</i>	Bed 74	66.90	200	9610	1925	466	264	14.0	2.1	3.9	9.6	4.57	2.46
<i>turneri - birchi</i>	Bed 74	67.20	200	9304	2107	463	269	15.2	2.4	3.8	9.8	4.08	2.58
<i>turneri - birchi</i>	Bed 74	67.50	200	9725	1895	511	245	14.2	2.0	4.7	8.8	4.40	1.87
<i>turneri - birchi</i>	Bed 74	67.80	200	9879	1984	499	216	14.5	2.2	4.8	7.6	3.45	1.58
<i>turneri - birchi</i>	Bed 74	68.10	200	10549	2043	506	249	15.6	2.3	4.9	9.1	3.96	1.86
<i>turneri - birchi</i>	Bed 74	68.40	200	11100	2182	564	293	16.6	2.4	5.0	10.6	4.42	2.12
<i>turneri - birchi</i>	Bed 74	68.70	200	11327	2234	548	292	17.0	2.8	4.4	10.6	3.79	2.41
<i>turneri - birchi</i>	Bed 74	69.00	200	10555	2075	630	265	15.7	2.2	5.3	9.9	4.50	1.87
<i>turneri - birchi</i>	Bed 75	69.30	200	10798	2084	603	282	16.2	2.2	5.7	10.1	4.53	1.77
<i>turneri - birchi</i>	Bed 75	69.60	200	10710	2073	601	270	16.0	2.2	5.3	9.8	4.45	1.85
<i>turneri - birchi</i>	Bed 75	69.90	200	10548	2032	575	276	15.7	2.0	4.8	9.9	4.95	2.06
<i>turneri - birchi</i>	Bed 75	70.20	200	10702	2057	589	270	16.0	2.1	5.0	9.7	4.62	1.94
<i>turneri - birchi</i>	Bed 75	70.50	200	10857	2082	604	264	16.2	2.2	5.8	9.5	4.32	1.64
<i>turneri - birchi</i>	bed 75	70.80	200	10780	2075	606	295	16.1	2.2	5.6	10.7	4.86	1.91

Table 2.08 (4 of 4).

Biostratigraphy	Horizon	Thick. (m)	Time Secs	Total Number of Counts Recorded			Total µr	Elemental Concentrations			Ratios		
				Total	K	U		Th	K %	U ppm	Th ppm	Th/K	Th/U
<i>turneri - birchi</i>	Bed 76	71.20	200	9734	1804	530	251	14.2	1.9	4.9	9.0	4.74	1.84
<i>turneri - birchi</i>	Bed 76	71.50	220	11957	2530	513	345	16.2	2.7	2.4	11.6	4.30	4.83
<i>turneri - birchi</i>	Bed 76	71.80	220	11093	2264	483	386	14.8	2.4	2.8	13.1	5.46	4.68
<i>turneri - birchi</i>	Bed 76	72.10	220	10900	2204	422	362	14.5	2.4	2.2	12.2	5.08	5.55
<i>turneri - birchi</i>	Bed 76	72.40	220	11629	2459	489	344	15.7	2.6	3.2	11.5	4.42	3.59
<i>turneri - birchi</i>	Bed 76	72.70	220	12707	2623	565	406	17.4	2.8	3.7	13.7	4.89	3.70
<i>turneri - birchi</i>	Bed 79	73.00	220	12548	2610	523	399	17.2	2.8	3.2	13.5	4.82	4.22
<i>turneri - birchi</i>	Bed 79	73.30	220	12606	2655	530	369	17.3	2.8	3.5	12.4	4.43	3.54
<i>turneri - birchi</i>	Bed 79	73.60	220	12246	2536	477	400	16.7	2.8	2.6	13.6	4.86	5.23
<i>turneri - birchi</i>	Bed 79	73.90	220	12405	2514	517	389	17.1	2.7	3.2	13.2	4.89	4.13
<i>turneri - birchi</i>	Bed 79	74.20	220	10765	2177	469	305	14.3	2.3	3.2	10.2	4.43	3.19
<i>turneri - birchi</i>	Bed 79	74.50	220	10424	2130	441	299	13.8	2.2	3.0	9.9	4.50	3.30
<i>turneri - birchi</i>	Bed 79	74.80	220	14008	2854	604	436	16.1	2.5	3.3	12.4	4.96	3.76
<i>turneri - birchi</i>	Bed 79	75.10	260	14339	3070	609	453	16.5	2.8	3.2	12.9	4.61	4.03
<i>turneri - birchi</i>	Bed 79	75.40	240	9564	1781	383	263	11.1	1.7	2.3	7.9	4.65	3.43
<i>turneri - birchi</i>	Bed 79	75.70	240	11530	2262	508	343	14.0	2.1	3.2	10.4	4.95	3.25
<i>turneri - birchi</i>	Bed 80	76.00	420	15975	2974	689	422	10.4	1.6	2.6	7.2	4.50	2.77
<i>turneri - birchi</i>	Bed 80	76.30	420	9658	1553	418	216	5.1	0.7	1.7	3.3	4.71	1.94
<i>turneri - birchi</i>	Bed 81	76.60	220	13143	2810	590	414	18.2	3.0	3.9	14.0	4.67	3.59
<i>turneri - birchi</i>	Bed 81	76.90	220	12263	2535	505	395	16.7	2.7	3.0	13.3	4.93	4.43
<i>turneri - birchi</i>	Bed 81	77.20	220	12145	2530	492	385	16.5	2.7	2.9	13.1	4.85	4.52
<i>turneri - birchi</i>	Bed 81	77.50	220	12509	2492	556	391	16.5	2.6	3.7	13.2	5.08	3.57
<i>turneri - birchi</i>	Bed 81	77.80	220	12031	2529	538	362	16.4	2.7	3.7	12.1	4.48	3.27
<i>turneri - birchi</i>	Bed 81	78.10	220	12048	2484	494	271	16.4	2.7	3.0	12.4	4.59	4.13
<i>turneri - birchi</i>	Bed 81	78.40	220	11305	2337	504	354	15.2	2.4	3.3	11.9	4.96	3.61

Table 2.02 Gamma-ray data-set for the Black Ven Marls that outcrop beneath Stonebarrow, Charmouth (SY 368930 - SY 380927). The 114 sets of measurements were collected from cliff section. All readings were taken with the B.P. GR-256 spectrometer. The stratigraphy represented between 71.20 m and 82.30 m was logged during the period 15th October - 20 th October 1993. The remainder of the formation was gamma-ray logged during the period 6th February - 16th February 1993. Measurements denoted by ** indicate a poor sample geometry. (1 of 4.)

Biostratigraphy	Horizon	Thick. (m)	Time Secs	Total Number of Counts Recorded				Total µr	Elemental Concentrations			Ratios	
				Total	K	U	Th		K %	U ppm	Th ppm	Th/K	Th/U
<i>obtusum - obtusum</i>	Bed 84	87.40	180	12394	2470	691	348	21.4	2.9	7.0	14.3	4.93	2.04
<i>obtusum - stellare</i>	Bed 86	87.70	180	10847	2100	625	278	18.3	2.4	6.7	11.2	4.67	1.67
<i>obtusum - stellare</i>	Bed 86	88.00	180	12938	2598	716	358	22.5	3.1	7.3	14.7	4.74	2.01
<i>obtusum - stellare</i>	Bed 86	88.30	180	11761	2273	597	336	20.1	2.8	5.7	13.8	4.93	2.42
<i>obtusum - stellare</i>	Bed 86	88.60	180	11765	2209	654	333	20.2	2.6	6.6	13.7	5.27	2.08
<i>obtusum - stellare</i>	Bed 86	88.90	180	11625	2280	638	270	19.9	2.7	6.9	10.9	4.04	1.58
<i>obtusum - stellare</i>	Bed 86	89.20	180	9188	1682	485	257	15.1	2.0	4.8	10.4	5.20	2.17
<i>obtusum - stellare</i>	Bed 86	89.50	180	10727	2090	569	259	18.1	2.5	6.0	10.4	4.16	1.73
<i>obtusum - stellare</i>	Bed 86	89.80	180	11150	2172	552	348	18.9	2.7	4.9	14.4	5.33	2.94
<i>obtusum - stellare</i>	Bed 86	90.10	180	12371	2485	637	383	21.3	3.1	5.9	15.8	5.10	2.68
<i>obtusum - stellare</i>	Bed 87	90.40	240	13818	2695	682	444	17.4	2.5	4.4	13.8	5.52	3.14
<i>obtusum - stellare</i>	Bed 87	90.70	240	11499	2301	563	302	13.9	2.1	4.1	9.1	4.33	2.22
<i>obtusum - stellare</i>	Bed 88	91.00	180	10791	2184	472	278	18.2	2.8	4.3	11.3	4.04	2.63
<i>obtusum - stellare</i>	Bed 88	91.30	180	9872	2081	382	297	16.4	2.8	2.7	12.3	4.39	4.56
<i>obtusum - stellare</i>	Bed 88	91.60	180	9847	2049	424	301	16.4	2.6	3.4	12.4	4.77	3.65
<i>obtusum - stellare</i>	Bed 88	91.90	220	11214	2365	477	343	15.0	2.5	3.1	11.5	4.60	3.71
non sequence	Coinstone	92.20	420	17686	3435	728	515	11.9	1.9	2.5	8.9	4.68	3.56
<i>raricostatium - densinodulum</i>	Bed 90	92.50	200	10461	2079	512	298	15.5	2.3	4.3	10.9	4.74	2.53
<i>raricostatium - densinodulum</i>	Bed 90	92.80	200	9787	2023	448	238	14.3	2.3	3.9	8.4	3.65	2.15
<i>raricostatium - densinodulum</i>	Bed 90	93.10	200	10548	2148	495	286	15.7	2.4	4.1	10.4	4.33	2.54
<i>raricostatium - densinodulum</i>	Bed 90	93.40	200	9218	1782	450	255	13.3	1.9	3.8	9.2	4.84	2.42
<i>raricostatium - densinodulum</i>	Bed 90	93.70	240	12843	2658	575	361	15.9	2.9	3.7	11.1	3.83	3.00
<i>raricostatium - densinodulum</i>	Bed 92	94.00	240	16216	3433	694	494	20.9	3.4	4.2	15.4	4.53	3.67
<i>raricostatium - densinodulum</i>	Bed 93	94.30	200	13368	2785	620	422	20.7	3.2	4.7	15.7	4.91	3.34
<i>raricostatium - densinodulum</i>	Bed 94	94.60	180	11747	2460	486	387	20.1	3.2	3.5	16.2	5.06	4.63
<i>raricostatium - densinodulum</i>	Bed 94	94.90	180	10469	2193	436	350	17.6	2.9	3.1	14.5	5.00	4.68
<i>raricostatium - densinodulum</i>	Bed 94	95.20	180	10499	2301	465	326	17.6	3.0	3.8	13.8	4.60	3.63
<i>raricostatium - densinodulum</i>	Bed 96	95.50	180	9975	2031	404	281	16.6	2.6	3.2	11.4	4.38	3.56
<i>raricostatium - densinodulum</i>	Bed 96	95.80	180	9393	1957	373	267	15.5	2.6	2.9	11.0	4.23	3.79

Table 2.09 (3 of 4).

Biostratigraphy	Horizon	Thick. (m)	Time Secs	Total Number of Counts Recorded			Total µr	Elemental Concentrations			Ratios		
				Total	K	U		Th	K%	U ppm	Th ppm	Th/K	Th/U
<i>raricostatium - densinodulum</i>	Bed 96	96.10	180	11696	2349	418	353	20.0	3.1	2.8	14.7	4.74	5.25
<i>raricostatium - densinodulum</i>	Bed 96	96.40	180	10417	2233	402	368	17.5	3.0	2.4	15.3	5.10	6.38
<i>raricostatium - densinodulum</i>	Bed 96	96.70	180	11303	2208	395	295	19.2	2.9	2.9	12.2	4.21	4.21
<i>raricostatium - densinodulum</i>	Bed 96	97.00	180	10117	2156	333	322	16.9	2.9	1.8	13.4	4.62	7.44
<i>raricostatium - densinodulum</i>	Bed 96	97.30	180	10137	2168	379	290	16.9	2.9	2.8	11.9	4.10	4.25
<i>raricostatium - densinodulum</i>	Bed 96	97.60	180	10312	2152	442	354	17.3	2.8	3.1	14.8	5.29	4.77
<i>raricostatium - densinodulum</i>	Bed 96	97.90	180	11258	2378	485	317	19.1	3.1	4.1	13.0	4.19	3.17
<i>raricostatium - densinodulum</i>	Bed 96	98.20	180	10862	2316	435	328	18.4	3.1	3.3	13.6	4.39	4.12
<i>raricostatium - densinodulum</i>	Bed 96	98.50	180	10846	2355	474	329	18.3	3.1	3.9	13.6	4.39	3.49
<i>raricostatium - densinodulum</i>	Bed 96	98.80	180	10476	2292	413	330	17.6	3.1	2.9	13.7	4.42	4.72
<i>raricostatium - densinodulum</i>	Bed 96	99.10	180	10336	2273	383	332	17.3	3.1	2.4	13.8	4.45	5.75
<i>raricostatium - densinodulum</i>	Bed 97	99.40	180	10811	2356	440	338	18.3	3.1	3.2	14.0	4.52	4.38
<i>raricostatium - densinodulum</i>	Bed 97	99.70	180	10297	2209	408	316	17.3	2.9	3.0	13.1	4.52	4.37
<i>raricostatium - densinodulum</i>	Bed 97	100.00	180	10528	2262	386	300	17.7	3.0	2.7	12.4	4.13	4.59
<i>raricostatium - densinodulum</i>	Bed 97	100.30	180	10981	2328	429	358	18.6	3.1	2.9	14.9	4.81	5.14
<i>raricostatium - densinodulum</i>	Bed 97	100.60	180	10652	2243	467	334	18.0	2.9	3.7	13.8	4.76	3.73
<i>raricostatium - densinodulum</i>	Bed 97	100.90	180	13240	2868	516	453	23.1	3.9	3.3	19.1	4.90	5.79
<i>raricostatium - densinodulum</i>	Bed 99	101.20	180	11493	2396	449	355	19.6	3.2	3.2	4.0	1.25	1.25
<i>raricostatium - raricostatooides</i>	Bed 100	101.50	180	12000	2593	457	404	20.6	3.5	2.9	16.9	4.83	5.83
<i>raricostatium - raricostatooides</i>	Bed 100	101.80	180	10464	2262	431	315	17.6	3.0	3.3	13.1	4.37	3.97
<i>raricostatium - raricostatooides</i>	Bed 100	102.10	180	10904	2324	412	389	18.4	3.1	2.3	16.3	5.26	7.09
<i>raricostatium - raricostatooides</i>	Bed 100	102.40	200	13245	2830	581	417	20.5	3.3	4.1	15.6	4.73	3.80
<i>raricostatium - raricostatooides</i>	Bed 100	102.70	200	12433	2545	515	388	19.0	3.0	3.5	14.5	4.83	4.14
<i>raricostatium - raricostatooides</i>	Bed 100	103.00	200	12515	2598	523	522	19.2	3.1	3.3	15.8	5.10	4.79
<i>raricostatium - raricostatooides</i>	Bed 100	103.30	200	9597	1824	420	309	14.0	2.1	2.9	11.4	5.43	3.93
<i>raricostatium - raricostatooides</i>	Bed 100	103.60	200	10335	2027	445	329	15.3	2.3	3.1	12.2	5.30	3.94
<i>raricostatium - raricostatooides</i>	Bed 102	103.90	180	9572	1924	406	300	15.8	2.5	3.1	12.4	4.96	4.00
<i>raricostatium - raricostatooides</i>	Bed 102	104.20	180	10310	2152	426	313	17.3	2.8	3.3	12.9	4.61	3.91
<i>raricostatium - raricostatooides</i>	Bed 103	104.50	180	10414	2161	475	361	17.5	2.8	3.6	15.0	5.36	4.17
<i>raricostatium - raricostatooides</i>	Bed 103	104.80	180	11427	2189	632	295	19.5	2.6	6.6	12.0	4.62	1.82
<i>raricostatium - raricostatooides</i>	Hummocky	105.10	180	10248	1837	654	212	17.2	2.0	7.8	8.2	4.10	1.05

Table 2.02 (4 of 4).

Biostratigraphy	Horizon	Thick. (m)	Time Secs	Total Number of Counts Recorded			Total u	Elemental Concentrations			Ratios		
				Total	K	U		Th	K %	U ppm	Th ppm	Th/K	Th/U
Hummocky	bed103	105.2	180	10248	1837	654	212	17.2	2.0	7.8	8.2	4.10	1.05
<i>jamesoni - taylori</i>	bed 105	105.5	260	9534	1786	447	217	9.9	1.5	3.1	5.9	3.93	1.90
<i>jamesoni - taylori</i>	bed 106	105.8	300	9412	1832	400	198	9.8	1.6	2.7	5.2	3.25	1.93
<i>jamesoni - taylori</i>	bed 107	106.1	300	12377	2108	647	247	11.6	1.4	4.3	5.7	4.07	1.33
<i>jamesoni - taylori</i>	bed 108	106.4	300	11924	2258	606	268	11.0	1.6	3.8	6.2	3.88	1.63
<i>jamesoni - taylori</i> **	bed 108	106.7	300	11896	2183	638	230	11.0	1.5	4.3	5.3	3.53	1.23
<i>jamesoni - taylori</i> **	bed 108	107.0	300	11396	2126	583	240	10.4	1.5	3.7	5.6	3.73	1.51
<i>jamesoni - taylori</i> **	bed 108	107.3	300	11521	2208	592	247	10.6	1.6	3.8	5.7	3.56	1.50
<i>jamesoni - taylori</i>	bed 108	107.6	300	11975	2343	576	262	11.1	1.7	3.6	6.1	3.59	1.69
<i>jamesoni - taylori</i> **	bed 108	107.9	300	11763	2315	539	255	10.8	1.7	3.2	6.0	3.53	1.88
<i>jamesoni - taylori</i>	bed 108	108.2	300	13138	2631	583	319	12.5	2.0	3.3	7.6	3.80	2.30
<i>jamesoni - taylori</i>	bed 109	108.5	240	10724	2159	521	249	12.8	2.0	4.0	7.4	3.70	1.85
<i>jamesoni - polymorphus</i>	bed 110	108.8	240	10559	2084	504	235	12.5	1.9	3.9	6.9	3.63	1.77
<i>jamesoni - polymorphus</i>	bed 110	109.1	240	10068	2047	456	207	11.8	1.9	3.5	6.0	3.16	1.71
<i>jamesoni - polymorphus</i>	bed 110	109.4	240	12674	2617	539	262	15.7	2.5	4.0	7.8	3.12	1.95
<i>jamesoni - polymorphus</i>	bed 110	109.7	240	12650	2597	662	289	15.6	2.4	5.3	8.6	3.58	1.62
<i>jamesoni - polymorphus</i>	bed 110	110.0	200	10891	2262	589	228	16.3	2.9	5.9	8.1	2.79	1.37
<i>jamesoni - polymorphus</i>	bed 110	110.3	200	10450	2177	544	215	15.5	2.4	5.4	7.6	3.17	1.41
<i>jamesoni - polymorphus</i>	bed 110	110.6	200	10103	2074	510	199	14.9	2.4	5.1	6.9	2.88	1.35
<i>jamesoni - polymorphus</i>	bed 110	110.9	200	10061	1998	493	242	14.8	2.2	4.5	8.7	3.95	1.93
<i>jamesoni - polymorphus</i>	bed 110	111.2	200	9535	1946	456	224	13.9	2.2	4.1	8.5	3.86	2.07
<i>jamesoni - polymorphus</i>	bed 110	111.5	200	10065	2025	556	233	14.8	2.2	5.4	8.2	3.73	1.52
<i>jamesoni - polymorphus</i>	bed 110	111.8	200	10345	2118	521	230	15.3	2.3	5.0	8.2	3.57	1.64
<i>jamesoni - polymorphus</i>	bed 110	112.4	240	11604	2364	583	250	14.1	2.2	4.7	7.3	3.32	1.55
<i>jamesoni - polymorphus</i>	bed 110	112.7	240	10967	2226	536	261	13.2	2.1	4.1	7.8	3.71	1.90
<i>jamesoni - polymorphus</i>	bed 110	113.0	240	9949	2028	433	206	11.6	1.9	3.9	6.0	3.16	1.54
<i>jamesoni - polymorphus</i> **	bed 110	113.3	200	9146	1776	409	198	13.2	2.0	3.7	7.0	3.50	1.89

Table 2.10 Gamma-ray data-set for the Belemnite Marls that outcrop between Stonebarrow and Seatown, Dorset (SY 380927 - SY 415918). Beds 103-110 were measured from the cliff exposure east of Westhay Water (SY 386925 - SY 391924). Measurements for beds 116-121 were obtained from the exposure between Golden Cap and Seatown (SY 410918 - SY 416917). A total number of 89 sets of measurements were collected in all. All readings were taken with the B.P. GR-256 during the period 20th October - 27th October 1993. (1 of 3.)

Biostratigraphy	Horizon	Thick. (m)	Time Secs	Total Number of Counts Recorded			Total µr	Elemental Concentrations			Ratios		
				Total	K	U		Th	K %	U ppm	Th ppm	Th/K	Th/U
<i>jamesoni - polymorphus</i>	bed 110	113.6	200	9057	1845	406	217	13.0	2.1	3.5	7.8	3.71	2.23
<i>jamesoni - polymorphus</i>	bed 110	113.9	240	11456	2373	515	242	13.9	2.3	3.9	7.1	3.09	1.82
<i>jamesoni - polymorphus</i>	bed 110	114.2	240	10022	2053	432	221	11.8	2.0	3.2	6.5	3.25	2.03
<i>jamesoni - polymorphus</i>	bed 110	114.5	240	10452	2148	460	219	12.4	2.0	3.5	6.4	3.20	1.83
<i>jamesoni - polymorphus</i>	bed 110	114.8	200	10147	2017	442	244	11.9	1.9	3.1	7.3	3.84	2.35
<i>jamesoni - polymorphus</i> **	bed 110	115.1	200	9492	1940	445	230	13.8	2.2	3.9	8.3	3.77	2.13
<i>jamesoni - polymorphus</i> **	bed 110	115.4	200	10442	2086	566	222	15.5	2.2	5.6	7.8	3.55	1.39
<i>jamesoni - polymorphus</i> **	bed 110	115.7	200	10544	2154	539	254	15.7	2.4	5.0	9.2	3.83	1.84
<i>jamesoni - polymorphus</i>	bed 110	116.0	200	10722	2205	523	236	16.0	2.5	4.9	8.4	3.36	1.71
<i>jamesoni - polymorphus</i>	bed 110	116.3	200	11093	2203	573	258	16.6	2.4	5.4	9.3	3.88	1.72
<i>jamesoni - polymorphus</i>	bed 110	116.6	200	11522	2334	644	264	17.4	2.5	6.4	9.5	3.80	1.48
<i>jamesoni - polymorphus</i>	bed 110	116.9	240	12441	2451	637	269	15.3	2.2	5.2	8.0	3.64	1.54
<i>jamesoni - polymorphus</i>	bed 110	117.2	240	9681	1912	444	220	11.2	1.8	3.3	6.5	3.61	1.97
<i>jamesoni - polymorphus</i>	bed 110	117.5	300	10427	1923	456	253	9.3	1.4	2.5	5.9	4.21	2.36
<i>jamesoni - polymorphus</i>	bed 110	117.8	240	9452	1863	426	223	10.9	1.7	3.1	6.5	3.82	2.10
<i>jamesoni - polymorphus</i>	bed 111	118.1	300	11140	2197	487	247	10.1	1.6	2.8	5.7	3.56	2.04
<i>jamesoni - polymorphus</i>	bed 111	118.4	300	9290	1687	396	201	7.9	1.2	2.3	4.6	3.83	2.00
<i>jamesoni - polymorphus</i>	bed 111	118.7	300	11787	2457	475	275	10.9	1.9	2.6	6.6	3.47	2.54
<i>jamesoni - polymorphus</i>	bed 111	119.0	240	9631	2032	422	213	11.2	1.9	3.1	6.3	3.32	2.03
<i>jamesoni - polymorphus</i>	bed 111	119.3	240	10521	2287	420	251	12.5	2.2	2.8	7.5	3.41	2.68
<i>jamesoni - polymorphus</i>	bed 111	119.6	240	10252	2196	447	261	12.1	2.1	3.0	7.8	3.71	2.60
<i>jamesoni - polymorphus</i>	bed 112	119.9	240	10629	2215	465	245	12.7	2.1	3.3	7.3	3.48	2.21
<i>jamesoni - polymorphus</i>	bed 112	120.2	240	10607	2174	474	241	12.6	2.1	3.5	7.2	3.43	2.06
<i>jamesoni - polymorphus</i>	bed 112	120.5	240	10873	2317	466	231	13.0	2.2	3.4	6.8	3.09	2.00
<i>jamesoni - polymorphus</i>	bed 112	120.8	240	10522	2270	415	235	12.5	2.2	2.8	6.9	3.14	2.46
<i>jamesoni - polymorphus</i>	bed 113	121.1	240	10341	2043	535	246	12.2	1.8	4.1	7.2	4.00	1.76
<i>jamesoni - brevispina</i>	bed 113	121.4	300	10446	2067	428	238	9.3	1.6	2.3	5.5	3.44	2.39
<i>jamesoni - brevispina</i>	bed 113	121.7	300	11739	2402	497	277	10.8	1.8	2.7	6.5	3.61	2.41
<i>jamesoni - brevispina</i>	bed 113	122.0	300	10945	2149	446	264	9.9	1.6	2.4	6.2	3.88	2.58
<i>jamesoni - brevispina</i>	bed 114	122.3	300	10260	1881	411	247	9.1	1.4	2.2	5.8	4.14	2.64
<i>jamesoni - brevispina</i>	bed 114	122.6	300	12799	2707	538	319	12.1	2.1	2.9	7.6	3.62	2.62

Table 2.10 (2 of 3).

Biostratigraphy	Horizon	Thick. (m)	Time Secs	Total Number of Counts Recorded			Elemental Concentrations			Ratios			
				Total	K	U	Th	U ppm	Th ppm	K %	U ppm	Th/K	Th/U
<i>jamesoni - brevispina</i>	bed 114	122.9	300	13085	2763	527	320	12.4	2.2	2.7	7.7	3.50	2.85
<i>jamesoni - brevispina</i>	bed 114	123.2	200	9029	1977	357	206	13.0	2.3	2.9	7.3	3.17	2.52
<i>jamesoni - jamesoni</i>	bed 115	123.5	200	9007	1860	378	242	12.9	2.2	2.9	8.0	3.64	2.76
<i>jamesoni - jamesoni</i>	bed 115	123.8	240	10038	2165	376	244	11.8	2.1	2.3	7.4	3.52	3.22
<i>jamesoni - jamesoni</i>	bed 115	124.1	240	9895	1965	397	254	11.6	1.9	2.5	7.6	4.00	3.04
<i>jamesoni - jamesoni</i>	bed 115	124.4	240	9340	1899	365	217	10.7	1.8	2.4	6.4	3.56	2.67
<i>jamesoni - jamesoni</i>	bed 115	124.7	240	9798	2002	423	248	11.4	1.9	2.8	7.5	3.95	2.68
<i>jamesoni - jamesoni</i>	bed 115	125.0	240	11045	2317	483	248	13.3	2.2	3.5	7.4	3.36	2.11
<i>jamesoni - jamesoni</i>	bed 115	125.3	200	9650	2055	409	230	14.1	2.4	3.4	8.3	3.46	2.44
<i>jamesoni - jamesoni</i>	bed 115	125.6	200	9603	2038	374	240	14.0	2.4	2.8	8.8	3.67	3.14
<i>jamesoni - jamesoni</i>	bed 115	125.9	200	9187	1932	420	236	13.2	2.2	3.5	8.5	3.86	2.43
<i>jamesoni - jamesoni</i>	bed 116	126.2	200	10539	2094	446	272	12.5	2.0	2.9	8.2	4.10	2.83
<i>jamesoni - jamesoni</i>	bed 116	126.5	200	10132	1978	424	250	11.9	1.9	2.9	7.4	3.89	2.55
<i>jamesoni - jamesoni</i> **	bed 117	126.8	200	9603	1949	403	214	11.1	1.9	2.8	6.3	3.32	2.25
<i>jamesoni - jamesoni</i> **	bed 117	127.1	200	10773	2259	419	246	12.9	2.2	2.0	7.3	3.32	3.65
<i>jamesoni - jamesoni</i> **	bed 118	127.4	200	10236	2091	404	275	12.1	2.0	2.5	8.3	4.15	3.32
<i>jamesoni - jamesoni</i> **	bed 118	127.7	200	9903	2066	406	227	14.5	2.4	3.4	8.2	3.42	2.41
<i>jamesoni - jamesoni</i>	bed 118	128.0	200	10841	2264	474	287	16.2	2.6	3.8	10.5	4.04	2.76
<i>jamesoni - jamesoni</i>	bed 118	128.3	200	10976	2360	547	285	16.4	2.7	4.8	10.4	3.85	2.17
<i>ibex - masseanum</i>	bed 118	128.6	200	11046	2362	518	304	16.5	2.7	4.3	11.2	4.15	2.60
<i>ibex - masseanum</i>	bed 118	128.9	200	10963	2346	501	296	16.4	2.7	4.1	10.8	4.00	2.63
<i>ibex - masseanum</i>	bed 118	129.2	200	10031	2013	413	289	14.7	2.3	2.9	10.6	4.61	3.66
<i>ibex - valdani</i>	bed 118	129.5	200	9611	2017	431	232	14.0	2.3	3.7	8.3	3.61	2.24
<i>ibex - valdani</i>	bed 118	129.8	200	9718	1954	443	239	14.2	2.2	3.8	8.6	3.91	2.26
<i>ibex - valdani</i>	bed 119	130.1	200	9453	1951	460	276	13.7	2.2	3.8	10.0	4.55	2.63
<i>ibex - valdani</i>	bed 119	130.4	200	9505	1953	467	251	13.8	2.2	4.1	9.1	4.14	2.22
<i>ibex - valdani</i>	bed 119	130.7	200	10209	2000	520	240	15.1	2.2	4.8	9.0	4.09	1.88
<i>ibex - valdani</i>	bed 120	131.0	200	10880	2182	578	286	16.3	2.4	5.3	10.3	4.29	1.94
<i>ibex - valdani</i>	bed 120	131.3	200	10800	2020	582	265	16.1	2.1	5.5	9.5	4.52	1.73
<i>ibex - valdani</i>	bed 120	131.6	200	10209	1994	568	240	15.1	2.1	5.5	8.6	4.10	1.56
<i>ibex - luridum</i>	bed 121	131.9	200	10413	2054	460	277	15.4	2.3	3.7	10.2	4.43	2.76

Table 2.10 (3 of 3).

Biostratigraphy	Height m	Time Secs	Total Number of Counts			Total µg	Elemental Concentration			Ratios	
			Total	K	U		Th	K %	U ppm	Th ppm	Th/K
<i>ibex - luridum</i>	0.0	140	10234	1978	435	335	3.3	3.5	17.9	5.42	5.11
<i>ibex - luridum</i>	0.3	140	9550	1819	451	337	2.9	3.8	17.9	6.17	4.71
<i>ibex - luridum</i>	0.6	140	10166	1914	489	336	3.0	4.6	17.9	5.97	3.89
<i>ibex - luridum</i>	0.9	140	9727	1856	436	326	2.8	3.9	19.1	6.82	4.90
<i>ibex - luridum</i>	1.2	140	10229	1978	460	361	3.2	3.6	19.3	6.03	5.36
<i>ibex - luridum</i>	1.5	180	12881	2518	570	477	3.2	3.1	19.9	6.22	6.42
<i>ibex - luridum</i>	1.8	140	9740	1862	442	294	3.0	4.2	15.6	5.20	3.71
<i>ibex - luridum</i> **	2.1	140	9036	1685	381	307	2.8	2.8	16.3	5.82	5.82
<i>ibex - luridum</i> **	2.4	140	9763	1835	376	373	3.1	1.7	20.0	6.45	11.76
<i>ibex - luridum</i>	2.7	140	9290	1835	444	342	3.0	3.6	18.2	6.07	5.06
<i>ibex - luridum</i>	3.0	140	9905	1853	489	304	2.9	5.1	16.0	5.52	3.14
<i>ibex - luridum</i>	3.3	140	9006	1639	386	298	2.7	3.1	15.8	5.85	5.10
<i>ibex - luridum</i>	3.6	180	11374	2172	491	408	2.8	2.6	17.0	6.07	6.54
<i>ibex - luridum</i>	3.9	180	11299	2081	517	376	2.6	3.5	15.4	5.92	4.40
<i>ibex - luridum</i>	4.2	180	11057	2118	495	380	2.7	3.1	15.6	5.78	5.03
<i>ibex - luridum</i>	4.5	180	10595	1970	446	350	2.5	2.6	14.4	5.76	5.54

Table 2.11 Gamma-ray data-set for the *luridum* Subzone of the *ibex* Zone that is exposed in Blockley Pit, Gloucestershire. (SP 182369). The gamma-ray logs were measured from a series of fresh sections in the pit. The measurements taken between 0 m and 4.2 m were obtained from a section exposed at the north end of the pit, measurements taken between 4.2 m and 9.3 m were obtained from a section exposed at the south east end of the pit and the remainder of measurements were obtained from a section at the south-south west end of the pit. The 36 sets of measurements were collected with the Edinburgh University GR-256 on the 10th October 1995. Measurements were taken with the detector placed perpendicular to the section and parallel to bedding, except for readings denoted by ** which indicates a poor sample geometry. (1 of 2).

Biostratigraphy	Height m	Time Secs	Total Number of Counts			Total μr	Elemental Concentration			Ratios		
			Total	K	U		Th	K %	U ppm	Th ppm	Th/K	Th/U
<i>ibex - luridum</i>	4.8	180	11957	2319	595	403	19.3	2.9	4.4	16.6	5.72	3.77
<i>ibex - luridum</i>	5.1	180	11970	2313	553	447	19.3	2.9	3.2	18.6	6.41	5.81
<i>ibex - luridum</i>	5.4	180	12194	2356	556	392	19.7	3.0	3.9	16.2	5.40	4.15
<i>ibex - luridum</i>	5.7	180	12127	2290	534	430	19.6	2.9	3.1	17.8	6.14	5.74
<i>ibex - luridum</i>	6.0	180	11865	2313	570	436	19.1	2.9	3.6	18.0	6.21	5.00
<i>ibex - luridum</i>	6.3	180	11560	2175	534	382	18.5	2.7	3.7	15.7	5.81	4.24
<i>ibex - luridum</i> **	6.6	180	11479	2172	514	419	18.3	2.7	2.9	17.3	6.41	5.97
<i>ibex - luridum</i> **	6.9	180	11804	2219	549	383	18.9	2.8	3.9	15.7	5.61	4.03
<i>ibex - luridum</i> **	7.2	180	12648	2374	598	431	20.6	2.9	4.7	17.8	6.14	3.79
<i>ibex - luridum</i> **	7.5	180	12440	2320	591	429	20.2	2.9	4.1	17.8	6.14	4.34
<i>ibex - luridum</i>	7.8	180	9970	1838	419	338	15.5	2.3	2.4	13.8	6.00	5.75
<i>ibex - luridum</i>	8.1	180	10072	1899	476	333	15.7	2.3	3.3	13.6	5.91	4.12
<i>ibex - luridum</i>	8.4	180	10269	1920	443	328	16.1	2.4	2.8	13.4	5.58	4.79
<i>ibex - luridum</i>	8.7	180	11455	2302	940	378	18.3	3.0	3.0	15.7	5.23	5.23
<i>ibex - luridum</i>	9.0	180	11008	2096	472	388	17.5	2.7	2.6	16.1	5.96	6.19
<i>ibex - luridum</i>	9.3	180	11484	2183	516	397	18.3	2.7	3.2	16.4	6.07	5.13
<i>ibex - luridum</i>	9.6	180	10830	2134	465	353	17.1	2.7	2.9	14.5	5.37	5.00
<i>ibex - luridum</i>	9.9	180	10685	2001	492	382	16.8	2.5	3.0	15.7	6.28	5.23
<i>ibex - luridum</i>	10.2	180	10342	1882	484	341	16.2	2.3	3.4	13.9	6.04	4.09
<i>ibex - luridum</i>	10.5	180	10203	1936	364	345	16.0	2.4	3.0	14.2	5.92	4.73

Table 2.11 (2 of 2)

ARTIFICIAL RADIOACTIVE CONTAMINATION AS A POSSIBLE,
ADDITIONAL SOURCE OF ERROR

The uppermost part of the *bucklandi* Subzone and the lowermost part of the *lyra* Subzone, between 110.4 m and 127.0 m, exposed at Hinkley Point, Somerset (ST 210465) was not measured. It is represented by foreshore which was entirely covered by *Fucus* (order Phaeophycophyta) during August and September 1995. This made gamma-ray measurements impractical.

Additionally, the GR-410 data-set, previously collected from this locality during August 1994, suggests artificial radioactive contamination of the foreshore released from the outflow pipe from the nuclear power station. Sets of gamma-ray measurement were collected from the foreshore just west of the outflow pipe (Figure 6.01, overleaf). The minimum distance from the outflow pipe was 80 cm. The gamma-ray signature (Figure 6.01) shows an increase in U and Th concentration within the raw data-set with the concentration of the radionuclides being similar (*e.g.* mean Th ppm = 20.01 and mean U ppm = 20.70 ppm). This gamma-ray signature is unusual and records the highest Th concentration in the raw GR-410 data-set for the Somerset coast (This data-set can be obtained from the author on request). The lower boundary of the signature collected from Hinkley Point foreshore occurs 60 cm below the dramatic increase in U and Th concentration with the lowermost two readings taken from the base of the cliff rather than from foreshore. The upper boundary coincides with highest stratigraphic sample collected from the foreshore at Hinkley Point. It is likely that the calculated increase in U and Th concentration is due to radioactive contamination from an artificial radionuclide released in the outflow pipe from the nuclear power station onto the foreshore and emits gamma-radiation that can be recorded in the U and Th energy windows in the GR-410 spectrometer (1.76 MeV to 2.62 MeV). Thus, even with robust GR-256 data, it is possible that any gamma-ray log collected from Hinkley Point cannot be reliably interpreted in terms of depositional stratigraphic trends.

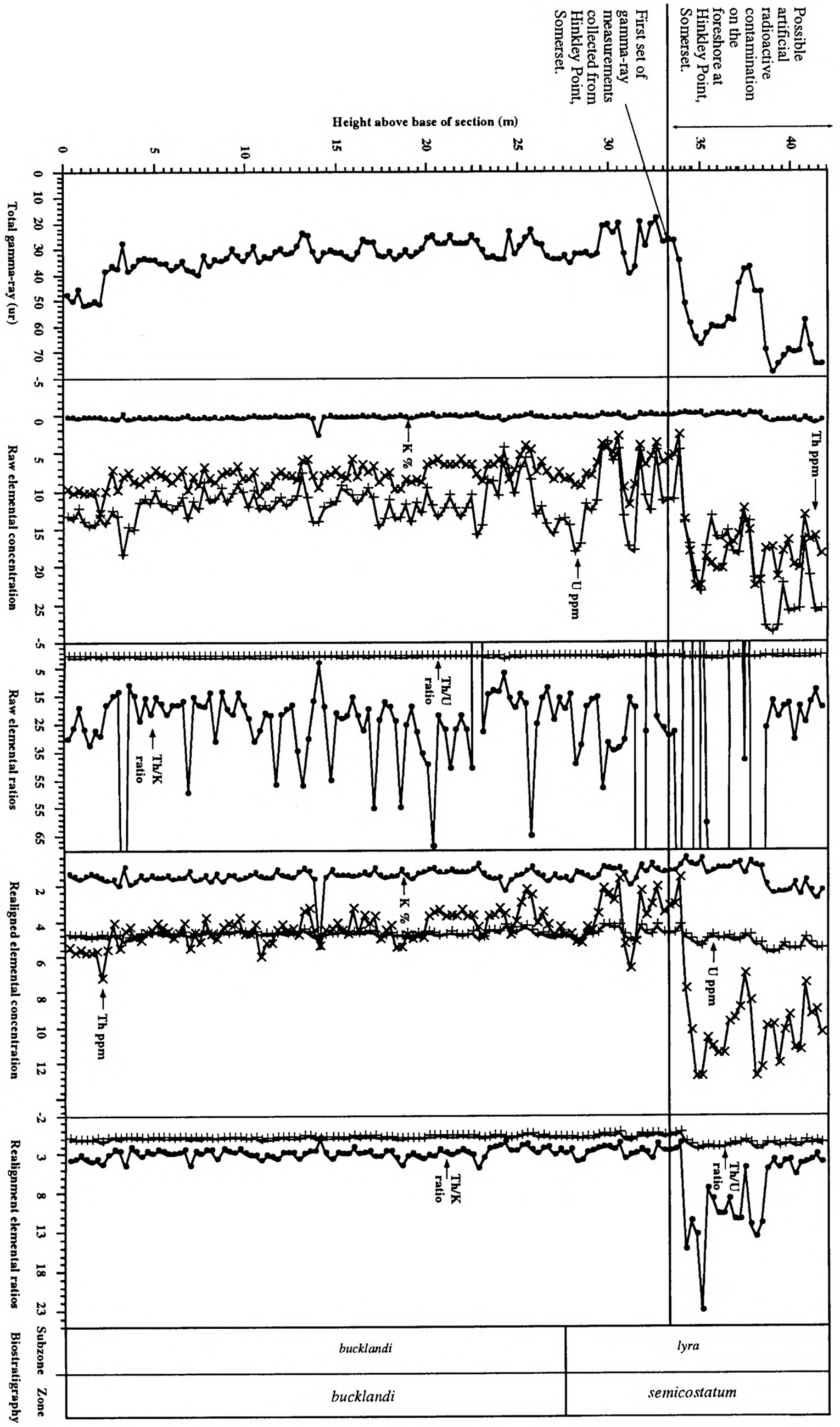


FIGURE 6.01 Total gamma-ray log, elemental-concentration logs and elemental-ratio curves for the Blue Lias exposed west of Klive Pill, Somerset (ST 139457 to ST 445144) and foreshore from Hinkley Point, Somerset (ST 210465). Raw data collected with the GR-410.

Figure 6.01